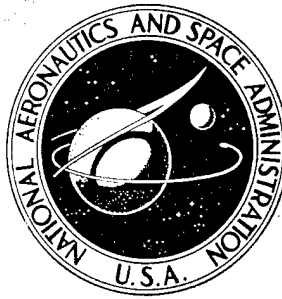


**NASA CONTRACTOR
REPORT**



NASA CR-1205(II)

NASA CR-1205(II)

**COMPENDIUM OF HUMAN RESPONSES
TO THE AEROSPACE ENVIRONMENT**

Volume II

Sections 7 - 9

20000920 202

Prepared by

LOVELACE FOUNDATION FOR MEDICAL EDUCATION AND RESEARCH

Albuquerque, N. Mex.

for

NATIONAL AERONAUTICS AND SPACE ADMINISTRATION • WASHINGTON, D. C. • NOVEMBER 1968

DISTRIBUTION STATEMENT A
Approved for Public Release
Distribution Unlimited

COMPENDIUM OF HUMAN RESPONSES TO THE
AEROSPACE ENVIRONMENT

Volume II
Sections 7 - 9

Edited by Emanuel M. Roth, M.D.

Distribution of this report is provided in the interest of
information exchange. Responsibility for the contents
resides in the author or organization that prepared it.

Fred B. Benjamin, D.M.D., Ph. D.
NASA Project Manager

Prepared under Contract No. NASr-115 by
LOVELACE FOUNDATION FOR MEDICAL EDUCATION AND RESEARCH
Albuquerque, N. Mex.

for

NATIONAL AERONAUTICS AND SPACE ADMINISTRATION

7. ACCELERATION

Prepared by

E. M. Roth, M. D., Lovelace Foundation
W. G. Teichner, Ph.D., R. L. Craig, M. D.
Guggenheim Center for Aerospace Health and Safety
Harvard School of Public Health

TABLE OF CONTENTS

7.	ACCELERATION	7-1
	Linear Sustained Acceleration	7-4
	Tolerance Criteria and Back-Angle Conventions	7-5
	$+G_z$ Acceleration	7-12
	Physiological Response	7-12
	Tolerance	7-12
	Interaction with other Stresses	7-12
	$-G_z$ Acceleration	7-17
	Physiological Responses	7-17
	Tolerance	7-17
	$+G_x$ Acceleration	7-17
	Physiological Responses	7-17
	Tolerance	7-19
	Interaction with Other Stresses	7-21
	$-G_x$ Acceleration	7-29
	Physiological Response	7-29
	Tolerance	7-29
	$\pm G_y$ Acceleration	7-35
	Physiological Response	7-35
	Tolerance	7-35
	Restraint and Protective Devices	7-35
	Performance Under Prolonged Linear Acceleration	7-38
	Vision	7-39
	a) Gross Vision	7-39
	b) Absolute Thresholds	7-40
	c) Brightness Discrimination	7-41
	d) Visual Acuity	7-41
	e) Visual Fields and Ocular Motility	7-44
	f) Pupillary Reactions	7-46
	g) Reading Tasks	7-46

Auditory Responses	7-46
Motor Performance	7-48
a) Body Movements	7-48
b) Controls	7-48
c) Cerebral Function	7-49
Training and Simulation	7-53
Rotary Acceleration	7-56
$\pm \dot{R}_y$ Tumbling	7-56
Combined R_y and Linear Acceleration	7-59
$\pm \dot{R}_x$ Roll Spin	7-61
$\pm \dot{R}_z$ Yaw Spin	7-62
Performance During Rotary Acceleration	7-63
Vestibular Interactions in the Rotary Environment	7-64
The Eye Movement Control System	7-77
Motion Sickness	7-82
Vestibular Illusions	7-90
The Visual Illusions	7-90
a) Autokinetic Illusions	7-91
b) Oculogyral Illusions	7-91
c) Oculogravic Illusions	7-93
The Non-Visual Illusions	7-94
a) The Audiogyral Illusion	7-95
b) Vertigo	7-95
Rotating Space Vehicles	7-96
Vestibular Responses	7-96
Operating Limits for Rotating Space Stations	7-106
Zero Gravity Environment	7-110
Cardiovascular Effects	7-110
Respiratory Effects	7-125
Metabolic Effects	7-126
Psychomotor Effects of Weightlessness	7-127
Vestibular Reactions	7-127
Vision	7-132
Extravehicular Activity	7-133

a) Gemini IV	7-133
b) Gemini VIII	7-138
c) Gemini IX-A	7-138
d) Gemini X	7-140
e) Gemini XI	7-142
f) Gemini XII	7-143
g) Maneuvering Equipment	7-145
h) Body Positioning and Restraints	7-148
i) Umbilical and Tether Combinations.	7-150
j) Capability of Astronauts in EVA	7-151
k) Flight Plans and Checklists	7-153
l) Scheduling of EVA and Training	7-154
m) Spacecraft Control During EVA	7-155
n) Medical Factors	7-156
o) Recommendations for Future EVA	7-156
Tether Lines for Astronaut Retrieval.	7-158
a) Conservative Methods	7-159
b) Nonconservative Methods.	7-164
Workspace and Equipment Simulation	7-166
a) Restraints	7-174
b) Tools	7-175
c) Fasteners	7-175
d) Locomotion aids	7-176
e) Work	7-176
Subgravity Environments.	7-177
Locomotion.	7-177
Performance of Tasks	7-188
Impact	7-190
The Biomechanical Factors of Impact	7-190
Physiological Response to Impact	7-195
Human Tolerance Limits.	7-199
On-Axis Impact	7-199
Off-Axis Impact	7-205

Impact by Missiles and Moving Objects	7-212
Restraint and Protective Systems	7-220
References	7-222

ACCELERATION

The spectrum of acceleration environments is extremely large and may vary in duration, magnitude, rate of onset and decline, and direction. Some acceleration exposures may be so mild that they have relatively no physiological or psychophysiological effects, or they may become so severe that they produce major disturbances. After a review of acceleration environment in general, specific sections on linear sustained acceleration in the three orthogonal axes, the rotating environment, angular acceleration, sub-gravity, zero gravity, and impact are presented. Vibration is covered separately in Vibration (No. 8).

Table 7-1a presents comparative nomenclature for the several systems used to describe the acceleration environment. The unit for the physiological acceleration is \underline{G} (system 4), as distinguished from the "true" displacement acceleration, generally designated by aerodynamicists, with the unit \underline{g} (system 1). The physiological acceleration represents the total reactive force

Table 7-1

Vehicle and Body Acceleration - Table of Equivalents

a. Comparative Nomenclature

Direction of motion	Table A Direction of acceleration		Table B Inertial resultant of body acceleration		
	Aircraft computer standard (System 1)	Acceleration descriptive (System 2)	Physiological descriptive * (System 3)	Physiological computer standard (System 4)	Vernacular descriptive
	System 1	System 2	System 3	System 4	
Linear					
Forward	$+a_x$	Forward accel.	^b Transverse A-P G Supine G Chest-to-back G	$+G_x$	Eyeballs in
Backward	$-a_x$	Backward accel.	^c Transverse P-A G Prone G Back-to-chest G	$-G_x$	Eyeballs out
Upward	$-a_z$	Headward accel.	Positive G	$+G_z$	Eyeballs down
Downward	$+a_z$	Footward accel.	Negative G	$-G_z$	Eyeballs up
To right	$+a_y$	R. lateral accel.	Left lateral G	$+G_y$	Eyeballs left
To left	$-a_y$	L. lateral accel.	Right lateral G	$-G_y$	Eyeballs right
Angular					
Roll right	$+p$		Roll	$-\dot{R}_x$	
Roll left	$-p$			$+\dot{R}_x$	
Pitch up	$+q$		Pitch	$-\dot{R}_y$	
Pitch down	$-q$			$+\dot{R}_y$	
Yaw right	$+r$		Yaw	$+\dot{R}_z$	
Yaw left	$-r$			$-\dot{R}_z$	

* The capital letter G is used as a unit to express inertial resultant to whole-body acceleration in multiples of the magnitude of the acceleration due to gravity. Acceleration due to gravity g_0 is 980.665 cm/sec² or 32.1739 ft/sec².

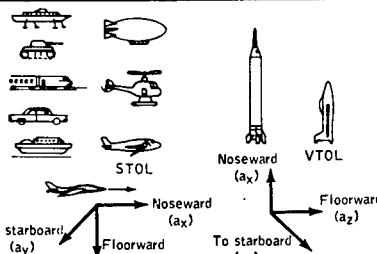
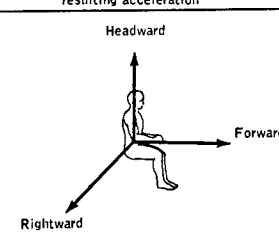
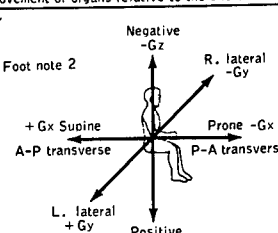
^b A-P refers to anterior-posterior.

^c P-A refers to posterior-anterior.

(After Gell⁽¹⁹⁴⁾)

Table 7-1 (continued)

b. Linear Motion

Vehicle coordinate systems			Human coordinate systems	
			Direction of applied force or resulting acceleration	Direction of kinetic reaction or inertial resistance and movement of organs relative to the skeletal frame
 <p>The zero point of the vehicle coordinate system along the longitudinal axis is arbitrarily set by the individual vehicle manufacturer.</p>				 <p>Foot note 2</p>
<p>1 2 3</p>			<p>4 5 6 7 8 Foot note 3</p>	
<p>(symbol)</p> <p> noseward → +ax tailward → -ax to starboard → +ay to port → -ay floorward → +az ceilingward → -az </p> <p>of the vehicle with the occupant placed</p> <p>prone crosswise head to starboard</p> <p>prone crosswise head to port</p> <p>prone, head toward nose</p> <p>prone, head toward tail</p> <p>supine crosswise, head to starboard</p> <p>supine crosswise, head to port</p> <p>supine, head toward nose</p> <p>supine, head toward tail</p>			<p> forward backward rightward leftward headward tailward, footward </p> <p> acting force and acceleration on the occupant. Because of this accelerative force the occupants' body instantaneously produces an opposing </p> <p> transverse A-P supine chest to back transverse P-A prone back to chest left lateral right lateral positive negative </p> <p> kinetic reaction or inertial resistance </p> <p> +Gx -Gx +Gy -Gy +Gz -Gz </p> <p> eyeballs in (EBI) eyeballs out (EBO) eyeballs left (EBL) eyeballs right (EBR) eyeballs down (EBD) eyeballs up (EBU) </p> <p> backward forward leftward rightward tailward headward </p> <p> and or </p> <p> heart movement relative to the skeletal frame and erect head </p>	

Inter-relationships between vehicle acceleration, the consequent force acting on the occupant, and terms used to describe directions of these variables are shown in the table. Possible inter-relationships are derived as follows: Direction of the vehicle acceleration, based on the above vehicle coordinate system, is selected in column 1. Position of an occupant with respect to the vehicle is selected in column 3. Direction of force acting on vehicle, column 1, combined with the occupant's position with respect to vehicle, column 3, determines direction of force with respect to occupant. Result then determines proper relationship to be selected in column 4. Once correct selection has been made, the two sentences, reading from left to right, list terms and symbols in present use describing directions of forces and accelerations of body, and organ movement relative to skeletal frame. Sentences also describe relationships that must exist because of Newton's laws of motion.

Footnotes:

1. Large letter, G, used as unit to express whole body acceleration in multiples of the acceleration of gravity. Acceleration of gravity, $g_0 = 980.665 \text{ cm/sec}^2$ or 32.1739 ft/sec^2 .
2. A-P, P-A refers to anterior-posterior, posterior-anterior.
3. Symbols ($\pm Gxyz$) represent orthogonal directions of kinetic reaction opposing applied force and thus units must be pounds of reaction force per pound of involved object. Laws of motion indicate that "G" may not represent an acceleration in situations and context depicted, and statement "a + Gx acceleration" would be a misnomer.

(After Pesman⁽⁴⁸⁰⁾)

Table 7-1 (continued)

c. Angular Motion

Vehicle coordinate systems			Human coordinate system		
<p>The zero point of the vehicle coordinate system along the longitudinal axis is arbitrarily set by the individual vehicle manufacturer.</p>			<p>Direction of heart rotation relative to skeletal frame</p>		
1	2	3	4	5	6*
		seated or standing facing noseward			
		seated or standing facing tailward			
		seated or standing facing to starboard			
		seated or standing facing to port			
		prone crosswise head to starboard			
		prone crosswise head to port			
		prone, head toward nose			
		prone, head toward tail			
		supine crosswise, head to starboard			
		supine crosswise, head to port			
		supine, head toward nose			
		supine, head toward tail			
		with respect to vehicle axis, imposes a			
		moment and angular acceleration on occupant. Because of this moment and inertia of the heart, the			
		left twist			
		right twist			

The inter-relationships between vehicle acceleration, the consequent force acting on occupant, and terms used to describe directions of these variables are shown in table. These various possible inter-relationships are derived as follows: Direction of vehicle acceleration, based on above vehicle coordinate systems, is selected in column 1. Position of occupant with respect to vehicle is selected in column 3. Direction of force acting on vehicle, column 1, combined with occupant's position with respect to vehicle, column 3, determines direction of force with respect to occupant. This result then determines proper relationship to be selected in column 4. Once correct selections have been made, the two sentences, reading from left to right, list terms and symbols in present use to describe the directions of forces and accelerations of body and organ movement relative to skeletal frame. Sentences also describe relationships that must exist because of Newton's laws of motion.

Footnote:
Statements true only when intersection of axes is below heart.

(After Pesman⁽⁴⁸⁰⁾)

divided by the body mass, and hence includes both displacement and resisted gravitational acceleration effects. It is thus seen that the physiological acceleration axes of system 4 represent directions of the reactive displacements of organs and tissues with respect to the skeleton. The Z axis is down the spine, with $+G_z$ (unit vector) designations for accelerations causing the heart, etc., to displace footward (caudally). The X axis is front to back, with $+G_x$ designations for accelerations causing the heart to be displaced back toward the spine (dorsally). The Y axis is right to left, with $+G_y$ designations for accelerations causing the heart to be displaced to the left. Angular accelerations which cause the heart to rotate (roll) to the left within the skeleton are specified by the $+\dot{R}_x$ unit vector, representing radians/sec² about the X axis. Angular velocities in the same sense are specified by the $+R_x$ unit vector, representing radians/sec about the X axis. Similarly, $+\dot{R}_y$ represents an angular acceleration producing a pitch down of the heart within the skeleton and $+\dot{R}_z$ represents yaw right of the heart within the skeleton.

System 4 is especially useful in specifying the exact angular position of a subject at any given instant on computerized gimballed centrifuges. It is recommended that systems 2 and 3 and the vernacular system not be used in describing the acceleration environment. They are included in Table 7-1 to allow translation of the different systems used in the older literature to the preferred System 4.

Figures 7-1b and 7-1c develop in greater physical and anatomical detail the equivalence of the different nomenclatures for the vehicular and human coordinate systems.

LINEAR SUSTAINED ACCELERATION

There is a difference in body response to accelerations of duration below and above approximately 0.2 second, related to the latent period for the development of hydrostatic effects. This duration will be used to delineate sustained acceleration from abrupt or impact type of acceleration. Other classifications such as brief acceleration (up to 10 seconds) and prolonged acceleration (greater than 10 seconds) may be used (178). An older classification defines abrupt acceleration as ranging from 0 to 2 seconds, brief acceleration as ranging from 2.1 to 10 seconds, long-term acceleration from 10.1 to 60 seconds, and prolonged acceleration as anything over 60 seconds (188). The following variables are of concern from the human point of view (72, 74, 178).

- Magnitude of the peak or peaks of acceleration
- Duration of the peak or peaks of acceleration
- Total duration of the acceleration from time of onset to completion of offset
- Direction of the primary or resultant acceleration with respect to the body axes (vector)
- Gradient of inertial effects along body in short-armed centrifuges

- Rate of onset and offset
- Types of end points used in determining tolerance (physiological and performance limits may be related but need not be same; portion of G profile when test performed)
- Types of G-protection devices and body restraints used; also the coupling between the individual and the vehicle of application (seat, couch, etc.)
- Body position, including specific back, head, and leg angles
- Environmental conditions such as temperature, ambient pressure and lighting
- Anthropomorphic form of the specific test animal's body and its components which modify the transmission of force (impedance)
- Age of subject
- Emotional factors such as fear and anxiety, confidence in self and apparatus, and willingness to tolerate discomfort and pain
- Motivational factors such as competitive attitude, desire to be selected for a particular space project, or specific pay, recognition, or awards
- Previous acceleration training and accumulative effects
- Techniques of breathing, straining, and muscular control; and G-protection devices

Tolerance Criteria and Back-Angle Conventions

Because various investigations are often of different intent, different criteria are used for what is and is not tolerable. The criteria used to terminate any given experiment can be assigned to categories as "subjective" (pain or discomfort) or "arbitrary" (time limit), or may be specifically noted. As is often the case, to reduce the number of points plotted on the graphs, only the highest runs (both amplitude and duration) of any series is used. Whenever the data to be presented are noted as representing the present upper limits of known, primarily subjective, tolerance, it should be recognized that there are many subjects who, for any given time, duration, and direction of acceleration, could not tolerate the exposure. As will be noted in tables and corresponding figures graphically expressing the tolerance data (7-5, 7-7, 7-9, 7-10, 7-11, 7-16, and 7-17), a duration attained by a single subject ($n = 1$) in a group of subjects (e.g., 1 of 4) is the longest of the group. Durations attained by more than one subject ($n > 1$) in a group of subjects (e.g., 3 of 4) are the longer of the group. The symbol (S) will be used when the subject terminates the experiment because of pain, fatigue, or dyspnea, or when he is not permitted to continue because of heart rate, ECG changes, or "blackout." The symbol (A) is used for termination of totally arbitrary nature, such as arbitrary time limits, or completion of

experimental measurements. Trauma listed are those reported in the references and are of a "serious" nature. The notation "none" does not exclude blackout, petechiae, fatigue, or discomfort. The term "aided" in the figures refers to countermeasures used in the corresponding tables.

Unfortunately, the effective axis of acceleration in operational situations seldom falls on any one orthogonal axis but is a vector with components of each. Most practical vectors are combinations of G_x and G_z with minor components of G_y (see Table 7-1). The nomenclature on angulation is usually given as the angulation of subject's trunk with respect to a plane normal (perpendicular) to the resultant acceleration axis. Figure 7-2a is a diagram of terminology used in the space program relating spacecraft configuration to geometric and physiological body angles. For Apollo an SA of 2° and ϵ of 6.5° is under consideration. The $+G_z$ component of any acceleration directly influences a subject's tolerance to any acceleration. The footward redistribution of blood produced by this direction of inertial force first influences the perfusion of blood through the subject's eyes and brain, causing loss of vision (blackout) and loss of consciousness, respectively. A subtle but important consideration at maximum tolerance levels of acceleration, is the relation between the anatomic $+G_z$ and the physiologic $+G_z$, the latter being termed Retinal-Aortic $+G_z$ (313, 315). This relation results because the eyeballs are in front of (ventral to) the anatomic G_z axis. That is, a line drawn from the root of the heart to the eyes and a line extended along the G_z axis and passing through the heart will include an angle of approximately 15° . In Figure 7-2b, the effective angle causing blackout, termed the Retinal-Aortic $+G_z$, is compared to the $+G_x$ and $+G_z$ component of any given acceleration. The ordinate in Figure 7-2b gives the percent of any acceleration vector amplitude in each of three axes ($+G_z$, $+G_x$, and Retinal-Aortic $+G$), all as a function of the back angle, equivalent to the sum of angles S.A. and ϵ of Figure 7-2a.

The "back angle" is therefore the amount of forward angulation of the subject toward the acceleration vector. The angle included between the subject's $+G_z$ axis and the plane normal (perpendicular) to the direction of acceleration is given as the abscissa. For example, if a subject is inclined 45° toward a $-10G$ acceleration, the acceleration is then termed either a $+10G_x$ or a $+10G_z$, and the resultant in the X-axis is about $+7G_x$, and the apparent $+G_z$ acceleration is also $+7G_z$. However, the Retinal-Aortic $+G_z$ is 15° forward and the effective vector component contributing to blackout, therefore, is about $+9G_z$. With regard to causing blackout, this is approximately 28% greater than is apparent from the $+G_z$ component used alone. Therefore, resolving the $+G_z$ component of a $+G_x$ acceleration is often not enough; one must also resolve the Retinal-Aortic axis component if he desires to realize the effective contribution to blackout or loss of consciousness.

Figure 7-2c gives the threshold $+G_x$ along the RFV vector needed to produce grayout in subjects oriented along different effective physiological angles (EPA) according to nomenclature of Figure 7-2a.

A diagram of a cone of vision. The vertical axis is labeled IX at the top and $-X$ at the bottom. A vertical line segment is labeled SV . A horizontal line segment is labeled SH . The horizontal axis is labeled $-Z$ on the left and $+Z$ on the right. A line segment is labeled VP . A line segment is labeled ARP . A line segment is labeled SA . A line segment is labeled ARA . A line segment is labeled RFV . An angle is labeled ϵ . A person is shown lying down, looking up at the vertex of the cone.

a. The Pilot Orientation and Grayout Terminology Proposed by the NASA Manned Spacecraft Center. The figure shows the relationship between the primary vector direction and pilot orientation employed to calculate the magnitude of sustained forward acceleration force applied along the axis of the column of blood above the heart. The relationship is expressed as follows:

where: X = magnitude of primary forward accelerative force applied along ARP in $+G_x$ units, and
 Z = magnitude of resultant accelerative force applied along ARP in $+G_z$ units.

PERCENT OF ACCELERATION AS VECTOR AMPLITUDE

RETINAL-AORTIC + G_z

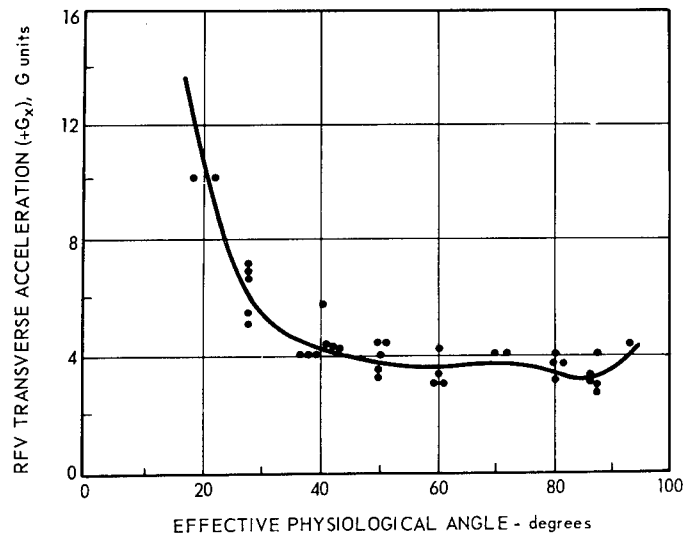
+ G_z

+ G_y

BACK ANGLE (FORWARD INCLINATION), DEGREES

(After Hyde⁽³¹³⁾),

Figure 7-2 (continued)



c. Susceptibility to Grayout as a Function of Pilot Orientation with Respect to the Primary Resultant Vector of a Transverse Acceleration (+G_x).

The terms RFV and EDA are defined in Figure 7-2a

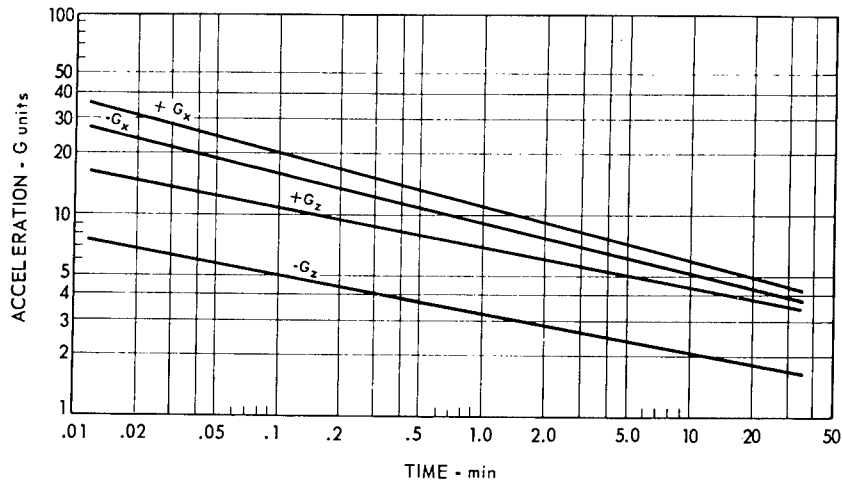
(After Chambers⁽⁷²⁾, adapted from Alexander et al⁽⁹⁾)

Tolerance to acceleration in the G_x and G_z vectors are compared in Figure 7-3. It must be emphasized that the endpoints and back angles for each curve are different and so this figure must at best, be considered only a very rough estimate of relative sensitivity of the human to these G vectors. (Figures 7-5 to 7-17 give more detailed threshold curves.)

Figure 7-4 also compares the G tolerance for the several axes. For clarity, the symbols indicating acceleration vector are applied to a vector regardless of the body attitude within that vector. Thus the triangles used for G_x data include accelerations where a subject is supine and where his legs or head might be raised. Although not all exposures are recorded, the diagram includes all available extreme exposures. It must also be noted that each data point represents a "plateau" of acceleration and not merely an incidental peak (109). Consequently, accelerations experienced in dynamic simulation of, for example, spacecraft launch and reentry are not included. Since it records only plateau acceleration, it ignores the G-time consumed in attaining the plateau. However, in the higher plateaus, depending on the rate of onset a significant G-time may be involved in reaching the level required, and thus, in terms of total impulse, the threshold is proportionately greater than at lower levels. The lines are an estimation of the maximum voluntary tolerance of healthy well-motivated men using conventional restraint harnesses, couches, and G-suits, but not water immersion, positive-pressure breathing, airbags, and so on. The figure shows that, exclusive of rates of onset, some areas are G-time limited

Figure 7-3
Crude Comparison of G-Tolerance in Four Vectors of G

a.

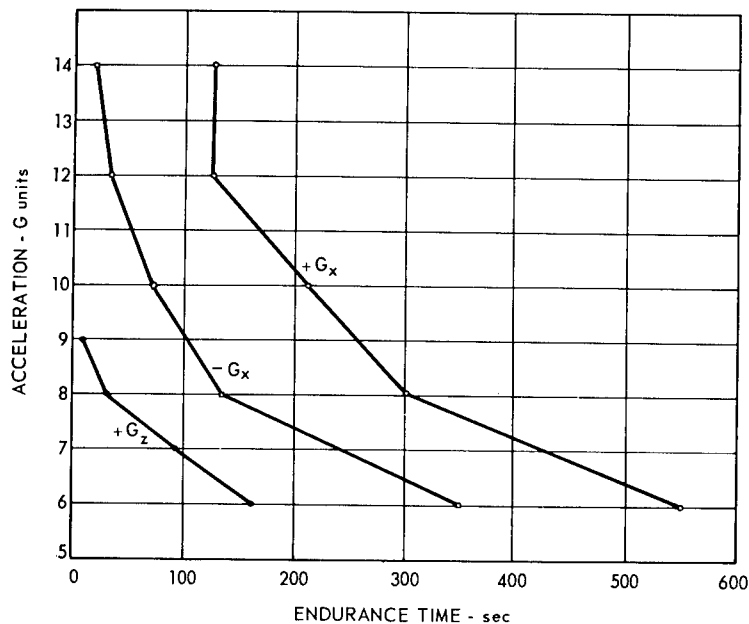


Average acceleration tolerance is shown for (+G_z), (-G_z), (+G_x), and (-G_x)

The end point criteria are different for each of the vectors and back angle may be different within each curve.

(After Chambers⁽⁷⁵⁾)

b.



Upper limits of voluntary endurance (as contrasted with average tolerance, shown above) are plotted for a group of highly motivated test pilots, preconditioned to the effects of acceleration and suitably restrained. The pilots were able to operate satisfactorily a side-arm control device to perform a tracking task throughout the times indicated.

(After Chambers⁽⁷²⁾, adapted from Chambers and Hitchcock⁽⁷⁸⁾)

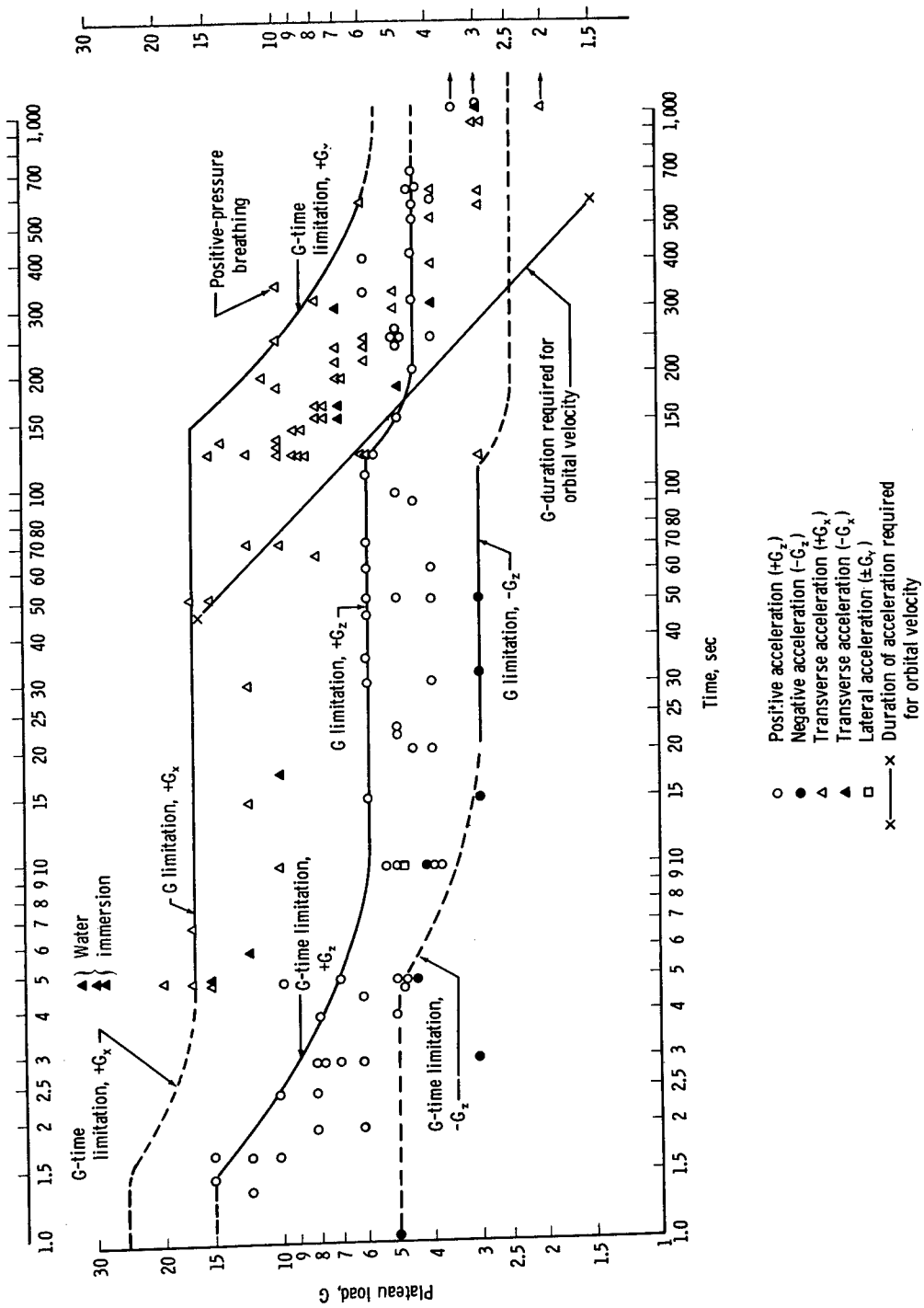


Figure 7-4

Human Experience of Sustained Acceleration (Data from many sources).

(After Fraser⁽¹⁷⁸⁾)

while others are G limited only. These threshold limits must be considered maximum levels and not ordinary working levels. Dashed lines represent extrapolations in face of inadequate empirical data.

The maximum total impulse of $G \times$ seconds required to achieve orbital velocity of 18,000 mph is 820 G-seconds, while escape velocity of 25,000 mph requires a total impulse of about 1,140 G-seconds. The duration and G load to give these products will vary from mission to mission. Acceleration profiles will be different for each booster stage during which the acceleration is continually changing. The duration \times acceleration product for orbital insertion is noted in Figure 7-4.

Between 1 and 1 3/4 seconds, $+G_z$, tolerance is apparently G limited at the level of 15G. Between 1 and 1 3/4 seconds and about 10 seconds it is G-time limited, tolerance decreasing with increase in time. Thereafter, another G-limited plateau occurs between 10 seconds and 2 minutes at a level of $6G_z$. Between 2 minutes and 3 minutes 20 seconds there is again a G-time limitation, leveling to a new G-limited plateau at $4\frac{1}{2}G_z$, which continues for an indefinite time. There may be a still further fall to $3G_z$, which has been experienced for an hour without reaching tolerance threshold. Even though the points are not plotted, it would appear that there is a G limit of $25G_x$ at the 1- to 1 1/2-second level (564). Thereafter, although there are data to support the hypothesis, it would seem reasonable to have a G-time limit dropping as indicated, and leveling at $+17G_x$ of the 4- to 5-second region. Thereafter the threshold is G limited at $+17G_x$ to the 2-minute mark, at which point a G-time limitation again occurs, gradually lowering the tolerance to about 5 or $6G_x$ at the 10-minute mark. In this region the data points unfortunately are vague. Data points for negative acceleration ($-G_z$) are very scanty but appear to indicate a G-limited plateau of $-5G_z$ for the first 4 to 5 seconds. This level seems high, since $-3G_z$ for 5 seconds is normally considered to be the tolerance threshold. In view of the data points available, however, it seems acceptable, bearing in mind that this level represents a maximum tolerance. Following this plateau there is a G-time limit reducing the tolerance to $-3G_z$ for at least 50 seconds and probably longer. Whether a further G-time limitation appears is not known and the dashed line is only conjectural.

The shape of the curves on the log-log plot provides an interesting corollary, namely, that one is observing here the failure of different systems with the establishment of new equilibria (178). Thus, while the interpretation is purely speculative, it may well be that in the $+G_z$ plot, one sees the effects of hydrostatic pressure on the cerebral circulation between 1 3/4 and 10 seconds, followed by a different failure at the 2-minute level. Many other speculations may be applied to the $+G_x$ and $-G_z$ plots.

The effects of G gradients along the body in short-armed centrifuges will be covered in the discussion of Figure 64 c, d, and e.

+G_Z Acceleration

Physiological Response

The sensations and symptoms that occur as a result of positive and negative acceleration have been reviewed by several authors (178, 184, 188). With slow increase in magnitude toward 2G, an increase in weight is observed, by the increased pressure on the buttocks in the seated position and drooping of the soft tissues of face and body. By 2 1/2G it is nearly impossible to raise oneself, and by 4G the arms and legs can hardly be lifted. Hydrostatic effects manifest themselves in the relaxed unprotected subject in the seated position after about 3 seconds' exposure to 3 or 4G, with progressive dimming (grayout) of peripheral vision. Tunneling of vision occurs at 3 1/2 to 4G and complete loss of vision (blackout) at 4 1/2 to 5G after a total plateau exposure of about 5 seconds. Hearing and consciousness are retained for a few seconds longer but are finally lost. In 50% of subjects of one study (177), mild to severe convulsions occur during the unconscious period, and recovery (assuming the stress is immediately reduced) is frequently accompanied by bizarre dreams, but this high a percentage is not commonly seen (169). Blackout and unconsciousness are sometimes associated with paresthesias, confused states, and, more rarely, gustatory sensations. No incontinence has been observed. During the onset, passive and compensatory physiological changes take place which will be discussed. Pain is not normally a feature, but the lower portions of the legs feel congested and tense; there may be muscular cramps and tingling. Inspiration becomes difficult, and eventually the subject exhibits a tendency to hold his breath in the mid-inspiratory position. Reaction times are prolonged and task performance is reduced even before the level of unconsciousness. If unconsciousness occurs, a loss of orientation for time and space persists for about 15 seconds after cessation of acceleration.

Summary charts and review of the cardiopulmonary changes in man during +G_Z are available (183, 367, 437) (See also Table 7-13c.)

Tolerance

Table 7-5a and graphic presentation of data in Figures 7-5b and c indicate maximum tolerance of one or more subjects to +G_Z. The graphic representations b and c distinguish between data points obtained with countermeasures (aided) and those without countermeasures (unaided) and give an overview of the comprehensive data of Table 7-5a. More details of +G_Z protection are given below under "restraint and protection devices". For the physiological end point, grayout, blackout, or unconsciousness are usually chosen. Data covering end points are seen in Figure 7-6a and b. (See also Table 7-19a.) Protective devices against +G_Z are discussed below (Table 7-18).

Interaction with other Stresses

Alteration of the ambient environment preceding, during, or following the acceleration exposure may alter the response to both environments. The effect of hypoxia and oxygen supplementation on +G_Z tolerance has been noted (60, 178, 188, 249). In view of the fact that hypoxia at a tissue

Figure 7-5

Maximum Tolerance to Prolonged +G_z

(See page 7-5)

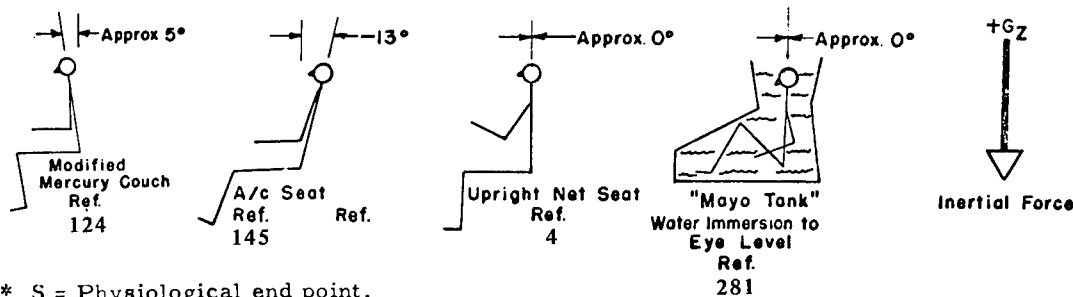
(After Hyde and Raab⁽³¹⁵⁾)

a.

Vector Magnitude (G)	Duration at G (Seconds)	Average Onset (G/Second)	Back Angle (Degrees)	Cause of Termination*	Trauma	Number of Subjects Attaining	Countermeasures	Support	Restraint	Reference
Unaided n = 1										
4.5	660	0.07	-13°	A	None	1 of 8	None	Aircraft Seat	Integrated Harness	423
4.0	1260	0.07	-13°	A	None	1 of 8	None	" "	" "	423
3.5	3600	0.07	-13°	A	None	1 of 8	None	" "	" "	423
Aided n = 1										
16.0	Peak	12.5 Sec. to Peak Sinusoidally	Approx. 0°	S	Irritation of Clotia and Pharynx	1	Hydrostatic Counter-pressure to Eye Level	"Mayo Tank" Modified Mercury Couch	Bungee Cords Helmet and Webbing Integrated Harness	281
6.0	390	?	Approx. 5°	S	None	1	Anti-G Suit	" "	" "	124
6.0	120	0.07	-13°	A	None	1 of 8	" "	Aircraft Seat	" "	423
5.0	300	0.07	-13°	A	None	1 of 8	" "	" "	" "	423
4.0	1200	0.07	-13°	A	None	1 of 2	" "	" "	" "	423
3.5	3600	0.07	-13°	A	None	1 of 4	" "	" "	" "	423
Unaided n > 1										
9.0	Peak	0.07	0°	A	None	2 of 31	None (M-1 Maneuvers)	Upright Net Seat	None	178
7.0	15-30	0.56	Approx. -10°	A	None	3 of 33	None	Aircraft Seat	? Integrated Harness	145
5.0	240	0.07	-13°	A	None	3 of 8	None	" "	" "	423
4.5	≥540	0.07	-13°	S	None	3 of 8	None	" "	" "	423
4.0	≥1200	0.07	-13°	A	None	3 of 8	None	" "	" "	423
3.5	>2700	0.07	-13°	S	None	3 of 8	None	" "	" "	423
3.0	3600	0.07	-13°	A	None	7 of 8	None	" "	" "	423
Aided n > 1										
10.5	Peak	12.5 Sec. to Peak Sinusoidally	Approx. 0°	A	None	2	Hydrostatic Counter-pressure to Eye Level	"Mayo Tank"	Bungee Cords	281
10.0	Peak	12.5 Sec. to Peak Sinusoidally	Approx. 0°	A	None	3 of 3	" "	" "	" "	281
7.0	15-30	0.56	Approx. -10°	A	None	13 of 30	Anti-G Suit	Aircraft Seat	? Integrated Harness	145
6.0	≥60	0.07	-13°	S	None	4 of 8	" "	" "	" "	423
5.0	≥240	0.07	-13°	A	None	6 of 8	" "	" "	" "	423
4.5	600	0.07	-13°	A	None	4 of 8	" "	" "	" "	423
4.0	≥720	0.07	-13°	S	None	2 of 2	" "	" "	" "	423
3.5	≥1340	0.07	-13°	S	None	4 of 4	" "	" "	" "	423
3.0	3600	0.07	-13°	A	None	2 of 3	" "	" "	" "	423

See also Figure 7-6 for tolerance levels using the criterion of vision.

Subject Configuration



* S = Physiological end point.

A = Arbitrary time limit end point

Figure 7-5 (continued)

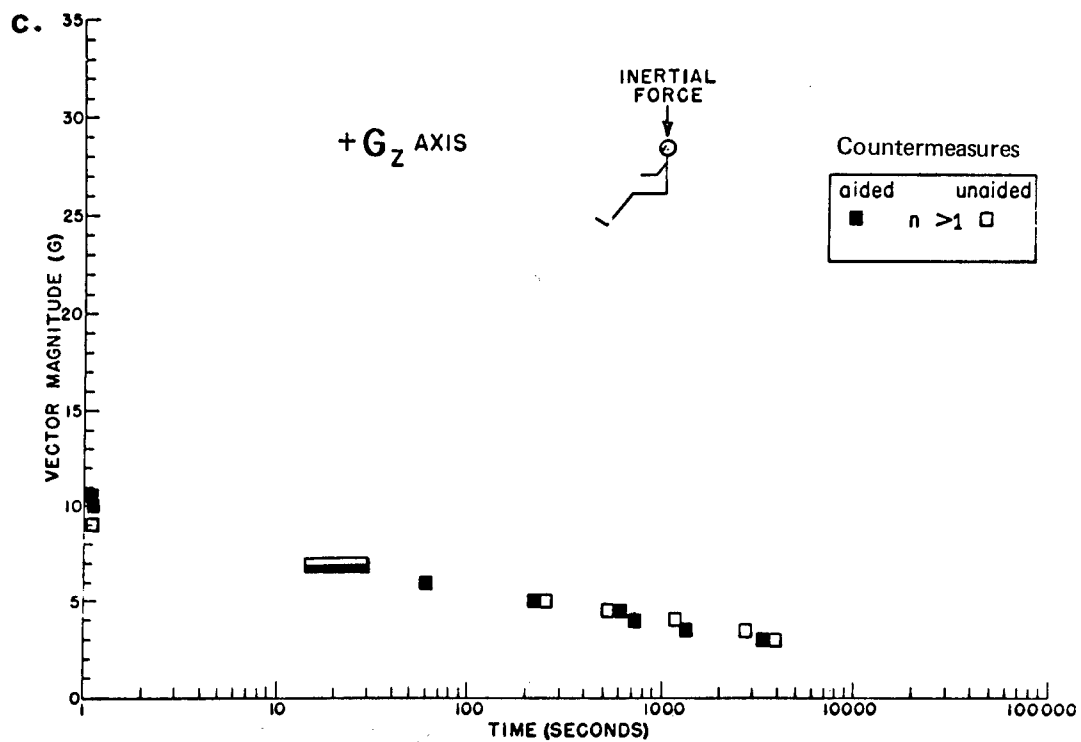
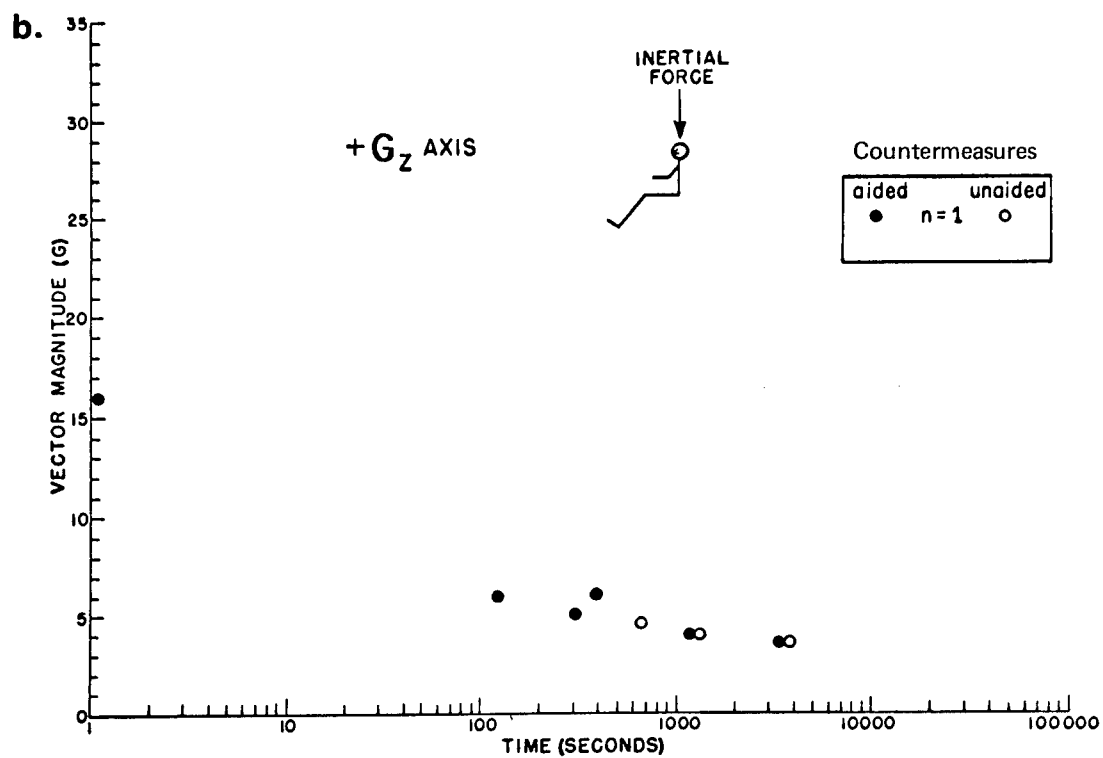
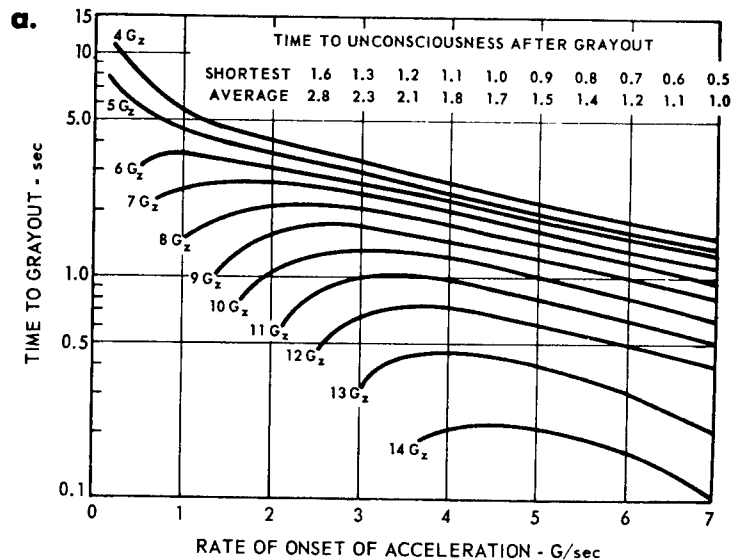


Figure 7-6

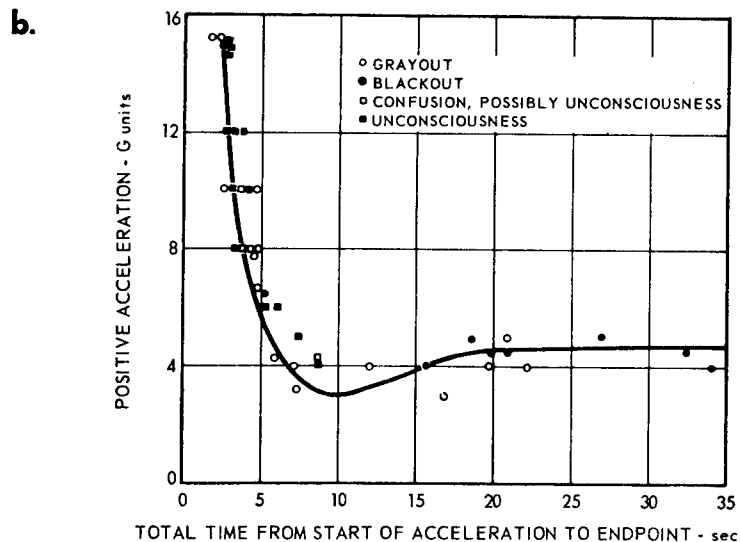
Grayout, Unconsciousness, and Rate of Onset of $+G_z$

(After Chambers⁽⁷²⁾, adapted from Stoll⁽⁵⁸⁷⁾)

This graph relates the onset rate of acceleration to time-to-end-point. It shows that for any given positive acceleration (G_z) from 4 to 14G, the time to grayout depends on how rapidly the acceleration level was reached. Further, the table inset in the graph shows the shortest times and the average times for unconsciousness to develop following grayout, each pair of values being related to an onset rate. For example, at onset rate of 4G/sec, the shortest time to unconsciousness was 1.1 sec, and the average 1.8 sec.



This graph shows human tolerance to positive G_z for varying rates of onset, G amplitudes, and exposure times.



level is responsible for the eye and brain defect during $+G_z$, hypoxia will aggravate and added oxygen will alleviate the symptoms of $+G_z$.

The effects of hypohydration have also received recent study (250, 251, 494, 599). These studies are of special importance in view of the hypohydration seen after weightlessness and heat stress. In one set of studies (251, 494, 599), two groups of male subjects who were hypohydrated approximately 3.6 percent of their total body weight either by means of a sauna bath (acute group) or a 48-hour water restriction period (chronic group) underwent four centrifugation runs at an acceleration buildup of $+3.7G/min$ - held at $6.0G$ until blackout occurred. The results indicate no significant difference in mean tolerance times between the acute and chronic group but a significant decrease (15 to 20%) in mean tolerance times (to blackout) between the normohydration and hypohydration groups. However, if subjects are hypohydrated over a period of 5 days to 5% of their body weight and passively centrifuged without muscular effort, no decrease in tolerance time is noted when compared to passively centrifuged controls (250). Similar results were obtained in other experiments with subjects dehydrated up to a 3% loss in body weight where decrease in $+G_z$ tolerance of 15 to 18% was noted (599).

The physiological mechanisms which help maintain the arterial pressure of the eye above the initial 20 mm Hg are increased stroke volume, tachycardia, and arterio- as well as veno-constriction aided by muscular efforts. The acute loss of water probably prevents adequate replacement of the critical free-circulating water by homeostatic mechanisms and thus degrades the anti-acceleratory compensation (352). Surprisingly, there is very little relationship between percent body weight loss, red cell volume, plasma volume, and total blood volume and tolerance time. Further work is required on the mechanism of hypohydration. The effects of prior zero gravity and bed rest on $+G_z$ tolerance will be discussed below in the zero gravity section.

As would be expected, heat and the resultant vasodilation decreases tolerance to $+G_z$. Exposure of men dressed in light summer flying suits to air temperatures of up to $160^{\circ}F$ for 1 hr in a gondola will decrease tolerance to $+G_z$ by up to 1 G unit (61). About 80% of this effect is seen at temperatures of $120^{\circ}F$. The effects of cold have not been studied in man, but in animals the level of acceleration is a significant factor. At $+30$ to $+40 G_z$, hypothermia in rats improves tolerance; but at $+20 G_z$, tolerance is actually decreased (586).

Radiation during a space mission may interact with acceleration stress. No data on the human are available. However, radiation given before and following exposure to $+G_z$, $-G_z$ and $+G_x$ was as effective in causing radiation death as in a $1G$ environment (603, 700). Soviet data indicate that accelerations of $+8G_z$ for 15 minutes and $+20G_z$ for 5 minutes prior to or during exposure to X-radiation (100 r) do not aggravate the usual radiation response in rodents but do alter the number of chromosomal abnormalities (173, 317). "Hypoxia" brought on by high G loads in mice and rats during or immediately following exposure reportedly can increase radiation tolerance (380). Conversely there is an increase resistance to 40-42 G of "back-to-chest" acceleration (which kills 50% of animals) for 1 to 7 days following exposures

of 250, 500, and 700 r of radiation (132). More recent data in dose range of 100-4000 R confirm this resistance (131). The significance of these findings to astronauts is far from clear.

-G_z Acceleration

Physiological Responses

With application of negative acceleration (-G_z) in the unprotected subject there is a feeling of facial suffusion and cranial fullness which is tolerable but unpleasant (178, 184, 188). This is accompanied by reflex cardiovascular changes which will be discussed. Increasing the magnitude to between -2G_z and -3G_z produces considerable facial congestion and throbbing headache. At about -3G_z for 5 seconds, blurring and graying of the vision occurs and in some subjects there is a reddening of the visual field or "redout", which is of debatable origin. (See Table 7-19). With the onset of acceleration, the arterial and venous pressure rise some 70 to 90 mm as measured in the carotid artery and jugular vein. An adequate arterial-venous (A-V) difference is initially maintained, but with increase in carotid sinus pressure, consequent on the increase in hydrostatic pressure, the resulting vagal stimulation produces bradycardia, decrease in cardiac output, and a secondary fall in arterial pressure while the venous pressure is still artificially maintained. Thus, the A-V difference approaches zero, and confusion or unconsciousness may arise. The change in systolic pressure per G unit decreases with increasing negative acceleration to an as yet unestablished asymptote. It has been suggested that redout is a distortion of vision caused by looking through the conjunctiva of the lower lid which is pulled upward over the eyeball by the negative acceleration. This is the commonly accepted explanation although it does not appear entirely satisfactory. A few individuals, with practice, may tolerate up to -5G_z for 5 seconds in the unprotected state. On cessation of acceleration, the congestion disappears slowly and may leave petechial hemorrhages, congested and hemorrhagic conjunctivae and edematous eyelids.

Tolerance

Table 7-7a and graphic presentation of these data in Figure 7-7b represent the maximum tolerance limits for at least one or more subjects.

+ G_x Acceleration

Physiological Responses

The higher G-load tolerated along this axis of the body has prompted much study in relation to launch and reentry of space vehicles (44, 73, 77, 178, 544). Application of up to +3G_x for about 2 minutes to a subject restrained in a contour couch will produce little effect other than a feeling of increased weight and pressure on chest and abdomen with a developing fatigue. At about 3G a slight difficulty in focusing may be observed along with slight spatial

Figure 7-7

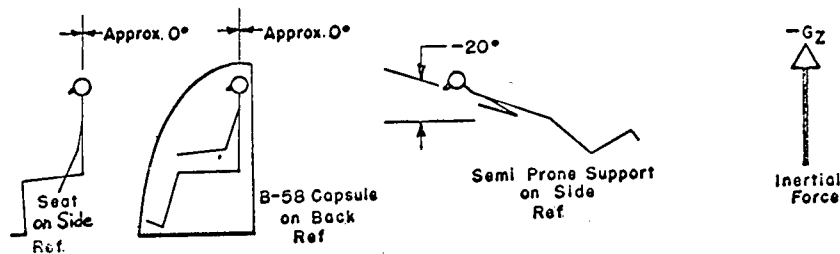
Maximum Tolerance to Prolonged +G_z
(See page 7-5)

(After Hyde and Raab⁽³¹⁵⁾)

a.

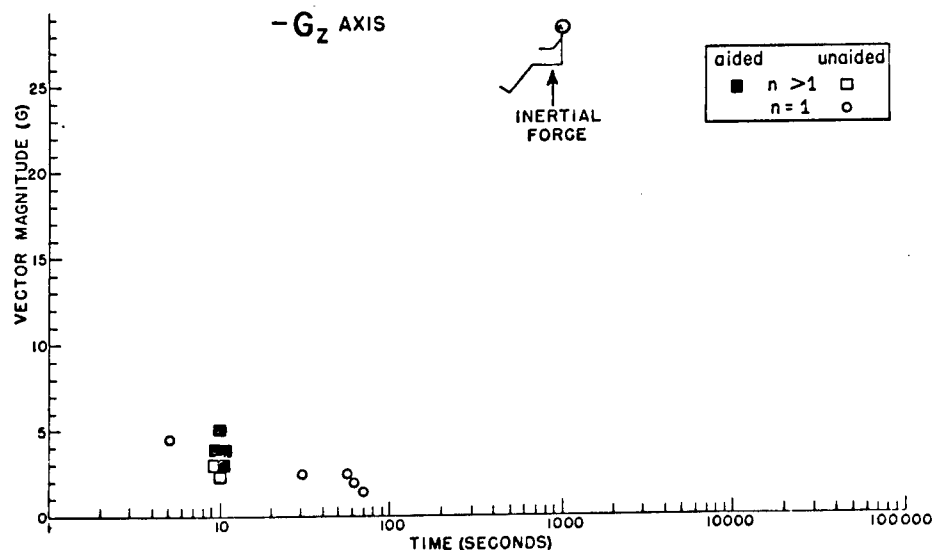
Vector Magnitude (G)	Duration at G (Seconds)	Average Onset (G/Second)	Back Angle (Degrees)	Cause of Termination *	Trauma	Number of Subjects Attaining	Countermeasures	Support	Restraint	Reference
Unaided n=1										
4.5	5	? Aircraft Maneuvers	?	S?	None	1	None	Aircraft Seat	Lap Belt	652
2.5	50		Approx. 0°?	S?	None	1	None	Aircraft Seat	Harness	4
2.5	30		Approx. 0°	A	None	1	None	B-58 Capsule on Back	Harness	4
2.0	60		?	A	None	1	None	Turntable	Harness	4
1.5	68		?	A?	None	1	None	Turntable	Harness	4
Unaided n>1										
3.0	10	>than 0.2	Approx. 0°	A	None	5 of 19	None	Seat	Harness	538
2.5	10		Approx. 0°	A	None	19 of 21	None	Seat	Harness	538
Aided n>1										
5.0	10	Usually	Approx. 0°	A	None	15 of 15	Pressure Helmet 25 mm Hg/G	Seat	Harness	538
4.0	10		Approx. 0°	A	None	15 of 15	" " " "	Seat	Harness	538
4.0	10		-20°	A	None	14 of 14	Body Position with Respect to Vector Pressure Helmet	Semiprone Support	Padded Wood Form	538
3.0	10		Approx. 0°	A	None	29 of 29	25 mm Hg/G	Seat	Harness	538

Subject Configuration



* S = Physiological end point
A = Arbitrary time-limit end point

b.



disorientation, each of which subsides with experience. In performance tasks, initially, there may even be some improvement. However, approaching $+6G_x$ there is a development of tightness in the chest, mild chest pain, some loss of peripheral vision, difficulty in breathing and speaking, decrease in depth of visual field, blurring of vision, and additional effort required in maintaining focus. In control performance tasks there is a tendency to overcontrol.

Toward $+9G_x$, chest pains and pressure become more severe. Breathing is difficult, requiring tensing of chest and stomach, and shallow respiration from a position of nearly full inspiration. Peripheral vision is further reduced, with increased blurring, occasional tunneling and greater concentration required to maintain focus. Occasional tears are observed. In control performance tasks there is a loss of feel, tendency to make inadvertent control inputs, and hesitation in making control inputs because of the possibility of inadvertent action.

By $+12G_x$, breathing difficulty is severe, with chest pain and marked fatigue. Peripheral vision is lost and central acuity diminished, with lacrimation. Control is very difficult and requires great concentration.

At $+15G_x$, some subjects report a recurrent complete loss of vision with extreme difficulty in breathing and speaking, loss of sense and feel, and extreme difficulty in control tasks. The pain experienced, when severe, is a gripping viselike sensation around the chest, and is also encountered in severe vertical sinusoidal vibration. Its origin is debatable but it is generally considered to arise from tissue stretching, or perhaps intercostal muscular spasm. Petechiae of the back and antecubital fossae occur regularly above $+6G_x$, and reflex cardiovascular changes and inertial pulmonary changes are observed which will be discussed later.

On cessation of high G_x the ensuing disability is variable and includes fatigue, an unsteady gait, dizziness, and occasional nausea, which may persist from 1 to 5 minutes. The dizziness and nausea, when it occurs, is probably related more to such artifacts as short centrifuge arm, head movements, or angular accelerations rather than to $+G_x$ per se.

Tolerance

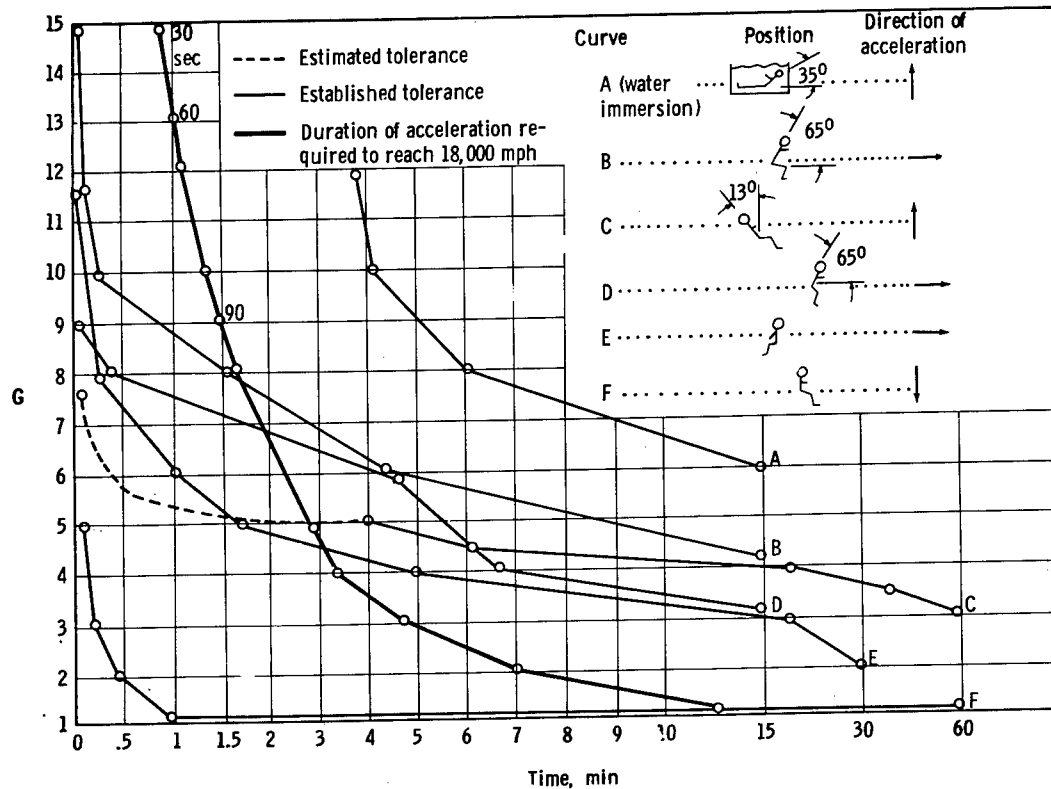
The relative amounts of G_x and G_z have been critical in experiments relating to tolerance along the G_x axis. Experiments have given different critical back angles for G_x tolerance, depending on the nature of the couch system. Examples will be given of the sensitivity of data to several different variables. One group of experiments are summarized in Figures 7-2b and 7-8a and b. The arrows in Figure 7-8 refer to direction of acceleration, not the direction of the inertial force (see Figure 7-1). Figure 7-8b illustrates the advantages and disadvantages of a variety of positions. Tolerance in the conventional seated position (B2) is limited at 8G by dyspnea and chest pain. In addition there is a component of negative G from the backward tilt of the trunk. If the angle of the trunk relative to the direction of acceleration is greater than 70° (SA + ϵ of Figure 7-2 < than 20°), quasi-pleuritic anterior chest pain can at times limit tolerance at about 7G, though this may be related to nature of the couch system. As the angle is decreased below 70° (SA + ϵ > 20°) (B3) there is more longitudinal application of the inertial force, and

Figure 7-8

Effect of Back Angle on Tolerance to $\pm G_z$

(Note that the directions of acceleration and not inertial directions are noted by arrows. The angles are not "back angles", but angles of the trunk relative to direction of acceleration.)

(After Bondurant et al⁽⁴⁴⁾)



a. Effect of Position on Tolerance to Acceleration

Position of greatest tolerance	Direction of acceleration	Position of lesser tolerance
A (water immersion) $\phi = 35^\circ$	↑	A
B $\phi = 65-70^\circ$	→	B1 $\phi = > 70^\circ$ B2 $\phi = < 65^\circ$ B3
D $\phi = 65^\circ$	→	D
E	→	E1 $\phi < 90^\circ$ E2

b. Variations in Position with Decrease Tolerance to Acceleration

blackout limits the tolerance at progressively lower levels. The best tolerances were found with the subject inclined in the direction of acceleration at greater than 65° to 70° angle ($SA + \epsilon < 20$ to 25 degrees). Blackout may occur in positions B and D, although position B has a higher threshold. The chief limiting factor in these positions is of course dyspnea. Asymptomatic patchiae also tend to occur.

In other experiments, back angles ($SA + \epsilon$) of 2 to 8 degrees were found to be most effective at high G_x (95, 109, 110). At 14 and 17° back angles, blackout limited exposure to $+20$ and $+23G_x$ respectively during a profile which reached peak in 20 seconds and decayed to zero in an equal time. At a back angle of 8° , difficulty in respiration leading to grayout limited the runs at $+25G_x$. No pain was experienced in the NASA contour couch. See Table 10a. It thus appears that back angles of 2 to 8° with hips flexed to bring knees to eye level offer the best all-around compromise for $+G_x$ acceleration. For Apollo, an SA of 2° with an ϵ of 6.5° and an aortic-retinal angle of 15° gives an EPA of 23° .

The optimal position for backward $-G_x$ is illustrated in E. An effective negative G_z component is introduced, however, if the head and trunk move forward (E1), with a reduction in tolerance dependent on the angle. If the legs are extended (E2) calf and thigh pain limit tolerance to about $-5G_x$.

Table 7-9a and graphic presentation of these data in Figure 7-9b and c summarize the tolerance experiments to $+G_x$ for angles of -17° to 0° . (Aided means countermeasures used.)

Table 7-10a and Figures and graphic presentation of these data in 7-10b and c summarize the tolerance experiments to $+G_x$ for back angles of $+5^{\circ}$ to 7° . (Aided means countermeasures used.)

Table 7-11a and graphic presentation of these data in Figure 7-11 b summarize the tolerance experiments to $+G_x$ for back angles of $+20^{\circ}$ to $+45^{\circ}$. (Aided means countermeasures used.)

During takeoff and reentry, the G_x loads in past space flights have had profiles with rise to short peaks. Figure 7-12 shows experience with peak $+G_x$ loads.

Interaction with other Stresses

Changes in the gaseous environment alter tolerance to $+G_x$ where thoracic dynamics are modified; the work of breathing is increased; and the pulmonary volumes, pressures and fluids shift. (see Figure 7-13) (14, 84, 178, 544, 546, 647). Collapse of lung segments or atelectasis are seen on x-ray (13, 294, 463). As might be expected from the elevated pulmonary vascular pressures (683) and the factors controlling vascular perfusion of the lung (663), there is little change in blood distribution up to $+8G_x$ (308) as contrasted to the $+G_z$ vector (59). A ventilation-perfusion defect probably results with unsaturation of hemoglobin and a hypoxic state (10, 15, 437, 505, 684). A decrease in diffusion capacity (L_{CO}) and pulmonary blood flow (Q_C) of 35%

Figure 7-9
Maximum Tolerance to Prolonged Accelerations +G_x
(See page 7-5)

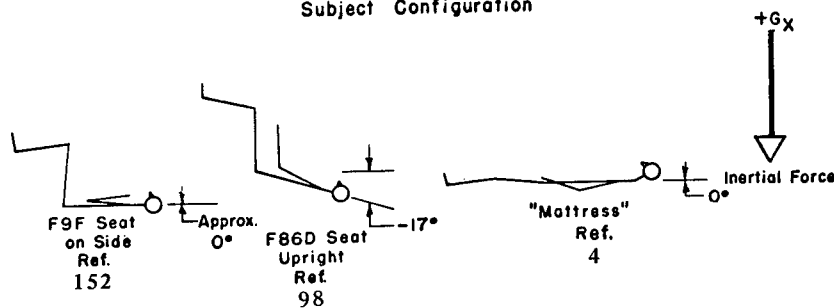
(After Hyde and Raab⁽³¹⁵⁾)

+G_x -17° to 0° Back Angle (SA + ε of Figure 7-2a)

a.

Vector Magnitude (G)	Duration at G (Seconds)	Average Onset (G/Second)	Back Angle (Degrees)	Cause of Termination*	Trauma	Number of Subjects Attaining	Countermeasures	Support	Restraint	Reference
Unaided n=1										
12.0	Peak	0.2	0°	S?	None	1	None	Mattress	None	4
10.0	150	?	0°	S	None	1	100% O ₂	Foam Matt.	None	646
8.6	Peak	0.5	-17°	S	None	1	None	F-86D Seat	Helmet and Lap Belt	98
8.0	195	?	0°	A	None	1	None	Mattress	None	4
8.0	13	0.5	-17°	S	None	1	None	F-86D Seat	Helmet and Lap Belt	98
6.0	390	"Gradual"	0°	A	None	1	None	Mattress	None	4
4.0	600	"Gradual"	0°	A	None	1	None	Mattress	None	4
3.0	610	"Gradual"	0°	A	None	1	None	Mattress	None	4
Aided n=1										
10.0	328	0.1 to 0.2	0°	S	None	1	19 mm Hg 100% O ₂ Positive Pressure Breathing	Foam Matt.	MA-2 Helmet	646
10.0	252	0.1 to 0.2	0°	S	6 Hour Hemoptysis	1	29 mm Hg 100% O ₂ Positive Pressure Breathing	Foam Matt.	MA-2 Helmet	646
+G _x -17° to 0° Back Angle n>1										
Vector Magnitude (G)	Duration at G (Seconds)	Average Onset (G/Second)	Back Angle (Degrees)	Cause of Termination	Trauma	Number of Subjects Attaining	Countermeasures	Support	Restraint	Reference
Unaided n>1										
15.0	5	8-10	Approx. 0°	Considered as Voluntary Limit	None	5 of 5	None	F-35P Seat on Side	Harness	152
10.0	≥130	?	0°	S	None	3 of 9	100% O ₂	Foam Matt.	None	646
8.0	>180	0.2	0°	A	None	7	None	Mattress	None	4
8.0	Peak	0.5	-17°	S	None	4	None	F-86D Seat	Helmet and Lap Belt	98
7.0	210	?	0°	A	None	7 of 8	None	Cotton Matt.	None	12
6.0	>360	0.2	0°	A	None	7	None	Mattress	None	4
6.0	270	?	0°	A	None	7 of 8	None	Cotton Matt.	None	12
5.0	330	?	0°	A	None	9 of 9	None	Cotton Matt.	None	12
5.0	>180	0.2	0°	A	None	6	None	Mattress	None	4
4.0	>600	"Gradual"	0°	A	None	7	None	Mattress	None	4
4.0	480	?	0°	A	None	9 of 9	None	Cotton Matt.	None	12
3.0	900	?	0°	A	None	9 of 10	None	Cotton Matt.	None	12
Aided n>1										
10.0	>200	0.1 to 0.2	0°	S	1 Subject Hemoptysis	4 of 9	19-29 mm Hg 100% O ₂ Positive Pressure Breathing	Foam Matt.	None	MA-2 Helmet

Subject Configuration



* S_e = Physiological end point
A = Arbitrary time limit end point

Figure 7-9 (continued)

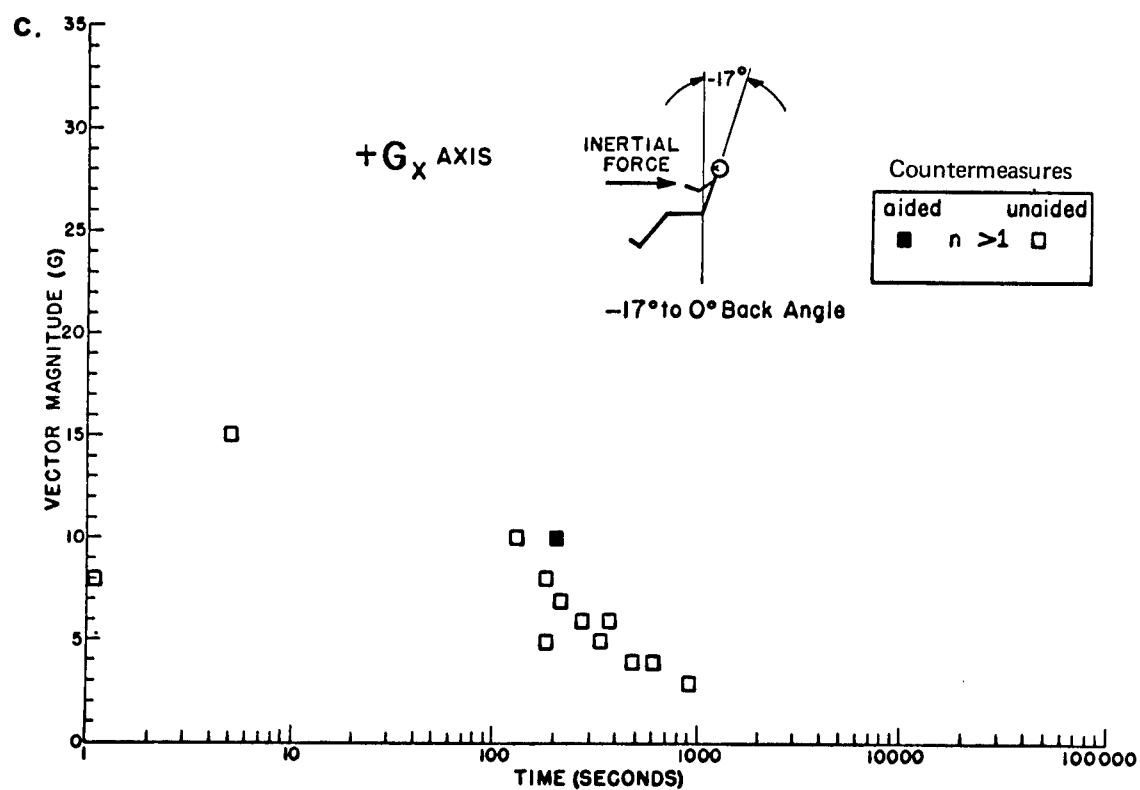
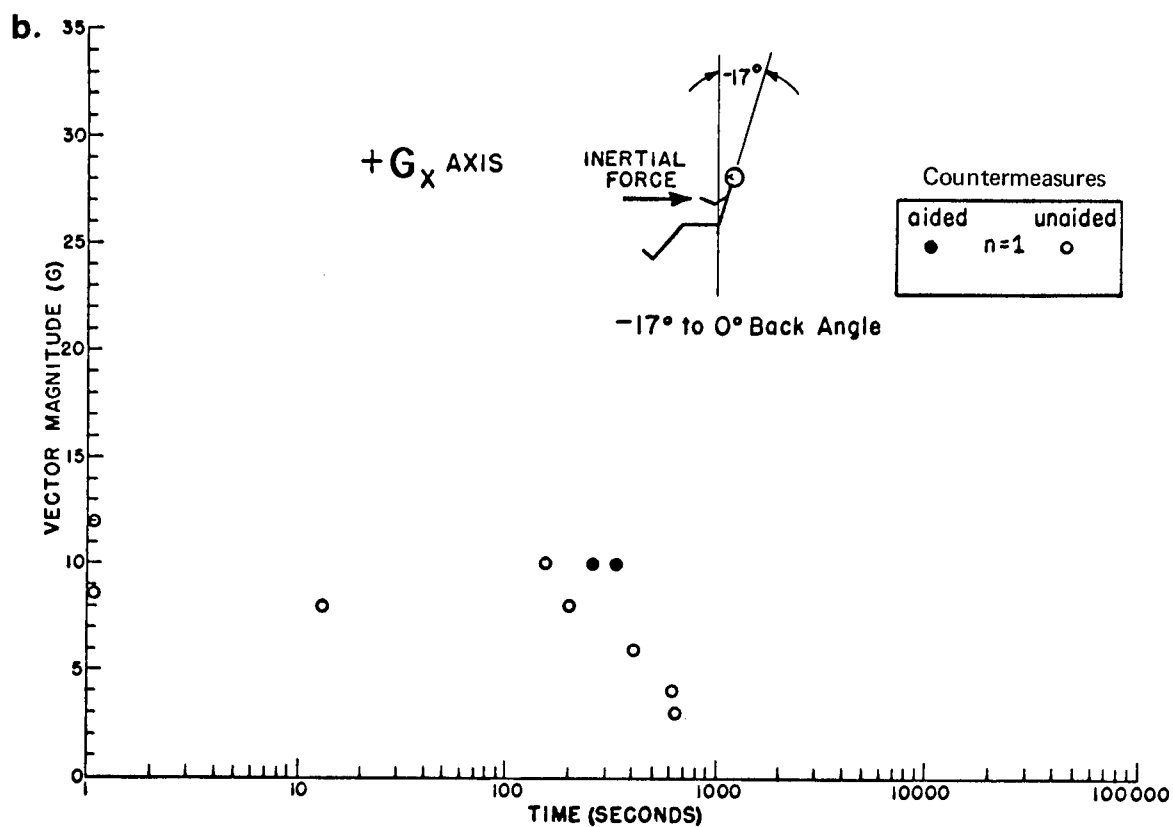


Figure 7-10
Maximum Tolerance to Prolonged Accelerations +G_x
(See page 7-5)
(After Hyde and Raab⁽³¹⁵⁾)

a.

+G_x 5° to 17° Back Angle (SA + ε of Figure 7-2a)

Vector Magnitude (G)	Duration at G (Seconds)	Average Onset (G/Second)	Back Angle (Degrees)	Cause of Termination*	Trauma	Number of Subjects Attaining	Countermeasures	Support	Restraint	Reference
Unaided n=1										
14.0	127	?	Approx. 5°	S?	None	1	None?	Contour Couch	Ref.	143
12.0	173	0.2	12°	S?	None	1	None	Net Seat	None	4
12.0	105	"Rapid"	12°	S?	None	1	None	" "	None	4
10.0	90	"Rapid"	12°	A	None	1	None	" "	None	4
9.0	270	0.2	12°	A	None	1	None	" "	None	4
8.0	240	?	12°	A	None	1	None	" "	None	4
6.0	540	0.1	12°	A	None	1	None	" "	None	4
6.0	500	?	12°	A?	None	1	None	Modified Mercury Couch	Helmet and Webbing	124
6.0	390	?	Approx. 5°	S?	None	1	None	Net Seat	None	4
4.5	850	"Gradual"	12°	S?	None	1	None	" "	None	4
4.0	660	?	12°	A	None	1	None	" "	None	4
3.0	1800	0.2	12°	A	None	1	None	" "	None	4
Aided n=1										
25.0	Peak	?	Approx. 10°	S?	None	1	Anti-G Suit?	Molded Couch	?	235
23.0	Peak	?	Approx. 10°	A	Inverted T-Wave	1	Anti-G Suit?	" "	?	235
20.7	Peak	1.0	17°	A	None	1 of 2	Anti-G Suit 100% O ₂	NACA Mod. 1 Contour Couch	Harness	109
8.0	600	"Rapid"	12°	A	None	1	Positive Pressure Breathing	Net Seat	A-13A Mask	4
Unaided n>1										
16.5	Peak	0.14 to 8.5G, then 0.32 to 16.5G	12°	A	None	5 of 7	None	Net Seat	None	99
12.0	≥110	0.2	12°	S?	None	3	None	" "	None	4
12.0	≥60	"Rapid"	12°	A	None	10	None	" "	None	4
12.0	45	1.0	12°	A	None	8	None	" "	None	4
10.0	≥60	"Rapid"	12°	A	None	3	None	" "	None	4
8.0	≥240	"Rapid"	12°	A	None	2	None	" "	None	4
8.0	≥85	0.2	12°	A	None	10	None	" "	None	4
6.0	>60	0.2	12°	A	None	6	None	" "	None	4
4.0	≥660	"Gradual"	12°	A	None	8	None	" "	None	4
Aided n>1										
23.0	Peak	?	Approx. 10°	A	1 Subject Inverted T-Wave	2	Anti-G Suit?	Molded Couch	?	235
20.7	Peak	1.0	10°	A	None	2 of 2	Anti-G Suit	NACA Mod. 1 Contour Couch	Harness	109

Subject Configuration

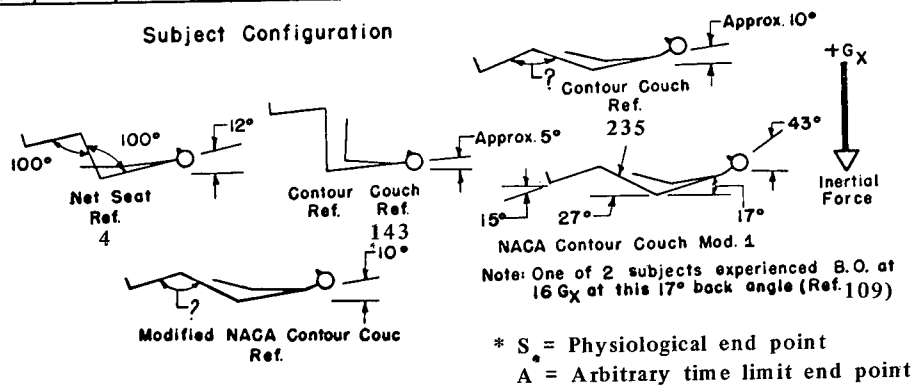


Figure 7-10 (continued)

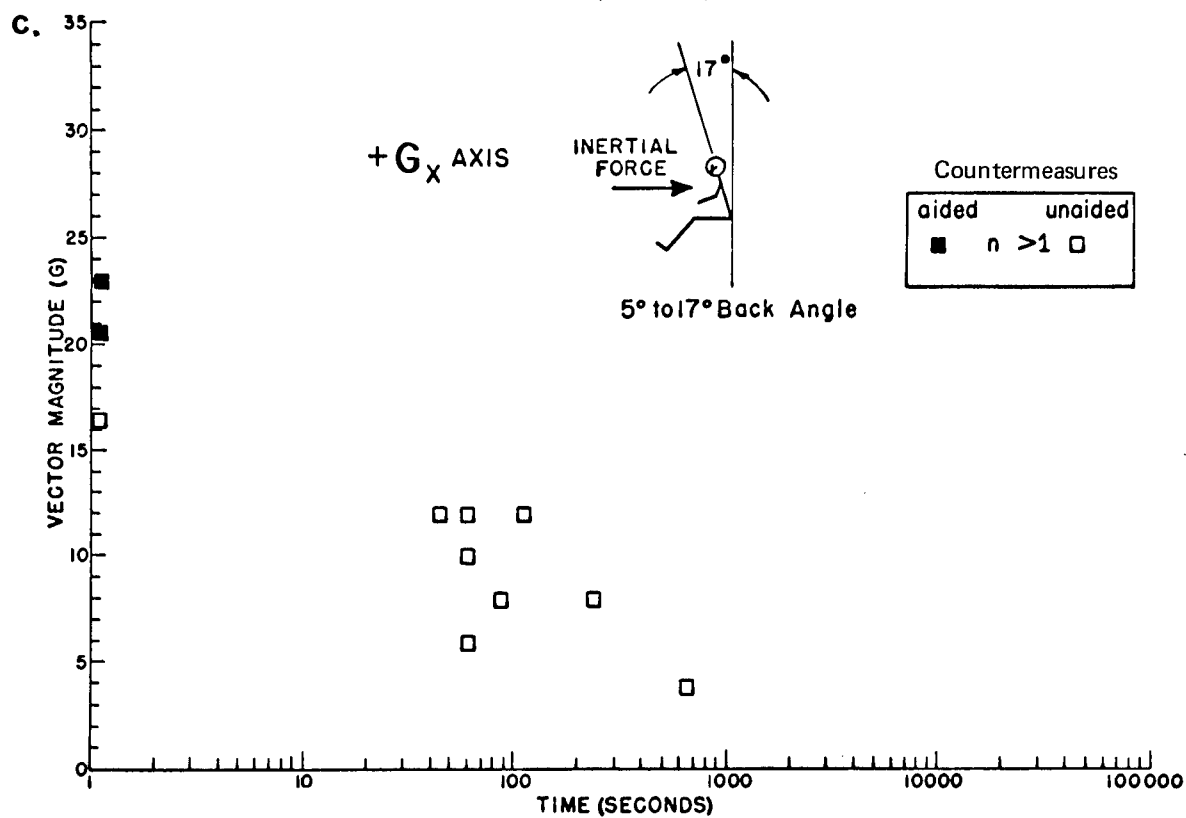
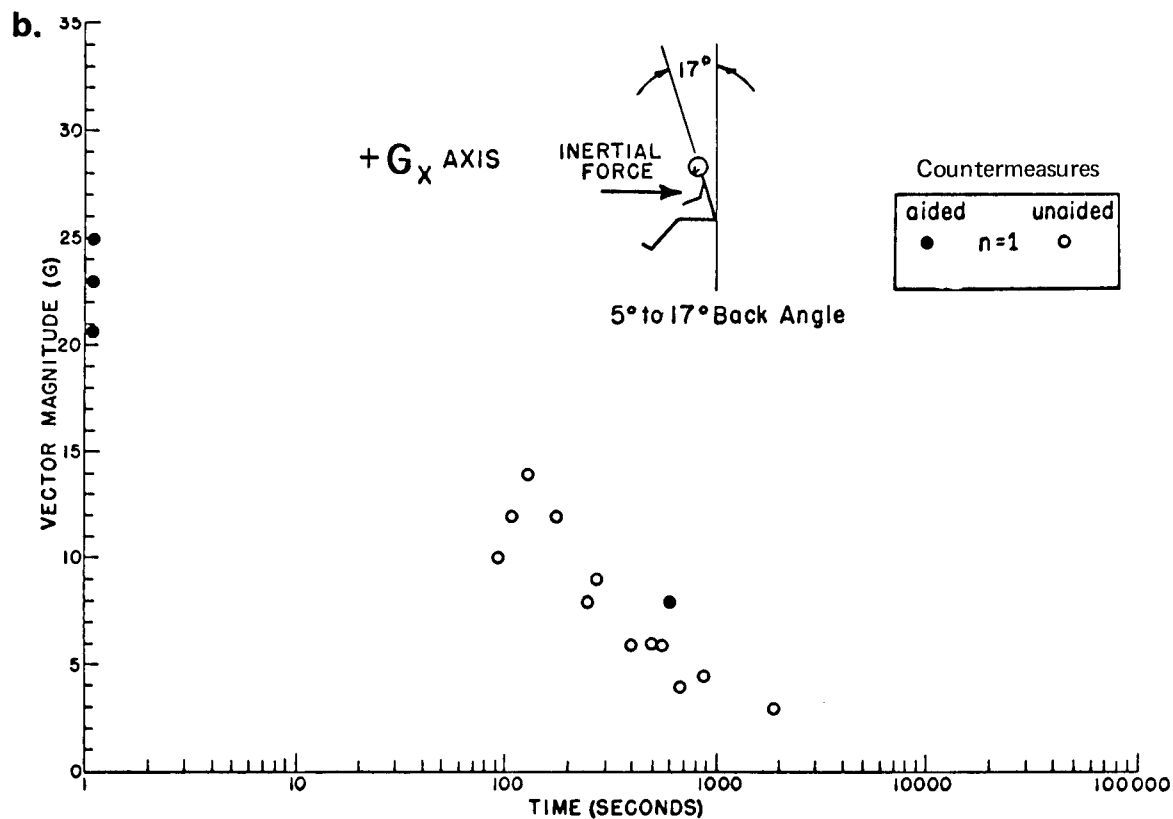


Figure 7-11
Maximum Tolerance to Prolonged Accelerations $+G_x$
(See page 7-5)

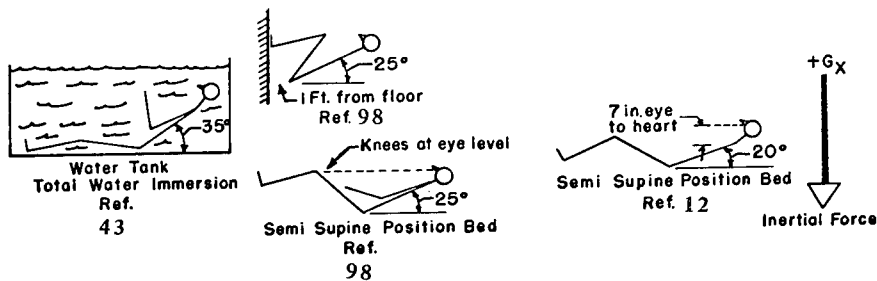
(After Hyde and Raab⁽³¹⁵⁾)

$+G_x$ 20° to 45° Back Angle (SA + ϵ of Figure 7-2a)

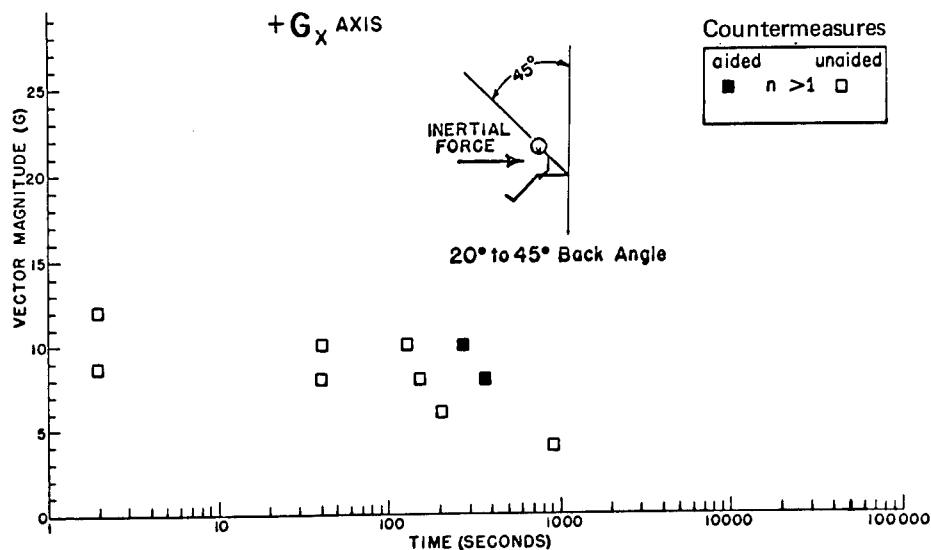
a.

Vector Magnitude (G)	Duration at G (Seconds)	Average Onset (G/Second)	Back Angle (Degrees)	Cause of Termination*	Trauma	Number of Subjects Attaining	Countermeasures	Support	Restraint	Reference
Unaided n>1										
12.0	2	0.5	25°	S	None	4	None	Seated, Legs Flexed Semisupine Position Bed	Helmet and Lap Belt	98
10.0	126	?	20°	S?	None	2 of 3	None	Seated, Legs Flexed Semisupine Position Bed	Straps	12
10.0	40	0.5	25°	S	None	2 of 6	None	Seated, Legs Flexed Semisupine Position Bed	Helmet and Lap Belt	98
8.7	2	0.5	25°	S	None	2	None	Seated, Legs Flexed Semisupine Position Bed	Helmet and Lap Belt	98
8.0	150	?	20°	A	None	3 of 3	None	Seated, Legs Flexed Semisupine Position Bed	Straps	12
8.0	≥ 40	0.5	25°	S	None	6 of 6	None	Seated, Legs Flexed Semisupine Position Bed	Helmet and Lap Belt	98
8.0	≥ 200	0.5	25°	S	None	3 of 6	None	Seated, Legs Flexed Semisupine Position Bed	Helmet and Lap Belt	98
4.0	900	0.5	25°	A	None	2 of 6	None	Seated, Legs Flexed Semisupine Position Bed	Helmet and Lap Belt	98
Aided n>1										
10.0	270	0.2	35°	A	None	5 of 6	Total Water Immersion Positive Pressure Breathing	35° Wedge	None	43
8.0	360	0.2	35°	A	None	6 of 6	Total Water Immersion Positive Pressure Breathing	35° Wedge	None	43

Subject Configuration



b.



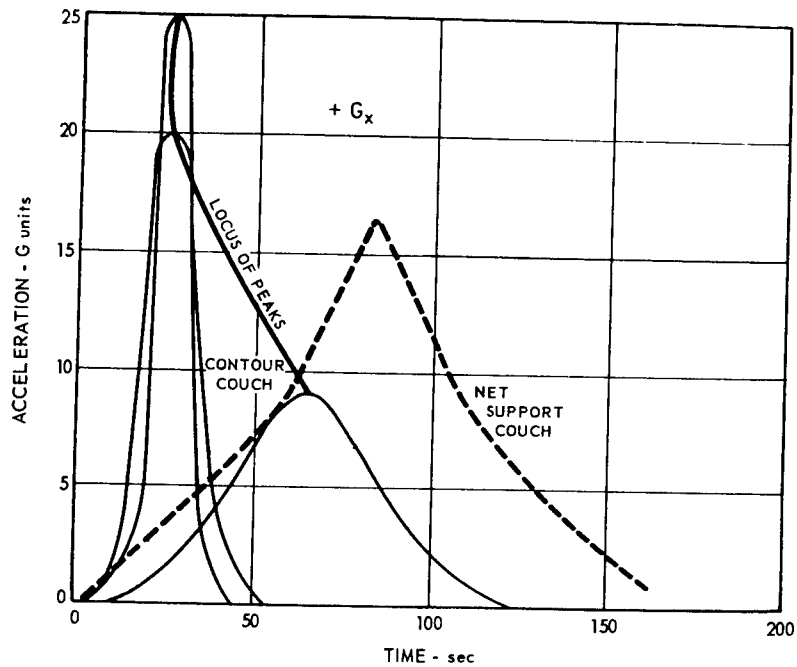


Figure shows the greatest acceleration-time histories that have been tolerated on centrifuges when special support structures and positioning are used. Solid lines show three curves which define about the same area of $+G_x$ times time. A heavy line connects the peaks of these three curves and locates the peaks of other curves enclosing the same area. The dashed line encloses a number of possible acceleration profiles related to space flight, all of which are tolerable, since the border of the envelope has been tolerated experimentally.

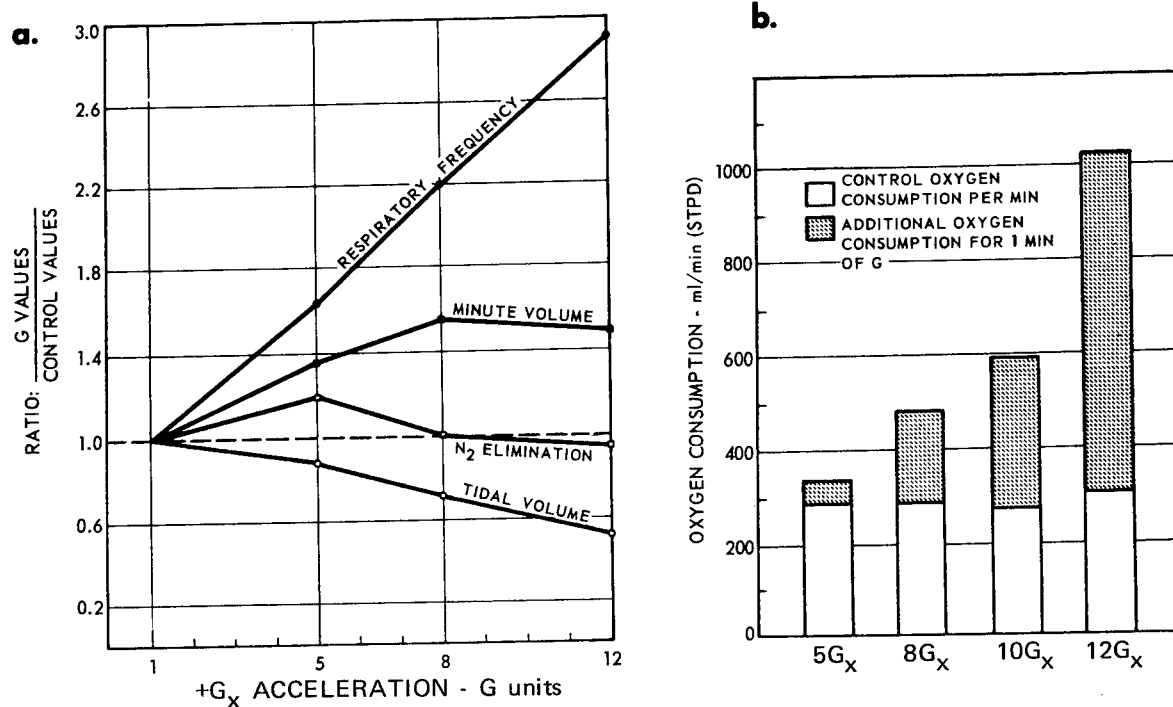
Figure 7-12

Maximum Tolerable Acceleration Profiles

(After Chambers⁽⁷²⁾, adapted from Bondurant et al⁽⁴⁴⁾, Clarke et al⁽⁹⁹⁾, Lawton et al⁽³⁶⁸⁾, Collins et al⁽¹⁰⁹⁾, and Collins and Gray⁽¹¹⁰⁾)

Figure 7-13

Ventilatory Responses to Forward Acceleration



Figures **a** and **b** show the effect of (+G_x) on respiratory frequency tidal volume, minute volume, and nitrogen elimination (a rough index of alveolar ventilation).

(Adapted from Zechman et al⁽⁶⁹⁹⁾)

c.

Respiratory Responses of 31 Pilots to +G_z and +G_x

		+G _z	+G _x					
			0° Back Angle			12° Back Angle		
			5G	8G		5G	8G	12G
Control vital capacity (liters)	mean	4.00	3.75	3.75		3.70	3.70	3.70
	S. D.	.48	0.45	0.45		0.48	0.48	0.48
Experimental vital capacity (liters)	mean	2.20	1.68	0.48		1.60	0.55	0.20
	S. D.	0.41	0.43	0.37		0.53	0.43	0.22
Control forced expiratory capacity (0.5 sec, percent)	mean	59%	59%	59%		55%	55%	55%
	S. D.	13%	11%	11%		12%	12%	12%
Experimental forced expiratory capacity (0.5 sec, percent)	mean	63%	80%	86%		77%	91%	94%
	S. D.	19%	18%	26%		20%	13%	13%

(After Hyde et al⁽³¹⁴⁾)

has been recorded (492). Less unsaturation is found in the $-G_z$ axis (546). Current models of cardiorespiratory dynamics during accelerative stress are available (413, 437, 533).

Figure 7-14 indicates the relationship between G profile, G load, the P_{O_2} of inspired air and the resultant time history of unsaturation. The relatively slow recovery of oxygen saturation in Figure 7-13c is probably due to atelectasis. Impairment of function brought about by the hemoglobin unsaturation in the $+G_x$ has been covered in Oxygen- CO_2 Energy (No. 10). Figure 7-15 compares the range of unsaturation and performance decrement brought about by 2 minutes of $+G_x$ while breathing air vs. breathing 100% oxygen at 5 psia. These data relate performance to that at equivalent altitude exposures through the arterial oxygen saturation.

The composition of gas breathed before acceleration appears to affect the rate of unsaturation as would be expected with a ventilation-perfusion defect (307). Positive pressure breathing also increases saturation and performance of several tasks to different extents at $+G_x$ up to 12 (79).

In one study of the problem it has been shown that tolerance to $+G_x$ in reentry profiles is unaffected by 4 weeks of prior bed rest (428). In other simulator studies as well as in flights of the Mercury and Gemini series, there was no indication that the transient $+G_x$ acceleration resulted in an operationally significant problem either during takeoff and reentry or while in orbit in a 100% oxygen mixture at 5 psia (35, 289, 505).

$-G_x$ Acceleration

Physiological Response

Less work has been done on backward or "eyeball out" acceleration (125, 178, 188, 538, 544, 546). In principle, the effects are similar to those of forward acceleration ($+G_x$), with modifications produced by the reversed direction of the vector. Thus, in $-G_x$ the chest pressure is reversed and respiration appears to be easier than in $+G_x$; also less unsaturation is experienced. However, since pressure is outward toward the restraint harness, there is a greater respiratory rate than in $+G_x$ and pain and discomfort from pressure on the harness may become severe at about $-8G_x$ even in the optimal position. Should the head be allowed to tilt forward, hydrostatic effects on the cerebral circulation become manifest at even lower $-G_x$ levels. Another major feature at -6 to $-8 G_x$ is interference with vision by alteration of tear clearance from the eyeball (544, 546) or lens displacement. Despite the greater respiratory comfort and lesser unsaturation of hemoglobin, $-G_x$ vector is disliked by operators, perhaps because of a feeling of insecurity engendered by inadequacies of restraint systems (544, 546).

Tolerance

Table 7-16 a and graphic presentation of these data in Figures 7-16b and c summarize the maximum tolerance to $-G_z$. (Aided means counter-measures used.)

Figure 7-14

Arterial Oxygenation During $+G_x$

(After Alexander et al⁽⁹⁾)

The following four graphs illustrate the effects of sustained transverse acceleration ($+G_x$) on the oxygen saturation of the arterial blood of 25 pilots in a supine position on the centrifuge. An ear oximeter was used to measure oxygen saturation throughout each of the various accelerations illustrated. All pilots breathed through an aviator's mask from a demand regulator.

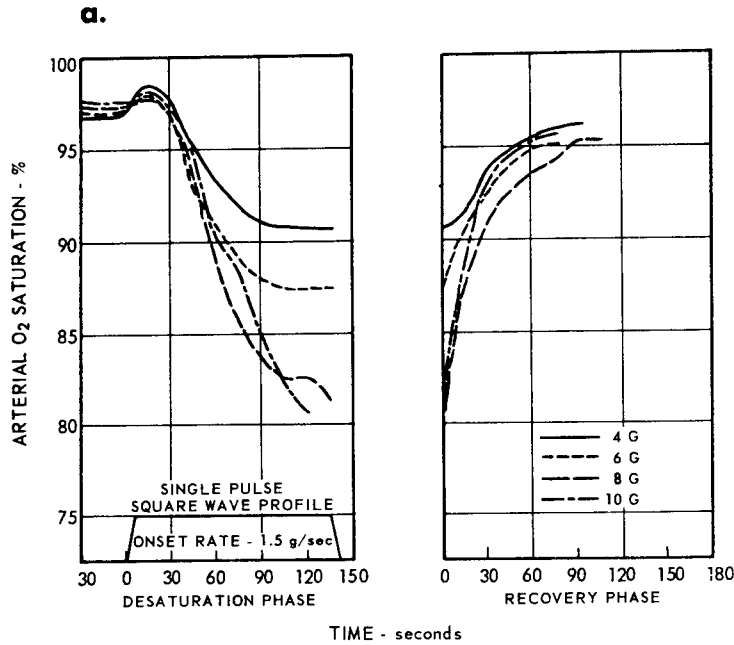


Figure a shows the arterial saturation during single pulse square wave profiles of acceleration while breathing air at 14.7 psia.

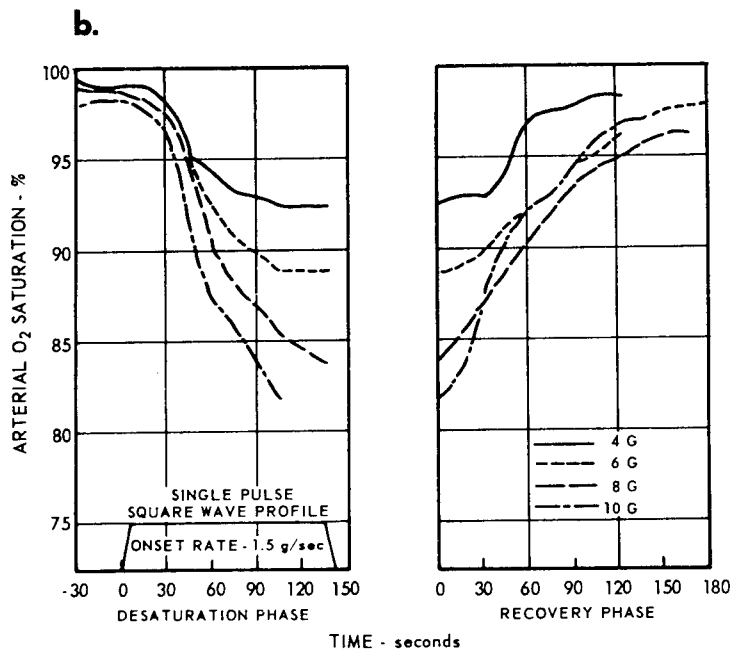


Figure b is a similar except that the pilots breathed pure oxygen at 5 psia and the gondola of the centrifuge was evacuated to 5 psia and they had breathed pure oxygen for 1 hour prior to the exposure.

Figure 7-14 (continued)

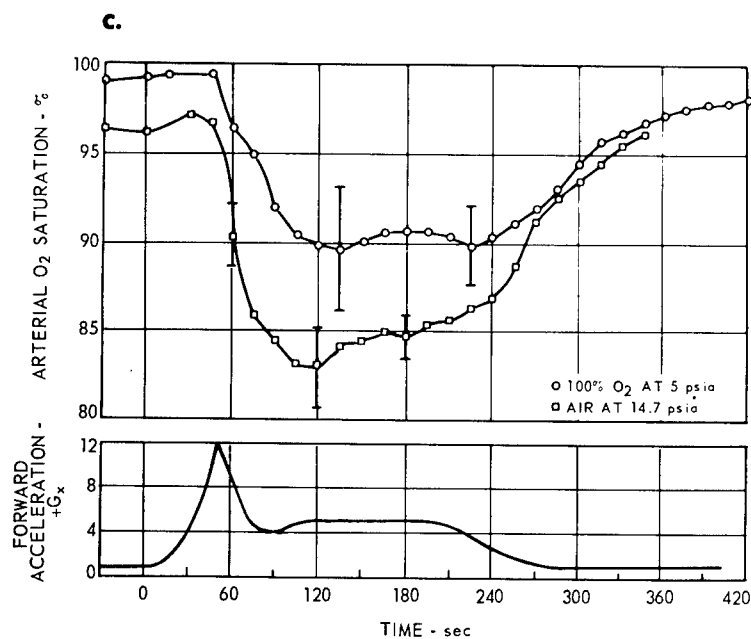


Figure c show arterial oxygen saturation breathing either air or oxygen as in Figures a and b during an acceleration profile representing one kind of re-entry pattern.

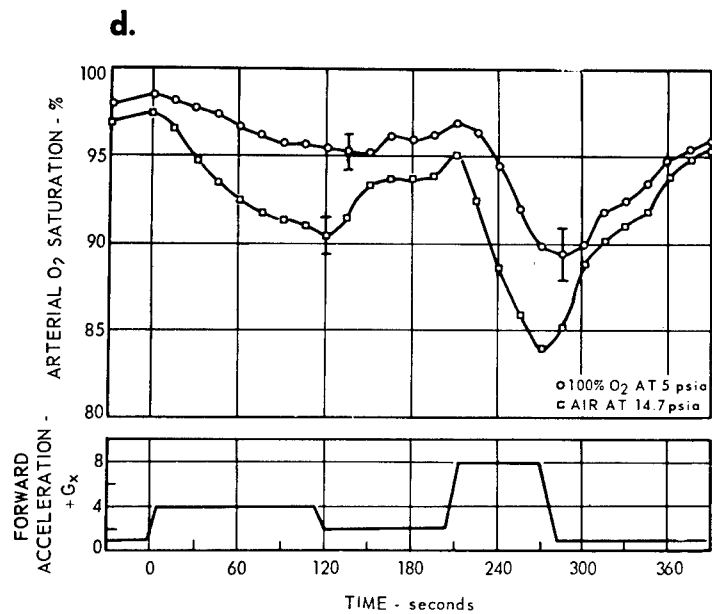


Figure d is similar to c except that a different type of re-entry pattern was simulated.

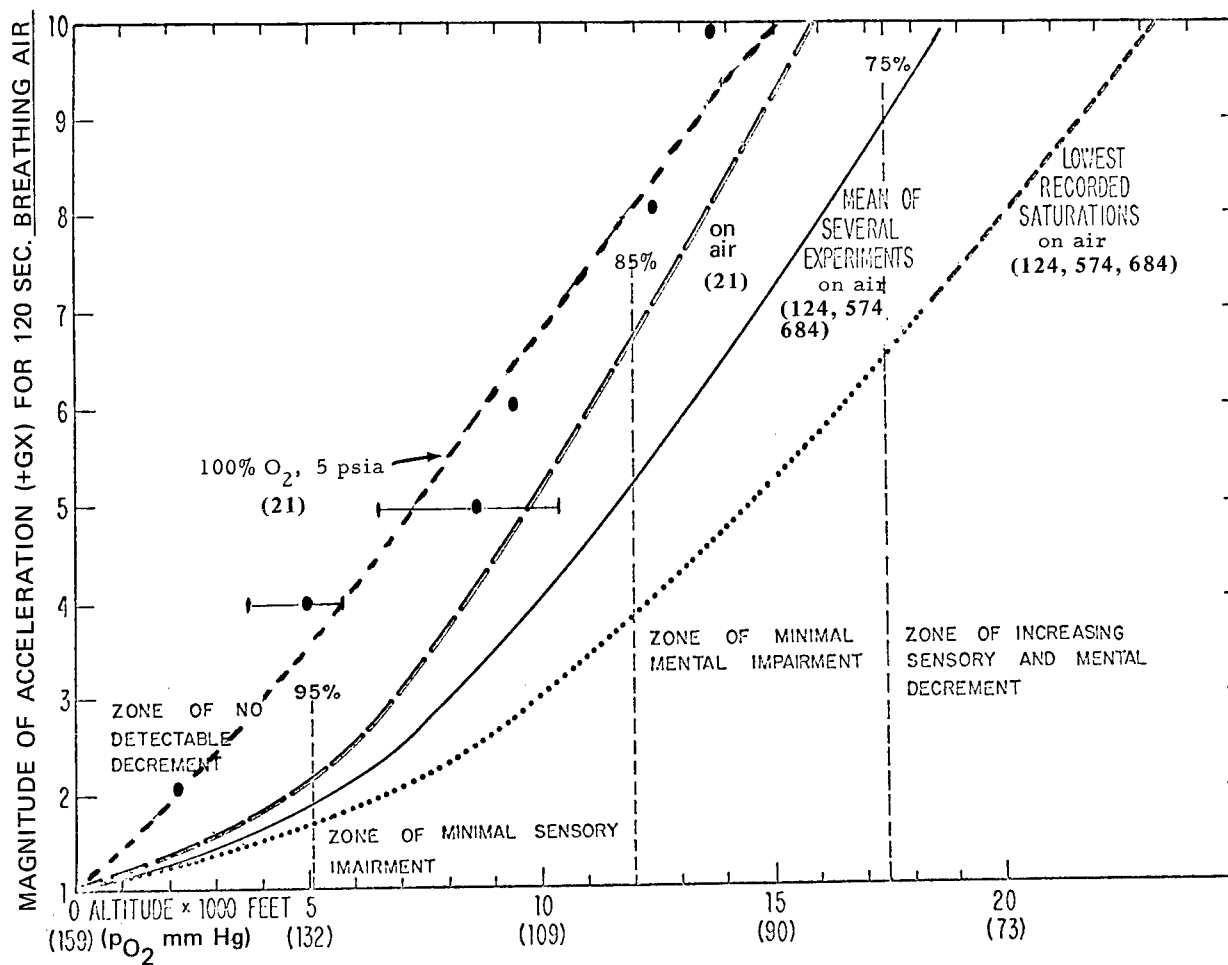


Figure 7-15

Impairment of Performance Predicted for Different $+G_x$ Levels Breathing Air and Oxygen at 5 psia Equated to Performance at Different Altitudes.

(After Teichner and Craig⁽⁶⁰⁵⁾, from data of Alexander et al⁽¹⁰⁾, Nolan et al⁽¹²⁴⁾, Wood et al⁽⁶⁸⁴⁾, and Steiner and Mueller⁽⁵⁷⁴⁾)

Figure 7-16

Maximum Tolerance to Prolonged Accelerations, $-G_x$
(See page 7-5)

(After Hyde and Raab⁽³¹⁵⁾)

a.

Vector Magnitude (G)	Duration at G (Seconds)	Average Onset (G/Second)	Back Angle (Degree)	Cause of Termination*	Trauma	Number of Subjects Attaining	Countermeasures	Support	Restraint	Reference
Complete Restraint n=1										
31.0	5	2.5	Approx. 0°	A?	Blood in Mucous	1	Total Water Immersion Positive Pressure in Lungs	G-Capsule	Water Immersion	235
28.0	Peak?	2.5	Approx. 0°	S	" " "	1	" " " " " "	" "	Water Immersion	235
26.0	Peak?	2.5	Approx. 0°	S	" " "	1	" " " " " "	" "	Water Immersion	235
12.0	6	0.5	-17°	S	None	1	None	F-86D Seat	Bernadini Restraint	98
11.0	11	0.2	-20°	S?	None	1	None	Scot Prone Bed	None?	4
10.0	90	0.2	-20°	S	None	1	None	Modified Prone Bed	Head Support Helmet	12
10.0	71	?	Approx. 5°	S?	None	1	None	Contour Couch	Ref. 548	143
10.0	18	0.5	-17°	S	None	1	None	F-86D Seat	Bernadini Restraint	98
8.0	65	0.5	-17°	S	None	1	None	F-86D Seat	Bernadini Restraint	98
7.0	300	?	Approx. 5°	S?	None	1	None	Modified Mercury Couch	Helmet and Webbing	124
7.0	240	?	Approx. 5°	S?	None	1	None	Modified Mercury Couch	Helmet and Webbing	124
7.0	210	?	0°	S?	None	1	None	Full Prone on Mat	None	4
6.0	140	0.5	-17°	S	None	1	None	F-86D Seat	Bernadini Restraint	98
5.0	180	0.5	-17°	A	None	1	None	F-86D Seat	Bernadini Restraint	98
4.0	300	0.5	-17°	A	None	1	None	F-86D Seat	Bernadini Restraint	98
3.0	1223	0.5	-17°	S	None	1	None	F-86D Seat	Bernadini Restraint	98
Partial Restraint n=1										
5.0	18	0.5	-17°	S	None	1	None	F-86D Seat	Integrated Harness	98
3.0	450	0.5?	-17°	S	None	1	None	F-86D Seat?	Integrated Harness	98
2.0	3600	?	-17°	A	None	1	None	F-86D Seat?	Integrated Harness	4
2.0	1800	0.5?	-17°	A	None	1	None	F-86D Seat?	Integrated Harness	98
Complete Restraint n>1										
15.0	5	8-10	Approx. 0°	Voluntary Limit	None	5 of 5	None	F-9F Seat Upright	Full Head Support	152
12.0	30	0.2	-20°	A	None	2 of 2	None	Modified Prone Bed	Head Support Helmet	12
12.0	≥3	0.5	-17°	S	None	4 of 4	None	F-86D Seat	Bernadini Restraint	98
10.0	120	0.2	-20°	A	None	4 of 9	None	Modified Prone Bed	Head Support Helmet	12
10.0	≥10	0.5	-17°	S	None	3 of 4	None	F-86D Seat	Bernadini Restraint	98
8.0	120	0.2	-20°	A	None	13 of 13	None	Modified Prone Bed	Head Support Helmet	12
8.0	>30	0.5	-17°	S	None	3 of 4	None	F-86D Seat	Bernadini Restraint	98
6.0	>50	0.5	-17°	S	None	4 of 4	None	F-86D Seat	Bernadini Restraint	98
5.0	≥80	0.5	-17°	S	None	4 of 4	None	F-86D Seat	Bernadini Restraint	98
4.0	>240	0.5	-17°	S	None	3 of 4	None	F-86D Seat	Bernadini Restraint	98
3.0	≥1200	0.5	-17°	A	None	2 of 4	None	F-86D Seat	Bernadini Restraint	98
3.0	900	0.2	-20°	A	None	10 of 13	None	Modified Prone Bed	Head Support Helmet	12
2.0	1200	0.5	-17°	A	None	2 of 2	None	F-86D Seat	Bernadini Restraint	98
Partial Restraint n>1										
5.0	≥5	0.5	-17°	S	None	4 of 5	None	F-86D Seat	Integrated Harness	98
3.0	>300	0.5?	-17°	S	None	4 of 4	None	F-86D Seat?	Integrated Harness	98
2.0	>1000	0.5?	-17°	S	None	2 of 3	None	F-86D Seat?	Integrated Harness	98

* S = Physiological end point

A = Arbitrary time limit end point

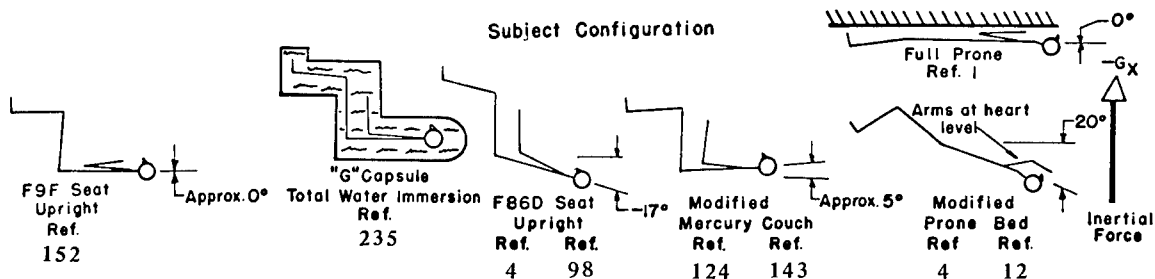
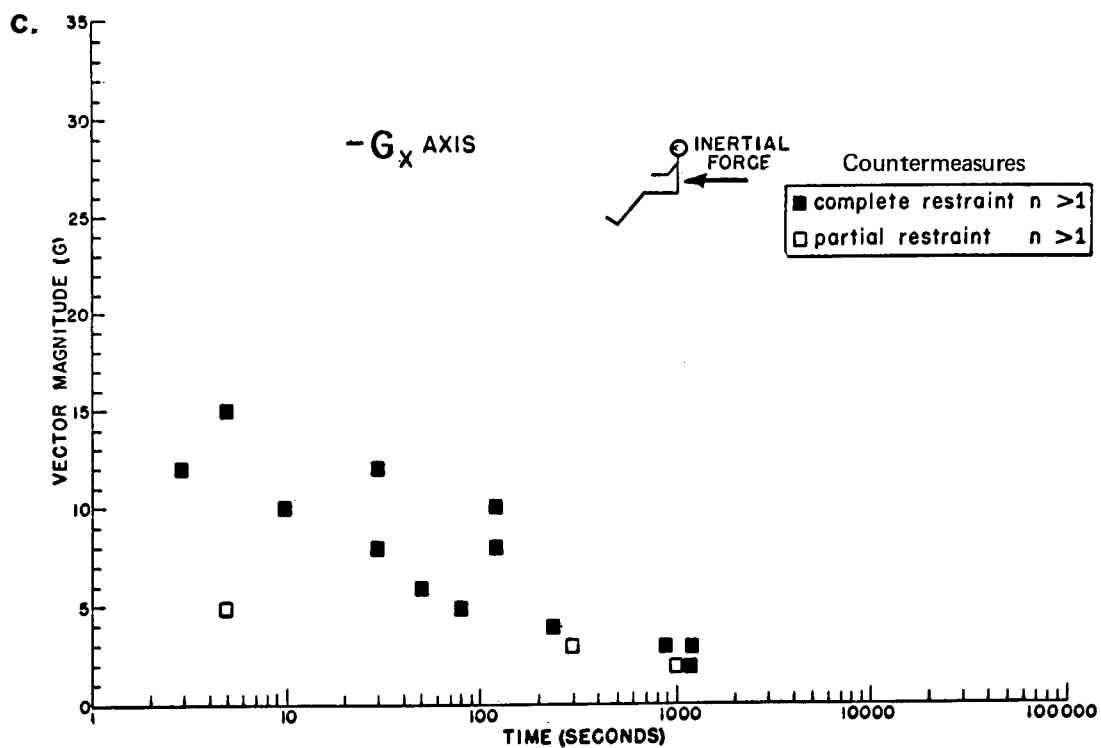
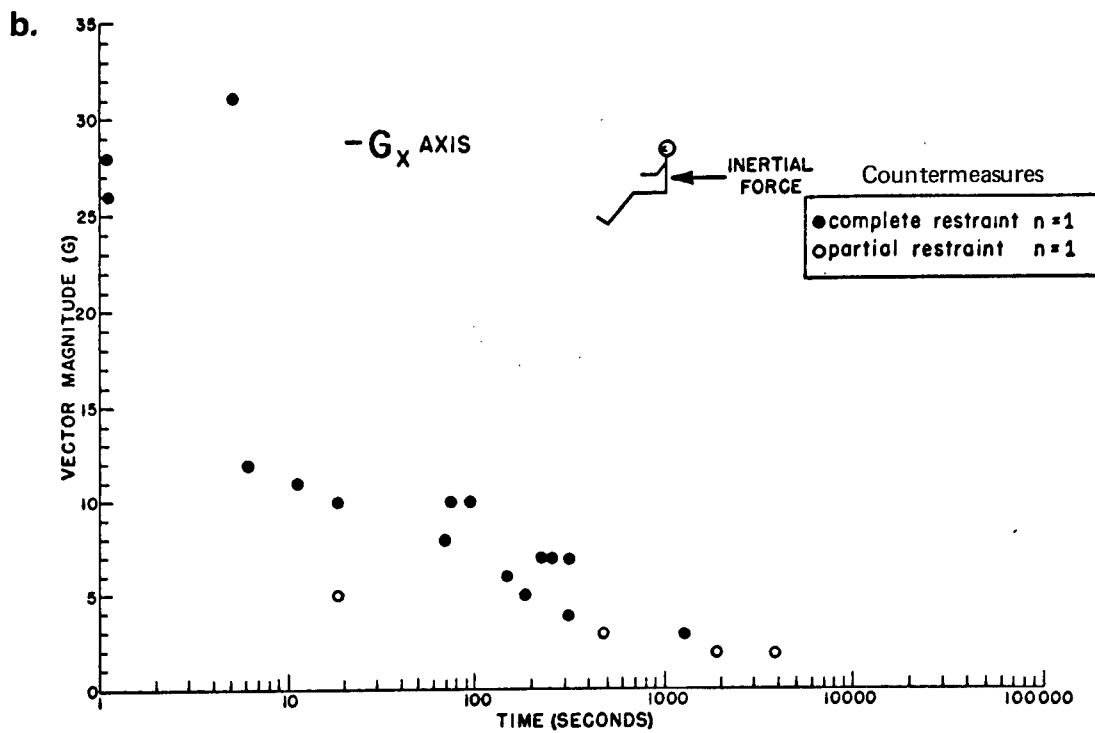


Figure 7-16 (continued)



(After Hyde and Raab⁽³¹⁵⁾)

$\pm G_y$ Acceleration

Physiological Response

Very little work has been done of the effects of $\pm G_y$ (93, 178, 188, 286, 294, 545). At $3G_y$ for 10 seconds lateral loads become uncomfortable, with pressure on the restraint system and a feeling of supporting the entire weight on the clavicle. This is accompanied by a movement of the hips and legs, and a yawing and rotation of the head toward the shoulder. Pressure effects were found to give rise to petechiae and bruising over the affected clavicles and, in the case of one subject at $-5G_y$ for 2 seconds during a total exposure of 14.5 seconds, to external hemorrhage and severe post-run headache. In addition, severe vascular engorgement with pain in the dependent forearm and elbow has been noted (286).

Tolerance

Table 7-17a and graphic presentation of these data in Figure 7-17b summarize maximum tolerance to $\pm G_y$ acceleration. (Aided means counter-measures used.)

Restraint and Protective Devices

The effects of restraint have been noted above in Figures 7-5 to 7-17. A tabular summary of the protective effect of different devices against $+G_z$ is presented in Table 7-18. The standard seat harness, normal in military aircraft, is inadequate for protection under sustained acceleration applied in the $+G_x$ vector, and still more so in the $-G_x$ (98). To counter this problem, custom-molded contour couches provide inclination of head, trunk, thighs, and legs, optimal both for acceleration tolerance and useful performance (95). They have been used in space flights to date.

These couches, while providing excellent support in the $+G_x$ vector, are inadequate in the $-G_x$ vector. For this vector, the "Ames system" is available that includes a posterior molded couch, a restraint helmet and supporting face and chin pieces secured into the mold, a chest and pelvic torso support, and nylon netting supports for upper arm, thigh, and lower leg (641). In addition, subjects wear a G-suit. This system, while cumbersome and not completely satisfactory under $-G_x$, was found to give the best restraint yet devised. Seats with raschel nylon net as the primary back, seat, and leg support surfaces are under development (483). They tend to provide excellent body support during extended acceleration up to $+16.5G_x$, semisupine. Under severe vibration and impact acceleration, however, undesirable rebound is encountered.

The ideal restraint system should provide:

1. Maximum comfort for long periods during all phases of the mission.
2. Maximum support and restraint during the sustained acceleration phases of the mission.

Figure 7-17

Maximum Tolerance to Prolonged $\pm G_y$ Acceleration

(See page 7-5)

(After Hyde and Raab⁽³¹⁵⁾)

a.

Resultant Vector Magnitude (G)	Component Vectors Magnitude (G)	Duration at G (Seconds)	Average Onset (G/Second)	Back Angle (Degrees)	Cause of Termination*	Trauma	Number of Subjects Attaining	Countermeasures	Support	Restraint	Reference
6.6	$\pm 26.6 G_y$	35	0.2	-13°	A	None	1	None	Modified Aircraft Seat	Harness Suit	2
5.6	$\pm 25.6 G_y$	25	0.2	-13°	A	None	1	None			2
5.4	$\pm 25.4 G_y$	40	0.2	-13°	A	None	1	None	(See Ref. for other particulars)		2
5.0	$\pm 25.0 G_y$	60	0.2	-13°	A	None	1	None			2
4.5	$\pm 24.5 G_y$	30	0.2	-13°	A	None	1	None			2

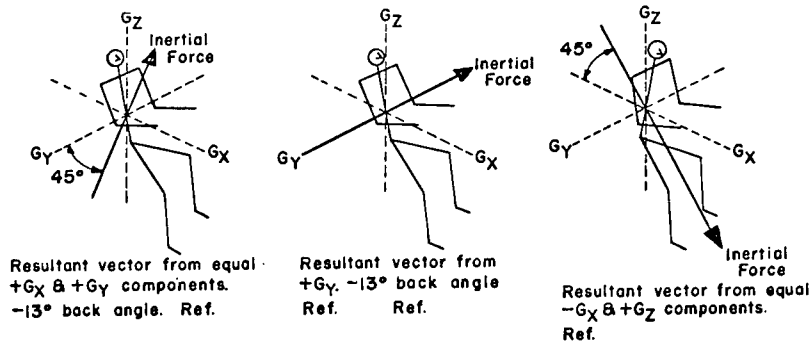
Combinations of Various Vectors

10.0	$\pm 7.1 G_x$ $\pm 7.1 G_y$	1	?	-13°	S?	None	1	None	Aircraft Seat Rotated 45° from Centrifuge Arm Axis	Harness Suit?	2
6.0	$\pm 4.2 G_x$ $\pm 4.2 G_y$	15	?	-13°	A	None	1	None			2
4.0	$\pm 2.8 G_x$ $\pm 2.8 G_y$	15	?	-13°	A	None	1	None			2
8.5	$\pm 6.0 G_x$ $\pm 6.0 G_z$	20	?	Approx. 5°	S	None	1	Anti-G Suit	Modified Mercury Couch	Helmet and Webbing	407
7.1	$\pm 5.0 G_x$ $\pm 5.0 G_z$	162	?	Approx. 5°	S	None	1	" " "	" " "	" " "	407
5.6	$\pm 4.0 G_x$ $\pm 4.0 G_z$	348	?	Approx. 5°	S	None	1	" " "	" " "	" " "	407

* S = Physiological end point

A = Arbitrary time limit end point

Subject Configuration



b.

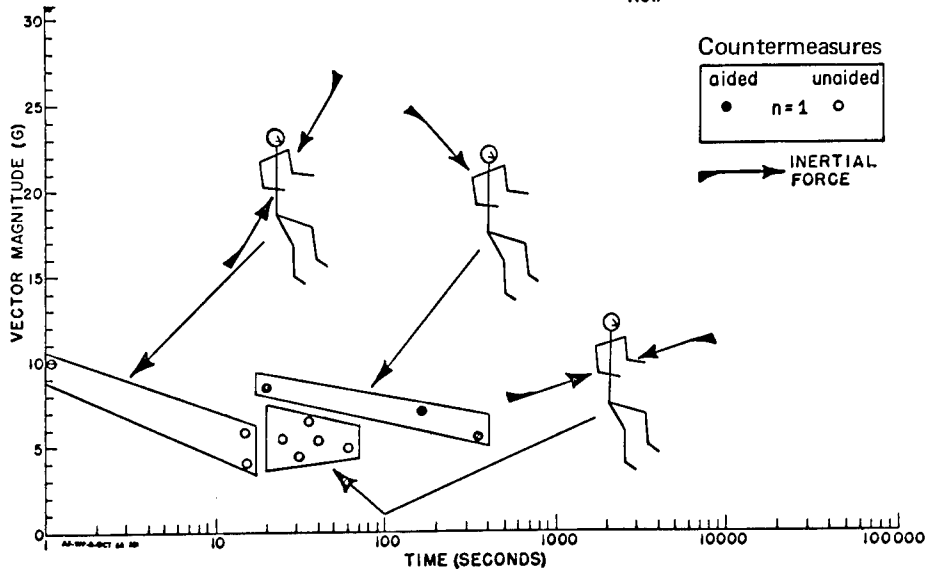


Table 7-18

Devices for Protection Against Positive (+G_z Axis) Acceleration(After Nicholason and Franks⁽⁴⁵⁷⁾)

Laboratory: RAF = Royal Air Force; RCAF = Royal Canadian Air Force;
 RAAF = Royal Australian Air Force; USAF = United States Air Force
 USAAF = United States Army Air Force; USN = United States Navy.

Anti-G Device	Description	Protection Against Visual Symptoms	References
1 Abdominal belts	Pneumatic belt connected to inflated bag situated under pilot; belt pressurized at 6 G to approximately 2 lb/in. ² ; additional device, pressurized by hand, exerted 25 mm Hg pressure at 5.8 G	None	169, 580, 581
2	Spencer acceleration belt inflated to 2-3 lb/in. ² approx 1 minute prior to acceleration	0.5 G	
3	Hydrostatic belt connected to 2-gallon water tank held at head level; during acceleration, belt filled with water and pressurized at the abdomen	0.5 G	
4 Arterial occlusion suit	Activated by G-controlled air pressure, occluding the femoral arteries; another suit occluded the brachial arteries	2.5 G	342, 682
5 Bandages	Applied to legs and abdomen	0.5-0.8 G	342
6 Hydrostatic pressure suits	Water-filled leggings, with pneumatic Spencer acceleration belt	0.5 G	583
7	Franks' flying suit (Canadian water-filled): Thigh, leg, and abdomen bladders were pressurized under gravitational stress and exerted tensing effect on limbs through an inextensible covering.	1.0-2.0 G	55, 129, 175, 501, 509, 510, 582
8		2.1 G	341
9		1.4 G	682
10		1.5 G	277
11	Franks' liquid-filled suit with superimposed G-graded air pressure	> 2.5 G	176
12 Pneumatic gradient pressure suits	Cotton aerodynamic anti-G suit (Australian air-filled): Overlapping bags in an inextensible outer covering; bags almost encircled limbs and body from feet to a few inches below the costal margin; provided 3 levels of pressure.	1.5-2.0 G	129, 399, 400, 585
13	Spencer-Berger rubber, air-filled suit: Bags partially covered body; ankle bladders pressurized at 1.25 lb/in. ² /G, calf and abdominal bladders at 1.13 lb/in. ² /G, bladders at 1.10 lb/in. ² /G.	1.3-1.6 G	129, 278, 342, 359, 360, 682
14 Single pressure suits	Spencer acceleration belt and stockings (Poppen Belt)	1.0 G	584
15	David Clark single pressure suit inflated at 1.2 lb/in. ² /G (developed from Spencer acceleration belt and stockings)	1.4 G	129, 359
16	RAF III suit: Essentially a copy of the David Clark single pressure suit, but with a split abdominal bladder and dual air inlet. Present day USAF and RAF suits have single air inlet serving leg and single abdominal bladder.	1.4-1.5 G	130, 501
17	Pneumatic lever suit: Bladder systems consisting of narrow-bore tubes passing down each side of the body from the low thoracic region to the ankle; inflated bladders applied tension to legs and abdomen through interwoven ribbons using capstan principle; 2.2 lb./in. ² /G pressure applied, starting with 2.0 lb/in. ² at 2 G.	1.5 G	130, 361
18 Water immersion	Mayo bath: Subject immersed in water to third rib level.	1.7 G	682
19	G capsule: Total immersion.	16.0 G	282

3. Adequate support during periods of low-frequency high-amplitude vibration.
4. An integral total-body restraint system.
5. Sufficient adjustments, including angular adjustability, to accommodate the 5th through the 95th percentile crew member.
6. Accommodation of pressure suits as well as regular flying suits.
7. Ultimate provision of an integrated arm-restraint device and a three-axis hand control.
8. Ultimate provision of an emergency encapsulation device.
9. Lightness, easy maintenance, durability, and crew appeal.

The effects of anti-G protective devices have been indicated on the tables above. Anti-G suits are most effective for loads along the retinal-aortic axis. While an anti-G suit in the G_x vector would not be expected to produce as dramatic results, it can make exposure to loads below $15G_x$ more comfortable and reduce the visual effects in subjects unpracticed in straining techniques (95). Above $15G$, the suit is of no benefit in increasing G tolerance, and, in fact, was found to make straining more uncomfortable. A water-filled immersion suit, does prevent the occurrence of petechiae but does not appear practical for space operations.

A short review of protection against linear accelerative stress is available (533).

Performance Under Prolonged Linear Acceleration

Performance under prolonged acceleration is quite sensitive to the variables covered above. Satisfactory performance demands adequate perception of appropriate stimuli, integration and correlation of these stimuli with previously established patterns, and coordinated effector action. Thus there are many ways in which exposure to acceleration may interfere with a pilot's performance. Major individual differences exist among pilots in their ability to perform piloting tasks during exposure to high G . Also, certain types and combinations of linear and rotary acceleration produce illusions, or false perceptions, of one's position and motion. These may occur in some pilots during or after the acceleration exposure and affect the performance end point. Since acceleration training results in physiological adaptation and conditioning to G , as well as learning to make performance compensation, acceleration training produces major improvements in performance proficiency during exposure to high G .

Perception may be disrupted by interference with the sensory process; integration and correlation may be impaired by disturbance of cerebral oxygenation; and effector action may be opposed by the forces developed. Of primary importance are the visual, vestibular, kinesthetic, and auditory senses.

Vision

The instrument display characteristics of a piloting task influence the measurement of performance capabilities of a pilot during exposure to high G. Among the more important display characteristics are: the position of the display instrument within the pilot's visual field, the degree of interpretation required of the pilot, the number of instruments that must be viewed by the pilot during high G, the amount of illumination, the amount of brightness contrast, the physical form in which the display information is presented, and the amount of visual instrument scanning that is required at high G (188,423).

a) Gross Vision

The effect of acceleration along the retinal-aortic axis has the most profound visual effects (see Figure 7-2a, b, and c) (675). The specific relationship of grayout, the dimming, peripheral light loss, and blackout to level, duration, and time of onset of G_z are seen in Figure 7-6a. These are the most frequently used behavioral measures of human tolerance to $+G_z$. There is considerable evidence indicating that these effects are the result of a decrease in arterial blood pressure at the eye and pooling of the blood in the lower extremities (178, 188). Typical tolerance values based on visual data obtained on 1000 subjects tested in the seated body position are summarized in Table 7-19a. These data are based on rates of development of 1 G per sec.

The visual effects of $-G_z$ are not well defined. "Redout" or red vision is perhaps the most interesting subjective symptom, yet the phenomenon has not been consistently observed. No authenticated cases of redout occurred on the human centrifuge at Wright-Patterson Air Force Base (290). Visual disturbances reported by subjects after 10 sec exposure to negative acceleration have been summarized and are shown in Table 7-19b. The category "diminished vision" includes such items as tear secretion and a tendency of the lower lid to cover the cornea. Funduscopic examination following the unprotected runs showed no alteration in retinal blood vessels. It can be seen that when air counterpressure was applied with the full pressure helmet, the pattern of visual symptoms changed. Subjects reported blurring of vision at the highest levels of acceleration only. At these levels the intensity of the symptoms was no greater than that experienced at $-2G_z$ without the protective helmet.

It has been reported that repeated exposure to $-G_z$ results in an increase in the time for the eyes to accommodate and a doubling of vision (290). The diplopia was attributed to edema in the tissues around the eye which disturbed the balance of the extraocular muscles. The symptoms subsided concurrently with the disappearance of edema in the facial tissue and linked the adverse effects of $-G_z$ to the vascular congestion of the head region, which produced petechiae, extravasation of fluid into the soft tissues, and hemorrhage into the sinus cavities. These symptoms are accompanied by severe pain.

A recent summary of Soviet work on cerebral blood volumes during $\pm G_z$ exposures is available (435).

Table 7-19

Visual Tolerance to Accelerative Stress

a. Visual Tolerance to $+G_z$ (N = 1000); Rate of G development is 1G/sec.

Criterion	Mean Threshold (G units)	Standard Deviation (G units)	Range (G units)
Loss of Peripheral Vision	4.1	± 0.7	2.2 - 7.1
Blackout	4.7	± 0.8	2.7 - 7.8
Unconsciousness	5.4	± 0.9	3.0 - 8.4

(After Cochran, Gard, and Norsworthy⁽¹⁰¹⁾)b. Frequency of Symptoms Reported by Subjects Exposed to Negative G_z for 10 Sec.

b. Frequency of Symptoms Reported by Subjects Exposed					
Symptoms	Acceleration in g				
	1	2	3	4	5
No protection					
Conjunctival Hemorrhage	0	0	40%		
Diminished Vision	0	0	40%		
Protected by full pressure helmet					
Diminished Vision	0	0	10%	20%	30%
Conjunctival Hemorrhage	0	0	0	0	0

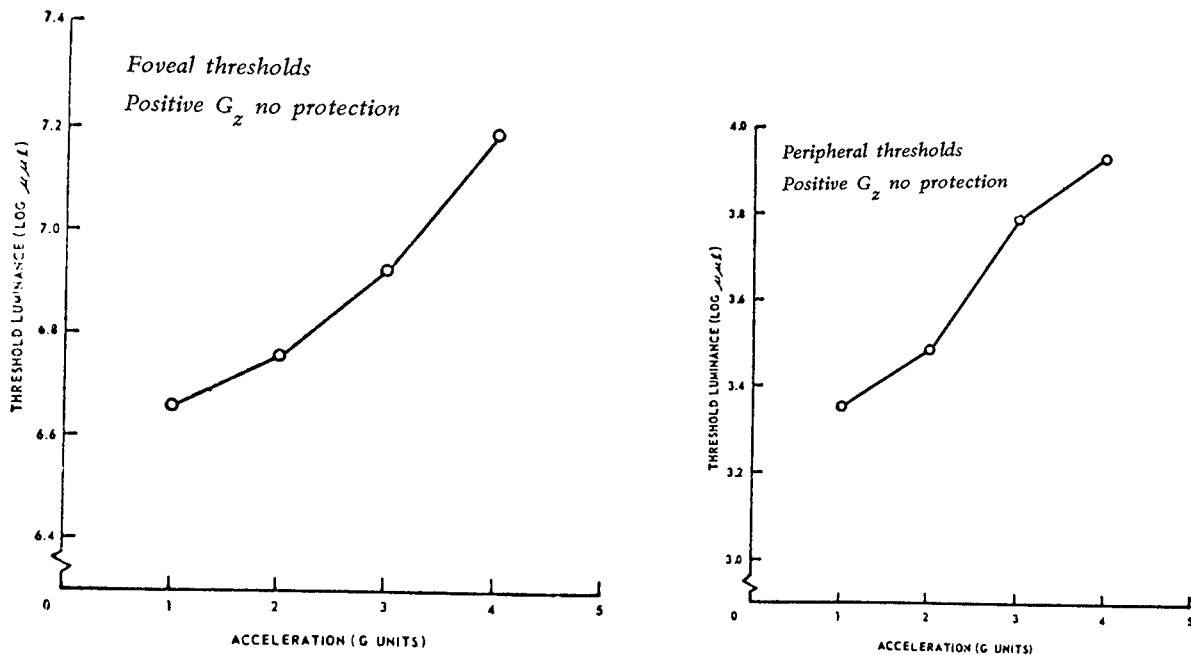
(After Sieker⁽⁵³⁸⁾)

In transverse acceleration, some loss of peripheral vision has been noted in $+6G_x$, increasing to marked loss at $+12G_x$, and recurrent blackout at $+15G_x$ (73). The onset of grayout in transverse G can be related to the "effective physiological angle" (EPA). (See Figure 7-2a.) The terminology of grayout thresholds for different effective physiological angles is illustrated in Figure 7-2c. Thus, in the current Apollo position, with a 15° aortic retinal angle, 2° back angle, and value of 6.5° for ϵ , the effective physiological angle will be 23.5° and grayout will be expected at about $7\frac{1}{2}G_x$.

b) Absolute Thresholds

There appears to be a continual change in absolute threshold of vision or the minimum light intensity at which a stimulus can be perceived under acceleration (673). Figures 7-20 a and b cover these data. At $+3G_z$ the foveal threshold was almost double that at 1G, and at $+4G_z$, it was 3.4 times that at $1G_z$, when measured at the 50% probability level. In the periphery the luminance of the stimulus has to be increased 1.5 times at $2G_z$, 3 times at $3G_z$, and 4 times at $4G_z$. Similarly, a decrease in differential threshold, the minimum perceptible difference between a pair of stimuli, is observed, most marked with positive acceleration and for low background luminance.

Figure 7-20
Foveal and Visual Thresholds Under Acceleration
(After White⁽⁶⁷³⁾)



a. Foveal Thresholds as a Function of Acceleration

b. Peripheral Thresholds as a Function of Acceleration

c) Brightness Discrimination

Visual brightness discrimination has been examined under four levels of background luminance, four levels of positive ($+G_z$) acceleration, and five levels of transverse ($+G_x$) (54). In Figure 7-21 for each of the four $+G_z$ conditions (1, 2, 3, and 5G) the visual contrast requirements increased as the background luminance decreased, and for any given background luminance the higher acceleration levels required more brightness contrast. Similar results were shown for the $+G_x$ exposures (1, 2, 3, 5, and 7G). The G_z acceleration consistently imposed higher contrast requirements than did the G_x . The effect of oxygen on brightness discrimination during acceleration has been studied (10, 79). The results are seen in Figure 7-22. Further data are available in Oxygen (No. 10).

d) Visual Acuity

Visual acuity, which is a foveal function, also decreases linearly with increase in acceleration. This decrease, however, is independent of body position and consequently is independent of change in hydrostatic pressure (50). Figure 7-23 indicates the loss of binocular visual acuity as a function of $\pm G_x$. This loss of acuity may be related to displacement of the lens in the direction of the acceleration vector or possibly to reflex cardiovascular changes in blood flow to the head.

In the $-G_x$ vector, visual disturbances become marked at $-G_x$ to $-8G_x$. No distortion is attributable to corneal deformation, but intermittent watering

Figure 7-21

Brightness Discrimination During $+G_z$ and $+G_x$

(After Braunstein and White⁽⁵⁴⁾)

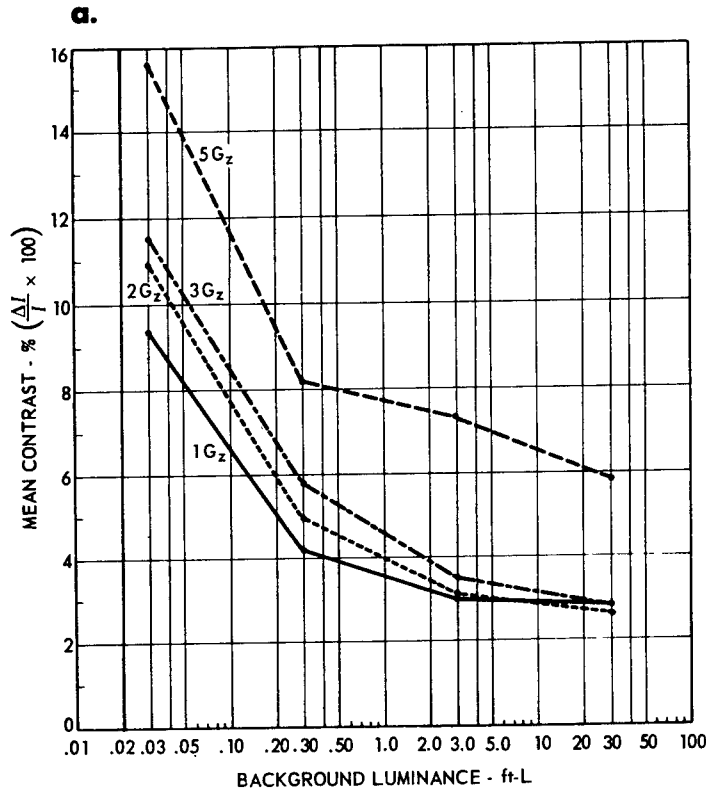


Figure a shows the relationship between brightness discrimination and background luminance at four levels of positive acceleration ($+G_z$).

The minimal detectable difference in intensity between a test patch and its lighted surround has long served as a test of visual sensitivity. The threshold difference has been found to be a function of basic energy level as well as contrast between the patch and its reference illumination; thus, the greater the background intensity, the smaller the ratio between the patch and the background required for detection. The data compiled in these graphs also illustrate an interaction between acceleration and the minimal discernible differential intensity (ΔI). The stimulus display used to collect these data consisted of a background subtending $8^\circ 4'$ visual angle positioned 28 inches from the eye and viewed monocularly through a circular aperture 17.5 inches from the eye. The test patch, projected upon the background, subtended a $1^\circ 28'$ visual angle.

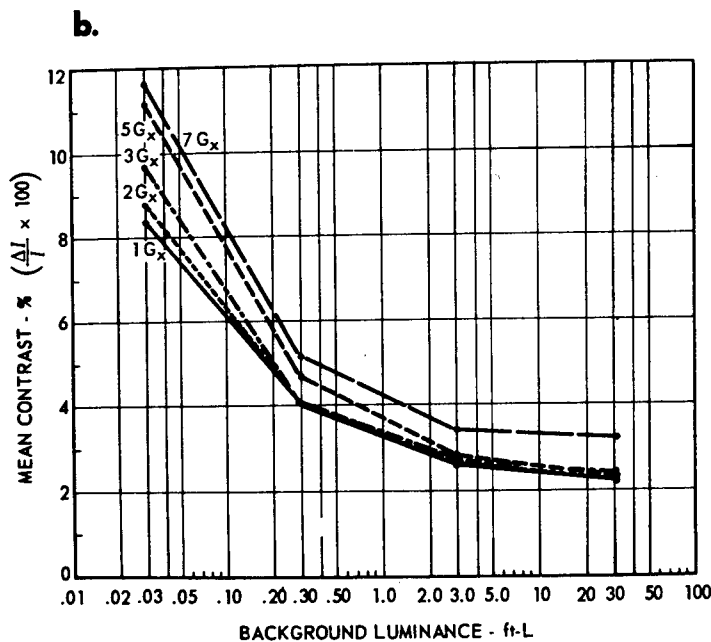


Figure b illustrates the relationship between brightness discrimination and background luminance at each of five levels of transverse acceleration ($+G_x$).

Figure 7-22

Oxygen and Brightness Discrimination During $+G_z$ and $+G_x$

(After Chambers et al⁽⁷⁹⁾)

Comparison of visual brightness discrimination is shown in figure a for subjects during exposure to $+G_z$ accelerations under three breathing conditions: normal breathing air; 100% O_2 ; and 100% O_2 with positive pressure. The positive pressure ratio was 0.75 inches of water per G.

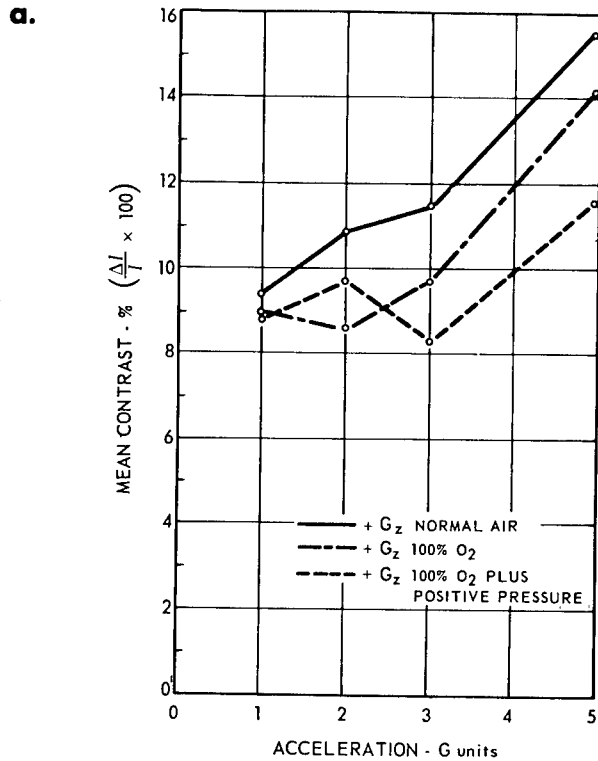
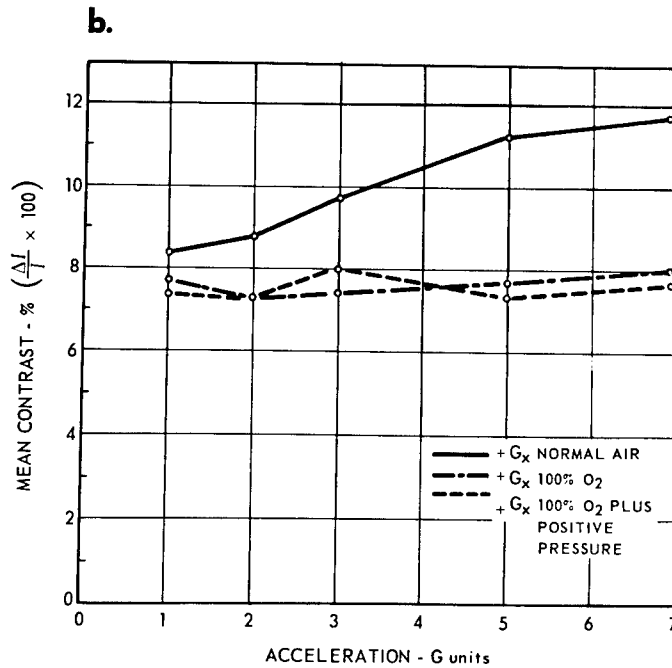


Figure b shows similar data during transverse acceleration ($+G_x$).



of the eyes distorted refraction of the cornea above $-6G_x$ (515). Changing body position exposes an individual to unusual gravitational forces other than the one to which the body is accustomed. Figure 7-24 shows deterioration of visual acuity produced by change in position.

e) Visual Fields and Ocular Motility

Very little work has been done in determining the degree of narrowing of the visual field that occurs with acceleration. At $+4.4G_z$ (range of $+3G_z$ to $+6.5G_z$) the field is narrowed to an arc of less than 46° (675). Figure 7-25 indicates the effect of retinal position on acceleration response as does Figure 7-20a and b. The limitation in ocular motility has been noted (26).

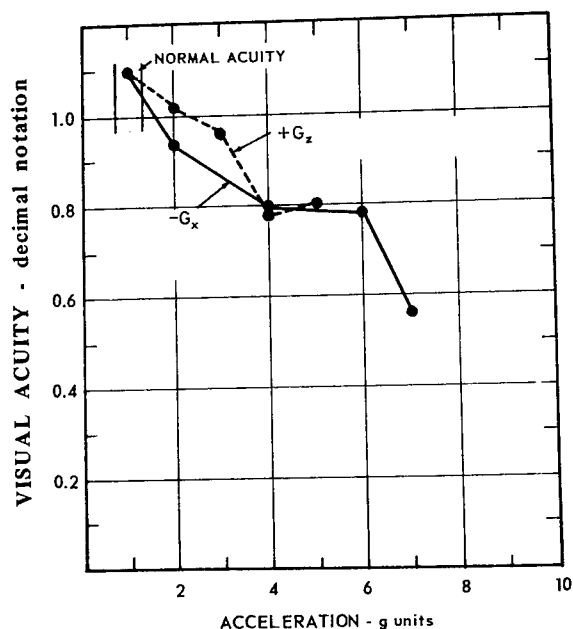


Figure 7-23

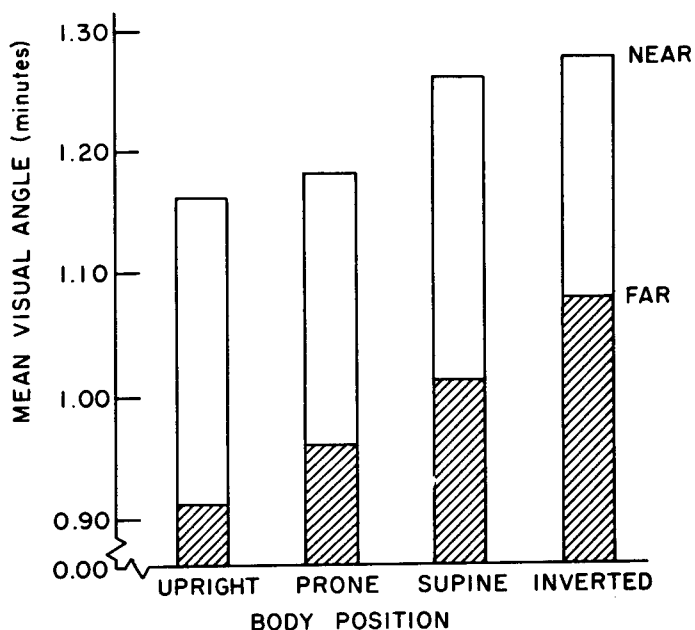
Binocular Visual Acuity Under Transverse Acceleration

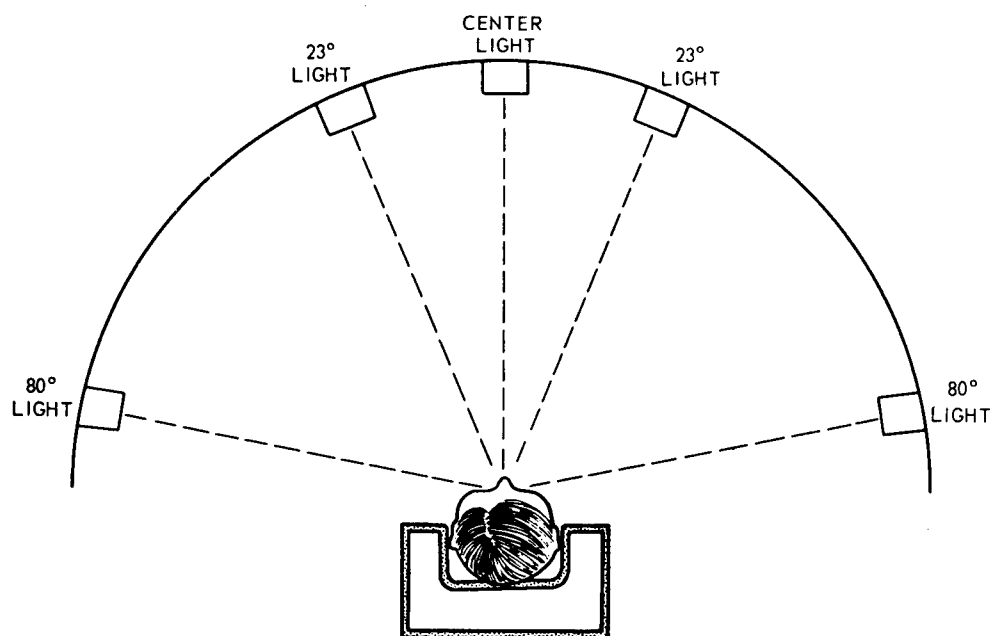
This graph shows binocular visual acuity as a function of acceleration. If a target is to be seen at $7 -G_x$, it must be twice the size of the threshold target at 1 G. See original data for standard deviations before directly applying these data.

(After White and Jorve⁽⁶⁷⁴⁾)

Figure 7-24
Binocular Visual Acuity as a Function
of Body Position

(Adapted from Pigg and Kama⁽⁴⁸⁶⁾)





One hundred fifteen subjects exposed to positive acceleration ($+G_z$) with a light array as shown in the diagram almost invariably lost the 80° light before loss of the light of 23° (23° LL). After completing the experiment it was decided to quantitate this in 30 subjects, and it was found that the 80° light loss (80° LL) occurred at a mean of $4.2 G_z$, standard deviation $\pm 0.7 G$; and in the same subjects, the 23° LL occurred at a mean of $4.5 G_z$, S.D. $\pm 0.8 G$. Central light loss (CLL) occurred at $5.3 G_z$, $\pm 0.8 G$.

This demonstrates also the reliability of the method used, since the original 115 subjects and the 30 subjects lost their 80° light at $4.24 G$ and $4.20 G$ respectively.

Comparison of 80° Light Loss, 23° Light Loss, and 0° Light Loss				
	Symptoms			
	Clear	80° LL	23° LL	CLL
Mean (G_z level)	3.8	4.2	4.5	5.3
Range (G_z level)	2.3-5.1	2.7-5.7	2.9-6.4	3.6-7.0
Standard Deviation	0.7	0.7	0.8	0.8
Duration of symptom- Mean (sec)		5.4	5.1	6.8
Duration of symptom- Range (sec)		1.9-17.0	1.9-11.9	2.1-23.4

Figure 7-25

Grayout Thresholds During $+G$

(After Chambers⁽⁷²⁾, adapted from Zarriello et al⁽⁶⁹⁸⁾)

f) Pupillary Reactions

Pupillary dilatation begins with loss of peripheral vision (26). The dilatation appears immediately upon exposure to acceleration, possibly a sympathetic response to anxiety (675). Accommodation ability is unaffected by acceleration (515).

g) Reading Tasks

Reading tasks of course demand an intact performance loop and are more than measures of vision. Acceleration forces up to $+2G_z$ do not appreciably degrade dial reading performance for luminances of 0.1 m-L but, as acceleration forces are increased, performance is significantly degraded (677). The reduction in acuity can be compensated for by increasing the luminance as indicated in Figure 7-26. At 42 m-L, acceleration levels up to $4G$ do not degrade dial reading performance while decreasing illumination to 4.2 m-L gives only a slight performance decrement.

The effect of G loads on other complicated visual-motor tasks has been reviewed (78, 178). Visual reaction time is more than a test of visual adequacy. A typical response is seen in Figure 7-27. The response time for discrimination of colored lights was longer under G_z acceleration than under normal conditions (77). During a 5-minute exposure to $+6G_x$, however, the response of each subject to 25 trials of light discrimination was slower than average; during a second 5-minute exposure it was still slower, but during the third series performance improved significantly. This suggests that the subjects had learned to adapt to acceleration stress and corroborates previous findings along this line (63, 64, 174).

Data are available on amelioration of visual effects of acceleration by anti- G suits (675).

Auditory Responses

It is well established that the sense of hearing is maintained after acceleration has reached a magnitude sufficient to cause blackout, although it does not appear to have been experimentally established whether loss of hearing occurs prior to, or with, unconsciousness. The point is not entirely academic; it is of practical importance to know whether an auditory warning will be heard after a visual warning is no longer perceived. Such evidence as there is indicates a progressive increase in reaction time to auditory stimuli as unconsciousness approaches (64). However, this increase in reaction time to auditory stimuli is denied by some investigators (177).

Vestibular Responses

Vestibular responses and illusions resulting from riding a centrifuge are covered below under "vestibular interactions in the rotary environment." Figures 7-43 to 7-48 present response of the otolith organs to changes in linear acceleration.

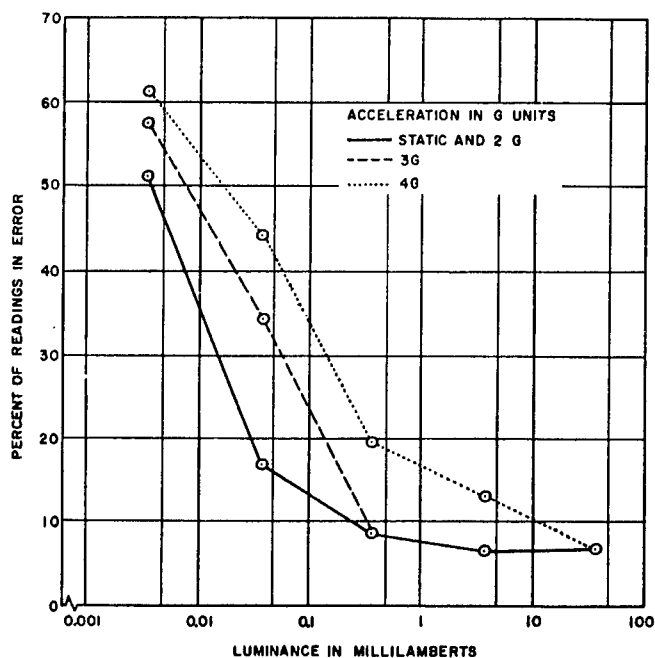


Figure 7-26

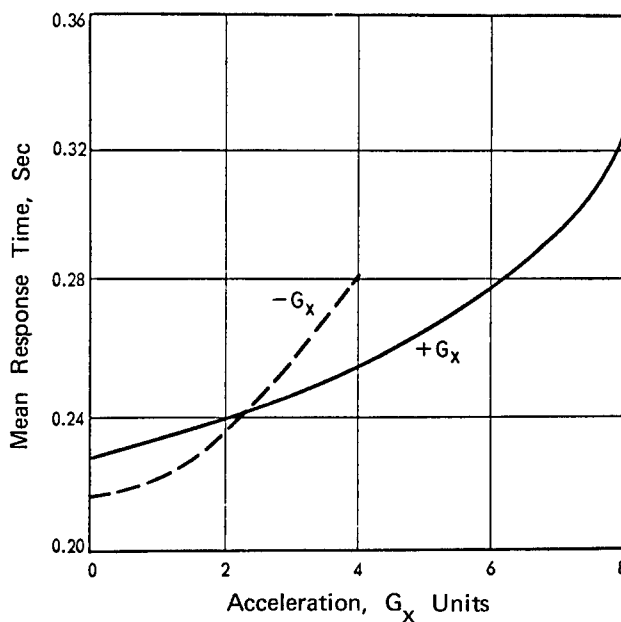
Effect of Acceleration ($+G_z$) on Dial Reading Accuracy as a Function of Luminance

(After White and Riley⁽⁶⁷⁷⁾)

Figure 7-27

Response Time During Transverse Acceleration

The two curves show mean response times (the time from appearance of a red signal light to the movement of the subject's hand from his lap) for five male college students, 20-25 years old, exposed to transverse accelerations. The solid line shows the combined response times for both right and left hand operation in more than 900 ($+G_x$) exposures up to $+8 G_x$. The dashed line shows the combined response times for both right and left hand operation in more than 500 ($-G_x$) exposures up to $-4 G_x$. The times required to reach and operate a horizontal lever, a toggle switch and a push button were longer as the accelerations increased, and variable times were recorded for left and right hand operation. Still longer times were needed for adjusting a rotating knob and a vertical "trim" wheel.



(Adapted from Kaehler and Meehan⁽³³⁰⁾)

Motor Performance

The characteristics of the control device used by the pilot in performing under G loads have a significant effect upon proficiency. These characteristics are: the number of axes of motion; the location of the axes of motion with respect to the G and the pilot's hand; stick force gradients along each mode of control; the centering characteristics along each mode of control; dead band zone; breakout force requirements; control friction; static and dynamic balance; damping characteristics; control throw; response time of control; control harmony; cross coupling characteristics; size and shape of grip; dynamic and static balance; and control sensitivity.

In general, acceleration impairs the ability of the pilot to sense changes in control characteristics that may occur as a function of specific acceleration vectors. This may be a direct effect of the acceleration forces on the receptors, effects on the central or autonomic nervous system, or an effect on circulatory and other physiological systems which indirectly affect the ability of the pilot to sense changes in his arm, hand, and fingers. Second-order motivational and emotional factors play an important role in these areas (224). In the operational situation, combined stresses and their integrated responses must also be considered (653).

a) Body Movements

Gross body movement is progressively impaired with increasing acceleration. Walking, crawling, and movement along a ladder against acceleration were very difficult at $+2G_z$ and impossible at $+3G_z$. Movement at right angles became impossible at $+4G_z$; parachute donning time was increased from 17 seconds at $1G$ to 75 seconds at $+3G_z$ (102). At $+6G_z$ to $+7G_z$ it is extremely difficult to reach a face-curtain seat-firing handle (86).

In the $+G_x$ vectors, the body, legs, and arms cannot be lifted at $8G_x$ and above. The unsupported head cannot be lifted above $9G_x$, although use of a counterweighted headgear allows relatively free movement up to $12G_x$ (57). Hand and wrist movement seem to be possible up to about $25G_x$.

b) Controls

Voluntary muscular exertion increases with increase in acceleration in a manner that is just sufficient to balance the change imposed by acceleration. This was studied in only one subject, using an ingenious electromyographic technique in analysis of the response of arm muscles during 10 to 50 lb pulls on an aircraft control stick under $+G_z$ to $+5G_z$ with the arm in flexed, intermediate, and extended positions (178).

The characteristics that should be borne in mind in designing control sticks have been noted above and are covered in greater detail in reference (73). Pilots can operate a right-hand control stick and a thumb switch on a contour couch up to $+25G_x$. Figure 7-28 covers typical responses to different types of control sticks for spacecraft use. Figures 7-29 and 7-30 cover tracking tasks using side-arm controls. The decrement caused by G_x acceleration on the operation of levers, switches, buttons, knobs, and wheels has been recorded (330).

Foot controls have also received study (95, 547). At $+5G_x$ it is difficult to hold the feet forward on rudder pedals. However, in the contour-couch positions, use of dorsiventral rotation at the ankles has some promise.

c) Cerebral Function

As covered above (see Figure 7-6), loss of consciousness and complete impairment of cerebral function occurs between $+3G_z$ and $+8G_z$, the specific level depending chiefly on biological factors, duration, and rate of onset. In the other vectors the subject normally reaches a tolerance threshold of another sort before unconsciousness occurs. On return to consciousness there is usually a short (5 to 15 second) period of confusion. Changes in the EEG consistent with the change in consciousness in $+G_z$ have been recorded (14, 529, 562). Animal data are available on EEG frequency analysis during $\pm G_x$ (3) There is no change in cerebral function as measured by flicker fusion frequency just before grayout at $+3.2G_z$ but it does drop slightly at $+4.8G_z$ (336). There is an increase in color naming and mental arithmetic time in subjects exposed to $+3.2G_z$ for 2 to 10 minutes (174). In shorter trials of only 1 minute, there was no change in performing arithmetic, tapping, number ranking, and word separation but changes were observed in color-naming and steadiness, where performance was poorer under acceleration.

In a complex test involving continuous and repetitive memorization of a portion of a sequence of random numbers, it has been found that subjects could perform this task as well at $+5G_x$ as at 1G, but the subjects stated that the mental strain was much greater at $+5G_x$ (74). In another task, monitoring a changing display of numbers and symbols and matching the current display with one presented some time before, immediate memory was shown unaffected to $+5G_x$ but impaired at $\pm 7G_x$ and above. In more recent studies of a 2-channel running memory task with 2 random binary series, no memory was found at $+3G_x$; significant deficits at $+5G_x$ and $+7G_x$, and still greater deficit at $+9G_x$ (502). Most of the deficit occurred in the latter half of the 2-minute and 18-second stress period. On the basis of these various tests it would appear that higher function is disrupted under acceleration, at least to the extent of interference with concentration.

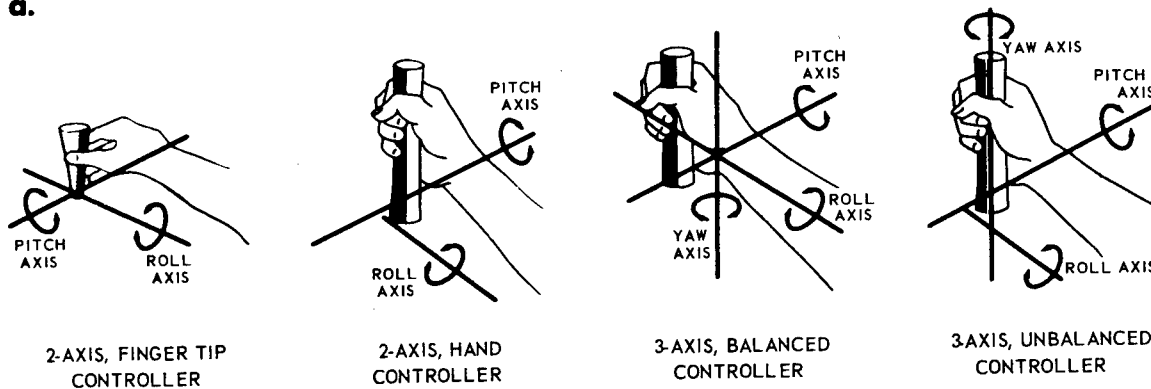
Tracking tasks are often used as operational tests of cerebral function and psychomotor behavior. Figures 7-28, 7-29, and 7-30 show typical findings. Within the parameters simulated, a pilot can adequately control his vehicle in a field of $+14G_z$ (125). Best control in the experiments of the type stated in Figure 7-29a was in the $+G_x$ vector, next in the $-G_x$, and least in the $+G_z$ (Figure 7-29b). With rates of onset varying from 0.1 to 2G per second, tracking performance declined above 0.75G per second. Even with the Ames restraint system, it has been found that tracking performance during $-G_x$ conditions was no better than during $+G_z$ despite the easier respiration (546).

The dominant effects of high, sustained acceleration stress on pilot response are increased filtering or attenuating at higher frequency of input commands. Reduction in the pilot's ability to cope with higher frequency components of the input command suggests that pilots should not be expected

Figure 7-28

Tracking, Controller Characteristics, and G Vectors
(After Chambers⁽⁷³⁾, and Chambers and Hitchcock⁽⁷⁸⁾)

a.



Shown in figure a are four types of right-hand side-arm controllers used in sustained acceleration studies on the human centrifuge. Under acceleration, each controller responds differently, and piloting performance is consequently influenced by both the type of control stick and the type of acceleration forces that are applied. Figure b illustrates that the mean tracking efficiency scores obtained by pilots using these controllers were influenced by the type of controller, the amount of damping and cross coupling, and the acceleration vector.

b.

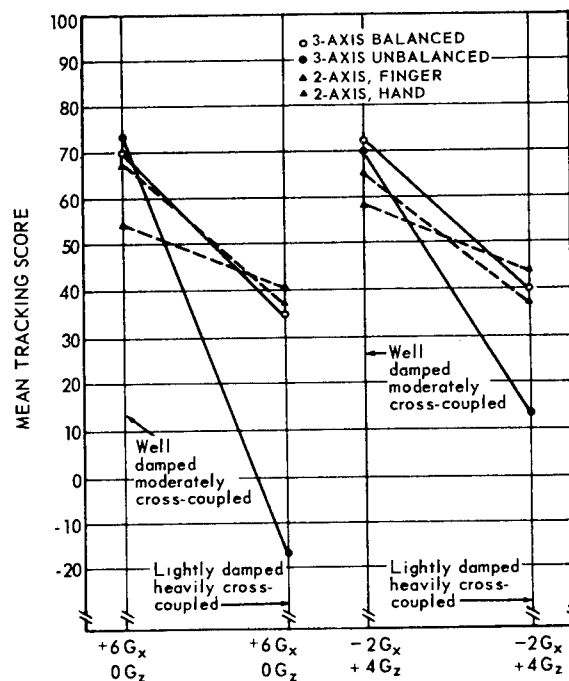


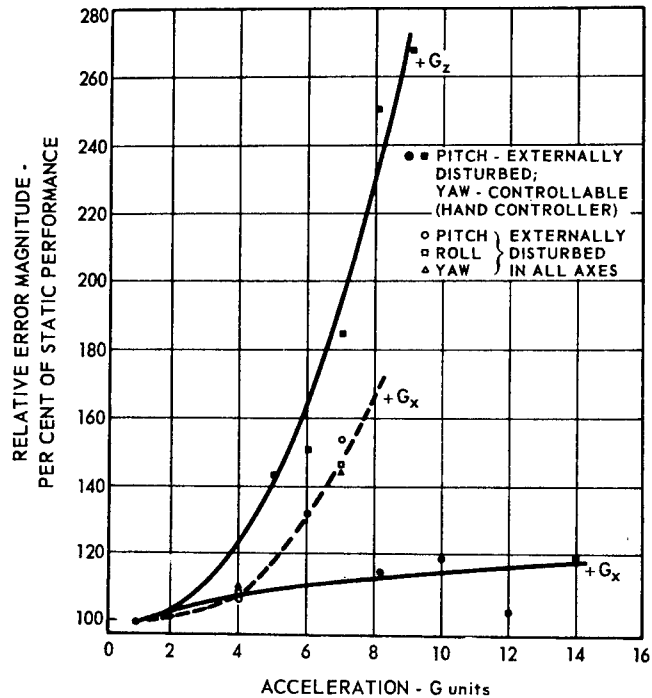
Figure 7-29

Effect of G Vector on Piloting Performance

a. G Vectors and Error Performance with Two Axis Hand Controller.

Performance of two separate piloting tasks is shown, plotted as functions of the magnitude and vector of acceleration exposure. The solid points represent a replotting of data from experiments by Creer et al. in which experienced pilots used a two-axis hand controller and performed a task in which programmed disturbances were introduced into the pitch axis only, but in which yaw error introduced by the pilot also contributed to the overall piloting task. The open points represent unpublished data from experiments at the USN Aviation Medical Acceleration Laboratory in which disturbances were introduced into all three axes by the computer, and compensatory control was effected by the pilots through a three-axis fingertip controller. It is apparent from this graph that changing the piloting task has an effect almost as great as that accompanying a change in acceleration vector.

(After Creer et al.⁽¹²⁵⁾, and USN Aviation Medical Acceleration Laboratory⁽⁴⁴⁶⁾)



b. The Effect of High Sustained Acceleration in +G_z and ± G_x on the Root-Mean-Square (RMS) Tracking Error

(After Creer⁽¹²³⁾)

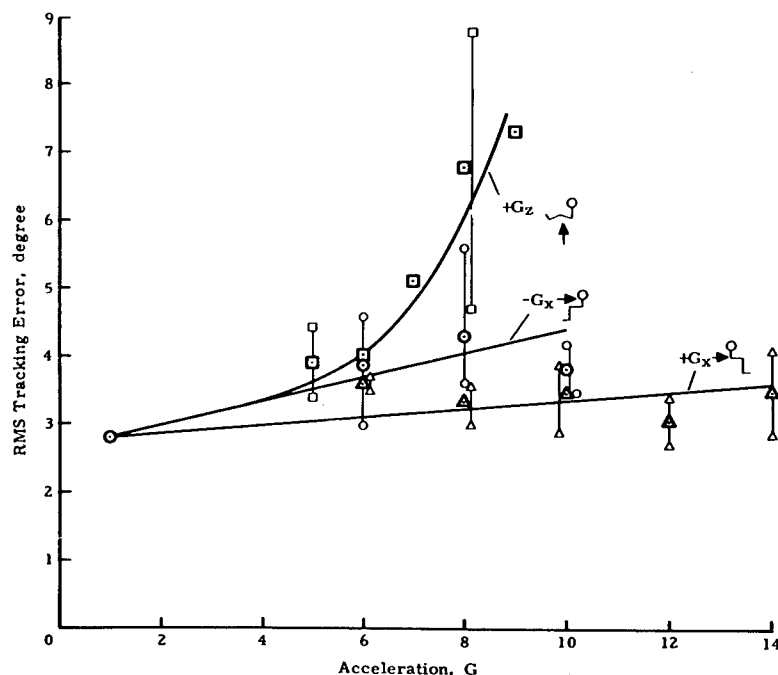


Figure 7-30

Tracking During Transverse Acceleration

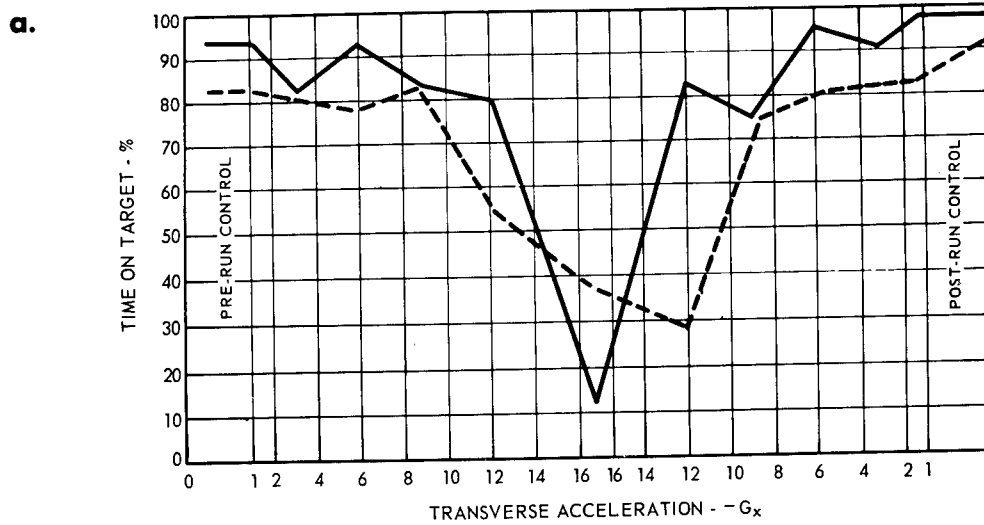
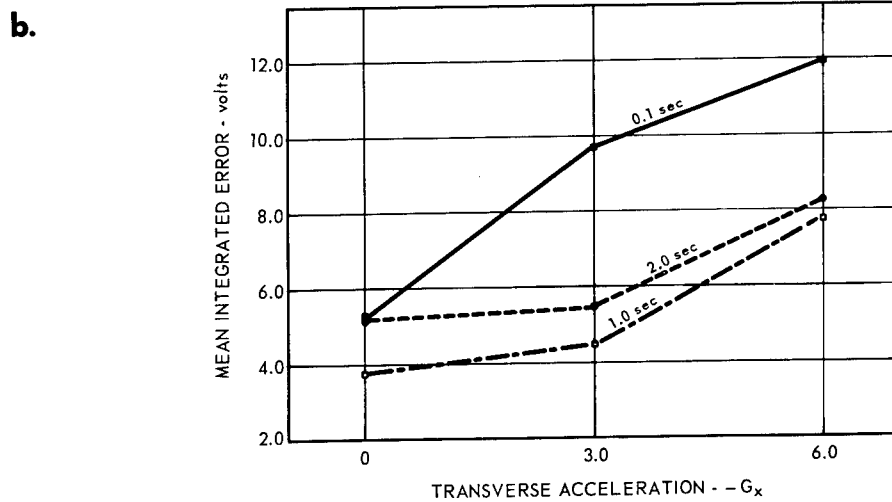


Figure a shows the decrement in tracking performance, using a 3.5 mm target in a dual pursuit task, for two subjects through a -16 G_x acceleration profile simulating re-entry.

(After Clarke et al⁽⁹⁹⁾)



Mean integrated error for tracking a display varying in the x-axis is shown as a function of increased acceleration and various time-lag constants. Notice that error is caused by both changing time-lag constants and acceleration.

(After Kaehler⁽³²⁹⁾)

to control moderate-frequency commands (1/2 cycles/sec or higher), or poorly damped, moderate-frequency, vehicle motions at high sustained accelerations (515).

The effect of takeoff and reentry profiles with G loads rising to transient peaks must also be considered as in Figure 7-30. The curves of Figure 7-31 compare the effects of rising G loads on a task representing control of an undamped vehicle by three-axis proportional control during a rise time of 15 seconds to various peak accelerations, each of which was maintained for 125 seconds. The results indicate the advantage of $+G_x$ in these conditions.

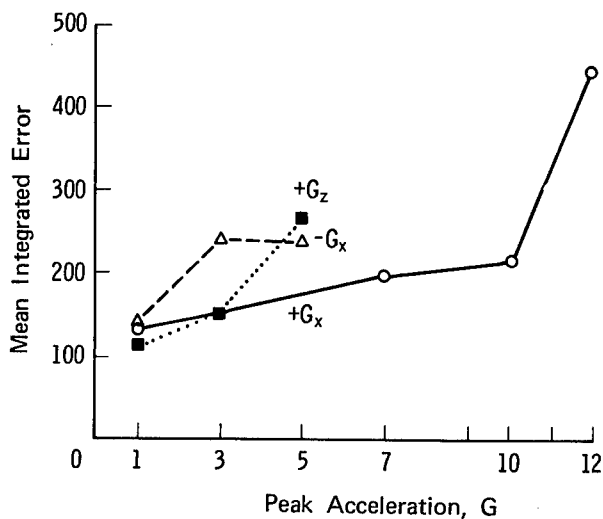


Figure 7-31

Comparison of the Effects of G Vector During Rise and Peak of Acceleration Upon Pilot Error of 12 Test Pilots in a Three-axis, Rate-damping Task.

(After Chambers and Nelson⁽⁸⁰⁾)

When pilots were exposed to a staging type of acceleration, characteristic of a two-stage and a four-stage launch vehicle with arrangement of controls so that pitch requires almost continuous control whereas yaw requires monitoring and occasional correction, little impairment is found up to the $7G_x$ limit, but the subjects observed that under acceleration they could concentrate on only a portion of the task requirements at a time. It should be remembered, however, that while a centrifuge can simulate an acceleration field, the motions through which it goes to achieve this are unlike those of an aircraft or spacecraft and may modify a performance response.

Training and Simulation

Simulation of specific space missions for training and systems design purposes also provides opportunity for performance study (76). Within the capacity of the simulator and the accuracy of the theoretical parameters of the mission, this can give a fair indication of the subject's ability to perform a specific mission, while at the same time provides an outstanding degree of training. Controls and displays, couches, space suits, and restraint systems can be tested and design changes made if astronaut performance is below the standard required for mission success under normal and emergency profiles.

In 12 simulated Mercury missions, 8 of which included centrifuge simulation of vehicle dynamics along with various other Mercury parameters, three general effects were noted in the course of this program:

1. Acceleration resulted in the insertion into the system of inadvertent control inputs. Such inadvertent inputs may be associated with excessive fuel utilization.
2. Acceleration generally disrupted the timing and precision of pilot control, although it would appear that the disruption which occurred, while obvious on the recording instruments, was not great enough to have a critical effect on the final adequacy of the performance.
3. Discrete task functions, such as an operation override, were affected by accelerations which preceded and/or followed them, though the operations themselves were performed under minimal acceleration loads.

In the Gemini program, launch profiles were prepared on magnetic tape for computer control of the centrifuge (76). In addition to normal launch and reentry profiles, zero lift reentry, fuel and engine failure aborts, premature ignitions and guidance system failure were simulated.

In a study of oxygen saturations during Apollo type profiles, a performance task simulating control of a vehicle during the acceleration phases of its mission was presented using a three-axis wrist controller and an "eight-ball" type of display (8). Error in three planes was integrated over time. Significant decrement in performance occurred during the simulated missions but it was not possible to say how much of the decrement was associated with the desaturation and how much was due to the acceleration per se.

During hundreds of acceleration tests conducted on astronauts, test pilots, and other subjects, specific characteristics of impaired piloting performance have been observed under high G_x . The following defects are taken directly from an excellent summary of the findings (76):

1. Increase in error amplitude as G duration and amplitude increases. Error amplitude is used most frequently as an indicator of performance. The vast majority of research on human behavior under acceleration has been done on tracking error amplitude scores. These scores are concerned with the difference between the obtained response and the desired response. Assuming that the subject can perform the task satisfactorily during static tests, any large tracking errors obtained during acceleration may be attributed to the stress.
2. Lapses or increasing unevenness and irregularity of performing the task. From time to time, the subject's performance may falter or may even stop temporarily. The subject is unable to maintain his performance at a consistently high level of proficiency. These may be called lapses, or expressions of increasing irregularity,

and they usually increase in frequency and duration as the adversity of the acceleration stress is increased. Lapsing is characterized by a very high level or almost perfect performance for a period of time and then the occurrence of relatively large errors. Following this brief lapse, performance again returns to normal, only to be followed by another lapse.

3. Performance oscillations.
4. Falling off or reduction in proficiency on some parts of a task while maintaining proficiency on other parts. Cessation of performance may occur on some parts of the task.
5. Changes in phasing and/or timing task components.
6. Reduction or cessation in performance output of some task components.
7. Inadvertent control inputs.
8. Failure to detect and respond to changes in the stimulus field. This occurs particularly often when the G force is from head-to-foot and blackout or grayout results. In such cases, the peripheral vision fails and responses to lights or other stimuli on the periphery also fail. This same failure to note changes in the visual field also becomes a leading factor when the array of dials and meters (containing both primary and secondary instruments) face the subject. Under acceleration attention tends to be focused on the primary instruments, and changes in secondary instruments may not be detected.
9. Errors in retrieving, integrating, storing and processing information.
10. Changes in the rate of performance or the sudden initiation of performance components non-essential to the task. In one particular example, subjects were required to press a button at least once per second while performing a tracking task under acceleration reaching $+10G_x$. One subject's rate of pressing tended to increase with acceleration until a final upper limit of nearly 250 responses per minute was reached. This contrasted sharply with the tendency of some other subjects to hold the response button in the depressed position during peak exposure.
11. Response lags and errors in timing. Increases in latency of response to discrimination stimuli. Also, there may be large changes in timing of component response sequences, or gross misjudgments of the passage of time.
12. Overcontrolling or undercontrolling, as during a transition phase.

13. Omission of portions of simple tasks, or of parts of complex perceptual motor tasks. These occur especially during overload when the subject may not process all of the stimulus information, such as the inputs necessary to perform the secondary parts of the task at the originally achieved level of proficiency.
14. Approximations. The pilot's behavior becomes less accurate, although the task does not increase in difficulty level. His responses become less precise, but minimally adequate to meet the required criterion of proficiency.
15. Stereotyping of responses and movements regardless of the stimulus situation. All of the stimuli appear to have an apparent equivalence to the subject during prolonged stress, for example. Inadvertent control inputs continue to be one of the most frequently encountered types of performance error during centrifuge simulations of spacecraft. These may be described as the insertion, by the astronaut of specific control inputs which are not intentional and of which he is unaware.

Performance during accelerative phases of the Mercury and Gemini flight programs was continually modified by changing stresses of other types such as vibration, anxiety, etc. Only general statements of performance adequacy by the astronauts are available. A summary of visual performance under these liftoff and reentry stresses is found on pages 2-72 and 2-73 of the Light Environment (No. 2). Mercury and Gemini programs attest to the fact that man can perform adequately under the conditions of sustained acceleration found during launch and reentry and indicate the likelihood of equally adequate performance in similar stressful conditions. Proposed acceleration profiles for nominal and abort modes of future missions to lunar and planetary surfaces are available (124, 371, 415, 527, 557, 691). Preliminary data are available on profiles for personal escape capsules (411).

ROTARY ACCELERATION

$\pm \dot{R}_y$ Tumbling

Tumbling (\dot{R}_y) became a problem with the development of aircraft ejection seats in jet aircraft. In the ejection situation, as in most operational situations, the problem is more than one of simple tumbling, since the tumbling takes place in a decelerative field which may, for a short time, be as high as 50G. In a space vehicle in a gravity-free state, however, simple tumbling could be a real problem, particularly if the reaction control system should fail after a spin had been imparted. Rotational accelerations have been initiated by faulty reaction controls as in Gemini VIII where $\pm \dot{R}_x$ tumbling was experienced (255).

In tumbling, the center of rotation is critical. A centrifugal force directed away from the heart produces an increment of pressure in both the venous and

arterial sides of the circulatory system. Flow would continue unabated were it not for the highly distensible venous bed. When pooling in this bed is sufficient, the return of blood to the heart will be inadequate and cardiac output will fall. If this fall produces a pressure drop in the cerebral circulation greater than the increase in hydrostatic pressure, cerebral hypoxia will ensue. When the center of rotation is moved caudad (footward), the hydrostatic column to the foot is shortened and a lesser degree of pooling can be expected. Conversely, of course, the negative acceleration ($-G_z$) effects on the cerebral circulation can be expected to increase. Movement of the center of rotation cephalad (headward) will increase the positive acceleration ($+G_z$) effects. Thus, the final effects are governed both by the rate of rotation and the position of the center of rotation.

Subjectively, vertigo ceases after the rotation reaches constant speed, provided the head is not moved. With center of rotation at the heart, 60 rpm is tolerable and even pleasant. Negative acceleration ($-G_z$) symptoms are manifest at 80 rpm and are tolerable at 125 rpm for only a few seconds. The effects of positive acceleration ($+G_x$) namely, numbness and pressure in the legs, develop slowly, but pain is evident at 90 rpm. No confusion or incipient loss of consciousness is observed, but in some subjects slight spatial disorientation, headache, nausea, or mental depression are noted for several minutes after the run. Repeated runs appear to increase the incidence of postrun nausea, headache, and depression. With the center of rotation at the level of the iliac crest, the symptoms more closely resemble those of negative acceleration ($-G_z$), with very unpleasant head pressure at 70 rpm. At higher rotation rates, 85 to 90 rpm, the head symptoms approach intolerability, although positive acceleration ($+G_z$) symptoms are unnoticed.

Since the hydrostatic pressure increases as the square of the distance from the center of rotation, the blood pressure response is complicated. The pressures in the arterial and venous side of the vascular tree and cardiac reflexes have been studied in animals (158, 657). Respiratory responses are complicated by the fact that the viscera and the diaphragm move downward with the radial acceleration and may stimulate stretch receptors in the lungs, with consequent inhibition of the inspiratory center. A similar apnea may be observed at high $+G_z$ levels.

Circulatory effects in humans spun about a center of rotation through the heart are illustrated in Figure 7-32a. It can be seen that the respiration is relatively unchanged.

With the center of rotation at the level of the iliac crest, physiological responses are seen in Figure 7-32b. Using an extrapolation from the data for dogs, and taking into account the difference in pressures introduced by different lengths of hydrostatic column in man and dog, it has been concluded that unconsciousness from circulatory effects alone would occur in man after 3 to 10 seconds at 160 rpm with the center of rotation at the heart, and at 180 rpm with the center of rotation at the iliac crest (658). Conjunctival petechiae occurred during exposures varying from 3 seconds at 90 rpm to 2 minutes at 50 rpm. Petechiae were also found on the dorsum of the foot of subjects who did not wear shoes. Physiological studies at lower spin rates in humans are under way (507).

Figure 7-32

Physiological Effects of Spinning a Human About a Center of Rotation Through the Heart
(After Weiss et al⁽⁶⁵⁸⁾)

a. Resources at 106 rpm.

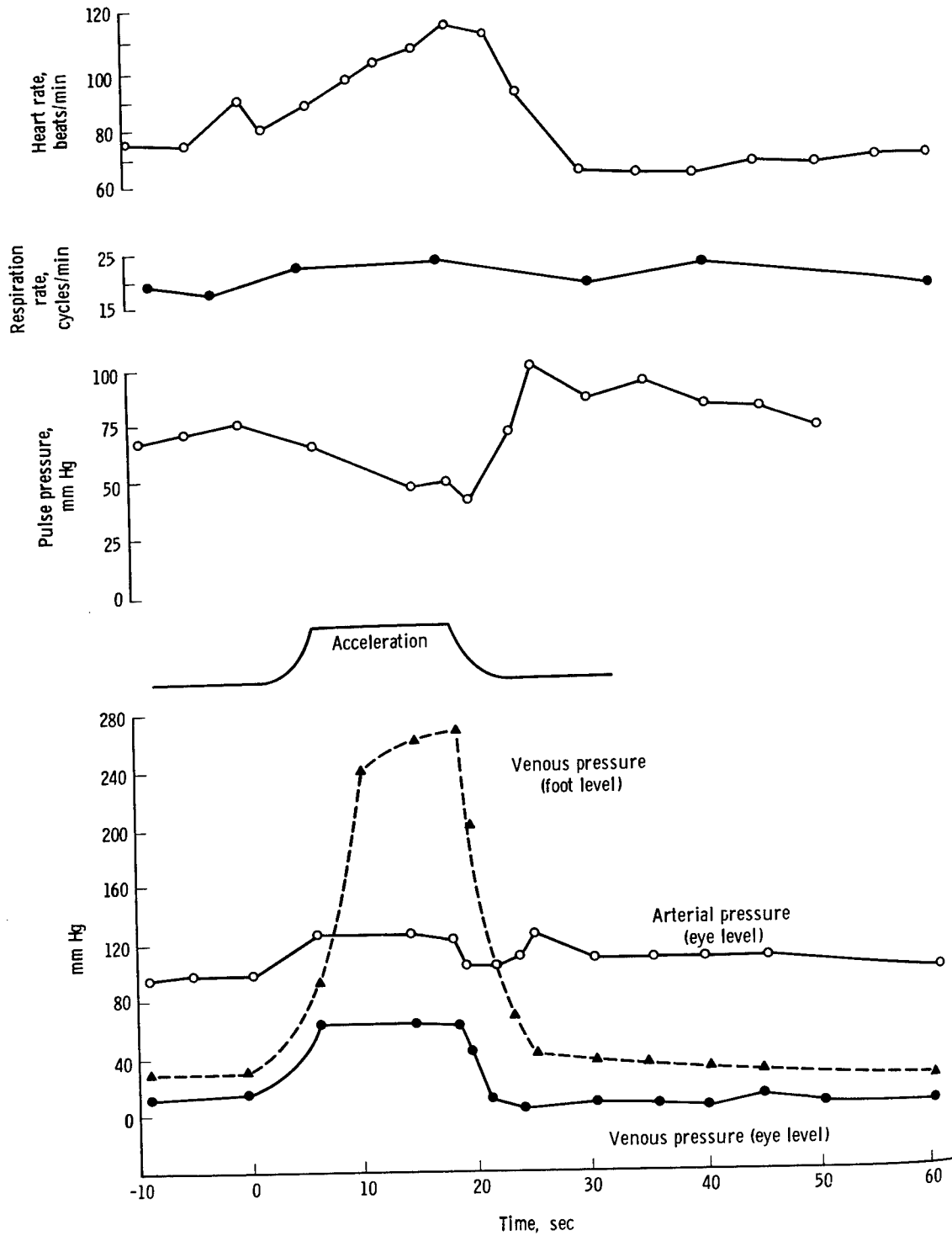
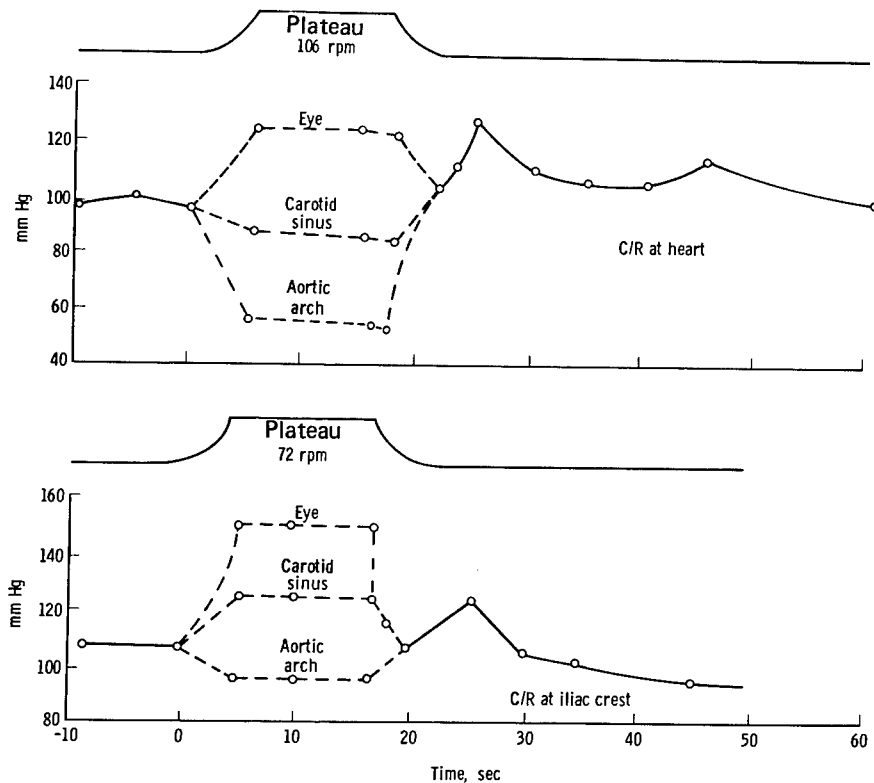


Figure 7-32 (continued)

b. Mean Arterial Pressures at Various Points with C/R at Heart and Iliac Crest



Combined \dot{R}_y and Linear Acceleration

When an acceleration field is added to tumbling, as in ejection, the response is different. It is not merely the summation of deceleration responses and tumbling responses, but, at least at rates of rotation below 100 rpm, the influence of the deceleration field appears paramount, though adequate quantification of this fact is lacking in studies on humans. Thus, when the rotation is in the pitch or yaw plane, the effect resembles severe sinusoidal vibration because of the repetitive oscillatory exposure to positive and negative acceleration (see Vibration, No. 8). Depending on the impedance and resonance of the body and organs, shear strains will occur and damage may result.

Postmortem studies of animals exposed to variable accelerations up to 35 G and rotations of 30 to 150 rpm in different attitudes show, 1 to 6 hours after exposure, tissue damage in the internal organs of all the animals, manifested by vascular congestion, edema, hemorrhage, formation of hyaline thrombi and separation of parenchymal liver cells (378).

Very little is known about the upper limits of human tolerance to simple tumbling or tumbling in a decelerative field. Most of the studies have involved animals. A summary of tolerance of humans to (\dot{R}_y) tumbling with no super-imposed linear deceleration is shown in Figure 7-33. It is probable, however,

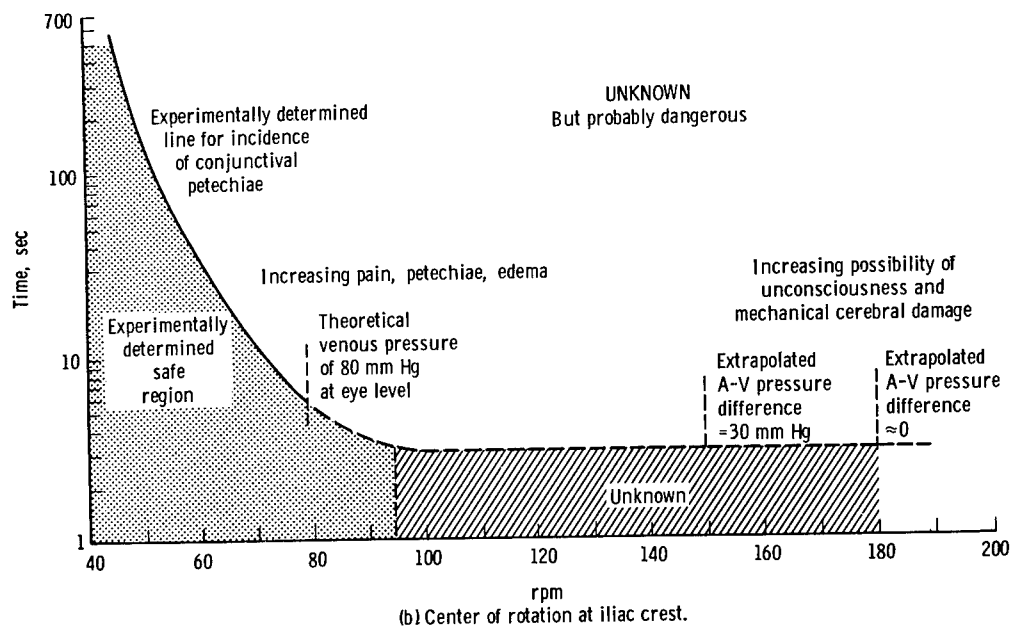
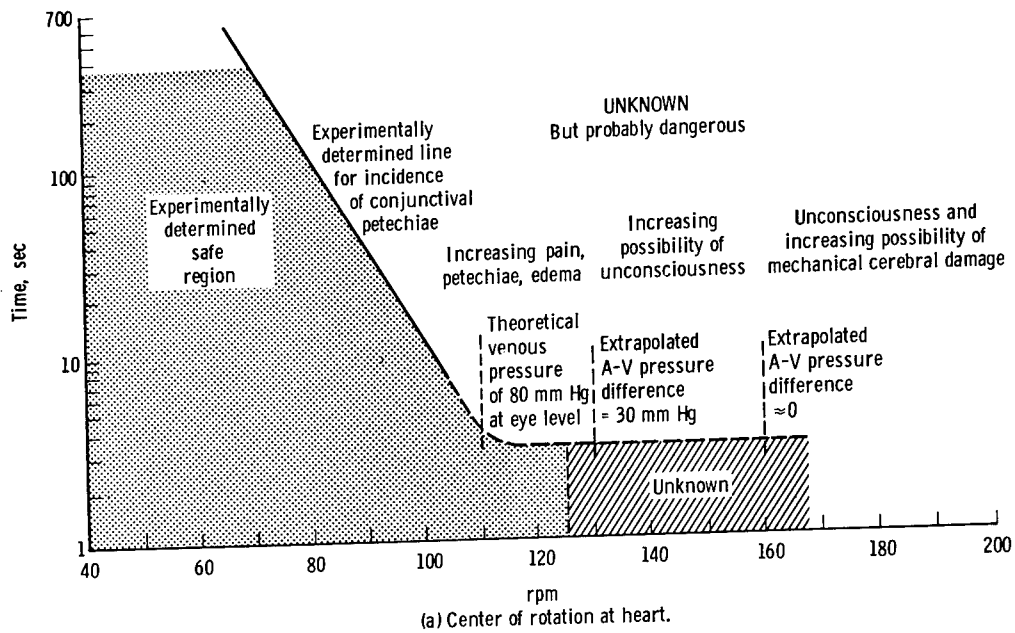


Figure 7-33

Human Tolerance to Simple Tumbling (No Superimposed Deceleration)

(After Edelberg⁽¹⁵⁷⁾)

that these limits err on the low side, and that work with an epicyclic centrifuge would provide more definitive data and show an increased threshold.

Extrapolation of animal data on combined linear deceleration and \dot{R}_y tumbling to humans is not clear (27, 157). At 200 rpm in simple tumbling, or at -10G_z negative acceleration, engorgement of tissues and vascular rupture may occur in animals, but when the two are combined these effects do not occur, nor do blood pressures attain the theoretical maximum expected from the hydrostatic pressures developed. The relative movement of human organs with respect to fixed structures depends on the natural frequency of the organ and the nature of the linear and sinusoidal forces being applied. Employing crude scaling factors, the curves of Figure 7-34 for human tolerance have been extrapolated from monkey to man. Study of dogs and accidental ejections of humans suggests that the combined accelerations are no more dangerous than the tumbling component when the linear deceleration is less than 15G. A large family of curves covering decay of linear acceleration from different peaks is required.

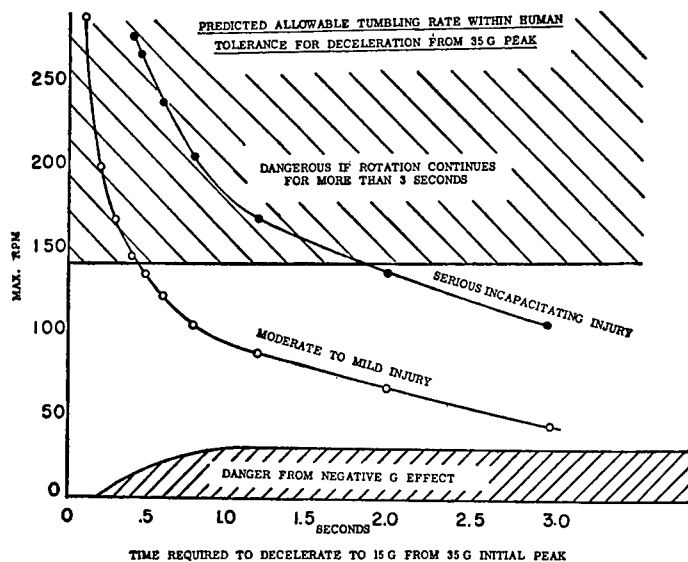


Figure 7-34

A Crude Estimate of Human Tolerance to Constant Rate of Tumbling in a G Field Decaying from 35 to 15 G.

(After Edelberg, in Gauer and Zuidema⁽¹⁵⁷⁾)

$\pm \dot{R}_x$ Spin

Very little is known about (\dot{R}_x) spin. It is assumed that the cardiovascular responses will be similar to those of \dot{R}_y tumbling with the axis passing through the same point along the longitudinal axis of the body. Current studies are in progress in this area (507).

A mixed \dot{R}_x and \dot{R}_z maneuver occurred accidentally in the Gemini VIII flight (255). Within a few minutes following the docking, the GT-8 Orbit Attitude and Maneuver System (OAMS) engine No. 8 initiated, without command, a series of sustained firing periods of varying lengths. These energy impulses caused the two joined vehicles to begin a lengthy period of uncontrolled maneuvering, predominantly in the roll mode. The firing of only one of the eight OAMS Yaw/Roll engines, as occurred in the accident, results in a combined

yaw/roll maneuver by the spacecraft. It is necessary to fire engines No. 7 and No. 8 to produce a pure yaw maneuver, and likewise, both engines No. 4 and No. 8 are required for a pure roll. Therefore, the spacecraft underwent a mixed yaw/roll maneuver (actually tumbled) during the firing of only engine No. 8. The maximum roll rate of 330-340° per second did not exist for more than 1 minute 9 seconds. The astronauts attempted almost immediately to stop the motion and decouple the two vehicles. However, due to disorientation resulting from vestibulo-ocular disturbance, their efforts to regain stability were seriously impaired. Armstrong's pulse reached 156 and performance was degraded. The effect of R_x on performance is covered on pages 7-63 & 64.

$\pm R_z$ Yaw Spin

Rotation of the seated subject in the vertical or Z axis (\dot{R}_z) is seen in relatively pure form in certain drogue chute stabilized ejection systems and is present more frequently as a component of more complex multi-axis rotation. Respiratory and cardiovascular effects concurrent with or secondary to labyrinthine stimulation, both caloric and rotational have been noted and studied (300,493). The effects noted have been inconsistent, small, and of transient nature, however, with rather low levels of angular acceleration and steady state velocity. The nausea, pallor and sweating of a subject exposed to severe angular acceleration are well known and emphasize potential autonomic reflexes. (See below.)

Less well studied than the reflex effects of angular acceleration is the potential cardiovascular stress resulting from the centripetal acceleration. At rotational speeds of 120 revolutions per minute, a considerable inertial force hindering venous return is present at hand or foot level. At high rotational speeds, this cardiovascular effect becomes the dominant factor affecting tolerance. Four rotational profiles have been studied combining two rates of angular acceleration (0.1 and 0.8 radians per second) and two maximum rotational speeds (60 and 120 rpm) (615). There was a three-minute plateau at peak velocity. Centripetal acceleration at hand/foot radius (0.5 meters) was 1.8 and 7.2 G at 60 and 120 rpm, respectively. Rotation at 60 rpm represented no significant stress. Three minute 120 rpm runs, however, caused progressive tachycardia; narrowing of pulse pressure; a drop in mean arterial pressure; petechiae, fullness and observed hyperemia of the hands; and decreased venous pressure - all pointing to peripheral pooling of blood with decreased central venous return. The rather striking overshoot of pressure seen during the rapid offset from 120 rpm further supports the concept of peripheral pooling. In the absence of a decrease in heart rate, the overshoot or pressure points to either a sudden increase in cardiac output or to a sudden increase in vasoconstriction. The increasing pulse pressure contrasting with the immediately preceding pattern of narrow pulse pressure and low arterial pressure suggests an increase in cardiac output secondary to a sudden increase in venous return. Tolerance to high R_z is probably limited by the ability of the circulation to maintain venous return.

Data are available on the personal opinions of pilots exposed to piloting tasks within combined G fields, obtained by adding angular acceleration from the motion and positions of two gimbals on the Johnsville centrifuge to the radial acceleration of the centrifuge arm (73).

Performance During Rotary Acceleration

With the high potential for multiaxial rotation during spacecraft control emergencies, it is important to know the range of conditions in which the pilot can be relied upon to exercise judgment and to maintain coordination of his faculties sufficiently to perform complex functions. Performance during tumbling has been studied by presenting visual and auditory signals which required a press-button response (658). No errors were observed up to 100 rpm with center of rotation at heart level, and no increase in reaction time was noted. In another test of motor performance the subject was required to simulate a manual ejection sequence. A very slight increase in reaction time was noted. In a rotary field of changing rate, however, the subjects had difficulty in locating a toggle switch so placed that it could not be seen.

Using the NASA Multi-Axis Test Facility, trained pilots exposed to complex rotations producing a resultant of up to 70 rpm have been tested for their ability to counteract the induced rotation by activating jet nozzles (617). Up to the limits studied, the pilots were able to perform their task with an error ranging from 6.5% to 18%, depending on the training and skill of the individual. Within the range measured, the rate of rotation did not affect performance. In this test, however, error was evaluated as the percentage of the total time the subject made an incorrect input, but the error score did not account for errors of omission. Repeated operation of a similar type rotational test showed that pilots were able to reduce their errors appreciably and improve technique by introducing several corrections simultaneously.

Although motion sickness would be expected to be encountered relatively infrequently with experienced pilots, intermittent rotation at rates of 50 rpm or greater for periods longer than 1 hour could induce motion sickness symptoms. Vestibular nystagmus can be encountered by all subjects tested when the acceleration is endured for at least ten seconds. However, if the subject concentrates on a centralized area of his instrument panel, the effects are reduced.

There has been no recorded simulation of \dot{R}_x spin during weightlessness. During the mixed \dot{R}_x and \dot{R}_z maneuver, in Gemini VIII, there appeared to be a decrease in performance proficiency (255). During \dot{R}_z spin, only the horizontal canal is stimulated. Laboratory studies have shown that, under various angular velocities as high as 60° per second, the roll and pitch motions produce a considerably greater rate of development of error in response to rotational stimuli than are exhibited by rotating in yaw motion (Reference 327 and Table 7-57). Even though two pairs of semicircular canals are stimulated in both roll and pitch (thereby making these two maneuvers more severe than yawing), pitch motion is not considered to be

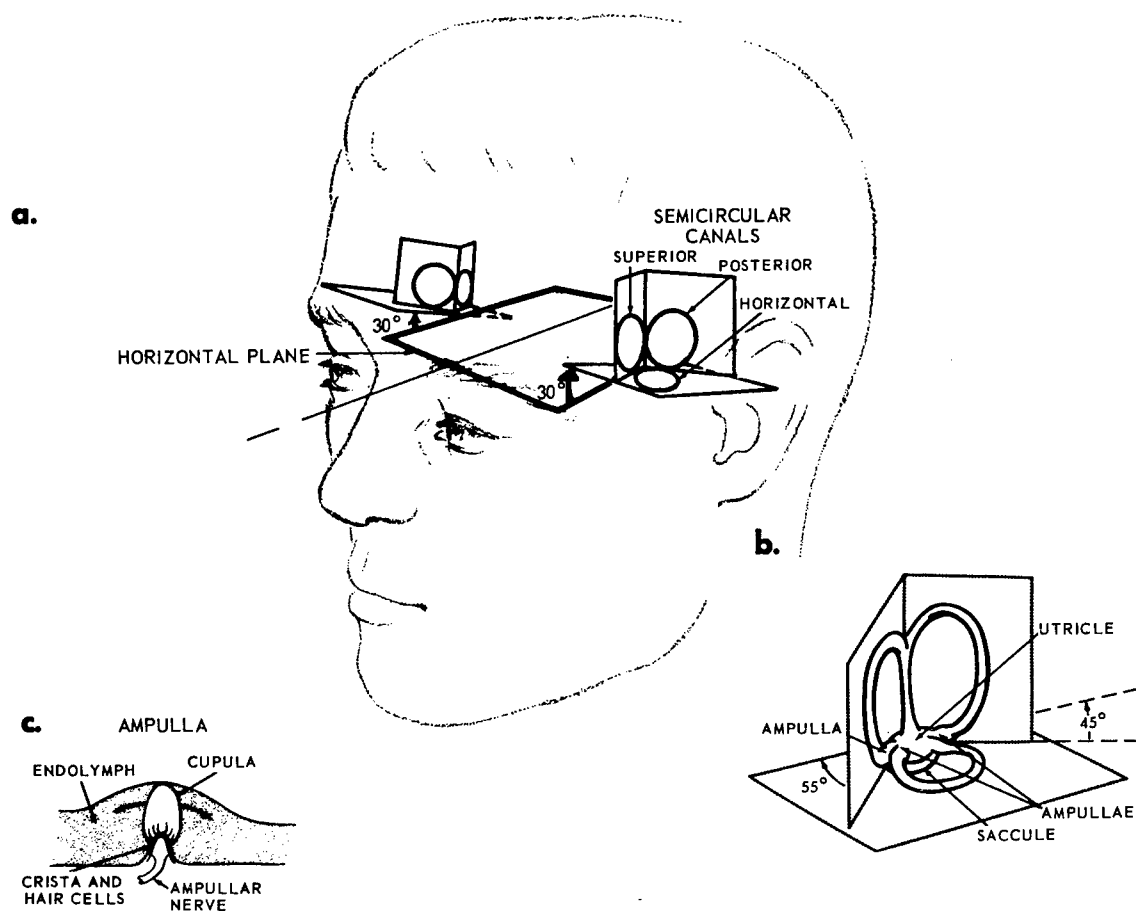
as deleterious to human behavior as rolling. The greatest physiological penalty is attached to rotational movement of the skull in its roll plane (326). As further proof that roll maneuvers are more severe than either yaw or pitch motion, optokinetic "following," i.e., tracking and focusing of the eye while the skull is in motion, has been shown to be very much less effective in the roll plane than in yaw or pitch. Roll movements on earth are relatively rare and short, but in flight where they may be sustained, the vestibular drive is quickly lost. Because of the virtual absence of visual tracking in this plane, substantial image slip then ensues (323). The problem of "image slip" is compounded when the vestibular signal is incorrect, e.g., during recovery from a roll maneuver (at which time the vestibulo-ocular response is reversed), because eye movement in the roll plane follows the misleading vestibular signal. The time constant for the exponential cupular damping of the eye is generally agreed to be 16 seconds in the yaw plane. In the pitch and roll planes, the time constant drops to a third of that for yaw. This unequal relationship yields a vectorial error in orientation (62).

Significantly, astronaut Armstrong was quoted as having said in debriefing interviews that during the emergency of Gemini VIII he could not "see" the circuit breakers which controlled the malfunctioning OAMS rocket engine (255). These breakers were located above his eye level. Apparently in response to Armstrong's report, the circuit breakers were relocated on the instrument panel for Gemini IX and subsequent flights. Whether this problem was due to image slipping or Coriolis-induced nystagmus (resulting from head movement) has not been discussed in official NASA reports released to date. Nevertheless, impaired vision is to be expected during accelerated rolling. Several less-than-optimum decisions were made, one of which (firing engines in both of the redundant Reentry Control Systems) necessitated an immediate abort of the mission at an unfavorable landing site.

It would be of value to determine the performance on a timed basis with higher resultants, and to include an imposed acceleration field or zero gravity. Current studies on the USAF Rotational Flight Simulator include effect of prior water immersion (507).

Vestibular Interactions in the Rotary Environment

The vestibular apparatus of the inner ear is made up of three semi-circular canals and two membranous sacs, housing the utricle and saccule. These organs function as acceleration detectors; the semicircular canals operating as detectors for angular acceleration and the utricle and saccule, as detectors for linear acceleration (162, 207, 266, 416, 443, 661). Figure 7-35 represents the anatomical configuration of the apparatus and its geometric placement in the skull. The neural signals produced under vestibular stimulation are integrated in the brainstem with signals from proprioceptors reporting the relationships of position among limbs, trunk, and neck. There or at higher levels, signals from skin pressure receptors, visual system, and stored intellectual information are integrated to coordinate movements of the limbs, head, eyes and present the body with awareness of the spatial environment. The interactions of these various systems in man-vehicle control are diagrammed in Figure 7-36 (91, 532).



The vestibular apparatus consists of symmetrical halves, located within the temporal bone on opposite sides of the head, where each forms part of the inner ear (see Figure 9-2). Each of the functions it carries out has been identified with a particular substructure.

Horizontal, superior, and posterior semicircular canals sense angular acceleration about three mutually perpendicular axes. The positions of the planes determined by those axes, relative to the co-ordinate axes of the head, are shown in the diagram above, in which it is apparent that the left superior canal is coplanar with the right posterior, the right superior with the left posterior, and the left horizontal with the right horizontal. Flow of endolymph fluid in a canal is sensed at the ampulla, a swelling on the canal, within which swings the cupula, a "door" of sulphomucopoly-saccharide material approximately equal in density to endolymph. This is hinged at a mount of cells, the crista, within which two types of receptor cells initiate nerve impulses in the ampullar nerve in response to movements of the cupula. The resting rate of discharge in the majority of the nerve fibers increases with cupula movement in one direction, and decreases in the other.

The utricle contains otoliths of calcium carbonate (specific gravity = 2.94) suspended in a gelatinous layer upon hair cells of the macula. Linear accelerations result in a displacement of the denser otolith mass relative to the hair cells. The bed of the otoliths is roughly horizontal when the head is erect.

Structures of the saccule are similar to those of the utricle, except that its bed is roughly 30° from vertical when the head is erect.

Figure 7-35

Anatomy of the Vestibular Apparatus

(After Guedry and Crocker⁽²⁶⁶⁾, adapted from Gernandt⁽²⁰⁷⁾)

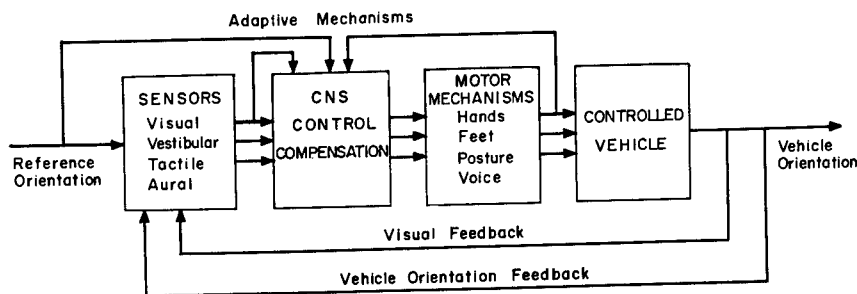


Figure 7-36
General Block Diagram of the Man-Vehicle Control Problem
(After Young and Li⁽⁶⁹³⁾)

The different nomenclatures suggested for providing separate mathematical identifications for vestibular acceleration stimuli and related vestibular responses which may act singly, simultaneously, or jointly in cross-coupled Coriolis configurations are summarized in Figures 7-1, 7-37, and 7-38. Figure 7-37 gives notation of instantaneous resultant kinematic vectors for linear and angular acceleration of the head along with the usual polarity conventions.

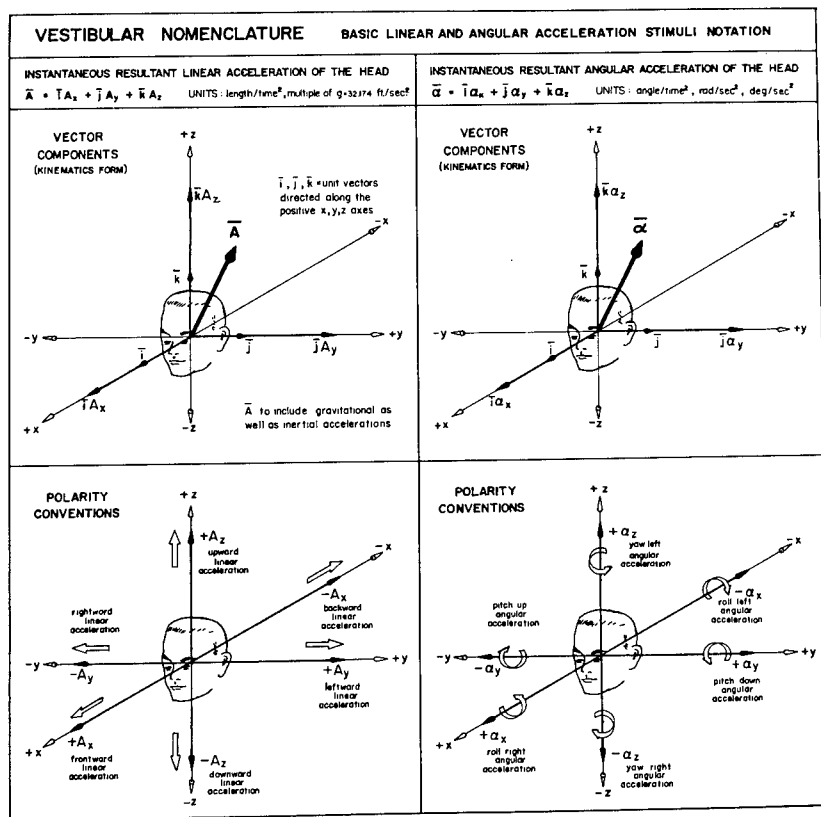


Figure 7-37
(After Hixson et al⁽³⁰²⁾)

Stimulation of the vestibular apparatus may produce abnormal responses under certain conditions. Studies have been performed on transient rotation and on prolonged rotation lasting several days. The most studied pair of canals is the horizontal, whose response to various patterns of acceleration is shown in Figure 7-38. The vertical canals appear to differ only quantitatively (327, 460). Position of the cupula can be inferred from measurements of movements of the eyes in a repeated flicking pattern known as nystagmus (258, 266, 268, 300, 301, 416). Angular velocity of the slow phase, computed by measuring the slope of oculographic tracings is related to cupula position. Subjective reactions, signalled continuously by movement of a control handle, or discretely by closing a switch, are a second output of information.

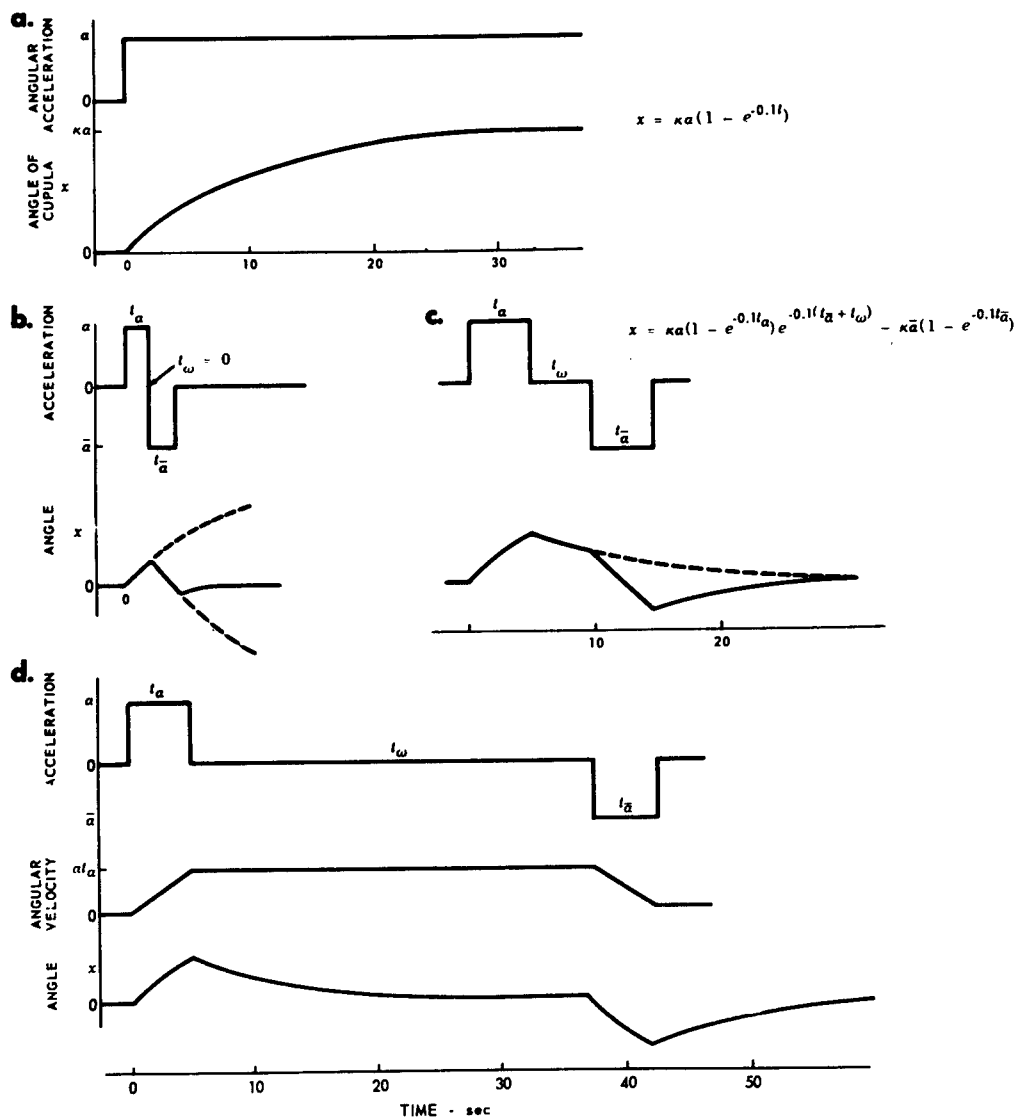
The relationship between an acceleration input and a subjective or nystagmus output show the effect of numerous other factors. The input acceleration may be so weak that time must elapse before the threshold of response is reached (Figures 7-39 and 7-40). Limits on displacement of the cupula plus nervous system adaptation may act to reduce output during prolonged acceleration (Figure 7-41). Mechanical response of the cupula may cause its position to lag an applied angular oscillation (Figure 7-42). Effects of an active visual presentation on thresholds of angular acceleration are under study (409). In all three pairs of semicircular canals, the displacement of the cupula can be approximated by a damped torsion pendulum model, described by a second order equation:

$$\frac{d^2x}{dt^2} + 2\zeta\omega_n \frac{dx}{dt} + \omega_n^2 x = \alpha(t) \quad (1)$$

Evidence that the equation is nonlinear is given for different values of angular acceleration (α) (300, 301). The frequency ω_n and possibly the damping coefficient ζ may be a function of cupula angle x and its derivatives.

The mechanics of the vestibular apparatus has received much sophisticated study from the point of view of its role in the feedback loop controlling postural control, motion, and sensory or spatial reference (119, 300, 301, 337, 389, 416, 417, 440, 694). The torsion-pendulum model of the horizontal canals and these differences in dynamics in some way can explain the subjective feeling in an aircraft that the instantaneous axis of rotation is different from that of the objective instantaneous axis of rotation. When data on the latency of sensation to constant angular acceleration around a vertical axis as a function of acceleration level is fitted with the exponential relation resulting from the torsion-pendulum equation, a long-time constant is obtained. The long-time constant for the sensation of rotation about the sagittal (roll) axis is approximately 7 seconds, compared to the 10-12 seconds found for the horizontal canals. The vertical canal threshold was found to be approximately 0.5 deg/sec² compared to approximately 0.14 deg/sec² for the horizontal plane (416).

Control system description of the linear accelerometer or gravoreceptor system of the utricle and saccule has lagged that of the semicircular canals (267). Figure 7-35 describes the utricular and saccular sensors. Recent



The response of the cupula to movements of the endolymph in the semicircular canal is analogous to that of a spring-mass system with viscous damping. Since the density of the cupula is close to that of endolymph, the inertial term in the resulting second-order equation is small relative to the damping term. Angular deflection of the cupula is described by solutions of the differential equation for particular patterns of acceleration, four of which are graphed above.

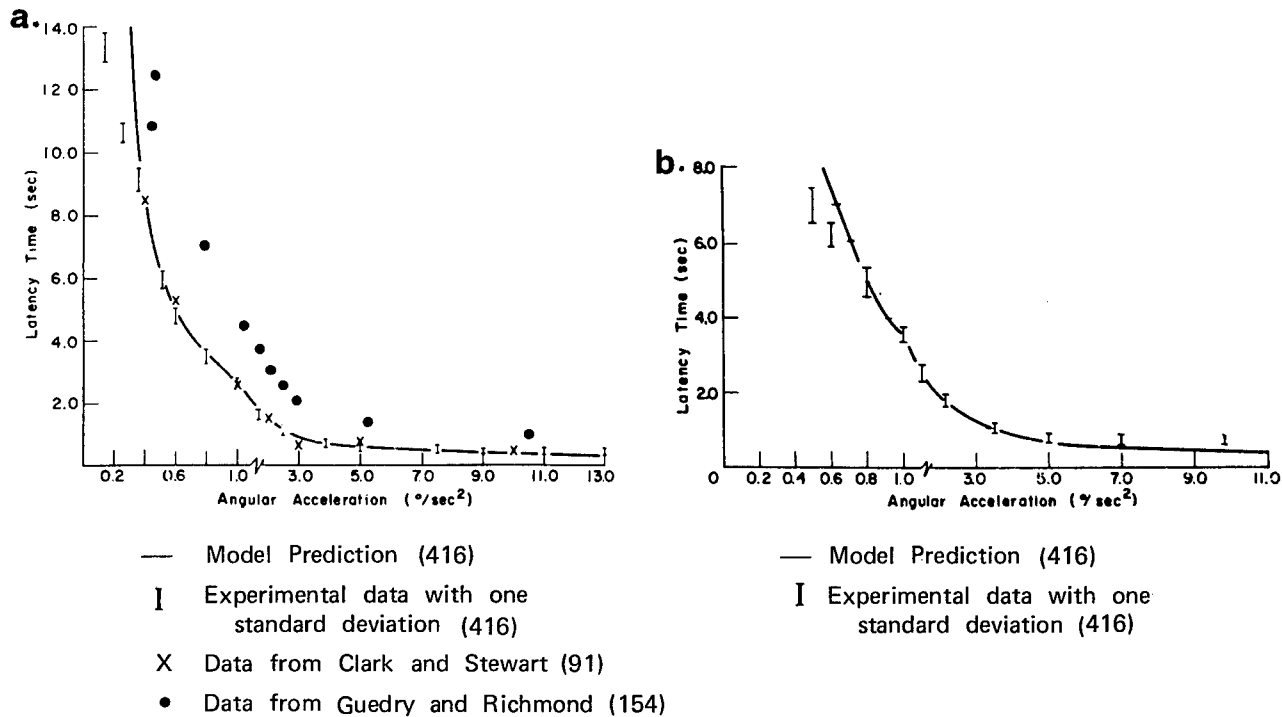
Figure 7-38

Dynamic Response to Angular Acceleration

(After Guedry and Crocker⁽²⁶⁶⁾, adapted from Guedry^(259, 262))

Figure 7-39

Threshold for Sensing Rotation About the Yaw (α_z or \dot{R}_z) and Roll (α_x or \dot{R}_x) Axes



a. Latency Times for Perception of Angular Acceleration About the Vertical Axis (Y_h)

Note scale change of angular acceleration

(Adapted from Meiry⁽⁴¹⁶⁾ and others noted.)

b. Latency Times for Perception of Angular Acceleration About the Roll Axis (X_h)

Note scale change of angular acceleration

(After Meiry⁽⁴¹⁶⁾)

It is usually assumed that a minimum cupula deflection, x_{\min} , must be exceeded for elicitation of vestibular reaction. When an angular acceleration, a , is suddenly applied, the time (t_{\min}) required for the cupula to deflect to the threshold value x_{\min} is a function of the applied acceleration; this time can be found by solving the differential equation of motion of the cupula.

The solution for a constant acceleration applied as a step function is the equation above.

The data points in Figures a and b are measurements of the time required by human subjects to sense and signal a response to low angular accelerations. They are directly predictive of the mean time elapsing between onset of an acceleration and motor response of an alerted individual, located close to the axis of rotation.

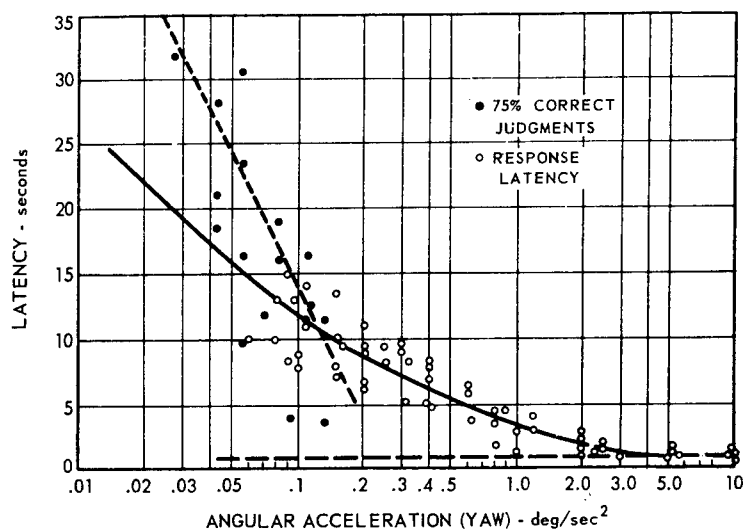
Because time for a decision and a motor output is included in the time to respond, these data cannot be used to find a_{\min} directly. However, analysis of the data on the assumption that the total decision and motor response time is a constant, on the order of 1 second yields an inferred value for threshold, a_{\min} , of 0.1 to 0.5 deg/sec², the least acceleration which, applied for an unlimited time, can be detected. Higher accelerations will be detected in less time, and combinations of time and acceleration lying in the quadrant above the curve will be detected with higher probability or by more of the population. Figure a shows variation in data for yaw axis or horizontal canals; the threshold of the latest model being 0.14 deg/sec². Figure b shows the threshold for the roll axis or vertical canals to be 0.5 deg/sec².

Figure 7-40

Perception of Angular Acceleration ($\pm\alpha_z$ or \dot{R}_z)

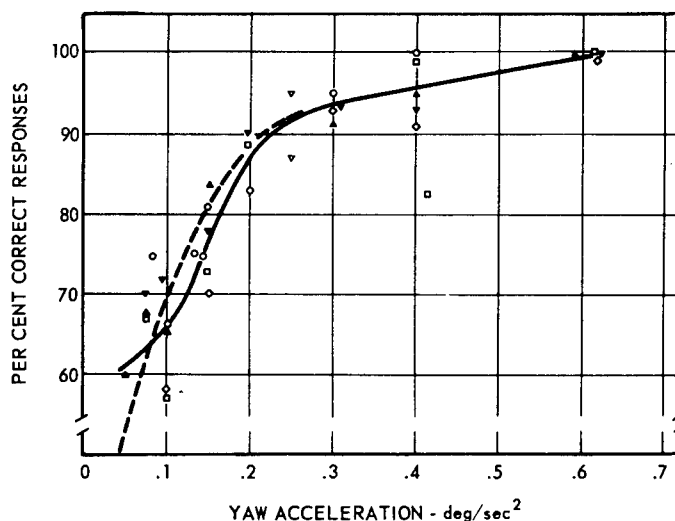
(After Chambers⁽⁷²⁾, adapted from Clark and Stewart⁽⁹¹⁾, and Mann and Ray⁽⁴⁰⁵⁾)

a.

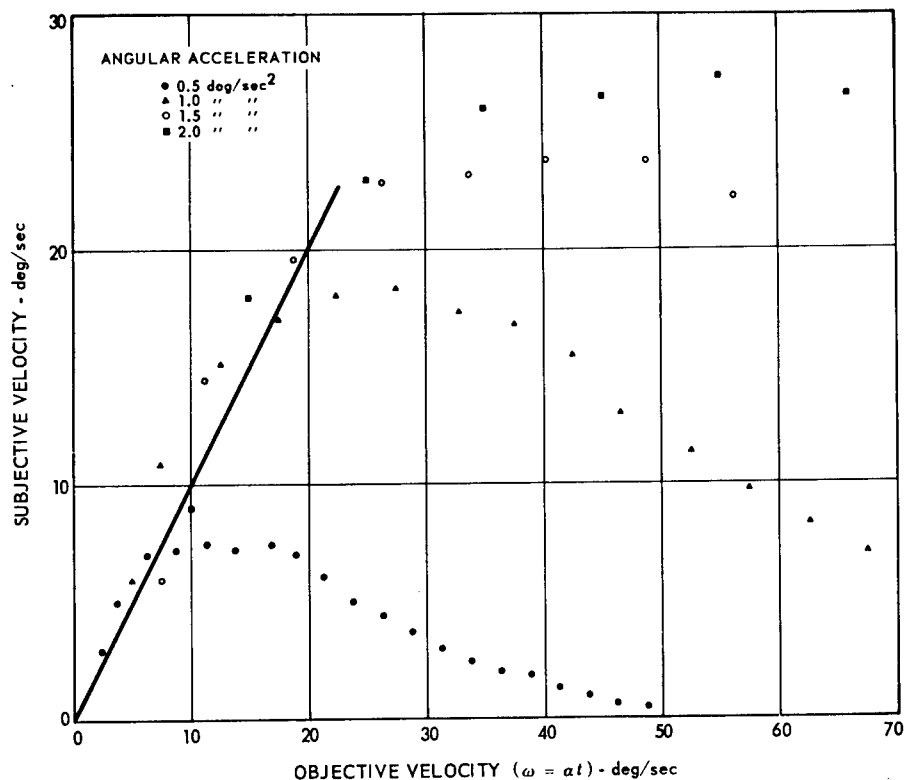


The times required to make judgments of the direction of rotation about the yaw axis are plotted as a function of the angular acceleration. The solid points indicate the time required to make judgments that are correct 75% of the time, as determined by Mann and Ray. The open points represent the time required to make judgments, whether the judgments are correct or not, and are redrawn from the data of Clark and Stewart.

b.



The per cent of direction-of-rotation judgments that are correct is plotted as a function of the level of angular acceleration. The 75% point is considered to be the threshold point. Also included are the 75% points from the data of Mann and Ray. (dashed line)



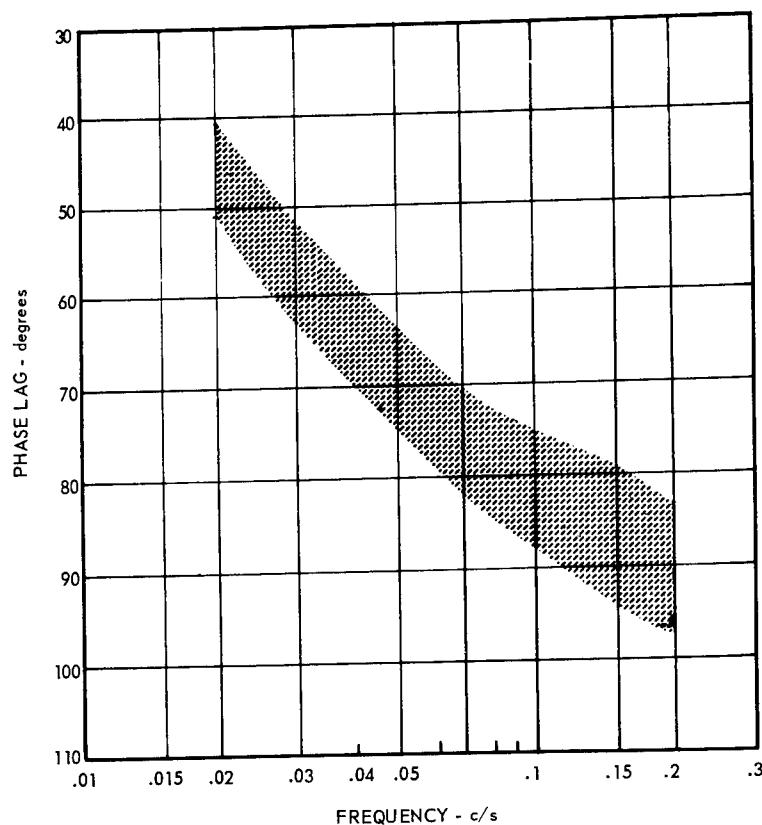
Points on this graph are values of angular velocity computed from subjects' reports of perceived 45° increments in displacement while subjected to constant angular acceleration on a turntable. Each point is the average of readings during four trials by each of ten subjects. A trial consisted of one acceleration and one deceleration, with sufficient time at constant velocity in between for sensations to decay. The average values mask a 25% decrease in response between the first and fourth trials, ascribed to habituation.

Note that subjective sensations fail to increase above a maximum level which is a function of the applied acceleration. Not immediately apparent is the fact that the time at which maximum subjective velocity occurs is the same for all levels of acceleration, and is approximately 30 seconds. According to the equation for the cupula (see 7-38), maximum deflection would be reached by that time. The fact that the response declines even while the cupula deflection is maintained must be attributed to adaptation, at the receptor or centrally, in the nervous system.

Figure 7-41

Perceived Vs. Actual Rotation

(After Guedry and Crocker⁽²⁶⁶⁾, adapted from Guedry and Ceran⁽²⁶⁴⁾)



The angle by which the reversal in nystagmus responses lags a sinusoidal angular acceleration stimulus is shown above as a function of frequency. The shaded region of the graph contains two standard deviations about the mean for six subjects experiencing a peak acceleration of 40 degrees per sec², at frequencies from 0.02 to 0.20 cycles/sec.

Phase lag is a function of stimulus magnitude as well as frequency, indicating the presence of non-linearities. At a peak acceleration of 10 deg/sec² and 0.02 cycles/sec it is between 10 and 20 degrees more than the values above; at 80 deg/sec² it may be less by 20 degrees.

The frequency response techniques used have proven to be sensitive to individual and left-right differences, and with them it has been possible to compute values of ζ and ω_n in the differential equation of motion of the cupula. The most interesting parameter is $2\zeta/\omega_n$, the ratio of damping to stiffness. Its value is a decreasing function of peak acceleration, evidence that the cupula stiffness increases with deflection.

In a subject with equilibrium difficulties, the value of $2\zeta/\omega_n$ for rightward acceleration of his head was measured to be only half that for leftward acceleration. Both values were lower than those of the normal subjects.

Figure 7-42

Phase Lag in Response to Angular Oscillation

(After Guedry and Crocker⁽²⁶⁶⁾, adapted from Niven and Hixson⁽³⁰²⁾, and Hixson and Niven⁽³⁰¹⁾)

studies have shed light on the nature of the transducer mechanism (165,316 , 389,662). The utricle appears to be a multidirectional sensor sensitive to specific force, and is stimulated by the shear acceleration in the plane of the otolith. Objective measurement of the sensitivity of the otolith organs have focused on the oculogravic illusion, the perceptual phenomenon of tilting surroundings one experiences when subjected to variations of the resultant force in his head axes system (52). Other sources of data are the human ability to locate the gravity vector when tilted in the frontal plane, and the objective measurements of compensatory counterrolling eye movements in response to alteration of the effective gravitational vector (283,524 , 643,680).

Static measurements of the subjective horizon for varying elevation of the head axes system (discrete rotations around the axis) render linear correlation of perception with the shear acceleration on the utricle (Figure 7-43). For an erect head, the shear on the macula is along an axis elevated

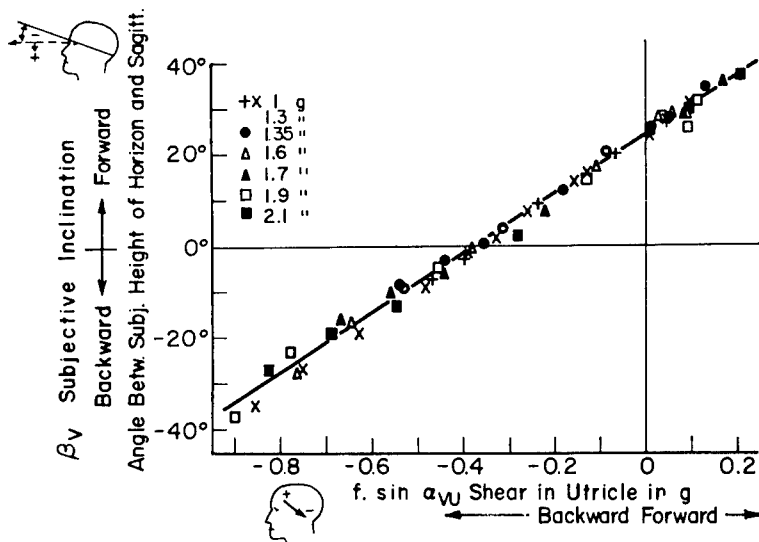


Figure 7-43

The Subjective Inclination (β_v)
Plotted as a Function of the
Shear Acceleration in the Plane
of the Utricle.

(After Schöne(524))

about 20° above the sagittal axis. Consequently the subjective horizon will correspond to the actual horizon for 0.4G backward shear acceleration on the otoliths. The measurements confirm the assumption that sensation is dependent upon the magnitude of the shear acceleration, since there is a linear relationship between shear and subjective perception. Experimentally this relationship is valid for $\pm 90^\circ$ of bending fore and aft. However, incomplete or rather erroneous spatial orientation is suggested by the slope of the line in Figure 7-43. Nevertheless, the sensor is responding to acceleration changes in the sagittal plane in agreement with its assumed characteristics.

Tilt in the frontal plane is associated with perception of the vertical when only gravity is present or perception of the resultant vector for exposure to gravity and linear accelerations. Psychophysical experiments show equal ability for reorientation without directional dependence (406). The observation confirms the expected symmetry of perception in the frontal plane, a feature

deduced on the basis of the structure of the utricle (416). The configuration produces shear acceleration components along two perpendicular directions. The resultant shear acceleration on the otoliths very closely obeys a $\cos^2\beta$ relation, where β is the angle of tilt. Counterrolling eye movements which rotate the eye in opposite direction to the body tilt show this relationship very closely (419).

Readjustments to the gravity vector are significantly more accurate immediately after the tilt compared to readings after 60 seconds of stay in tilted position (406). Moreover, the amount of adaptation in this experiment is of the order of 60 percent of the initial angle of tilt. These findings are supported independently by additional experiments which show the effect of angular rate upon readjustment but almost no influence of the period of exposure to the tilt if longer than 30 sec. (171).

The dynamic sensitivity of the horizontal system has been recently described in experiments establishing the phase relation between the subjective sensation of linear velocity and the objective linear velocity for sinusoidal linear oscillation (416). Figure 7-44 is a plot of subjective phase lag versus

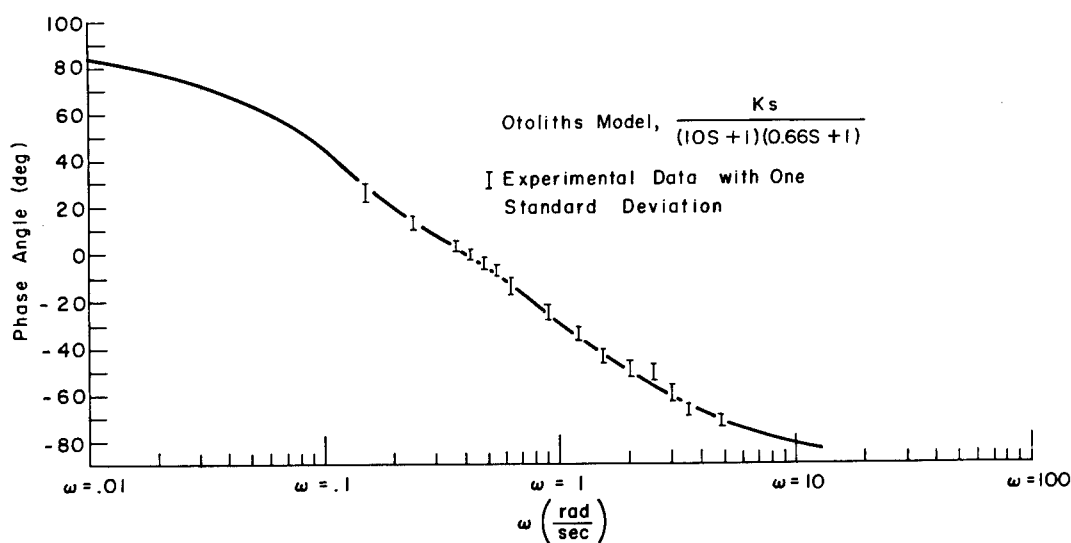


Figure 7-44

Subjective Perception of Motion Reversal Phase Versus Frequency
for Linear Acceleration Along the Horizontal, Earth Fixed Axis.

(After Meiry⁽⁴¹⁶⁾)

frequency of stimulation. The phase lag is the phase difference between the time that the body, in the erect position, actually reverses its velocity and the time the subject indicated the change of velocity. At very low frequencies the subject leads the stimulus velocity in swing experiments (642). Over a fairly wide range of frequencies, man has approximately the correct phase relationship (zero lag), and as frequency increases, he develops more and more phase lag, approaching 90° at high frequencies. These phase data can

easily be fitted by a linear minimum-phase model which does not include any pure delay. The resulting transfer function from input acceleration to subjective sensation of velocity will take the form of:

$$\frac{\text{subjective velocity (s)}}{a_{X_e} (s)} = \frac{K}{(10s + 1)(0.66s + 1)} \quad (2)$$

where a_{X_e} = linear acceleration along the horizontal earth-fixed, X_e axis.

The frequency response of the otoliths from an input velocity along the X_e axis to subjective velocity is shown in Figure 7-45. The gain constant K has not yet been measured. This equation corresponds to a second-order differential equation identical to the form of the torsion-pendulum model of the

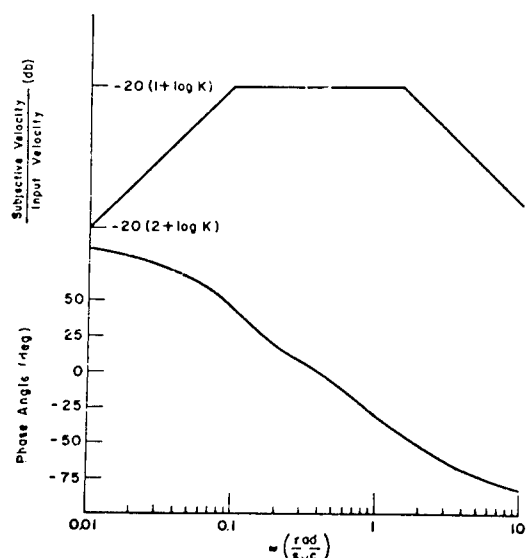


Figure 7-45

Bode Plot of Otoliths Model

(After Meiry⁽⁴¹⁶⁾)

semicircular canals. The major difference lies in the value of the short-time constant, which is 0.66 second compared to approximately 0.1 second.

Threshold of perception for the utricle is significant in terms of minimum deviation in orientation detectable by the sensor. If threshold is associated with minimum displacement of the otolith, the latency time to detect input acceleration of a certain magnitude will correspond to the duration of travel of the otolith from rest position to the threshold deflection. Consequently, the threshold of the utricle is defined as the minimum acceleration which the sensor will detect, provided the stimulus persisted for a sufficiently long period. For the otolithic organ, measurements of threshold and latency times in the sagittal plane have been determined. The response of the model for the otoliths to a step of acceleration is given by (423, 694):

$$\text{Subjective perception (t)} = a_{X_e} K(1 + 0.07e^{-1.5t} - 1.07e^{-0.1t}) \quad (3)$$

If one associates the physical vector of displacement of the otoliths with subjective perception, the threshold will correspond to some minimum travel d_{\min} such that:

$$d_{\min} = a_{X_e} K(1 + 0.07e^{-1.5\tau} - 1.07e^{-0.1\tau}) \quad (4)$$

with a unique relation between the latency times τ measured and the magnitude of the input acceleration, a_{X_e} .

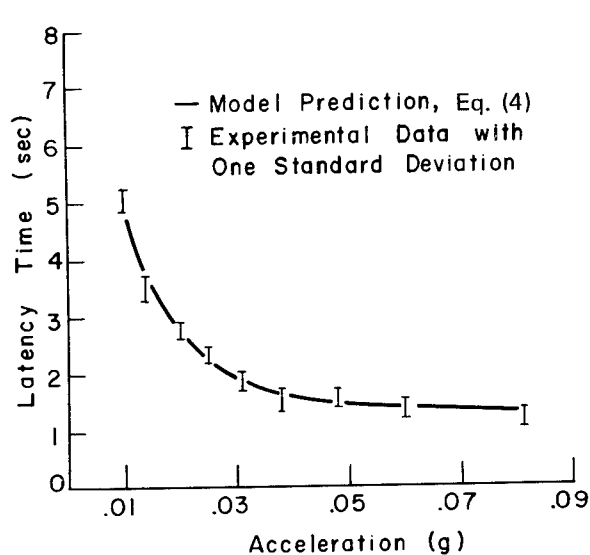
Two immediate observations are apparent from Equation (3): (1) the effect of the term $0.07e^{-1.5t}$, drops off almost completely after one second; (2) a very slow increase of the factor multiplying the input acceleration during the first second. One can expect then that a wide range of accelerations will be perceived with latency times of about one second.

Figure 7-46a represents the mean latency times of the three subjects for the supine position as a function of input acceleration. The solid line in the theoretical curve from Equation (4) referred to the experimental measurement at 0.01G. An excellent agreement between experimental results and theoretical prediction, over the whole range covered in the experiment, is noticed. Figure 7-46b shows the experimental latency times for the seated

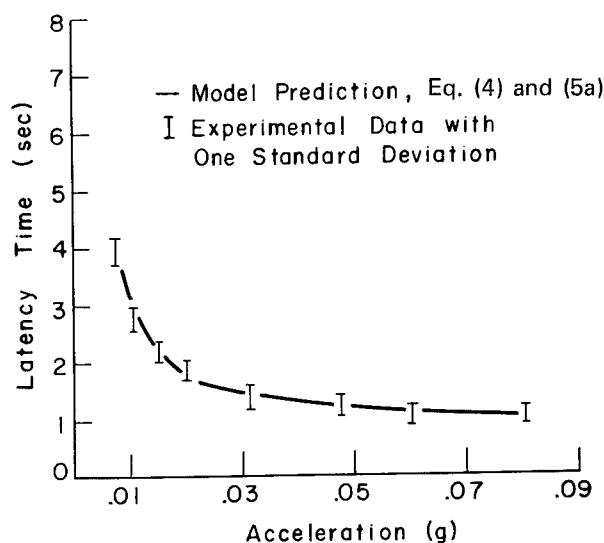
Figure 4-46

Latency Times for Perception of Horizontal Linear Acceleration

(After Meiry⁽⁴¹⁶⁾)



a. Supine Position



b. Upright Position

upright position. According to the shear theory there is a difference of shear accelerations between the supine and the upright experimental positions. Since measurements of acceleration along the earth-fixed X_e axis were made, the shear acceleration on the otoliths (assumed 30° elevated above the sagittal axis) is:

$$0.866 \text{ ng}_e = a_o \text{ upright} \quad (5a)$$

$$0.5 \text{ ng}_e = a_o \text{ supine} \quad (5b)$$

where ng_e = input acceleration along X_e axis and

a_o = shear acceleration on the otoliths.

From these relations, the theoretical, expected latency times for the upright position are shown as the solid line in Figure 7-46b which correspond well with empirical data also indicated.

Dynamically, the otoliths function as linear velocity meters for motions with frequencies within the range 0.016 cps to 0.25 cps. The threshold of perception of linear accelerations is about 0.005G in the plane of the otoliths. The thresholds of perception for the otoliths, based on 75 percent correct vector detection are 0.01G for supine head and 0.006G for upright head. These new estimates correspond to previous thresholds of 0.009 to 0.012G for the supine head (642).

The mathematical models for the semicircular canals and the otoliths are summarized in Figure 7-47 (416). Each sensor model consists of a linear second order portion followed by a non-linearity corresponding to the threshold of perception. This overall model of the vestibular system is an engineering description of the motion information perceived by the human. A "specification" summary for the vestibular sensors is given in Table 7-48. It must be remembered that these models represent only a simplified system free of the complicated cross-coupling which obviously exists between the different sensor systems (694).

The Eye Movement Control System

Eye movements are controlled with respect to a target or reference by a multi-input control system (323, 416). The horizontal eye movement control system stabilizes the eye in the presence of body and head rotations. Three sensory systems, the vestibular system, the neck proprioceptors and the eye itself (by visual tracking), are considered to participate in the control system. Figure 7-49 is a block diagram model for this multi-input, horizontal, eye-movement system with experimentally determined transfer functions.

Inputs arise from rotation of the head in space and rotation of the head with respect to the trunk, as well as from linear acceleration of the body and head. The semicircular canals respond to the net rotation of the head with respect to the body and the rotation of the body and vehicle with respect

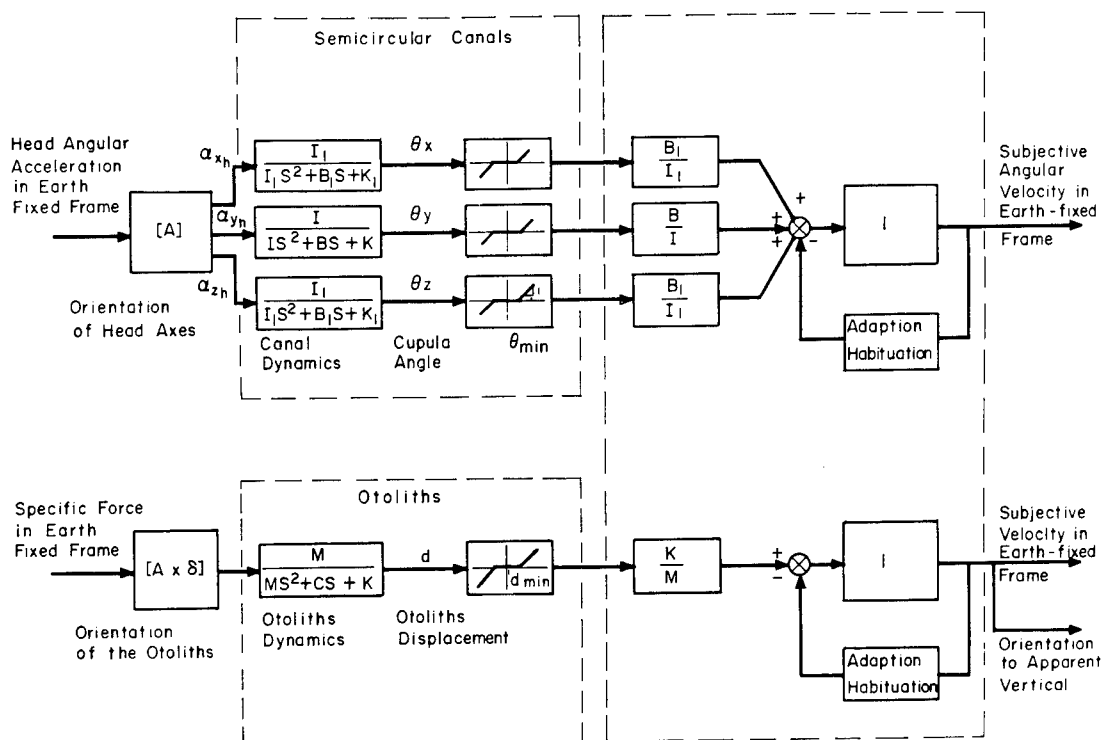


Figure 7-47

Block Diagram of the Vestibular System
(After Meiry⁽⁴¹⁶⁾)

Sensor	Semicircular Canals	Utricle
Input Variable	Angular Acceleration	Specific force in the Plane of the Otolith
Sensitive Axis	Sensitive to Angular Accelerations about an Axis Perpendicular to the Plane of the Canals	Sensitive to Accelerations in the Plane of the Otolith
Output Variable	Subjective Sensation of Angular Velocity; Vestibular Nystagmus	Subjective Sensation of Tilt and Linear Velocity; Counterrolling Eye Movements
Sensor Transfer Function	$H(s) = \frac{\text{subjective angular velocity}}{\text{input angular velocity}}$ $\text{Rotation about the Sagittal Head Axis } X_h \text{ (Roll)} \quad (a_x)(\dot{R}_x)$ $H_{xh}(s) = \frac{7s}{(7s+1)(0.1s+1)}$ $\text{Rotation about the Vertical Head Axis } Y_h \text{ (Yaw)} \quad (a_y)(\dot{R}_y)$ $H_{yh}(s) = \frac{10s}{(10s+1)(0.1s+1)}$ $\text{Rotation about the Lateral Head Axis } Z_h \text{ (Pitch)} \quad (a_z)(\dot{R}_z)$ $H_{zh}(s) = \frac{7s}{(7s+1)(0.1s+1)}$	$\frac{\text{subjective velocity}}{\text{input velocity}} = \frac{Ks}{(10s+1)(0.66s+1)}$
Threshold of Perception	$\alpha_{xh} = 0.5^\circ / \text{sec}^2$ $\alpha_{yh} = 0.14^\circ / \text{sec}^2$ $\alpha_{zh} = 0.5^\circ / \text{sec}^2$	$a_o = 0.005g$

Table 7-48

Summary of Control Data for the Vestibular System.

(After Meiry⁽⁴¹⁶⁾)

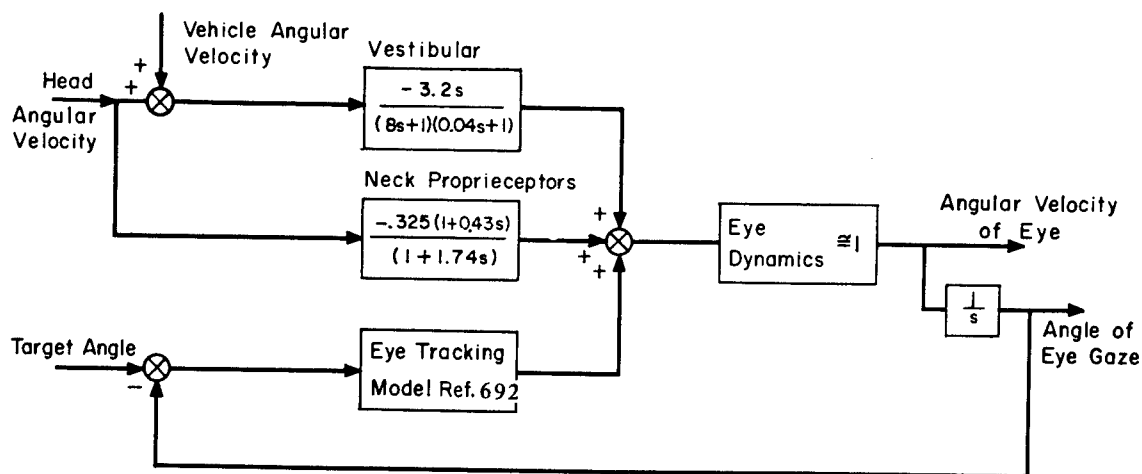


Figure 7-49

Model for Multi-input Horizontal Eye Movement Control System

(After Meiry⁽⁴¹⁶⁾)

to space. The neck proprioceptors obviously respond to head rotation and movement of the head with respect to the neck.

Vestibular nystagmus can be used as an indication of semicircular-canal phase relationships (300, 301, 416). The results of these vestibular investigations are shown in the frequency response of eye velocity compared with input velocity of Figure 7-50a. The data agree with the torsion-pendulum models with transfer function as indicated in Figure 7-49. The resulting eye movements are relatively small, which is one of the reasons that they are not readily observed. It is not clear whether the results represent a feed forward in the sense of a Von Holst type or whether it is a proprioceptive feedback.

The frequency response of eye velocity with respect to input velocity for neck is shown in Figure 7-50b. The analytic approximation of Figures 7-49 and 7-50 is:

$$\frac{\text{Eye velocity}}{\text{Input velocity}} = \frac{-0.325 (1+0.43 S)}{(1+1.74 S)}$$

The form of this transfer function is a lag-lead network indicating the possibility of position-plus-rate proprioceptive feedback in the neck. Combining this model for stimulation of the neck only with the previous model for stimulation of the vestibular system only, to get the model which matches data for combination of head and neck movement (Figure 7-49), the result is perfect agreement as shown in Figure 7-50c, the empirical frequency response for combined vestibular and neck stimulation.

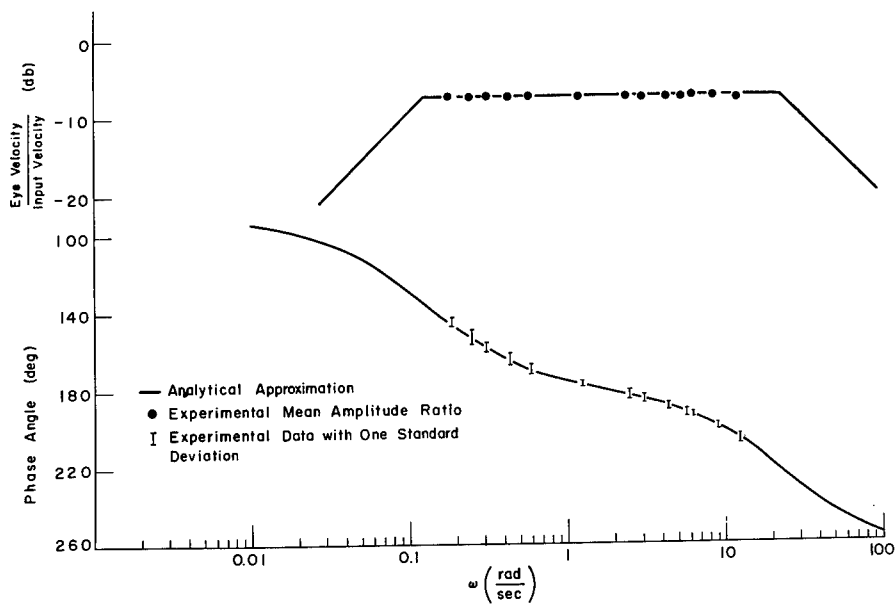
Data are available on the control dynamics of the eye movement system in tracking tasks with varying visual feedback (692, 694). From these data, it is clear that while compensatory eye movements attributed to the vestibular

Figure 7-50

Bode Plots of Compensatory Eye Movements Elicited
by Vestibular and Neck Proprioception

(After Meiry⁽⁴¹⁶⁾)

a. Vestibular Compensatory Eye Movements (Slow Phase)



b. Compensatory Eye Movements by Neck Proprioception

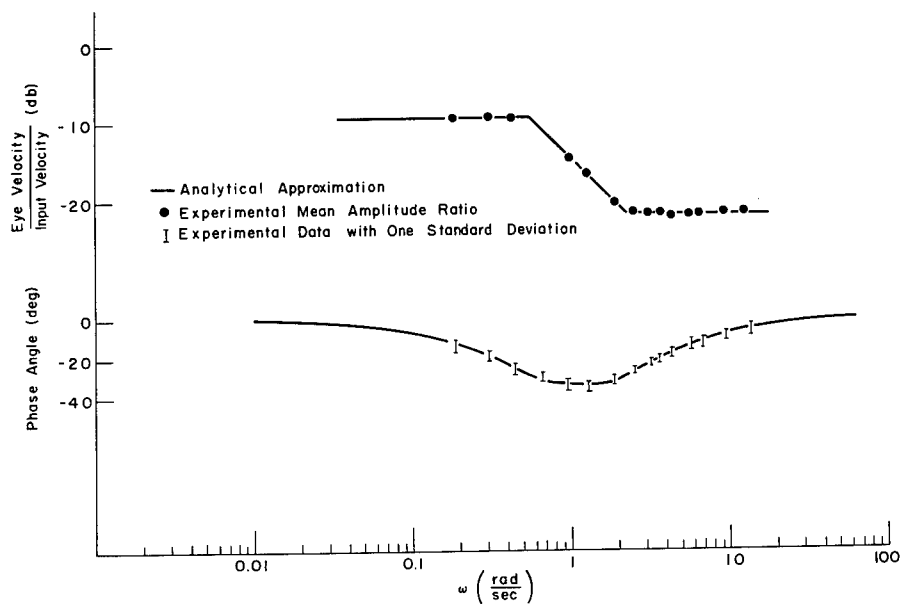
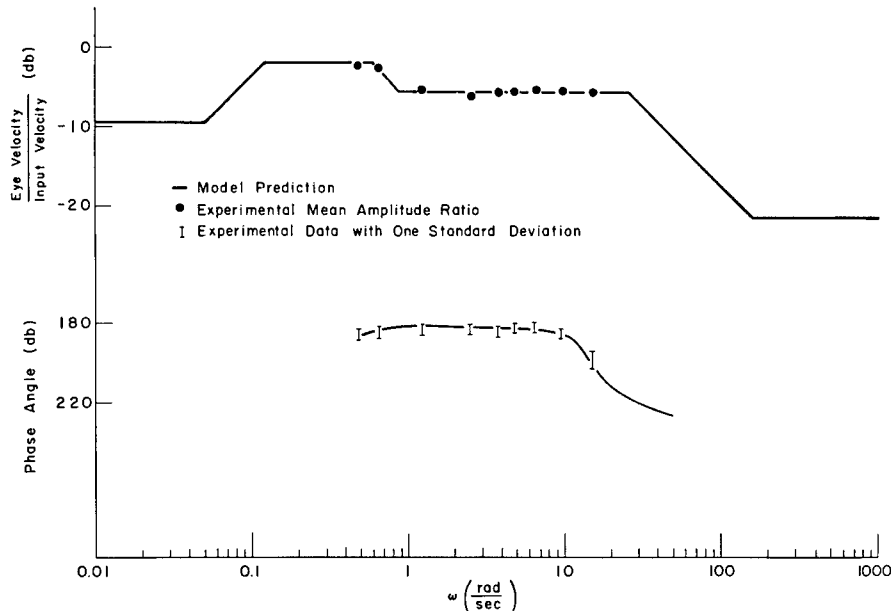


Figure 7-50 (continued)

c. Compensatory Eye Movements (Vestibular and Neck Proprioception)



system and the neck proprioceptors are of the nature of reflex responses with no voluntary control, tracking movements of the eye depend upon the wish to maintain a certain object, in the immediate vicinity, under observation. Regardless of their origin, eye movements during periods of motion disturbances are controlled to keep the eye position stationary with respect to an environment which is judged as stationary too.

Table 7-51 summarizes qualitatively the experimental results obtained in the above experiments (416). In the presence of fixation points, rotation of the skull with respect to the body or rotations of the body as a whole tend to displace the stationary picture observed by the eye. The eye is stabilized in space within ± 0.5 degrees when the fixation is on the moving surrounding. For an earth-fixed fixation point, the eye compensates with essentially a constant amplitude ratio and minimal phase lag in response to input frequencies of rotations up to 2 cps. The linearity of the summing point prior to the motor mechanism of the eyeball was established experimentally for addition of vestibular and proprioceptor signals (see Figure 7-50). Therefore, the assumption of additive property for the visual tracking branch too is plausible and experiments show quantitatively such behavior.

With the vestibular system stimulated, eye movements are smooth and regular, free of harmonics. When the vestibular system is unstimulated, wave shape of the eye movements loses similarity to the input sinusoid for frequencies above 0.8 cps. The visual tracking loop alone, which is a position control system, shows similar distortion of the wave shape of eye movements for high input frequencies (692). However, with the vestibular system stimulated and with visual fixation, the wave shape regularity of eye movements is

Table 7-51
Space Stabilization of Eye
(After Meiry⁽⁴¹⁶⁾)

	No Fixation Point	Environmental Fixation	Earth-fixed Fixation
Vestibular	Partial Compensation Of Rotational Rate over Frequencies from 0.02 cps to 4.0 cps	Maintain Eye Angle within $\pm 0.5^\circ$ up to 2 cps	Full Compensation up to 2 cps
Neck Proprieceptors	Partial Compensation of Rotational Rate Below 0.15 cps	Poor Compensation above 1 cps	Maintain Eye Angle within $\pm 0.5^\circ$ up to 2 cps
Vestibular and Neck Proprieceptors	Partial Compensation of Rotational Rate up to 4.0 cps	Maintain Eye Angle within $\pm 0.5^\circ$ up to 2 cps	Full Compensation up to 2 cps

preserved for input frequencies close to 2.5 cps. In view of these findings and considering the semicircular canals as angular velocity meters, one can conclude that the vestibular system provides the rate information for the eye movement control system, the visual tracking monitors mainly the deviation of the eye from a given fixation point (416).

Preliminary models with some empirical data are available on the relative roles of vestibular, visual, and proprioceptive cues in the vehicle control system (Figure 7-36) (532, 644, 689, 692, 694). Optimum angular rate control data are also available for unusual vehicular configurations of future space operations (97, 254, 319).

Motion Sickness

Motion sickness is a convenient generalization referring to a syndrome that may be produced in a variety of ways. The symptoms vary with the individual differences of the subject and possibly with the exact nature of the stimulus situation. Car sickness, train sickness, boat sickness, air sickness, elevator sickness, motion picture sickness, etc., are examples of the syndrome. Nausea and vomiting are the cardinal symptoms of motion sickness. The earliest to develop are psychological; first to appear are a decreased spontaneity and increased carelessness in the performance of routine duty. This may progress to the point of drowsiness, and yawning is the first obvious sign. Cold sweat and facial pallor appear. Subjectively, the experience may be reminiscent of fear, though introspectively no fear is present. The full syndrome may certainly develop in the absence of any conscious fear. As symptoms progress, salivation and swallowing occur, then nausea and vomiting. There is malaise or a general feeling of sickness

which may be differentiated from that accompanying vomiting due to other causes. Early there is muscle tenseness that later gives way to weakness and trembling, with an unsteady gait. Physiological responses simulate those of an autonomic discharge (218, 573).

Movement of endolymph in the canals induced by factors other than angular acceleration in the plane of the canal may produce bizarre nystagmic, postural, and subjective responses (266). One such factor is "caloric stimulation" by warm or cool water in the external auditory canal, which circulates the endolymph by natural convection and is often used as a test for vestibular function. Another is the inequality among Coriolis accelerations acting on different particles of fluid which occurs when the head is tilted while rotating. Responses show that the rotation perceived is about an axis at right angles to that of head tilt (Figure 7-52).

The semicircular canals may interact with the otoliths in producing motion sickness. The otoliths assume a resting position when the head is stationary under gravitational acceleration. Changes in the direction of acceleration acting on the otolith, due to movement of the head or due to an additional acceleration (linear, centrifugal, or Coriolis), will act to move the otoliths upon the sensory bed. The nature of the resulting perception depends upon the contribution of the canals as well as other inputs such as pressures on the skin. On a centrifuge operated in 1 G, the changing vector resultant of centrifugal and gravitational acceleration is not immediately perceived as tilt despite the sensation of leaning against the cab. Here, input from the canals is lacking, and the subject's estimate of the angle of tilt shows a considerable exponential lag (236). For instance, if a centrifuge reaches constant angular velocity within 6 seconds, the subject's perception of tilt, as indicated by a manual alignment of a line of light with the apparent horizontal, requires 40 seconds to reach 95% of final value. An oscillating linear acceleration of the entire body may be interpreted in different ways. Normal subjects report an immediate experience of linear velocity and are able to make fairly accurate estimates of the amplitude of body displacement (266).

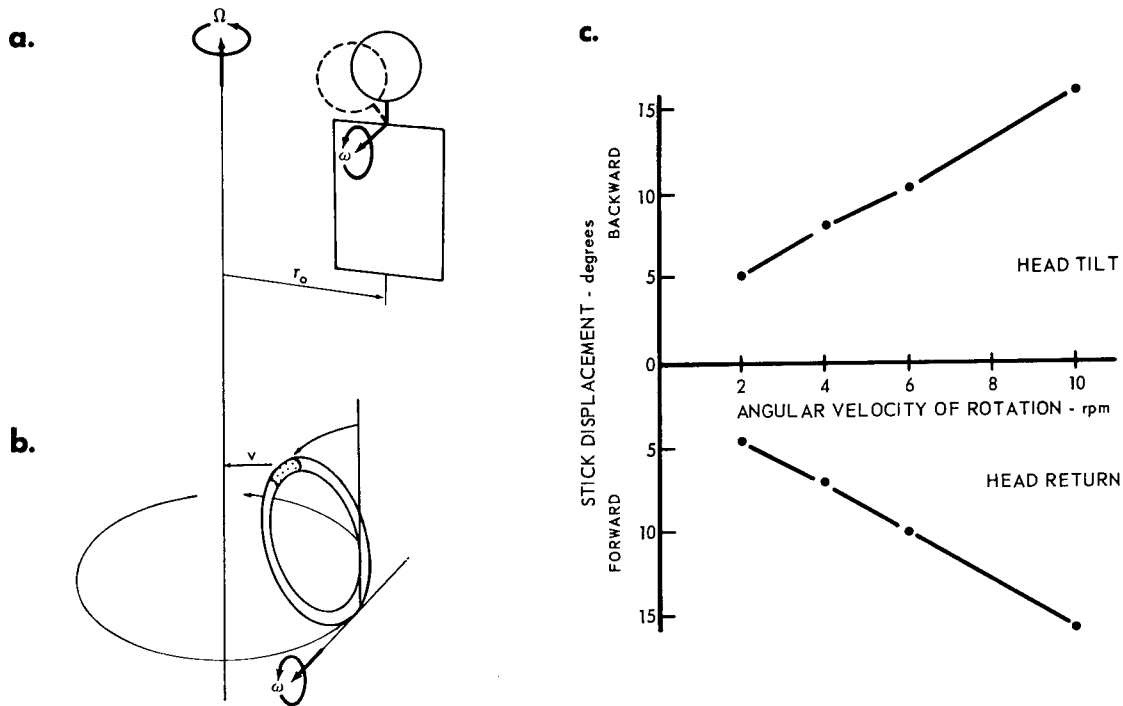
There appears to be an increased sensitivity to motion sickness with linear motion around the frequencies $1/4$ to $1/3$ cps (383). For the high frequencies, the attenuation in dynamics of the otoliths indeed serves as a limit on the input accelerations; while for frequencies below $1/4$ cps, probably equipment limitations on maximum acceleration are the cause for absence of sickness (see Figures 7-46, 7-48, and Table 7-47). Vertical reciprocating movement excites motion sickness more than similar motion in other directions (407). Reclining so as to change the head orientation often prevents completion of the syndrome in the 1 G Earth environment.

Visual stimuli alone can cause the symptoms to appear (117, 122, 345). Presentation of a visual environment which is a distorted representation of a real environment appears to be a major factor contributing to the sickness (573). Conflict between the otolithic, labyrinthine, kinesthetic and visual inputs can combine to give the most serious problems (89, 407). Head movement relative to body movement may also play a key role in that the fixation of the head in relation to vehicular movement relieves air sickness (321). There seems to be a difference in the probability of motion sickness for drivers or pilots, as opposed to the passengers. The continual task

Figure 7-52

Head Tilt During Rotation

(After Guedry and Crocker⁽²⁶⁶⁾, adapted from Guedry and Montague⁽²⁶⁸⁾)



When a subject is rotating at a constant angular velocity (figure a), a tilt of his head in a direction which changes the radius vector to the center of rotation will cause him to experience a sensation of tilt in a plane perpendicular to that of the original tilt. The sensation is due to movement of fluid in the canals caused by purely mechanical forces.

If an enlarged model of one of the canals, consisting of a liquid-filled transparent torus (figure b), is moved through an arc as shown, circulation of the liquid will be observed. The necessary conditions for circulation are that the torus must be rotating and that the radius of its center from the axis of rotation must be changing.

The liquid is circulated by the resultant of Coriolis accelerations $2(\Omega \times \dot{r})$ due to the individual velocity \dot{r} of each element of the fluid. If the torus translates only, so that \dot{r} is constant, then the resultant will be zero. Similarly if it rotates only, so that the radius of its center is constant, accelerations in the half of the torus moving away from the axis will be equal and opposite to those in the half moving toward the axis.

When the subject is seated at the axis of rotation, tilt of his head in any direction will fulfill the conditions for Coriolis circulation in at least two of the canals. The magnitude of the response is a function of the rate of head tilt (ω), the total angle of tilt, and of the speed of rotation (Ω). The response can be measured both by nystagmus (see 7-53) and by voluntary outputs.

Figure c shows the control stick movement by the subject used to indicate apparent angular displacement of a target light following head tilt. Average values of the peak stick displacement were a function of angular velocity. Each point is the average of 8 runs on 6 subjects (total of 48 runs) during which the subject tilted his head 30° to the right in 0.5 sec while being rotated clockwise. After the illusion had decayed, he returned his head to the upright position producing an illusion in the opposite direction.

appears to provide distinct inhibitory factors. Introspective evidence indicates that there are two techniques by which motion sickness may be deferred. The subject must either concentrate upon the task of continual tracking of some steady reference, such as the horizon, or he must choose the opposite extreme, that of complete attention within a narrow frame of reference which is fixed in relation to his own body, particularly his head (115, 617).

Conflicting stimulation of the visual, vestibular, and proprioceptive systems can produce, as well, deficiencies in sensory-motor coordination, including control of posture (288). Different types of conflict situations can be classified with respect to the time of exposure required to produce symptoms. Examples of four experimental situations are described in Figures 7-53, 7-54, and 7-55. The first three situations (I, II, III) are rotations that involve conflict between the semicircular canal sensory input and other kinesthetic receptors, including the otoliths. Subjects exposed to these situations show a high incidence of nausea in relatively brief exposures (10 minutes). The last three situations (II, III, IV) produce a physical disturbance of the visceral contents. In situation IV, vertical linear accelerations were sufficient to cause motion sickness, although requiring a longer exposure time.

Nystagmographic data are available for many different rotary environments (18, 71, 115, 258, 324, 327, 362, 370, 373, 430, 460). (See also references in Table 7-57). Relationship between vestibular nystagmus and visual response is under study (114, 260). Linear acceleration may contribute to the nystagmic responses (461). Quantitative techniques now under development should permit a better understanding of these phenomena (56). Hypoxia plays a relatively small role in altering these responses (448).

Susceptibility to motion sickness shows significant variability among individuals. Furthermore, the response of a given individual may show a decrease with repeated stimulation (146, 218). Habituation of nystagmic responses through repeated stimulation is of considerable practical interest in rotating environments (56, 111, 115, 121, 370, 659). Habituation, as in figure skaters, may be associated with decrease in the amplitude of the primary slow phase eye displacement, but the number of eye movements and the duration of nystagmus is the same for experienced and non-experienced individuals (113). Durations of turning sensations are shorter for skaters; and for both groups, active visual sensation significantly shortens or terminates subjective sensation.

Conflicts due to head tilt cease in time to produce nystagmus and subject responses as motion sickness subsides (see Figure 7-56). The transference of habituation from one type of head tilt to another in rotary acceleration appears to be rather strong for duration of sensation and nystagmus, but not for visual reactions (148). The significance of these findings to rotating space vehicles is covered below.

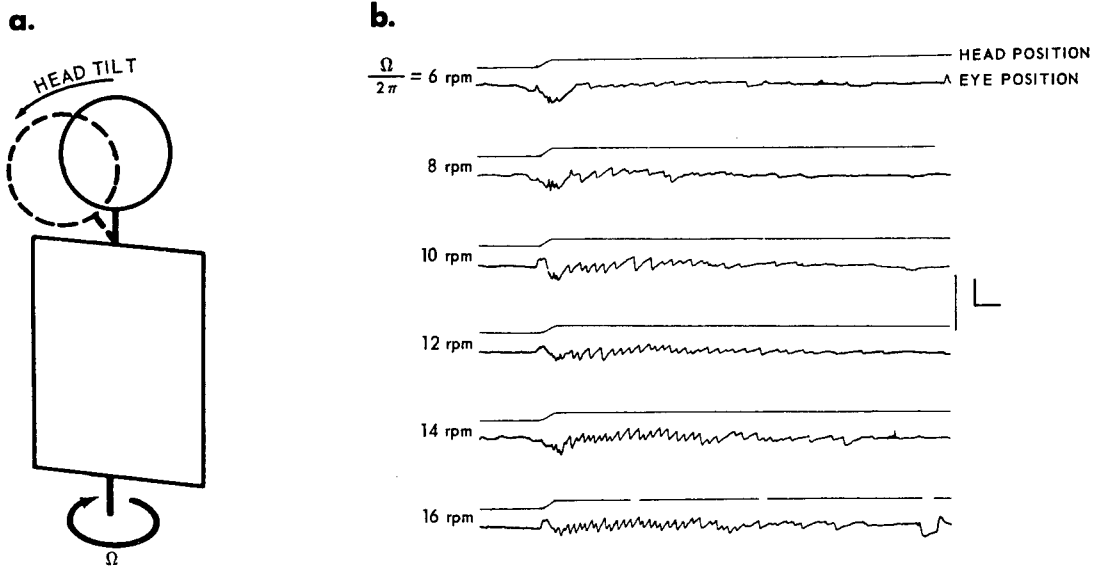
Table 7-57 summarizes the symptomatic and nystagmic effects of rotary stimulation of the semicircular canals. Respiratory and biochemical responses

Figure 7-53

Motion Sickness from Head Tilt

(After Guedry and Crocker⁽²⁶⁶⁾, adapted from Guedry and Montague⁽²⁶⁸⁾)

Situation 1.



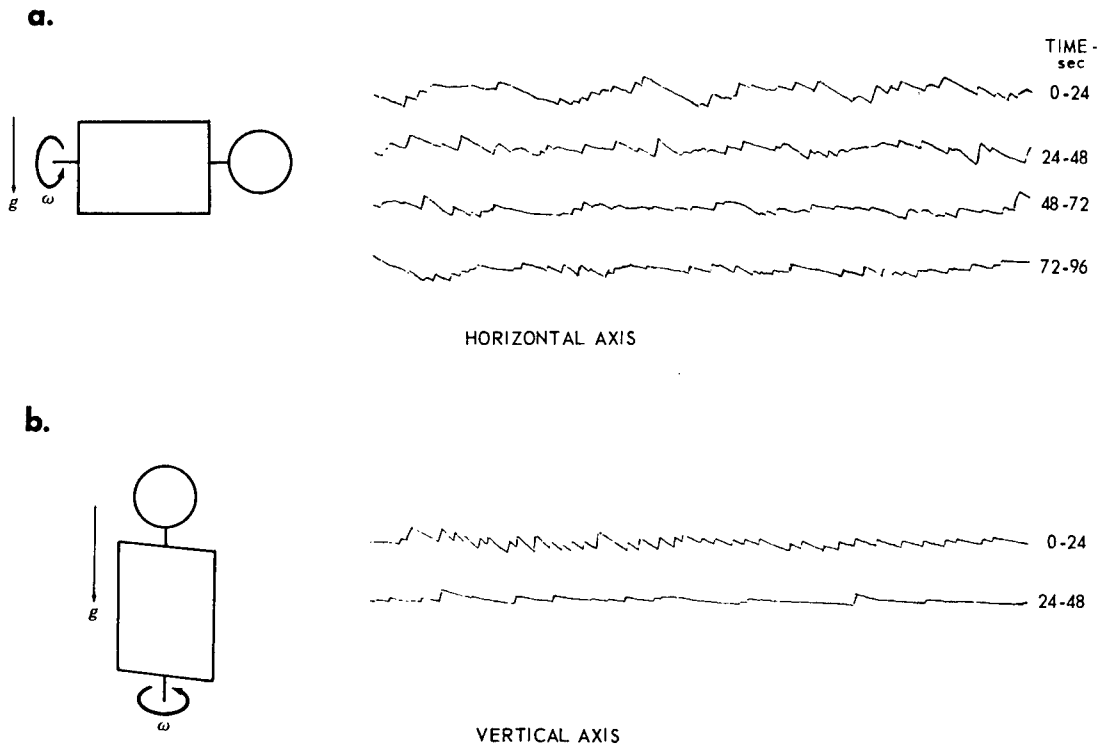
While the body is rotating at constant angular velocity, tilting the head to one side produces a sensation of pitching forward, if the head tilt is to the left during clockwise rotation. This sensation is accompanied by corresponding vertical movements of the eyeballs (nystagmus). For a given head movement (75° to the right in one second), the intensity and duration of effect, exemplified by the nystagmus records in Figure b, is a function of the angular velocity of the platform. The calibration marker shows 1 second and 40° vertical eye movement.

Figure 7-54

Motion Sickness from Rotation

(After Guedry and Crocker⁽²⁶⁶⁾, adapted from Guedry⁽²⁵⁸⁾)

Situation II.



Rotation at constant velocity about a horizontal axis, with gravitational acceleration perpendicular to the axis of rotation, produces a nystagmus response sustained long after the sensory response of the semicircular canals has decayed. The continual reorientation of the otoliths relative to gravity may be the reason for the sustained nystagmus.

Evidence for that inference comes from the companion case of rotation about a vertical axis. Strong nystagmus begins with the acceleration to constant angular velocity, and then decays along the theoretical time course of semicircular canal response.

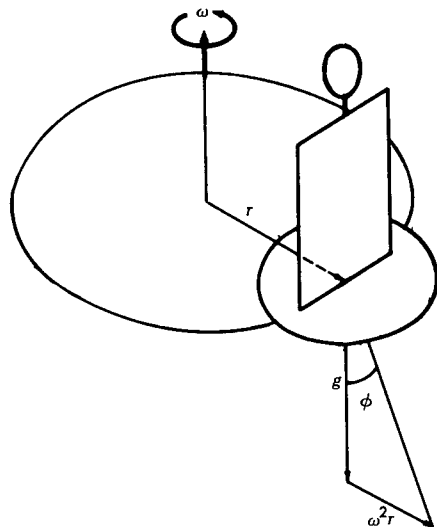
Rotation about a vertical axis is not a potent cause of motion sickness so long as the subject's eyes are closed. Prolonged rotation about a horizontal axis carries with it the self-contradictory vestibular input which can cause motion sickness independent of the visual input.

Figure 7-55

Motion Sickness from Counter-Rotation and Oscillation

Situation III.

a.



b.

SYMPTOMATOLOGY OF MOTION SICKNESS IN NORMAL SUBJECTS, SEQUENTIAL EXPERIMENTS IN COUNTER ROTATING ROOM						
EXPERIMENTAL CONDITIONS		I	II	III	IV	V
		20 RPM 2 min φ15°15' Head fixed Eyes closed	12 RPM 2 min φ5°36' Head fixed Fixate Vertical Line	30 RPM 10 min φ31°31' Head fixed Eyes closed	30RPM 10 min φ31°31' Head fixed Eyes open	10-30 RPM 10 min φ3°54'-31°31' Head moving Eyes open
"MOTION-SICK" SUBJECTS	JO	NONE	NONE	DISCOMFORT S-A* I PALLOR II	VOMITED PALLOR III SWEAT III DISORIENT II DISCONT. 7min	NAUSEA III PALLOR III SWEAT II DISCONT. 4 min
	MO	DISCOMFORT I S-A I PALLOR I	NAUSEA I INC SALIVA I PALLOR I SWEAT I	DISORIENT* S-A	NAUSEA III DESIRE BM PALLOR III SWEAT III	
	GR	NAUSEA I SWEAT I	NONE	NAUSEA I PALLOR II SWEAT II DISCONT. 2 min	NAUSEA II PALLOR II SWEAT II DISCONT. 2 min	NAUSEA I PALLOR II SWEAT II DISCONT. 2 min
REGULAR SUBJECTS	BA	S-A	NONE	S-A	S-A	
	FO	NONE	NONE	NONE	NONE	
	GI	NONE	NONE	NONE	NONE	
	KR	DIZZY I SWEAT II	SWEAT II	SWEAT II	DISCOMFORT I QIZZY I SWEAT I	
	ME	NONE	NONE	NONE	NAUSEA III PALLOR II SWEAT I	
	NI	NONE	NONE	NONE	NONE	
	MU	NONE	NONE	NONE	NONE	
	TO	PALLOR I	NONE	NONE	NONE	
	WO	NONE	NONE	NONE	NONE	

*STOMACH AWARENESS

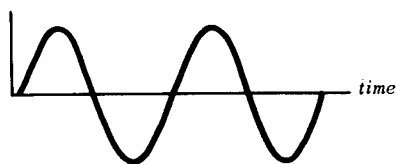
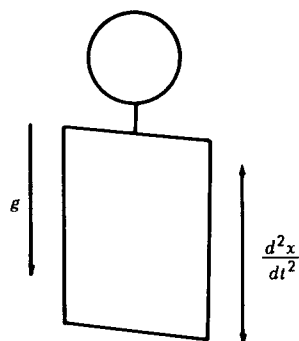
* BEFORE ROTATION BEGAN

In the apparatus used in Situation III, the platform carrying the subject rotated counter to the main centrifuge at a radius (r) of 2 feet, so that the subject faced the same direction throughout each revolution. For this reason, the direction of centrifugal acceleration ($\omega^2 r$) varied relative to his body. Since the subject had no net angular velocity, the semicircular canals received no stimulus. Subjects selected for motion sickness susceptibility reacted to all levels of the contradictory stimuli. The group of unselected normal subjects included one who reacted with nausea to strong stimulation.

(After Guedry and Crocker⁽²⁶⁶⁾, adapted from Graybiel and Johnson⁽²⁴²⁾)

Situation IV.

c.



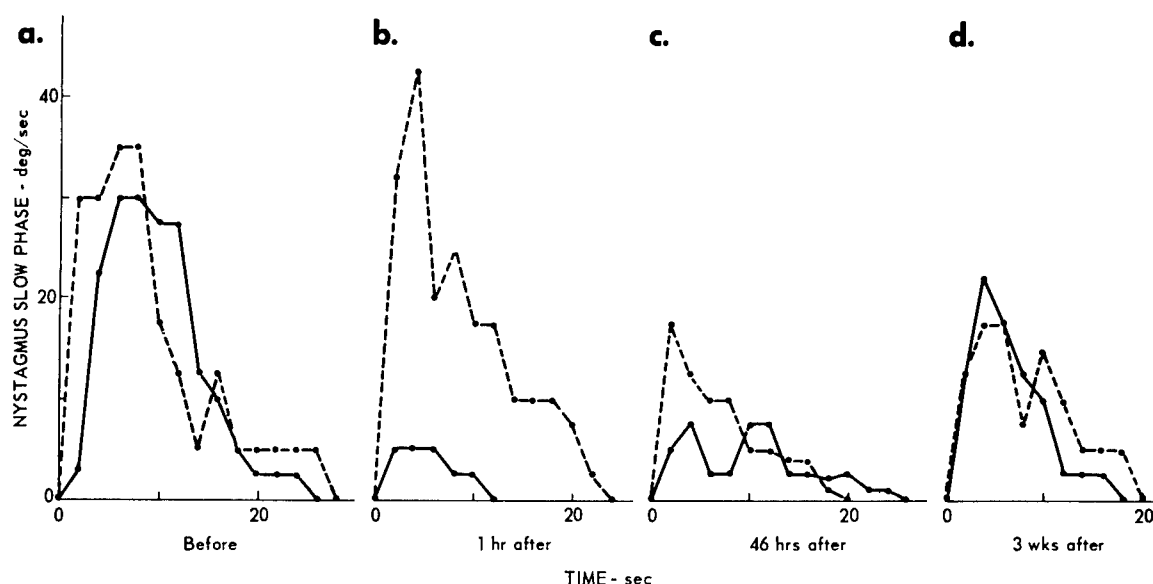
Vertical linear oscillation (7-foot peak-to-peak wave at 22 cycles per minute) produced sickness in 53% of a group of naval officers in 20 minutes.

(After Guedry and Crocker⁽²⁶⁶⁾, adapted from Wendt⁽⁶⁶¹⁾)

Figure 7-56

Habituation to Rotation

(After Guedry and Crocker⁽²⁶⁶⁾, adapted from Guedry⁽²⁵⁷⁾, and Guedry⁽²⁵⁹⁾)



Habituation to rotation is a reduction of response to repetitive sensory stimulation. Response to conflicting vestibular, visual and proprioceptive information may be measured by recordings of nystagmus and from reports of subjective sensations. Reduction in response may be due to any of three processes:

- 1) Reduced attention to a repetitive stimulus. Response may be reduced after only two or three stimulus presentations, perhaps through a general loss of alertness. The response may reappear in its original intensity when the subject is aroused, either by a change in the stimulus itself or by an extraneous event.
- 2) A conditioned reaction which competes with the subject's normal response and may, with repetition, become adequate to nullify subjective or nystagmus responses. Habituation of this type requires many trials to develop, is not abolished by arousal, and usually reduces the incidence of nausea and vomiting, at least for identical vestibular, visual, and proprioceptive stimulus patterns. Change in the conditions, such as stopping the rotation or, especially, reversing its direction, may yield more intense responses, since the conditioned reaction then supplements the reaction to the unaccustomed direction of rotation.
- 3) A general suppression of response to accustomed and even some unaccustomed patterns of stimulation. This form of habituation can be detected for a period of weeks after the stimulation has ended, and may afford a fairly generalized protection against motion sickness.

Habituation of the second and third types is achieved most rapidly under a particular set of conditions, in which the subject's arousal is maintained, as by a mental task, as he initiates the vestibular stimulation intentionally and makes an active effort to fixate on a visual target under normal illumination.

The figures above show the way in which habituation of the second and third types develops with time. The graphs show nystagmus velocity as a function of time following head tilt to the left during rotation clockwise (dotted line) and counter clockwise (solid line). After initial testing (figure a), the subject lived 12 days in a room rotating 10 rpm in a counterclockwise (ccw) direction. When tested one hour after returning to non-rotating surroundings (figure b), the diminished response to head tilt during ccw rotation and enhanced response during cw rotation are signs of the reaction conditioned during the 12 days to compete with the normal reactions. By 46 hours, responses to head tilt while rotating in either direction (figure c) showed suppression below initial levels. This suppression was still evident three weeks later (figure d).

have also been studied in man (107,616). Any one of these situations may occur in space vehicles rotating around the noted axes (120,325).

One must also consider the effect of radiation on the vestibular mechanism. Preliminary studies indicate that ionizing radiation will affect vestibular activity (431). Doses greater than several hundred rads of x-ray and α particles given to the vestibular apparatus of animals can alter nystagmographic responses (396). Response of several vestibular reflexes of cats to 910 MeV α -particles is now under study (182). Whether or not the doses of space radiation anticipated will harmfully synergize with weightlessness and rotary acceleration for space operations is still open to question (see Ionizing Radiation No. 3).

The malaise, nausea, and vomiting associated with motion sickness can be a serious hazard in space operations by degrading performance and contaminating the cabin in the weightless environment (see Contaminants, No. 13 and zero gravity of this section). Drug prophylaxis and therapy for motion sickness has received recent review (62, 237, 511,681). Hyosine (scopolamine) still appears to be the drug of choice especially when combined with amphetamine. Drowsiness, vertigo, and dry mouth limit its usefulness at high doses. Meclizine (Bonamine) and Cyclizine (Marezine) are the most effective of the antihistamines with therapeutic ratios approaching that of hyosine. The phenothiazine tranquilizers do not appear to be as effective as the above drugs. Soviet studies have been directed at alteration of symptomatic and nystagmographic responses after vestibular stimulation by electric current (7.5 mA., D.C.) applied through moveable electrical contacts on the ear and neck (639). Both increases and decreases in response have been obtained by this means. Further study is needed before the significance of this work to space flight becomes clear.

Vestibular Illusions

At the conscious level, motion sickness leads to illusions. As with the other symptoms, illusory phenomena arise when vestibular, kinesthetic, and visual cues are in conflict giving rise to "cross modality" interactions (288). During aircraft flight, many kinds of illusions occur because of sudden changes in linear acceleration or departure of the aircraft from a straight path. These may be compounded by adverse weather or night-flight conditions which restrict visibility and add fear and anxiety. The many flight illusions have been reviewed (45, 90, 172, 466, 488). Their relation to zero gravity will be covered in the zero gravity section on pages 7-127 to 7-132. An Air Force training device is currently being used to study these phenomena (219).

The Visual Illusions

This class of illusions usually involves error in interpreting the visual environment, which gives the pilot information about the horizon, altitude, location of other vehicles and obstacles, position in formation, vehicle attitude, and so on. Lights form the major portion of his night visual field. Errors in the perception of lights include those of recognition, position, and movement. Fatigue may cause loss of binocular vision, a single light may

split and appear as two or more lights. Stimulation from angular acceleration may cause nystagmic eye movements in which slow sweeps of the eye (in a direction opposite to the rotation) accompany positive acceleration (see Figures 7-53 to 7-56 and Table 7-57). Interaction with voluntary eye movements and ocular reflexes, when nystagmus is present, may cause serious difficulty in reading instruments.

(1) Autokinetic Illusions (See also Light, No. 2)

A single fixed point of light may appear to move in random fashion when viewed steadily against a dark background (160, 161, 252). This can be demonstrated by staring fixedly at a fairly bright, isolated star. A subject asked to localize such a light usually reports this to be impossible, because of the apparent movement of the star. After a short delay before onset, movement is reported in apparently random directions. Median duration of the movement is about 10 seconds, and voluntary control over it is slight. The effect is abolished only with difficulty. Alternately blinking lights used on current vehicles tend to destroy the illusion. Moving the eyes and avoiding steady fixation also tends to prevent it. Eye muscle imbalance rather than vestibular factors appear at fault (170, 216).

(2) Oculogyral Illusions (OGY)

These visual illusions may result when a pilot is subjected to rotary motion. It is caused by a reflex response consisting of movements of the eyeball following semicircular canal stimulation (90, 163, 166, 241, 269, 324, 325, 326, 327, 679). The direction of apparent motion is in accord with the sensation of rotation during acceleration. If the subject is rotated to the right, a visual target fixed in relation to the subject appears to move in that direction. Movement gradually comes to a standstill after which it may appear to shift slowly to the left. When rotation rate is stabilized, apparent motion ceases. Sudden deceleration causes the visual target to have rapid apparent motion to the left, with a successive stage in which apparent motion is to the right. The pilot may interpret this as motion of the craft. After recovering from a spin to the left which involves large accelerations, a pilot will sense a turning to the right, and if he attempts to correct for this illusory turning, he will cause the airplane to spin to the left again. This reflex response of the eyeballs cannot be eliminated, and the only remedy is to train the pilot to ignore the sensations it produces.

The threshold for the OGY is approximately 0.2° to 0.3° of angular acceleration per second; however, reported threshold values in the literature vary from $2.00^\circ/\text{sec.}^2$ to $0.035^\circ/\text{sec.}^2$ (405, 245). OGY has been studied in human subjects with real targets, afterimages and simultaneous presentation of the two. It seems that the apparent movement is associated with efferent activity in the agonist to the slow-phase efferent activity present as a result of labyrinthine stimulus. The magnitude of the oculogyral illusion varies in relation to the rate of angular acceleration, position of the head, illumination of the target and background, acoustic noise, and the experience of the individual. In ordinary daylight the apparent motion of a target is seen only after a relatively high rate of angular acceleration. Strong illusions can be initiated with small angular accelerations in the darkness. Therefore, the

Table 7-57

Rotary Stimulation of the Semicircular Canals: Man
(After Guedry⁽²⁶¹⁾)

Abbreviations and Symbols: K = constant; α = angular acceleration; t = duration of α ; T = time constant; SE = standard error; ~ = approximately.

Stimulus		Factors Affecting Response Intensity	Response			Reference
Characteristics of Rotation	Head Orientation (Principal Organ Stimulated)		Motion Sensation ¹	Eye Movement ¹	Motion Sickness	
1 Brief angular acceleration to constant rotation (10 rpm) around earth-vertical axis; head at center of rotation	Horizontal plane of skull in plane of rotation (Lateral semicircular canals)	$K\alpha(1-e^{-t/T})^2$; mental alertness; visual stimulation; habituation	Spinning around earth-vertical axis. T of response, 10.2 ± 0.9 sec (SE) ^{2,3} . Stopping produces spinning sensation in opposite direction but with similar characteristics.	Nystagmus in horizontal plane, around earth-vertical axis. T of response, 15.6 ± 0.6 sec (SE) ^{2,3} . Stopping produces similar response but reversed in direction.	Negligible in absence of visual conflict.	162 259 266 327
2	Sagittal plane of skull in plane of rotation (Superior and posterior semicircular canals)	$K\alpha(1-e^{-t/T})^2$; mental alertness; visual stimulation; habituation	Spinning around earth-vertical axis. T of response, 5.3 ± 0.35 sec (SE) ^{2,3} . Stopping produces spinning sensation in opposite direction but with similar characteristics.	Nystagmus in sagittal plane, around earth-vertical axis. T of response, 6.6 ± 0.35 sec (SE) ^{2,3} . Stopping produces similar response but reversed in direction.	Negligible in absence of visual conflict	259 327
3	Frontal plane of skull in plane of rotation (Superior and posterior semicircular canals)	$K\alpha(1-e^{-t/T})^2$; mental alertness; visual stimulation; habituation	Spinning around earth-vertical axis. T of response, 6.1 ± 0.6 sec (SE) ^{2,3} . Stopping produces spinning sensation in opposite direction but with similar characteristics.	Nystagmus in frontal plane, around earth-vertical axis. T of response, 4.0 ± 0.2 sec (SE) ^{2,3} .	Negligible in absence of visual conflict	259 327
4 Brief angular acceleration to constant rotation (10 rpm) around earth-horizontal axis; head at center of rotation	Horizontal plane of skull in plane of rotation (Lateral canals; otoliths and other gravity-sensitive structures)	Same as for entry 3, but complicated by continual reorientation of gravity-sensitive structures	Rotation around earth-horizontal axis. T indeterminate. Response persists throughout rotation. Stopping produces very short reversed responses or none at all.	Nystagmus in horizontal plane, around earth-horizontal axis. Response persists throughout rotation. Stopping produces short reversed response. T undetermined during rotation. After rotation, T = 6.8 sec	Nausea in ~50% of men tested during 5-min exposure. Associated effects with longer exposure: sweating, pallor, vomiting, antidiuresis.	32 119 120 258 604
5	Sagittal plane of skull in plane of rotation (Superior and posterior canals; otoliths and other gravity-sensitive structures)	Same as for entry 3, but complicated by continual reorientation of gravity-sensitive structures	Same as for entry 4	Nystagmus in sagittal plane, around earth-horizontal axis. Time characteristics same as for entry 4.	Same as for entry 4	459
6 Constant rotation (15 rpm) about one axis (ω -axis), plus head rotation about an orthogonal axis	Changing relative to plane of rotation (Semicircular canals and otoliths)	Angular displacement: head-tilt axis; angular velocity: head-tilt axis and ω -axis	Rotation about a 3rd axis approximately orthogonal to head-tilt axis and ω -axis	Nystagmus about a 3rd axis approximately orthogonal to head-tilt axis and ω -axis	Nausea in ~50% of men tested after 6 head movements during 4-min exposure. Associated effects: sweating, pallor, vomiting, antidiuresis	4 46 240 265 268 604

¹ Recorded with subject in dark. ² During normal head movements, nystagmus slow-phase velocity is opposite in direction and directly related in magnitude to the angular velocity of the skull (328). ³ Time constants from estimates made by G. Melvill Jones (327). ⁴ Time constant does not apply to a single canal or pair of canals because no single pair was in the plane of rotation.

pilot would be expected to experience the oculogyral illusion as a result of the small angular accelerations experienced while flying at night.

In space operations, complex illusory behavior is possible when rotatory vectors are continually changing (255, 324, 325, 327).

(3) Oculogravic Illusions (OGI)

Conflicting sensory information supplied by the eye and otolithic sense organs can cause an illusion consisting of the apparent displacement of objects in space as well as body displacement (87, 89, 236, 239, 247, 420, 462). Upon change of gravitational vector, dimly illuminated objects in the visual field will move and assume new positions in space after a lag period (89). Presence of a strong visual framework will tend to prevent the change from primary visual orientation to vestibular, and diminish the effect; but there is little adaptation or habituation effect upon repeated exposure.

The illusion may be described as follows (488): If a subject faces toward the line of the resultant force, he perceives an apparent change in body position as though he were being tilted backwards. An object on the horizon will appear to shift above the horizon. Conversely, facing away from the resultant force results in the sensation of being tilted forward and an object will appear below the horizon. If a subject is at right angles to the resultant force, a horizontal line will appear to rotate clockwise if the direction of the resultant force is from the left and counterclockwise if the direction of the resultant force is from the right. For example, if a subject faces the center of a centrifuge while viewing a fixed light during exposure to acceleration which attains 3.0 G within three seconds, with onset of rotation, he feels he is changing position and the light is rising. The apparent change is described as a sensation of being slowly tilted backward along with the chair and centrifuge platform; thus, the illusion includes both apparent exterior motion and body displacement. When centripetal acceleration reaches 1.5 G, the subject reports a sensation of being on his back in a horizontally placed chair fixed to a vertical platform with walls of the centrifuge rotating around him. The opposite sensation occurs when the centrifuge is stopped.

The threshold for a perceived change in direction of horizontal or vertical is 1.5° (248). This is equal to a G increase of 0.00034; however, calculations reveal that this corresponds to 0.02 G at right angles to the gravity vector. Further work is needed to better establish the quantitative value of the OGI threshold.

There has been much theoretic speculation on the possible cause of this illusion. Neither ocular nystagmus nor ocular rotations can explain the phenomenon. The movement of the eyes from nystagmus results in a rapid apparent motion of an object in space but without displacement of the object. A visual afterimage is displaced in the same direction as a target, whereas the target and afterimage separate with ocular nystagmus. It has been postulated that "a psychophysiological mechanism which has no correlate in the retinal image" is a cause of the phenomenon (236). Since the otolithic organs are the organs for the perception of linear accelerations, the illusion

is probably correlated with their stimulation or with a central mechanism associated with their function (239), and those of eyeball control (679).

During normal (\dot{R}_Z) spin, a pilot feels he is being forced slowly forward, or backward, depending on the pilot's position relating to the center of rotation. He identifies the apparent displacement of his body with changing attitude of aircraft through sensory contact (body pressure senses) with the airplane. During inverted (\dot{R}_Z) spin, the opposite effect would occur due to changed axis of rotation and body position. Blindfolded subjects perceive rapid positive acceleration ($+G_Z$) as backward tilt and rapid deceleration as forward tilt. These sensations are interpreted as changing altitude, climbing in the case of positive acceleration and diving in the case of negative acceleration. A linear acceleration increment of about $0.1 + G_X$ is interpreted as a climb at a 20° to 25° angle. A deceleration of about the same magnitude may be interpreted as a dive at a 15° angle below horizontal. Static tilt of the body laterally from vertical can also displace the visual localization of the horizontal (420, 421). Kinesthetic cues from a horizontal floor may abolish this effect (88).

The elevator illusion is a special case of the oculogravic phenomenon in which the resultant vector changes only in magnitude and not in direction (462). Subjects tend to perceive illusory movement of real targets and visual after-images during vertical accelerations greater or less than 1 G. Apparent movement of real targets is downward when $G < 1$ and upward when $G > 1$; for a visual afterimage the directional relationships are reversed. There is no well-defined displacement of a real target whereas marked displacement occurs with a visual afterimage. When viewed in combination, the same relationships are maintained. The change from 1 G to zero G, causes an involuntary upward eye movement in normals which lasts at least 150 milliseconds. The failure to demonstrate this in the labyrinthine defective subject suggests that the change is reflexive and probably otolithic in origin. This illusion may play a role during orbital insertion in space operations.

The Non-Visual Illusions

Illusions of this type may result solely from accelerative stimulation of vestibular and kinesthetic sense organs. Such illusions are marked by perceived rotation during and following actual rotation and by changes in linear acceleration (670). A subject may sense the onset of rotation but lose the sensation when rotation becomes constant. After a momentary lag or during deceleration, an illusion of turning in the opposite direction occurs. Rotation evokes a number of responses in the neck, limbs, and trunk. The head may show slow sweeping motions in a direction opposite rotation during positive acceleration. Sudden deceleration brings compensatory movements in head and limbs. If a blindfolded subject in a counter-clockwise rotating chair is told to stand with his arms raised straight out in front of him, he may stand with his head and arms to the left, right arm up, left arm down. A radical change in head position at this time may endanger his balance.

Rotating chair experiments have been used to illustrate how deceleration while in \dot{R}_Z spin, with reduced visual field, might affect pilot judgment. The

pilot quickly senses onset of spin but sensation fades and vanishes as speed becomes constant. During deceleration, the pilot feels he is turning in a direction opposite the actual turn.

(1) The Audiogyral Illusion

The ears also return faulty information as a result of rotary deceleration. A sound source in front of the subject was reported as arising from left of center following left spin. The audiogyral illusion might affect a pilot who has become oriented to the afterburner or rocket sound. Following spin to left, the pilot might perceive the sound as coming from right of rear. Similarly, spin to right would dislocate the sound to left of rear.

(2) Vertigo

Vertigo may be defined as the subjective loss of spatial orientation with respect to the direction of "up." Vertigo may be induced by many physiological and/or psychological factors often related to the conflicting vestibular and local visual cues to verticality (90, 325, 466, 614, 622, 624, 697). These result from a combination of the illusions noted above.

(a) Sensation of Climbing While Turning

In a properly banked turn, acceleration tends to force the body firmly into the seat in the same manner as when the aircraft is entering a climb or pulling out of a dive. Without visual references, an aircraft making a banked turn may be interpreted as being in a climbing attitude, and the pilot may react inappropriately by pushing forward on the control column.

(b) Sensation of Diving While Recovering from a Turn

The positive G-forces sustained in a banked turn are reduced as the turn is completed. This reduction in pressure gives the flyer the same sensation as going into a dive and may be interpreted in this way. He may overcorrect by pulling back on the control column and cause the aircraft to stall.

(c) Sensation of Diving Following Pull-out from a Dive

The accelerative forces on the body during the pull-out from a dive are reduced after recovery is complete. This reduction in G-forces may be falsely identified as originating from another dive.

(d) Sensation of Opposite Tilt While Skidding

If skidding of the aircraft takes place during a turn, the body is pressed away from the direction of turning. This may be falsely perceived as a tilt in the opposite direction.

(e) The Coriolis Phenomenon

(See Figure 7-52). This is a severe loss of equilibrium in which vertigo results (66, 268, 447). When the pilot is rotating with the aircraft and then moves his head out of the plane of rotation, there is a differential stimulation of two sets of semi-

circular canals. For example, if during a spin the pilot moves his head forward or backward, an additional pair of semicircular canals is stimulated and extreme dizziness and nausea may be suddenly produced. Constant angular velocity of less than $1^\circ/\text{sec}$ with the appropriate head movement may permit the Coriolis response (217). Training by repeated exposure of the Coriolis effect can produce resistance (146, 147, 218, 432, 433, 447). (See also discussion of Rotating Space Stations on page 7-96).

(f) Sensation of Reversed Rotation

If a rotary motion persists for a short period and is then discontinued, there is a sensation of rotation in the opposite direction. This occurs in a spinning aircraft when the pilot has poor visual reference to the Earth. After recovery from a spin to the left, there is a sensation of turning to the right. In attempting to correct for this, the pilot puts the aircraft back into the spin to the left. Flyers have given this illusion the sinister name of "graveyard spin."

The most important psychological factor results from the presentation to the pilot of two different vertical indications. This requires his decision with respect to which of these is "correct," and this decision in itself may result in a loss of orientation. Such a situation often develops when the body-sensed vertical is in disagreement with the vertical indicated by the attitude instrument. There are many degrees of vertigo. They range all the way from what is commonly called the "leans" (wherein the pilot feels that he is slightly tilted with respect to the instrument-indicated vertical), to the outright situation where the pilot can even be flying upside down without knowledge that such is the case. Pilot instructions emphasize the necessity of remaining on instruments even during weather which might permit intermittent contact flight. Pilot training insists that the pilot learn to disregard his body sensations and only concern himself with the indicated vertical on the instrument panel. The very act of visual fixation may play a role (112, 617).

The effects of training against the many forms of vertigo by repeated exposure to vertiginous stimuli are clear-cut (45, 56, 107, 146, 147, 218, 432, 433, 447). Brief screening tests for selection of flight training candidates free of vestibular sensitivity are now under study (11). An Air Force spatial orientation trainer for control of illusions is now under design (219).

A recent bibliographic review of the Soviet literature in vestibular physiology is available (549).

Rotating Space Vehicles

Vestibular Responses

In view of some uncertainty regarding the effect of zero gravity on body systems and housekeeping functions, the rotation of vehicles has been suggested as a possible method of supplying an artificial gravity (376, 388, 454, 591). The movement of the head and body in a rotating space vehicle

imposes on the semicircular canals of Figure 7-35 angular accelerations which include the factors noted in Figure 7-58 (588). Equations have been presented covering cross coupling accelerations to be expected (588). The total angular velocities experienced by the head are the sum of the various angular velocities acting

$$\left. \begin{aligned} \omega_{hx} &= \omega_{h\phi} + \omega_V \cos \theta_e \cos \psi_e \\ \omega_{hy} &= \omega_{h\theta} - \omega_V \cos \theta_e \sin \psi_e \\ \omega_{hz} &= \omega_{h\psi} + \omega_V \sin \theta_e \end{aligned} \right\} \quad (6)$$

where ω_V , the rotational velocity of the vehicle, is assumed to be constant and aligned with the inertial X axis.

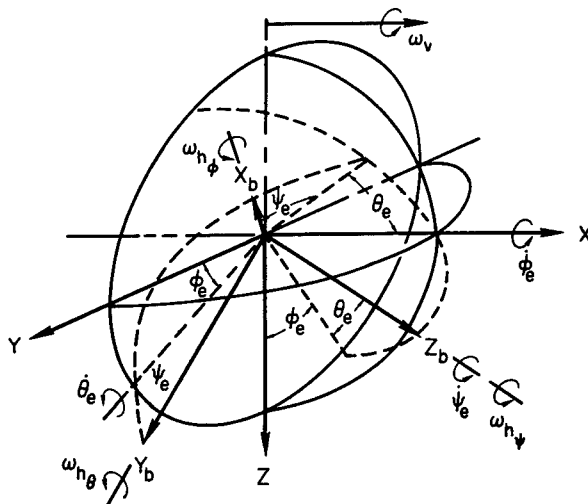
The derivatives of equations (6) with time will then give the angular accelerations experienced by the head when moving, where $\dot{\omega}_{hx}$, $\dot{\omega}_{hy}$, and $\dot{\omega}_{hz}$ are the angular accelerations of the head in inertial space - the accelerations which will stimulate the semicircular canals - and $\dot{\omega}_{h\phi}$, $\dot{\omega}_{h\theta}$, and $\dot{\omega}_{h\psi}$ are the angular accelerations of the head in the rotating frame of reference.

$$\left. \begin{aligned} \dot{\omega}_{hx} &= \dot{\omega}_{h\phi} - \omega_V (\sin \theta_e \cos \psi_e \dot{\theta}_e + \cos \theta_e \sin \psi_e \dot{\psi}_e) \\ \dot{\omega}_{hy} &= \dot{\omega}_{h\theta} - \omega_V (\cos \theta_e \cos \psi_e \dot{\psi}_e - \sin \theta_e \sin \psi_e \dot{\theta}_e) \\ \dot{\omega}_{hz} &= \dot{\omega}_{h\psi} + \omega_V \cos \theta_e \dot{\theta}_e \end{aligned} \right\} \quad (7)$$

Further

$$\left. \begin{aligned} \dot{\phi}_e &= (\omega_{h\phi} \cos \psi_e - \omega_{h\theta} \sin \psi_e) \frac{1}{\cos \theta_e} \\ \dot{\theta}_e &= (\omega_{h\phi} \sin \psi_e + \omega_{h\theta} \cos \psi_e) \\ \dot{\psi}_e &= \omega_{h\psi} - \tan \theta_e (\omega_{h\phi} \cos \psi_e - \omega_{h\theta} \sin \psi_e) \end{aligned} \right\} \quad (8)$$

A substitution of Equations (8) in Equations (7) then gives the general expression for the angular accelerations that will be experienced while moving the head in a rotating space vehicle having constant velocity. There results the following expressions:



$a_{G\theta}$ cross-coupled nodding acceleration

$\omega_{G\psi}$ cross-coupled turning acceleration

$a_{G\phi}$ cross-coupled rolling acceleration

$\omega_{G\theta} = \int a_{G\theta} dt$

$\omega_{G\psi} = \int a_{G\psi} dt$

$a_{G\phi} = \int a_{G\phi} dt$

θ_n nodding displacement

ψ_n turning displacement

ϕ_n rolling displacement

θ_e, ψ_e, ϕ_e Euler angular displacement using the order of rotation

t time

$\theta_G = \iint a_{G\theta} dt^2$

$\psi_G = \iint a_{G\psi} dt^2$

$\phi_G = \iint a_{G\phi} dt^2$

θ_{sc} backward tilt of semicircular canals from $X_b Y_b$ plane

ψ_{sc} rotation of semicircular canals from $X_b Z_b$ plane

X, Y, Z inertial space axes

X_b, Y_b, Z_b body axes

$\omega_{h\theta}$ nodding velocity — a fore and aft motion of the head at the neck or from the whole body

$\omega_{h\psi}$ turning velocity — a motion about the neck or long-body axis

$\omega_{h\phi}$ rolling velocity — a sideways motion of the head or from the body

These are angular head motions and may be from motions at the neck and shoulders or from body bending, etc.

ω_v vehicle rotational velocity

ω_{h_x} total angular velocity of head about rolling axis

ω_{h_y} total angular velocity of head about nodding axis

ω_{h_z} total angular velocity of head about turning axis

Subscripts: (See Figure 7-35)

lr, ll right and left lateral canals, respectively

pr, pl right and left posterior canals, respectively

ar, al right and left anterior canals, respectively

A dot over a symbol indicates its first derivative with respect to time.

Figure 7-58

Vectorial Representation of Head Orientation and Angular Motion in a Rotating Space Vehicle (After Stone and Letko⁽⁵⁸⁸⁾)

$$\left. \begin{aligned} \dot{\omega}_{n_x} &= \dot{\omega}_{n_\phi} - \omega_V (\omega_{n_\theta} \sin \theta_e + \omega_{n_\psi} \cos \theta_e \sin \psi_e) \\ \dot{\omega}_{n_y} &= \dot{\omega}_{n_\theta} - \omega_V (\omega_{n_\psi} \cos \theta_e \cos \psi_e - \omega_{n_\phi} \sin \theta_e) \\ \dot{\omega}_{n_z} &= \dot{\omega}_{n_\psi} + \omega_V (\omega_{n_\theta} \cos \theta_e \cos \psi_e + \omega_{n_\phi} \cos \theta_e \sin \psi_e) \end{aligned} \right\} \quad (9)$$

These Equations (9) as noted describe the total angular acceleration that would be experienced for any orientation of the head and for any head motion when in a vehicle rotating at constant angular velocity.

When the vehicle is not rotating ($\omega_V = 0$);

$$\left. \begin{aligned} \dot{\omega}_{n_x} &= \dot{\omega}_{n_\phi} \\ \dot{\omega}_{n_y} &= \dot{\omega}_{n_\theta} \\ \dot{\omega}_{n_z} &= \dot{\omega}_{n_\psi} \end{aligned} \right\} \quad (10)$$

which are the equations expressing our normal experiences (ignoring the subliminal effects of earth's rotation).

The differences between Equations (9) and (10) are thus the angular accelerations caused by the vehicle rotation and are herein called the cross-coupled angular accelerations.

$$\left. \begin{aligned} \alpha_{G_\phi} &= -\omega_V (\omega_{n_\theta} \sin \theta_e + \omega_{n_\psi} \cos \theta_e \sin \psi_e) \\ \alpha_{G_\theta} &= \omega_V (\omega_{n_\phi} \sin \theta_e - \omega_{n_\psi} \cos \theta_e \cos \psi_e) \\ \alpha_{G_\psi} &= \omega_V (\omega_{n_\theta} \cos \theta_e \cos \psi_e + \omega_{n_\phi} \cos \theta_e \sin \psi_e) \end{aligned} \right\} \quad (11)$$

These accelerations are those sensed by the semicircular canals and are the cause of the disquieting effects experienced in rotating devices particularly when the vision is restricted to the rotating frame of reference.

Equations (9) are the accelerations experienced by the head. The stimulation of each semicircular canal may also be of interest. The canal system is approximately orthogonal but is oriented in the head so as not to be aligned with the body axis system. This orientation varies with individuals so that the lateral canals are tilted back from 15° to 30° up in the front and the anterior and posterior canals are turned somewhere from 35° to 65° about an axis tilted back and about normal to the plane of the lateral canals (561). These differences may contribute to the different sensitivities to motions that exist among people. The stimulation of the canals is expressed as follows:

$$\left. \begin{aligned}
 \dot{\omega}_{sc_{lr}} &= \dot{\omega}_{n_x} \sin \theta_{sc} + \dot{\omega}_{n_z} \cos \theta_{sc} \\
 \dot{\omega}_{sc_{ll}} &= \dot{\omega}_{n_x} \sin \theta_{sc} + \dot{\omega}_{n_z} \cos \theta_{sc} \\
 \dot{\omega}_{sc_{ar}} &= \dot{\omega}_{n_y} \cos \psi_{sc} - \dot{\omega}_{n_x} \cos \theta_{sc} \sin \psi_{sc} + \dot{\omega}_{n_z} \sin \theta_{sc} \sin \psi_{sc} \\
 \dot{\omega}_{sc_{al}} &= -\dot{\omega}_{n_y} \cos \psi_{sc} - \dot{\omega}_{n_x} \cos \theta_{sc} \sin \psi_{sc} + \dot{\omega}_{n_z} \sin \theta_{sc} \sin \psi_{sc} \\
 \dot{\omega}_{sc_{pr}} &= \dot{\omega}_{n_x} \cos \theta_{sc} \cos \psi_{sc} + \dot{\omega}_{n_y} \sin \psi_{sc} - \dot{\omega}_{n_z} \sin \theta_{sc} \cos \psi_{sc} \\
 \dot{\omega}_{sc_{pl}} &= \dot{\omega}_{n_x} \cos \theta_{sc} \cos \psi_{sc} - \dot{\omega}_{n_y} \sin \psi_{sc} - \dot{\omega}_{n_z} \sin \theta_{sc} \cos \psi_{sc}
 \end{aligned} \right\} \quad (12)$$

These equations are based on the arbitrary assumption that the angular acceleration vectors of the canals are positive outward from the head and downwards. A substitution of Equations (9) into Equations (12) leads to expressions for the total angular acceleration experienced by each semi-circular canal. Table 7-59 shows the angular accelerations that would exist in a rotating space vehicle (or other rotating system) in the separate canals of the right ear. Assuming the range of orientation of the canals noted above, it is evident that in a nodding motion the stimulation of a given canal, particularly the anterior and posterior canals, can vary nearly 3 to 1 among various people. Further, in a turning motion of the head, a 2 to 1 variation in canal stimulation is possible among various people. These differences possibly could cause some people to adapt less readily to rotation than others, especially those with the greater stimulation, i.e., those with canals tilted 30° back and rotated 65° (588).

In rotating space vehicles the astronauts normally will be oriented when standing or sitting with the long body axis perpendicular to the axis of rotation which is represented by the value of $\theta_e = 0$. The head is then moved about that point of reference. The significant force acting is the centrifugal force along the long axis of the body (Z_b) and the otoliths are affected by this force only. Because of the presence of gravity on Earth it is absolutely impossible to simulate on Earth the situation just described. Thus, simulation is a compromise of the sundry factors acting.

Table 7-60 expresses the angular accelerations experienced in a rotating reference frame for various orientations of the long body axis (Z_b) from the vehicle rotational vector. The value of $\theta_e = 0$ (the long body axis perpendicular to the rotational axis) is the actual orientation that will exist in rotating space vehicles. The others represent conditions of simulation possible on Earth.

The results of Table 7-60 indicate greatly different cross-coupled angular accelerations for the three situations. An adaptation to one situation may not

Table 7-59

Canal Stimulation for Various Orientations of the Canals in the Head

(After Stone and Letko⁽⁵⁸⁸⁾)(Assume $\psi_e = \phi_e = \theta_e = 0$ with the head moving steadily through these values for consideration of this table)

Canal acceleration	$\theta_{sc} = 15^\circ$		$\theta_{sc} = 30^\circ$	
	ψ_{sc}		ψ_{sc}	
	35°	65°	35°	65°
Head nodding				
$\dot{\omega}_{sc_{tr}}$	$0.9659\omega_V\omega_{h\theta}$	$0.9659\omega_V\omega_{h\theta}$	$0.8660\omega_V\omega_{h\theta}$	$0.8660\omega_V\omega_{h\theta}$
$\dot{\omega}_{sc_{ar}}$	$0.1484\omega_V\omega_{h\theta}$	$0.2346\omega_V\omega_{h\theta}$	$0.2882\omega_V\omega_{h\theta}$	$0.4532\omega_V\omega_{h\theta}$
$\dot{\omega}_{sc_{pr}}$	$-0.2120\omega_V\omega_{h\theta}$	$-0.1094\omega_V\omega_{h\theta}$	$0.4096\omega_V\omega_{h\theta}$	$0.2113\omega_V\omega_{h\theta}$
Head turning				
$\dot{\omega}_{sc_{tr}}$	0	0	0	0
$\dot{\omega}_{sc_{ar}}$	$-0.8192\omega_V\omega_{h\psi}$	$-0.4226\omega_V\omega_{h\psi}$	$-0.8192\omega_V\omega_{h\psi}$	$-0.4226\omega_V\omega_{h\psi}$
$\dot{\omega}_{sc_{pr}}$	$-0.5736\omega_V\omega_{h\psi}$	$-0.9063\omega_V\omega_{h\psi}$	$-0.5736\omega_V\omega_{h\psi}$	$-0.9063\omega_V\omega_{h\psi}$

Table 7-60

Angular Accelerations for Various Orientations of Subjects in a Rotating Space Vehicle

(After Stone and Letko⁽⁵⁸⁸⁾)(a) $\psi_e = \phi_e = 0^\circ$

θ_e (a)	0°	-45°	-90°
$\dot{\omega}_{n_x} = \dot{\omega}_{n\phi} - \omega_V$	0	$-0.7071\omega_{n\theta}$	$-\omega_{n\theta}$
$\dot{\omega}_{n_y} = \dot{\omega}_{n\theta} - \omega_V$	$\omega_{n\psi}$	$0.7071(\omega_{n\phi} - \omega_{n\psi})$	$\omega_{n\phi}$
$\dot{\omega}_{n_z} = \dot{\omega}_{n\psi} + \omega_V$	$\omega_{n\theta}$	$0.7071\omega_{n\theta}$	0

(b) $\psi_e = 90^\circ; \phi_e = 0^\circ$

θ_e (a)	0°	-45°	-90°
$\dot{\omega}_{n_x} = \dot{\omega}_{n\phi} - \omega_V$	$\omega_{n\psi}$	$0.7071(\omega_{n\psi} - \omega_{n\theta})$	$-\omega_{n\theta}$
$\dot{\omega}_{n_y} = \dot{\omega}_{n\theta} - \omega_V$	0	$0.7071\omega_{n\phi}$	$\omega_{n\phi}$
$\dot{\omega}_{n_z} = \dot{\omega}_{n\psi} + \omega_V$	$\omega_{n\phi}$	$0.7071\omega_{n\phi}$	0

^aThe total angular accelerations are obtained by multiplying ω_V by the specific column of concern and adding the result to $\dot{\omega}_{n\phi}$, $\dot{\omega}_{n\theta}$, and $\dot{\omega}_{n\psi}$ as noted.

indicate adaptation to another because of the grossly different stimulations involved. The use of $\theta_e = 0$ would seem most appropriate for simulation since the Z_b lies in the plane of rotation, although not along the resultant G vector.

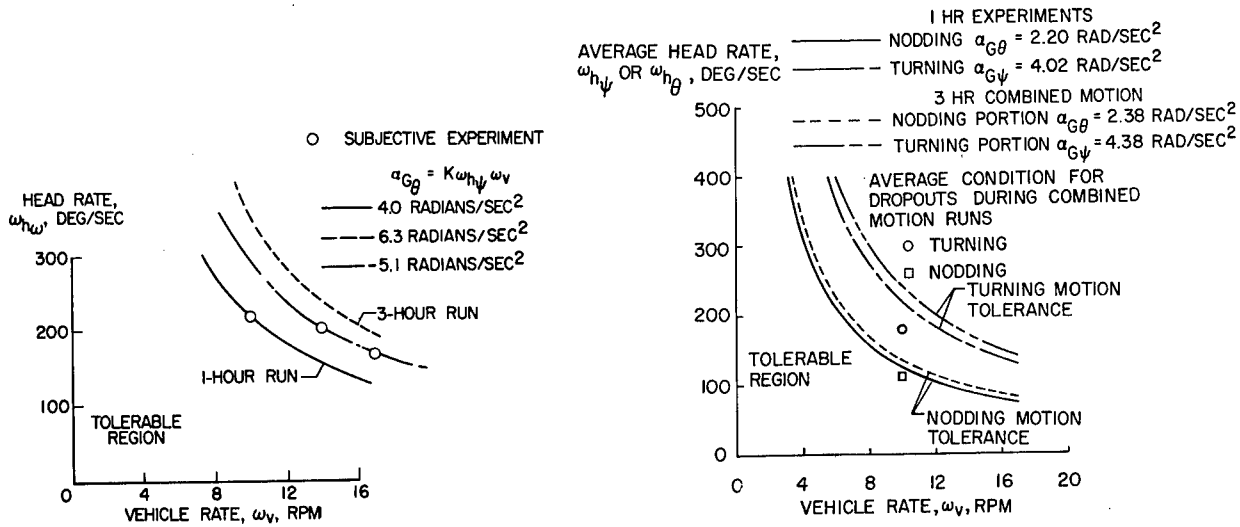
Recent studies on ground-based simulators have covered conditions where $\theta_e = 90^\circ$ (69, 242, 244, 256, 257, 259, 588); where $\theta_e = 0$ (454, 588, 589); and where $\theta_e = 45^\circ$ (50, 51, 451, 452, 453, 454, 455, 456).

Figures 7-55a and b, 7-56, and 7-58 review the physiology of movement in rotating rooms under 1 G where the axis of the body is parallel to the axis of rotation which is, in turn, parallel to the Earth-G vector ($\theta_e = 90^\circ$). Habituation to these effects are noted in Figure 7-56. More recent data are recorded on habituation, visual deprivation, vestibular testing, and biochemical responses in this type of rotatory environment (107, 180, 257, 339, 340). Nystagmographic data are available comparing ($\theta_e = 90^\circ$) conditions with conditions in which subjects are oriented with long-body axis radial to the axis of rotation ($\theta_e = 0$) (263). More recent studies from the NASA Langley Research Center shed some light on cross-coupling effects of nodding, turning, and moving in chronic rotation for $\theta_e = 0$ (69, 588, 589). The results can be summarized in Figure 7-61a, b, and c for head movements and symptoms found in a rotation simulator where feet were 15 ft from center of rotation. These are described in greater detail in References (588, 589). The head rates are the maximum voluntarily tolerated at any given vehicular rotation rate. These plots of head rate vs. the vehicle rate of rotation are hyperbolas along which the product of head rate ($\dot{\omega}_h$ or $\dot{\omega}_h$) times the vehicle rate of rotation (ω_v) is constant. These curves are, therefore, loci of constant cross-coupled angular acceleration. If the significant element in the disquieting effects of rotation lies principally in the tolerance to cross-coupled angular acceleration, constant values of this acceleration form boundaries of tolerance to rotation. This would imply that on a slowly rotating vehicle the subject could use and tolerate head motions with larger rates than he could on a rapidly rotating vehicle.

The results shown in Figure 7-61a are for head turning motions. The solid line results from an hour-long experiment wherein the rotation of the vehicle was increased in steps from 0 to 17 rpm. All subjects tolerated the motion to 10 rpm which is the data point upon which the solid curve is based. The cross-coupled angular acceleration for this condition is 4.0 rad/sec², and is an average for all subjects. The values of cross-coupled angular acceleration are based on the maximum values of head rates of rotation which are the peaks in the variation of head rate with time (589). Although there is a wide range of individual experience from this average value, all subjects were tolerant of 10 rpm and performed well. The other data points shown beyond this boundary and indicated by the dash-dot curve are average values for those subjects that tolerated rates of rotation greater than 10 rpm. As the vehicle rate of rotation was increased to 14 and 17 rpm these subjects decreased their rate of head motion in such a manner as to maintain a cross-coupled angular acceleration of 5.1 rad/sec². This is indicative of the fact that subjects adjust to a given situation to maintain tolerable conditions. The dotted curve in Figure 7-61a is based on the maximum head rates used during

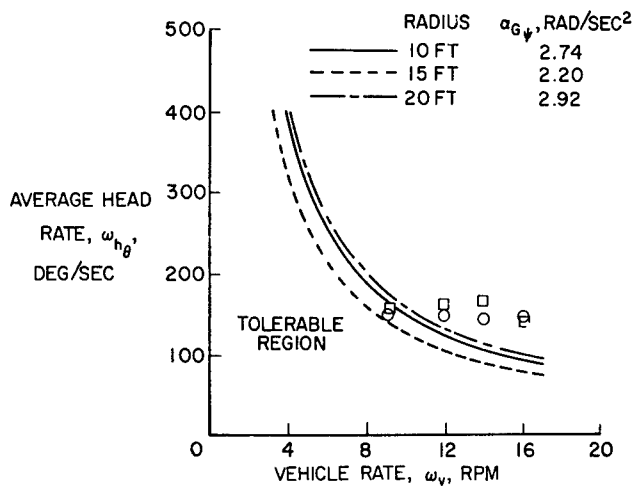
Figure 7-61

Tolerance to Cross-Coupled Accelerations While Turning and Nodding Head
(After Stone and Letko⁽⁵⁸⁸⁾)



a. Effect of Head Turning Rate and Duration of Exposure (15 ft Radius)

b. Effect of Duration of Exposure (15 ft Radius)



c. Effect of Different Radii on Tolerance to Cross-Coupled Angular Accelerations While Nodding Head

a 3-hour run at a constant vehicle rate of rotation of 10 rpm. The subjects of this experiment continued to increase their head rates as the test progressed and values used on this plot are those used at the end of the 3 hours. The differences between the solid and dotted curves are an indication of the adaptation that occurred in 3 hours. The fuzziness of vision and the general apprehension that existed in the short experiments disappeared from the subjects within an hour during these 3-hour runs. The tolerable cross-coupled angular acceleration for the case is more than 50 percent greater than for the shorter experiments.

The solid curve in Figure 7-61b is for a 1-hour experiment wherein the vehicle rate of rotation was increased stepwise from 0 to 10 rpm. At this last rate of rotation there was one subject who dropped out and four others who became uncomfortable. The test was therefore not extended to higher values of rotational rate. The cross-coupled angular acceleration for this case is based on the peak nodding head motions for those subjects that tolerated 10 rpm and is about 2.1 rad/sec^2 . This cross-coupled angular acceleration is only one-half of that generally established for turning head motions of Figure 7-61a. Again, the induced motion sensation that occurs when nodding the head is a turning motion for which the lateral canals are primarily affected. The time constant of the semicircular canals in response to head turning is about twice as large as the time constant for nodding and rolling motions. Cross-coupled angular accelerations which stimulate a turning sensation cause about one-half the tolerance level in a sense of motion where the time constant is twice as large as for other motions. The implication that there is some relation of the acceleration and the time period of cupula motion after an applied acceleration is apparent. However, during the tests discussed herein, there were few times when the head was still for 10 to 15 seconds, the time constant for lateral stimulation. An integration of the cross-coupled angular acceleration for the length of the time constant therefore may not be related to the tolerance boundaries shown regardless of the implications (588).

The other data shown in Figure 7-61b are for an experiment where both nodding and turning motions were used in a combined and random fashion. The dotted curve and the dash-double dotted curve are derived from these data. This experiment was run for 3 hours at a constant vehicular angular velocity of 10 rpm. The two to one ratio in turning to pitching motions is evident. The increase in tolerance for the 3-hour experiment over the 1-hour experiment is indicated by the shift upwards of the curves for nodding alone as well as for turning from the dash-dot curve which is replotted from Figure 7-61a. Adaptation to the combined motion appears slower than that to the individual motion of turning where a 50-percent increase occurred. This compares with about 5-percent increase in tolerance shown in Figure 7-61b even for the turning motion portion of the combined motions. Whether this is a result of increased work load where the subjects are concerned with two tasks or whether adaptation occurs more slowly when combined motions are used is a question requiring additional study. It has also been noted that the cross-coupled turning motion induced by nodding changes direction when the head is nodded back of its normal position and then moved forward. Such a change in direction of the induced stimulation may be more uncomfortable than the mere existence of the stimulation in one direction. Preventing

backward movement of the head by a collar is worthy of consideration if this proves true.

The effects of changing the radius of rotation are noted in Figure 7-61c where the average rates of tolerable head rotation are plotted for the radii of 10 and 20 feet as well as for the 15 ft radius of Figure 7-61 a and b, and, as noted before, show no decrease with vehicle rate of rotation. There is only a slight difference between the 10- and 20-foot radii, 2.74 rad/sec and 2.92 rad/sec, (157 and 167 degrees/sec) respectively. Both of these are somewhat larger than the value of 2.20 rad/sec (126 degrees/sec for the 15-foot radius. The cause probably relates to the previous discussion of head amplitude. Actually, at 16 rpm a cross-coupled angular acceleration of 4.52 rad/sec (260 degrees/sec) was tolerated. These results indicate no significant effect of radius of rotation indicating that performance and tolerance are essentially independent of radius. This conclusion would imply that the semicircular canals alone influence performance and tolerance for the conditions studied at least. Further, it implies the otoliths do not affect the results for the range of conditions studied, as the centrifugal force felt on the soles of the feet of the subjects ranged from slightly over $1/4 G$ to $1 \ 3/4 G$. The inclination of the total linear-acceleration vector ranges, respectively, from 74° to 30° from the long body axis, for these conditions.

Studies have been made at a 20-foot radius in the General Dynamics MRSS simulator under the condition of $\theta_e = 45^\circ$ (451, 455). The subjects were rotating at 12.2 rpm in a gimbaled room so that when standing perpendicular to the floor, the long axis of the subject's body along the resultant G vector was 45° from the spin plane. By seating the subject so that his body was depressed 45° downward toward the axis of rotation, the body was made coplanar with the plane of rotation with position similar to that of the Langley study. Adaptation is possible at the $\theta_e = 45^\circ$ to $\theta_e = 0^\circ$ for head nods (Y-axis turns in the plane of rotation) but not for Z-axis turns (90° from the plane of rotation). The Langley and General Dynamics studies suggest that head turns in a revolving space station should preferably be executed in the plane of system rotation for optimal performance during crew adaptation to rotation and that instruments on bulkhead be so placed as not to require head movements more than 45° out of the plane.

Comparison has been made on the General Dynamics MRSS simulator of different rotation rates (7.5, 10, and 12.0 rpm) on rotary tracking performance at a 20-foot radius (50). Perceptual-motor ability, with a rotary tracking designed to elicit untoward Coriolis effects, suggests that satisfactory hand-eye coordinations can be performed in space vehicles rotating at all of these velocities. Performance at 10.0 rpm was significantly better than at the other two rpm's showing least decrement and the fastest adaptation.

The Coriolis force acting in rotating vehicles is of considerable concern (see Figure 7-52). In a rotating space station the floor normally used lies in a plane always parallel to the axis of rotation. When moving on this floor the astronaut can move along the floor in a direction parallel to the axis of rotation for which the Coriolis force is zero or he can move along the floor perpendicular to the axis of rotation for which the Coriolis force causes the astronaut to become effectively heavier or lighter as he increases or

decreases the centrifugal force. There is the possibility of degrading performance as one approaches weightlessness when moving counter to the direction of rotation. It is not felt, however, that any disquieting effects would occur from this situation (588). In a study of this problem, tests of equilibrium and walking along the radius also show less decrement but also less adaptation at 10 rpm than at 5, 7.5, or 12 rpm (454). Subjects in the walking tests had begun to adapt to the rotating system by making the necessary compensations to overcome Coriolis forces and carried this learning process over into the tests during post-rotation where deviations to the right of path suddenly became errors to the left in the static environment. No such post-rotation effect was evident in the balancing tests, where recovery was immediate when the room stopped spinning. The subjects who were confined to bunks during rotation did not show any post-rotation disorientation.

Studies have also been made on several psychomotor functions during 4 days of rotation at 6 rpm and 19-foot radius in the MRSS (452, 453, 456). This gives a G of 0.23 which would be increased to 0.49 G at a 40-foot radius. Data are available on perimetric and orthoscopic tests of vision, caloric tests, oculogyral illusion, ballistic aiming, brachial and digital proprioception, visual and blind tandem walking, steadiness, logical inference, response analysis, time estimation, and mathematics. In all of these tests except for tandem standing and tandem walking with eyes closed, subjects performed effectively and adapted rapidly with no need for static readaptation upon step-wise spin-down. These two tests showed no improvement with time; and along with digital proprioception, poor performance 8 hours post-rotation. The deletion of visual cues and kinematic stimuli to the deep proprioceptors may account for the sensitivity of these tests to inertial change arising from radial movements in the absence of a strongly orienting visual framework.

Operating Limits for Rotating Space Stations

In view of these data, one can speculate on tentative design limits for future space stations. Previous attempts had been made before adequate empirical data were available (144, 388). The basic problem is one of maintaining the angular velocity at a tolerable maximum, with a spin radius adequate to keep the G level and Coriolis/gravity ratio within satisfactory ranges.

A choice of G from 1/5 to 1 appears suitable. The limits for Coriolis/gravity ratio are as yet not clear. In orbital flight, the force acting upon any particle inside can be described by the expression (21):

$$F = m(a + \omega^2 r + 2\omega v \sin \theta)$$

where: F = total force on the particle

m = mass of the particle

a = linear acceleration of the particle
with respect to the vehicle

ω = angular velocity of the vehicle

r = radial distance from the axis of
rotation to the particle

v = linear velocity of the particle with
respect to the vehicle
 θ = angle between axis of rotation and
direction of " v "

The first term within the parenthesis represents linear acceleration. The second term is the rotogravity acceleration and is directed away from the axis of rotation of the vehicle. The last term is the Coriolis acceleration. While Coriolis acceleration varies linearly with the angular velocity of the vehicle, rotogravity varies exponentially. The Coriolis acceleration is independent of the spin radius, while rotogravity is dependent. It is desirable from the engineering aspect to have a short radius. With a short radius, either the G level must be kept low or the angular velocity high. Reducing the G by shortening the radius has no concurrent effect upon the Coriolis force, thus increasing the critical Coriolis/gravity ratio. Reducing the angular velocity with constant radius produces the same undesirable effect.

The MRSS studies noted above indicate that for Z-axis head turns of 70° or 1.2 radians/second in the rotary pursuit task and with the room rotating at a constant angular velocity of 0.75, 1.0, and 1.2 radians/sec. (43, 57 and 69 degrees/sec), the cross-coupled product (rms values) equals respectively 0.9, 1.2 and 1.4 radians/sec.² (52, 69 and 80 degrees/sec.²). Each of these values is in excess of earlier empirical figures for suggested nausea threshold of (cross-coupled) 0.6 radians/sec.² (3.6 degrees/sec.²) and more than one order of magnitude above the threshold estimate of cross-coupled 0.06 radians/sec.² (3.6 degrees/sec.²) for Coriolis awareness (92) (see also Figure 7-61). The cross-coupled thresholds for nausea and Coriolis detection are currently being evaluated (449). They appear sensitive to the specific canals being stimulated and, therefore, to the range of motion of the head relative to the spin axis as well as to the angular rates of spin and of head movement. Such factors as crossing the plane of rotation and duration of exposure may play a role. For example, the threshold appears to be dependent on the position of the head but, in general, it falls right around $3.6^\circ/\text{sec}^2$ which is the same as $0.06 \text{ rad}/\text{sec}^2$ (or $0.06 \text{ rad}^2/\text{sec}^2$) as stated in Ref. (92). The threshold is highly dependent on the time of stimulus. The $3.6^\circ/\text{sec}^2$ was derived at $5.7^\circ/\text{sec}$. through a 90° head turn at 6 rpm ($36^\circ/\text{sec}$.). When head rotation rates were increased to 17.2° and $22.9^\circ/\text{sec}$., the threshold for oculogyral illusions jumped as high as 18° to $24^\circ/\text{sec}^2$. This last value is even more dependent on position of head turn in the plane perpendicular to the plane of rotation. Periodic turnings of the head at intervals that are small (a few secs.) relative to the accepted period of the normal cupula (20-30 seconds) produce little vestibular response after the initial turn, probably as a result of the cupula damping coefficient (51, 589). The improved motor performance at about 10 rpm and 20 foot radius suggests that there is an optimum range, with the G increasing exponentially and the Coriolis forces linearly as the angular velocity rises, wherein the G attenuates the effect of the Coriolis forces to a greater degree than it retards performance (50). More data are needed on this "inertial buffer zone."

In view of these findings a revised comfort zone for spin rate vs. spin radius has been suggested as shown in Figure 7-62 (591). The gravitational level at the upper bound, is 1 G. The lower bound, determined from

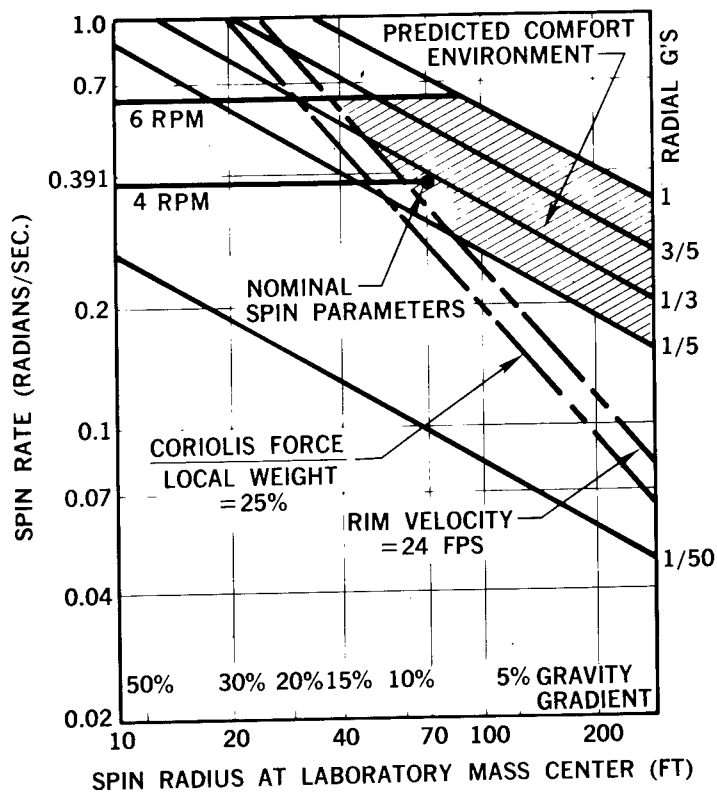


Figure 7-62
Tentative Rotational Limits
in Space Vehicle Design
(After Stone and Piland⁽⁵⁹¹⁾)

parabolic flight studies, is usually taken to be about $1/5$ G, which is required to provide adequate friction for locomotion (28, 497, 591). When the man moves tangentially within the vehicle, the Coriolis force which adds to or subtracts from the centrifugal force causes the man to become "heavier" or "lighter," depending on his walking direction. This condition would not seem difficult to adapt to unless he should become excessively heavy or too light for proper traction, or the change from the normal artificial gravity was such as to be disturbing. If the rate of walking is arbitrarily selected to be 4 ft/sec (relatively brisk), difficulty in walking would not necessarily appear between gravity levels of $1/6$ to 1.0 G and rotational rates up to 4 rpm. However, a gravity level within these limits may not be sufficient to allay all ataxia (lack of normal coordination) problems. The proportional change in gravity level as one moves about or moves things about may be disturbing and difficult to accommodate to if it exceeds some proportion of the basic "G" level. A criteria selection in this respect would require experimentation to determine at what level of change difficulty may be encountered.

Motion perpendicular to the floor occurs when moving radially such as climbing toward or away from the center of rotation. This particular motion undoubtedly would only be performed occasionally by an individual, but the characteristic Coriolis forces involved may be frequently encountered when raising and lowering objects. The criterion to be considered for radial motion would be one where the Coriolis force would not exceed a certain percentage of the normal weight (at that gravity level) of the object or person. Analysis of vectors indicates the resultant gravity vector would tend to make

climbing seem like it is being performed on a tilted ladder. Possibly the best solution would be to arrange the ladders such that the crew members are forced against the ladder by this acceleration. There would then be up and down sides of a ladder. Movement of dropped objects would also be a minor consideration in setting Coriolis force /weight ratios.

Radius arms of greater than 40 ft are generally thought to be required to produce gravity gradients below 15% (see Figure 7-64 and related discussion). From the physiological standpoint, the implications of a gravity gradient environment are vague and most difficult to establish. The fact that a person is heavier when he squats than when he is standing erect seems of little significance. However, one may consider that the hydrostatic pressure distribution within the body may be of significance. The gravity gradient in rotating vehicles causes a nonlinear hydrostatic pressure distribution in the body fluid systems and is thus different than that on Earth. In the Earth's environment, that portion of the pressure distribution due to gravity in an erect man's fluid system, such as the cardiovascular system, varies linearly with his height on Earth. Actually, the nonlinear pressure distribution in the rotating environment is a function of the square of the radii involved. The ratio of the pressures at the heart and feet, for example, should be a certain portion of that in Earth gravity (see Figure 7-64).

The final bound depicted on this curve is based on space station rim velocity; at too low a velocity, an astronaut's walking counter to rotation would reduce the gravitational levels appreciably below those intended. This figure shows that radius arms of about 70 ft are generally desirable; however, this distance may be difficult to achieve in practice with configurations being contemplated today.

In addition to this spin envelope, the general principles that should be observed in a rotating space station design can be summarized as: (388)

1. Radial traffic should be kept to a minimum.
2. Transport across the spin axis and human activity at the spin axis should be prohibited unless the hub is nonrotating.
3. The living-working compartment should be located as far as possible from the axis of rotation.
4. The compartment should be oriented so that the direction of traffic--i.e., the major dimension of the compartment--is parallel to the vehicle spin axis.
5. Crew duty-station positions should be oriented so that, during normal activity, the lateral axis through the crew member's ears is parallel to the spin axis. In conjunction with this requirement, the work-console instruments and controls should be designed so that left-right head rotations and up-down arm motions are minimized.
6. Sleeping bunks should be oriented with their long axes parallel to the vehicle spin axis.

7. The presence of confusing visual stimuli should be minimized. For example, the apparent convergence of the vertical from any two points separated tangentially should be played down by proper interior decoration and, except for necessary observation ports, which should be covered when not in use, the living-working compartment should probably be windowless.

A factor often overlooked is the high rpm desired for vehicle stability (351, 363, 453). Disturbances, such as docking impacts and active or passive changes in crew or hardware mass, may cause many combinations of structural and force-field oscillations, most of which could be significantly detrimental to crew function. The stimuli to the labyrinth due to vehicle instability can complement those due to the crewman's active head movements. The wobble or spin axis precession and precession of the vehicular angular momentum vector, more easily generated in vehicles of low mass and spin rate, may present the crewman with illusions of complex and ever-varying tilting of the floor as his body perceives the resultant of the linear acceleration oscillating along his longitudinal body axis and the linear acceleration normal to this axis. Simultaneous dynamic mass unbalances along both transverse axes would increase the complexity of the vector pattern and the resulting disturbances. Much more work is required especially at the higher spin rates before the tentative limits of Figure 7-62 become meaningful.

ZERO GRAVITY ENVIRONMENT

Zero or nulled gravity, the major novelty in the orbital environment, has been the object of many speculative and empirical studies. Data now available on physiological and performance responses in orbital flights up to 14 days duration (35, 444, 591) complement earlier studies in parabolic flight maneuvers (22, 23, 197, 202).

A chart briefly summarizing the effects of zero gravity in drop tower, parabolic flight and orbital testing is shown in Table 7-63a. Table 63b presents more specific findings from immersion, bed rest, parabolic flight and orbital studies in the older literature.

Responses to zero gravity may be classified as cardiovascular, respiratory, metabolic, and psychomotor responses. These are covered below. Many of the clinical problems predicted for prolonged exposure to this condition have received recent review (62), and the reader is directed to this study for a more detailed clinical picture than is presented here.

Cardiovascular Effects (62)

By means of bed rest and water immersion, ground-based experiments have attempted to simulate long term weightlessness by minimizing the effect of intravascular hydrostatic pressures due to gravity (1, 37, 38, 153, 225, 229, 231, 232, 353, 354, 355, 391, 392, 393, 424, 426, 429, 576, 579, 599, 618, 619, 625, 632, 633, 635, 636, 637, 666, 688). Much of the data

Table 7-63

Response of Humans and Animals to Null Gravity

a. Physiological Effects of Weightlessness on Man and Animals

Animal	Dynamic Conditions	Effects	Reference
Sensory and Neurophysiological Effects			
1	Man	Subgravity tower	Upward deviation when aiming a stylus and attempting to hit a bull's-eye ("overshoot")
2			Increased tapping rate and distribution of marks in "upper right" sector of test chart
3	Man	Aerodynamic flight parabola ^{1,2}	Upward deviation when aiming a stylus and attempting to hit a bull's-eye ("overshoot")
4			Difficulty in placing crosses in diagonally arranged squares, especially when blindfolded ("overshoot")
5			Apparent motion and displacement of a real target in the direction of gravity ("oculogravic illusion")
6			Apparent motion and displacement of an afterimage in the direction opposite to that of gravity ("oculogravic illusion")
7			Retardation in speed of execution of motor functions in the absence of discoordination symptoms
8			Loss of gravitational vertical; sensation of floating, being lifted, and flying upside down
9			Shortening of illusions of counter-rotation and afterrotational nystagmus after a series of parabolic flights
10			Mass-weight discrimination changed in weight-lifting task
11			Recovery from acceleration stress impaired before and after weightless state
12		Cargo aircraft	23 of 45 subjects became motion sick
13		Fighter aircraft	5 of 16 subjects became motion sick
14			6 of 18 subjects became motion sick
15		Suborbital flight, MR 4 ^{1,2}	Grissom: tumbling sensation during transition from accelerated flight to weightlessness
16		Orbital flight ^{1,2}	Glenn: brief forward tumbling sensation
17		MA 6	Schirra: sensation of traveling upside down
18		MA 8	Cooper: sensation of traveling upside down
19		MA 9	Cooper: sensation of traveling upside down
20		Vostok 2	Titov: vertigo, nausea, rolling, sensations of illusion
21		Vostok 3	Nicolayev: sensations of illusion and traveling upside down
22		Vostok 4	Popovich: sensations of illusion and traveling upside down
23		Vostok 5	Bykovsky: decreased oculomotor activity; asymmetry of nystagmoid movement
24		Vostok 6	Tereshkova: decreased oculomotor activity; asymmetry of nystagmoid movement
25		Voskhod 1	Feoktistov and Yegorov: sensations of illusion and traveling upside down. Yegorov: mild nausea
26	Cat	Aerodynamic flight parabola	Labyrinthine posture reflex (righting reflex) ceased to function after several seconds of weightlessness
27	House mouse	Aerodynamic flight parabola	Mice without labyrinthine function less disoriented than normal mice

(After Gerathewohl and von Beckh⁽²⁰³⁾)

Table 7-63 (continued)

a. Physiological Effects of Weightlessness on man and Animals (continued)

Animal	Dynamic Conditions	Effects	Reference
27	Rabbit	Subgravity tower	Righting reflex inhibited when subjects blindfolded
28		Aerodynamic flight parabola	Oculomotor reflex opposite to direction of gravity
29	Pigeon	Aerodynamic flight parabola	Posture reflex failed whether subjects were blindfolded or not; random movements and floating
30	Water turtle	Aerodynamic flight parabola	Inability to project head when attempting to aim accurately at offered bait. Turtles without labyrinthine function have advantage.
31	Goldfish	Aerodynamic flight parabola	Swimming upside down, on the side, etc.
Respiratory Effects			
32	Man	Aerodynamic flight parabola	Recovery from acceleration stress impaired before and after weightless state
33		Orbital flight Mercury flights	Slightly decreased pulmonary activity
34		Vostok 3, 4	Nicolayev, Popovitch: slightly decreased pulmonary activity
35		Voskhod 2	Velyayev, Leonov: two- to threefold increase in pulmonary ventilation
36	Dog	Orbital flight, Sputnik II	Laika: decrease in frequency of respiration
Cardiovascular Effects			
37	Man	Aerodynamic flight parabola	Recovery from acceleration stress impaired before and after weightless state
38		Orbital flight ⁵ Mercury flights	Cardiac activity increased
39		Vostok 1-6; Voskhod 1	Increased pulse fluctuations in the duration of cardiac cycle; cardiac activity reorganized; tendency toward lowered cardiac activity
40		Postorbital flight MA 8	Schirra: orthostatic hypotension persisted several hours after landing
41		MA 9	Cooper: orthostatic hypotension, accompanied by accelerated pulse and blood pressure responses, persisted 9-19 hr after landing
42		Vostok 1-6	Orthostatic hypotension
43	Dog	Orbital flight, Sputnik II	Laika: heart rate took 3 times longer to return to normal than in preflight laboratory experiments in which the dog was exposed to G profiles similar to those of the launching acceleration
Metabolic Effects			
44	Man	Orbital flight MA 7	Carpenter: mobilization of skeletal minerals
45		Gemini IV	White, McDivitt: bone mass losses
46		Voskhod I, II	Some strain on lipid metabolism; increase in cholesterol levels

1 Disorientation, which can be extreme without visual cues, was prevented during orbital flights by maintenance of visual control. ² Since these short exposures (> 1 minute) to weightlessness were necessarily preceded and followed by phases of G loads, the experiments revealed the effects of alternating acceleration and weightlessness rather than the effects of weightlessness per se. ³ The extent to which weightlessness alone is responsible for the deconditioning phenomenon is difficult to assess, since astronauts are also exposed to multiple stresses, such as dehydration, high temperature, recumbency, and muscular inactivity during orbital flights.

Table 7-63 (continued)

b. Response to Weightlessness Found in Early Experiments

	<u>Short-term Effects</u>	<u>Orbital Flight Data</u>	<u>Submersion Effects</u>	<u>Bed-rest Effects</u>
	Free-fall, frictionless devices, Keplerian trajectory, * Mercury ballistic flights	Project Mercury (441) primarily (Vostok flights V1 and V2 (638))	Head-out submersion (HOS) Complete submersion (CS)	Normal subjects
<u>General Metabolism</u>				
Metabolic rate	--	Low-residue balanced diet pre-flight; low-caloric intake inflight	Decreased (230)	Decrease 6 - 9% (37, 134, 602)
Body weight	--	Observed losses due to low-caloric intake and dehydration	Variable (230, 238)	Variable depending on caloric balance (37, 134, 602)
Body temperature	--	Elevated due to thermal stress	Depends on water temperature (34, 230, 238)	No effect
Water Balance	--	Diuresis in one, low intake and low or normal urine volume in three Mercury astronauts	Diuresis during both HOS (230) and CS (232)	Diuresis (37)
Electrolyte balance	--	Post-flight Na ⁺ and Cl ⁻ retention with rehydration	Na ⁺ losses, HOS (230)	Equilibrium (134)
<u>Musculoskeletal System</u>				
Nitrogen balance	--	Not measured	Equilibrium or negative (230, 238)	Equilibrium or negative, depending on method of calculation (37, 134, 602)
Muscle girth and strength	--	No change	Little or no change reported (230, 238)	Only slight wasting, little or no loss in strength (37, 134, 602)
Calcium excretion	--	No increased excretion	--	Sustained loss despite supine bicycle exercise (39)
<u>Cardiovascular System</u>				
Resting responses				
Pulse	Abrupt decrease in heart rate on transition to weightlessness* (279)	Normal values at rest, work, and sleep	--	+0.5 beats/minute per day (602)
Pressure	Influenced by prior G; resting value decreased while weightless* (279)	Normal values at rest, work, and sleep	Reduced pulse pressure (228)	Increase (602)
Stroke volume	--	--	--	Probable decrease (602)
Cardiac output	--	--	--	No major change (602)
Peripheral resistance	--	--	--	No marked change (602)
Blood volume	--	Reduced in dehydration	Plethora, elevated hematocrit (230) Deterioration (228, 230)	-9.3% (602)
Tilt-table response	Abrupt decrease in heart rate on transition to weightlessness* (279)	Transient faintness due to orthostasis on capsule egress with elevated heart rate--188; confirmed by tilt-table test post-flight		Deterioration (34, 134)
Acceleration tolerance	No change	No apparent effect; good performance on reentry	Decreased--small but significant (34, 230)	--
Exercise tolerance				
Work capacity	--	Maintained; work subjectively easier; pulse rate response slightly greater and slightly slower in return to normal	Decreased (228)	Decreased, but capacity can be maintained by supine exercise (39)
Vasomotor activity	--	--	--	Response to supine exercise indicates effective arterial vasomotor activity but decreased venomotor tone (37)

* In the body of the table, those data taken under the conditions of the Keplerian trajectory are marked with an asterisk.

Table 7-63 (continued)

b. Response to Weightlessness Found in Early Experiments (continued)

	<u>Short-term Effects</u>	<u>Orbital Flight Data</u>	<u>Submersion Effects</u>	<u>Bed-rest Effects</u>
	Free-fall, frictionless devices, Keplerian trajectory, * Mercury ballistic flights	Project Mercury--MA-9(441) Vostok flights V1 and V2(638)	Head-out submersion (HOS) Complete submersion (CS)	Normal subjects
<u>Mechanical Effects</u>				
Swallowing	No problem with proper food containers and training* (279)	No problem with proper food containers and training	--	--
Urination	No problem (365, 384)	No problem; bladder sensation normal	--	--
Free objects	Dust, droplet, and food crumb problem* (279)	Dust, droplet, and food crumb problem	--	--
<u>Sensations</u>				
Falling	Induced by prior G; absent when free-floating* (539)	Not experienced	--	--
Motion sickness	Related to G-transition* (383)	One subject (Titov)	--	--
Orientation	Orientation unrestrained decays in dark, and tactile sensations become important; any surface can become floor for the individual* (539)	Perceives earth or vehicle relative to self	Otolithic sensitivity decreased in certain postures (365, 384)	--
Illusions	"Oculoagravic" illusion observed*(384); no significant difference in semicircular canal sensitivity when weightless compared to 1G-- Oculogyral illusion*(204)	Change in apparent position of objects in peripheral visual fields; head motion not disorienting	Illusions related to sensory monotony (384)	--
Vision	Small decrement in visual acuity* (279)	Sightings indicate importance of pattern vision; no apparent decrement in acuity, color vision, or light sensitivity	--	--
<u>Performance</u>				
Mass discrimination	Difference threshold twice as large for masses as compared to weights (279)	--	--	--
Motor	Body restraint, hand-holds, tethers and adhesive footgear required for effective performance, closed force tools recommended; eye-hand coordination and object positioning shows overshooting, slight decrement in switch operation; rapid adaptation to altered motor requirements* (539)	No operational decrement in restrained subject, as evidenced by reentry performance	Vigilance, discriminative reaction time, and complex task performance show small decrements, HOS(279) overshooting and applied force changes related to water displaced, CS (434)	--
Sleep	Disorientation on sudden awakening* (384)	Frequent dozing; oriented rapidly on awakening (one subject)	Diminished requirement (230, 231)	--

* In the body of the table, those data taken under the conditions of the Keplerian trajectory are marked with an asterisk.

in this section are taken directly from a recent summary of these research efforts (62). The extrapolation to operational space conditions of cardiovascular findings in individuals exposed to prolonged bed rest or complete water immersion must be guarded, however, for these conditions do not completely eliminate the effects of gravity on the cardiovascular system. The degree of physical and cardiovascular "fitness" maintained under such conditions with periodic exercises, does not match exactly those found on space flight.

Most observations of cardiovascular responses of astronauts exposed to weightlessness have been made in the immediate post-flight period. Cardiovascular data for American missions (up to 14 days) (35, 142, 139, 398), and Soviet missions (up to 5 days) have been reported (19, 35, 190, 333, 439, 474, 542, 543). Findings must again be viewed with caution. Confinement, limited physical activity during missions, and post-flight fatigue are factors affecting the cardiovascular system similar to those which have been predicted for weightlessness. Post-flight data may, on occasion, have also reflected the effects of dehydration, and physiologic events which are associated with the vague feeling of "let-down" often experienced after a prolonged emotionally and physically stressful event.

In up to 42 days of bed rest, 7 days of complete water immersion and 14 days of weightlessness, recordings of systolic and diastolic pressures, pulse-rate, heart sounds, and electrical activity of the heart have remained within normal limits, even in the face of marked physical inactivity which led to diminished exercise tolerance (62). Soviet studies of bed rest for up to 20 days have shown somewhat wider but not serious cardiovascular changes called the "myocardial hypodynamia syndrome" (472). It appears unlikely that prolonged weightlessness would significantly alter cardiac function if cardiac work capacity is maintained through physical exercise while in orbit.

Cardiovascular adaptation to prolonged weightlessness results in lowering of blood volume with decreases in both the plasma and red cell fractions of the blood. In conditions of bed rest and complete water immersion, healthy subjects have consistently demonstrated an acute fall in plasma volume, accompanied by a diuresis and a loss of weight. Most of this initial contraction of blood volume has occurred during the first 24 to 48 hours of exposure to these conditions (354). The maximum decrease in plasma volume observed has usually been in the range of 500-700 ml, or about 10 percent of the body weight (231, 354, 424, 426). Figure 7-65b (crosses) shows the wide scatter found from person to person, all on a similar bed-rest protocol for equal time. Although decrease in blood plasma leads to hemoconcentration, prolonged bed rest studies have demonstrated that over a period of many days the hematocrit returns to normal values, presumably due to rehydration of the plasma or suppression of red-cell production (354, 426, 427). It should be pointed out, however, that in spite of some evidence to the contrary, bed rest studies of up to 42 days in duration have yielded data indicating that after a typical initial decrease, blood volumes tend to return toward pre-exposure values (134, 636).

Post-flight data on the command pilots and pilots of the 4 and 8 day Gemini missions indicated that the blood volume also decreases in the

weightless environment (35, 139) (see Figures 10-41 a and b). A 7 to 15 percent decrease of blood volume occurred during these missions. The decrease in plasma volume was 4 to 13 percent. As compared to bed rest studies, the loss of red cell mass was accelerated, possibly due to a combination of the 5 psia-100% oxygen environment and vitamin E deficiency (356, 357, 504, 505). (See Oxygen-CO₂ - Energy, No. 10.) A weight loss of usually 2 to 5 percent of body weight, recorded after these and previous space missions may be due only in part to this decrease of blood volume. Weight loss did not correlate with mission duration or plasma volume, and pre-flight weights and plasma volumes were restored rapidly by fluid intake in the post-flight period (35, 650). Immediately after the 14 day Gemini mission, the blood volumes of both astronauts were the same as those recorded pre-flight. An increase of plasma volume at some time in the mission had compensated for a decrease of red cell mass similar to that observed after the 4 and 8 day missions. Plasma volume decreases mostly during the first 48 hours of bed rest, and then changes little over a period of several weeks (355).

The cause of the decrease in blood volume and the diuresis which occur during bed rest, complete water immersion and probably weightlessness has been summarized as follows (62). Negation of the gravitational component of intravascular hydrostatic pressure due to gravity leads to a headward redistribution of blood. Central venous channels are distended, leading to stimulation of central venous blood volume receptors, located mainly in the right atrium (185, 186, 187). Through reflex pathways, antidiuretic hormone production is probably inhibited. The resulting increase in plasma water excretion reestablishes normal central venous volume. Due to one or more possible mechanisms involving venous and possibly arterial volume sensors as well as osmoreceptors, aldosterone production is suppressed, leading to a variable natriuresis or sodium excretion (62). The constancy of osmotic composition appears to be sacrificed in favor of the constancy of blood volume (391). No direct evidence of a diuretic factor appearing in the blood plasma has been found (185). Renal hemodynamics do not seem to be altered to a significant degree (391).

Dehydration brought on by thermogenic and non-thermogenic sweating at the terminal phases of the mission, decreased water intake, accompanied by thirst depression during the mission and depression of ADH by stress may have all played a role in producing some of the post-flight dehydration seen in the Gemini program (62, 333, 444, 650). The daily time course of dynamic changes in the volume of blood, and in its plasma and red cell fractions in the weightless environment cannot be predicted at the present time. Rebound of blood volume may be attributed to expansion of the venous circulation as peripheral venous tone decreases in adaptive response to weightlessness. On the other hand, the rebound of volume might be also due to decreased sensitivity of blood volume receptors in adaptation to chronic exposure to relatively high central venous pressure.

One result of the loss of blood and extravascular volume is orthostatic intolerance. This has been shown after space flight (35) as well as after water immersion and bed rest simulation in the many references noted above. Exposure to a tilt table test, a provocative test of orthostatic

intolerance, results in an excessive increase in heart rate, an excessive narrowing of pulse pressure and a fall in systemic arterial blood pressure while passively maintaining the erect posture (627). Failure of cardiovascular compensation to gravity leads to the so-called vasodepressor reaction, the manifestations of which are presumably due to an overwhelming increase in parasympathetic nervous system activity (353, 393). This reaction is characterized clinically by pallor, nausea, dimming of vision, sweating, "air-hunger," and eventually loss of consciousness, arising from an acute fall in systemic arterial blood pressure, occasioned by bradycardia and a decrease in peripheral vascular resistance.

Signs and symptoms of orthostatic intolerance have consistently appeared after as little as one week of bed rest (37, 134, 393, 427, 602) (see Figure 7-64a) and 6 to 12 hours of complete water immersion (227, 229, 231, 233, 393). Orthostatic intolerance was observed after the 9 and 34 hour, one-man Mercury missions, and for periods of up to 50 hours after the 4, 8, and 14 day, two-man Gemini missions (35, 142). The 14-day Gemini pilot experienced a vasodepressor tachycardiac reaction during his first post-flight tilt; his responses to subsequent tilts were similar to those of the other Mercury and Gemini astronauts. The time for the return of the normal pre-flight response to tilt has not correlated with either the duration of space flights to date, or decreases in blood volume which occurred. In the 14-day flight, both pilot and copilot had normal tilt responses by the second post-flight day.

It has not been determined with certainty what cardiovascular adaptations to simulated and actual weightlessness might have occurred to account for the decreased orthostatic tolerance that resulted from exposure to these conditions (62). On standing upright, cardiovascular reflex mechanisms increase heart rate and augment adrenal epinephrine output to strengthen cardiac muscle contraction. Arteriolar tone is also increased in dependent parts of the body to maintain the required distribution of cardiac output to these parts. Venous pooling in the lower regions of the body is minimized to assure an adequate return of blood to the heart. This appears to be accomplished mainly by a reflex increase in venous tone, by the restricting effect of skeletal muscle tone on venous distension, by the pumping action of contracting leg muscles on the veins and by venous valve competence (516). Through mechanisms outlined above, blood volume must also be maintained in the face not only of gravitational pooling of blood, but also of transudation of protein-free fluid into the extravascular spaces of the lower extremities caused by excess intravascular over extravascular pressures, especially in loosely bound tissues. The tension created in tissues as fluid is forced into them would also serve to restrict venous distension.

The decrease of blood volume and reabsorption of fluid transudate from tissues of the lower extremities during exposure to weightlessness would diminish orthostatic tolerance. Any decrease of blood volume in a normal active individual from any cause, such as blood loss or dehydration, will result in a strain being placed on normal mechanisms required to maintain cardiovascular integrity in the upright position. The observations that there has been no correlation between the amount of blood volume decrease and the degree of orthostatic intolerance resulting from prolonged bed rest, and that post-flight Gemini astronauts demonstrated orthostatic intolerance for many

hours after their blood volumes returned to pre-flight levels, suggest that cardiovascular adaptations to weightlessness other than decrease in blood volume contributed to this orthostatic intolerance (35, 139, 142). Loss of skeletal muscle tone and vascular tone, especially in the arterioles and veins of dependent parts of the body, may predispose to orthostatic intolerance by failing to maintain normal distribution of cardiac output and by allowing excessive pooling of venous blood and fluid transudation (35, 427). Diminished responsiveness of vasoconstrictor mechanisms after deconditioning might be reflected by decrease of urinary norepinephrine excretion during upright tilt (225, 227, 608). More data are needed on these mechanisms especially on the roles of in-flight exercise and post-flight fatigue in alteration of responses.

The operational significance of the degree of tilt table intolerance as has been seen in space flights is not clear. The tilt table test is a rather severe test of homeostatic capacity. One may speculate that adaptation to subsequent accelerative, thermal, dehydrative, hemorrhagic and, possibly, hypoxic and exercise stress may be reduced (62, 82, 250, 251, 352, 494, 623, 650, 667). Quantitative data on these reductions are available only from these simulator studies. Tolerance to Gemini reentry profiles, predicted from bed rest simulation, (428) has been corroborated in flight (35).

Prevention of these cardiovascular and fluid adaptations to weightlessness may be of some value in space operations (62, 591). Techniques are:

EXERCISE	ACCELERATIVE
PRESSURE	Space station rotation
Positive pressure-cuff	Short-radius centrifuge
Lower body negative pressure	Trampoline
Pressure breathing	DRUGS
Hypoxia	Aldosterone
Elastic leotard	Antidiuretic hormones
Cardiovascular conditioning suit	Plasma expanders

Periodic physical exercise and maintenance of an optimum level of physical "fitness" during space missions has been suggested as a way of minimizing the decrease of blood volume associated with weightlessness (38, 426, 450) (see Figure 7-65b). Exercise of the lower extremities might reduce the tendency to venous pooling by maintaining muscle tone, strength and mass, and possibly the capacity of vasoconstrictor mechanisms to respond to intravascular hydrostatic forces due to gravity (31, 471, 590). However, a number of isotonic and isometric exercise regimens have reportedly had no really significant effect on either the blood volume or the degree of orthostatic intolerance associated with prolonged bed rest (62). Bungee cord exercises during the 8 and 14 day, two-man Gemini missions were also not protective, even though the cardiovascular response to a

calibrated work load might for the most part have been maintained by these exercises (35, 439). That exercise will be a useful method for specifically preventing the cardiovascular adaptations to weightlessness is doubtful, but further study in this area still appears indicated.

Various combinations of periodically inflated cuffs placed proximally on the extremities have been used in attempts to prevent cardiovascular adaptations to weightlessness. Periodic increase of hydrostatic pressures, especially in the extremities, may maintain not only venomotor capacity, but an optimum level of extravascular tissue tension during prolonged space missions (69, 141, 393). It may also reduce the degree of central venous volume overload, and thereby prevent the decrease of blood volume associated with weightlessness. Periodic inflation of cuffs placed around all four extremities of subjects immersed up to the neck in water for 6 hours or during two weeks of bed rest, conferred protection from the equivalent of lunar orthostatic intolerance as tested by a 10 degree tilt (229, 425, 625). On the other hand, a variety of cuff configurations applied during a number of water immersion and prolonged bed rest studies have been unsuccessful in preventing either decrease of plasma volume or orthostatic intolerance (68, 395, 578, 628, 631, 632). Periodic inflation of lower extremity cuffs on the pilots of the 8 and 14-day two-man, Gemini missions was also ineffective in lessening post-flight orthostatic intolerance, even though there appeared to be some decrease in the degree of post-flight pooling of blood in the lower extremities as judged by the strain gage technique (141, 439). A recent review of cuffs in the Gemini program and under simulation is available (629). It has been concluded that in the light of failure to establish definite effectiveness of extremity cuffs in many simulated and actual weightless exposures to date, further consideration of the use of cuffs in the space flight situation is probably not warranted (628, 631).

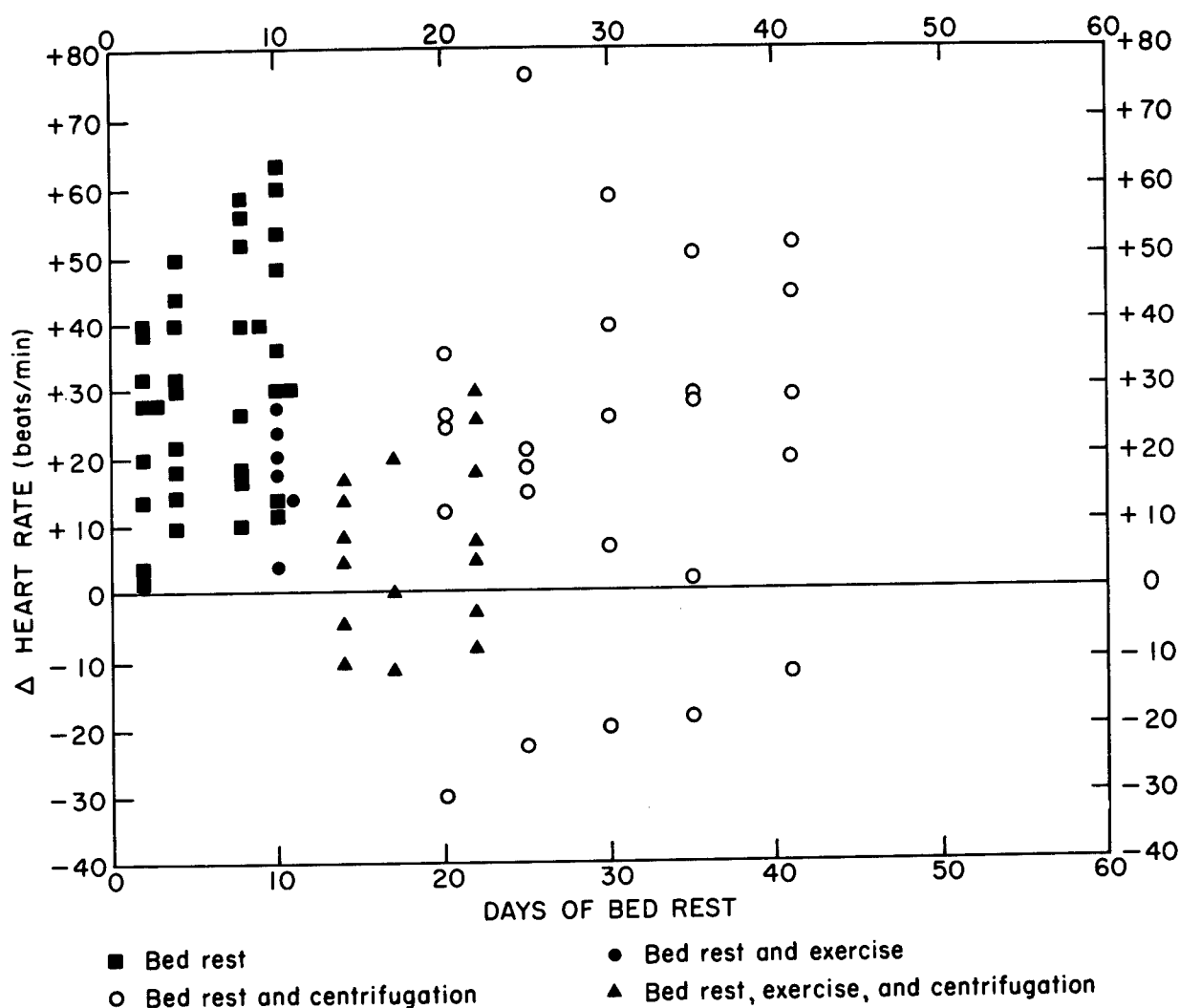
Since its effect on the cardiovascular system is similar to that of increasing the gravitational component of hydrostatic pressure, it has been suggested that lower body negative pressure may force pooling of blood in the lower part of the body, thus increasing transudation of fluid, rehydration, and restoration of tension in tissues of the lower extremities (215, 355, 575). A number of studies have shown that lower-body negative pressure in as short a period as 2 days can either prevent or restore the decreases of plasma volume and orthostatic tolerance which result from prolonged bed rest (38, 108, 215, 358, 394, 427, 577, 579). The mechanism is under study (516, 667). It would also seem feasible and tactically more simple than application of negative pressure, to cover the upper torso with an inflatable positive-pressure jerkin and accomplish the same hydrostatic effects.

Periodic centrifugation has also been assessed for its effectiveness in preventing orthostatic intolerance resulting from prolonged bed rest (467, 590, 591, 667, 672, 676). As few as four 7.5-min. rides at $+4G_z$ (foot level) on a short-arm centrifuge (from 1/2 to 3 gravity-hours) largely prevents orthostatic intolerance as judged by syncope. However, heart rate and blood pressure responses to tilt, and decrease of plasma volume during bed rest appear only slightly affected by this measure. Figure 7-64a compares the effects of this type of centrifugation and exercise on orthostatic intolerance; and Figure 7-64b, changes in plasma volume brought about by bed rest (669).

Figure 7-64

Centrifugation, Acceleration Gradients, and Exercise in the Prophylaxis
Against Cardiovascular Conditioning of Bed Rest

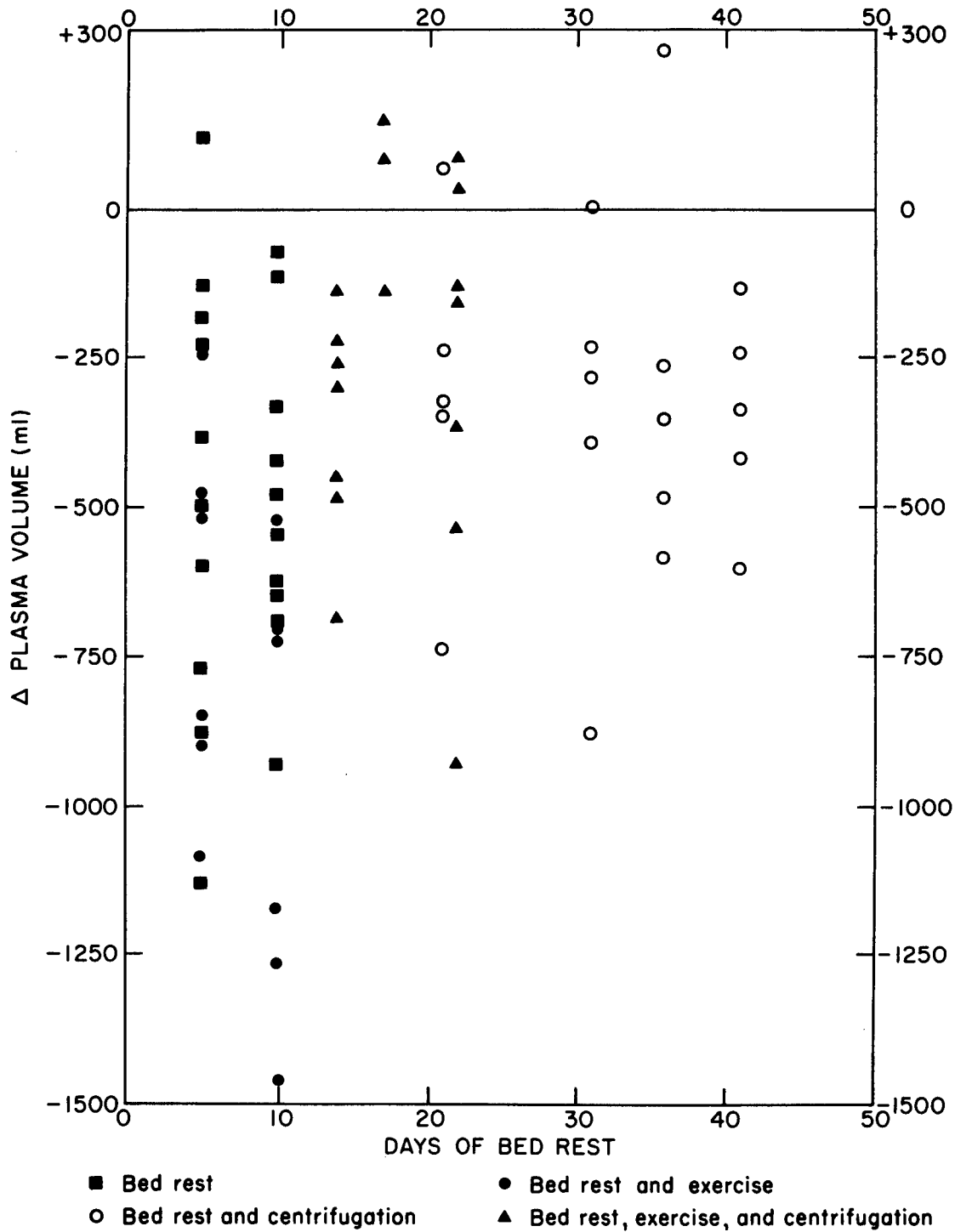
a. Comparative Effects of Centrifugation and Exercise on the Highest
Orthostatic Heart Rates Following Bed Rest (See text)



(After White⁽⁶⁶⁹⁾, drawn from the data of White et al^(667, 676), and Nyberg et al⁽⁴⁶⁷⁾)

Figure 7-64 (continued)

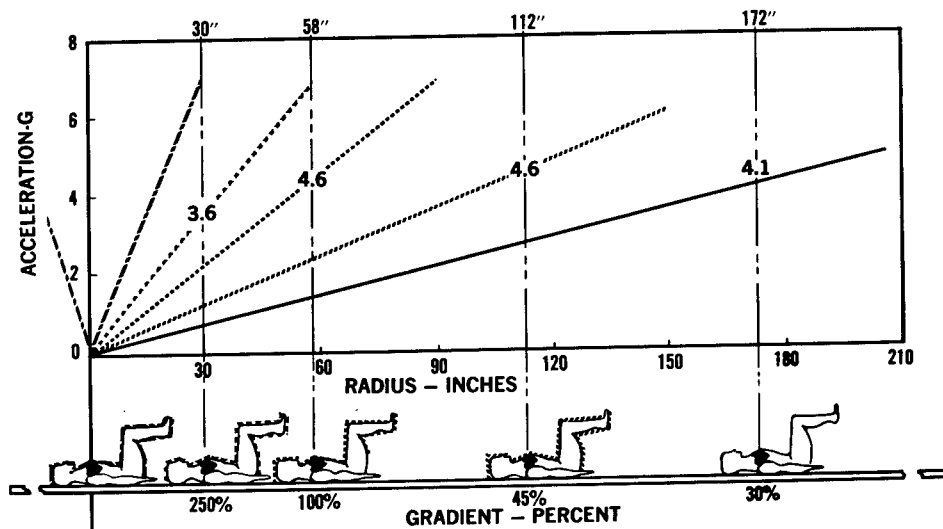
b. Comparative Effects of Centrifugation and Exercise on the Decrease of Plasma Volume Produced by Bed Rest (See Text)



(After White⁽⁶⁶⁹⁾, drawn from the data of White et al^(667, 676), and Nyberg et al⁽⁴⁶⁷⁾)

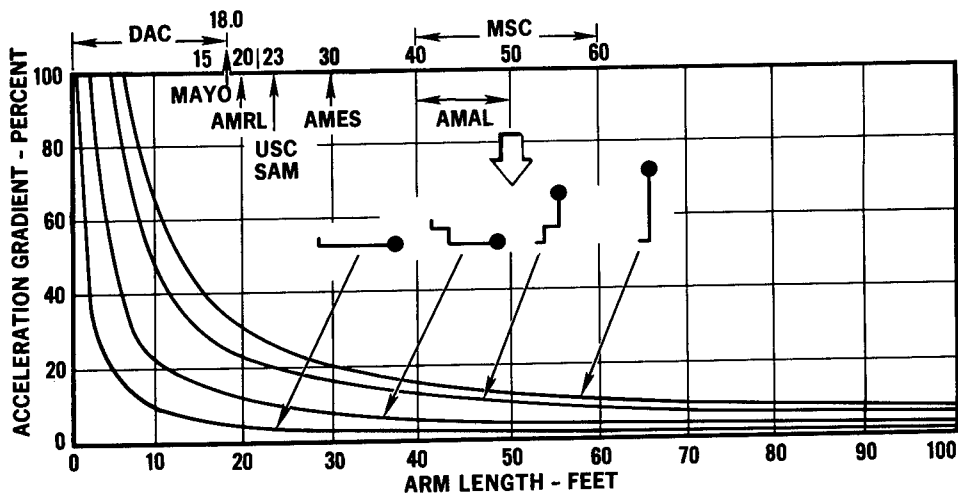
Figure 7-64 (continued)

c. Acceleration Gradients at Different Centrifuge Radii



(After Collier et al⁽¹⁰⁸⁾)

d. Acceleration Gradient Across the Body for Different Radii and Body Positions.

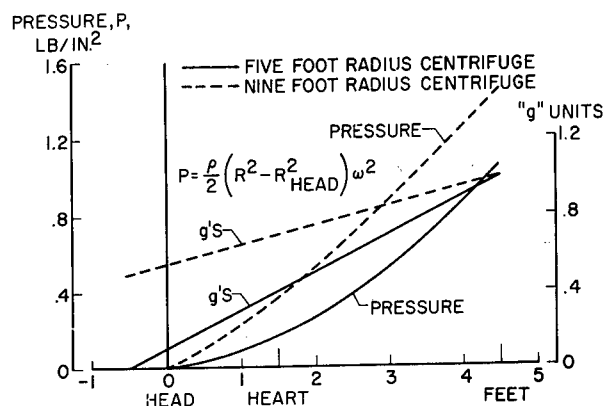


(After Collier et al⁽¹⁰⁸⁾)

e. Pressure Along a Column of Fluid on Small Centrifuges.

Length of column equals the height of seated man.

(After Stone et al⁽⁵⁹⁰⁾)



In these two figures, the centrifugation and exercise profiles within each experimental group are the same, though they may be different from group to group. The wide scatter of the data are evident. Interestingly, the steep heart-to-foot acceleration gradient of up to 256 percent created by these measures did not preclude movement of the head, arms and legs; and motion sickness was not a problem for the well-trained individual when exposed to high angular rates and modest head or limb movements.

Figures 7-64c and d indicate the geometrical considerations determining acceleration gradients. Figure 7-64e indicates the G-gradients and fluid pressures attainable in spacecraft with on-board centrifuges. The validity of on-board centrifuges as reentry simulators are now under study (590). The optimum G-time profiles for minimizing deconditioning are as yet not known nor is the optimum gradient (418). At the lower end of the G_z spectrum, +1.75 G_z for 20 minutes, four times a day (integrated 4.7 G-hrs at foot level) alleviated syncopal and heart rate responses to 70° head-up tilt following 10 days of bed rest (667). Gradients of 20 to 219 percent have been studied using various radii (468, 676). Discomfort of the legs and slightly less tolerance to blackout were noticed with the shorter radii. Further testing of periodic centrifugation appears indicated.

It is considered that the weight, power, volume, and control penalties imposed by a short-radius centrifuge could be made reasonable for future spacecraft if the need and effectiveness of this measure are well established (590, 676). Perhaps one of the best defined examples of a short-radius centrifuge design is one designed for the 260-inch-diameter Manned Orbital Research Laboratory (MORL) (150), which is basically a zero gravity configuration and capable of accommodating one or two men. It has two completely enclosed one-man cabs which can be positioned to provide a range of gravity vector directions, and which are attached to a 108-inch-diameter drive ring. The centrifuge assembly is mounted on three sets of rollers, one of which is driven by a 1-horsepower, shunt-wound dc motor, operating through a V-belt drive. Two speed ranges are available if the belt pulleys are shifted. The centrifuge provides up to 1 G (20 rpm) for therapeutic purposes, and as high as 9 G for reentry simulation. The design penalties incurred by this particular centrifuge configuration in the six-man MORL system are:

1. A weight penalty of 300 pounds (centrifuge structure and drive system).
2. Approximately 1600 ft³ of volume unavailable for other purposes.
3. Sixty watts of power required for 1.3 hours daily.
4. An additional 7 pounds of attitude control propellant per day to null centrifuge torques.
5. Crew time of 3.9 man-hours/day spent attending the centrifuge (two men riding in gondolas and one man observing) lost from overall available work time.

Artificial gravity by rotation of the entire space vehicle is another concept. For therapeutic value, continuous artificial gravity by rotation has

the potential of being as beneficial as the centrifuge in eliminating the adverse effects of weightlessness and could be considerably more convenient and comfortable for the crew. One can use the MORL in a spinning mode. The basic laboratory is separated from the SIV-B launch stage by a system of cables, and with the SIV-B stage acting as a counterweight, the entire configuration is rotated to achieve the desired gravity field within the laboratory. As an example, at a radius of 70 feet from the common center of mass of the spinning configuration to the outer floor of the laboratory, a gravity level of 0.333 G can be achieved by rotating the deployed system at 4 rpm. The inclusion of this spin capability in the basic zero gravity MORL had considerable effect on the laboratory design. The major impact was the increase in weight of the structure, reaction control, and flight electronic systems to accommodate this additional operating mode. The total changes in dry launch weight of the laboratory/SIV-B combination amounts to 3400 pounds and requires about 600 pounds of additional propellant to circularize the orbit from an initial elliptical orbit. Therefore, the impact of the spin capability on the initial launch of the laboratory involves a decrease in discretionary payload capability of approximately 4000 pounds. Fewer consumables, experiments, etc., can thus be carried on the initial launch, and more severe demands are placed on the subsequent logistics schedules. In addition to the initial launch penalties, the spin capability includes a major increase in reaction control propellant consumption rate. Increased drag and moments of inertia, deployment, and spinup requirements all increase the orbital propellant requirements. For the MORL in the spinning mode, the orbit-keeping requirements are increased by about 200 pounds of propellant per month, and the attitude control expenditures are raised by almost 400 pounds per month. These increases in overall propellant consumption total 600 pounds per month or approximately 80 percent over the basic zero gravity configuration.

Designs are available for three large rotating manned orbital space station configurations (382). Each is basically a 24-man station, rotating to provide artificial gravity at the operational floor levels. Each configuration could provide for the experiment program requirements by performing the zero-gravity-dependent experiments in the counterrotating hub where the gravity level goes to zero. For these larger rotating vehicles, there are similar, but more complex, problems as those associated with the MORL spinning mode. Besides a tremendous launch weight, the aerodynamic and gravity gradient torques and the orbit-keeping requirements will involve very high propellant consumption rates, although a lesser number of spin/despin operations will be involved since docking would be accomplished at the zero gravity hub. Although these are highly complicated vehicles requiring subsystems of increased complexity to support the mission, there may be a requirement for such vehicles in the future.

Adverse vestibular effects of rotating space stations have been covered above on page 7-96.

A few other protective measures which have been suggested for use in space have been studied. Presumably to stimulate peripheral vasomotor reflexes otherwise dormant during exposure to weightlessness, variants of positive pressure breathing (PPB) have been applied. They appear to have a significant effect in improving the orthostatic intolerance resulting from

head-out water immersion and bed rest (309, 310, 311, 630). Hyperventilation associated with this PPB may have played a role in altering peripheral vasoconstrictor reflexes. Periodic bouncing exercise on a railed cart between two trampolines has been carried out on prolonged bed rest subjects (82). It was thought that the vascular stimulation of exercise, as well as the repetitive "sloshing" of blood, would serve to maintain the capacity of both veins and arteries to compensate adequately for intravascular hydrostatic forces due to gravity. Although this measure was found ineffective, it might warrant further testing.

Chemical methods have also been attempted. The administration of pitressin, with and without concomitant waterloading to subjects immersed to the neck in water has prevented the diuresis, and associated decrease in plasma volume, but not the orthostatic intolerance which results from water immersion (309, 310, 395). The administration of 9-alpha, fluoro-hydrocortisone for a short period of time towards the end of prolonged bed rest exposures did return blood volume to normal and to levels often above normal, but did not prevent the orthostatic intolerance resulting from these exposures (312, 576, 578). This drug also produced occasional nausea, an effect which would be highly undesirable in the space situation. Based on the fact that many of the physiologic responses to hypoxia are opposite to those of weightlessness, individuals have been exposed to 10,000 - 12,000 ft altitudes during bed rest (108, 354, 577, 579). Although exposure to mild hypoxic conditions did prevent the decrease in red cell mass which occurred during bed rest exposures at ground level, it did not reduce the orthostatic intolerance produced by bed rest.

The "anti-G" suit in the form of an elastic gradient leotard often used to prevent fainting of individuals suffering from postural hypotension, has been used with some success against orthostatic intolerance following six hours of head-out immersion (395) as well as following bed rest (426, 631). About 5 to 15 pounds of weight per crewman is all that would be required. This approach appears most feasible if the need should arise.

Cardiovascular conditioning suits are now under study (649). Such suits may weigh from 20 to 100 lbs and would be worn from 2 to 6 hrs/day with 1/2 to 1 hr donning and doffing times. Preliminary estimates of weight tradeoffs for the different techniques covered above are available (591).

Respiratory Effects

The effects of zero gravity on respiratory function have been recently reviewed (437). There appears to be no gross defect expected from the slight alteration of the normal vertical pressure gradient in the lung. The effects of gravity on the inhalation of pulmonary contaminants is covered in Contaminants, (No. 13).

Metabolic Effects

The lack of gravitational stress on bone and muscle has often been cited as a deconditioning factor in zero gravity. Restriction of exercise with bed rest has often been shown to cause calcium depletion in bone with resultant bone fragility and urinary calculus problems. The subject has been reviewed in great detail (53, 62, 390, 450, 465, 634). Current experience to date in the Gemini program has indicated that with the appropriate exercise and dietary intake of calcium, decalcification of bone should not be a major problem in future space flight (402, 444). Control of dietary factors other than calcium which are related to the maintenance of bone in optimum functional state needs further study. Hypoxia, equivalent to 12,000 ft altitude, can reverse the calcium, phosphorous, nitrogen, potassium, and sodium loss associated with bed rest (390). Direct monochromatic photon techniques have improved bone densitometry so that changes of < 5% can be detected (65, 156).

In the orbital flight of Gemini VII, there was no significant decrease in exercise tolerance as measured by cardiac rate response to a test work load while seated in the cabin (139, 444). Extravehicular work decrement as a result of platform instability and possibly carbon dioxide retention has been covered in Oxygen-CO₂ - Energy, (No. 10). Maintenance of muscle tone and bone density by exercise has been considered by several groups and is being actively used in the space program (53, 139, 331, 398, 450).

The H₂O and electrolytes excretion during the Gemini flights has been studied and correlated with post-flight plasma/serum electrolytes (140, 444). Urinary sodium excretion decreased slightly during flight. Immediately post-flight, there was a retention of sodium so that its excretion was sharply diminished. Then a short time later there was a marked rise in urinary sodium levels as the retained sodium was being excreted. The urinary excretion of chloride was found, as expected, to parallel that of sodium, with a slight decrease during flight, a marked decrease during the first 24 hours after being out of the craft, and then a return to pre-flight levels. The amount of potassium excreted in the urine during the 14-day in-flight period was significantly less than the amount excreted either before or after the flight.

Post-flight water and sodium retention was attributed to the elevation of aldosterone output and postulated as a compensatory mechanism for increased water and sodium excretion during early weightless flight (see above). The cause of the elevation of aldosterone output during mid-flight is not clear. More data are needed on the aldosterone output in the first 48 hours. There was an as yet unexplained decrease in urinary hydroxycorticosteroids during mid-flight with elevations only pre- and post-flight (444). This is contrary to an expected increase resulting from chronic stress and may indicate the relative lack of mid-flight stress.

Elevations of norepinephrine in the early and late stages of flight are attributed to anxiety and gravitational stress related to takeoff and landing (139, 444). Epinephrine output varied from man to man. Norepinephrine reflects physical stress, while epinephrine more accurately reflects the degree of emotional stress. Hydroxyproline, which is a component of bone collagen, expected to be increased in the urine, was relatively unchanged.

Difficulties with the urine collection device during flight precluded accurate quantitative evaluation of these results. The possibility of synergism with 5 psia-100% oxygen must also be kept in mind.

Psychomotor Effects of Weightlessness

Effect of zero gravity on psychomotor performance has received much study, review and speculation (22, 23, 197, 202, 206, 366, 383, 398, 412, , 522, 591). Table 7-63 a and b reviews some of the psychomotor effects found in simulators and in orbit. Table 7-65 reviews the psychomotor effects of weightlessness found while subjects were floating free in large aircraft cabins during parabolic flight (366).

Data are also available on other specific intravehicular and extravehicular tasks in parabolic and ground-based simulators such as suit donning (517), handholds, (320, 398, 485, 519) torqueing and hand-tool use (127, 155, 159, 320, 464), walking techniques and aids (279, 458, 535, 541), orbital work techniques (118, 159, 350, 398, 525, 526, 537, 645) maneuvering devices (253, 398, 607, 621, 645), and tether lines (20, 377, 436, 489, 490, 520). Recent reviews and critiques of all of these techniques are available (167, 464 , 487, 591). A major concern is with the vestibular function, but cerebral function, energetics and other factors must also be considered.

Vestibular Reactions

The response of the otolith organs and semicircular canals have been discussed above under rotational acceleration. The effect of zero gravity in eliminating the chronic 1 G output from the otolith organs might be expected to produce the symptoms of vertigo and motion sickness because of the alteration of cross-modal, sensory interactions (288, 573). (See Table 7-63 and previous discussion of motion sickness). However, the otolith organ responds to changes in acceleration (416). One should therefore expect no sensation of falling or being upside down except possibly during active movement of the body and the head in zero gravity or during transitions from +G to zero G conditions.

Simulations in parabolic flight have indicated that nausea and vomiting responses, experienced by some subjects, appear to require a functional labyrinth and are related to transitions into and from zero G rather than to zero G itself (197, 202, 338, 383). Sensations of rolling over backwards and being upside down are also experienced during transitions from + to zero G, and the opposite sensation in transitioning from zero G to +G in parabolic flight, when the visual frame of orientation was reduced or eliminated. When free-floating in a large cabin, the illusion of being upside down is often experienced in parabolic flight (243).

American experience in orbit was free of nausea, vomiting, or serious illusory phenomena even during movement of the head (412, 444). Selection, training and relative stability or lack of rotation of the spacecraft may have

Table 7-65

Factors Detected While Free-Floating in Large Aircraft Cabins

(X = conditions affecting factor)

(After Gerathewohl⁽²⁰¹⁾, from the data of Simons and Gardner⁽⁵³⁹⁾)

Subjective Sensations (subject's observations)	Light Conditions			Weightless Conditions			Maneuver Conditions				Aircraft Rotation	Summary, Applications and Hazards
	Light Cabin	Dark Cabin and Moon	Dark Cabin	Low Friction	Free Body	G-Free Support and Stimulation	Rapid G Transition	Stress	Short Time Period			
1. <i>Exhilaration</i> from surface freedom	x	x	x	x		x	x	x				Enjoyment increased in light cabin (knowledge of freedom), G-free support tends to induce an exciting and enjoyable environment. G-free training should be based on the advantages of such an environment.
2. <i>Comfort</i> of non-tactual support					x	x						Simpler bed and chair required, exercise required. Emphasis should be on man's position as focus, rather than cabin orientation within a vehicle.
3. <i>Lack of falling</i> sensation					x	x	x					Sudden vehicle accelerations induce falling sensations, while G-free training quickly dispels anticipated falling sensations. Slow G transitions reduce sensations during this phase.
4. <i>Knowledge and control of limb position</i> (orientation)	x				x	x	x		x			Positions were known during all conditions. Overshooting occurs in darkness but knowledge of results aids quick adjustment. Rapid motions perceived as weight.
5. <i>Knowledge and control of body position</i> in aircraft (orientation)	x				x	x	x		x			Posture orientation proposed as <i>basic reference plane</i> , for visual-gravitational conflict of subjective vertical is not a problem with posture identification. Man rather than vehicle should be design focus. The cockpit is 'floor oriented' whereas our space position may be 'man oriented.' Attitude and position information necessary to flight path knowledge can be related to basic reference plane. False rotation and loss of rotation knowledge noted.
6. <i>Knowledge of vehicle attitude</i> (orientation)	x	x	x				x		x		x	Knowledge of surface location decreased in darkroom and apprehension and accidents increased because of inability to prepare for surface contact. Observers often unable to differentiate between subject motion and aircraft motion about subject without comparative G-free mass. G-free posture indoctrination (item 5) reduces need for vehicle information.
7. <i>Concern over collisions</i>	x	x	x	x	x	x		x				Difficulty in self rotation produces collision anxiety. Padding requirements are extensive, open machinery absolutely taboo. Training flights excellent for reducing overcontrol.
8. <i>Illusions</i> (target motion)		x				x	x	x			x	The apparent upward displacement of the visual target (oculo-gravic illusion) may not be a design problem with proper display information. Self propulsion units must have low thrust (low G) levels due to line of sight and deceleration program requirements. Autokinesis should be investigated with subjects moving in still visual field.
9. <i>Sense of zero, partial and excessive G's</i>	x	x	x	x	x	x	x					Lack of visual stimulation (dark cabin) increased sensitivity to G; G-free body systems tend to pick up strong sensations with minute stimulations (?) (Weber-Fechner law). Development of G cues may aid worker handling materials where small accelerations of mass and man are important factors.
10. <i>Sense of heaviness</i> after zero-G period					x	x	x		x		x	Variable control forces may aid psychomotor adjustment upon re-entry.

Table 7-65 (continued)

Factors Detected While Free-Floating in Large Aircraft Cabins

Subjective Sensations (subject's observations)	Light Conditions			Weightless Conditions			Maneuver Conditions				Summary, Applications and Hazards
	Light Cabin	Dark Cabin and Moon	Dark Cabin	Low Friction	Free Body	G-Free Support and Stimulation	Rapid G Transition	Stress	Short Time Period	Aircraft Rotation	
11. Decrease in clothing pressure					x	x	x				Movies of loose clothing reveal that apparel tends to oscillate out of phase on moving limbs. Crews in shirt sleeve environments should wear form fitting, easily flexed clothing with elastic cuffs on limb extremities. The sensation could serve as a tactile perception of weightlessness.
12. Nausea and motion sickness	x			x	x	x	x	x	x	x	Rapid G transition and perceptual-sensation conflicts cause discomfort; may be valuable crew selection criterion.
13. Decrease in span of attention	x					x	x	x	x	x	During the excitement of the moment subjects forget their task. Criterion for crew selection might be their adaptation rate to unusual environment over short periods. Emergency tasks should be assigned to restrained workers. Task analyses should include a reorientation constant for free-floaters; omnidirectional displays should be developed.
14. Harness irritations					x	x					Harnesses tightened for 1-G behavior tend to limit G-free limb activity.
15. Change in cabin pressure										x	Changing cabin pressures were mistaken for weightless stimulations of the ear organs.
Performance Factors (Observable by subject or observer)											
16. Swimming motions	x			x	x	x			x		These 'swimming in air' motions were unsuccessful attempts to translate, stabilize and turn; however, they tended to interfere with attitude control and disappeared after a few exposures (self rotation). Rotation training can be accomplished on simple swivel chairs.
17. Body resilience motions				x		x	x				Passive subjects tend to leave surfaces following sudden relaxation of excessive G-compressed tissues. Compressible objects should be tethered. Sleeping subjects should be restrained against their own accelerations.
18. Cross-coupled motion				x	x	x					3-d spinning subjects should extend limbs and thus reduce rpm. Any external force adds a linear component to the tumble. Stabilization gyros must be available for controlled rotation, before, during and after translation. Moments of inertia computed from segmented man models should include the transfer of energies between the muscular interactions of the various segments.

Table 7-65 (continued)

Factors Detected While Free-Floating in Large Aircraft Cabins

Subjective Sensations (subject's observations)	Light Conditions		Weightless Conditions				Maneuver Conditions				Summary, Applications and Hazards
	Light Cabin	Dark Cabin and Moon	Dark Cabin	Low Friction	Free Body	G-Free Support and Stimulation	Rapid G Transition	Stress	Short Time Period	Aircraft Rotation	
19. Sloppy, pendulous motion					X	X					Self induced accelerations tend to oscillate a G-free body causing unstable work performance, poor translation, and poor attitude and position control. Unharnessed operators should not be required to perform gross motions requiring discriminating movements. Open force systems must be avoided and man should work against himself.
20. Ease of self propulsion				X	X	X					Improper launches cause excessive motions, inadvertent tumbling, and rotating translations. Subjects can train for accomplishing straight and stable flight paths.
21. Difficulty in walking				X	X	X	X				Attempts at walking propel the worker from the surface. Handholds, rails, and foot devices are being developed.
22. Change of relaxed posture					X	X	X				Subjects' limbs tend to contract toward the center of mass (fully relaxed subjects). Bed, chair, and control position designs should be affected.
23. Difficulty in absorbing inertia against a surface	X	XXX	XXX								The inability to self-rotate accurately and prepare for impact compels workers to absorb their previous launching forces haphazardly (lighted cabin). Exhilaration promotes overcontrol, which decreases with exposure. Cautious training, padded living areas, and attitude control aids are basic requirements.
24. Helplessness between surfaces (light cabin served as base line)		X	X	X	X	X					Suspended subjects are often incapable of surface return. Training methods should include proper methods of expending mass to achieve translation.
25. Rigidity of powered tools				X	X	X					Tools may be a source of stabilization, but are difficult to align and reposition. Motors impart forces to G-free capsules.
26. Suspension of dust and objects				X		X					Filters, screens, air circulation are required; smooth configuration of objects is a necessity.
27. Inadequacy of open containers, tethers		X	X	X		X	X				Covers, mounts, and tethers must be designed.

Note: x Indicates conditions affecting factor.

been factors. There is a report by Borman in Gemini VII that he experienced, on occasion, a vague sensation of being upside down.

Soviet experience has been variable (467). Titov, who was an experienced acrobatic pilot and given pre-flight vestibular training, developed unpleasant sensations in Vostok 2 which he described as being similar to the sensation of being rocked back and forth. These gave rise to vertigo and dimming of vision (189, 191, 226). Whenever Titov would turn his head quickly, the vertigo increased and he had the sensation that objects were floating. The cosmonaut noted that not only turning his head, but also the flashing of objects in the viewing screen ("flight of the earth") caused unpleasant sensations. Despite the disturbances, Titov did not suffer any depersonalization reactions in post-flight sequelae. Nicholaev and Popovich in Vostok 3 did not become ill but had illusory sensations of traveling upside down on shift from acceleration to weightlessness (226). The vehicle reportedly rotated on its axis at a rate of 1 rotation every 20-40 seconds. In Vostok 5, Bykovsky experienced no abnormal sensations, but symmetry of nystagmoid movement was noted (7, 193). In Vostok 6, Treshkova had the same nystagmoid asymmetry, and reportedly experienced a "psychotic episode" which lasted for several days post-flight (701). Several references to psychotic behavior with full-blown hallucinations and illusions have been made in the Soviet literature on weightlessness (226, 369).

In Voskhod 1, Feoktistov and Yugarov had sensations during the entire flight, with eyes open and closed, of traveling upside down (189, 690, 695, 696). As with Titov, head movement and moving lights produced vertiginous sensations and nausea in Yugarov, who was a physician and the least experienced pilot of the cosmonauts. No post-flight sequelae were noted.

It is reported that with entry into orbit, "the feeling of easiness appeared and the nervous and psychic distress decreased. At the same time self-observations of the cosmonauts confirmed that the complex of the flight factors specifically affects the state of the 'statokinetic analyzer' (36). This was expressed in illusory conceptions on the spatial position of the body and in sensory and vegetative reactions appearing during sharp movements of the head (Yugarov and Feoktistov). They noted the illusion of the body position turned over, both when their eyes were opened and when they were closed in the whole period of weightlessness, up to the beginning of the effect of acceleration during the reentry. Along with illusions, especially in the middle of the flight, an unpleasant sensation of slight 'short-time giddiness' was observed when the head was turned sharply (Feoktistov and Yugarov). In this connection, while performing working operations, the space pilots tried to make motions more smoothly than under conventional ground conditions. Of great importance was the observation of the astronauts to the effect that the character and degree of illusions and giddiness were equally pronounced in free flight and during stabilization of the ship (by rotation). After 1 1/2 to 2 hours of the flight, Yugarov noted the first signs of 'vestibular-vegetative reactions' expressed in a decrease of appetite and in unpleasant sensations in the pit of the stomach, which are regarded by him as the first symptoms of nausea. These phenomena were most pronounced on the fifth orbit of the flight. Feoktistov noted similar symptoms, but they were less pronounced. After sleep, the vestibular-vegetative syndrome vanished almost

completely and the space pilots actively continued to fulfill their flight program. On the basis of these data, Yugarov considers weightlessness one of the unfavorable factors of space flight requiring serious study by physicians. Analysis of fulfilling the flight assignment and of individual elements of labor activity showed the Yugarov's performance was somewhat reduced during the orbital flight. To conduct active experimental work, Feoktistov was to spare much greater nervous and physical efforts than under ground conditions. During the whole flight Komarov's (the well-trained pilot) performance was at a high level."

In-flight and post-flight studies of the vestibular apparatus in this flight showed no changes in the sensitivity thresholds of the otolith apparatus (695). Slight asymmetry of nystagmus after head rotation was noted in Yugarov but not in Komarov (696). In Voskhod 2, Leonov claims to have had some difficulty in orientation of up and down, only when in the airlock with limited visual cues, but no illness. No problems were noted in his extravehicular program in spite of the spacecraft rotation. The role of the slow rotation of the Russian spacecraft in producing the difference in responses is still not clear in that stabilization of Voskhod 1 had no effect on symptoms (695). Prior rotation may have been a factor in this study. Extra-vestibular impulses from the intestinal tract and elsewhere have also been implicated by the Soviets (343).

In Soviet flights, handwriting and other complex psychomotor tests involving high frequency tracking responses showed improvement with time in orbit and even a better performance, as in the case of some of the writing tests, than under a 1 G acceleration (189, 333, 695). Some flight operations in the early orbits took up to two times longer than in pre-flight simulation on the ground. Pre-flight vestibular training is a major factor in the Soviet program (258, 373, 690, 695, 697).

Vestibular responses have been measured during zero gravity parabolic and orbital flight. Coriolis forces are usually experienced during maneuvers in normal but not in labyrinthine defective subjects (106). Experience of the inversion illusion also requires a normal labyrinth (243). The actual nystagmic response to Z-axis rotation is no different in parabolic flights than on the ground (318). The visual illusion of target rotation upon rolling of an aircraft is also no different in 1 G and zero G parabolic flight (500).

Vision

The determination of the visual horizontal in a dark field from previous seat cues in spacecraft is no different in orbit than in similar studies on Earth, suggesting the relative normality of tactile and kinesthetic cues. Ocular counterrolling response to tilt is also unchanged in orbit, suggesting normal responses of the otolith organ (246). Defective counterrolling responses as well as lack of response to caloric stimulation, however, have been noted in short-term parabolic flights (246, 422). Analysis of vestibular responses in subjects who become ill in the weightlessness of parabolic flight indicates a high level of sensitivity to the usual nystagmic tests and weak inhibition by other sensory inputs (696).

Studies indicating normal visual acuity in orbital flight have been covered in Light, (No. 2). In parabolic flights, there appears to be a very slight improvement in the brightness discrimination threshold, possibly due to a decrease in frictional and damping forces in the orbit with resultant increase in retinal mobility (671). In transient weightlessness there is no significant effect on binocular depth perception (518).

Extravehicular Activity

The extravehicular activity in Gemini flights has been recently summarized (398). The following coverage is taken directly from this study.

Table 7-66a reviews all the extravehicular phases of the Gemini program giving nomenclature of systems and duration of experience. Extravehicular activity (EVA) was accomplished on 5 of the 10 manned Gemini missions. A total of 6 hours and 1 minute was accumulated in five extravehicular excursions on an umbilical (Figure 7-66a). An additional 6 hours and 24 minutes of hatch-open time was accumulated in six periods of standup EVA including two periods for jettisoning equipment. The total extravehicular time for the Gemini Program was 12 hours and 25 minutes. Because of problems encountered during the equipment evaluation, emphasis was shifted from maneuvering equipment to body restraint devices.

Each of these missions will be summarized. More complete time lines are available (398).

a. Gemini IV

Two of the objectives of the Gemini IV mission were to establish the initial feasibility of EVA and to evaluate a simple maneuvering device. The life support system was a small chestpack called the Ventilation Control Module (VCM), with oxygen supplied through a 25-foot umbilical hose assembly. The Hand Held Maneuvering Unit (HHMU) was a self-contained, cold-gas propulsion unit which utilized two 1-pound tractor jets and one 2-pound pusher jet. The G4C space suit was worn with an extravehicular coverlayer for micrometeorite and thermal protection. While outside the spacecraft, the pilot also wore a special sun visor designed for visual protection.

The hatch was opened at 4 hours 18 minutes ground elapsed time (g.e.t.). The pilot was outside the spacecraft for 20 minutes. The results established the feasibility of simple EVA without disorientation. The utility of the HHMU for self-propulsion without artificial stabilization was tentatively indicated, although the total available thrust of 20 seconds was too brief for a detailed evaluation of stability and control. The extravehicular pilot evaluated the dynamics of a 25-foot tether, and was able to push out from the surface of the spacecraft under gross control. The umbilical tether caused the pilot to move back in the general direction of the spacecraft. The tether provided no means of body positioning control other than as a distance limiting device. Ingress to the cockpit and hatch closure were substantially more difficult than anticipated because of the high forces required to pull the hatch fully closed.

Table 7-66

Summary of Extravehicular Activities

a. Extravehicular Activity in Gemini Program

(After Machell (ed.)-NASA-(MSC)(398))

Mission	Life support system	Umbilical length, ft	Maneuvering device	Umbilical EVA time, ^a hr:min	Standup EVA time, ^{a,b} hr:min	Total EVA time, ^a hr:min
Gemini IV	VCM ^c	25	HHMU ^d	0:36	--	0:36
Gemini VIII	ELSS ^e - ESP ^f	25	HHMU	--	--	--
Gemini IX-A	ELSS - AMU ^g	25	AMU	2:07	--	2:07
Gemini X	ELSS	50	HHMU	0:39	0:50	1:29
Gemini XI	ELSS	30	HHMU	0:33	2:10	2:43
Gemini XII	ELSS	25	--	2:06	3:24	5:30
EVA totals				6:01	6:24	12:25

^aTime from hatch opening to hatch closure.^bIncludes mission equipment jettison time.^cVentilation Control Module.^dHand Held Maneuvering Unit.^eExtravehicular Life Support System.^fExtravehicular Support Package.^gAstronaut Maneuvering Unit.

b. Hand-Held Maneuvering Unit Used in Gemini

(After Machell (ed.)-NASA-(MSC)(398))

Hand Held Maneuvering Unit Characteristics			
	Gemini IV	Gemini VIII	Gemini X
Propellant, gas	Oxygen	Freon-14	Nitrogen
Thrust, tractor or pusher, lb	0 to 2	0 to 2	0 to 2
Specific impulse (calculated), sec	-	33.4	63
Total impulse, lb-sec	40	600	677
Total available velocity increment, ft/sec	6	54	84
Trigger preload, lb	15	15	5
Trigger force at maximum thrust, lb	20	20	8
Storage tank pressure, psi	4000	5000	5000
Regulated pressure, psi	120	110 ± 15	125 ± 5
Nozzle area ratio	50:1	51:1	51:1
Weight of propellant, lb	7	18	10.75
HHMU weight, lb	7.5	3	3

Table 7-66 (continued)

c. Summary of Gemini Extravehicular Tasks
(After Machell (ed.)-NASA-(MSC)(398))

EVA tasks	Body restraints used	Forces required	Ease of accomplishment
Removal of 7 in ² of nylon Velcro strip, Gemini XI	Handholds	Finger, hand, and body	Satisfactory
Translation between two points, Gemini X	None	Establish velocity vector when leaving first point	Satisfactory
GATV tether attachment to spacecraft docking bar, Gemini XI	Handholds	Body control and forces from hands, arms, legs, and torso	Unsatisfactory
Experiment package deployment or retrieval (S009, S010, and S012), Gemini IX-A, X, and XI	Handholds	Body control and forces from fingers, hand, and body	Satisfactory
Unstowage and extension of the AMU controller arm (during AMU checkout), Gemini IX-A	Foot stirrups	Torquing and forces from hands, arms, and body	Unsatisfactory
Unstowage and installation of the telescopic handrail, Gemini XII	Waist tethers	Alignment, body control, and forces from fingers, hands, and body	Satisfactory
GATV tether attachment to the spacecraft docking bar, Gemini XII	Waist tethers	Body control and forces from fingers, hands, and body	Satisfactory
Translation between two points along the surface of the spacecraft on Gemini IX-A, X, and XII	Handrail	Body control and forces from fingers, hands, and body	Satisfactory
Experiment package deployment; bolt-torquing operations, Gemini XII	Waist tethers	Alignment, torque, body control, and forces from finger, hand, and body	Satisfactory
Connector operations, Gemini XII	Waist tethers	Alignment, body control, and push/turn, blind push/turn, and push/push	Satisfactory
Cutting operations, Gemini XII	Foot restraints	Body control, finger, and hand	Satisfactory
Removal of 200 in ² of nylon Velcro strip, Gemini XII	Foot restraints	Finger, hand, and body	Satisfactory

Table 7-66 (continued)

d. Restraint Devices Used During Gemini Extravehicular Activities
(After Machell (ed.)-NASA-(MSC)⁽³⁹⁸⁾)

Configuration of restraint device	Gemini mission			
	IX-A	X	XI	XII
Rectangular handrail	X	X	X	X
Large cylindrical handbars (1.38-in. diameter)	X			X
Small cylindrical handrails (0.317-in. diameter)				X
Telescoping cylindrical handrail				X
Fixed handhold			X	X
Flexible Velcro-backed portable handhold	X			
Rigid Velcro-backed portable handhold				X
Waist tethers				X
Pip-pin handhold/tether attachment device				X
Pip-pin antirotation device				X
U-bolt handhold/tether attach device				X
Foot stirrups	X			
Foot restraints				X
Standup tether		X	X	X
Straps on space suit leg			X	X

Table 7-66 (continued)

e. Summary of Hazards During Extravehicular Activity
(After AFSC⁽⁵⁾)

CONDITION	METHOD OF HAZARD REDUCTION	EMERGENCY PROCEDURE
Environmental		
Solar radiation	Use of visor and shielding afforded by structures	Wait for blindness to pass or wait for rescue
Particle radiation	Avoid regions of high flux density	Withdrawal to craft
Micrometeorite flux	Use of shielding afforded by structures	Return to craft
Vacuum	Suit maintenance and checkout	Use of emergency oxygen system and/or crew rescue bag
Spacecraft discharge	Avoid attitude changes or jettisoning waste during EVA	Remove particles from face plate
Electrical potential	Provide electrical path among structures touched by astronaut. Danger from this source has not been determined	(unknown)
Garment/Life Support		
Tears	Maintenance and checkout, short missions, avoid sharp objects, avoid narrow passages	Rescue if trapped, self-release to be avoided
Condensation on face plate	Short missions, frequent rest	Rest, wait for plate to clear, return to craft
Loss of communication	Check out communications frequently	Return to craft
Crew Morphology/Health		
Vertigo	Avoid sudden movements, training	Rest or rescue
Rapture	Selection and training	Rest, communication
Dissociation	Training	Activity, communication
Fatigue	Training, frequent rest	Rest, return to craft
Fear	Training, communication bio-monitoring, return if fear increases with time	Perform familiar activity, return to craft, communicate
Bends	Denitrogenation procedure, slow change in pressure	Increase pressure, then reduce pressure slowly
Heat exhaustion	Monitor physiological variables, short missions, rest	Rest
Nausea	Selection and training, diet control, avoidance of fatigue	Reschedule EVA so man not required (return to craft at first symptom)
Operating Procedures		
Tangle umbilical	Training, monitoring of procedure by standby astronaut	Stop movement, allow standby to free lines
Caught between moving structures	Communications with other crewmen, training, improve design to avoid EVA near moving structures	Rescue

The hatch-locking mechanism malfunctioned, which further complicated the task of ingress. In coping with the hatch-closing problems, the metabolic heat output of the extravehicular pilot exceeded the cooling capacity of the VCM. The pilot was greatly overheated and experienced slight visor fogging at the completion of ingress, although he had been cool while outside the spacecraft. Several hours were required for the pilot to cool off after completion of the extravehicular period; however, no continuing aftereffects were noted. Because of the hatch-closing problems, the hatch was not opened for jettisoning the extravehicular equipment.

The inflight experience showed that substantially more time and effort were required to prepare for the EVA than had been anticipated. The increased hazards of EVA dictated meticulous care in the inflight checkout before the spacecraft was depressurized. The flight crew found the use of detailed checklists a necessary part of the preparations for EVA. In summary, the Gemini IV mission proved that EVA was feasible and indicated several areas where equipment performance needed improvement.

b. Gemini VIII

The primary objectives for EVA during the Gemini VIII mission were evaluation of the Extravehicular Life Support System (ELSS), the HHMU and the Extravehicular Support Package (ESP). The ELSS was a chestpack unit with an increased reserve oxygen supply and a substantially greater thermal capacity than the VCM used during Gemini IV. The ESP consisted of a backpack unit containing an independent oxygen supply for life support, a larger propellant supply for the HHMU, and an ultrahigh frequency radio package for independent voice communications. A detailed evaluation was planned of the HHMU with the pilot on a 75-foot lightweight tether. The Gemini VIII mission was terminated before the end of the first day because of a spacecraft control system malfunction; therefore, no EVA was accomplished.

Equipment design proved to be quite complex, with a substantial number of late modifications during preparation for the Gemini VIII mission primarily because the chestpack had to interface with (1) the 25-foot ELSS umbilical, (2) the 75-foot electrical tether, and (3) an ESP line for oxygen. Acceptable designs and procedures were established; however, the handling procedures were more difficult than was desired. Although the equipment provided for the Gemini VIII EVA was not used in orbit, its use in training and in preparation for flight provided initial insight into the problems of complicated equipment connections.

c. Gemini IX-A

The prime objective of the Gemini IX-A EVA was to evaluate the ELSS and the Air Force Astronaut Maneuvering Unit (AMU). The AMU was a backpack which included a stabilization and control system, a hydrogen peroxide propulsion system, a life support oxygen supply, and an ultrahigh frequency radio package for voice communications. The mission profile planned for the

EVA was very similar to the profile intended for Gemini VIII. The hatch was to be opened at sunrise of a daylight period when good communications could be established with the tracking stations in the continental United States. The first daylight period was to be devoted to familiarization with the environment and to conducting simple evaluations and experiments. The following night period was to be spent in the adapter equipment section of the spacecraft checking out and donning the AMU. The second daylight period was to be spent evaluating the AMU. Then, the pilot was to return to the cockpit, discard the AMU, perform a simple scientific photographic experiment, and ingress.

The Gemini IX-A EVA proceeded essentially as planned for the first daylight period. Higher forces than expected were required to move the hatch in the partially open position, but this condition did not cause immediate difficulty. While outside the spacecraft, the pilot discovered that the familiarization tasks and evaluations required more time and effort than the ground simulations. Minor difficulty was also experienced in controlling body position. Before the end of the first daylight period, the pilot proceeded to the spacecraft adapter and began the preparations for donning the AMU. The tasks of preparing the AMU required much more work than had been expected, principally because of the difficulty in maintaining body position relative to the foot bar and hand bars. At approximately 10 minutes after sunset, the visor on the helmet began to fog. The fogging increased in coverage and severity until the crew were forced to discontinue the activities with the AMU. After sunrise, the fogging decreased slightly, but increased again when the extravehicular pilot expended appreciable effort. Although the AMU was donned, it was not evaluated. The EVA was terminated early because of the visor fogging. The pilot experienced more difficulties in moving the hatch when it was in the intermediate position; however, the forces required to close and lock the hatch were normal.

Postflight evaluation indicated that the ELSS was functioning normally. The task of preparing the AMU and the lack of adequate body restraints resulted in workloads which exceeded the design limits of the ELSS. Visor fogging was attributed to the pilot's high respiration rate and to the resulting high humidity in the helmet. The pilot reported that he was not excessively hot until the time of ingress. The performance of the ELSS heat exchanger may have degraded at this time because of depletion of the evaporator water supply.

Several corrective measures were initiated for the problems encountered during the Gemini IX-A EVA. To minimize visor fogging, an antifog solution was to be applied to the space suit helmet visors immediately before EVA on future missions. Each extravehicular task planned for the succeeding missions was analyzed in greater detail concerning the type of body restraints required and the magnitude of the forces involved. An overshoe type of positive foot restraint was installed in the spacecraft adapter section to be used for Gemini XI and XII. Also, underwater programs were initiated in an attempt to simulate the weightless environment more accurately than zero-G aircraft simulations. Prior to the Gemini X and XI missions, the underwater simulations were used only for procedure validation, but not for training or development of time lines. For the Gemini XII mission, underwater simulations were used for crew training and time line development.

d. Gemini X

The prime objective of the Gemini X EVA was to retrieve the Experiment S010 Micrometeorite Collection package from the target vehicle that had been launched 4 months earlier as part of the Gemini VIII mission. The package was to be retrieved immediately after rendezvous with the Gemini VIII target vehicle, and the umbilical EVA was to last approximately one daylight period. Also planned were the evaluation of the HHMU, the installation of a new S010 experiment package on the target vehicle, the retrieval of the Experiment S012 Gemini Micrometeorite Collection package from the spacecraft adapter section, and the performance of several photographic experiments. Photography was scheduled for 1-1/2 orbits during a period of standup EVA.

The EVA equipment included the ELSS, an improved HHMU, and the new 50-foot dual umbilical. One hose in the umbilical carried the spacecraft oxygen to the ELSS. The other hose carried nitrogen to the HHMU. The umbilical was designed so that the HHMU and all oxygen fittings could be connected before the hatch was opened; however, the nitrogen hose for the HHMU had to be connected while outside the spacecraft cabin. The configuration and operation of this umbilical were simpler than those of the Gemini VIII and IX-A equipment, but the 50-foot umbilical required a substantial increase in stowage volume. For the standup EVA, short extension hoses were connected to the spacecraft Environmental Control System (ECS) to permit the pilot to remain on the spacecraft closed-loop system while standing. The pilot also used a fabric strap standup tether to hold himself in the cockpit, thereby avoiding any loads on the extension hoses.

The standup activity began just after sunset at an elapsed flight time of 23 hours 24 minutes and proceeded normally for the first 30 minutes. The pilot was satisfactorily restrained by the standup tether, and since there were no unusual problems with body positioning, ultraviolet photographs of various star fields were taken. Immediately after sunrise, both crewmembers experienced eye irritation and tear formation which interfered with their vision. The crew elected to terminate the standup EVA at this time.

The eye irritation subsided gradually after ingress and hatch closure. The cause of the eye irritation was not known, but was believed to have been related to the simultaneous use of both compressors in the spacecraft oxygen-supply loop to the space suits. Prior to the umbilical EVA, an additional cabin depressurization was conducted to verify that there was no significant eye irritation when only one suit compressor was used and the cabin was decompressed.

The Gemini X umbilical EVA was initiated at an elapsed time of 48 hours 42 minutes, immediately after rendezvous with the Gemini VIII target vehicle. The target vehicle was completely passive with no electrical power available

because of the long staytime in orbit. The pilot retrieved the Experiment S012 Gemini Micrometeorite Collection package from the exterior of the spacecraft adapter, moved outside to connect the nitrogen umbilical supply line for the HHMU, and then returned to the cockpit. Meanwhile, the command pilot was flying the spacecraft in close formation with the target vehicle. With the docking cone of the target vehicle approximately 5 feet away, the pilot pushed off from the spacecraft and grasped the outer lip of the docking cone. In moving around the target vehicle to the location of the Experiment S010 Agena Micrometeorite Collection package, the pilot lost his hold on the smooth lip of the docking cone and drifted away from the target vehicle. He used the HHMU to translate approximately 15 feet back to the spacecraft. The pilot then used the HHMU to translate to the target vehicle. On his second attempt to move around the docking cone, he used the wire bundles and struts behind the cone as handholds, and was able to maintain satisfactory control of his body position. Retrieval of the Experiment S010 Agena Micrometeorite Collection package was accomplished without difficulty; however, the pilot elected at this time to discard the replacement S010 package rather than risk losing the one he had just retrieved. The pilot, carrying the package, used the umbilical to pull himself back to the cockpit. At this time, the spacecraft propellant had reached the lower limit allotted for the EVA and station keeping operation. The EVA was terminated. During ingress, the pilot became entangled in the 50-foot umbilical. Several minutes of effort by both crewmembers were required to free the pilot from the umbilical so that he could continue to ingress. The hatch was then closed normally.

Fifty minutes later, the crew opened the right hatch and jettisoned the ELSS chestpack, the umbilical, and other equipment not required for the remainder of the mission.

During the umbilical EVA, the pilot reported the loss of the 70-mm still camera used during the EVA. The camera had been fastened to the ELSS with a lanyard, but the attaching screw came loose. Also, it was discovered that the Experiment S012 Gemini Micrometeorite Collection package was missing. The package had been stowed in a pouch with an elastic top, but appeared to have been knocked free while the 50-foot umbilical was being untangled.

The principal lessons learned from the EVA phase of this mission were:

- (a) Preparation for EVA was an important task and the full time attention of both crewmembers was desirable. Performing a rendezvous with a passive target vehicle and simultaneous EVA preparation caused the crew to be rushed and did not allow the command pilot time to give the pilot as much assistance as had been planned.
- (b) The tasks of crew transfer and equipment retrieval from another satellite were accomplished in a deliberate fashion without an excessive workload.
- (c) Formation flying with another satellite during EVA was accomplished by coordination of thruster operation between the command pilot and the extravehicular pilot.

(d) Equipment which was not securely tied down was susceptible to drifting away during EVA, even when precautions were being taken.

(e) The bulk of the 50-foot umbilical was a greater inconvenience than had been anticipated. The stowage during normal flight and the handling during ingress made this length undesirable.

e. Gemini XI

The prime objectives of the Gemini XI EVA were to attach a 100-foot tether between the spacecraft and the target vehicle and to provide a more extensive evaluation of the HHMU. In addition, several experiments, including ultraviolet photography, were scheduled for the standup EVA. The umbilical EVA was scheduled for the morning of the second day so that the spacecraft/target vehicle tether evaluation could be accomplished later that day.

The equipment for the Gemini XI EVA was the same as for the Gemini X mission, except that the dual umbilical was shortened from 50 to 30 feet to reduce the stowage and handling problems. An Apollo sump-tank module, which was mounted in the spacecraft adapter section, incorporated two sequence cameras that were to be retrieved during EVA. The HHMU was also stowed in the adapter section. A molded overshoe type of foot restraint was provided for body restraint when performing tasks in the adapter equipment section.

The Gemini XI umbilical EVA began at an elapsed flight time of 24 hours 2 minutes; almost immediately, there were indications of difficulty. The first significant task after egress was to position and secure the external sequence camera. After the camera was secured, the pilot indicated that he was fatigued and out of breath. The pilot then moved to the front of the spacecraft and assumed a straddle position on the rendezvous and recovery section in preparation for attaching the spacecraft/target vehicle tether. While maintaining position and attaching the tether, the pilot expended a high level of effort for several minutes. After returning to the cockpit to rest, the pilot continued to breathe very heavily and was apparently fatigued. In view of the unknown amount of effort required for the remaining tasks, the crew elected to terminate the EVA prior to the end of the first daylight period. Ingress and hatch closure were readily accomplished.

The Gemini XI standup EVA was initiated at an elapsed time of 46 hours 6 minutes, just before sunset. The crew began the ultraviolet stellar photography as soon as practical after sunset; the photography of star patterns was readily accomplished. The extravehicular pilot operated at a very low work level because he was well restrained by the standup tether. As in the Gemini X standup EVA, the crew had little difficulty with the standup tasks. After completing the planned activities, the pilot ingressed and closed the hatch without any difficulty.

Discussions with the crew and analysis of the onboard films revealed that several factors contributed to the high rate of exertion during the umbilical activity and the subsequent exhaustion of the pilot.

(a) A high rate of physical effort was required to maintain the desired position on the rendezvous and the recovery section of the spacecraft because of the lack of body restraints.

(b) The zero-g aircraft simulations had not sufficiently duplicated the extravehicular environment to demonstrate the difficulties of the initial extravehicular tasks.

(c) The pilot had experienced difficulty in donning the extravehicular visor on his helmet with the space suit pressurized. As a result, he had become partially fatigued and overheated prior to opening the hatch.

(d) The requirement to perform a mission-critical task immediately following egress did not allow the pilot time to become accustomed to the environment. This factor probably caused the pilot to work faster than was desired.

(e) The high workloads may have resulted in a concentration of carbon dioxide in the space suit helmet high enough to cause the increased respiration and the apparent exhaustion. Although no measurement of carbon dioxide concentration was made during the mission, an increase had been shown during testing of the ELSS at high workloads. For workloads which exceed design limits, the carbon dioxide concentration may reach values that cause physiological symptoms, including high respiration rates, and decreased work tolerance.

The Gemini XI umbilical EVA results failed to substantiate the confidence generated by the relatively successful Gemini X umbilical EVA. In order to provide a better understanding of the basic techniques for performing EVA tasks, the umbilical EVA planned for Gemini XII was redirected from an evaluation of the AMU to further evaluations of body restraints and workloads.

f. Gemini XII

The prime objective of the Gemini XII EVA was to evaluate the type of body restraints and the associated workload required for a series of representative tasks. Other objectives were attachment of the spacecraft/target vehicle tether and ultraviolet stellar photography. The extravehicular equipment for the Gemini XII mission included a new work station in the adapter equipment section, a new work station on the Target Docking Adapter (TDA), and several added body restraints and handholds. The pilot's extravehicular equipment was essentially identical to that of Gemini IX-A.

The flight crew training for the Gemini XII EVA was expanded to include five sessions of intensive underwater simulation training. During these sessions, the pilot followed the planned flight procedures and duplicated the planned umbilical EVA on an end-to-end basis. The procedures and times for each event were established and used to schedule the final inflight task sequence. The underwater training supplemented the extensive ground training and zero-g aircraft simulations.

To increase the margin for success and provide a suitable period of acclimatization before the performance of any critical tasks, the standup EVA was scheduled prior to the umbilical activity. The planned EVA timeline was interspersed with 2-minute rest periods. Procedures were established for monitoring the heart rate and respiration rate of the extravehicular pilot; the crewmembers were to be advised of any indications of a high rate of exertion before the condition could become serious. Finally, the pilot was trained to operate at a moderate work rate, and flight and ground personnel were instructed in the importance of workload control.

The first standup EVA was very similar to the previous two missions. The ultraviolet stellar and the synoptic terrain photography experiments were accomplished on a routine basis. During the standup activity, the pilot performed several tasks designed for familiarization with the environment and for comparison of the standup and umbilical EVA's. These tasks included mounting the extravehicular sequence camera and deploying a handrail from the cabin of the spacecraft to the TDA on the target vehicle. The pilot also retrieved the Experiment S010 Micrometeorite Collection package and several contamination sample disks from the adapter section. The standup activity was completed without difficulty.

The umbilical EVA preparations proceeded smoothly. The hatch was opened within 2 minutes of the planned time. The use of waist tethers during performance of the initial tasks on the TDA enabled the pilot to rest easily, to work without great effort, and to connect the spacecraft/target vehicle tether in an expeditious manner. The pilot activated the Experiment S010 Agena Micrometeorite Collection package on the target vehicle for possible future retrieval. Before the end of the first daylight period, the pilot moved to the spacecraft adapter section where he evaluated the work tasks of torquing bolts, making and breaking electrical and fluid connectors, cutting cables and fluid lines, hooking rings and hooks, and stripping patches of Velcro. The tasks were accomplished using either the foot restraints or the waist tethers. Both systems of restraint proved to be satisfactory.

During the second daylight period of the umbilical activity, the pilot returned to the target vehicle and performed tasks at a small work station on the outside of the docking cone. The tasks were similar to those in the spacecraft adapter section and, in addition, included use of an Apollo torque wrench. The pilot evaluated working with the use of one or two waist tethers and without a waist tether. At the end of the scheduled EVA, the pilot returned to the cabin and ingressed without difficulty.

A second standup EVA was conducted. Again, this activity was routine. All the objectives were satisfactorily completed.

The results of the Gemini XII EVA showed that all the tasks attempted were feasible when body restraints were used to maintain position. The results also showed that the EVA workload could be controlled within desired limits by the application of proper procedures and indoctrination. Finally, perhaps the most significant result was that the underwater simulation duplicated the actual extravehicular actions and reactions with a high degree of

fidelity. It was concluded that any task which could be accomplished readily in underwater simulation would have a high probability of success during the actual EVA.

g. Maneuvering Equipment

The maneuvering equipment used in the Gemini Program is summarized in Table 7-66a and b. The propellant gas storage-tank installation for Gemini XI was identical to the Gemini X configuration and provided the same operational characteristics, except a 30-foot dual umbilical was used instead of the 50-foot dual umbilical. Also in the Gemini XI mission, the HHMU was stowed in the spacecraft adapter section rather than in the cabin. Greater detail on the design rationale is available (398).

The original plan for the use of the extravehicular maneuvering equipment was to evaluate the Hand Held Maneuvering Unit (HHMU) during the Gemini IV, VIII, X, and XI missions, and the Air Force Astronaut Maneuvering Unit (AMU) during the Gemini IX-A and XII missions. The HHMU was the only maneuvering device actually evaluated in orbit. The evaluations of maneuvering equipment planned for Gemini VIII, X, and XI were not completed because of problems with other systems. The AMU was not carried on Gemini XII because of the increased emphasis on the evaluation of body restraints.

Prior to the development of the HHMU utilized on the Gemini IV mission, several experimental hand-held gas-expulsion devices were evaluated at the air-bearing facility of the NASA MSC, Houston. The following conclusions were derived from early investigations.

- (a) For translation, the tractor mode was inherently stable and easiest to control.
- (b) Parallel tractor nozzles placed far apart produced much lower thrust losses from gas-impingement than nozzles placed side by side and canted outward.
- (c) Because of the lack of finger dexterity in pressurized space suit gloves, the trigger which operated the pusher and tractor valves should be controlled by gross movements of the hand.
- (d) Because arm and hand movements were constrained by the pressurized space suit, the handle of the HHMU was redesigned.
- (e) Because of the necessity to easily align the thrust with the center of gravity of the operator, the thrusters were oriented at specific angles to insure easy aiming.
- (f) Attitude control was improved by utilizing a proportional thrust system, rather than an off-on system, for controlling thrust level.

Details of training procedures are available (398). These include air bearing and inertia coupling training devices. Pilot responses corroborated the value of training devices employed. The Gemini IV pilot accomplished the first propulsive EVA maneuvering in history. Concerning the response

characteristics of the HHMU, the pilot stated that thrust levels from 0 to 2 pounds were satisfactory. These levels provided adequate translational and rotational control without an overly sensitive response.

The Gemini X pilot was to perform an extensive evaluation of the HHMU, including precise angular attitude changes and translations. However, the flight plan for the EVA required that a number of other activities be accomplished before this evaluation. One of these planned activities was to transfer to the target vehicle at very short range and to retrieve the Experiment S010 Agena Micrometeorite package attached near the docking cone. With respect to ability to transfer the control skills acquired on the 3-degrees-of-freedom air-bearing simulators to the 6-degrees-of-freedom that actually existed in space, the Gemini X pilot stated that the transfer was made easily and naturally. This pilot was, perhaps, a little surprised to find that the pitch control was more difficult than yaw control. Because of the very low body inertia about the yaw axis, yawing motions could be generated more rapidly with the HHMU than either pitch or roll motions. During his brief periods of maneuvering with the HHMU no rolling motions had been experienced. This was significant because: (1) based upon indications of the inertia coupling model, and upon the experience obtained during the Gemini IV EVA, the pilot had trained specifically to avoid rolling motions, and to stop them immediately if they should occur, and (2) in the absence of rolling motions, control with the HHMU was reduced to a simpler problem involving yawing rotations, pitching rotations, and linear translations.

The Astronaut Maneuvering Unit (AMU) was a backpack device which contained the necessary systems to permit an extravehicular crewman to maneuver in space independent of spacecraft systems. The AMU was carried on Gemini IX-A under Air Force Experiment D012 and was originally planned to be carried on Gemini XII. However, the Gemini XII flight plan was subsequently revised, and the AMU was not included. Although a maneuvering evaluation was not accomplished in orbit, a large effort was expended in preparing for the evaluation. The planning for the AMU dominated the EVA flight plan for Gemini IX-A. Complete data on the AMU are available (398).

A significant result of the simulations was the development of an AMU flight technique by the NASA flight crew which differed greatly from the flight technique devised by the contractor. The technique developed by the contractor for a rendezvous followed these lines: (a) Facing the target, introduce a closing velocity with the aft-firing thrusters; (b) When line-of-sight drift is observed against the background, roll until the vertical thrusters are aligned with the direction of drift and fire the up-firing or down-firing thrusters as required to stop the drift; (c) Repeat as required until close to the target; (d) Take out the closing velocity and contact the target.

The technique developed by the flight crew was as follows: (a) Facing the target, introduce a closing velocity with the aft-firing thrusters; (b) After the closing velocity is established, yaw right or left up to 90 degrees. When line-of-sight drift is detected, correct by firing forward, aft, up, or down thrusters as required to stop the drift. (c) Repeat as required until rendezvous is imminent; and (d) Yaw back to a facing-the-spacecraft attitude, take

out the closing velocity, and contact the target. In simulations, this "over-the-shoulder" rendezvous technique provided faster response for less fuel and was much easier to learn than the earlier method of roll and vertical firing. In some cases, the technique also permitted the pilot to see the target and the starting point without special maneuvers.

Because of the severe visor fogging which occurred during the AMU preparation activities in flight, the crew discontinued the AMU experiment. At sunrise, the EVA pilot disconnected the AMU electrical connection, connected the ELSS umbilical, and returned to the cabin, leaving the AMU power on. The AMU remained in the adapter with the systems activated for flight until retrofire.

Termination of the EVA precluded an evaluation of most of the AMU performance capabilities. However, the backpack successfully withstood a Gemini launch and a 2-day exposure to the space environment. Most of the functions of checkout and donning were performed prior to the termination of AMU activities. Although the AMU was transmitting telemetry data following power-up during the predonning activity, failure of the Gemini data recorder precluded the recovery of quantitative analysis of AMU data performance. Analysis of the AMU systems, therefore, was based primarily on the debriefing comments by the flight crew.

All AMU systems exercised during the mission were in an acceptable condition for flight when the AMU evaluation was terminated. Some difficulty was experienced with the reception of the AMU voice signal by the command pilot. Subsequent investigations failed to pinpoint the exact cause of the problem. However, for the expected Gemini XII AMU mission, a third antenna for reception of AMU transmissions was added in the adapter section. Since one of the adapter floodlights did not function on Gemini IX-A, a design change was made to shock-mount the floodlights for Gemini XI and XII. One of the penlights provided for backup failed to operate. A pair of these penlights was subjected to a simulated launch environment mounted on the AMU tether bag as they were on Gemini IX-A. Both functioned properly after the test, and no further action was taken. The preparation and donning of the AMU was a complex procedure involving serial operations. The primary cause of AMU donning problems on Gemini IX-A was the lack of adequate body restraints. A new foot restraint system for AMU donning was designed for Gemini XII before the AMU was deleted from the mission. Several changes were made to the AMU after Gemini IX-A to simplify the donning and changes were made to other EVA equipment to simplify all EVA tasks.

The AMU experience on Gemini IX-A indicated that the training requirements for a flight of this type of device were quite extensive. The Gemini IX-A EVA pilot spent 140 hours in the various AMU training activities. Training for the AMU flight started with introductory briefings about 7 months before the scheduled flight of Gemini IX-A. This training for flight of the AMU was very demanding on the crew's time. This should be considered in planning future EVA maneuvering missions.

h. Body Positioning and Restraints

The requirement for body restraints during extravehicular activity (EVA) was indicated on Gemini IV. After depletion of the propellant in the Hand Held Maneuvering Unit (HHMU), the pilot evaluated the umbilical as an aid for body positioning and for moving through space. It was concluded that the umbilical was usable only as an aid in moving to its origin, and that handholds would be required for other movements on the outside of the spacecraft. The significance of the requirement was emphasized when body restraint problems contributed to the premature termination of the Gemini IX-A and Gemini XI EVA missions. During the Gemini XII mission, with adequate restraint provisions, a great variety of EVA tasks were performed. For the Gemini XII EVA, 44 pieces of equipment were provided for extravehicular body restraint in contrast to the 9 pieces provided for Gemini IX-A EVA. The restraints and tasks of the Gemini program are summarized in Tables 7-66c and d.

The first major EVA work task attempted during the Gemini Program was the checkout and donning of the Astronaut Maneuvering Unit (AMU) on Gemini IX-A. The original restraint provisions for this task were two handbars and a horizontal footbar. Velcro pile on the footbar was intended to mate with Velcro hook on the pilot's boots; however, before the mission, the need for additional body restraint for this task was demonstrated during tests in the zero-G aircraft. A pair of foot stirrups was added to the horizontal footbar, and on subsequent tests in the zero-G aircraft, the checkout of the AMU was easily accomplished. The pilot forced his feet into the stirrups. The frictional force restrained his feet and allowed both hands to be free for working.

During the Gemini IX-A EVA, the pilot was unable to maintain body position using only the foot stirrups. The tasks that required the use of both hands, such as tether connections, were exceedingly difficult because the pilot had to stop working every few seconds and use his hands to regain proper body position. The foot stirrups were unsatisfactory when the pilot was unstowing the AMU controller arms. When he bent forward and applied a downward force to the controller arm, he created a moment which caused his feet to come out of the stirrups. In addition to the work involved in performing the tasks, the inadequacy of the foot restraints caused the pilot to exert a continuously high workload to maintain control of his body position. Heat and perspiration were produced at a rate that exceeded the removal capability of the life support system, and fog began to form on the space suit visor. This fogging increased until the pilot's vision was severely restricted, forcing him to discontinue his attempts to don and use the AMU. As a result, new requirements for foot restraints were developed, and the investigation of underwater simulation of zero G was initiated. Equipment modifications were also incorporated to simplify the EVA tasks on subsequent missions.

Analysis of the Gemini IX-A body-restraint problem resulted in the following criteria for design of new foot restraints: motion must be restrained in all six degrees of freedom; the foot restraints must position the EVA crewman for convenient access to the intended work task; and release of the feet must not depend on the action of any moving mechanism. Molded fiberglass foot restraints incorporating these features were designed for the Gemini XI and XII spacecraft. These restraints were custom-fitted to the pilot for each flight and were mounted on a platform attached to the inside

surface of the spacecraft adapter equipment section. During the zero-G aircraft training, the Gemini XI and XII flight crews evaluated the foot restraints and found them to be satisfactory for all applicable tasks. The Gemini XII flight crew also evaluated the restraints in underwater zero-G simulation tests with the same results.

The initial evaluation of the underwater zero-G simulation was conducted by the Gemini IX-A pilot shortly after the mission. The underwater mockup equipment was similar to the Gemini IX-A spacecraft, and the pilot completed the AMU donning procedures previously attempted in flight. The pilot concluded that the underwater zero-G simulation very nearly duplicated the actual flight. The extravehicular tasks planned for Gemini X, XI, and XII were performed in the underwater zero-G simulation and recommendations were made concerning the required restraints and the feasibility of proposed tasks. The simulations for Gemini X and XI were performed using contractor test subjects. For Gemini XII, the prime and backup pilots both participated in underwater simulations for procedures development and training. Underwater simulation of zero G was particularly applicable to the problems of body positioning and restraints.

Minor restraint problems were encountered during the Gemini X EVA, but performance of the planned tasks was not seriously affected. The pilot had difficulty controlling his body position while using the outer edge of the target vehicle docking cone as a handrail. Attachment of the umbilical nitrogen fitting also involved minor difficulty because one of the adapter section handrails had not fully deployed. The tasks were accomplished with one hand, while the other hand was used for restraint.

For the Gemini XI mission, the tether for the spacecraft/Gemini Agena Target Vehicle (GATV) tether evaluation was assembled and stowed so that the pilot could attach the tether to the spacecraft docking bar with one hand. With the other hand, he could use one of three handholds on the back surface of the docking cone to maintain position. However, the pilot had been trained to have both hands free, and he had been able to wrap his legs around the spacecraft nose and to wedge his legs into the docking cone. The pilot was able to place himself in the position by arm force using the handholds provided. In the zero-G aircraft simulations, the pilot was able to move from the hatch, to force himself into the restrained position, and to make the complete tether hookup in about 30 seconds. In orbit, however, this positioning technique proved extremely difficult, and the pilot expended a great deal of energy during the 6 minutes that were required to move from the hatch and to make the tether hookup. The resulting fatigue was the major factor in his inability to continue the flight plan for the EVA. Similar to the Gemini IX-A pilot, the principal expenditure of energy by the Gemini XI pilot was the effort required to overcome the forces of the space suit to maintain the desired body position. The frictional forces induced by the pilot in wedging his legs into the docking cone were not sufficient to overcome the tendency of the pressurized suit to straighten itself out and push him out of the docking cone.

The following restraints were found to be most satisfactory in the Gemini Program:

- Foot restraints as used on Gemini XII for rest and localized work
- Waist tethers as used on Gemini XII for rest and localized work (slightly greater freedom of movement was possible with waist tethers than with foot restraints)
- Rectangular handrail for transit across a spacecraft surface
- Pip-pin devices for combination tether attachment points and handholds where flush-surface installations were required
- U-bolts for simple attachment points where flush-surface installations were not required

Details of the design of the restraint devices noted in Table 7-67d are available (398).

i. Umbilical and Tether Combinations

Several types of umbilical and tether combinations were designed, fabricated, and used in accomplishing the extravehicular activities of the Gemini Program to provide structural, fluid, and electrical linkage with the spacecraft and to limit the distance between the extravehicular crewman and the spacecraft. (See Table 7-66a.) The basic function of the umbilicals was to provide a structural attachment, electrical leads for voice communications and biomedical data, and an oxygen supply line. In one case, the 75-foot tether for the Extravehicular Support Package (ESP) supplied only a structural member and electrical leads. And, the 50-foot and 30-foot umbilicals flown on Gemini X and Gemini XI, respectively, included a nitrogen supply line for the HHMU. A 25-foot umbilical was flown on Gemini IV, VIII, IX-A, and XII. The 75-foot tether was to have been used during the ESP evaluation planned for Gemini VIII. Complete data on design and function of these umbilicals are available (398).

The feasibility of using umbilicals for EVA in the vicinity of the spacecraft was established. The umbilicals produced no unfavorable torques or forces on the EVA pilots. However, some difficulty was experienced during ingress with the bulk of the 50-foot umbilical used for the Gemini X EVA. The donning of the umbilicals was easy, and a complete system checkout could be made before opening the hatch. The incorporation of a supply line for the propulsion system of the HHMU proved satisfactory, and this concept has possible future application for power tools as well as for maneuvering units.

The umbilical concept was particularly applicable to near-vehicle operations, or operations in close quarters where the bulk of a life support pack would have been undesirable. The difficulty of long tether dynamics was experienced by Gemini IV pilot who found that a maneuver would have taken more fuel than he had wanted to expend with the gun, so he gave a little tug

on the tether and came back in. "This is the first experience I had with tether dynamics and it brought me right back to where I did not want to be. It brought me right back on top of the spacecraft, by the adapter section."

j. Capability of Astronauts in EVA

One of the early discoveries by pilots performing EVA was the dominant effect of small forces in the weightless environment. The lack of a large gravity force made the second-order forces significant, although they had previously been neglected. Each small force exerted on the pilot resulted in a displacement velocity which, in most cases, interfered with the task he was attempting to perform. Also, the pilots seemed to have difficulty in rationalizing the forces and the resulting motions in zero G without adequate simulation and training. It was not until after several hours of extravehicular experience in the space environment had been obtained that a practical appreciation of these second-order forces was achieved. As a result of this knowledge, an increased emphasis was placed on the design and use of body restraint devices. In the Gemini XII mission, the pilot demonstrated methods to perform the assigned EVA tasks more efficiently.

Some of the early experiences in EVA indicated the possible existence of external body forces which caused the pilot to float up, away from the Earth. The Gemini IX-A pilot commented as follows in the postflight debriefing:

"My work load, I felt, was harder than it should be. It was harder than it should be because of position control or maintaining yourself in the stirrups in the adapter. All of our work had been built around the fact that in zero G, you would stay there unless you perturb your body position with some external force or motion. This is not true. It was a continuous work load just to stay put in zero G. I always tended to roll back over to the right and over the top of the spacecraft. So, in addition to these other things, it was a case of position maintenance."

Later Gemini missions included an investigation of external forces during EVA. Objects were placed in a free position inside the spacecraft, with the hatch opened and closed, while the crews watched for any tendencies for movement of the objects. Also, the pilots attempted to position themselves in a stationary position with respect to the spacecraft and to observe the motions caused by any external forces. No preferred direction of motion was observed in any of these evaluations, although some movement invariably ensued. The Gemini XII pilot reported that, if such forces existed, they were much smaller than the magnitude of known small forces such as those associated with the body tether. The results of this investigation also verified that small forces were significant in the motions of the pilot's body or of other objects in the EVA environment. Small forces applied with the fingers or the hand induced body motions and could be used for body positioning at low rates. The following factors, which reflect the knowledge gained from investigations of some of the later Gemini pilots, may have lead to the initial reports of unknown body forces:

- (a) Forces were induced by the space suit tending to return to the neutral position.
- (b) Body motions resulted from inadvertent application of small forces by the pilot.
- (c) Spacecraft outgassing when the hatch was first opened, induced an outward force on all loose items in the cabin, including the pilot.
- (d) Small perturbations in spacecraft motion caused primarily by attitude control limit cycling may have induced body motions relative to the spacecraft.
- (e) Inability to set up an initial condition of no movement may have led to the impression of external forces.

The effort required to perform assigned EVA tasks was greater than planned on several EVA missions. A major part of the effort was due to the pilot working against the pressurized space suit. The Gemini space suit tended to assume a unique neutral position and to maintain that position. Therefore, if a pilot was unable to perform an assigned task with the suit in the neutral position, he had to work against the space suit to complete the task. While this factor had been anticipated, the magnitude of the effort had not been fully appreciated until the gravity bias force was eliminated. Suit forces of considerable magnitude were encountered when the pilots attempted to change from the neutral suit position, such as moving the arm toward the head area or toward the feet. The magnitude of these forces exerted by the pilot was a function of the displacement from the neutral position of the suit. However, the pilots were able to minimize the suit forces by training for assigned EVA tasks in high-fidelity simulations and by becoming familiar with optimum methods of operating in their own suits.

Experience in EVA indicated that a pilot was in better condition to perform his assigned EVA task successfully if he had had an opportunity to familiarize himself with the EVA environment. The pilots performing the EVA in the Gemini Program had no previous experience in a sustained weightless environment; they approached the tasks without complete knowledge of how to operate in the space suit or to control body positions and attitudes. They were operating in a new environment, and a period of acclimatization improved pilot performance.

Unless the pilot was adequately restrained, his capability for useful work during EVA was severely limited. Pilots were able to perform relatively difficult tasks without adequate restraint, but only with an excessive expenditure of energy. The problem was that the pilot expended a large percentage of his energy in overcoming the space suit forces and in maintaining body position. Two pilots terminated their planned EVA prematurely because the lack of adequate body restraints resulted in high workloads and in high energy expenditures. However, it was also demonstrated that, with proper familiarization, useful work could be continued for long periods of time, if the pilot was provided with adequate body restraints and if the work was paced properly. An ideal sequence included rest periods of 2 to 3 minutes every 5 to 15 minutes depending on the work performed. If the pilot was properly restrained, his normal capabilities were limited principally by

the mobility limits of the space suit. Examples of the tasks performed by Gemini pilots are shown in Table 7-66c.

In addition to the lack of adequate restraints and the lack of space suit mobility, the EVA pilot's capabilities were limited by the design of the EVA hardware. Early experience indicated that performance of EVA tasks was frequently more difficult in orbit than on the ground. In some cases, tasks were more difficult because of minor incompatibilities between the hardware design and the EVA operational environment. The extensive underwater simulation before the Gemini XII mission served to identify this type of hardware problem and to facilitate correction. Hardware designs that were found to be suitable in a valid underwater simulation were also suitable for use in orbit.

The command pilot's capabilities were also limited during EVA. The normal functions of spacecraft control, systems monitor, replacement of voice tape cartridges and film magazines, and general equipment management were complicated by the restrictions of operating in the pressurized space suit. Since the command pilot was responsible for directing the entire EVA operation, he received detailed training in all equipment and procedures. The resulting familiarity enabled effective exercise of the command function. Because of the extensive involvement of the command pilot, a detailed analysis of his tasks and time lines was also needed in the preparation of the EVA flight plan.

k. Flight Plans and Checklists

One of the many factors to be considered in EVA flight planning was the writeup of EVA procedures. Detailed checklists were used during Gemini EVA. The Gemini crews consistently used the checklists either as a step-by-step sequence of the tasks to be performed or as a check to see that various tasks had been completed. The detail included was commensurate with the requirements of the tasks to be performed. The checklist included procedures for preparing for the EVA, for performing the EVA, and for ingress. The checklist also provided information concerning equipment location and unstowage, operation, restowage, and concerning the crew function and interface with the equipment. Since the stowed equipment for the later Gemini missions included items for numerous experiments and inflight tasks, the preparation for EVA required substantial handling of loose equipment. A written plan of action was necessary to insure the completion of all the tasks within the time allowed. Velcro was used to hold the checklist in position.

Early EVA experience indicated the necessity of a detailed checklist for extravehicular tasks. With extravehicular tasks, such as the checkout and donning of the AMU, the procedures were complex and required a specific sequence. Most EVA tasks consisted of individual steps with a specific sequence required for successful completion. Hence, the pilots were confronted with the sequencing of the steps for completing each task, as well as the sequencing of all the tasks to be completed in the EVA flight plan. The efficiency of operation outside the spacecraft was enhanced by reference to a

comprehensive set of extravehicular procedures. Besides defining the sequence, the procedures for Gemini XII also provided a realistic time line for EVA which had been developed during underwater zero-G simulations. The Gemini XII experience reflected the benefit of the use of underwater simulations for development of procedures and time lines.

The EVA checklist was a byproduct of the crew training program. The checklist was the focal point for all items related to EVA, and it was updated because of the following: modifications to procedures resulting from crew training and procedures development; modifications to equipment; changes to the flight plan or mission because of other factors. Review and validation by the crew during their training was repeated after each revision of the checklist. The flight procedures were in final form when the crew training was completed.

1. Scheduling of EVA and Training

Maximum ground tracking coverage during EVA allowed the flight control network to monitor systems performance with maximum communication between the ground and the spacecraft. The Gemini EVA was basically experimental; and, for the overall mission, the EVA could occur at almost any time. EVA was normally scheduled in orbits when the spacecraft was over the United States, since these orbits afforded maximum tracking coverage. Only 4 revolutions of every 15 gave the desired coverage, and this caused a restriction in the flight planning.

An additional restriction was imposed on the flight plan by the extensive preparation and postingress cleanup time required for EVA. A 2-hour umbilical EVA on a typical Gemini mission occupied about 7 hours of flight time. Three and one-half hours were required for EVA preparation, 2 hours for actual EVA, and about 1-1/2 hours for restowage after EVA. Total elapsed time for a standup EVA was less, since standup EVA required only about 2 hours for preparation. In either case, EVA consumed a significant portion of a mission day. Whenever possible, this period was uninterrupted. The many items of hardware unstowed for EVA made continuity highly desirable. Any other activity during EVA preparation complicated both activities because of the loose hardware in the cabin.

Familiarization with the EVA environment also had overall flight plan implications. No pilot encountered any disorientation problems during EVA; however, the desirability of an initial period of familiarization was best satisfied by avoiding mission-critical activities immediately following the initial egress.

Night EVA operations were limited to either the standup activity, in which the pilot was restrained in the cockpit, or to activities in the spacecraft adapter section. The EVA pilots carried out these night operations successfully. Adequate lighting was the only constraint identified. A relatively low level of lighting was provided in the adapter section, and this lighting was found

adequate in Gemini IX-A and XII. Both the Gemini IX-A and XII pilots indicated that, with appropriate lighting, transit along fixed handrails appeared feasible for night operation.

The extravehicular crew training conducted in the zero-G aircraft for each Gemini mission was valuable for many of the inflight tasks. The value of the actual training was enhanced by the use of up-to-date flight hardware for which design and procedure validation had already been accomplished. The mission results indicated that for extended tasks, such as AMU donning and spacecraft/target-vehicle tether attachment, data from the short periods of weightlessness were misleading. The rest periods between the weightless parabolas prevented assessment of fatigue as a factor. Also, these rest periods led to the tendency to start each segment of the tasks with more favorable initial conditions than would be experienced in a continuous task. The zero-G aircraft simulation was effective only for short period tasks such as egress and ingress.

m. Spacecraft Control during EVA

Control of spacecraft attitude and position during EVA was complicated by several factors. Tests showed that significant damage to EVA equipment could result if the spacecraft control thrusters were fired when the equipment was within the direct impingement envelope of the thrusters. To avoid such damage, the flight crews coordinated thruster operation and the EVA pilot's movements. The pilot kept track of the position of the umbilical and of his position and notified the command pilot when certain thrusters could be fired safely. This coordination was particularly important during the umbilical EVA on Gemini X when the command pilot was station-keeping with the Gemini VIII GATV. Coordination between the pilots enabled them to accomplish the task without equipment damage.

Another complication to spacecraft attitude control was the significant torques introduced by the EVA pilots. During the umbilical EVA on Gemini IX-A, the pilot may have caused noticeable attitude excursions when he moved about on the external surface of the spacecraft. The control system was off at the time. When he was in the adapter section and the control system was reactivated, there were frequent thruster firings, especially whenever the pilot moved vigorously. The use of an automatic control mode tended to relieve the command pilot of the task of counteracting the disturbances introduced by the EVA pilot.

Although the spacecraft exterior was designed to withstand the extremes of heat inputs from direct solar radiation and of radiation heat losses to deep space, the Gemini spacecraft interior was not so designed. Opening the hatch for EVA exposed the spacecraft interior to these conditions. On Gemini IX-A, there was an overheating problem, and some of the paint on the top of the ejection seat headrest and on the seat pan was blistered. Review of the time line indicated that the seat was only exposed to the sun for approximately 30 minutes. Subsequent analysis showed that in thin metal structures, such as the ejection seat, the surface temperature could reach 200° to 300°F within 20 minutes exposure to direct sunlight. A study of the

shadowing using a scaled mockup was made to determine the sun angles which could be tolerated. For Gemini XI and XII, a fixed inertial attitude was maintained during the umbilical EVA, using the GATV attitude control system. The attitude was chosen to avoid direct sunlight on the interior of the cockpit, even with the right hatch open.

n. Medical Factors

Medical experience gained as a result of Gemini EVA has provided information which will be valuable in preparing for future EVA missions. There were no indications that the ability of man to do work was significantly altered during EVA. [See O₂ - CO₂ - Energy, (No. 10).] The major factors which produced the highest workload during EVA were engineering design problems which were resolved for Gemini XII. The success of Gemini XII EVA demonstrated that when these factors were understood properly, the medical response to EVA was very close to prediction. Evaluation of physiological factors during EVA in Gemini was limited by the lack of more extensive instrumentation. Much was learned about the physiological responses to EVA from simulations such as sea-level practice exercises and the zero-G underwater simulations. However, without specific knowledge of the thermal and environmental conditions, a complete analysis of the physiological aspects of EVA could not be accomplished. Specific measurements which were lacking were the carbon dioxide concentration, the dew point in the space suit helmet, the space suit inlet and outlet temperatures, and the body temperature. The electrocardiogram and the rate and depth of respiration were useful but only partially effective in assessing total physiological performance during EVA.

The successful completion of the Gemini EVA program indicated that EVA life support system planning had been essentially sound. The success of Gemini XII indicated that within the limitations of our experience, time lines and work levels could be tailored so that flight objectives could be accomplished. There were no medical contraindications to the type of EVA accomplished in the Gemini Program.

o. Recommendations for Future EVA

- (a) EVA should be considered for future missions where a specific need exists, and where the activity cannot be accomplished by any other practical means. Since EVA involves some increased hazard, it should not be conducted merely for the purpose of doing EVA.
- (b) In future EVA missions, consideration should be given to body restraints, proper task sequence, workload control, realistic simulation, and proper training.
- (c) Underwater simulation should be used for EVA procedures development and crew training in conjunction with zero-G aircraft simulations and ground simulations.

Work levels and metabolic rates should be measured inflight. Inflight work levels should be controlled by designing tasks so that they could be accomplished readily, by providing additional body restraints, by allowing a generous amount of time for each task, and by establishing planned rest periods between tasks. Equipment retention during EVA should be considered a problem for all items which are not tied down or securely fastened. By the extensive use of equipment lanyards, the loss of equipment can be avoided.

(d) The Hand Held Maneuvering Unit should be evaluated further in orbital flight with emphasis on stability and control capabilities. Other maneuvering systems which incorporate stabilization systems should be evaluated for comparison.

(e) Priority efforts should be given to improving the mobility of space suits with emphasis on arm, shoulder, and glove mobility. For the 2-hour EVA mission, glove mobility restrictions caused hand fatigue in both training and flight situations.

(f) In future Extravehicular Life Support Systems, consideration should be given to cooling systems with greater heat removal capacity than the gaseous cooling systems used in the Gemini Program. The bulk and encumbrance of sizable chest-mounted units should be avoided. Any life support system should be capable of supporting the anticipated peak workloads.

The size and location of the ELSS chestpack was a constant encumbrance to the crews. The design was selected because of space limitations within the spacecraft, and the crews were continually hampered in two-handed operations by the bulk of the chest-mounted system. The use of gaseous oxygen as the coolant medium in the space suit was a limiting factor both in the rejection of metabolic heat and in pilot comfort. The use of a gaseous system required the evaporation of perspiration as a cooling mechanism. Heavy perspiration and high humidity within the suit occurred on the two missions where the workloads apparently exceeded the planned values. Special effort should be made to control the workload within the capabilities of the ELSS and the space suit for nominal and emergency conditions.

(g) Qualification test programs for future EVA life support systems should include detailed component testing; should be conducted in a flight-serviced configuration, whenever appropriate; should include manned testing on representative off-nominal mission profiles; and should require that the contractor take the lead in all qualification testing of his equipment.

(h) Vacuum chamber tests should be included in the preparations for future EVA missions. Both the prime and backup crews should participate in these tests using EVA flight hardware.

(i) Detailed EVA flight plans and crew procedures should be established as early in the hardware development cycle as possible,

so that the impact of design or procedures changes can be evaluated. The ease of accomplishing EVA tasks appeared to correlate with the sequence in which they were scheduled. A period of acclimatization to the extravehicular environment appeared desirable. Those pilots who had completed a standup EVA first appeared to be more at ease during the umbilical EVA. It appears that critical EVA tasks should not be scheduled until the pilot has had an opportunity to familiarize himself with the environment.

(j) Training programs for further EVA missions should include configuration control procedure to insure that the training hardware is maintained in representative flight configuration. Although considerable attention was given to maintaining the training hardware in an authentic configuration, the efforts were not always successful. The use of the actual flight hardware in final simulations was the principal method for insuring crew familiarity with the flight configuration.

(k) Planning for future EVA missions should include consideration of the Gemini EVA experience and results.

A Soviet model of extravehicular dynamics has recently been presented (491). American models are discussed relative to Tables 16-5 and 16-6.

Table 7-66c covers the hazards anticipated during extravehicular activity. A more complete discussion of these hazards is available (62).

Tether Lines for Astronaut Retrieval

Problems in using tethers or cable for human retrieval techniques have been examined by relatively few investigators (20, 436, 520). The problems encountered with tethers in rendezvous and docking of large components have been pointed out in an orbital-operation study (640).

Problems exist for short as well as long tethers. During Gemini IV, it was discovered that the attachment of the tether to the sill of the hatch tended to force White perpendicular to the hatch area rather than out in front of the craft. When he maneuvered to the forward part of the capsule, the tether carried him along a large arc up and over the top of the craft and back into the adaptor area. It appeared difficult for him to push off at an angle from the surface of the craft. When he did exercise this maneuver, the craft tended to pitch down (about two degrees per second) under his pushing force and the direction of White's motion tended to be perpendicular to the surface. He admitted that it was difficult to maneuver himself to specific points on the craft. However, White reported that it was easy to return to the hatch area using the tether. He experienced no high velocity contact with the vehicle. This implies that the value of his training in maneuvering in a weightlessness environment should not be underestimated (398).

Figure 7-67a summarizes the approaches that have been proposed. The basic problem is not materially altered whether the system involves an astronaut and carrier vehicle or two other objects in orbit. The difficulties stem mainly from the fact that, in the absence of external forces, the system conserves angular momentum. The magnitude of the retrieval problem thus becomes a function of the system's initial conditions, primarily tether length and relative velocity of astronaut to carrier vehicle. Unfurling flexible lines without fouling is a hardware-design problem.

a. Conservative Methods. The simplest method of conservative retrieval (angular momentum assumed to be retained in the system without adverse effect) involves direct reel-in of the astronaut. When the astronaut's radial velocity is small compared to his tangential, the line tension varies inversely with the third power of the tetherline length. Unless the angular momentum is relatively low, directly reeling in the astronaut, or other body, may cause excessively high line tension or radial acceleration. Figure 7-67b summarizes the basic problem of the conservative techniques when using long tether lines. Study was made of conservative retrieval of an astronaut rotating at the initial rate of 0.001 rad/sec (5 fps tangential velocity), which is less than what is present due just to being in orbit. As he is reeled in from 5000 to 25 ft, the astronaut heads toward an extreme final condition of 400 rpm and 1200 G.

Figure 7-67

Retrieval of Astronauts in Orbit by Tether Lines

a. Comparison of Retrieval Philosophies

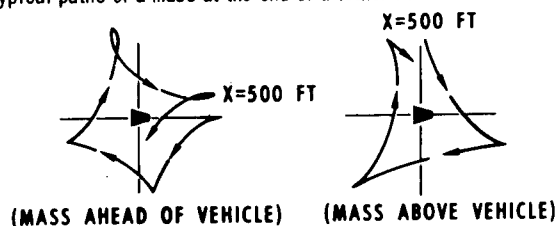
(After Beasley and Brissenden⁽²⁰⁾)

Philosophies of retrieval	ASPECTS OF PHILOSOPHY						
	Relative energy requirement	Relative weight requirement	Relative time requirement	Complexity	Operational control	General technical feasibility	Remarks
A. Nonconservative.							
Environmental	Small	Negligible	Excessive	Simple	Easy	Poor	Forces are too small to aid retrieval.
Multiple-body deployment	Nominal	Small	Arbitrary	Fairly simple	Easy	Excellent	Several techniques available; requires throw-away mass.
Thrusting							
Space-vehicle translation	Small	Small	Arbitrary	Simple	Easy	Good	Uses onboard store of propellant.
Space-vehicle torquing	Nominal	Moderate	Arbitrary	Fairly complex	Fairly easy	Fair	Normally less efficient than translating.
Astronaut translation	Nominal	Very little	Arbitrary	Complex	Fairly easy	Excellent	Propellant expedient; may be complex in emergencies; favorable in normal operations.
B. Conservative.							
Direct	Large	Excessive	Arbitrary	Simple	Easy	Poor	Normally exceeds tolerances on human.
Angular-momentum exchange							
Rotate-space vehicle	Large	Moderate	Arbitrary	Fairly complex	Fairly difficult	Fair	Depends on large mass ratios.
Internal storage	Large	Considerable	Arbitrary	Complex	Fairly easy	Poor	Requires large angular-momentum storage.
Snaring	Large	Considerable	Moderate	Complex	Difficult	Poor	Normally entails excessive mechanical features.

Figure 7-67 (continued)

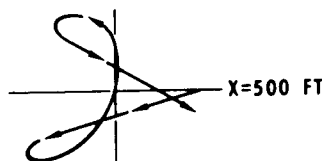
b. Dynamics of a Long Tether Line
(After Mueller⁽⁴³⁶⁾)

An obvious method of astronaut locomotion, equipment transfer and retrieval of an incapacitated EVA-performing space-worker is the use of tether lines. However, the retrieval of a mass, attached to a long tether line, presents serious hazards. Impulsive jerks on a long tether line by a man inside a spacecraft causes the mass to follow a path in a plane different from that of the spacecraft, depending on the initial location of the mass and the amount of force applied to the tether. Two typical paths of a mass at the end of a tether line after an initial impulse are shown below.

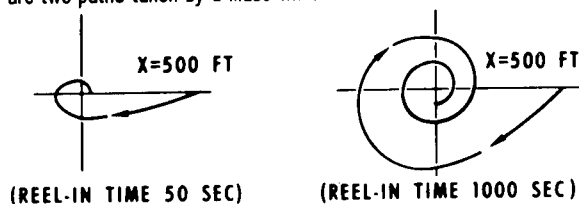


This method of retrieval will ultimately result in the interception of the mass, but it requires from seven minutes to an hour and presents the additional hazard of the mass colliding with the ship at an intolerable velocity.

An alternative to jerking the line is to maintain a constant tension on the tether. However where no tangential velocity exists, this process is also time consuming (25 min or more) and describes an erratic path as shown below.



Another method of retrieving a mass at the end of a line is to simply reel the line in at a constant speed. In such an operation, the mass follows a spiral path toward the spaceship, the exact trajectory depending on the speed with which the line is reeled in. Below are two paths taken by a mass which has been reeled in at different speeds.



Though intersection of the mass and craft is possible by this technique, it requires considerable time to safely reel the mass in. Or, if the distance of mass to craft is too great, the mass could be approaching the spacecraft at a great velocity with a centripetal acceleration of 40 g's or more.

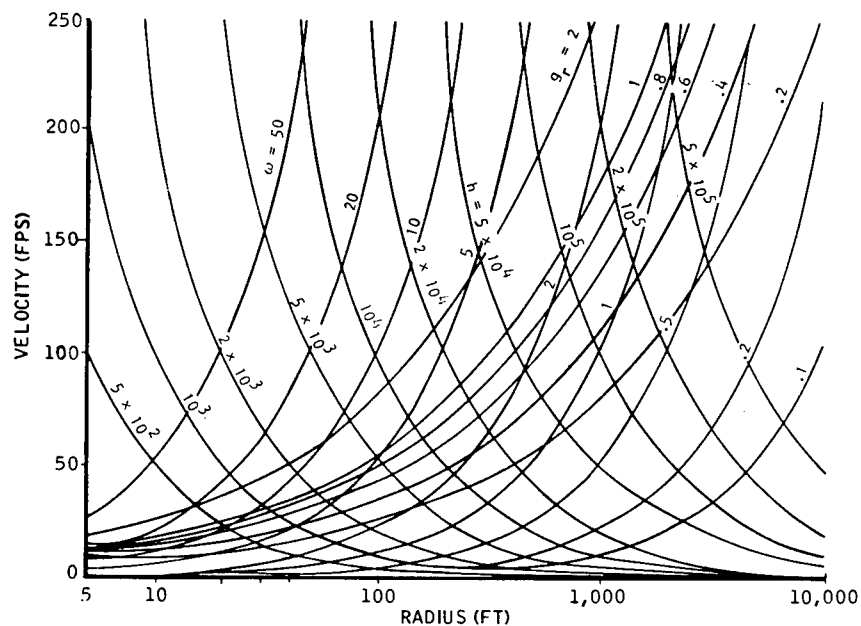
Figure 7-67 (continued)

c. Dynamic Parameters of Astronaut Versus Tether Length

(h = specific angular momentum, ft^2/sec ; ω = angular velocity, rpm;
 g_r = radial acceleration, Earth's g 's; ordinate is reel-in rate)

(After Beasley and Brissenden⁽²⁰⁾)

SEMILOG
COORDINATES



LOG-LOG
COORDINATES

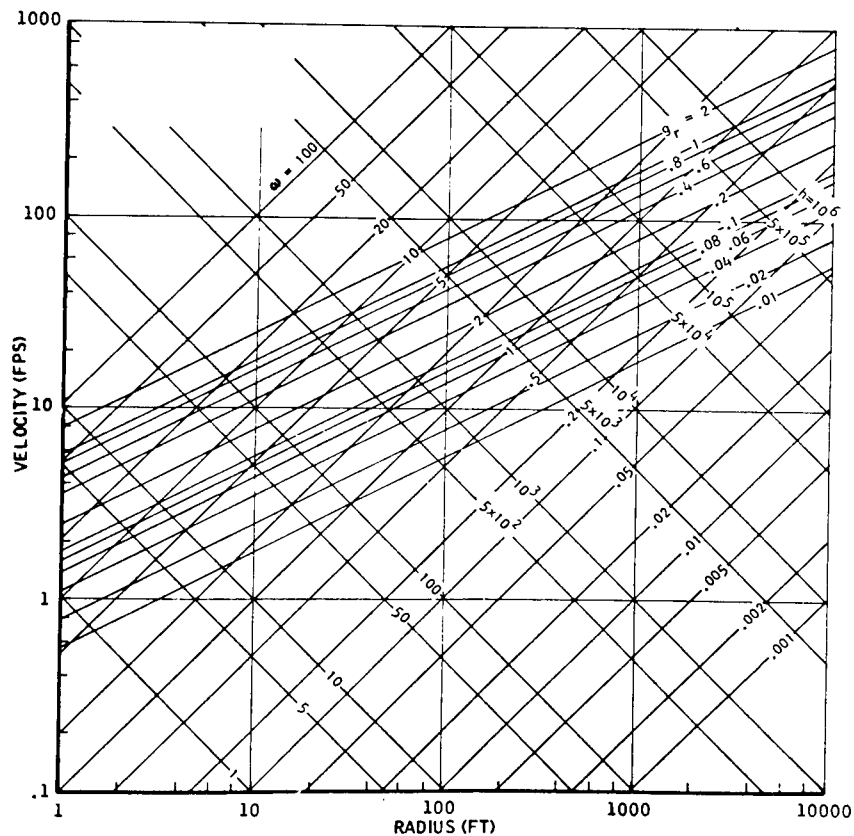
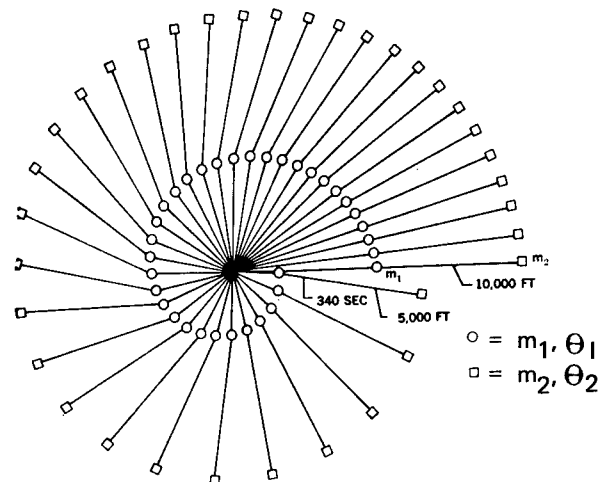


Figure 7-67 (continued)

- d. Three-Body Retrieval at Constant Reel-in Speed of 10 Fps
Shown at 10-sec Intervals Up to 340 Sec from 10,000 ft
($m_1 = 10$ slugs for man; $m_2 = 2$ slugs for anchor)

(After Beasley and Brissenden⁽²⁰⁾)



Reel-in from 100 to 500 seconds (t)

t	R_1	θ_1	θ_2	T_1	T_2
100	4000	63.6	52.6	11	3
200	3008	157.4	131.2	16	5
300	2017	282.6	278.8	26	12
350	1524	21.5	9.0	42	16
400	1029	152.2	127.3	47	30
450	534	299.4	289.4	79	42
490	132	60.9	86.7	48	52
494	94	86.8	103.2	87	53
496	75	117.7	111.5	149	65
498	56	165.3	119.9	193	79
500	35	229.5	128.5	143	77

In the case just described, the angular momentum is assumed to be contained largely in the retrieved body, by virtue of its velocity and large displacement from the system's mass center. This assumption is valid in most cases of astronaut retrieval. The conditions cited can be eased somewhat by transferring some or all of the system's angular momentum to the spacecraft.

The angular momentum must display itself in the angular velocity of either the retrieving spacecraft or in an onboard momentum-storage device, such as a flywheel. Angular momentum storage by either of these methods has severe limitations, showing up as flywheel saturation or excessive spin on the retriever.

If the line tension rather than line length is to be controlled, the trajectory of the astronaut about the retrieving body can be modified so that an arbitrary approach distance, however small, can be achieved without exceeding a nominal line tension. That is, the astronaut might be retrieved by extending a snare to an appropriate point. As the approach distance becomes small, the tangential velocity increases, thereby imposing high energy-absorption requirements on the snaring device.

The upper part of Figure 7-67c presents in graphic form data covering the dynamic parameters of astronaut motion in terms of tether length. By being plotted on semi-log coordinates, it shows relations between distance, reel-in rate, angular velocity, momentum, and centripetal acceleration. It can be seen that conservative retrieval systems rapidly encounter difficulties at high values of angular momentum. The lower part of Figure 7-67c, a plot of the same dynamic parameters on log-log coordinates, provides a more workable plot for obtaining trajectories for specific retrieval techniques. On this plot, limiting value lines can be drawn for a given retrieval mode or technique. For example, assume that the centripetal acceleration and angular velocity are limited to values below 0.25 G and 2 rpm. This, then, defines the boundaries for retrieval operations to the lower right half of the figure. Within these boundaries, various techniques for dissipation of angular momentum can be used and the resultant trajectories plotted, thereby giving energy requirements.

Recent computer studies have been made of the conservative retrieval problem for Gemini EVA conditions (489, 490). These studies show that line-wrap is a recurring problem associated with retrieval system using a tether-line attached to a rigid body spacecraft. Though generally considered to be unacceptable, line-wrap might be considered acceptable under conditions when velocity is less than 5 ft/sec. With the astronaut so close to the spacecraft when line-wrap begins, he could conceivably come in contact with the surface of the spacecraft in such a manner that he will reach the spacecraft. Unfortunately, however, the angular velocity becomes larger than the acceptable limits in some cases. Line-wrap could possibly be avoided by actively controlling the attitude of the spacecraft using the attitude control system. This "controlled" tetherline system, however, requires additional equipment to sense the orientation of the line with respect to the attachment point, to calculate the necessary attitude corrections, and to display these corrections to the astronaut inside the spacecraft. Not enough time was available before the

Gemini extravehicular experiments for the development and testing of such a system to avoid line-wrap.

b. Nonconservative Methods. The constancy of momentum, giving conservative techniques severe inherent limits for general retrieval, forces a look at nonconservative techniques (Table 7-76a). This implies angular-momentum dissipation during the retrieval maneuver-by the action of an outside torque on the system. For many cases, one or more of the common thrusting devices, such as rocket propulsion, present the most expedient method of providing this torque. Thrust can be applied effectively at any point except the system's mass center. The effectiveness, however, is proportional to the moment of the applied thrust about the mass center.

The ultimate objective of all non-conservative methods is to reduce undesirable relative velocity between astronaut and space vehicle. Since momentum (not kinetic energy) must be removed, it is generally expedient in terms of energy efficiency to remove this velocity from the least massive of the bodies when the system exhibits its least relative velocity. In other words, it is often desirable to apply thrust to the astronaut before retrieval is started. But this could require equipment much more complicated than if it were to be done at the spacecraft. The spacecraft would have to be able to tolerate, of course, the orbital perturbation.

It is also possible to introduce a third body to the system configuration where the astronaut is held by two tether lines; one to the spacecraft and another to a distal anchor as shown in Figure 7-67d. A large portion of the total angular momentum could conceivably be transferred to this body during the retrieval operation. To be effective, the third mass must be remote with respect to the other two primary masses - vehicle and astronaut. Proper deployment of this tethered "anchor mass" during retrieval causes most of the total angular momentum to show up as anchor-mass linear tangential velocity about the center of mass of the system. An alternate approach using a third body has been proposed using the astronaut's inoperative propulsion unit as the anchor mass (377). The astronaut would detach the propulsion unit from his back and leave it at the end of the tetherline to act as the third body. No deployment would be necessary in this approach. The astronaut would pull himself along the tetherline toward the spacecraft at a constant rate. Computer studies have compared the three distinct types of extravehicular astronaut retrievals by use of a flexible tetherline (489, 490). The models obtained were for the case of constant line-tension retrieval, direct reel-in retrieval at constant speed, and anchor mass retrieval. The equations were used on a typical man-vehicle configuration and the feasibilities of the three retrieval techniques were investigated. The program made use of the rotational equations of motion for a rigid body spacecraft, the translational equations of motion for a "point-mass" man and a "point-mass" anchor, and the equations of constraint relating the distance between the Gemini spacecraft, the astronaut, and the anchor mass. The trajectories of the astronaut and the anchor mass with respect to the spacecraft, the forces of constraint on the astronaut, and the angular-velocity components of the spacecraft are determined by solving the equations using various initial conditions for the astronaut, the anchor mass, and the spacecraft under typical orbital conditions.

The solution to the equations describing the retrieval techniques show that the anchor mass technique appears to be the most promising, while the constant line tension technique appears to be the most disastrous approach to tetherline retrieval.

Figure 7-67d shows a quantitative digital solution for retrieving the astronaut at a constant 10 fps for this three-body case. The anchor mass (third body) is initially at 10,000 ft and the astronaut is at 5000 ft. During the reel-in the anchor mass remains 5000 ft outboard of the astronaut. The angular momentum is continually exchanged between the astronaut and the anchor mass, which oscillates through a moderate angular deadband. The astronaut is retrieved within 35 ft, with practically all of the momentum stored in the anchor mass and tetherline tension on neither mass exceeding 200 lbs. The chart shows only one revolution, while the full retrieval required three revolutions, as indicated in the inset table. During this retrieval, the system never rotated faster than 1 rpm. At the completion of the maneuver, the anchor mass remained a considerable distance from the remainder of the configuration. For this reason, its linear velocity would not need to be large for the anchor mass to contain a relatively large amount of angular momentum.

Two methods would allow this third body to be introduced at the time a retrieval is started: (1) If the mass center of the station-astronaut system was in or near the station, a third mass sent out from the station would have a "downhill" potential decay, producing a radial acceleration outward to the astronaut and, with a proper bypass guide, beyond the astronaut on a subsequent reel. (2) A simple triggering mechanism could release some mass from the astronaut himself (such as a spent backpack unit or other disposable or predetermined weight) to serve as the third body.

Both of these methods are undergoing analytical scrutiny (20). The total system behavior is momentum-conservative until the anchor mass is released. At that point the angular momentum which has been transferred to it is also removed from the system. Calculations are now in progress to identify, for all methods, the trajectories of the third mass that allow absorption of a large fraction of the system's angular momentum. Where the momentum of the retrieved body oscillates through zero, release of the anchor mass would remove all of the momentum at this point.

There are other means of exerting torque on the system besides mass expulsion - reaction with the environment through solar-radiation pressure, aerodynamic drag, gravity gradient, and numerous other natural phenomena; but these, at best, show only marginal utility for most of the systems considered (20).

The three-body techniques are now under study in ground-based simulators (20). Oscillations develop from momentum exchange between the two masses. As the retrieved mass is brought in, it speeds up, causing the anchor mass to lag, and providing a component of line tension opposing the direction of travel. As the retrieved mass slows down, the anchor mass goes

slightly ahead, and so on. These oscillations continue until the inner mass is completely retrieved. Then, as mentioned earlier, the anchor mass is released as the momentum of the retrieved body oscillates through zero. This is easily recognized when the retrieved body is at rest at the end of one oscillatory cycle, and the anchor mass is at maximum relative rotational speed.

Workspace and Equipment Simulation

The workspace environment in zero gravity has been studied in parabolic simulators (539, 540). (See Table 7-65 and page 126 for bibliographic summary). Time and contact data are available on the motions of unsuited and pressure-suited subjects as they performed lunging, egressing, and landing tasks. Motions of suited subjects generally take 30% more time than those of unsuited subjects in both 1 and zero G. All motions required about 35% more time in zero G than in 1/6th G of the lunar surface. Zero gravity tended to increase the total mobility but this was countered by over-control and lack of fixation to the work site. Cyclogrammometric techniques have been used to determine muscular coordination patterns during zero-gravity parabolic flights (83).

A preliminary investigation has been made into the feasibility of using handrails as an aid to the astronaut in moving from one location to another within or outside a space vehicle (607). Eight subjects wearing flying coveralls (one of whom also performed the tests wearing an inflated full-pressure suit) moved from one point to another aided by a single handrail or two parallel handrails during parabolic flights. Eight conditions were investigated with the parallel handrails spaced from 6 to 36 inches apart and one with the single handrail. All subjects were successful in moving across the surface and turning around using both the single and parallel handrails. Motion picture films were taken to evaluate the body positions and ease of movement. The most common position appeared to be one in which the elbows and knees were slightly bent and the torso was nearly parallel to the surface. The parallel handrails spaced from 16 to 24 inches apart appeared to provide the greatest body stability. Optimum handrail diameters between 0.75 and 2.00 inches (cross-section) have been recommended (5). Optimum translational velocities using handholds are about 0.8 fps (5).

Time scores were recorded of a subject donning and doffing a "Phase B" Apollo Prototype Space Suit inside and outside a donning bag, while in the weightless condition (517). The total times for each of the three donning trials were, in order, 181 seconds (inside the bag), 165 seconds (outside the bag), and 154 seconds (inside the bag). Difficulties encountered in donning the suit are mentioned. The total time for the one doffing trial (inside the bag) was only 95 seconds. Neither the bag nor the space suit was vented or pressurized for the tests.

To provide the astronaut with a means of locomotion in weightlessness the use of magnetic boots and suction cup or Velcro shoes has been tested to allow the astronaut to walk within the spacecraft (279, 541). For the performance of various routine tasks with other objects, the use of Velcro,

magnets, air currents, and electrostatic attraction devices has been proposed to force the objects being used to remain in place and not drift from the working area. (See section on Gemini Flights.)

Washing and bathing can be accomplished using sponge cloths, and dental and oral hygiene could be accomplished in a similar manner as on Earth except that the toothpaste and water would be swallowed. Electric razors with vacuum attachments for catching cut hairs could be used for shaving and haircutting (see Contaminants, No. 13). Human waste collection could be performed with the aid of airflow toilets (149). These techniques for personal maintenance and convenience are quite feasible but, in some cases, offer engineering problems that need to be solved.

Underwater simulation has also been used for study of time-motion parameters and optimization of hatches, workspace, tools and aids (2, 133, 196, 381, 410, 484, 609). Shirtsleeve or pressure suited conditions may be simulated. Task and motion analyses correlate well with data obtained in parabolic flight. In simulating the motions of bodies in zero gravity under an applied force or moment, the mass, moment of inertia of the subject must be considered. This can be done with underwater simulation except that hydrodynamic drag, lift and moment, which are all foreign to a space environment, are introduced. A successful underwater simulation is one where mass and inertia simulation is achieved and the extraneous forces and moments are either reduced to negligible values or the results are corrected to show what would have occurred in space. For example, metabolic rates taken from subject's working underwater would be reduced by the amount of energy that would have been required to overcome the underwater drag effects in doing his work (687). However, water drag will reduce the effort required by the subject to hold his pressure suit in a position opposing the tendency of the suit. It is also possible that damping by water of the velocities imparted to a locomotion aid or in the motion of a subject would be helpful in that he would not have to expend as much energy to slow down or stop these velocities.

Due to a steady loss of momentum to neighboring water layers, the damping forces imposed by the water upon the moving subject tend to constantly decelerate the motion. No energy is required in space to sustain a motion of uniform speed because there is virtually no retarding force; the same motion is possible in water only when additional energy is supplied. The scaling analysis thus involves the calculation of this additional energy expenditure for overcoming water drag. The value of drag energy can then be scaled off from the total energy expenditure to extrapolate zero-gravity, zero-ambient-drag situations.

A theoretical analysis is available identifying a model design technique which utilizes hydrodynamic mass and hydrodynamic moment of inertia to achieve mass and inertia simulation (222). The technique, applicable to simulating modules in space, also results in little hydrodynamic drag, lift and moment. Laboratory tests have verified the design technique and established that valid simulations are possible when mass simulation is achieved and the $W/C_D A$ is greater than 150 pounds per square foot. The same

principles described above for achieving simulations of motions of inert modules also apply to simulating manned space activities. The main difference is that now the underwater model and the space subject are constrained to have the same size and shape. The hydrodynamic drag, lift and moment cannot be altered but must be evaluated and the proper adjustments applied. The hydrodynamic mass and hydrodynamic moment of inertia must also be evaluated and added to the physical mass and moment of inertia of the suited man. Obviously, mass and inertia simulation cannot be achieved when the space subject and the underwater subject are identical. However, the effects of the hydrodynamic drag and hydrodynamic mass can be measured and the results can be applied to the measured body motions to determine the motions occurring in space.

Drag effects are negligible when tasks are performed at velocities of about 2 fps (0.6 m/sec) or less. Figure 7-68 represents the estimated drag envelopes for aircraft and water immersion calculated from the average drag coefficient for zero-roll (zero-side slip) taken from wind tunnel data (521). The total drag, D , is expressed as:

$$D = C_D q A = C_D \left(\frac{1}{2} \rho V^2 \right) A \quad (11)$$

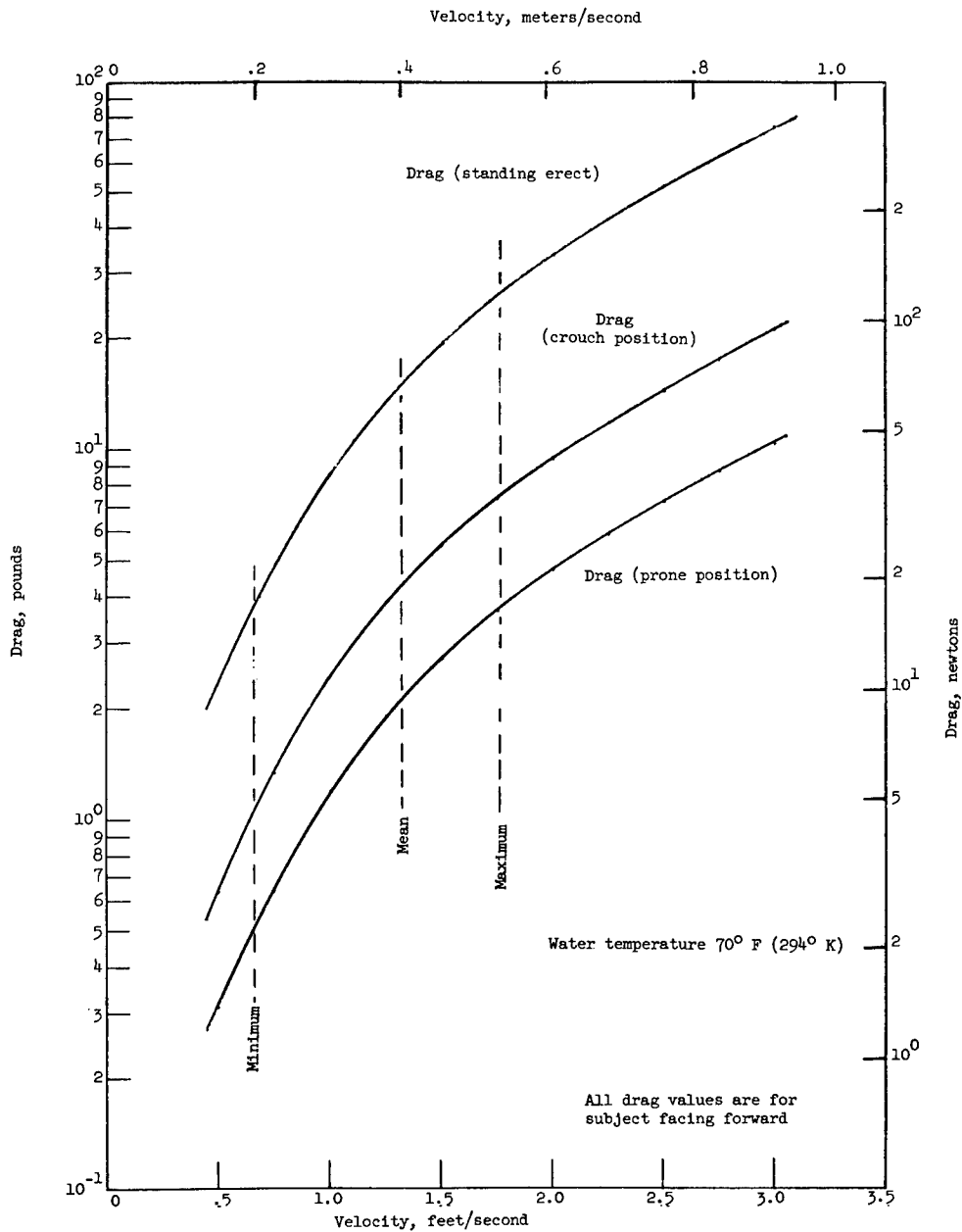
Where: C_D is the drag coefficient, V = velocity of body and ρ = density of the medium, and A is the projected area normal to V . The drag coefficient of an average clothed man in a wind tunnel at a speed of 100 to 200 fps is between 1.0 and 1.3 for the standing positions, and 5 to 10 percent less without clothing (521). For pressure-suited subjects, the curves of Figures 7-68a, b, and c may be used to determine the drag area under different conditions (196, 223, 609). The effective drag area ($C_D A$), ranges from 1.6 to 9.6 ft² depending on the garment configuration and orientation. Figure 7-68c shows the drag generated as a function of velocity. At a velocity of 1 foot/second, drag in the prone position is seen to vary from 1.6 to 3.6 pounds for the configurations tested. A large portion of this drag is attributable to the position of the hands. When the hands are in the mobility aids position (i.e., extended in front of the subject), a significantly larger frontal area is presented.

Table 7-69 compares the calculation of drag area obtained in water simulation, aircraft trajectories, and wind tunnel (473). By the principle of dynamic similarity, it was concluded from the two available sources that the drag coefficient C_D for the standing position of the human body immersed in water is between 1.0 and 1.3 when the velocity of motion is below 2 fps. As the comparison showed, the size of the subject, either clothed or pressure-suited, seems to have no effect on the magnitude of the drag coefficient. Before the accumulated information on drag coefficients can be used in the water-immersion simulation, it is advisable to narrow down the range of 1.0 to 1.3 and to determine specifically its values for various maneuvering positions. For improving the accuracy of scaling and the prediction of actual space conditions, further detailed drag tests in water are necessary. Table 7-69b gives only the values of drag areas for those positions which are likely to exist in a programmed task. Until accurate C_D values for complicated maneuvering attitudes are available from elaborate drag tests in

Figure 7-68

Variation of Calculated Drag with Velocity for Water-Immersion and Aircraft Tests

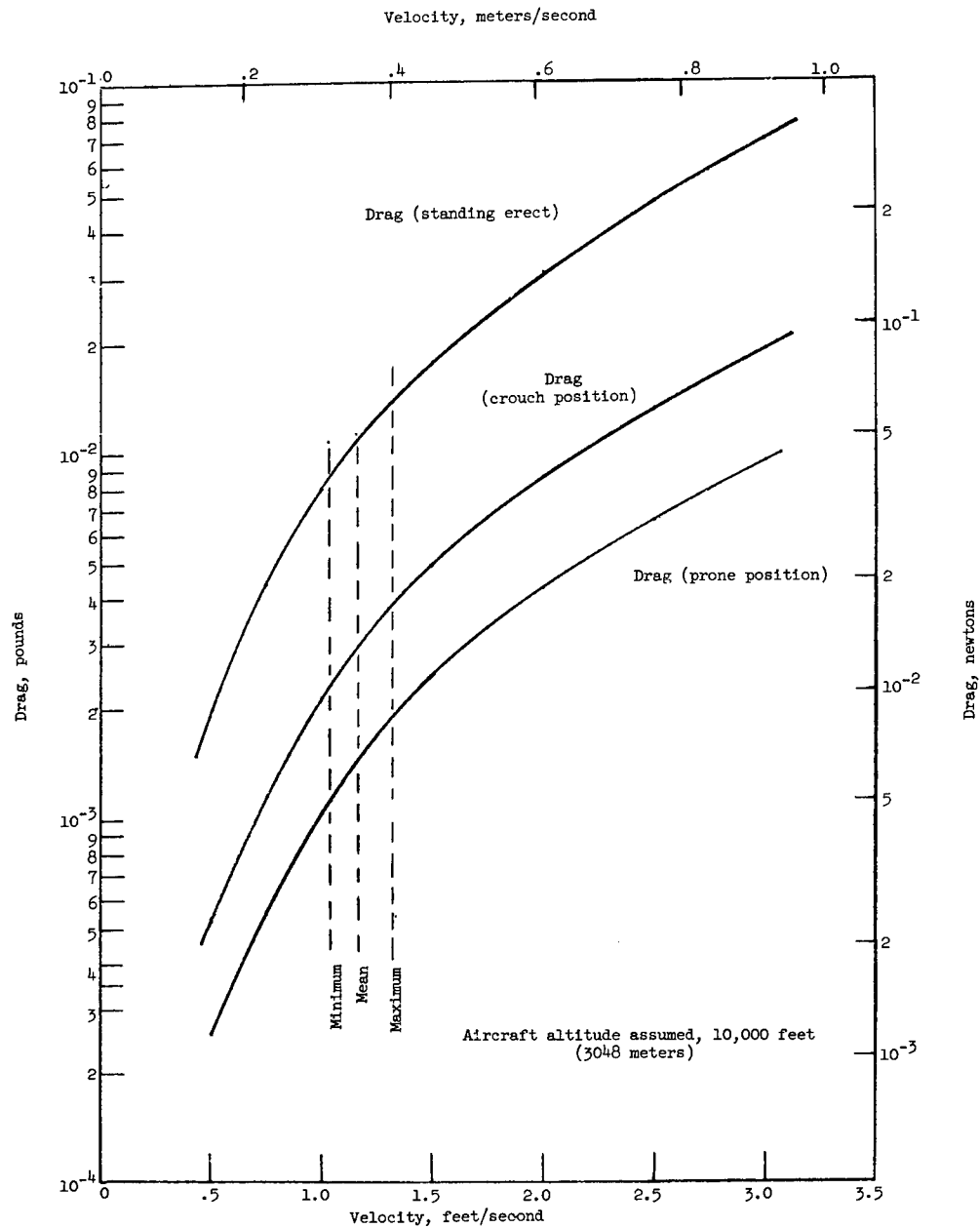
a. Water-Immersion Simulation



(After Trout et al⁽⁶⁰⁹⁾)

Figure 7-68 (continued)

b. Aircraft Simulation

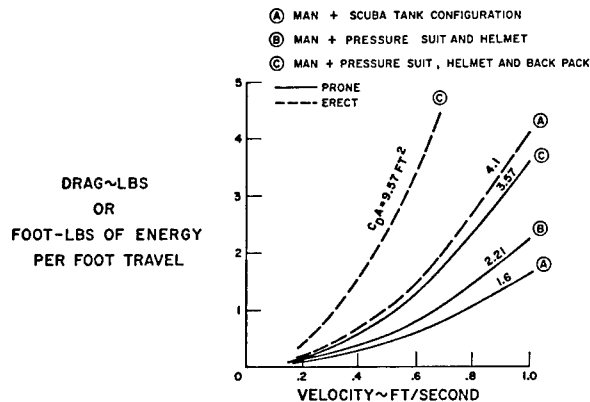


(b) Aircraft simulation.

(After Trout et al⁽⁶⁰⁹⁾)

Figure 7-68 (continued)

c. Variation of Hydrodynamic Drag of Man Under Water in Different Garments. (Hands in Mobility Aids Position)



(After Goldstein⁽²²³⁾ and General Electric Co.⁽¹⁹⁶⁾)

Table 7-69

Drag Area and Hydrodynamic Mass for Nude and Clothed Subjects

a. Comparison of Drag Area in Different Conditions for Clothed Subjects *

$$A_D = C_D A = \frac{D}{q}, \text{ FT}^2$$

Body Position	Water-Immersion Simulation	Aircraft Trajectory Simulation	Wind Tunnel Investigation
Standing	8.7	9	9
Crouch	2.4	2.4	2 to 3
Prone	1.2	1.15	1.2

* In arriving at the results, the densities $\rho_{\text{water}} = 1.94 \text{ lb-sec/ft}^4$ and $\rho_{\text{air}} = 0.7385 \times 0.00238 = 0.00176 \text{ lb-sec/ft}^4$ for altitudes of 10,000 ft have been assumed.

(After Pao⁽⁴⁷³⁾)

b. Calculated Average Drag Area of Clothed Subjects in Water, $A_D, \text{ Ft}^2$ *

Body Position	Yaw Angle, ψ	A_D
Standing	0°	8.70
Sitting	0°	5.74
Supine	180°	0.962

* Due to the suit constraints, it is unlikely that any of the two squat positions of the wind tunnel tests can be achieved.

(After Pao⁽⁴⁷³⁾)

Table 7-69 (continued)

c. Hydrodynamic Mass of Human Body
 $(1 \times 10^4 < R_N < 4 \times 10^5)$

Configuration (Hands in Mobility Aid Position)	Hydrodynamic Mass Factor $\sim K_h$
Man-Scuba Gear-Prone	0.6
Man-Scuba Gear-Erect	1.0
Man-Pressure Suit-Backpack-Prone	0.7
Man-Pressure Suit-Backpack-Erect	1.0

(After General Electric Co. (196))

d. Mass Comparison (Space Subject Versus Underwater Subject)

Subject to be Simulated	Mass in Space	Underwater	
		Physical Mass \sim Slugs M_p	Apparent Mass, i.e. Physical Mass plus Hydrodynamic Mass \sim Slugs (Note 1) M_A
Man \sim Nude (150 lb)	4.65	4.65	7.4
Man and Pressur- ized Space Suit (Note 2) (175 lb)	5.45	5.45 <u>3.75</u> (Note 3) 9.20	14.6
Man and Pressure- ized Space Suit and Backpack (Note 2)	5.45 <u>1.85</u> 7.30	9.20 <u>5.45</u> (Note 4) 14.65	23.5

Notes

1. Hydrodynamic Mass of man in prone position with hands in mobility aid position.
2. Neutrally buoyant when underwater.
3. Ballast or water for neutrally buoyant pressurized suit.
4. Ballast for neutrally buoyant backpack

(After General Electric Co. (196))

water, these data can be adopted for determining the approximate C_D value in preliminary model analyses. Such mathematical models are being studied for extrapolating underwater data to the zero gravity gaseous environment (473, 687). To really evaluate the drag force during underwater maneuvering, it is necessary to know the history of the positions and velocities of every segment of the pressure-suited subject. This is accomplished by employing accelerometer recordings of the segment joints of the body (349). Such methods of measurement make it possible to determine not only the segment translations, but also pure rotations about the centroid of the segment. Because of the restraints imposed by the pressure suit and the concern for mission safety, EVA may well be limited to low speeds, which also limit the range of Reynolds numbers of underwater motions for programmed tasks.

If acceleration histories occurring in space for a given impulse are to be obtained, special care must also be taken to achieve correct mass simulation (485). This may require employing a man in Scuba gear to simulate a man in space with a bulky space suit and backpack. If it is not possible, because of other test requirements, to achieve mass simulation and if acceleration simulation is required, the data obtained must be adjusted for the effect of the mass mismatch. The apparent mass (M_a) is related to the physical mass (M_p), by the hydrodynamic mass factor (K_h):

$$M_a = M_p (1 + K_h)$$

Table 7-69c presents the observed hydrodynamic mass factor and Table 7-69d presents a comparison of the apparent mass underwater and the mass in space. The results indicate that the acceleration response to a given impulse observed underwater is generally representative of the response of a significantly more massive body. This is due to the additional mass introduced by a pressurized suit ballasted with water or weight, the backpack and the hydrodynamic mass.

Data are available on the efficacy of underwater simulation of construction and maintenance tasks in orbit (687). The following conclusions are taken directly from this report. Metabolic data will be covered in O₂ - CO₂ - Energy, (No. 10). Weightless simulation at low limb and body velocities appears to be better accomplished by neutral buoyancy simulation than by the six-degrees-of-freedom simulator. The extent of man's capabilities to perform maintenance and assembly tasks in weightlessness is much greater than had been originally anticipated. With appropriately designed tools, restraint devices, locomotion aids, and task sequences it appears that any foreseeable manual task can be accomplished in weightlessness. This observation must be tempered with a complete lack of knowledge on the problems of mass manipulation. In addition, great emphasis must be attached to proper design of EVA hardware. Manual construction of large rigid or inflatable structures such as antennas or shelters can be accomplished manually in weightlessness, but detailed "hand-by-hand" task analyses must be conducted in developing procedures for any EVA or IVA in large volumes and complete and detailed simulation should be used to check out all work projected. Whenever subjects take short-cuts in the task sequence that appear to be work improvement steps, these deviations from the task procedures

most frequently lead to difficulty. No object, including tools, fasteners, and hardware, can be considered acceptable without proof of acceptability testing by simulation. The general conclusion from the tests conducted imply that little of the hardware used was acceptable in its present "off-the-shelf" configuration. Some of the more specific recommendations were as follow:

a. Restraints

- The lineman's position, or variations of it, was the most sought-after position used by the subject, but was hard to attain with rigid restraints.
- The effectiveness of a restraint configuration is inversely proportional to the amount of time the subject spends seeking and obtaining the "best" position from which to work.
- Both dexterity and force are dependent of the stability and the positioning of the subject.
- The foot-strap and cage restraints were generally better than any other restraint concept tested. The Gemini XII type of strap restraint is best for tasks requiring force opposing the tension of the straps, for tasks requiring prolonged dexterous work in place and for tasks requiring force not opposing the position tension. The birdcage restraint system is best for tasks requiring mobility while restrained.
- Strap restraints at the waist of the subject are not satisfactory when used alone but are effective and essential when used in conjunction with the foot-strap and cage restraints. Their continued use is expected in any restraint mechanism to be developed and tested.
- In configurations used in this program the mechanisms for lengthening and shortening the straps were too small for adequate handling by the pressurized glove.
- Stability of a work position is proportional to the number of limb contact points the subject can obtain.
- Restraints that require many connections and disconnections during positional changes are too time consuming.
- Restraints with free pivoting at connection points are undesirable.
- Stable positioning required the use of hands and legs to maintain the position.
- Two-hand freedom is essential for "good" EVA work and is dependent on the restraint configuration.
- Since all restraints tested had design faults, it is concluded that no restraint can be completely eliminated as a potentially successful restraint mechanism.

b. Tools

- Off-the-shelf adjustable wrenches should not be used for EVA assembly and erection.
- Socket-type wrench sets, if used for EVA assembly and erection, will require modification to assure positive locking of the interchangeable connections.
- Screwdriver use should be avoided for EVA erection, assembly, and maintenance tasks.
- Tool performance improves with the improved stability of positioning.
- When the subject was well positioned to the work spot and had a stable position, little difference could be noted in the variety of wrenches tested.
- Pliers and pincher-type handles require modification to allow manipulation with one hand.
- The simple flexible lanyard used in these tests for tool retention is inadequate. (See also inadequacy of lanyards in the Gemini program).
- Hammer blow accuracy is interfered with by suit resistance.
- Testing of all tools to be used during EVA in the neutral buoyance water-immersion simulation is required to assure their adequacy. Consideration should be given to adapting the current EVA power tools and those forthcoming to the water environment and to assure neutral buoyancy of both tools and work objects.

c. Fasteners

- A need exists for a clamp that may be manipulated with one hand to position, adjust, engage, and release.
- Off-the-shelf clamps are not acceptable for EVA assembly and erection.
- A requirement exists to establish ways and means of handling, retaining, and controlling bolts, nuts, and fasteners that are not captive.
- A positive, quick-locking fastener with high holding capability is required for EVA assembly and erection.
- The internal wrenching bolts were the most desirable bolts tested and the slotted head bolts the least desirable.
- Bolts with head sizes of less than 1/2 in. and lengths of less than 1 in. are undesirable for EVA because of their handling difficulty.
- Fasteners for EVA erection and assembly should be standardized and of a minimum number of sizes.

d. Locomotion aids

- Rigidity of locomotion aids is desirable.
- Locomotion aids without protrusions are the most desirable to prevent the EVA worker from snagging his suit or equipment.
- Since all locomotion devices seem to work reasonably well, the guide rule for selection should be one of simplicity.
- Carrying packages in one hand while traversing is an uneconomical way of performing work in the water immersion simulation, and an effort should be undertaken to correct this by providing attaching points to the suit or other suitable means for transporting materials in a manual manner.

e. Work

- EVA erection and assembly tasks should have step by step procedures developed by a simulation technique using real hardware to prove the concept, develop procedures, and provide the training necessary to assure success of the mission in space.
- In tasks where several tools are used there exists a problem of tool presentation and retention.
- Two-handed tasks should be eliminated from EVA tasks whenever possible.
- A direct frontal extension of the arm requires more effort and discomfort than does a "hooking" extension of the arm.
- Deviation from check-list task procedures should be allowed only when the task sequence has been proven unworkable.
- Each step of EVA assembly and erection should be planned, tested and set in a check-list task sequence for performance compliance.
- The pressurized glove of the suit does not provide appropriate feedback from tools or hardware to the EVA worker. This fact requires the subject to see the work he performs.
- Any requirement for the EVA worker to use two tools simultaneously should be eliminated.
- Whenever possible, two-handed task requirements are often broken down by subject innovations into one-handed task elements.
- Accessibility and positioning are compound problems complicated by pressure suit limitations, restraint configuration used, vision, and task demand. Free volume space about the work spot is therefore not an acceptable definition of accessibility for EVA work.

SUBGRAVITY ENVIRONMENTS

Locomotion and work on lunar and planetary surfaces follow dynamics which are quite different from those on Earth (372, 408, 503, 559). The energetics of locomotion on the lunar surface have been discussed in Oxygen - CO₂ - Energy, (No. 10).

Locomotion

From the discussions above on motion sickness and zero gravity, it can be expected that with reduced stimulation of the otolithic and proprioceptive sensors, in the absence of vision, man may have difficulty in judging the vertical. Against this possibility is the fact that the threshold for the otolith is about 0.003 to 0.01 G which is far less than the 1/6th G of the lunar surface. It is not clear how this level of gravity will affect the balance and locomotor mechanism of adapted astronauts under visual deprivation, a highly unlikely situation.

Studies on the Langley inclined-plane lunar simulator have been directed at analyzing the human gait at 1/6th G (295). A plot of the locomotive index (η) or the ratio of leg swing to leg stroke, calculated from the data for all the subjects and test conditions as a function of average locomotive speed is presented in Figure 7-70a. The curves are faired through the two sets of data points to denote general trends. Although the two curves denote similar

Figure 7-70

Locomotor Effects of Subgravity

(After Hewes et al(295))

- a. Locomotive Index or Ratio of Leg Swing to Leg Stroke
Plotted Against Velocity at 1 G and 1/6 G.

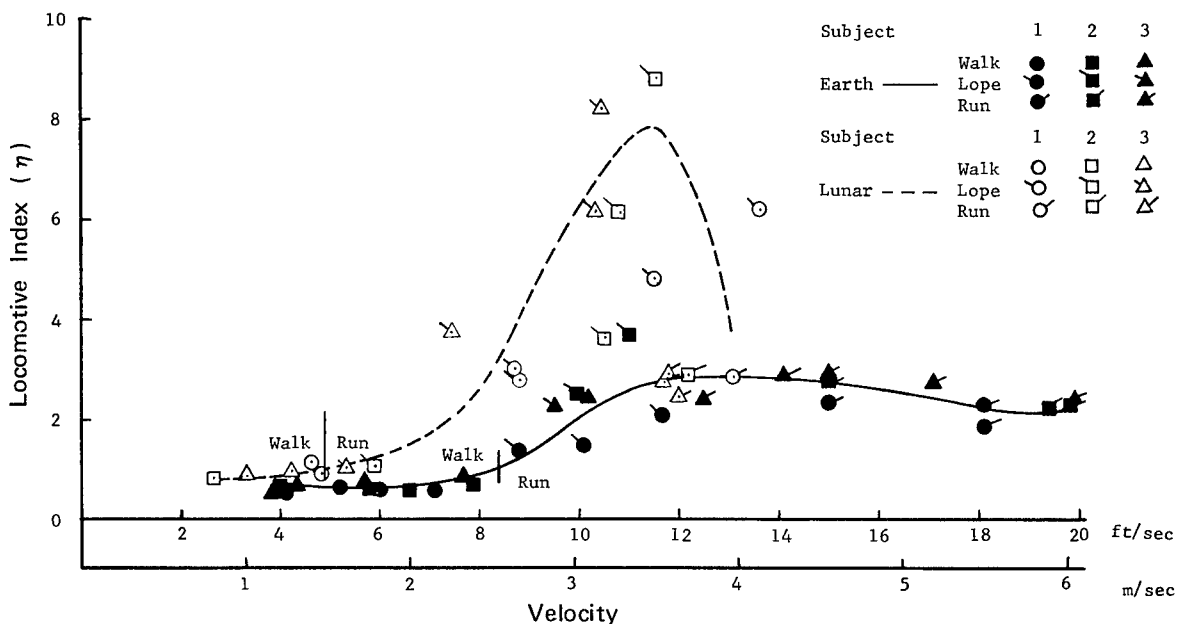
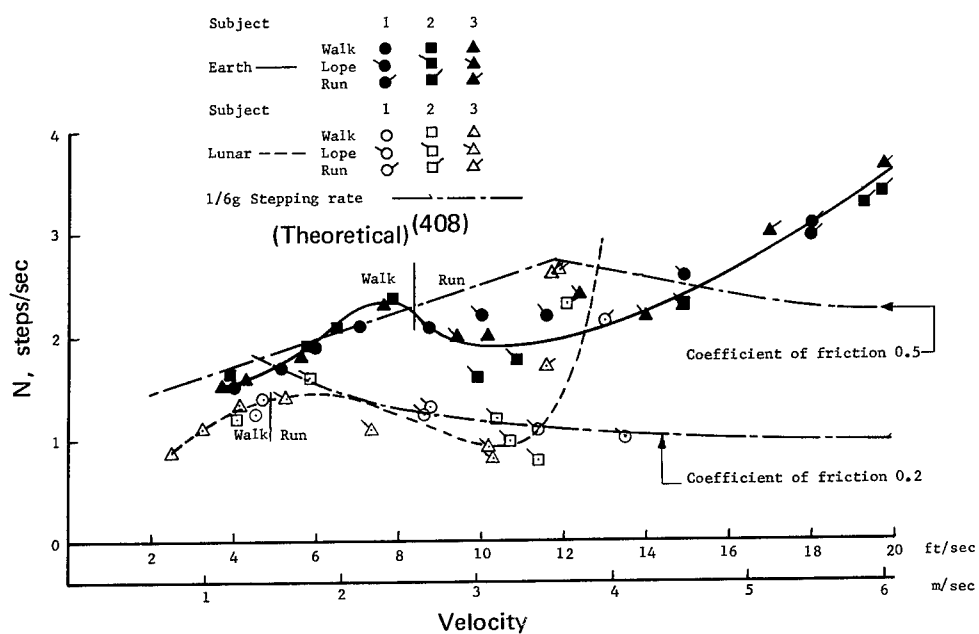
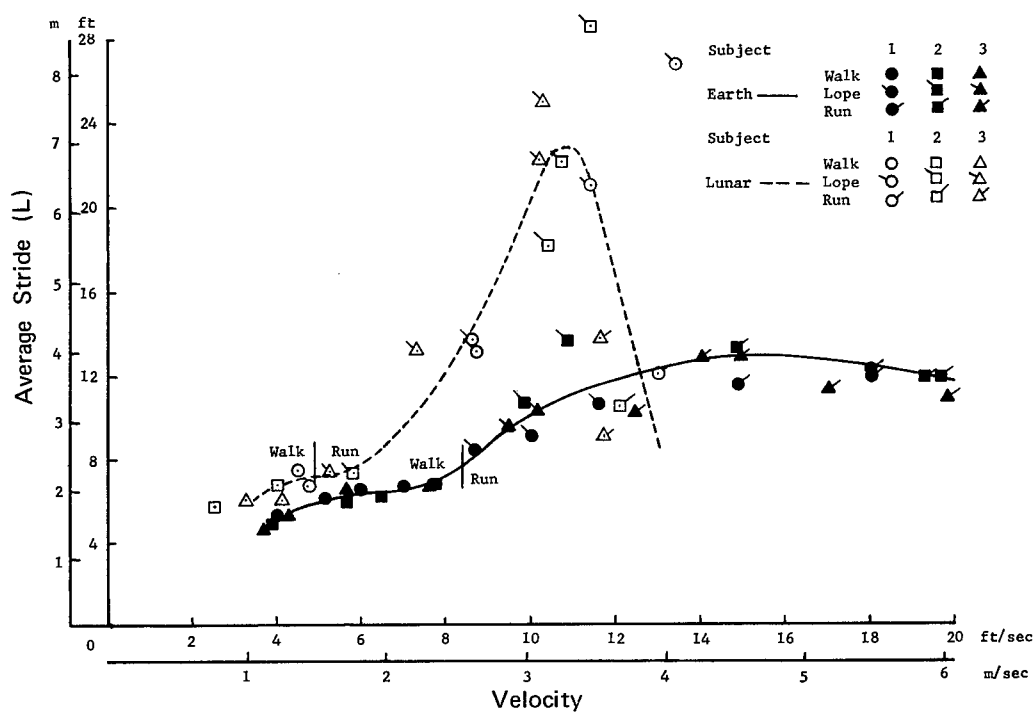


Figure 7-70 (continued)

b. Average Stepping Rate Plotted Against Velocity at 1 G and 1/6 G (lunar)



c. Average Stride Plotted Against Velocity at 1 G and 1/6 G (lunar)



trends, they also show significant differences. However, the number of "1/6th G" data points below the dashed line raises question as to the validity of recurved nature of the lunar plot. The average transition speed on the moon (the speed at which $\eta = 1$) for the three subjects was about 5 fps (1.5 m/sec) or about 60 percent of the 8.3 feet-per-second (2.5 m/sec) speed for the Earth gravity condition. The location of the data points along the abscissa indicates that the maximum running speeds achieved by the test subjects for the lunar condition were approximately 13 fps (4 m/sec), which is about 60 percent of the 20 fps (6 m/sec) maximum running speed for the Earth condition and considerably faster than the limit of 0.91 fps (1 km/hr) previously theorized (408). Man not only will walk slower but also will run slower on the moon than on Earth by about 40 percent. These two related effects are attributed to the reduced weight and corresponding loss of traction experienced in lunar gravity.

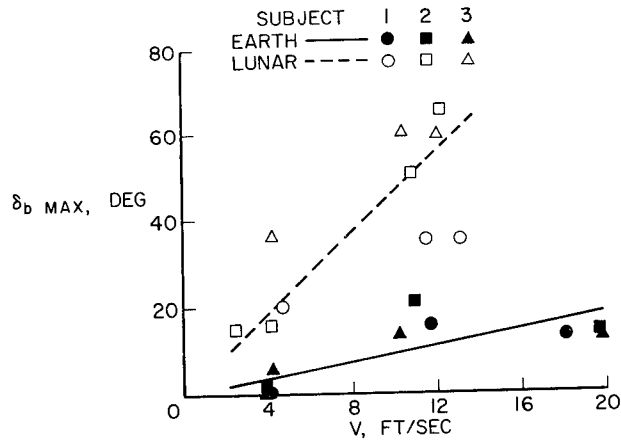
In spite of the type of gait employed, different physical characteristics of the three subjects tested and practice effects, there was a fairly well-defined variation of the stride and stepping rate with velocity, as shown in Figures 7-70b and c where the data for stepping rate and stride are plotted against average locomotive speed. This is attributed to the greater familiarity with Earth gravity and to the less constraining effects of lunar gravity. The trends of the gait parameters with speed of locomotion for the two gravity conditions as denoted by the shape of faired curves are similar. However, there are significant differences in the absolute values of the stride and stepping rate at any given speed. At practically all speeds, the subjects were able to take longer strides with corresponding lower stepping rates for the lunar condition, taking fewer steps to cover a given distance. This effect was most pronounced in the range between 6 and 12 feet per second (1.8 to 3.7 m/sec) where the stride was greater and the stepping rate was lesser by a factor as large as 2. This difference may play a role in determining the relatively low energy expenditures in walking on the moon. For the Earth gravity tests, the loping gait was usually employed in the speed range of about 9 to 15 feet per second (2.7 to 3.7 m/sec) and sprinting produced substantially higher speeds up to about 20 feet per second (6 m/sec). On Earth the higher running speed range did not change the stride appreciably and the higher speeds were achieved primarily as the result of increased stepping rate. Practically no difference in the maximum loping speeds existed between the two conditions. The highest speeds for the lunar condition were also achieved by the use of the sprint gait. The theoretical points in Figure 7-70b were calculated for two values of friction coefficient, both of which are appreciably lower than those for the simulator tests. There appears to be very little correlation between the theoretical and empirical other than the close match of the theoretical curve with the 1G test data at the lower speeds.

The body position during these different locomotor patterns in subgravity have been photographed and analyzed (295). Body-point analyses show that as the speed of locomotion increases, the lean angle of the back with respect to the vertical (δ_b) increases differently in the two gravity conditions. This is shown graphically in Figure 7-71a.

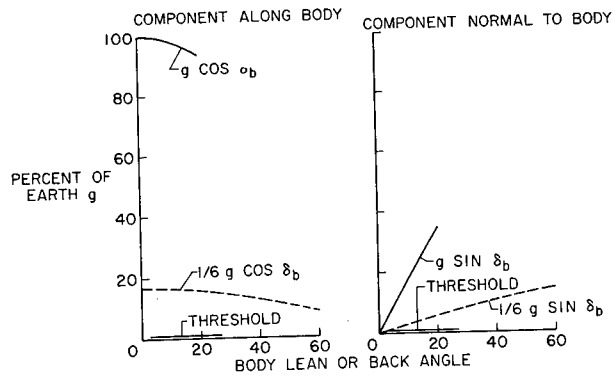
Figure 7-71

Body Lean During Locomotion in Simulated Lunar and Earth Gravity

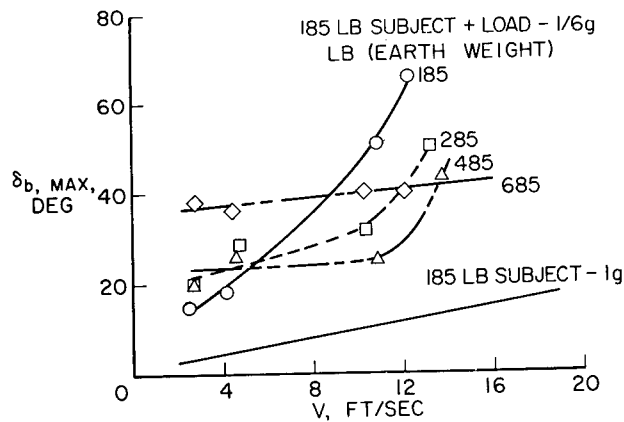
(After Hewes et al⁽²⁹⁵⁾)



a. Maximum Body Lean or Back Angle Versus Locomotion Rate at 1 G and 1/6 G.



b. Gravity Components Versus Body Lean or Back Angle for 1 G and 1/6 G.



c. Maximum Body Lean or Back Angle Versus Locomotion Rate with Subject Carrying Various Loads.

Figure 7-71b shows how the body lean or back angle affects the component of gravity along and perpendicular to the subject's body. The components are simply sine and cosine functions of the body-lean angle in the figure. The data in the figure illustrate that even though the component along the body in simulated lunar gravity is decreased by 50 percent when leaning from 0° to 60° , it is still considerably greater than the threshold value indicated by the solid horizontal line. The component normal to the body increases with body lean, but the maximum obtained for simulated lunar gravity at 60° is much less than that obtained at the maximum body-lean angle of 20° used in Earth gravity. In carrying a backpack, as the weight of the subject plus weight of his load approaches that of the man with no load in Earth gravity, the rate increase of lean generally decreases and is more nearly like that for man with no backpack in Earth gravity as seen in Figure 7-71c. The large body lean used by the subject in simulated lunar gravity is probably related to traction and to the mechanics of locomotion. Since the subject carried the weights in a frame mounted on his back, the initial upper body lean or back angle was required to keep the resultant center of gravity over his hip joint. This initial lean accounts for the large upper-body-lean angles used, even at low locomotion velocities, by the weight-carrying subject. Despite these unusual body-lean angles, the subject had no trouble in maintaining his balance while walking or running on the simulator.

Figure 7-72a shows that hip flexion angles are larger for the lunar condition than for Earth gravity, indicating that the legs were carried farther forward in the lunar gait than in Earth gaits. This is attributed to the fact that with the large body inclinations noted, the legs had to be carried farther forward to maintain balance. This, in turn, resulted in decreased knee flexion and gave the subject an appearance of walking stiff-legged for the lunar simulation. It appears likely that the normal knee action is not required for lunar walking, with the weight on the legs relatively low.

As shown in Figure 7-72b there was also a difference in rates of limb motion between Earth walking and simulated lunar walking. The maximum angular rates for hip-and-knee motions for lunar walking were about one-half that for Earth walking.

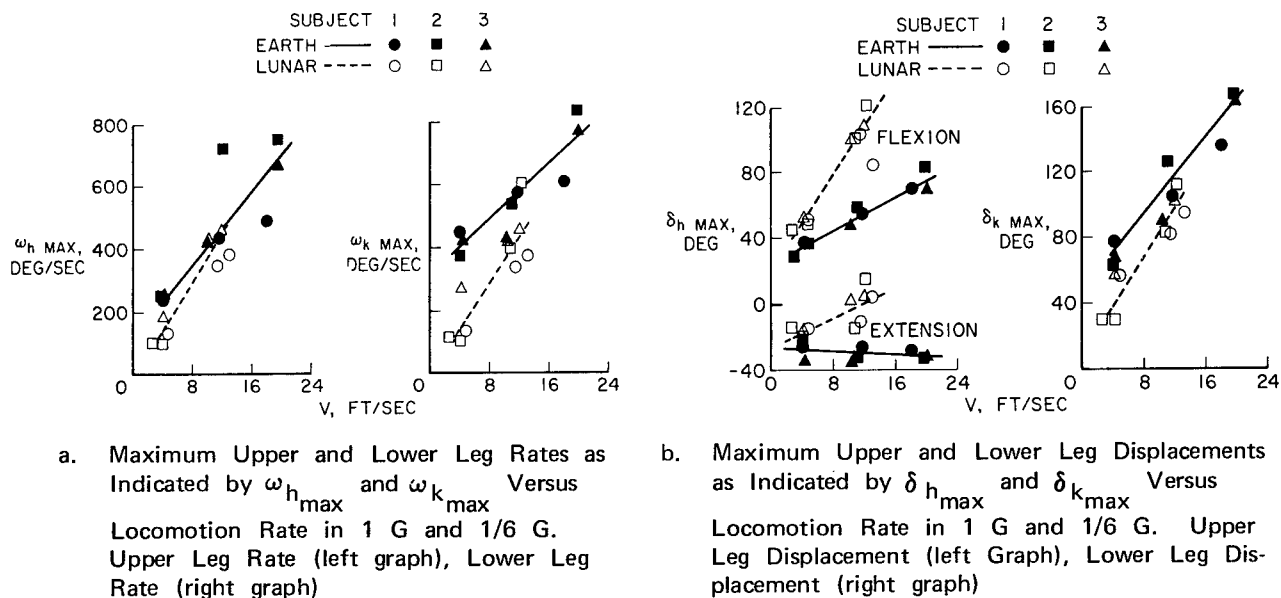
For Earth conditions, the arms appear to play a very active role in achieving a coordinated and balanced gait as indicated by the swinging secondary motion in opposition to the primary motion of the leg member on the same side of the body. In contrast, the arms seem to play a relatively minor role in the case of the gaits under $1/6$ th G inasmuch as the arms are carried high and forward with a minimum of swinging motion. It is noted that for the loping gait under $1/6$ th G that the arms usually were used with a slight up-and-down pumping motion in unison with each jumping step. It is possible that some of the constraints of the body support cables for the lunar simulation tests might have provided compensating moments that would have altered these secondary motions.

The results of these experiments generally indicate that the subjects are able to adapt their limb motions to the decreased gravity conditions and are able to maintain equilibrium even while running at about 13 ft/sec (295). The rate of simulator constraints in permitting this equilibrium to be maintained

Figure 7-72

Leg Movements During Locomotion on Earth and in Simulated Lunar Gravity

(After Hewes et al (295))



is not made clear. The more natural loping pace during lunar simulation is probably due to the lower weight which makes it relatively easy to develop the long leaping steps carrying the subject distances up to about 28 feet (8.5 m), relieving him of the work of sustaining his own weight except during the very brief period when there is contact with the surface. The stepping rates for lunar walking and loping are comparable and, if it is assumed that the internal work expended by the subject merely to move his legs back and forth is a direct function of stepping rate, one might predict that the work for the two gaits is the same and that because of the higher speed of loping, the loping gait should be more efficient (295). Two factors, however, intercede. The high loping gait, requiring relatively greater anti-gravity work per step than the walking gait even in the 1/6th G, makes it less efficient than fast walking. Also, the flexion of joints required for the loping gait is more severe than in fast walking. Since the pressure-volume-work required to flex suit joints is an exponential function of the flexion angle, relatively more energy is probably required in loping in spite of the reduced stepping rate (503). Preliminary studies of energy requirement for the two gaits suggest that loping does take more energy to cover a given distance than does the fast walking or running (686). For instance, in an inflated Gemini suit, running on a hard surface at 12.8 km/hr takes about the same amount of energy as loping at 9.7 mph. Regardless of gaits being compared, the total work required of a lunar explorer will be appreciably less than that required to cover the same distance here on Earth. See Oxygen-CO₂-Energy, (No. 10).

The effects of inflated space suits on locomotion must also be considered (559, 560). Tests have been made on the Langley simulator with a "soft type"

prototype Apollo suit. Though the simulator imposes some resistance to motion; it does not appear to stabilize many of the unusual swaying gait patterns brought on by the suit in 1/6 G parabolic flight tests. The inflated suit tends to decrease the rate of natural stride and forward lean caused by the reduced gravity as seen in Table 7-73a.

For both gravity conditions the time to reach a point 20 feet from the origin increased slightly because of the increasing bulk and constraint as changes from normal clothing to the fully pressurized suit were made. Furthermore, the times for the lunar-gravity tests were approximately twice those for the Earth-gravity conditions as a result of the reduced foot traction. The average maximum velocity reached for the 1/6 G condition is approximately 40 to 50 percent of that for the 1 G condition. The values, however, are probably not the maximum attainable because of distance restriction on the simulator. Pressurizing the suit for both gravity conditions reduced the average maximum velocities by 20 to 30 percent.

Jumping capability in 1/6 G and at 3.5 psia suit pressure are seen in Table 7-73b and summarized in Figure 7-73c. Subjects jumped about twice the distance under 1/6 G that they could achieve under 1 G for any condition of clothing. Pressurizing the suit reduced the distances obtained by 30 to 40 percent in both gravity conditions. This reduction was attributed by the subjects directly to the increased restrictions of the suit. Large amounts of body lean required for takeoff created timing and balance problems that were overcome by practice. To reach 6 ft platforms and land with balance, up to 3 steps were needed in the takeoff run.

Climbing may actually be easier in 1/6 G. Results are summarized in Table 7-73d. Ascent or descent of stairs could be accomplished at any desired pace. In fact, it was found easier to jump to the landing. The descent of the stairs was a more exacting task than ascending, especially in the pressurized suit, as the subject could see neither the platform nor where the stairs started and, consequently, had to judge where the steps were located with respect to his position. No handrails were used.

Climbing a ladder with normal clothing in simulated lunar gravity posed no serious problem as long as a slow deliberate pace was used to allow time for proper placement of the feet on the rungs of the ladder. The same result was true for tests with the space suit unpressurized. With the pressurized suit, however, the effort required to move the legs and feet was noticeably increased as a result of the increased stiffness of the knee and hip joints. Also stiffening of the shoulder and elbow joints increased the effort required to place the hands onto the ladder rungs. Because of restriction of shoulder movement, climbing a pole was impractical while wearing the pressure suit at 1 G but proved to be a relatively simple task at 1/6 G.

Kneeling in the pressurized suit at lunar gravity was accomplished by first trying to assume a squatting position and then leaning forward to a kneeling position. Although the maneuver was not hard to execute, the restrictions (bunching in the popliteal area) of the suit allowed the subjects to flex only a limited amount. This position, in turn, caused the subjects to lean forward

Figure 7-73

Locomotor and Work Task Performance in Space Suits Under Lunar Gravity

a. Typical Results of Walking and Running Tests of Two Subjects

(After Spady et al⁽⁵⁶⁰⁾)

	Earth gravity						Lunar gravity					
	Normal clothing		Unpressurized suit		Pressurized suit		Normal clothing		Unpressurized suit		Pressurized suit	
	Subject		Subject		Subject		Subject		Subject		Subject	
	1	2	1	2	1	2	1	2	1	2	1	2
Walking												
Average stride, ft	5.0	5.3	5.0	5.3	2.5	2.0	5.0	4.5	5.0	4.0	5.0	3.0
Average velocity, ft/sec	5.0	5.0	5.0	5.0	1.5	1.4	3.2	3.5	3.0	3.3	2.3	2.6
Body lean angle, deg	1 to 2						10 to 20					
Running												
Average stride, ft	5.0	6.0	5.0	6.0	4.0	4.0	5.0	5.0	5.4	5.0	5.0	4.5
Average time to travel 20 feet, sec	1.2	1.6	3.2	3.4	4.0	4.0	4.9	4.1	6.5	6.0	8.3	9.0
Maximum velocity, ft/sec	12.0	11.0	12.0	10.0	8.2	8.2	6.5	6.0	5.7	5.4	4.3	3.7
Body lean angle, deg	2 to 5						20 to 30					

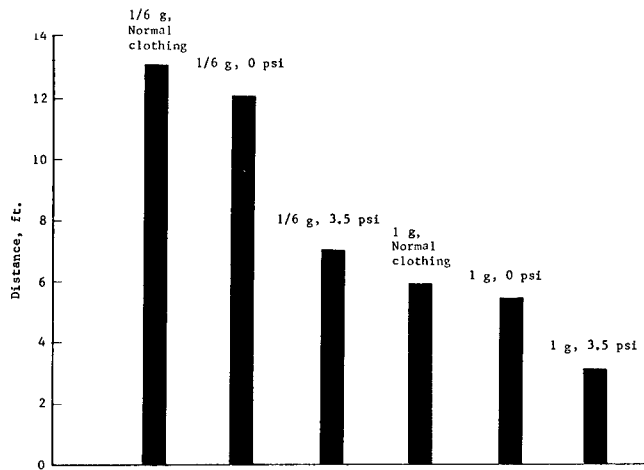
b. Jumping Characteristics in Pressurized Suits at 1/6 G

(After Spady et al⁽⁵⁶⁰⁾)

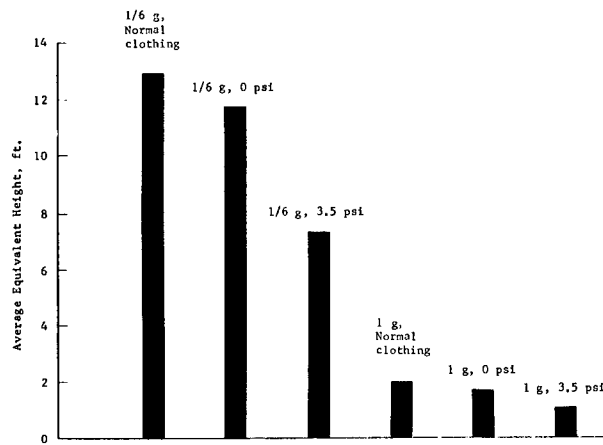
	Earth gravity						Lunar gravity					
	Normal clothing		Unpressurized suit		Pressurized suit		Normal clothing		Unpressurized suit		Pressurized suit	
	Subject		Subject		Subject		Subject		Subject		Subject	
	1	2	1	2	1	2	1	2	1	2	1	2
Vertical jumping												
Jump height, ft	1.9	---	1.6	1.5	1.0	1.0	13.8	---	11.8	12.2	7.7	8.5
Peak push-off acceleration, g units	3.0	---	1.7	1.6	1.5	1.9	1.0	---	1.5	1.5	1.4	2.1
Broad jumping												
Jump distance, ft	6.2	---	5.5	7.0	5.0	4.5	13.0	---	13.0	13.0	11.0	9.0
Average forward velocity, ft/sec	---	---	12.0	5.7	10.0	8.3	---	---	6.2	5.5	4.9	3.8

Figure 7-73 (continued)

c. Jumping Capability in Pressurized Suits at 1/6 G
(After Spady et al⁽⁵⁶⁰⁾)



The average horizontal distances obtained during broad jump tests.



The average vertical heights obtained during the vertical jump test. (The values listed are the average of 5 jumps each by 2 subjects).

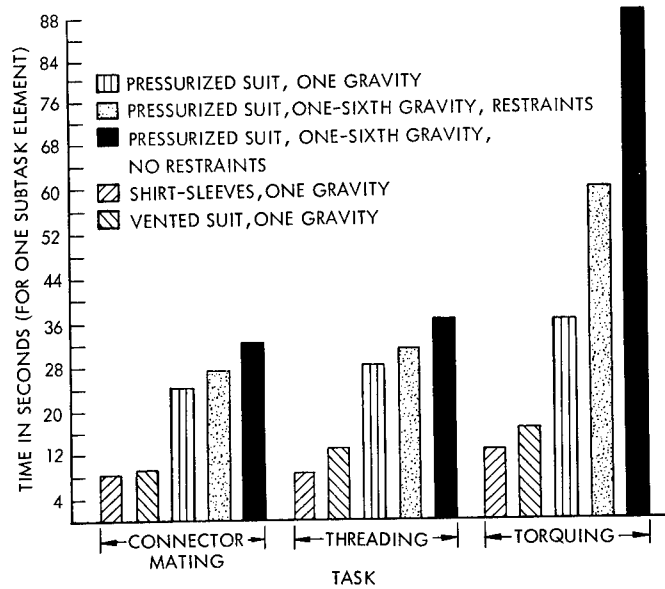
d. Averaged Results of Climbing Tests of Two Subjects
(After Spady et al⁽⁵⁶⁰⁾)

	Earth gravity						Lunar gravity					
	Normal clothing	Unpressurized suit	Pressurized suit	Normal clothing	Unpressurized suit	Pressurized suit						
Ladder climbing												
Subject	1	1	1	1	1	1	1	1	1	1	1	1
Hand placement	Rungs	Side pieces	Rungs	Side pieces	Rungs	Side pieces	Rungs	Side pieces	Rungs	Side pieces	Rungs	Side pieces
Climbing rate, ft/sec	2.7	---	1.2	1.1	0.2	---	2.4	---	2.1	1.5	1.0	0.8
Pole climbing												
Subject	1	2	1	2	1	2	1	2	1	2	1	2
Climbing rate, ft/sec	1	---	Not attempted		Not attempted		1.7	---	2	1.7	0.6	0.9
Average hand stroke, ft	0.5	---					1	---	1	0.9	0.5	0.6

Figure 7-73 (continued)

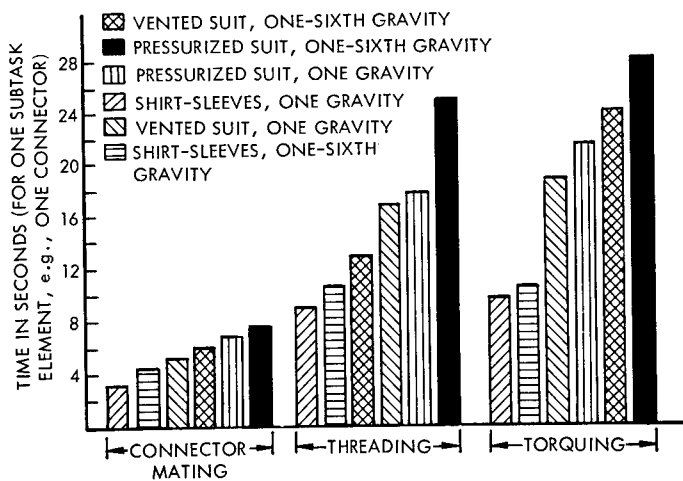
e. Effect of Simple Restraints on Performance of Poorly Trained Subjects on a Lunar Gravity Simulator (See text)

(After Seminara⁽⁵³⁰⁾)



f. Effect of Training and Restraint on Tasks Performed in Figure 7-73e

(After Seminara⁽⁵³⁰⁾)



over the knees as they touched the floor, and required the subjects to brace themselves with their hands to keep from falling forward.

Kneeling with the aid of a support stick (a 1-1/2 inch-diameter aluminum pole 6 feet long) made the task easier. If the subjects were lying face down, standing was accomplished by simply pushing against the floor with the hands and arms with sufficient force to regain a standing position. In the case where the subjects were in a supine position, they found it difficult to regain an upright position, though less so with support sticks. Subjects were able to perform the many tasks without becoming overly fatigued for periods up to about 3 hours in the lunar-gravity condition. At the same time, fatigue was encountered in much shorter times when the subjects performed in Earth gravity.

In general, subjects reported that sensations and efforts in the lunar simulator were much like those in short-term parabolic flight at equivalent level of subgravity. (See references above on simulation of zero gravity tasks in parabolic flight). An explorer wearing a pressurized space suit on the moon should, with practice, be able to walk and run provided, of course, that the terrain is relatively firm and not too rough. He should also be able to perform many other self-locomotion tasks such as jumping and climbing and may be able to out-perform his Earth counterpart with the exception of body motions requiring rapid accelerations, especially along surfaces of low traction. Experiments with a 6-degree-of-freedom simulator indicate that a 300 pound man-suit-backpack has a substantial inertia at any running velocity and a small moment of force available for altering direction even with high-friction surfaces (686). One must be cautious in predicting operational capacity of encumbered man on the lunar surface without specific simulator studies of the function in question.

Studies are currently under way on the effect of backpack weight and suit pressurization on human performance in simulated lunar gravity (559). The effect of a state-of-the-art, Apollo, full pressure suit at 0 and 3.7 psig on a subject's lunar locomotive gaits can be summarized as follows: (1) Pressurizing the suit did not appreciably affect either the stepping rate or the maximum walking speed in lunar gravity, but it had a marked effect on both in Earth gravity, (2) In general, the stepping rates were lower and the corresponding stride length longer in simulated lunar gravity than in Earth gravity.

The effect of backpack loads on the lunar locomotive gait of subjects in shirt sleeves can be summarized as follows: (1) in simulated lunar gravity the subject could carry backpack loads of up to 500 Earth-pounds (2225 Newtons) while standing, walking, loping, and sprinting, (2) The amount of load being carried did not significantly affect the lunar gait characteristics; however, the greater loads did increase the stepping rate of the lunar lope, (3) The subjects were of the opinion that the 500-pound load seemed to be approaching the maximum load they could carry with confidence while sprinting. In these experiments, two subjects were required to carry loads ranging from 100 to 500 Earth-pounds in lunar gravity for approximately 45 minutes while performing various walking, sprinting, and loping tests. Although the subjects who performed these tests in only the shirt-sleeve condition did become tired, particularly with the maximum loads, they both thought that they could have

continued for a significantly longer period. The load was found to be easier to control if it was securely strapped to the subject; however, care was taken to insure that the backpack straps did not impede the subject's respiration. In several incidents where the subject's respiration was impaired by the straps, headaches were experienced after leaving the simulator. Subjects were able to fall to a prone position and then regain a standing position, with no difficulty even with the 500-lb load; however, the technique used depended on the load being carried. For the light loads it was not necessary for the subjects to use the arms for braking purposes when falling and they could regain a standing position, simply by pushing the body upward with the arms. In contrast, for the heavy loads the arms were required to provide a braking action and the same technique was used to regain a standing position as is normally employed in Earth gravity.

Performance of Tasks

Performance of tasks on the lunar surface is complicated by several factors beyond the subgravity. Inflated space suits degrade performance of maintenance and other tasks in the subgravity environment (530, 536). The light environment is also most unfavorable with glare, shadows, blinding reflections from tools, suits, and vehicular structures (531). See also Light Environment, (No. 3).

Table 7-70e and f presents data obtained from a lunar gravity simulator (LMSC-LUNARG) on degradation of performance of typical maintenance tasks (530, 536). The unit supports 5/6ths of the subjects' weight by 9 negator spring motors attached to a cable-reeling system. An Apollo A4H training suit was used with C-3 Helmet. Figure 7-70e shows the effects of suit pressurization restraints (simple foot restraints and tethers) and gravity levels on performance of connector mating, threading and torquing. This study was performed in the absence of optimized training and restraints. The pressurized suit and 1/6 G were the greatest factor. The 1/6th gravity did not degrade all tests to the same degree, torquing being much more sensitive than connector mating.

Subsequent studies were performed with subjects trained to peak proficiency, all using restraint systems. Figure 7-70f shows that training and restraint has a marked effect in reducing the time to perform manual tasks on the lunar surface; but it still may take up to 32% longer to perform these tasks on the lunar surface than on Earth.

Although errors of trained, harnessed subjects in 1/6th gravity increased 340% over errors in one gravity and 159% over errors in 1/6th gravity (harnessed) these increases were not statistically significant. Subjectively, the threading task proved to be the most difficult to perform in one gravity whereas, the torquing task was identified as the most difficult to perform in 1/6th gravity.

In estimating performance times for lunar intravehicular tasks in shirt-sleeves, it was suggested that a 25.67% increment in performance time should be made over comparable Earth-based performances.

Although considerable attention is currently being given to performance aids for assisting the astronaut in the zero-gravity environment (see above), relatively little attention has been devoted to a comparable study of performance aids required to facilitate lunar maintenance and operational tasks (306). The above studies suggest that handholds should be provided for the astronaut primarily as a method for obtaining a satisfactory position relative to the task. However, if possible, the astronaut should not be required to use his hands in steadying his position relative to his equipment task since this would limit his ability to use both hands in accomplishing tasks. Further, it appears that a one-hand grip would not be sufficient to steady his position for many tasks. Properly spaced and distributed toe holds and tether anchor points appear to offer promise in helping to steady the astronaut's position for tasks involving force application such as the torquing task. A single tether located from the navel area of the suit to the task appears to be the best candidate (306). However, further research is required. It has also been pointed out that the pressurized suit prohibited performance in extreme positions. In addition to the tethers and handholds just cited, extravehicular work may require lunar ladders or toe holds on the side of structures where work is required above the astronaut's shoulders. Also, work areas extremely close to the lunar surface should be avoided where possible. Tools which grip the components may be desirable to reduce time and especially errors. Also, the size of the components, such as nuts and bolts, should be considered. This research agrees with past recommendations that equipment components and parts should be made large enough for the astronaut to handle with a pressurized glove to minimize errors (306). Effects of thermal and visible-light control surfaces on tools should also be considered (531).

In predicting the time to be allotted for any given task, the effect of the lunar visual environment on performance should also be considered within the context of the totality of environmental characteristics that may affect performance; namely, lunar gravity, the high risk vacuum environment, space suit encumbrances, lunar surface characteristics and shelter confinement. Control panel tasks have been performed by two subjects in the LMSC lunar environment test bed (530) under optimum illumination at 100,000 ft altitude, in a pressurized Litton Mark II hard space suit, and suspended by LUNARG, a lunar gravity simulator. Test subjects performed the control tasks as part of an extravehicular sortie associated with five days of confinement within a simulated lunar shelter. Under these conditions, the following performance time increases over baseline shirtsleeves performance were obtained: digi-switch task - 60%, potentiometer task - 84%, valve task - 104%. Under 1G conditions in the presence of solar illumination an average increase in performance time of 28% over normal illumination conditions was reported for the digiswitch task (531). A 50% decrement was noted under the worse conditions with sun shining from the rear. Percentage increases for the potentiometer setting task were less dramatic, although an increase in performance time of 18% was required under the worse conditions. The valve task showed no consistent performance change due to illumination. It was not possible to integrate illumination simulation into the 1/6th G study.

In attempting to develop realistic performance times for lunar astronaut workday activities, it should be considered that the effects of the lunar illumination environment may not be simply additive to other environmental factors.

A best estimate from these two sources of data is that control tasks of the type examined will require approximately 100% more time on the lunar surface than required by the shirtsleeves operator in one gravity. It is also anticipated that the astronaut will lose time in finding a favorable position with respect to sunlight direction (531).

IMPACT

Acute acceleration may occur at many points along a space mission profile. These may be planned as in the normal landing and docking impact or accidental.

Data are available on the dynamics of water impact in general (116) and Apollo water and Earth landings in particular (33, 592, 593). The Apollo command module will descend to an Earth landing by parachute. Vertical parachute descent velocity using three chutes has been calculated not to be greater than 8.5 m/sec (27.9 ft/sec) while the horizontal velocity imparted by cross-winds could be up to 15.2 m/sec (50 ft/sec). Under maximum conditions of descent, the resultant velocity would be 17.5 m/sec (57.3 ft/sec). Vertical decelerative peaks at the vehicle center of about 20 G with rise times of 4 to 8 milliseconds are anticipated in water and Earth landings. Test impact profiles at the couch level are available (513).

By their very nature, impact studies are dangerous. Most laboratory studies with humans start with purposely low levels of force, which are increased only up to the point of voluntary tolerance limited by pain or discomfort and under the control of the subject. The experiment may accidentally proceed to the point of considerable damage, so that even the "voluntary end point" is not a uniform end point condition. The use of experimental animals in place of human subjects is of very limited value. For example, mice and rats can tolerate many times more impact and vibration G levels than can a human (347). Sensitivity to duration must be considered. It is perhaps a difference in physiological sensitivity, as well as an expression of the differences in body size, the arrangement of the limbs, the different suspension and weight of organs, and other anatomical dissimilarities. Black bears have been used in impact studies, since bears come close to approximating the size and the body mass distribution of man (601). Impact data have also been collected from information about accidental falls -- the estimated forces required to produce injury and death, heights, direction of impact, etc. (551, 553, 596). These data, rough as they are, help to establish lethal limits. Those who study accidental falls can distinguish both physical and biological factors which influence the result.

General reviews of impact acceleration are available (94, 164, 211, 213, 221, 438, 651).

The Biomechanical Factors of Impact

Impact forces are extremely complex, being influenced by velocity, duration of deceleration, type of protection, position of the body, magnitude of

force, state of relaxation, etc. These forces are variously transmitted to an extremely complex physical system, the human body. In an effort to reduce this complexity to manageable levels, mechanical analogs of the body have been devised (16, 105, 168, 209, 347, 445, 478, 534). The hope is that eventually there will be enough information about body masses, impedance of segments, coupling, damping, and other important features of the models so that they may be used in making predictions about the effects of the random multi-vectored, and often sequential forces that are at play in operational impact conditions.

In some critical organs, the damage may occur at a cellular or subcellular level with no gross evidence of the shear, tensile, and compressive forces at play. More knowledge of the ultrastructural organization of cells must be made available to allow extension of current models to the molecular level.

The direction of impact forces are indicated by the linear G symbols noted in Figure 7-1.

The human body consists of a bony structural skeleton, held together by tough fibers, which provides mechanical support and a lever system on which the muscles act. The slightly curved vertebrae or spinal column is the basic structural component and consists of a number of vertebrae acting as load carrying elements and separated by supporting tissues which act as shock absorbers and connecting links (292). The rib cage and abdominal cavity contain the visceral organs (heart, lungs, liver, etc.) which are fairly massive components, suspended freely by connective tissues from a muscle and bone support. The basic constituents such as bone tissue, ligaments and muscle exhibit mechanical properties such as elasticity, compressibility, shearing and tensile strength. Unfortunately, similar physical properties for specific critical organs are often not available. Data on the strength of the vertebrae (126, 271, 292, 479, 512), lower limbs (299), skull and facial bones (135, 271, 273, 379, 595, 702), and other bones (271), are available. Some of these properties are shown in Table 7-74.

Table 7-74
Physical Properties of Human Tissue
(After Goldman and Von Gierke⁽²²¹⁾)

	TISSUE, SOFT	BONE, COMPACT	
		FRESH	EMBALMED, DRY
Density, g/cm ³	1-1.2	1.93-1.98	1.87
Young's Modulus, dyne/cm ²	7.5×10^4	2.26×10^{11}	1.84×10^{11}
Volume compressibility, * dyne/cm ²	2.6×10^{10}	—	1.3×10^{11}
Shear elasticity, * dyne/cm ²	2.5×10^4	—	7.1×10^{10}
Shear viscosity, * dyne sec/cm ²	1.5×10^2	—	—
Sound velocity, cm/sec	$1.5-1.6 \times 10^5$	3.36×10^5	—
Acoustic impedance, dyne sec/cm ³	1.7×10^5	6.0×10^5	6.0×10^5
Tensile strength, dyne/cm ²	—	9.75×10^8	1.05×10^9
Shearing strength, dyne/cm ² , parallel	—	4.9×10^8	—
perpendicular	—	1.16×10^9	5.55×10^8

* Lamé elastic moduli.

Impacts tend to look like a $1/2$ cycle vibration of large magnitude, but, in fact, are composed of a wide spectrum of frequencies because of their non-periodic nature. When the body is exposed to comparatively low frequency vibrations, resonances occur which can be measured directly and detected as well by the low tolerance level of the subject to a particular frequency of vibration. The mechanical body system for the low-frequency range below 100 Hz can be approximated partially or in toto by a lumped parameter system, i. e., a system consisting of rigid bodies and restraining elements of negligible mass. Calculation of the response of such a system to static, transient or dynamic forces presents a "network" rather than a field problem. The characteristic of such a system can be determined experimentally by studying its resonance behavior when exposed to steady state vibrations by varying frequency (105, 136, 137, 138). Usually the system can then be analyzed in terms of effective masses, elasticities, dampings, couplings, etc. The smaller the masses involved, the higher is the resonance frequency of the subsystems. For example, the main torso resonances of the sitting or standing man are between 4 and 6 Hz (105), whereas the resonance of the head relative to the shoulder is in the order of 30 Hz (137). Mechanical impedance, i. e., the complex ratio of the alternating force transmitted to the body to the resulting velocity of the area of application has been measured for small areas of the body surface (214) and also for the sitting and standing human subject exposed to whole body vibrations (30, 103, 137, 209, 403, 655, 656). Typical impedance functions derived from impact data are demonstrated in Figure 7-75. (See also impedance curves in Vibration, No. 8). The impedance magnitudes and phase angles reveal critical frequencies at approximately 7 Hz and 12 Hz. The impedance magnitude tends toward zero at low frequencies and, except for the sitting and standing positions during vibration, toward higher values at higher frequencies. It should be pointed out that the location of resonances obtained from transient data may not always be the same as those obtained under vibration conditions (49).

Impedance is related to the concept that the mechanical energy, per se, transferred from the environment to the man is primarily deterministic of biologic effects (655, 656). The impedance model then is essentially an energy transfer model. As such, its purpose is to delineate the energy exchange characteristics of the human body. There are several pertinent aspects to the energy characteristics; the distribution of the real or dissipated energy over the frequency range, the distribution of the reactive or stored energy over the frequency range, and the total amount of each. The development of the energy transfer model has certain implications as regards tolerance. The model defines the energy transfer patterns and, while it gives no a priori estimate of absolute levels, it does indicate that certain types of environments will be more likely to present tolerance problems than others. This means that one can set about designing protection systems without a complete knowledge of the tolerance levels and be assured that, whatever the tolerability, the protection system will offer the minimum energy transfer and therefore the maximum protection. There is another implication in the use of the energy transfer model.

The energy transfer to the human from the environment can be given in terms of the impedance and the power density spectrum of the velocity. This

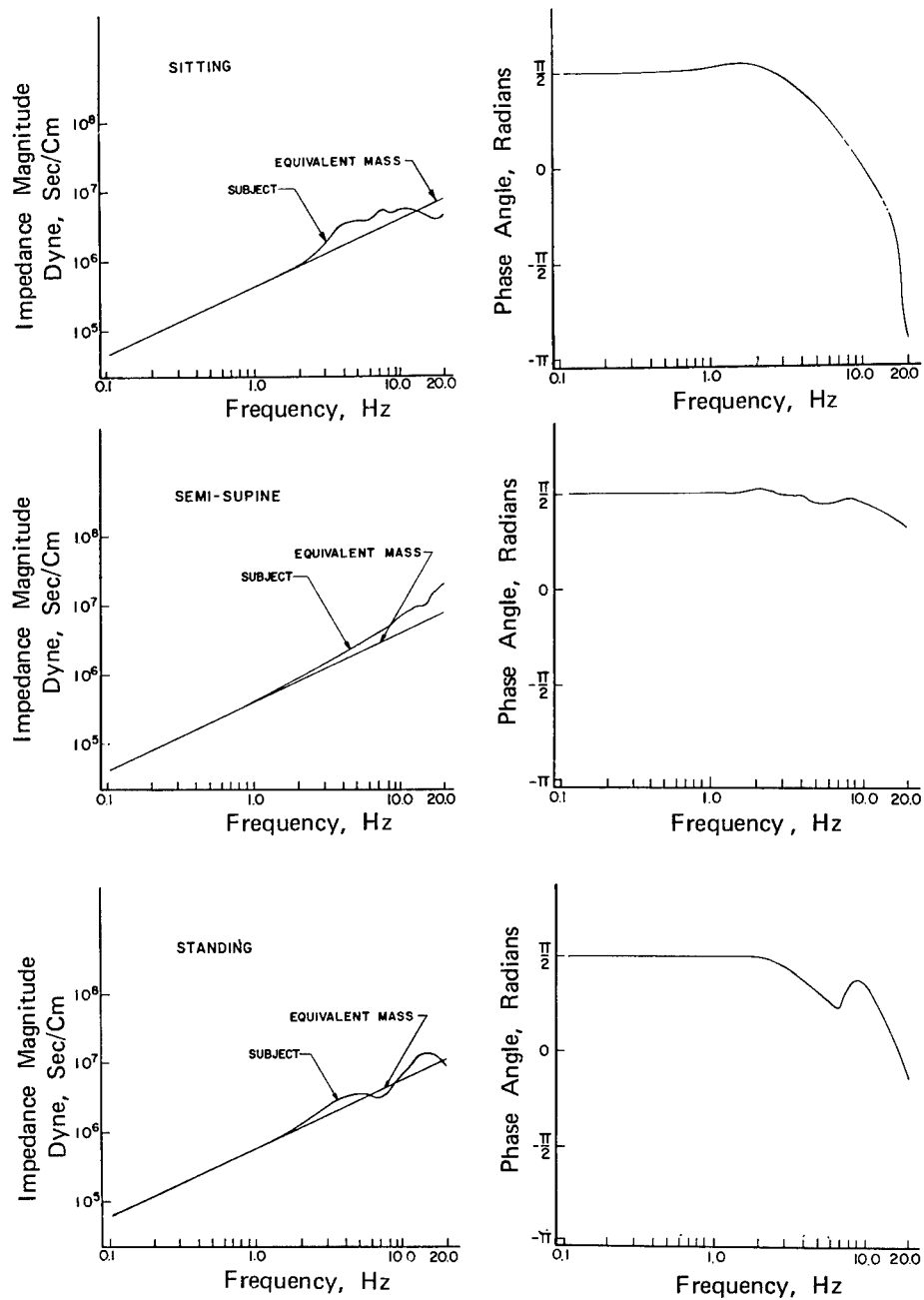


Figure 7-75

Human Mechanical Driving Impedance Determined in the Transient (Impact) Environment

(After Weis et al⁽¹⁹⁵⁵⁾)

means that one can reduce a particular acceleration-time history to its power spectrum in order to judge its effect. This has the advantage that it eliminates the need for approximating very erratic acceleration-time histories. Therefore, impedance along with the phase angle permits calculation of the coupling of mechanical energy transmitted to the body under different modes of application and protection.

Under small amplitude vibration conditions, with ideal support and restraint, the human body response is sufficiently linear to allow meaningful conclusions to be drawn from impedance data. With high intensity vibration and large magnitude impact environments, due to the inherent nonlinearities of the human body and associated support and restraint system, the impedance results must be interpreted with extreme caution (104). Under conditions of impact, relative displacement of "critical mass" or in effect "critical spring deflection" is often a more useful measure of tolerance (477). (Vide infra).

Above roughly 100 Hz, lumped-parameter models become more and more unsatisfactory; a distributed-constant, continuous medium must be introduced to describe the wave phenomena observed in these frequency ranges (209, 210, 214, 469, 655). The characteristics of their propagation and the increased damping of vibrations at higher frequencies tend to localize the effects of such stimuli. Rapid blows and some mechanical shock patterns require the consideration of wave phenomena, whereas lumped parameter systems are usually sufficient for treating the responses to the vibration and impact patterns connected with whole body motions. Even such organs as the eye with a high natural frequency may be considered with the lumped-parameter model if the impact is experienced through the remainder of the body. Direct impact to the head may require the distributed-constant treatment.

When time of exposure to acceleration is less than 1 second, and no blood shifts can occur, physiological effects are caused by localized pressures and relative tissue displacements, which develop into pathological injuries if the mechanical stress limits of the tissue are exceeded (see Figure 7-81). The physical response of the body and its organs, and the dependence of this response on the duration and shape of the acceleration time function, can be calculated when the appropriate mechanical system representative for the body in the particular situation is known (16, 168, 347, 348, 364, 374, 445, 475, 534). A small analogue computer is available for these studies (475). Unusual acceleration profiles in accidental or operational situations, nonlinearities in response of tissue and limitation of complete directional data for the whole body tend to limit use of these models to first-order approximations for design purposes.

In general, one can expect maximum effect of impact acceleration functions if the impact duration is of the same order of magnitude or longer than the natural periods of the body systems (212). From the dynamic response factor for the transient response of linear structures to shock, excitation follows a pattern as illustrated in Figure 7-76 which shows curves of equal physical displacement of organs (tolerance curve) as a function of maximum acceleration and pulse duration. It is important to note that, if the pulse duration is much shorter than the natural period of a system, $\tau/T_0 < 0.3$,

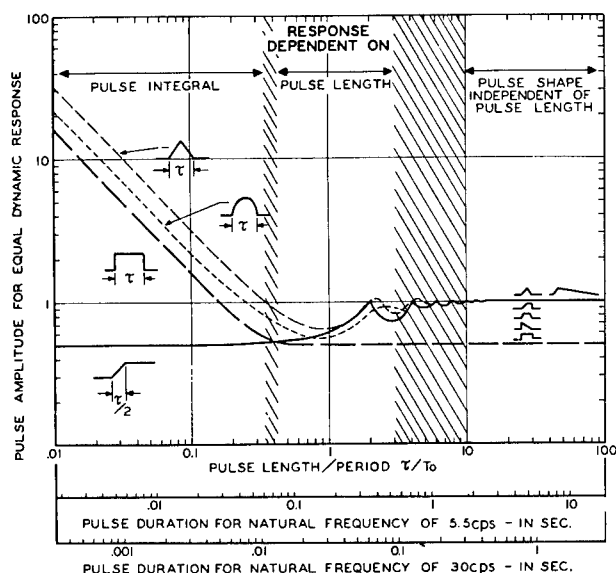


Figure 7-76

Theoretical Impact Tolerance Curves of a One-Degree-of-Freedom System

The curves show for various types of pulses the pulse height (as a function of the ratio of pulse length to natural period of the system) which is necessary to achieve the same maximum displacement of the system. (T = natural period of the system; τ = pulse duration). The additional pulse duration scales on the abscissa are for a system having its resonance at 5.5 cps (main body resonance) and for a system with its resonance at 30 cps (head resonance).

(After Von Gierke⁽²¹¹⁾)

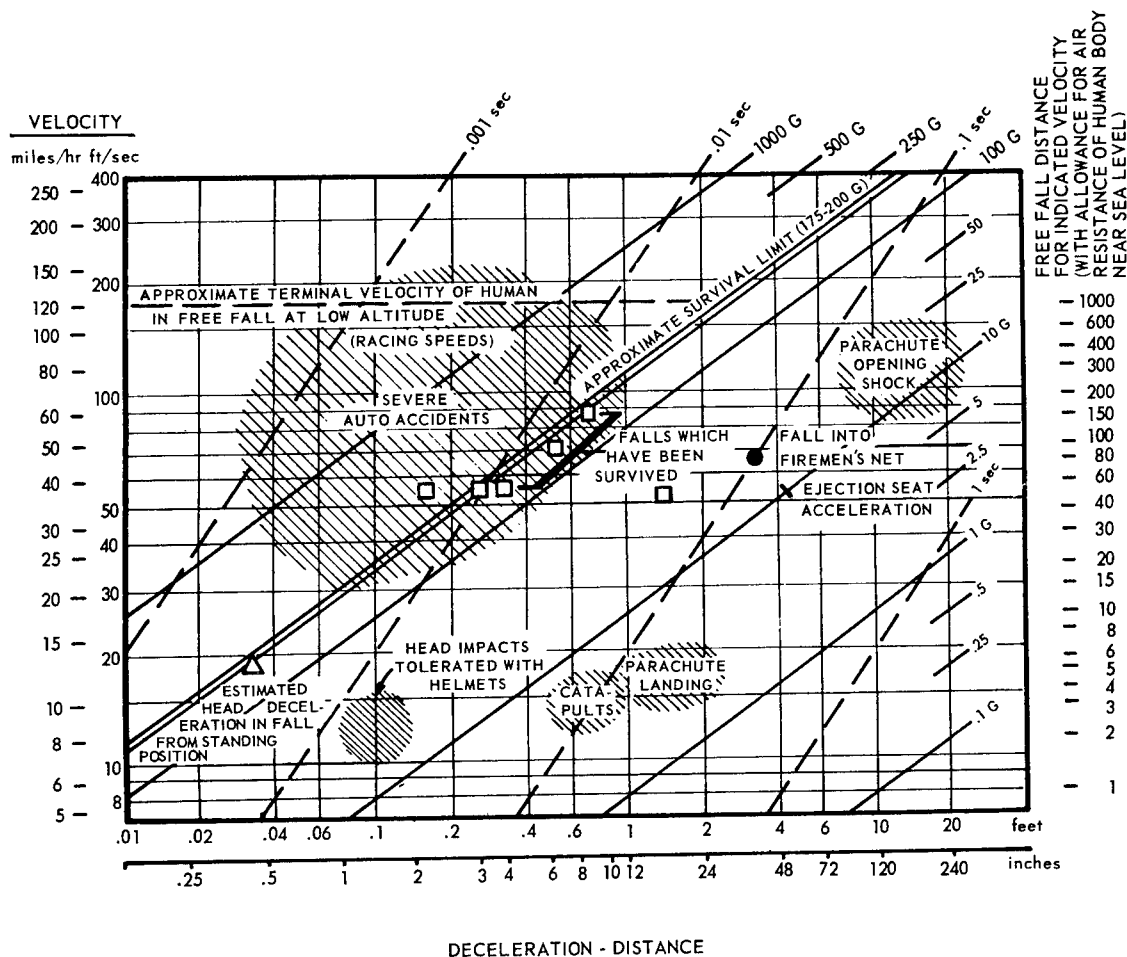
the response is only dependent on the acceleration-time integral, "impulse." It is equal to the difference in velocity of the system before and after impact and ceases to be a direct function of the peak acceleration (596). (See Figures 7-82 and 7-92). If τ/T_0 is larger than approximately 3, the response becomes independent of the pulse duration and more dependent on pulse height and pulse shape. In this range the rise pattern of the pulse (rate of onset) can change the response within a factor of two. In the range $0.3 < \tau/T_0 < 3$, pulse shape, height, and pulse duration are of influence. These curves of Figure 7-76 represent undamped responses. The more complicated damped responses are more typical of the real-world situation (16). These are mentioned below in the discussion of Figure 7-81.

Physiological Response to Impact

The main difficulties in interpreting experimental data are; correct interpretation of the results of measuring instruments, the effect of seat and harness configuration, lack of standard acceleration input patterns, orientation of the subject, differences in response of individual subjects and the often unreproducible nature of the experiments. Qualitatively, experiment has shown that the major factors influencing human tolerance to short duration accelerations are:

- (a) direction of application of input
- (b) magnitude of the input acceleration
- (c) duration of the input
- (d) rate of application of the acceleration ("rate of onset")
- (e) orientation of the body

For each direction of application there is a different limiting structure and symptom pattern (213). Figure 7-77 summarizes some of the exposures for which critical deceleration loads and times of application are known. For



This chart brings together a variety of impact and deceleration experiences by plotting the data from a number of sources on the common axes of deceleration distance and velocity. Stopping time and impact force in G units are shown as secondary scales. The data points with hollow squares are for free falls of 50-150 ft with survival. There are many other cases of more extreme and less extreme impacts with survival, for free falls from 5 to 275 ft (Snyder 551), but deceleration distance is not always available. The line labeled "approximate survival limit" must be used with caution, since many biophysical factors influence the injury due to deceleration.

Figure 7-77

Impact Experience

(After Webb⁽⁶⁵¹⁾, adapted from Roth⁽⁵⁰⁶⁾, and data of Snyder⁽⁵⁵¹⁾)

acceleration forces parallel to the spine, compression of the spinal column limits voluntary tolerance (126, 303, 364, 512, 596). Persistent neuralgic and sciatic-like pains resulted from such exposures. For forces transverse to the longitudinal axis, for which tolerance limits are higher, symptoms of various degrees of shock were the first signs limiting voluntary tolerance (29, 481, 563, 564, 567, 568, 569). Subjects turned pale, perspired, and exhibited transient rises in blood pressure. In one case, brief attacks of low blood pressure and albuminuria were observed for about six hours after the run. More severe loads resulted in unconsciousness. At the maximum acceleration loads applied, immediate effects were sometimes not pronounced, but delayed effects occurred with gradual onset over the next 24 hours. So far no evidence of cumulative effects due to repeated exposure to impact forces close to voluntary tolerance limits has been reported; however, the number of subjects and exposures are too limited, and physiological and psychological tests are too crude to permit valid differentiation of subtle effects of such stress from the changes which occur with time in individuals unexposed to impact.

In accidental situations, with impact forces high enough to produce pathological damage, injury to the head is the most frequent and most severe manifestation (221, 481). More than 75 percent of crash fatalities in aircraft have been found to result from head injuries. They usually occur from heavy blows to the head by solid objects as a result of crash deceleration rather than from the action of acceleration forces on the head structure as a whole. Injury to the neck, specifically to the cervical spinal cord at the first vertebra, seems to occur from backward flexion and extension of the neck when the whole body is accelerated from back to front without head support (181, 305, 470). This "whiplash" type of injury is very common in rear end automobile collisions. Other types of concussion result from heavy blows to the skull with deformation or fracture of the skull and shear strains throughout the brain (100, 135, 271, 273, 379, 702). More severe skull deformations or fractures cause contusions of various degrees. Within the conditions studied, the total energy required for skull fracture varies from 400 to 900 in. -lbs., with an average often assumed to be 600 in. -lbs., (6.8×10^8 ergs). The shape and elastic properties of the object injuring the head and exposure time are of prime importance in determining the degree of injury (see also Figure 7-89 and Table 7-94).

Damage from impact forces to other areas besides the head structure are bruises, tissue crushing, bone fracture (271), and rupture of membranes or organ capsules (17, 100, 287). Damage of varying degree to the vertebrae is most common (271, 298, 479, 512). Internal injuries, such as are observed in aircraft accidents, have rarely occurred in experimental situations with humans. These injuries, frequently the cause of death, are probably produced by forces of relatively long duration (211). (See section on Impact by Missiles and Moving Structures).

Symptoms and signs resulting from "off axis" impact under the Apollo restraint system are noted in Table 7-87b.

In addition to these gross responses to impact, there are general biological responses. These are summarized in Table 7-78.

Table 7-78

General Biological Effects of Impact

(Adapted from Taylor⁽⁶⁰⁰⁾)

A review of experimental experiences with impacts produced by short track deceleration devices has shown that there are numerous physiological changes following impacts in the transverse ($\pm G_x$) direction when the peak forces range from 15 to 25 G, and onsets range from 400 to 1000 G/sec. These are transient changes, and occur in subjects who are entirely uninjured in the mechanical sense of bone fracture or detectable tearing of tissues and organs. (See also the subjective responses of men exposed to lateral and off-axis impacts in 7-86). The physiological changes are summarized in the following table.

Effect	Notes
Shock	Blood pressure 90/60 mm Hg routinely seen 15-30 sec after impacts producing 15-20 $\pm G_x$ peaks, where onset rate was 500 G/sec. Lower pressures observed after greater impacts.
Bradycardia	Slight slowing of heart rate (bradycardia) following 15 G peak impacts facing forward ($-G_x$), and greater slowing in backward facing impacts ($+G_x$). The effect was related to activity of the vagus nerve, since atropine blocked the bradycardia. At greater peak accelerations, greater slowing occurred.
Transient neurological changes	Subjects appeared to be stunned for 10-15 seconds at 20 G peak accelerations (onset at 400 and 800 G/sec), and abnormal slow wave patterns were seen on the electroencephalogram for several minutes following peak impacts at 25 $+G_x$, 1000 G/sec onset. Other changes included increased muscle tone, euphoria, loquacity, hand tremor, decreased coordination, and gross involuntary movements in head, arms, and trunk. Increased deep tendon reflexes were commonly present after $\pm 15 G_x$, and after a peak impact of 25 G reflexes were absent for several seconds, then hyperactive for about a minute.
Changes in blood platelets	One hour after impacts with +20 G_x peaks and onsets of 400 or 800 G/sec, blood platelets were found to be reduced. A week later the platelet count was higher than the control value.
Psychological changes	Psychological evaluation with the Kahn symbol arrangement test showed changes which increased with $+G_x$ impacts from 10 to 25 G peak accelerations.
General stress reactions	Changes were seen in the indicators of adrenal gland activity, and various changes occurred in chemical constituents of the blood.

The post-impact bradycardia or slowing of the heart is a function of the acceleration profile and the subject orientation (see Table 7-78). Individual variation in response to a given impact profile is recognized. Under physiological stimulation cardiac rate may change abruptly, followed by a gradual return to pre-stimulus levels after stimulus cessation. Physiological stimuli may be hormonal or neural in origin. The immediate onset of slowing in response to impact is consistent with a neural stimulus. Cardio-inhibitory reflexes of the body can be initiated from baroreceptors in the aortic arch and carotid sinus and by visceral afferents in the lung, gastro-intestinal tract, and skeletal muscle. Visceral afferent nerves originating in nearly all tissues and organs except the skin produce bradycardia (513). Stretch receptors in the lung can initiate reflex cardiac slowing (128). During headward deceleration ($-G_z$), stretching (distortion) of the lung can occur which initiates the cardio-inhibitory reflex. Because impact duration is so brief, vascular fluid shifts are an unlikely source of stimulation to cardio-inhibitory reflex areas. However, it is apparent that the inertial effects of a headward deceleration ($-G_z$) would produce a transient increase in the hydrostatic pressure sensed by the baroreceptors, which in turn respond to this pressure increase by reflex slowing of heart rate.

If an impact pulse is of a duration less than 50 milliseconds, the cardio-inhibitory reflex resulting in slowing of the heart rate is apparently not permitted to occur. Conversely, beagle dogs and macaque monkeys show tachycardia when exposed to $-G_z$ deceleration of 20 G magnitude with a plateau of peak impact lasting 15 to 20 milliseconds, and a trapezoidal deceleration profile. The tachycardia can be prevented by use of propranolol, a beta-adrenergic blockade (558).

Damage to the respiratory systems is often seen in impact studies. This ranges from minor functional changes in maximum ventilation (280) to contusion and hemorrhage (49). Restraint straps and structures may themselves be responsible for lung damage (49, 220, 514).

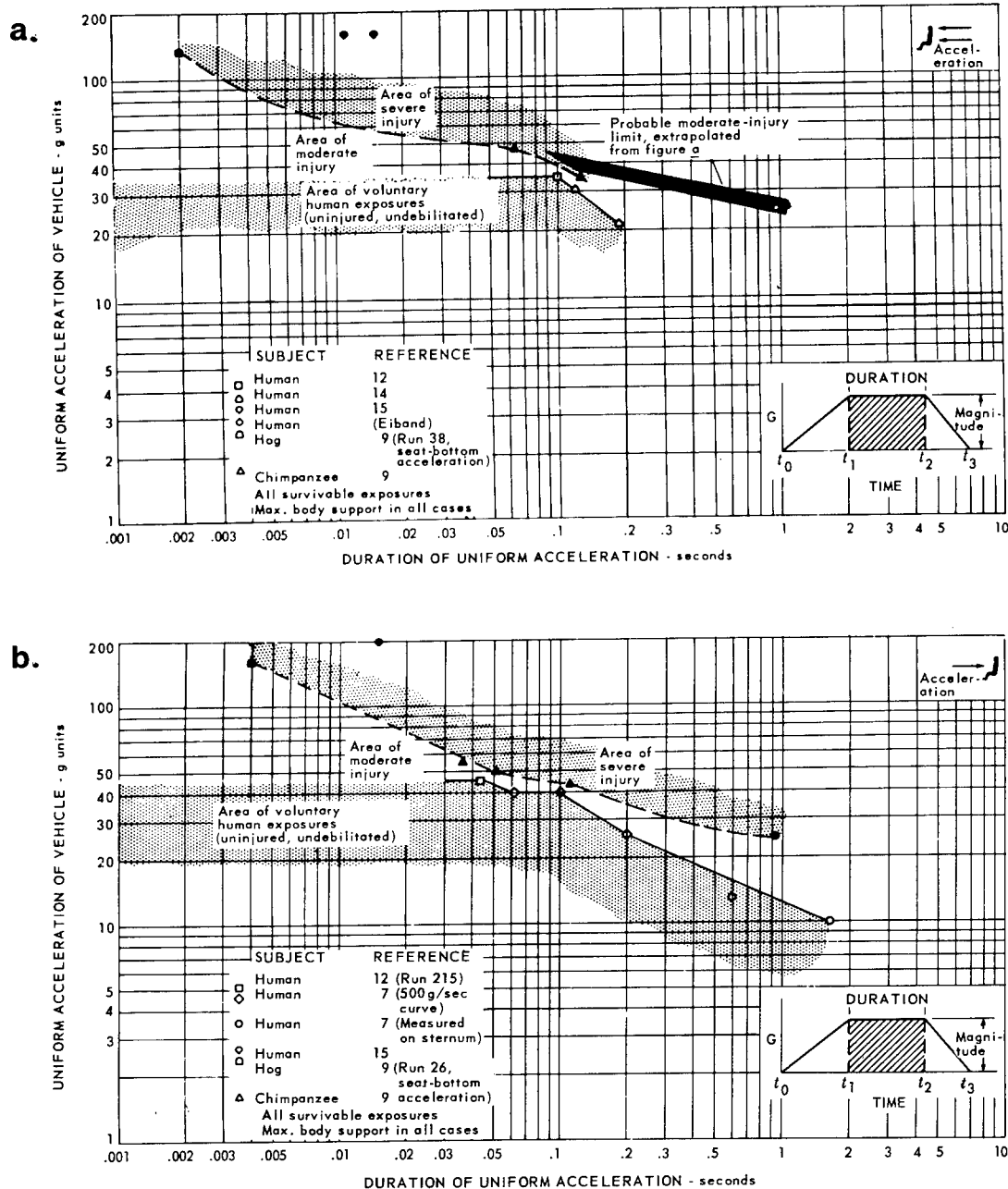
Human Tolerance Limits

Approximate tolerance limits for the sitting human subject with maximum body support have been summarized for impact loads in the direction of the four main body axes (164, 385, 552, 563, 566, 569). Unfortunately, evaluation of the tests is only available in terms of idealized trapezoidal force functions with peak acceleration, duration, and rate of onset as the only parameters evaluated. These do not permit analysis of the complete force pattern including restraint variables.

On-Axis Impact

Tolerance to spineward acceleration ($+G_x$) as a function of magnitude and duration of impulse is illustrated in Figure 7-79a. For sternumward acceleration ($-G_x$), Figure 7-79b is similar but roughly in the order of 25% lower. In the longitudinal axis, tolerance to headward acceleration ($+G_z$), in Figure 7-80a exceeds tolerance to footward acceleration ($-G_z$). (Figure 7-80b).

Figure 7-79
Abrupt Transverse Decelerations
(After Webb⁽⁶⁵¹⁾, adapted from Eiband⁽¹⁶⁴⁾)



These two graphs show the durations and magnitudes of abrupt transverse decelerations which have been endured by various animals and man, showing areas of voluntary endurance without injury, moderate injury, and severe injury. Graph a summarizes (+G_x) data (chest to back acceleration) and b shows (-G_x) data (back to chest acceleration). Reference numbers on the graphs are those in the original reports.

More recent data on $-G_z$ impacts are available (58,297). Included in Figure 7-80a is a tolerance curve based on German World War II data relative to compressive strength tests performed on the human spine. This curve is used as limit criteria for ejection seats and is so marked (512).

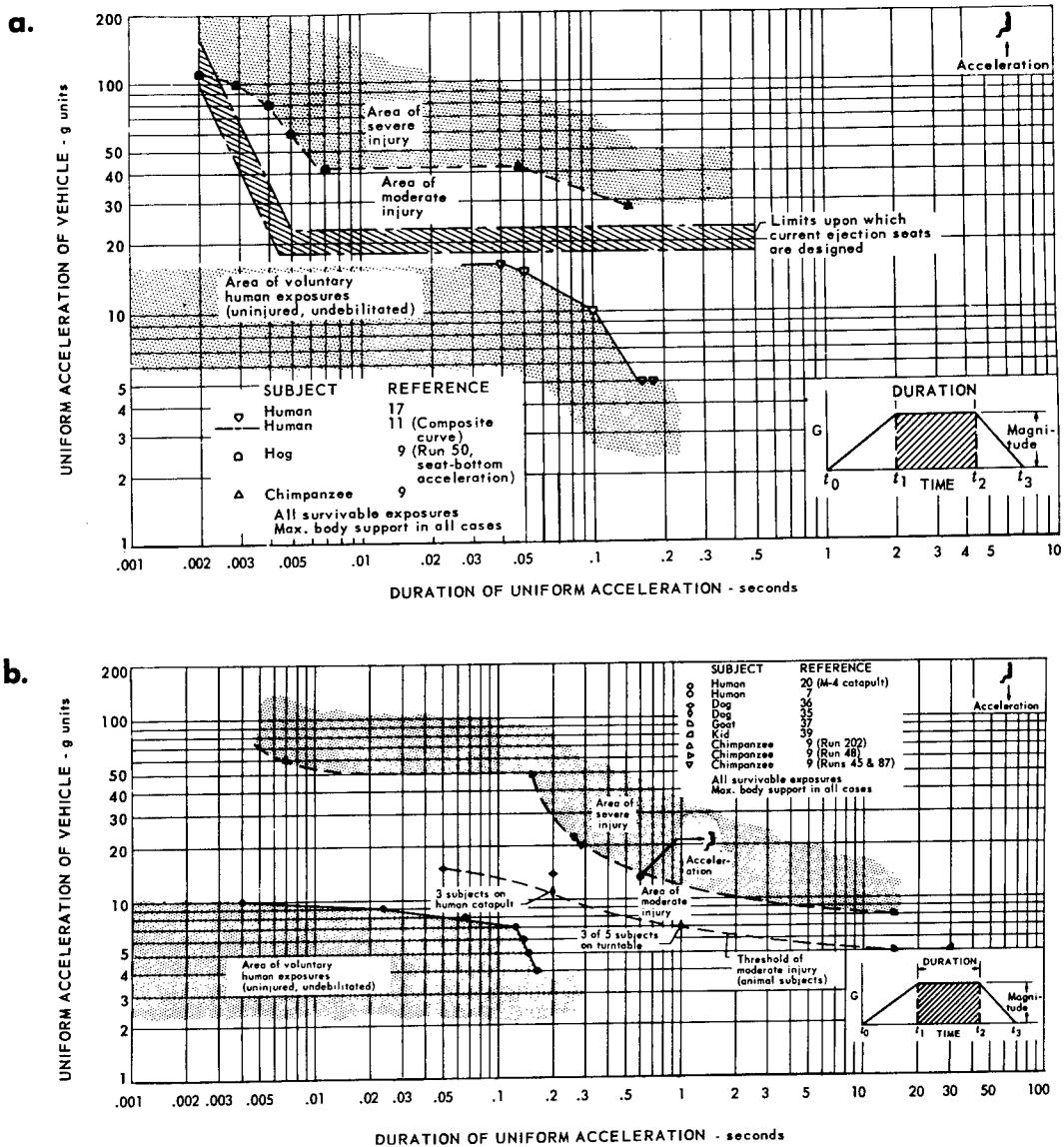
For the impulse durations illustrated, changes in the rate of onset had marked effects on human response (164, 563, 567, 568, 569). For example, in Figure 7-80 peak acceleration of approximately 45G (0.09 sec duration) with a rate of onset of 500 G/sec results in no signs of shock whereas 38G's (0.03 sec) at higher than 1300 G/sec rate of onset produced definite shock signs. A higher rate of onset usually implies a higher content of high frequency energy in the acceleration pulse and this implies a higher energy transfer to the human. Unfortunately, the data are too few and too often uncontrolled with respect to restraint system for adequate interpretation (304, 445). Also, tolerance limits cannot be set by models based on non-tolerance limiting experiments. The total energy limits must be given in terms of the amount of energy which causes biologic injury. The summary charts which are available must be applied with caution (164, 221).

Design curves for ejection seat and escape capsules (6, 195) have often neglected the dynamic overshoot of man and have been vague regarding the relationships between rate of onset and duration, especially in the region of short duration (304, 310). For example, whole body deceleration of 50 pound chimpanzees at $-30G_z$ using a trapezoidal deceleration profile with a plateau of 50-60 milliseconds duration resulted in G amplification of 2.0 to 2.5 times the sled G as detected by a miniature accelerometer mounted on the calvarium (558). Attempts are being made to expand design criteria to cover these variables (612). In view of these gaps, the general form of curves in Figures 7-79 and 7-80 merits some comment (445). It can be seen in Figure 7-80a that for duration times up to 0.01 sec the tolerance level drops off linearly (log - log scale) as the duration time increases. This is shown in Figure 7-81a and can be explained in terms of dynamic response, since the acceleration achieved by the man takes a finite time to develop. When full overshoot is attained (at about 0.01 sec) any further increase in the duration time does not increase the man's response for a given input level, until the "long" duration regime is approached when hydraulic effects become noticeable and reduce the tolerance level still further (see also Figure 7-76).

It is clear that there is a considerable unknown area between the region of voluntary human exposure and the known region of injury. In the headward case, Figure 7-80, this unknown area covers over 20G in the ordinate, which includes the region of most interest in space operations. In addition, the boundaries are not particularly well defined and a few more reliable points might well change the general shape of the curves, particularly in the impulse region. The method of analysis of the results was in no way rigid as the deduction of a plateau level and duration time from a complex acceleration trace is no easy task and various combinations of the two parameters are equally correct. The hog points shown in Figure 7-80a were apparently obtained from a single experiment which is not particularly valid, since the experiment represented an end point. The reverse argument is also true since it is difficult to fit criteria based on a trapezoidal input to the complex acceleration-time histories encountered in practice. (See Figures 7-86 and 7-91).

Figure 7-80

Abrupt Longitudinal Decelerations
(After Webb⁽⁶⁵¹⁾, adapted from Eiband⁽¹⁶⁴⁾)



These two graphs show the durations and magnitudes of abrupt decelerations in the G_z (longitudinal) direction which have been endured by various animals and man, showing areas of voluntary endurance without injury, moderate injury, and severe injury marked by shading. Graph **a** shows data of $+G_z$ acceleration (headward), and **b** shows data for $-G_z$ acceleration (tailward). Reference numbers on the graphs are those in the original reports.

Recent attempts have been made to supplement the empirical curves with preliminary computer models employing impedance and resonance techniques (445). An analysis of headward accelerations ($+G_z$ of Figure 7-80) has shown that the maximum plateau input acceleration can probably be taken as 40G with some degree of confidence. The selection of an equivalent spinal frequency (ω) is not so well defined. Because of the shortage of results in the impulse region, the most reliable evidence can be taken from the critical velocity change deduced from drop tests which gives a value for ω of 225 rad/sec (596).

In the transverse, backward direction ($+G_x$ of Figure 7-79a), the plateau tolerance line falls at a value of 45G for the input acceleration and the most sensible position for the impulse tolerance line corresponds to an equivalent frequency of 95 rad/sec, which is somewhat higher than the value suggested by the evidence from accident survival. The adoption of the more pessimistic tolerance line appears justified since it satisfies the few sled test points available and accident cases usually represent extreme end points. No satisfactory conclusions could be made from the transverse forward data ($-G_x$ of Figure 7-80b) but a frequency of 95 rad/sec, as for the backward case, is suggested. From a physiological standpoint, the plateau tolerance level might be lower than that for the backward direction because of the position of the spine relative to the internal organs. There is some experimental evidence to support this fact and until more relevant tests have been conducted, it is suggested that the allowable peak input acceleration is taken as 35G.

These tentative values suggested for use with the single degree of freedom, undamped dynamic model are given in Table 7-81b. It should be remembered that these values are applicable to an undamped model. Damping will introduce changes in the tolerance levels which have been considered to be small enough to be ignored at this stage of model development. Analytic results are also available for two and three degrees of freedom models (445). These bring out the factors determining the drop in tolerance levels at the longer durations of Figures 7-79 and 7-80. The exact shapes of the curves are determined sequentially by tolerance of the head, lumbosacral and spine-abdomen system as the duration of impulse is increased.

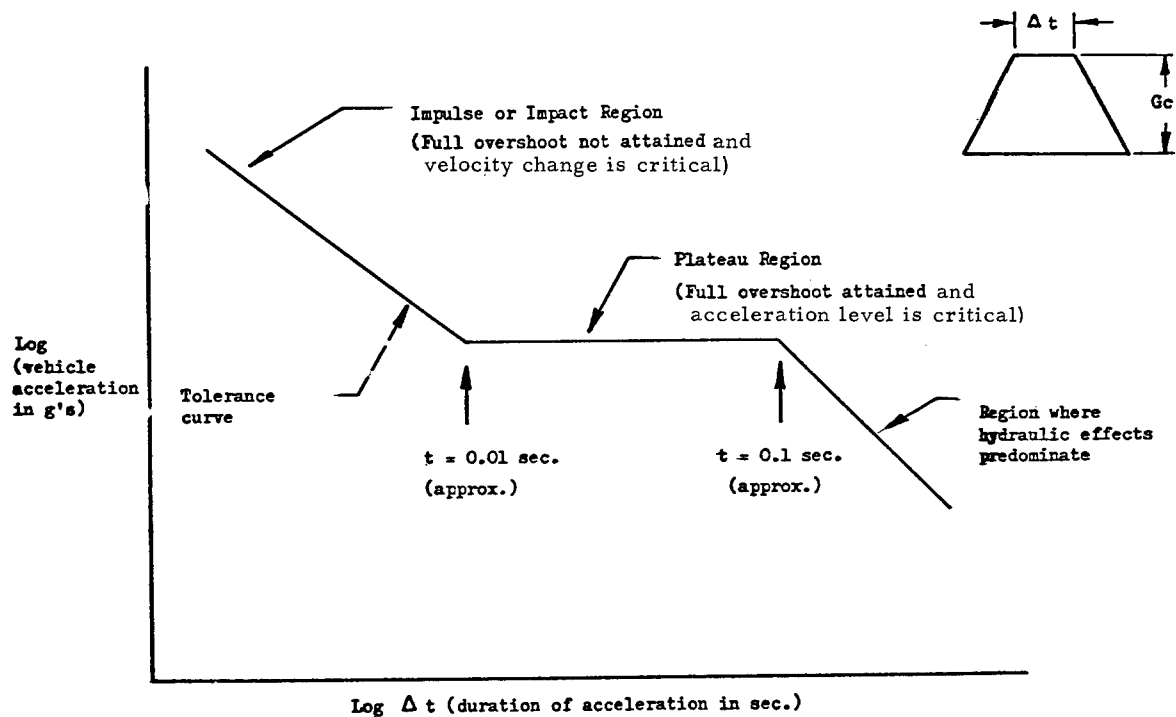
The factors discussed in Figures 7-79, 7-81 may be presented in another form and compared with previous estimates of backward acceleration tolerance, $+G_x$. Figure 7-82 represents this comparison. The curves of Reference 652 were calculated to define the dividing line between mild injury (no damage) and severe injury such as shock and retinal hemorrhage in humans, in terms of velocity change and average acceleration force. There are few human experiments at the high accelerations. Animal data support the shape and approximate location of the curve (347). Because of an error found in the original calculations, they were recalculated and plotted as shown. Good agreement is noted except for the 0 to 0.02 region where the earlier model of Reference 652 shows a greater permissible velocity. It can be seen that for exposures of less than 0.02 to 0.06 seconds, the change in velocity rather than the acceleration level determines tolerance as predicted by Figure 7-76. More human data are needed to define the curve at low durations of exposure.

Figure 7-81

Modeling of Impact Acceleration Regimes

(After Stanley Aviation Corp.⁽⁴⁴⁵⁾)

a. Definition of Tolerance Factors



b. Tentative Impact Tolerance Parameters for Use with Single Degree of Freedom Undamped Dynamic Models (See Figure 7-81a)

Parameter	Impact Direction		
	Headward (+G _z)	Backward (+G _x)	Forward (-G _x)
Equivalent Frequency	225 rad/sec	95 rad/sec	95 rad/sec
Maximum Allowable Mass Acceleration	+80 G _z	+90 G _x	-70 G _x
Impulse Region	0 to 0.009 sec	0 to 0.02	0 to 0.02
End of Plateau	.09 sec	.06 sec	.08 sec

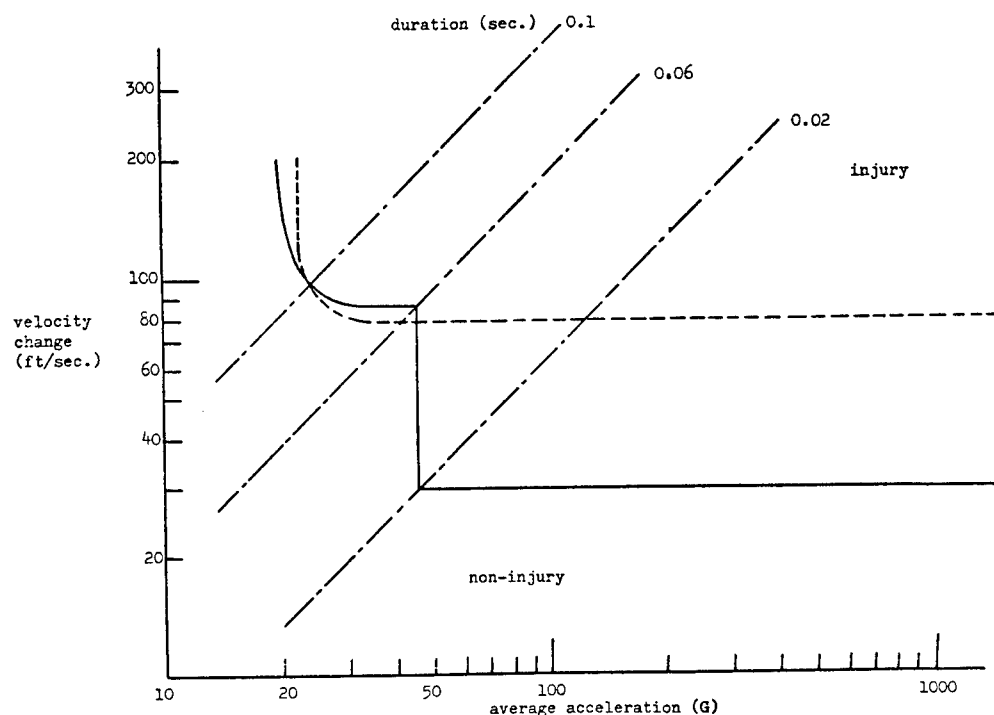


Figure 7-82

Tolerance to Short-Duration Accelerations as a Function of Velocity Change and Average Acceleration

(After Stanely Aviation Corp. (445))

Figure 7-83 indicates the peak accelerations that have been survived without permanent injury. Figure 7-84 shows the greatest vertical impact subjects would voluntarily endure and the type of symptoms noted at given rates of onset. Data are available on the survival of free falls into water (553).

Another way of defining impact sensitivity is in terms of impact force per unit area and duration. For the shorter times on the left half of Figure 7-85, the body is thought to act as a rigid mass; for the longer times to the right, effects are caused by shifts in body fluids and tissues. The data points are taken from human experiments in drop towers, falls, and rocket sleds, with various restraint devices. The two shaded areas define approximate areas of effect in terms of impact pressure for any duration. Body position affects these results.

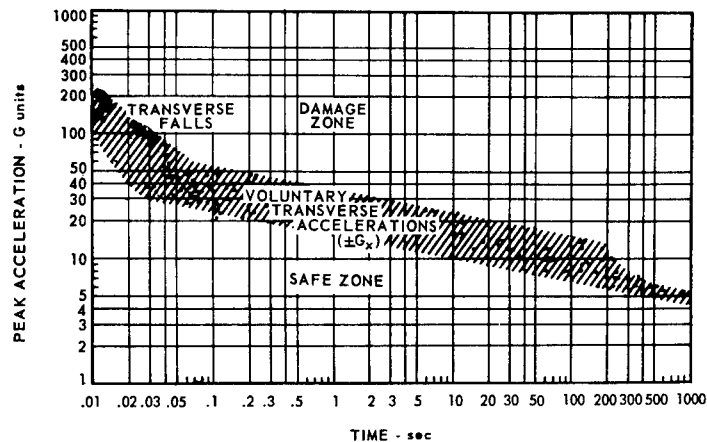
Off-Axis Impact

There are relatively few data on "off axis" impact profiles in restraint systems used in space operations (482). Figure 7-86 represents some of the acceleration profiles and responses noted in subjects exposed to these accelerations while seated in form-fitting couches used in Project Mercury. The impact modes predicted at the couch in Apollo landings have been reviewed (593). Data are now available for predicting impact tolerance with the Apollo restraint system. To obtain the results, two hundred eighty-eight

Figure 7-83

Tolerance to Peak Accelerations

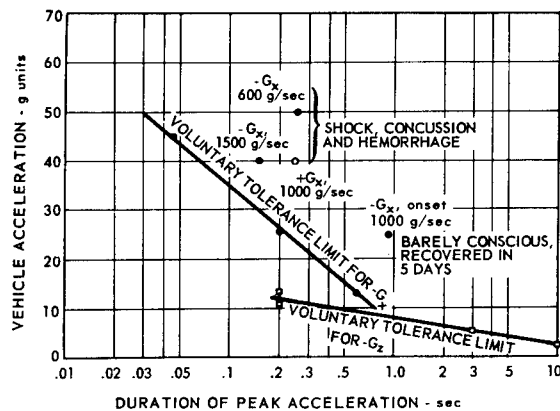
a.



This shows peak transverse accelerations which have been survived without permanent injury in a variety of situations, including data from falls (below 0.03 sec), short track impact facilities (0.03 to 0.1 sec), high speed sled runs (0.1 to 1.0 sec), and centrifuge studies (2-1000 sec). Peak accelerations lying below the band of data would be assumed to be non-injurious, while those above the plotted data would be presumed to produce severe injury or death.

(After Webb⁽⁶⁵¹⁾, adapted from Thompson⁽⁶⁰⁶⁾)

b.

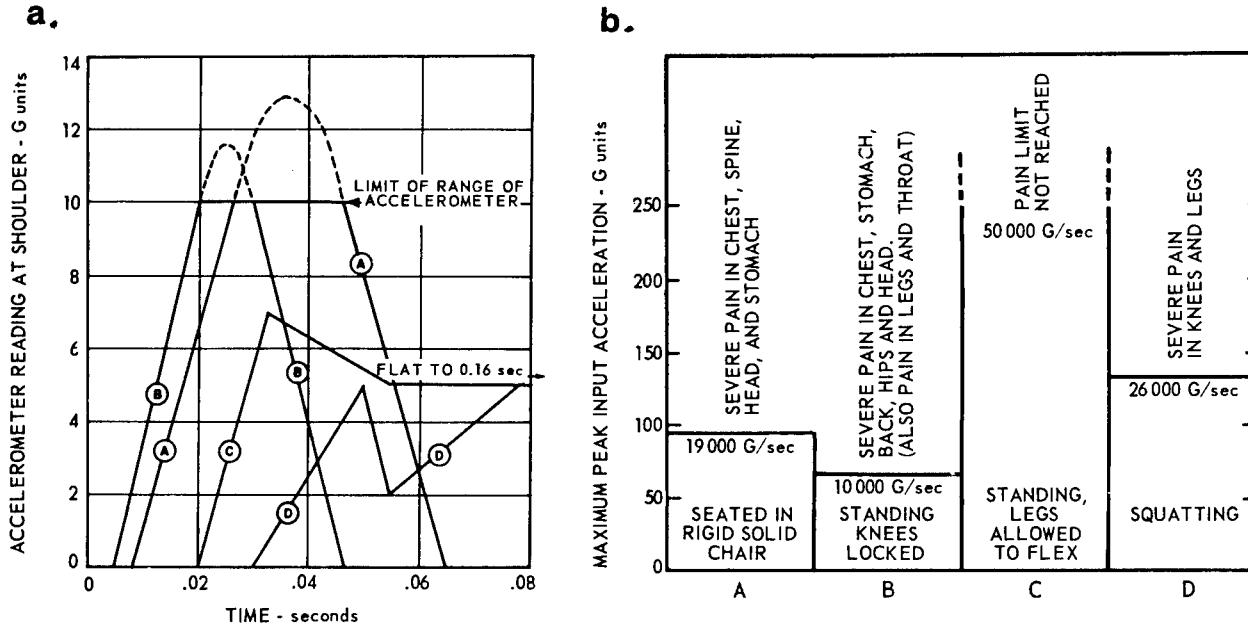


The two lines connect data points for the highest peak accelerations – transverse, $-G_x$ and negative, $-G_z$ – which carefully restrained subjects have voluntarily endured without injury on high speed rocket sleds which are decelerated to give the vehicle accelerations and times shown. The four points above the lines show accelerations which produced reversible but none-the-less serious injury in transverse acceleration ($\pm G_x$) runs.

(After Webb⁽⁶⁵¹⁾, adapted from Blockley⁽⁴²⁾, and Stapp^(564,565,567,568,569))

Figure 7-84

Tolerance to Vertical Impact
(After Webb⁽⁶⁵¹⁾, adapted from Swearingen⁽⁵⁹⁶⁾)



The greatest impact which subjects would voluntarily endure during test drops in several positions is shown. In chart a the time histories of impact are drawn from readings of accelerometers located on the subjects' shoulders, while in b the symptoms for the four different drop positions are related to the maximum peak accelerations. There were 13 subjects and a total of some 500 test drops.

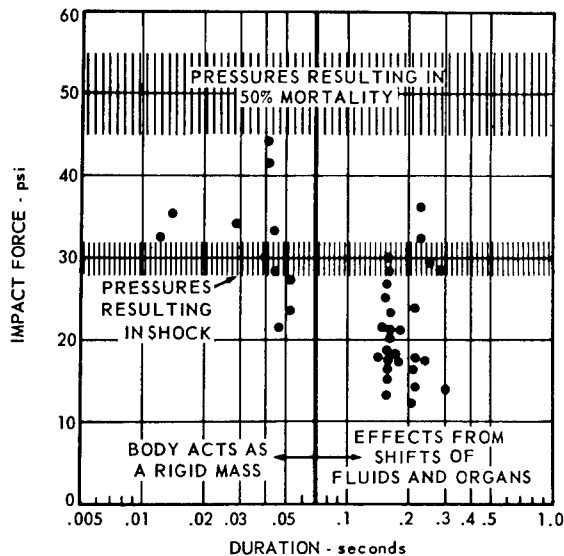


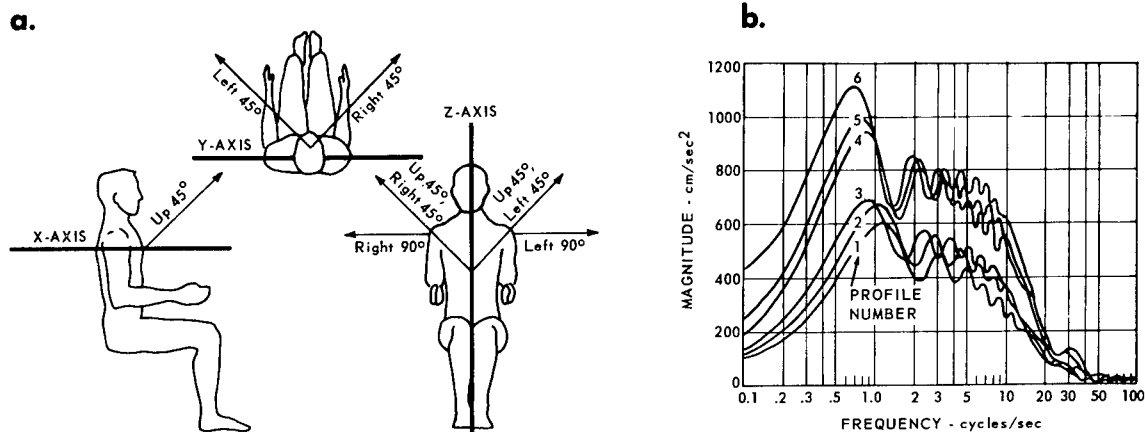
Figure 7-85

Tolerance to Impact as Related to Impact
Force Per Unit Area

(After Webb⁽⁶⁵¹⁾, adapted from Thompson⁽⁶⁰⁶⁾)

Figure 7-86

Impacts Off Axis

(After Webb⁽⁶⁵¹⁾, adapted from Weis⁽⁶⁵⁴⁾)

Early data are illustrated here on the tolerability of impacts laterally applied and applied off the major X, Y, and Z body axes. The directions of impact for five body positions 45° off axis, and for left and right lateral positions (on the Y-axis) are shown in **a**. Using a vertical drop tower device which decelerates the falling vehicle when a shaped plunger enters water, the experimenters exposed some 20 subjects to six different acceleration profiles while in each of the seven body positions. The subjects were carefully restrained and supported on a form-fitting couch, and wore the helmet used in Project Mercury. Peak accelerations ranged from 13.4 to 26.6 g, and onsets from 426 to 1770 g/sec; the power density spectra of the six acceleration profiles are shown in **b**. There were no injuries produced. Some transient changes were seen in the electrocardiograms, such as premature ventricular beats. The subjects said they would be willing to endure the impacts again. Their subjective comments are summarized in the table below.

c. SUBJECT RESPONSES

Orientation	Acceleration Profile Number					
	1	2	3	4	5	6
Right 45°	None	None	"Slight pain" in center of forehead lasting 5 minutes.	"Slight pain" above left ear in skull.	Complained bitterly but diffusely - EKG shows abrupt rhythm changes and four premature ventricular contractions.	Complained bitterly but diffusely.
Up 45°	None	Transient pain in occiput.	Transient pain in occiput - developed severe pain in neck four hours post-test, gone in a. m.	None	Slight head pain - pain about T ₂ or T ₃ ; * transient - developed severe muscle pain at point of left scapula - gone 24 hours.	None
Left 45°	Transient pain in occiput moving to temples.	None	None	None	None	Mild pain radiating from right midaxillary line at level of 11th rib to left iliac crest, transient.
Left 45°, up 45°	None	None	None	Fleeting pressure under chest belt.	Mild pain beneath chest strap - mild pain about C ₈ or T ₁ * in midline posterior.	None
Right 45°, up 45°	None	None	None	None	"Wind knocked out."	"Wind knocked out."
Right 90°	None	None	Skinned right elbow.	Pain in right calf.	Pain in right calf.	"Knocked wind out."
Left 90°	None	None	Pain in right trapezius.	None	"Wind knocked out."	One premature ventricular contraction 2 minutes post-test and one 11 sec pre-test.

*T₁, T₂, T₃ - first, second and third thoracic vertebrae; C₈ - eighth cervical vertebra.

human impact experiments were accomplished on a linear decelerating device at variable axes of impact (81). The acceleration profile of each run was not stated. However, it was indicated that the rate of onset (G/sec) of impact was varied in most orientations in addition to the magnitude of G. Two tests were performed at each combination of position, G level and rate of onset. The G level (measured on the sled) ranged from 5.5 to 30.7, the rate of onset varied from 300 to 25,000 G/sec and the sled brake entry velocity ranged from 2.8 to 13.7 m/sec (9.3-45.0 ft/sec). A proposed Apollo restraint system was used in all human tests. Figure 7-87a represents the direction of forces applied and the orientation on the impact device. Tables 7-87b and c represent the symptoms noted and post-impact examination findings.

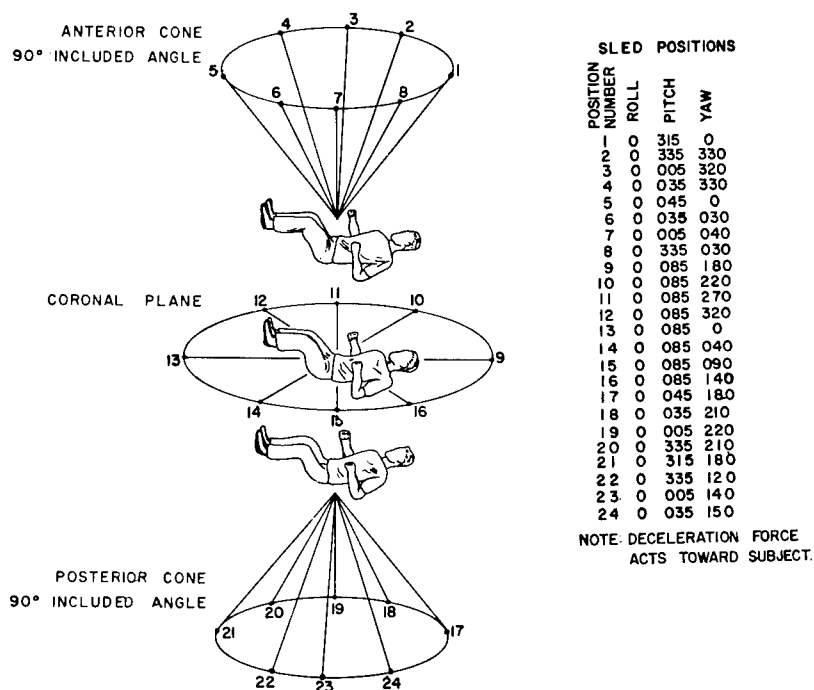
It was observed that impact forces produced effects to the nervous, cardiorespiratory and musculo-skeletal systems. Neurological effects of impact were momentary stunning and disorienting. A consistent effect to the cardiovascular system was transitory post-impact slowing of the heart rate in those body orientations in which the decelerative force acts in a footward direction (inertial force acts headward). Respiratory effects of impact were momentary shortness of breath and chest pain. Effects to the musculo-skeletal system were soreness and spasm of muscle groups of the neck and back. No effect to the human subject was severe enough to exceed human tolerance, significant incapacitation or undue pain.

Figure 7-87

Off-Axis Impact with the Apollo Restraint System

(After Brown et al⁽⁵⁸⁾)

a. Deceleration Force Vector Orientation for Apollo Impact Tests



The numbered lines represent the direction of forces applied to the subject during impact. The columns on the right indicate the translation of forces orientations into seat position.

Figure 7-87 (continued)

b. Subjective Complaints

Pos. No.	Seat Orientation (Roll-Pitch-Yaw)	Complaint Tests Total Tests	Category ^a of Complaints	Complaint ^b G Range	Sled G Range
1	000-315-000	2/14	4,9	13.2-24.6	5.7-26.3
2	000-335-330	3/10	7,8,10,10	17.3-21.0	6.0-21.0
3	000-005-320	2/14	4,8,9,9,10	17.5-25.6	9.2-25.6
4	000-035-330	4/12	1,1,4,4,6	18.5-25.0	10.5-25.0
5	000-045-000	5/14	2,4,4,4,5,5,6,9,9,9	5.9-25.0	5.9-25.0
6	000-035-030	6/12	2,4,4,5,8,9,9,10	18.5-24.5	10.2-24.5
7	000-005-040	4/11	2,4,4,6,7,9	14.2-23.5	10.0-23.5
8	000-335-030	1/14	4,9	19.5	8.0-24.7
9	000-085-180	1/2	2,4,10	9.8	9.8-11.8
10	000-085-220	2/13	4,10,10	13.9-15.4	5.9-16.0
11	000-085-270	0/2	No Complaints	—	17.4-18.7
12	000-085-320	2/21	1,1,4	15.7-17.8	6.4-19.5
13	000-085-000	0/2	No Complaints	—	9.4-11.1
14	000-085-040	1/13	4	14.6	5.8-18.2
15	000-085-090	0/2	No Complaints	—	11.6-13.5
16	000-085-140	3/14	4,5,5	15.1-16.0	5.5-18.9
17	000-045-180	9/17	1,1,2,2,3,3,3,5,5,5,5,5,6,7,7,7,7,8,8,8,9,10,10	15.0-26.1	15.0-26.1
18	000-035-210	8/20	1,1,2,2,3,4,5,6,6,6,7,7,7,8,9	15.2-23.2	10.5-28.9
19	000-005-220	5/16	1,5,5,6,9,9	16.5-28.2	16.5-30.0
20	000-335-210	1/6	2	19.8	15.8-21.7
21	000-315-180	1/10	2,3	19.0	15.8-21.9
22	000-335-150	0/8	No Complaints	—	15.0-21.9
23	000-005-140	8/19	2,2,4,5,6,8,9,9,9,9,9,10	16.4-30.7	16.3-30.7
24	000-035-150	8/19	1,1,2,2,5,5,5,6,6,7	11.0-29.3	11.0-29.3

(a) Subjective complaints were compiled into ten categories. The numbers under column heading "Category of Complaints" correspond to the categories of complaints listed below. In some tests more than one complaint was registered.

1. Headache — Incidence at impact, duration up to several hours.
2. Stunning/disorientation — Incidence at impact but of brief duration.
3. Blurred vision/spots before eyes — Incidence at impact but of brief duration
4. Neck/back muscle spasm/strain — Delayed onset, lasting up to several days.
5. Chest pain — Incidence at impact but of brief duration.
6. Shortness of breath — Incidence at impact but of brief duration.
7. Abdominal visceral displacement sensation — At impact.
8. Joint pain — Delayed onset and lasting up to several days.
9. Lower extremity muscle spasm/pain — Delayed onset and lasting up to several days.
10. Upper extremity muscle spasm/pain — Delayed onset and lasting no longer than 1 day.

(b) Complaint G Range indicates the range of impact levels at which complaints occurred, as measured on the sled.

c. Significant Post-Impact Physical Exam Findings

Significant Physical Findings	Test Position	Test Numbers	Sled G
Harness Burns	2	1537	20.0
(all first degree)	7	1552	23.0
Dazed and Disoriented (lasting no longer than two minutes post-impact)	17	1163 1187 1204 1205 1456	17.4 18.9 21.7 25.8 19.6
	19	1295	30.0
	24	1303 1182 1403	28.1 24.6 16.5
	9	1387	9.8
	1	1517	17.2
	21	1610	19.0
Respiratory Difficulty	17	1187	18.9
(lasting no longer than one minute post-impact)	23	1191	19.5
	18	1215 1216	24.6 23.2
	24	1217 1403	23.7 16.5
Blood Pressure Difference (20 mm Hg at pre and post run physical exam)	19	1295	30.0
Pulse Difference	23	1192	19.4
(20 beats/min at pre and post run physical exam)	17	1456	19.6
	24	1441	20.2
	12	1819	19.5
Engorged Retinal Vessels	17	1204	21.7
	3	1487	9.2
Back and/or Neck Pain and	17	1205	25.8
Decreased range of Motion	1	1517	17.2
	5	1559 1591	25.1 21.0

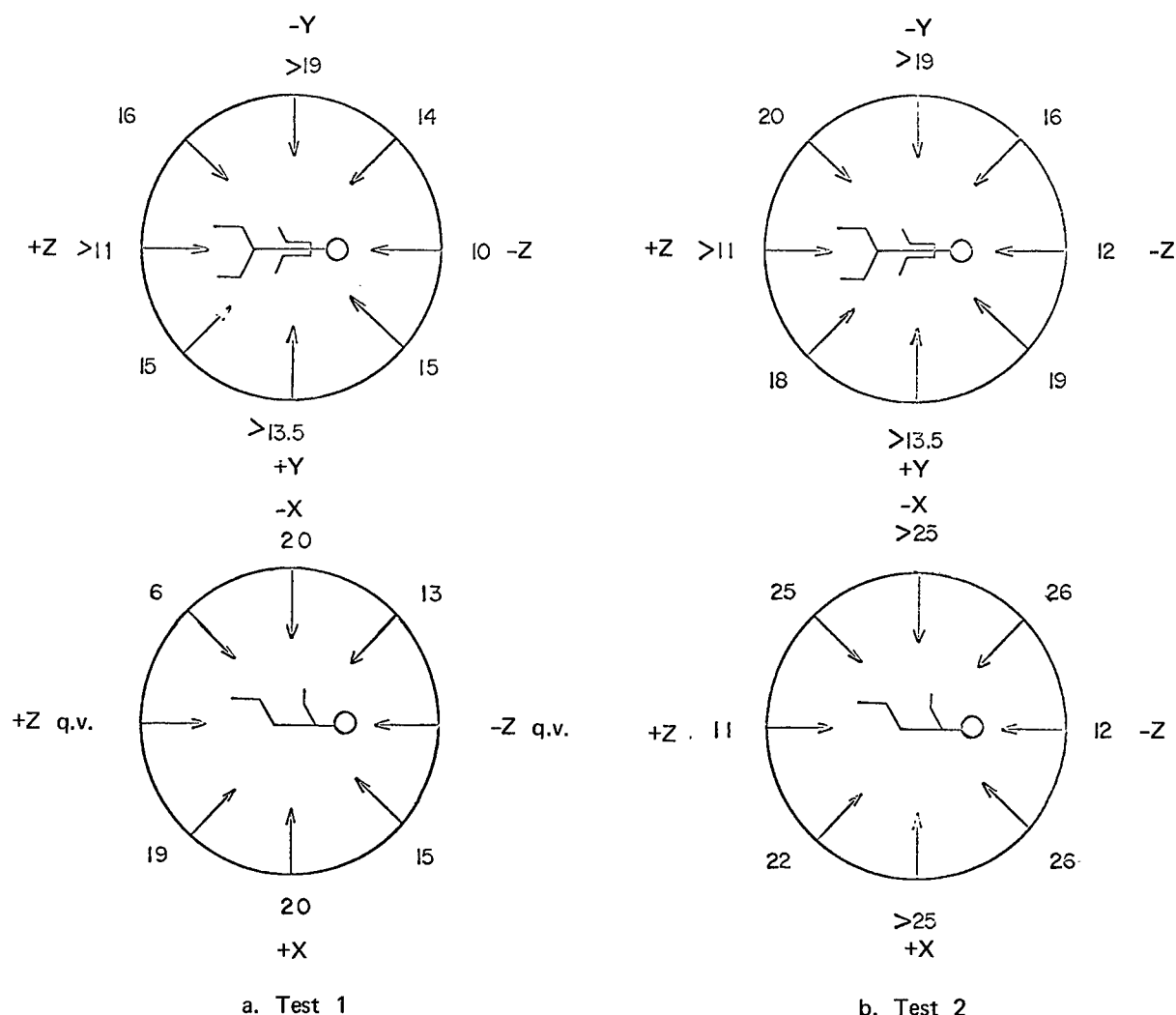
Figure 7-88 summarizes the impact levels tolerated with only transient discomfort as taken from Tables 7-87 b and c. Preliminary data are also available for a less restrictive and less complex Apollo restraint system (508). During studies of restraint and positional factors in Apollo landing, several data points were found at which trauma occurred (570). A forward facing subject tipped back 45° in pitch sustained simultaneous compression and hyperflexion of the trunk by force vectors at right angles which produced persistent soft tissue injury in the 6th, 7th, and 8th thoracic area, from impact of 25.0 G at 960 G per second in 97.0 milliseconds; loose restraints contributed to whole body resonance amplification of impact. In a similar restraint system at 83 peak G at 10,000 G/sec. in the 45° backward pitch and forward facing position a black bear sustained a 6th lumbar vertebra fracture and recuperable internal injuries.

Figure 7-88

Impact Levels Tolerated on 2 Tests Without Complaint.

Data are given in G-units with recorder on sled.

(Adapted from Brown et al⁽⁵⁸⁾)



With a less sophisticated harness restraint system, the occurrence of compression deformities of the 4th and 5th thoracic vertebrae has been reported in a human test subject exposed in laboratory experiments to an impact acceleration profile similar to that produced by ejection seat rockets. This injury was presumed to be the result of an impact profile having a peak acceleration of 18.8 G, a rate of onset of 420 G per second and a baseline duration of approximately 100 milliseconds. The subject's long axis was inclined backward 34° from the vertical force vector. Use of head restraint, impact attenuation, and mechanical retraction of harness restraint to prevent slack and relative body motion are recommended (see below).

Summary tables of the tolerance and response of man and animals to impact loads at variable axes are available (552, 566). Data have been presented on survival of animals at G loads of up to 400 G at onset rates of over 200,000 G/sec. in full containment restraints at various body axes (386). A summary of studies on bears is also available (601).

Impact by Missiles and Moving Objects

Injuries, due to the impact of missiles arising from debris energized by blast pressures, winds, ground or floor shock, and sometimes gravity, depend upon a number of factors. Among them are the mass, velocity, character, density, and angle of impact of the missiles whether or not penetration or perforation occurs; the area and organ of the body involved; the amount and kind of clothing if any; and the immunological status and general health condition of the injured individual (100, 664). Much data are available on wound ballistics and the nature of damage in penetrating wounds. Much more needs to be known about the wounding power of both penetrating and nonpenetrating missiles, particularly those much larger than conventional projectiles traveling at relatively lower velocities, as seen in the injuries caused by flying debris (40, 41). Quantitative evaluations rely heavily on animal studies supplemented by careful analysis of human accidents and upon cautious experiments involving man.

The mechanism of tissue damage by impact of small objects has been recently reviewed (208, 209). From these studies it appears that if a relatively small object hits a body surface overlying soft tissue, the energy is absorbed in the surrounding tissue and does not bring about a motion of the whole body or a spreading of the energy over farther distances, with exciting oscillations in subsystems formed as a cause of tissue or geometric discontinuities. Interesting insight into the phenomena occurring here can be obtained by treating the tissue as a homogeneous, infinite medium having the viscoelastic properties observed for body tissue (Figure 7-74). Results of such calculations indicate that most of the energy spreads through the tissue in the form of shear waves and not of compression waves. As an example the spectra of the energy transmitted to the tissue by three blows of different velocity but equal displacement (tissue indentation) are illustrated in Figure 7-89 (208). The graph also indicates a dividing line between shear and compression waves, which can be obtained from the impedance function for the tissue surface of the area struck. For frequencies below the dividing line, energy is propagated primarily in shear waves; for frequencies above, in compression waves. Only

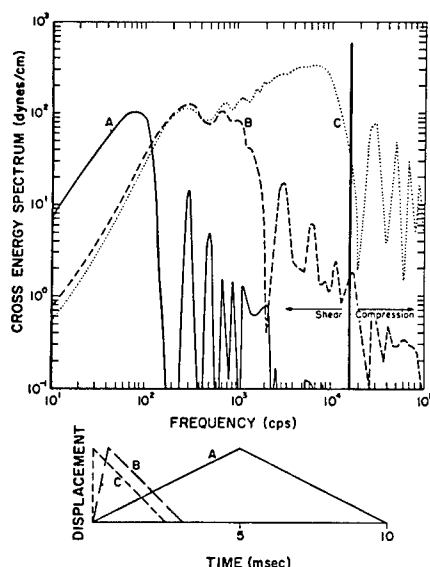


Figure 7-89

Transferred Energy Spectrum (Magnitude) for Constant Displacement Blows of Different Velocity to Soft Body Tissue. The Displacement-Time Function Is Plotted on the Lower Part of the Figure.

(After von Gierke^(208, 209))

very rapid blows produce compression waves of appreciable magnitude in tissue and it appears that in most practical cases the tissue damage from blows results from the shearing action of the transmitted energy. Calculations of the type illustrated in Figure 7-89 were helpful in evaluating the physics of energy transmission in blows to brain tissue (head injury). (70, 208).

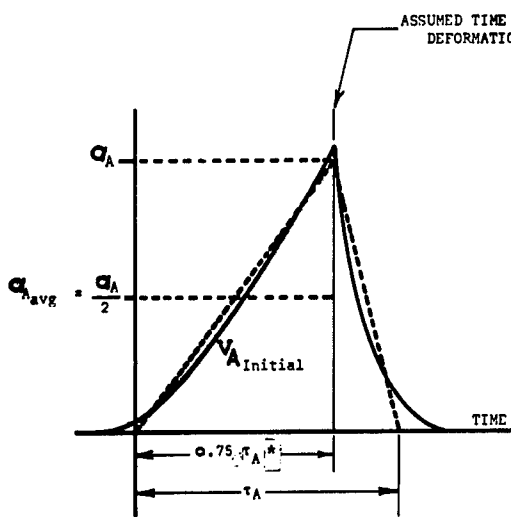
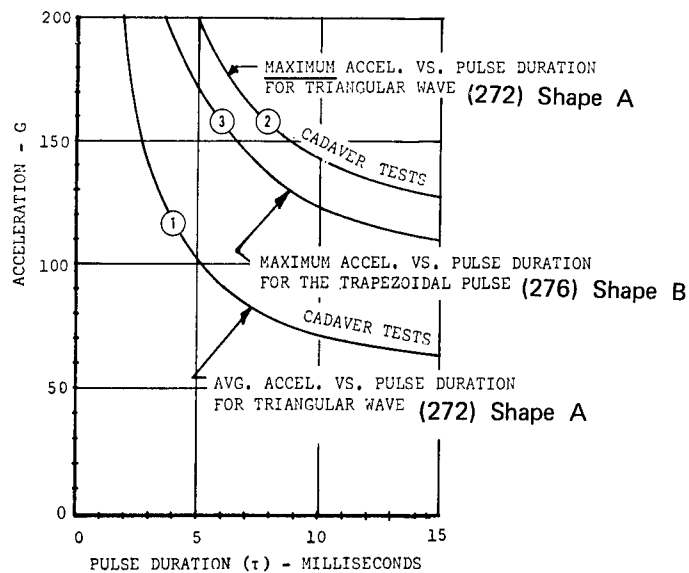
The sensitivity of the individual organ systems to damage appears to vary with the type of blast phenomenon (17, 664). Tolerance to the three types of blast follows these organ patterns in decreasing order of sensitivity:

Primary blast: (air blast)	1. Eardrums, 2. Lungs and Circulatory System, 3. Gut, 4. Liver and spleen, 5. Central nervous system.
Secondary blast: (missiles)	1. Liver and spleen, 2. Central nervous system, 3. Heart, 4. Lungs.
Tertiary blast: (impact after body translation)	1. Central nervous system, 2. Circulatory system (especially aortic rupture), 3. Liver, 4. Lungs.

Tentative criteria for secondary missile damage in humans are shown in Table 7-94b.

There are few quantitative studies of trauma to the abdominal organs (287). Data are available on liver trauma in dogs (100).

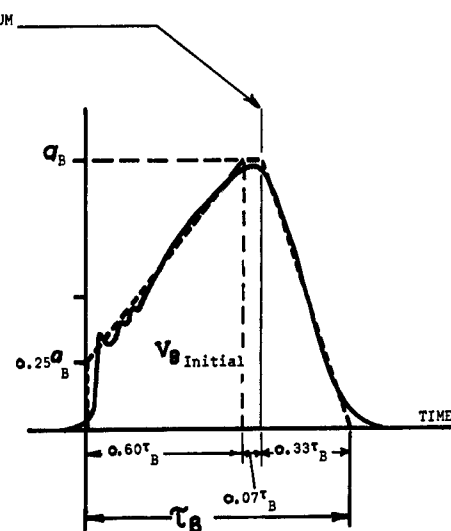
The tolerance of the head to impact has received much study (70, 100 , 271, 272, 273, 276, 208, 296, 375, 379, 499, 550, 702). Data on the tolerable G-duration profile for linear fracture (concussion) end point has been recorded as shown in Figure 7-90. The acceleration-duration relationship is obtained from tests on cadavers (272). In Curve 1, the average accelerations ($a_{A_{avg}}$) and pulse duration (τ) are those illustrated below as shape A. Based upon a triangular pulse shape, the peak of maximum acceleration a_A is twice the



Shape A

Approximate pulse shape as obtained in cadaver tests.

* The $0.75\tau_A$ value was assumed in the absence of the actual $a-t$ curves.



Shape B

Approximate pulse shape as recorded in AvSER helmet tests.

Figure 7-90

Acceleration-Time History in Humans, Based on Head Impacts on Cadavers, Animals, and on Clinical Observations of Humans
(After Haley et al (276))

average acceleration as shown in Curve 2. It is not known whether head tolerance to pulses of other shapes can be extrapolated from Curves 1 and 2; however, it is assumed that pulses which do not differ greatly from the basic triangular pulse and which possess the same energy per unit mass (same velocity change) will cause similar damage to the human brain. Attenuation by helmets tends to cause a trapezoidal pulse, shown as shape B (276). Curve 3 is the tolerance calculated for such trapezoidal curves. The physiological response to impact of the head has received recent review (296).

The mechanics of damage to the chest and lung by impact with small missiles is related to damage by air blast (49, 209, 664). See also Pressure, (No. 12). A mathematical model of the chest dynamics under these conditions is available (48). The cause of death is usually lung hemorrhage with secondary gas embolization of the systemic circulation. An index of damage for the dog is the ratio of lung mass to body mass, L (%), and is related to the velocity of impact, V_o (cm/m/sec) and the ratio of missile mass to dog mass, M (%), for flat circular impacts of 7 cm in diameter by the Equation (49):

$$V_o L^{-0.7} = 1.915 + 1.544 M^{-1} \quad (13)$$

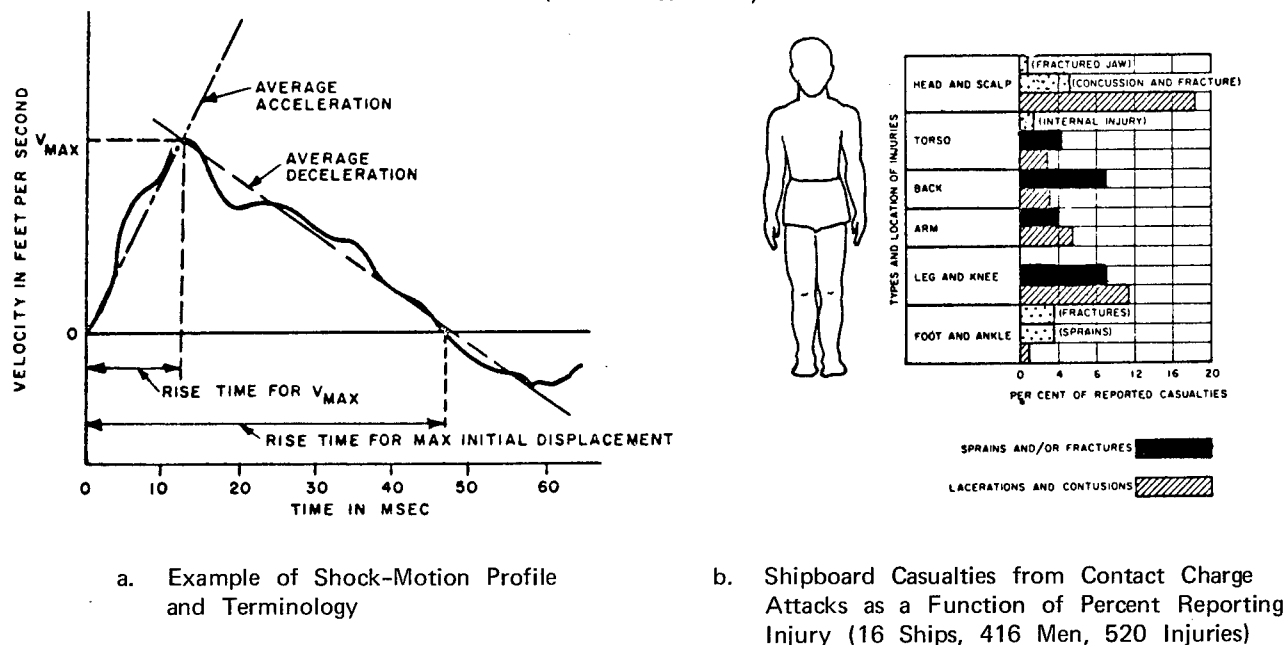
Scaling of these data to man is now under study (47).

Damage, occurring as a consequence of gross translation of the body induced mostly by blast pressures and winds, but with ground or floor shock, gravity, and a blow from a large missile often contributing, can be accelerative or decelerative in character. Either may be serious but abrupt decelerative trauma is characteristically associated with high and early lethality (496, 664). Significant factors include the velocity change at impact, the time and distance over which deceleration occurs, the character and nature of the decelerating surface and the area of the body involved. Though trauma to the head is known to be highly hazardous, it is likely that blunt blows over the liver and spleen and other portions of the abdominal wall may also be quite dangerous at relatively low impact velocities (17, 100, 287). Blunt blows by restraint straps are always a problem (554).

Explosions beneath the seat in ejection or beneath the floor of a vehicle can cause a structure to impact against the foot or buttock of a crewman. The response to this type of impact has been studied in naval warfare where the deck of ships propelled upward by underwater explosions may impact against the foot of a stiff-legged subject or the buttock area of a seated subject (298). The typical velocity record and casualty partition for these motions are noted in Figure 7-91. This velocity record has two main phases: an acceleration phase which lasts about 10 msec, and a deceleration phase which lasts about 40 msec. The average acceleration during the initial phase can be well above 50 G. The deceleration is about 2 to 3 G. Figure 7-91b shows the frequency of injury to the various body regions found in surveys after underwater explosions during wartime conditions. The head and body lacerations, contusions, and abrasions arise from secondary falls or contact with ceiling structures with multivector trajectories.

Tolerance to impact loads on the feet and buttocks in $+G_z$ acceleration has been studied (298). In the case of impact on the sole of the foot with leg

Figure 7-91
Motion Profiles and Casualties Produced by Upheaval
of a Deck from Explosion Beneath
(After Hirsch⁽²⁹⁸⁾)

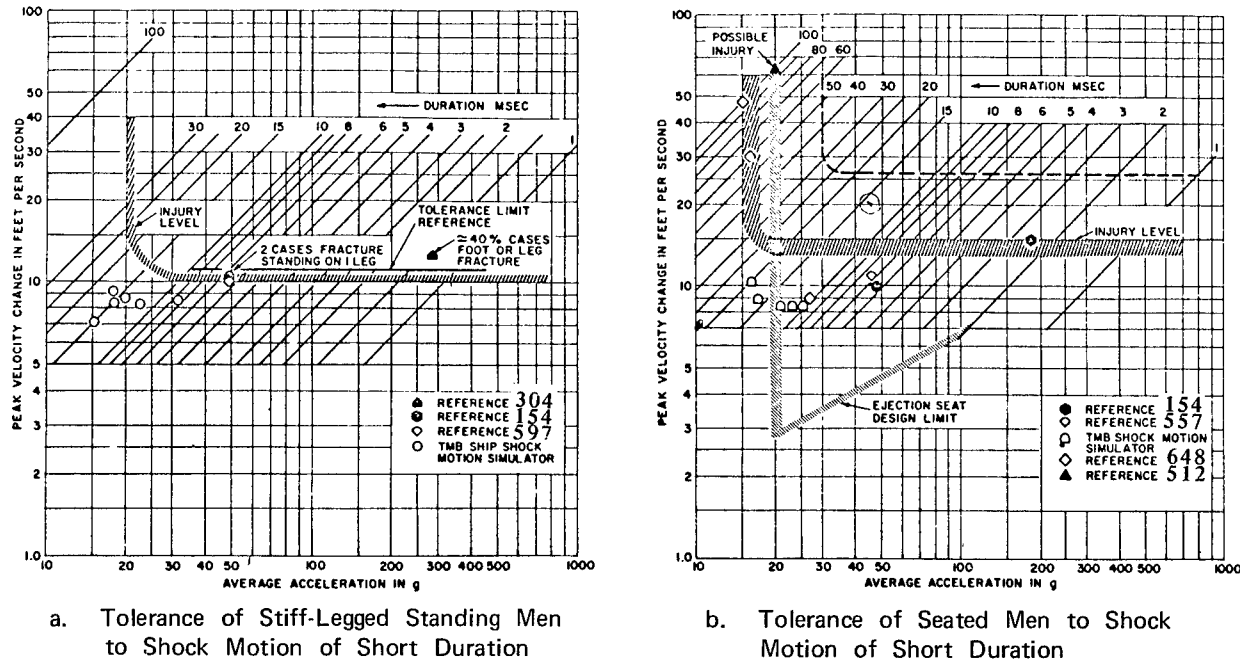


extended, the crushing load for the human leg was determined to be 1500 lbs, applied in axial compression between the knee and foot (151, 299). Such a load results in fracture of the distal tibia, a mode of failure commonly observed in ship-shock injuries to the lower leg. Thus an axial loading of 3000 lbs applied to two equally-loaded stiff legs will probably cause them to break. This means that a 160-lb man, when standing stiff-legged and subjected to a constant acceleration of about 20 G, will suffer bone fracture of the foot or ankle. This value of 20 G has been entered in Figure 7-92a as the vertical asymptote describing the slowly-applied G tolerance of the stiff-legged man. Calculation of the remainder of the curve was accomplished by assuming that the duration is short compared to the natural period of the system and using the relationship:

$$V_o = 5.13 \frac{g_o}{f} \text{ fps} \quad (14)$$

where V_o is the limiting velocity; g_o is the static acceleration sensitivity in gravitational units; f is the natural frequency of the excited system in cycles per second (347). The limiting velocity V_o for a standing man with a static tolerance of 20 G and a natural frequency of 10 Hz appears to be 10 fps, shown as a limiting value in Figure 7-92a. A few empirical studies on cadaver legs are plotted in this figure. Such data are of value in the design of lunar or planetary landing vehicles where the crew may be standing upright during landing.

Figure 7-92
Tolerance of Men to $+G_z$ When Standing and Seated
(After Hirsch(298))



In the seated man, the affected bones are the vertebrae. An excellent review of this problem is in publication (292). Fractures to the vertebrae will occur with crushing loads varying from 1600 to 2900 lbs (512). A later study reported that 40 percent of any lumbar vertebrae will fracture at loads of about 1400 lbs (479). These vertebrae were selected from subjects under 60 years of age. This same investigation showed that the intervertebral disk has the same ultimate strength as the vertebrae. If it is assumed that the vertebral strength is indeed uniform in the lower back region, then the location of fracture in a properly aligned spine will be at the lowest vertebra, L5, which bears about 60 percent of the body weight (512). A static acceleration of about 15 G applied to a 160-lb man, can cause injury to the lower vertebrae. If the maximum estimate of 2900 lbs for the ultimate strength of the L5 vertebra is used, then a static acceleration of about 30 G will be required to cause injury. This discrepancy is reflected throughout the literature concerning the tolerance limit of the spine. Tolerance values varying from 10 to 28 G have been given (648, 685), but the subject is now under reevaluation (126). Curves predicting the probability of vertebral (T8 - L5) endplate fracture, compression fracture and proportional limits for different age groups have been published (292, 571, 572). A band presenting the slowly-applied G -tolerance limit of 15 G_z is plotted as a vertical asymptote in the tolerance curve shown in Figure 7-92b. The dashed line shows the 30-G limit.

Using Equation (14), the limiting velocity V_0 for a seated man with a static tolerance of 15 to 30 G and a natural frequency for the upper torso of 6 cps ranges from 13 to 26 fps (298). These values are shown in Figure 7-92b

by the band and dashed line along with several empirical points (see also Figure 7-80). It is probable that the injury level lies close to the 20-G asymptote for long-duration pulses. This is in agreement with the design-limit for ejection seats, a limit which was derived from static-loading tests on fresh cadavers (164). In setting this limit, it was assumed that higher accelerations could be tolerated when the time duration of the pulse was less than 5 msec. This design curve is plotted in Figure 7-92b for comparison with existing data and present tolerance estimates (see also Reference 668).

After undergoing the initial compressive-phase response just described, the unrestrained man will be thrown off the deck or floor with some kickoff velocity. While this velocity in itself will not cause injury, it will have important bearing on his velocity at the termination of flight, when injury can occur. The kickoff velocities of men in the standing and seated positions have been measured for a variety of input pulses from tests of the Taylor Model Basin ship shock simulator and in full-scale tests (298). The ratio of peak deck velocity, V_d , to kickoff velocity, V_k , has been plotted as a function of the ratio of rise time to peak velocity (t_p) to natural period of man (T) in Figure 7-93. The curves follow the form:

$$V_k/V_d = 2.7(t_p/T)^{0.44} \quad (15)$$

T is 100 msec for standing man and 167 msec for seated man (298). He will leave the deck and fly upward with a kickoff velocity which varies from about 60 percent to 120 percent of the peak deck velocity, depending on his position and the rise time to the peak velocity of the deck. Data are available on the movement of body parts during such exposure (298).

Table 7-94a is a tentative summary of the velocity limits for large structures and Figure 7-94b, for small structures impacting against humans (665).

Treatment of trauma in space operations has received recent review (62).

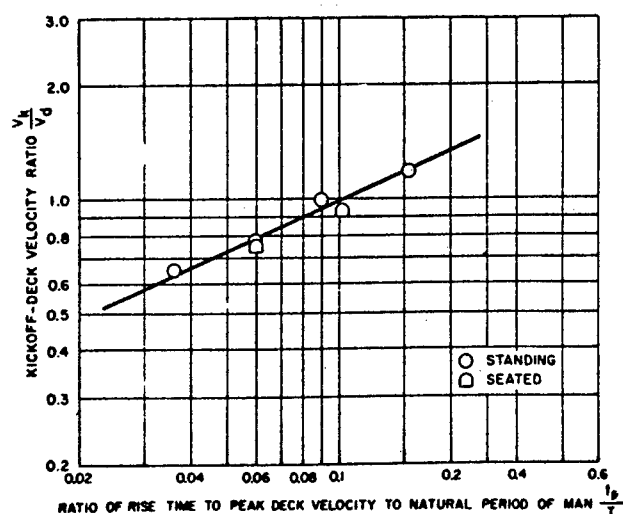


Figure 7-93

Ratio of Kickoff to Peak Deck Velocity as a Function of Ratio of Rise Time to Peak Deck Velocity to Natural Period of Man

(After Hirsch⁽²⁹⁸⁾)

Table 7-94
Criteria for Impact Tolerance in Humans
(After White et al⁽⁶⁶⁵⁾)

a. Tentative Criteria for Limiting Impact Velocities in Humans

Condition Critical Organ or Event	Related Impact Velocity ft/sec
<u>Standing Stiff-legged Impact</u>	
Mostly "safe"	
No significant effect	<8 (?)
Severe discomfort	8 - 10
Injury	
Threshold	10 - 12
Fracture threshold (heels, feet and legs)	13 - 16
<u>Seated Impact</u>	
Mostly "safe"	
No effect	<8 (?)
Severe discomfort	8 - 14
Injury	
Threshold	15 - 26
<u>Skull Fracture</u>	
Mostly "safe"	10
Threshold	13
50 per cent	18
Near 100 per cent	23
<u>Total Body Impact</u>	
Mostly "safe"	10
Lethality threshold	20
Lethality 50 per cent	26
Lethality near 100 per cent	30

b. Tentative Criteria for Indirect Blast Effects Involving Impact from Secondary Missiles

Kind of Missile	Critical Organ or Event	Related Impact Velocity ft/sec
Nonpenetrating 10-lb object	Cerebral Concussion:*	
	Mostly "safe"	10
	Threshold	15
	Skull Fracture:*	
	Mostly "safe"	10
	Threshold	15
Penetrating 10-gm glass fragments	Near 100 %	23
	Skin Laceration:**	
	Threshold	50
	Serious Wounds:**	
	Threshold	100
	50 %	180
	Near 100 %	300

* Data from Lissner & Evans⁽³⁷⁹⁾, Zuckerman & Black⁽⁷⁰²⁾, Gurdjian, Webster & Lissner⁽²⁷³⁾

** Represent impact velocities with unclothed skin. A serious wound arbitrarily defined as a laceration of the skin with missile penetration into the tissues of depth of 10 mm or more.

Restraint and Protective Systems

Human tolerance to abrupt accelerations is decisively dependent on the body support and restraint systems (24, 58, 164, 438, 552, 563, 566, 569). It is clear that the seat structure is used to reinforce the skeleton and should be coupled as tightly and directly as possible to it. The load should be distributed uniformly over as wide an area as possible to avoid force concentrations with resulting bending and shearing displacements of body parts. Recent studies are available covering the dynamics of seat cushioning, restraint systems, and a physiological index of hazard (445, 476, 477). Theoretically, one can set about designing protection systems without a complete knowledge of the tolerance levels and be assured that, whatever the tolerability, the protection system will offer the minimum energy transfer and therefore the maximum protection.

The basic problem is to minimize the amount of power exchange by the human with the environment (477, 655, 656). The protection system should have a characteristic such that, when interposed between the human and the environment, it modifies the environment to minimize the transmittal of energy at the frequencies where the impedance is absolutely or relatively highest. In fact, velocity transfer function of the protection system should be the reciprocal of the impedance magnitude. However, there is an aspect of protection system design which cannot be specified by the impedance method. This is the absolute level or the total energy which can be transmitted with safety. In other words, there is no specification on how much energy the protection system must dissipate within itself in order to keep the body displacements below the critical threshold for damage.

Lap-belt, shoulder straps, lap-belt tie-down straps, thigh straps, chest straps, full head support, arm rests and suitable hand holds, and toe straps have all been used in various combinations to achieve adequate body restraint. The importance of tying the various parts of the body to the seat support varies with the direction of the impact (164, 213, 554, 569). Data are available on the dynamic response of restraints and secondary effect on subjects during impact testing (569). For $+G_z$ acceleration in the normal seating position, for example, the acceleration force throws the man back into the seat. A non-deflecting seatback, a full-height head rest restricting lateral head motion, leg and foot support are of main importance. Tie-down straps are only necessary to restrict rebound motions and to protect against secondary impact forces from other directions. For other impact directions where no structure comparable to the back of a seat is available to support the body in the force direction, the restriction of possible motions of body parts by tie-down straps becomes of paramount importance (58, 179, 234, 476, 508, 569). Recent studies have centered on full-body support in $-G_x$ configurations through the use of molded couches made from polyurethane foam or unicellular polyvinyl foam rubber shock absorbant material which greatly enhance survivability of a large biological subject to high deceleration loads. Chimpanzees weighing 50 pounds survived $-147G_x$ of onset rate of 13,000 G/sec with a sled brake entrance velocity of 131.5 ft/sec. Duration of peak G was 20 milliseconds (558).

The use of tie-down suits, (for example, vests or full-support webbing nets), has a high potential to reduce force concentrations and to combine maximum body support with comfort (386, 620). Pressure suits with integrated internal restraint systems have been given preliminary study (414). To allow normal mobility of pilots and crews when not subjected to impact loads, inertia locks have been proposed to allow relatively slow motions of the man but freeze his position when rapid impact forces act on the body (213).

Many attempts have been made to incorporate energy absorbing devices either in a harness or a seat structure (221, 476, 593, 596). If they are used it is important to note that they can reduce peak acceleration but not transferred momentum; therefore their usefulness has to be carefully evaluated depending on the expected force-time pattern (213, 655, 656). Cyclic strain impact attenuations are now under study (404). Hydraulic and damped-spring systems as well as crushable structures with non-linear characteristics (styrofoam, aluminum honeycomb structures) have been tested to reduce ground impact loads (284, 445, 476, 594). These techniques have been employed in the Apollo landing system (593). The individually-fitted, contoured, plastic couches selected as body support for the NASA space program combine most of the discussed principles for protection against spineward acceleration (uniform support, crushable material) with optimum positioning and support for sustained acceleration (58, 445, 688). Multidirectional systems studied with animals may become of practical value for winged reentry vehicles (24).

Restriction of head motion during impact loads appears to be a factor worthy of a tradeoff study relative to the restriction of overall movement from an operational point of view (508). Protection of the head against blows or flying objects is achieved by rigid helmets which distribute the impact loads over the whole head area and prevent force concentrations. Recent reviews of helmet design and test methods for impact protection are available (275, 276, 296, 498, 610). (See also Figure 7-90.)

An overview of mechanical and human factors in designing aircraft for crash survival is now available (88). Preliminary studies have been made of the impact environment as related to independent personal escape capsules in space operations (411). Many data have been gathered on safety and restraint systems for automobile crashes. Discussions of recent concepts are available (528, 555).

REFERENCES

- 7-1. Abbott, H. M., Duddy, J. H., Weightless Simulation Using Water Immersion Techniques: An Annotated Bibliography, LAC-SB-65-2, Lockheed Aircraft Corp., Sunnyvale, Calif., 1965.
- 7-2. Adams, C. R., Bulk, G. K., Zero Buoyancy: Simulation of Weightlessness to Evaluate Psychophysiological and Anthropomorphic Parameters that Affect Space Station Design, Aerospace Med., 38: 518-520, May, 1967.
- 7-3. Adey, W. R., Kado, R. T., Walter, D. O., Results of Electroencephalographic Examinations under the Influence of Vibration and Centrifuging in the Monkey, AFOSR-67-1857, reprinted from Recent Advances in Clinical Neurophysiology, Electroenceph. Clin. Neurophysiology Suppl. 25, Widen, L., (ed.), Elsevier Publishing Co., Amsterdam, 1967, pp. 227-245. (This study supported by contract AF (49) 638-1387).
- 7-4. Aerospace Medical Research Laboratories, Centrifuge Log Book, Wright-Patterson AFB, Ohio, 1961.
- 7-5. Air Force Systems Command, Headquarters, AFSC Design Handbook 1-6, System Safety, Andrews AFB, Washington, D. C., First Ed., Rev. 1, Jan. 20, 1968.
- 7-6. Air Force Systems Command, Headquarters, Handbook of Instructions for Aircraft Designers, ARCDM-80-1, Andrews AFB, Washington, D. C., Apr. 1960.
- 7-7. Akulinichev, I. T., Yemelyanov, M. D., Maksimov, D. G., Oculomotoric Activity in Cosmonauts during Orbital Flight, Izv. Akad. Nauk SSSR (Biol.), No. 2: 274-278, 1965.
- 7-8. Alexander, W. C., Sever, R. J., Fedderson, W. E., et al., Acceleration (+G_x) Induced Hypoxemia and Crew Performance, Aerospace Med., 35: 257, 1964.
- 7-9. Alexander, W. C., Sever, R. J., Hoppin, F. G., Hypoxemia Induced by Sustained Forward Acceleration in Pilot's Breathing Pure Oxygen in a Five Pounds Per Square Inch Absolute Environment, NASA-TM-X-51649, July 1965.

- 7-10. Alexander, W. C., Sever, R. J., Hoppin, F. G., Hypoxemia Induced in Man by Sustained Forward Acceleration While Breathing Pure Oxygen in a Five Pounds per Square Inch Absolute Environment, Aerospace Med., 37(4) Sect. 1: 372-378, Apr. 1966.
- 7-11. Ambler, R. K., Guedry, F. E., Jr., The Validity of a Brief Vestibular Disorientation Test in Screening Pilot Trainees, NAMI-947, Naval Aerospace Medical Institute, Pensacola, Fla., Oct. 1965.
- 7-12. Ballinger, E. R., Dempsey, C. A., The Effects of Prolonged Acceleration on the Human Body in the Prone and Supine Positions, WADC-TR-52-250, Wright Air Development Center, Wright-Patterson AFB, Ohio, July 1952.
- 7-13. Banchemo, N., Cronin, L., Nolan, A. C., et al., Blood Oxygen Changes Induced by Forward (+G_x) Acceleration, AMRL-TR-64-132, Aerospace Medical Research Labs., Wright-Patterson AFB, Ohio, Dec. 1964.
- 7-14. Barer, A. S., Golov, G. A., Zubavin, V. B., et al., Physiological Reactions of the Human Organism to Transverse Accelerations and Means of Raising the Resistance to Such Forces, NASA-TT-F-274, 1964. (Translation of paper presented at the XV International Astronautical Congress, Warsaw, Poland, Sept. 7-12, 1964).
- 7-15. Barr, P. O., Hypoxemia in Man Induced by Prolonged Acceleration, Acta Physiol. Scand., 54: 128-137, 1962. (Also AMRL-TDR-62-137, Apr. 1963).
- 7-16. Barrett, S., Payne, P. R., Response of a Linear Damped Dynamic System to Selected Acceleration Inputs, AMRL-TR-65-40, Aerospace Medical Research Labs., Wright-Patterson AFB, Ohio, Apr. 1965.
- 7-17. Baxter, C. S., Williams, R. D., Blunt Abdominal Trauma, J. Trauma, 1: 241-248, 1961.
- 7-18. Bayevskiy, R. M., Methods of Investigating the Vestibular Apparatus, NASA-TT-F-10125, May 1966. (Translated from Fiziologicheskkiye Metody V Kosmonavtike, Chap. 10, 1965, pp. 246-250).
- 7-19. Bayevskiy, R. M., Gazenko, O. G., Reaction of the Human and Animal Cardiovascular System Under Conditions of Weightlessness, NASA-TT-F-8895, June 1964. (Translation of Reaktsiya Serdechnov Sosudistoy Sistemy Cheloveka i Shivotnykh v Usloviyaka Nevesomosti, 2(2): 307-319, 1964).

- 7-20. Beasley, G. P., Brissenden, R. F., Straly, W. H., et al., Retrieving the Tethered Astronaut, Astron. Aeron., 3: 72-77, Jan. 1965.
- 7-21. Beauchamp, G. T., Adverse Effects Due to Space Vehicle Rotation, paper presented at the 7th Annual Meeting, American Astronautical Society, Dallas, Texas, Jan. 16-18, 1961.
- 7-22. von Beckh, H. J., Experiments with Animals and Human Subjects under Sub and Zero-Gravity Conditions during the Dive and Parabolic Flight, J. Aviat. Med., 25: 235-241, June 1954.
- 7-23. von Beckh, H. J., Human Reactions during Flight to Acceleration Preceded by or Followed by Weightlessness, Aerospace Med., 30: 391-409, June 1959.
- 7-24. von Beckh, H. J., Multi-Directional G-Protection during Experimental Sled Runs, Aeromedical Field Lab., Holloman AFB, N. M., Reprint from Xth International Astronautical Congress, London, 1959, pp. 671-682.
- 7-25. von Beckh, H. J., A Summary of Motion Sickness Experiences in Weightless Flights Conducted by the Aeromedical Field Laboratory, in Symposium on Motion Sickness with Special Reference to Weightlessness, Mar. 1960, Wright-Patterson AFB, Ohio, AMRL-TDR-63-25, Aerospace Medical Research Labs., Wright-Patterson AFB, Ohio, June 1963, pp. 67-72.
- 7-26. Beckman, E. L., Duane, T. D., Coburn, K. R., Limitation of Ocular Motility and Pupillary Dilatation in Humans Due to Positive Acceleration, NADC-MA-6140, Naval Air Development Center, Johnsville, Pa., 1961.
- 7-27. Beckman, E. L., Ziegler, J. E., Duane, T. D., et al., Preliminary Studies in Primates Subjected to Maximum Simple Accelerative Loads, NADC-MA-5301, Naval Air Development Center, Johnsville, Pa., May 1953.
- 7-28. Beebe, D. E., Force Analysis of Walking at Reduced Gravity, (M.S. Thesis), Air University, Wright-Patterson AFB, Ohio, Aug. 1964.
- 7-29. Beeding, E. J., Mosely, J. D., Human Deceleration Tests, AFMDC-TN-60-2, Air Force Missile Development Center, Holloman AFB, N. M., Jan. 1960.
- 7-30. von Bekesy, G., Uber die Empfindlichkeit des Stehenden und Sitzenden Menschen Gegen Sinusformige Erschutterungen, Akust. Ztschr., 4: 360, 1939.

- 7-31. Beller, B. M., Dong, E., Ord, J. W., et al., A Study Designed to Determine the Effectiveness of Vigorous Supine Exercise in Preventing Bed Rest Deconditioning: II. Cardiovascular Responses, paper presented at the 37th Annual Scientific Meeting, Aerospace Medical Association, Las Vegas, Nev., Apr. 18-22, 1966.
- 7-32. Benson, A. J., Bodin, M. A., Interaction of Linear and Angular Accelerations on Vestibular Receptors in Man, Aerospace Med., 37(2): 144-154, Feb. 1966.
- 7-33. Benson, H. E., Water Impact of the Apollo Spacecraft, J. Spacecraft, 3(8): 1282-1284, Aug. 1966.
- 7-34. Benson, V. G., Beckman, E. L., Coburn, K. R., et al., Effects of Weightlessness as Simulated by Total Body Immersion upon Human Response to Positive Acceleration, Aerospace Med., 33: 198-203, 1962.
- 7-35. Berry, C. A., Coons, D. O., Catterson, A. D., et al., Man's Response to Long-Duration Flight in the Gemini Spacecraft, in Gemini Midprogram Conference, NASA-SP-121, Manned Spacecraft Center, Houston, Texas, Feb. 23-25, 1966, pp. 235-261.
- 7-36. Billingham, J., Russian Experience of Problems in Vestibular Physiology Related to the Space Environment, in Second Symposium on the Role of the Vestibular Organs in Space Exploration, Ames Research Center, Moffett Field, Calif., Jan. 25-27, 1966, NASA-SP-115, 1966, pp. 5-13.
- 7-37. Birkhead, N. C., Blizzard, J. J., Daly, J. W., et al., Cardio-dynamic and Metabolic Effects of Prolonged Bed Rest, AMRL-TDR-63-37, Aerospace Medical Research Labs., Wright-Patterson AFB, Ohio, 1963.
- 7-38. Birkhead, N. C., Blizzard, J. J., Issekutz, B., Jr., et al., Effect of Exercise, Standing Negative Trunk and Positive Skeletal Pressure on Bed Rest-Induced Orthostasis and Hypercalciuria, AMRL-TR-66-6, Aerospace Medical Research Labs., Wright-Patterson AFB, Ohio, 1966.
- 7-39. Birkhead, N. C., Haupt, G. J., Blizzard, J. W., et al., Effects of Supine and Sitting Exercise on Circulatory and Metabolic Alterations in Prolonged Bed Rest, The Physiologist, 6: 140, 1963. (Abstract)
- 7-40. Blocker, T. G., Jr., Blocker, V., Graham, J. E., et al., Follow-Up Medical Survey of the Texas City Disaster, Amer. J. Surg., 97: 605-623, 1959.

- 7-41. Blocker, V., Blocker, T. G., Jr., The Texas City Disaster - A Survey of 3000 Casualties, Amer. J. Surg., 78: 756-771, 1949.
- 7-42. Blockley, W. V., Study on Tolerance Limits for Extreme Decelerations, Unpublished paper, Webb Associates, Yellow Springs, Ohio, 1962.
- 7-43. Bondurant, S., Blanchard, W. G., Clarke, N. P., et al., Effect of Water Immersion on Human Tolerance to Forward and Backward Acceleration, WADC-TR-58-290, Wright Air Development Center, Wright-Patterson AFB, Ohio, July 1958.
- 7-44. Bondurant, S., Clarke, N. P., Blanchard, W. G., et al., Human Tolerance to Some of the Accelerations Anticipated in Space Flight, U. S. Armed Forces Med. J., 9: 1093-1105, 1958. (Also WADC-TR-58-156)
- 7-45. Bonner, R. H., Spatial Disorientation - Current Concepts and Aeromedical Implications, SAM-Review 7-63, School of Aerospace Medicine, Brooks AFB, Texas, Aug. 1963.
- 7-46. Bornschein, V. H., Schubert, G., Die Reizparameter des Vestibularen Coriolis - Effektes, Z. Biol., 110: 269-275, 1958.
- 7-47. Bowen, I. G., Lovelace Foundation for Medical Education and Research, Albuquerque, N. M., personal communication, 1967.
- 7-48. Bowen, I. G., Holladay, A., Fletcher, E. R., et al., A Fluid-Mechanical Model of the Thoraco-Abdominal System with Applications to Blast Biology, DASA-1675, Defense Atomic Support Agency, Washington, D. C., June 1965.
- 7-49. Bowen, I. G., Fletcher, E. R., Richmond, D. R., et al., Biophysical Mechanisms and Scaling Procedures Applicable in Assessing Responses of the Thorax Energized by Air-Blast Overpressures or by Non-Penetrating Missiles, DASA-1857, Defense Atomic Support Agency, Washington, D. C., Nov. 1966.
- 7-50. Brady, J. F., Newsom, B. D., Large Excursion Rotary Tracking of Target and Target Light in a Space Station Simulator Revolving at 7.5, 10.0 and 12.0 RPM, Aerospace Med., 36(4): 332-342, 1965.

- 7-51. Brady, J. F., Urmston, R. E., Newsom, B. D., Rotary Tracking Performance in a Space Station Simulator Revolving at 5 RPM, GDA-63-1287, General Dynamics Convair Division, San Diego, Calif., Nov. 1963.
- 7-52. Brandt, U., Cause and Practical Importance of the Oculogravic Illusions, Acta Oto-laryng., 54: 127-135, 1962.
- 7-53. Brannon, E. W., Rockwood, C. A., Jr., Potts, P., The Influence of Specific Exercises in the Prevention of Debilitating Musculoskeletal Disorders; Implication in Physiological Conditioning for Prolonged Weightlessness, Aerospace Med., 34(10): 900-906, 1963.
- 7-54. Braunstein, M. L., White, W. J., The Effects of Acceleration on Brightness Discrimination, J. Opt. Soc. Amer., 52: 931-933, 1962.
- 7-55. Briggs, F. E. R., Franks' Anti Blacking-Out Suit, FPRC-301 (a), Flying Personnel Research Committee, Air Ministry, London, May 1941.
- 7-56. Brown, J. H., Crampton, G. H., Concomitant Visual Stimulation Does Not Alter Habituation of Nystagmic, Oculogyral or Psychophysical Responses to Angular Acceleration, AMRL-664, Army Medical Research Lab., Fort Knox, Ky., Mar. 1966.
- 7-57. Brown, J. L., Acceleration and Human Performance, in Selected Papers on Human Factors in the Design and Use of Control Systems, Sinaiko, H. W., (ed.), Dover Pub., Inc., N. Y., 1961.
- 7-58. Brown, W. K., Rothstein, J. D., Foster, P., Human Response to Predicted Apollo Landing Impacts in Selected Body Orientations, Aerospace Med., 37(4): 394-398, 1966.
- 7-59. Bryan, A. C., Macnamara, W. D., Bates, D. V., et al., Effect of Acceleration on the Distribution of Pulmonary Blood Flow, J. Appl. Physiol., 20(6): 1129-1132, 1965.
- 7-60. Burgess, B. F., The Effect of Hypoxia on Tolerance to Positive Acceleration, NADC-MA-5804, Naval Air Development Center, Johnsville, Pa., Mar. 1958.
- 7-61. Burgess, B. F., The Effects of Temperature on Tolerance to Positive Acceleration, Aerospace Med., 30: 567-571, 1959.

- 7-62. Busby, D. E., Clinical Space Medicine: A Prospective Look at Medical Problems from Hazards of Space Operations, NASA-CR-856, 1967.
- 7-63. Canfield, A. A., Comrey, A. L., Wilson, R. C., et al., The Effect of Increased Positive Radial Acceleration upon Discrimination Reaction Time, J. Exp. Psychol., 40: 733-737, 1950.
- 7-64. Canfield, A. A., Comrey, A. L., Wilson, R. C., A Study of Reaction Time to Light and Sound as Related to Increased Positive Radial Acceleration, J. Aviat. Med., 20: 350-355, 1949.
- 7-65. Cameron, J. R., Sorenson, J., Measurement of Bone Mineral in Vivo: An Improved Method, Science, 142(3589): 230-232, Oct. 11, 1963.
- 7-66. Caporale, R., Investigation of the Threshold Value, Riv. Med. Aeron. Spaz., 27(3): 325-352, 1964.
- 7-67. Caporale, R., Righting Reflex in Rabbits during Short Periods of Subgravity, Riv. Med. Aeron., 28: 10-25, 1965. (Text in Italian).
- 7-68. Cardus, D., Effects of 10 Days Recumbency on the Response to the Bicycle Ergometer Test, Aerospace Med., 37(10): 993-999, 1966.
- 7-69. Cardus, D., Beasley, W. C., Vogt, F. B., A Study of the Possible Preventive Effects of Muscular Exercises and Intermittent Venous Occlusion on the Cardiovascular Deconditioning Observed after 10 Days Recumbency: Experimental Design, NASA-CR-692, 1967.
- 7-70. Caveness, W. F., Walker, A. E., (eds.), Head Injury Conference Proceedings, University of Chicago, 1966, sponsored by the National Advisory Neurological Diseases and Blindness Council, J. B. Lippincott, Philadelphia, Pa., 1966.
- 7-71. Cennachi, V., Fenu, G., Problems Concerning Nystagmus Caused by Stimulation of the Vertical Semicircular Canals, Clin. Otorinolaring., (Cagliari), 13: 445-466, 1961, article translated by Federal Aviation Agency, Washington, D. C., FAA-T-32, Aug. 1963.
- 7-72. Chambers, R. M., Acceleration, in Bioastronautics Data Book, Webb, P., (ed.), NASA-SP-3006, 1964, pp. 31-52.

- 7-73. Chambers, R. M., Control Performance under Acceleration with Side-Arm Attitude Controllers, NADC-MA-6110, Naval Air Development Center, Johnsville, Pa., 1961.
- 7-74. Chambers, R. M., Long Term Acceleration and Centrifuge Simulation Studies, Naval Air Development Center, Johnsville, Pa., Apr. 1963.
- 7-75. Chambers, R. M., Operator Performance in Acceleration Environments, in Unusual Environments and Human Behavior, Burns, N. M., Chambers, R. M., Hendler, E., (eds.), The Free Press of Glencoe (The Macmillan Company), N. Y., 1963, pp. 193-320.
- 7-76. Chambers, R. M., Hitchcock, L., Acceleration Training for Astronauts and Test Personnel, Naval Air Development Center, Johnsville, Warminster, Pa., in Collected Papers Presented at the Twenty-Second Meeting of the AGARD Aerospace Medical Panel, NATO, Sept. 2-6, 1965, Fuerstenfeldbruck Air Base, Munich, Germany, 1965, pp. 429-468.
- 7-77. Chambers, R. M., Hitchcock, L., Effects of Acceleration on Pilot Performance, NADC-MA-6219, Naval Air Development Center, Johnsville, Pa., Mar. 1963.
- 7-78. Chambers, R. M., Hitchcock, L., Effects of High G Conditions on Pilot Performance, in Proceedings of the National Meeting of Manned Space Flight, N. Y., Apr. 30-May 2, 1962, Institute of the Aerospace Sciences, N. Y., 1962, pp. 204-227.
- 7-79. Chambers, R. M., Kerr, R., Effects of Positive Pressure Breathing on Performance during Acceleration, NADC-MA-6205, Naval Air Development Center, Johnsville, Pa., July 1962. (AD-298009).
- 7-80. Chambers, R. M., Nelson, J. G., Pilot Biomedical and Psychological Instrumentation for Monitoring Performance during Centrifuge Simulations of Space Flight, NADC-MA-6308, Naval Air Development Center, Johnsville, Pa., Oct. 1963.
- 7-81. Chandler, R. F., The Daisey Decelerator, ARL-TR-67-3, Aeromedical Research Lab., Holloman AFB, N. M., May 1967.
- 7-82. Chase, G. A., Grave, C., Rowell, L. B., Independence of Changes in Functional and Performance Capacities Attending Prolonged Bed Rest, Aerospace Med., 37: 1232-1238, 1966.

- 7-83. Chekirda, I. F., Coordination Structure and Reconstruction Phases of Motor Habits under Conditions of Weightlessness and Accelerations, in Space Biology and Medicine, 1(4): 135-141, 1967, JPRS-43762, Joint Publications Research Service, Washington, D. C., 1967. (Translation of Kosmicheskaya Biologiya i Meditsina, 1(4): 87-92, 1967).
- 7-84. Cherniack, N. S., Hyde, A. S., Watson, J. F., et al., Some Aspects of Respiratory Physiology during Forward Acceleration, Aerospace Med., 23: 113-120, 1961.
- 7-85. Chernov, V. N., Yakolev, V. I., Research on the Flight of a Living Creature in an Artificial Earth Satellite, ARS J. (Russian Suppl.), 29(10) Pt. I: 736-742, Oct. 1959.
- 7-86. Christy, R. L., Effects of Radial and Angular Accelerations, in Aerospace Medicine, Armstrong, H. G., (ed.), The Williams and Wilkins Co., Baltimore, Md., 1961, Ch. 16.
- 7-87. Clark, B., Graybiel, A., Contributing Factors in the Perception of the Oculogravic Illusion, Amer. J. Psychol., 76: 18-27, Mar. 1963.
- 7-88. Clark, B., Graybiel, A., The Egocentric Localization of the Visual Horizontal in Normal and Labyrinthine-Defective Observers as a Function of Head and Body Tilt, NAMI-991, Naval Aerospace Medical Institute, Pensacola, Fla., Jan. 1967.
- 7-89. Clark, B., Graybiel, A., Factors Contributing to the Delay in the Perception of the Oculogravic Illusion, NSAM-944, Naval School of Aviation Medicine, Pensacola, Fla., Aug. 1965.
- 7-90. Clark, B., Graybiel, A., Vertigo as a Cause of Pilot Error in Jet Aircraft, J. Aviat. Med., 28: 469-478, Oct. 1957.
- 7-91. Clark, B., Stewart, J. D., Perception of Angular Acceleration about the Yaw Axis of a Flight Simulator: Thresholds and Reaction Latency for Research Pilots, Aerospace Med., 33: 1426-1432, Dec. 1962.
- 7-92. Clark, G. C., Observation of a Human Experiencing 2 G for 24 Hours, paper presented at the 31st Aerospace Medical Association Meeting, Miami Beach, Fla., May 11, 1960.
- 7-93. Clark, C. C., Some Body Displacements and Medical Effects of Lateral Accelerations during Navy Centrifuge Simulation of Ejection Capabilities from the Army AO Aircraft, NADC-MA-6044, Naval Air Development Center, Johnsville, Pa., Apr. 1961.

- 7-94. Clark, C. C., Faubert, D., A Chronological Bibliography on the Biological Effects of Impact, MAR-ER-11953, Martin Co., Baltimore, Md., Sept. 1961.
- 7-95. Clark, C. C., Gray, R. F., Hardy, J. D., et al., A Discussion of Restraint and Protection of the Human Experiencing the Smooth and Oscillating Acceleration of Proposed Space Vehicles, NADC-MA-5914, Naval Air Development Center, Johnsville, Pa., 1959.
- 7-96. Clark, C. C., Hardy, J. D., Crosbie, R. J., A Proposed Physiological Acceleration Terminology with Historical Review, in Human Acceleration Studies, NAS-NRC-913, National Academy of Sciences, National Research Council, Washington, D. C., 1961, Sect. IV, The Use of G or g, pp. 39-42.
- 7-97. Clark, H. J., Optimum Angular Accelerations for Control of a Remote Maneuvering Unit, AMRL-TR-66-20, Aerospace Medical Research Labs., Wright-Patterson AFB, Ohio, Mar. 1966.
- 7-98. Clarke, N. P., Bondurant, S., Leverett, S. D., Human Tolerance to Prolonged Forward and Backward Acceleration, J. Aviat. Med., 30: 1-21, Jan. 1959. (Also WADC-TR-58-267. AD-155749).
- 7-99. Clarke, N. P., Hyde, A. S., Cherniack, N. S., et al., A Preliminary Report of Human Response to Rearward-Facing Reentry Accelerations, WADC-TN-59-109, Wright Air Development Center, Wright-Patterson AFB, Ohio, July 1959.
- 7-100. Clemedson, C. J., Hellstrom, G., Lindgren, S., The Relative Tolerance of the Head Thorax and Abdomen to Blunt Trauma, Surgeon General, Swedish Armed Forces, Riddargatan 13, Stockholm, Sweden, paper to be published.
- 7-101. Cochran, L. B., Gard, P. W., Norsworthy, M. E., Variation in Human G Tolerance to Positive Acceleration, NAV-SAM-NM-001-059.02.10, Naval School of Aviation Medicine, Pensacola, Fla., Aug. 1954.
- 7-102. Code, C. F., Wood, E. H., Lambert, E. H., Limiting Effect of Centripetal Acceleration on Man's Ability to Move, NAS-NRC-CAM-436, National Academy of Sciences, National Research Council, Division of Medical Sciences, Washington, D. C., May 1945.

- 7-103. Coermann, R. R., Comparison of the Dynamic Characteristics of Dummies, Animals and Man, in Impact Acceleration Stress Symposium, Brooks AFB, Texas, Nov. 27-29, 1961, NAS-NRC-977, National Academy of Sciences, National Research Council, Washington, D. C., 1962, pp. 173-184.
- 7-104. Coermann, R. R., The Mechanical Impedance of the Human Body in Sitting and Standing Position at Low Frequencies, ASD-TR-61-492, Aeronautical Systems Div., Wright-Patterson AFB, Ohio, Sept. 1961. (AD-413478).
- 7-105. Coermann, R. R., Ziegenruecker, G. H., Wittmer, A. L., et al., The Passive Dynamic Mechanical Properties of the Human Thorax-Abdomen System and of the Whole Body System, Aerospace Med., 31: 443-455, 1960.
- 7-106. Colehour, J. K., The Effects of Coriolis Acceleration during Zero Gravity Flight on Certain Hematological and Urinary Parameters in Normal and Labyrinthine Defective Subjects, NAV-SAM-MR-005.13-0004-2, Naval School of Aviation Medicine, Pensacola, Fla., and NASA, May 1964.
- 7-107. Colehour, J. K., Graybiel, A., Biochemical Changes Occurring with Adaptation to Accelerative Forces during Rotation, NAMI-959, Naval Aerospace Medical Institute, Pensacola, Fla., Apr. 1966. (Also in Aerospace Med., 37(12): 1205-1207, 1966).
- 7-108. Collier, D. R., Havens, D. E., White, W. J., Alleviation of Cardiovascular Deconditioning in Orbital Laboratories through Centrifugation, Douglas Aircraft Co., Inc., Missile and Space Systems Division, Santa Monica, Calif., 1964.
- 7-109. Collins, C. C., Crosbie, R. J., Gray, R. F., Pilot Performance and Tolerance Study of Orbital Re-entry Acceleration, NADC-LR-64, Naval Air Development Center, Johnsville, Pa., 1958.
- 7-110. Collins, C. C., Gray, R. F., Pilot Performance and Tolerance Studies of Orbital Re-entry Acceleration, NADC-LR-90, Naval Air Development Center, Johnsville, Pa., Sept. 1959.
- 7-111. Collins, W. E., Adaptation to Vestibular Disorientation. I. Vertigo and Nystagmus Following Repeated Clinical Stimulation, FAA-AM-65-18, Federal Aviation Agency, Oklahoma City, Okla., May 1965.

- 7-112. Collins, W. E., Adaptation to Vestibular Disorientation. III. Influence on Adaptation of Interrupting Nystagmic Eye Movements with Opposing Stimuli, FAA-AM-66-37, Federal Aviation Agency, Oklahoma City, Okla., Sept. 1966.
- 7-113. Collins, W. E., Adaptation to Vestibular Disorientation. VII. Special Effects of Brief Periods of Visual Fixation on Nystagmus and Sensations of Turning, FAA-AM-67-12, Federal Aviation Administration, Oklahoma City, Okla., May 1967.
- 7-114. Collins, W. E., Adaptation to Vestibular Disorientation. VIII. "Coriolis" Vestibular Stimulation and the Influence of Different Visual Surrounds, FAA-AM-67-19, Federal Aviation Administration, Oklahoma City, Okla., Aug. 1967. (Also in Aerospace Med., 39(2): 125-130, 1968).
- 7-115. Collins, W. E., Vestibular Responses from Figure Skaters, Aerospace Med., 37(11): 1098-1104, 1966.
- 7-116. Collopy, F. H., Determination of the Water Impact Shock Environment, in The Shock and Vibration Bulletin, Bull. 35, Pt. 7, Naval Research Lab., Washington, D. C., Apr. 1966, pp. 77-86.
- 7-117. The Concept of Motion on Sensitivity, Inter. Record Med. and Gen. Practice Clin., 168(6): 371-376, 1955.
- 7-118. Cording, C. R., Extravehicular Maintenance and Techniques, General Electric Co., Valley Forge, Pa., in AIAA 2nd Manned Space Flight Meeting, Dallas, Texas, Apr. 22-24, 1963, pp. 86-91.
- 7-119. Correia, M. J., Guedry, F. E., Jr., Influence of Labyrinth Orientation Relative to Gravity on Responses Elicited by Stimulation of the Horizontal Semicircular Canals, Project No. MR005.13-6001, Rep. 100, Naval School of Aviation Medicine, Pensacola, Fla., 1964.
- 7-120. Correia, M. J., Guedry, F. E., Jr., Modification of Vestibular Responses as a Function of Rate of Rotation about an Earth-Horizontal Axis, NAMI-957, Naval Aerospace Medical Institute, Pensacola, Fla., Mar. 1966.
- 7-121. Cramer, R. L., Dowd, P. J., Moore, E. W., et al., The Changing Parameters of the Habituating Vestibular System, SAM-TR-67-85, School of Aerospace Medicine, Brooks AFB, Texas, Sept. 1967.

- 7-122. Crampton, G. H., Young, F. A., The Differential Effect of a Rotary Visual Field on Susceptibles and Nonsusceptibles to Motion Sickness, J. Comp. Physiol. Psychol., 46(6): 451-453, 1953.
- 7-123. Creer, B. Y., Pilot Performance during Acceleration, in Environmental Biology, Altman, P. I., Dittmer, D. S., (eds.), AMRL-TR-66-194, Aerospace Medical Research Labs., Wright-Patterson AFB, Ohio, Nov. 1966, pp. 261-263.
- 7-124. Creer, B. Y., Smedal, H. A., Wingrove, R. C., Centrifuge Study of Pilot Tolerance to Acceleration and the Effects of Acceleration on Pilot Performance, NASA-TN-D-337, Nov. 1960.
- 7-125. Creer, B. Y., Stewart, J. D., Douvillier, J. G., Influence of Sustained Accelerations on Certain Pilot Performance Capabilities, Aerospace Med., 33: 1086-1093, 1962.
- 7-126. Crocker, J. F., Higgins, L. S., Phase IV, Investigation of Strength of Isolated Vertebrae, TI-1313-66-2, Technology Inc., Dayton, Ohio, May 1966.
- 7-127. Daisey, F. K., Space Power Tool, RTD-TDR-63-4227, Research Technology Division, Wright-Patterson AFB, Ohio, Oct. 1963.
- 7-128. Daves, G. S., Mott, J. G., Widdicombe, J. G., Respiratory and Cardiovascular Reflexes from the Heart and Lungs, J. Physiol., 115: 258-291, 1951.
- 7-129. Davidson, S., Evaluation of Methods of Resistance to G, FPRC-599, Flying Personnel Research Comm., Air Ministry, London, Oct. 1944.
- 7-130. Davidson, S., Report on the RAF, IAM Liaison Visit to Canada and the United States, (no number), Royal Air Force, Farnborough, Hants, England, 1945.
- 7-131. Davydov, B. I., Endurance of External Acceleration Increased as a Result of Exposure to Ionizing Radiation, NASA-TT-F-10349, Oct. 1966. (Translation of Doklady Akademii Nauk SSSR, 168(3): 691-693, 1966).
- 7-132. Davydov, B. I., Antipov, V. V., Saksonov, P. P., Reaction of Irradiated Organism when Affected by Acceleration of Critical Magnitude, in FTD-TT-65-170, Cosmic Research, 3(2): 256-268, 1965, Foreign Technology Division, Wright-Patterson AFB, Ohio.

- 7-133. Dean, R. D., Langan, R. P., Simulated Weightlessness under Neutral Buoyancy, in Proceedings of the Interdisciplinary Symposium on Apollo Application Programs, Jan. 12-13, 1966, Huntsville, Ala., NASA-TM-X-53558, Dec. 1966, pp. 229-240.
- 7-134. Deitrick, J. E., Whedon, G. D., Shorr, E., Effects of Immobilization upon Various Metabolic and Physiologic Functions of Normal Men, Amer. J. Med., 4(1): 3-36, Jan. 1948.
- 7-135. Denny-Brown, D., Russell, W. R., Experimental Cerebral Concussion, Brain, 64: 93-164, 1951.
- 7-136. Dieckman, D., Einfluss Horizontaler Mechanischer Schwingungen auf den Menschen, [Influence of Horizontal Mechanical Swinging on Man] , Int. Z. Angew. Physiol., 17(1): 83-100, 1958.
- 7-137. Dieckman, D., Einfluss Vertikaler Mechanischer Schwingungen auf den Menschen, [Influence of Vertikal Mechanical Oscillations in Man] , Int. Z. Angew. Physiol., 16(6): 519-564, 1957.
- 7-138. Dieckman, D., Mechanische Modelle fur den Vertikal Schwingenden Menschlichen Korper, [Mechanical Models for the Vertically Swinging Human Body] , Int. Z. Angew. Physiol., 17(1): 67-82, 1958.
- 7-139. Dietlein, L. F., Some Physiological Considerations of Space Flight: Weightlessness, in Manned Spacecraft: Engineering Design and Operation, Purser, P. E., Faget, M. A., Smith, N. F., (eds.), Fairchild Publications, Inc., N. Y., 1964, Chapt. 14, pp. 125-135.
- 7-140. Dietlein, L. F., Harris, E., Experiment M-5, Bioassays of Body Fluids, in Gemini Midprogram Conference, NASA-Manned Spacecraft Center, Houston, Texas, Feb. 23-25, 1966, NASA-SP-121, 1966, pp. 403-406.
- 7-141. Dietlein, L. F., Judy, W. V., Experiment M-1, Cardiovascular Conditioning, in Gemini Midprogram Conference, NASA-Manned Spacecraft Center, Houston, Texas, Feb. 23-25, 1966, pp. 381-391.
- 7-142. Dietlein, L. F., Judy, W. V., Experiment M-1, Cardiovascular Conditioning, in A Review of Medical Results of Gemini 7 and Related Flights, Kennedy Space Center, Fla., Aug. 23, 1966, NASA, Space Medicine Directorate, Office of Manned Space Flight, 1966, pp. 1-35.

- 7-143. DiGiovanni, C., Jr., Chambers, R. M., Physiologic and Psychologic Aspects of the Gravity Spectrum, New Eng. J. Med., 270(1): 31-35, Jan. 1964.
- 7-144. Dole, S. H., Design Criteria for Rotating Space Vehicles, RAND-RM-2668, Rand Corporation, Santa Monica, Calif., Oct. 1960.
- 7-145. Dorman, P. J., Lawton, R. W., Effect of G Tolerance on Partial Supination Combined with the Anti-G Suit, J. Aviat. Med., 27(6): 490-496, Dec. 1956.
- 7-146. Dowd, P. J., Resistance to Motion Sickness through Repeated Exposure to Coriolis Stimulation, Aerospace Med., 36(5): 452-455, 1965.
- 7-147. Dowd, P. J., Speed of Recovery from Coriolis Stimulation in Motion Sickness in Relation to Pilots and Non-pilots, SAM-TR-66-63, School of Aerospace Medicine, Brooks AFB, Texas, July 1966.
- 7-148. Dowd, P. J., Cramer, R. L., Habituation Transference in Coriolis Acceleration, Aerospace Med., 38: 1103-1107, Nov. 1967.
- 7-149. Douglas Aircraft Co., Inc., Report on the Optimization of the Manned Orbital Research Laboratory (MORL) System Concept. Vol. IV. Systems Analysis - Flight Crew, Santa Monica, Calif., NASA contract NAS1-3612, Sept. 1964.
- 7-150. Douglas Aircraft Co., Inc., Report on the Optimization of the Manned Orbital Research Laboratory (MORL) System Concept. Vol. XIII. Laboratory Mechanical Systems - Artificial Gravity Systems, Santa Monica, Calif., NASA contract NAS1-3612, Sept. 1964.
- 7-151. Draeger, R. H., et al., A Study of Personnel Injury by Solid Blast and the Design and Evaluation of Protective Devices, Research Project X-517, Rep. 1, Naval Medical Research Inst., Bethesda, Md., Mar. 1945.
- 7-152. Duane, T. D., Beckman, E. L., Ziegler, J. E., et al., Some Observations of Human Tolerance to Exposures of 15 Transverse G, NADC-MA-5305, Phase III, Naval Air Development Center, Johnsville, Pa., July 1953.
- 7-153. Duddy, J. H., Weightless Simulation Using Water Immersion Techniques: An Annotated Bibliography, SB-65-2 (Rev. 2) Lockheed Missiles and Space Co., Sunnyvale, Calif., Dec. 1967.

- 7-154. Durkovic, R. G., Hirsch, A. E., Personnel Injuries and Estimated Shock Motions on Yms 368 during a Mine Attack, DTMB-C-1318, David Taylor Model Basin, Washington, D. C., May 1962. (Confidential Rep.)
- 7-155. Dzendolet, E., Rievley, J. F., Man's Ability to Apply Certain Torques while Weightless, WADC-TR-59-94, Wright Air Development Center, Wright-Patterson AFB, Ohio, Apr. 1959. (AD-220363).
- 7-156. Edeiken, J., Jefferson Medical College Hospital, Dept. of Radiology, Philadelphia, Pa., personal communication on unpublished manuscript, 1968.
- 7-157. Edelberg, R., The Physiology of Combined Accelerations, in Gravitational Stress in Aerospace Medicine, Gauer, O. H., Zuidema, G. D., (eds.), Little, Brown and Co., Boston, 1961, pp. 140-149.
- 7-158. Edelberg, R., Weiss, H. S., Charland, P. V., et al., The Physiology of Simple Tumbling, WADC-TR-53-139, Part I, Wright Air Development Center, Wright-Patterson AFB, Ohio, Jan. 1954.
- 7-159. Edwards, D. K., Stauffer, E. J., Pine, A., et al., Study of Astronaut Capabilities to Perform Extravehicular Maintenance Functions and Assembly in Weightless Conditions, LS-166-1 Vol. I, Garrett/AiResearch Manufacturing Div., Los Angeles, Calif., Dec. 1965.
- 7-160. Edwards, W., Autokinetic Movement of Very Large Stimuli, J. Exp. Psychol., 48: 493-495, 1954.
- 7-161. Edwards, W., Two- and Three-Dimensional Autokinetic Movement as a Function of Size and Brightness of Stimuli, J. Exp. Psychol., 48: 391-398, 1954.
- 7-162. van Egmond, A. A. J., van Groen, J. J., Jongkees, L. B. W., The Function of the Vestibular Organ, Pract. Oto-rhino-laryng., Suppl. 2, 14: 3-109, 1952.
- 7-163. van Egmond, A. A. J., van Groen, J. J., Jongkees, L. B. W., The Mechanics of the Semicircular Canal, J. Physiol., 110: 1-17, 1949.
- 7-164. Eiband, A. M., Human Tolerance to Rapidly Applied Accelerations: A Summary of the Literature, NASA-Memo-5-19-59E, June 1959.

- 7-165. Engstrom, H., Lindeman, H. H., Ades, H. W., Anatomical Features of the Auricular Sensory Organs, in Second Symposium on the Role of the Vestibular Organs in Space Explorations, NASA-Ames Research Center, Moffett Field, Calif., Jan. 25-27, 1966, NASA-SP-115, pp. 33-46.
- 7-166. Epple, R. G. E., The Human Pilot, AE-61-4 Vol. III, USN, Bureau of Aeronautics, Washington, D. C., Aug. 1954.
- 7-167. Ernst, F. H., Smith, R. B., An Experimental Investigation under Zero-Gravity Conditions of Tethered Worker Maintenance Techniques, (Thesis), GA-63, Air Force Institute of Technology, Air University, Wright-Patterson AFB, Ohio, Aug. 1963.
- 7-168. Feder, H. C., Root, E. H., Dynamic Response Analysis of $+G_x$ Impact on Man, ARL-TR-64-11, Aeromedical Research Lab., Holloman AFB, N. M., Nov. 1964.
- 7-169. Ferwerda, T., Report of the U. S. Medical Corps Tests at Naval Air Station, Anacostia, Royal Air Force, Farnborough, Hants, England, 1941.
- 7-170. Fiorentini, A., Ronchi, L., Problems Related to Visual Performance of Pilots, Istituto Nazionale di Ottica, Arcetri-Firenze, Italy, 1965. (AD-630475).
- 7-171. Fleishman, E. A., The Perception of Body Position, Effect of Speed, Magnitude and Direction of Displacement on Accuracy of Adjustment to an Upright Position, Research Bulletin 53-1, Human Resources Research Center, Lackland AFB, Texas, Jan. 1953.
- 7-172. Fogel, L. J., The Position- and Motion- Sensing Channel, in Biotechnology: Concepts and Applications, Fogel, L. J., Prentice Hall, Englewood Cliffs, N. J., 1963, pp. 145-165.
- 7-173. Frank, G. M., Livshits, N. N., Arsen'yeva, M. A., et al., The Effects of Combined Space Flight Factors on Some Bodily Functions, JPRS-39159, Joint Publications Research Service, Washington, D. C., Dec. 1966. (Translation from Izvestiya Akademii Nauk SSSR, Ser. Biol., Moscow, No. 5, Sept. 1966, pp. 625-642).
- 7-174. Frankenhaeuser, M., Effects of Prolonged Gravitational Stress on Performance, Acta Psychologica, 14: 92-108, 1958 and Nordisk Psykologi, 10: 48-64, 1958.
- 7-175. Franks, W. R., Test Flights with Hydrostatic Suit, FPRC-301, Flying Personnel Research Comm., Air Ministry, London, May 1941.

- 7-176. Franks, W. R., Carr, J. A., Martin, W. R., et al., Use in Increase in Weight of a Mass under G to Provide Source of Compressed Air for F.F.S. (AB/BG System), C-2722, National Research Council, Canada, Sept. 28, 1944.
- 7-177. Franks, W. R., Kerr, W. K., Rose, B., Some Effects of Centrifugal Force on the Cardiovascular System in Man, J. Physiol., 104: 9P-10P, 1945.
- 7-178. Fraser, T. M., Human Response to Sustained Acceleration, NASA-SP-103, 1966.
- 7-179. Freeman, H. E., A Research Program to Develop a 60 "G" Personnel Restraint System, in Impact Acceleration Stress Symposium, Brooks AFB, Texas, Nov. 27-29, 1961, NAS-NRC-977, National Academy of Sciences, National Research Council, Washington, D. C., 1962, pp. 259-264.
- 7-180. Fregly, A. R., Kennedy, R. S., Comparative Effects of Prolonged Rotation at 10 RPM on Postural Equilibrium in Vestibular Normal and Vestibular Defective Human Subjects, NSAM-920, Naval School of Aviation Medicine, Pensacola, Fla., Mar. 1965.
- 7-181. Friede, R. L., Specific Cord Damage at the Atlas Level as a Pathogenic Mechanism in Cerebral Concussion, J. Neuropath. Exp. Neurol., 19: 266-279, 1960.
- 7-182. Gaffey, C. T., Montoya, V. J., The Vestibular Apparatus as Influenced by Localized High-Energy Irradiation, in Joint NASA-AEC Program in Space Radiation Biology, Progress Report, Fall 1967, UCRL-17751, University of California, Lawrence Radiation Lab., Berkeley, Calif., Sept. 1967, pp. 125.
- 7-183. Gauer, O. H., Physiological Effects of Acceleration and Exercise: Man. Part III. Changes in the Cardiovascular System during Positive G, in Environmental Biology, Altman, P. I., Dittmer, D. S., (eds.), AMRL-TR-66-194, Aerospace Medical Research Labs., Wright-Patterson AFB, Ohio, Nov. 1966, pp. 256.
- 7-184. Gauer, O. H., The Physiological Effects of Prolonged Acceleration, in German Aviation Medicine, World War II, Vol. 1, Superintendent of Documents, U. S. Government Printing Office, 1950.
- 7-185. Gauer, O. H., Physiological Problems of Weightlessness and Basic Research, in Proceedings First International Symposium on Basic Environmental Problems of Man in Space, Björstedt, H., (ed.), Springer-Verlag, N. Y., 1965, pp. 160-168.

- 7-186. Gauer, O. H., Eckert, P., Kaiser, D., et al., Fluid Metabolism and Circulation during and after Simulated Weightlessness, Second International Symposium on Basic Environmental Problems of Man in Space, International Astronautical Federation - International Academy of Astronautics, Paris, France, 1965.
- 7-187. Gauer, O. H., Henry, J. P., Circulatory Basis of Fluid Volume Control, Physiol. Rev., 43: 423-481, July 1963.
- 7-188. Gauer, O. H., Zuidema, G. D., (eds.), Gravitational Stress in Aerospace Medicine, Little, Brown and Co., Boston, 1961.
- 7-189. Gazenko, O., Medical Studies on the Cosmic Spacecrafts Vostok and Voskhod, NASA-TT-F-9207, Dec. 1964. (Translation from Akademiya Nauk SSSR, Otdeleniye Fiziologii. Komissiya Po Issledovaniyu i Osvoyeniyu Kosmicheskogo Prostranstva, 1964, pp. 1-38).
- 7-190. Gazenko, O. G., Gyurdzhian, A. A., On the Biological Role of Gravity, USSR Academy of Sciences, Moscow, USSR, (Presented at COSPAR Symposium, Florence, Italy, May 8-20), 1964.
- 7-191. Gazenko, O. G., Gyurdzhian, A. A., Physiological Effects of Gravitation, NASA-TT-F-376, Aug. 1965. (Translation of paper presented at the Eighth Plenary Meeting and Sixth International Space Science Symposium, Buenos Aires, May 10-21, 1965)
- 7-192. Gazenko, O. G., Kuznetsov, A., Further Biological Investigations on Rockets, paper presented at the Second World and Fourth European Congress of Aviation and Space Medicine, Rome, Oct. 27-31, 1959.
- 7-193. Gazenko, O. G., Parin, V. V., Chernigovskii, V. N., Space Physiology, Some Results and Outlooks of Experimental Investigations, ANL-Trans-209, Argonne National Laboratory, Argonne, Ill., July 1965. (Translated from abstract of report at Plenary session of the 10th Meeting of the All-Union I. P. Pavlov Physiological Society at Yerevan, Oct. 22-28, 1964).
- 7-194. Gell, C. F., Table of Equivalents for Acceleration Terminology. Recommended by the Acceleration Committee of the Aerospace Medical Panel, AGARD, Aerospace Med., 32(12): 1109-1111, 1961.

- 7-195. General Dynamics/Convair, Capsule Escape System Specifications, FZC-4-344 (G), San Diego, Calif., Feb. 1961.
- 7-196. General Electric, Crew Systems Simulation Results of a Water Immersion Simulation Program, GE-67SD4306, Missile and Space Div., Valley Forge Space Technology Center, Philadelphia, Pa., June 10, 1967.
- 7-197. Gerathewohl, S. J., Comparative Studies on Animals and Human Subjects in the Gravity-Free State, J. Aviat. Med., 25: 412-419, 1954.
- 7-198. Gerathewohl, S. J., Effect of Low-Gravity on Physiological Processes, in Conference on the Role of Simulation in Space Technology, Virginia Polytechnic Institute, Blacksburg, Va., Aug. 17-21, 1964, Circular No. 4, Part D, pp. XXIII-1 - XXIII-36.
- 7-199. Gerathewohl, S. J., Effects of Weightlessness on Man during U. S. Sub-Orbital and Orbital Flights, in Sixth International and Twelfth European Congress of Aviation and Space Medicine, Rome, Oct. 1-5, 1963, Lectures, Vol. I, pp. 399-428, Discussion, pp. 435-436.
- 7-200. Gerathewohl, S. J., Personal Experiences during Short Periods of Weightlessness Reported by Sixteen Subjects, Astron. Acta., 2: 203-217, 1956.
- 7-201. Gerathewohl, S. J., Principles of Bioastronautics, Prentice-Hall, Englewood Cliffs, N. J., 1963.
- 7-202. Gerathewohl, S. J., Weightlessness: The Problem and the Air Force Research Program, Air Univ. Quart. Rev., 10: 121-141, 1958.
- 7-203. Gerathewohl, S. J., von Beckh, H. J., Physiological Effects of Weightlessness: Vertebrates, in Environmental Biology, Altman, P. I., Dittmer, D. S., (eds.), AMRL-TR-66-194, Aerospace Medical Research Labs., Wright-Patterson AFB, Ohio, Nov. 1966, pp. 264-266.
- 7-204. Gerathewohl, S. J., Stallings, H. D., Experiments during Weightlessness: A Study of the Oculo-Agravic Illusion, J. Aviat. Med., 29: 504-516, July 1958.
- 7-205. Gerathewohl, S. J., Stallings, H. D., The Labyrinthine Posture Reflex (Righting Reflex) in the Cat during Weightlessness, J. Aviat. Med., 28: 345-355, Aug. 1957.

- 7-206. Gerathewohl, S. J., Strughold, H., Stallings, H. D., Sensomotor Performance during Weightlessness, Eye-Hand Coordination, J. Aviat. Med., 28: 7-12, Feb. 1957.
- 7-207. Gernandt, B. E., Vestibular Mechanisms, in Handbook of Physiology, Section 1, Neurophysiology, Vol. 1, American Physiological Society, Washington, D. C., 1963, Chapt. 22, pp. 549-564.
- 7-208. von Gierke, H. E., On the Dynamics of Some Head Injury Mechanisms, in Head Injury Conference Proceedings, University of Chicago, 1966, Caveness, W. F., Walker, A., (eds.), J. B. Lippincott Co., Philadelphia, Pa., 1966, pp. 383-396.
- 7-209. von Gierke, H. E., Response of the Body to Mechanical Forces - An Overview, in Lectures in Aerospace Medicine, Sixth Series, Feb. 6-9, 1967, School of Aerospace Medicine, Brooks AFB, Texas, pp. 325-344.
- 7-210. von Gierke, H. E., Transmission of Vibratory Energy through Human Body Tissue, in Medical Physics, Vol. 3, Glasser, O., (ed.), The Year Book Publishers, Inc., Chicago, 1960, pp. 661-669.
- 7-211. von Gierke, H. E., Transient Acceleration, Vibration and Noise Problems in Space Flight, in Bioastronautics, Schaefer, K. E., (ed.), Macmillan Co., N. Y., 1964, pp. 27-75.
- 7-212. von Gierke, H. E., Vibration and Noise Problems Expected in Manned Space Craft, Noise Control, 5: 8, 1959.
- 7-213. von Gierke, H. E., Hiatt, E. P., Biodynamics of Space Flight, Progress in the Astronautical Sciences, 1: 343-401, 1962.
- 7-214. von Gierke, H. E., Oestreicher, H. L., Franke, E. K., et al., Physics of Vibrations in Living Tissue, J. Appl. Physiol., 4: 886-900, 1952.
- 7-215. Gilbert, C. A., Stevens, P. M., Forearm Vascular Responses to Lower Body Negative Pressure and Orthostasis, J. Appl. Physiol., 21(4): 1265-1272, July 1966.
- 7-216. Gillies, J. A., (ed.), A Textbook of Aviation Physiology, Pergamon Press, Oxford, England, 1965.
- 7-217. Gillingham, K. K., Some Notes on the Threshold of the Vestibular Coriolis Effect and Its Significance to Aircrew, SAM-TR-65-55, School of Aerospace Medicine, Brooks AFB, Texas, Aug. 1965.
- 7-242

- 7-218. Gillingham, K. K., Training the Vestibule for Aerospace Operations, Aeromedical Review 8-65, School of Aerospace Medicine, Brooks AFB, Texas, Sept. 1965.
- 7-219. Gillingham, K. K., Cramer, R. L., Dowd, P. J., et al., Design Criteria for the Spatial Orientation Trainer, SAM-TR-67-90, School of Aerospace Medicine, Brooks AFB, Texas, Oct. 1967.
- 7-220. Goldberg, N. M., Roentgenogram of the Month, Diagnosis: Probable Pulmonary Contusion, Dis. Chest, 52: 397-398, Sept. 1967.
- 7-221. Goldman, D. R., von Gierke, H. E., The Effects of Shock and Vibration on Man, Lecture and Review Series No. 60-3, Naval Medical Research Institute, Bethesda, Md., Jan. 1960.
- 7-222. Goldstein, S. E., Input to Proposal for Stimulating Astronaut Activity in Weightlessness Condition, GE-MSD-PIR-57E74, Dec. 1966.
- 7-223. Goldstein, S. E., Tests to Validate an Underwater Model Design Technique and to Determine the Hydrodynamic Mass and Drag of a Man, GE MSD TIS Report to be published.
- 7-224. Goodall, McC., Sympathoadrenal Response to Gravitational Stress, J. Clin. Invest., 41: 197-202, 1962.
- 7-225. Goodall, McC., McCally, M., Graveline, D. E., Urinary Adrenaline and Noradrenaline Response to Simulated Weightless State, Amer. J. Physiol., 206(2): 431-436, 1964.
- 7-226. Gorbov, F. D., Kuznetsov, O. N., Lebedev, V. I., The Simulation of Psychosensory Disorders Resulting from Temporary Weightlessness, JPRS-38140, Joint Publications Research Service, Washington, D. C., Oct. 1966. (Translation of article in Zhurnal Nevropatologii i Psikhiatrii, LXVI, Issue 1: 81-88, Oct. 1966).
- 7-227. Graveline, D. E., Cardiovascular Deconditioning: Role of Blood Volume and Sympathetic Neurohormones, in Life Sciences and Space Research II, A Session of the Fourth International Space Science Symposium, Florkin, M., Dollfus, A., (eds.), John Wiley and Sons, Inc., N. Y., 1964, pp. 287-298.

- 7-228. Graveline, D. E., Effects of Posture on Cardiovascular Changes Induced by Prolonged Water Immersion, ASD-TR-61-563, Aeronautical Systems Div., Wright-Patterson AFB, Ohio, Oct. 1961.
- 7-229. Graveline, D. E., Maintenance of Cardiovascular Adaptability during Prolonged Weightlessness, Aerospace Med., 33: 297-302, Nov., 1962
- 7-230. Graveline, D. E., Balke, B., The Physiological Effects of Hypodynamics Induced by Water Immersion, SAM-60-88, School of Aviation Medicine, Brooks AFB, Texas, Sept. 1960.
- 7-231. Graveline, D. E., Balke, B., McKenzie, R. E., et al., Psychobiologic Effects of Water-Immersion-Induced Hypodynamics, Aerospace Med., 32: 387-400, May 1961.
- 7-232. Graveline, D. E., Jackson, M. M., Diuresis Associated with Prolonged Water Immersion, J. Appl. Physiol., 17(3): 519-524, May 1962.
- 7-233. Graveline, D. E., McCally, M., Body Fluid Distribution: Implications for Zero Gravity, Aerospace Med., 33: 1281-1290, 1962.
- 7-234. Gray, R. F., Full Body Support Systems, in Impact Acceleration Stress Symposium, Brooks AFB, Texas, Nov. 27-29, 1961, NAS-NRC-977, National Academy of Sciences, National Research Council, Washington, D. C., 1962, pp. 265-270.
- 7-235. Gray, R. F., Webb, M. G., High G Protection, NADC-MA-5910, Naval Air Development Center, Johnsville, Pa., Feb. 1960.
- 7-236. Graybiel, A., Oculogravic Illusion, AMA Archives of Ophthalmol., 48: 605-615, 1952. (Also: Proj. No. NM001-59.01.27, Naval School of Aviation Medicine, Pensacola, Fla., Dec. 1951).
- 7-237. Graybiel, A., The Problem of Man's Gravitoinertial Force Environment in Space Flight, NASA-CR-81787, 1966.
- 7-238. Graybiel, A., Clark, B., Symptoms Resulting from Prolonged Immersion in Water: The Problem of Zero-G Asthenia, Aerospace Med., 32: 181-196, 1961.
- 7-239. Graybiel, A., Clark, B., Validity of the Oculogravic Illusion as a Specific Indicator of Otolith Function, Aerospace Med., 36(12): 1173-1181, 1965.

- 7-240. Graybiel, A., Clark, B., Zarriello, J. J., Observations on Human Subjects Living in a "Slow Rotation Room" for Periods of Two Days, AMA Arch. Neurol., 3: 55-73, 1960.
- 7-241. Graybiel, A., Hupp, D. I., The Oculo-Gyral Illusion: A Form of Apparent Motion Which May be Observed Following Stimulation of the Semicircular Canals, Naval School of Aviation Medicine, Pensacola, Fla, Nov. 1945. (AD-467975).
- 7-242. Graybiel, A., Johnson, W. H., A Comparison of the Symptomatology Experienced by Healthy Persons and Subjects with Loss of Labyrinthine Function When Exposed to Unusual Patterns of Centripetal Force in a Counter-Rotating Room, USN-SAM and NASA Joint Rep. 70, Naval School of Aviation Medicine, Pensacola, Fla., June 1962.
- 7-243. Graybiel, A., Kellogg, R. S., The Inversion Illusion in Parabolic Flight: Its Probable Dependence on Otolith Function, NAMI-974, Naval Aerospace Medical Institute, Pensacola, Fla., July 1966.
- 7-244. Graybiel, A., Kennedy, R. S., Knoblock, E. C., et al., Effects of Exposure to a Rotating Environment (10 RPM) on Four Aviators for a Period of Twelve Days, Aerospace Med., 36(8): 733-754, 1965.
- 7-245. Graybiel, A., Kerr, W. A., Bartley, S. H., Stimulus Thresholds of the Semicircular Canals as a Function of Angular Acceleration, Amer. J. Psychol., 56: 21-36, 1948.
- 7-246. Graybiel, A., Miller, E. F., Billingham, J., Vestibular Experiments in Gemini Flights V and VII, Aerospace Med., 38(4): 360-370, 1967.
- 7-247. Graybiel, A., Miller, E. F., Newsom, B. D., et al., The Effect of Water Immersion on Perception of the Oculogravic Illusion in Normal and Labyrinthine-Defective Subjects, NAMI-1016, Naval Aerospace Medical Institute, Pensacola, Fla., Sept. 1967.
- 7-248. Graybiel, A., Patterson, J. L., Jr., Thresholds of Stimulation of the Otolith Organs as Indicated by the Oculogravic Illusion, J. Appl. Physiol., 7: 666-670, 1955.
- 7-249. Greeley, P. O., Jorgenson, H., Clark, W. G., et al., Effect of Anoxia on G Tolerance, NAS-NRC-CAM-480, National Academy of Sciences, National Research Council, Washington, D. C., Oct. 1945.

- 7-250. Greenleaf, J. E., Matter, M., Jr., Bosco, J. S., et al., Effects of Hypohydration on Work Performance and Tolerance to +G Acceleration in Man, Aerospace Med., 37(1): 34-39, 1966.
- 7-251. Greenleaf, J. E., Matter, M., Jr., Douglas, L. G., et al., Effects of Acute and Chronic Hypohydration on Tolerance to +G Acceleration in Man: 1. Physiological Results, NASA-TM-X-1285, Sept. 1966.
- 7-252. Gregory, R. L., Zangwill, O. L., The Origin of the Autokinetic Effect, Quart. J. Exp. Psychol., 15: 252-261, 1963.
- 7-253. Griffin, J. B., Feasibility of a Self-Maneuvering Unit for Orbital Maintenance Workers, ASD-TDR-62-278, Aeronautical Systems Division, Wright-Patterson AFB, Ohio, June 1962.
- 7-254. Grodsky, M. A., Crew Performance Studies for Manned Space Flight, Martin-Marietta Corporation, Baltimore, Md., Dec. 1965. (NASA Contract NASw-1187).
- 7-255. Grose, V. L., Deleterious Effect on Astronaut Capability of Vestibulo-Ocular Disturbance during Spacecraft Roll Acceleration, Aerospace Med., 38: 1138-1144, Nov. 1967.
- 7-256. Guedry, F. E., Jr., Comparison of Vestibular Effects in Several Rotating Environments, in Symposium on the Role of the Vestibular Organs in the Exploration of Space Pensacola, Fla., Jan. 20-22, 1965, NASA-SP-77, 1965, pp. 243-255.
- 7-257. Guedry, F. E., Jr., Habituation to Complex Vestibular Stimulation in Man: Transfer and Retention of Effects from Twelve Days of Rotation at 10 RPM, NSAM-921, Naval School of Aviation Medicine, Pensacola, Fla., 1965.
- 7-258. Guedry, F. E., Jr., Orientation of the Rotation-Axis Relative to Gravity: Its Influence on Nystagmus and the Sensation of Rotation, USN-SAM and NASA Joint Rep. No. 96, Naval School of Aviation Medicine, Pensacola, Fla., 1964. (Also in: Acta Otolaryng. (Stockholm), 60: 30-48, 1965).
- 7-259. Guedry, F. E., Jr., Psychophysiological Studies of Vestibular Function, in Contributions to Sensory Physiology, Neff, W. D., (ed.), Academic Press, N. Y., 1965, Vol. I., pp. 63-135.
- 7-260. Guedry, F. E., Jr., Relations Between Vestibular Nystagmus and Visual Performance, NAMI-1008, Naval Aerospace Medical Institute, Pensacola, Fla., May 1967.

- 7-261. Guedry, F. E., Jr., Rotatory Stimulation of the Semicircular Canals: Man, in Environmental Biology, Altman, P. I., Dittmer, D. S., (eds.), AMRL-TR-66-194, Aerospace Medical Research Labs., Wright-Patterson AFB, Ohio, 1966, p. 247.
- 7-262. Guedry, F. E., Jr., Some Effects of Interacting Vestibular Stimuli, AMRL-261, Army Medical Research Labs., Fort Knox, Ky., Mar. 1957.
- 7-263. Guedry, F. E., Jr., Visual Control of Habituation to Complex Vestibular Stimulation in Man, NAV-SAM and NASA Joint Rep. 95, Naval School of Aviation Medicine, Pensacola, Fla., May 1964.
- 7-264. Guedry, F. E., Jr., Ceran, S. J., Derivation of "Subjective Velocity" from Angular-Displacement Estimates Made during Prolonged Angular Accelerations: Adaptation Effects, AMRL-376, Army Medical Research Lab., Fort Knox, Ky., Feb. 1959.
- 7-265. Guedry, F. E., Jr., Collins, W. E., Graybiel, A., Vestibular Habituation during Repetitive Complex Stimulation: A Study of Transfer Effects, J. Appl. Physiol., 19: 1005-1015, 1964.
- 7-266. Guedry, F. E., Jr., Crocker, J., Vestibular System, in Bioastronautics Data Book, Webb, P., (ed.), NASA-SP-3006, 1964, Section 19, pp. 363-381.
- 7-267. Guedry, F. E., Jr., Harris, C. S., Labyrinthine Function Related to Experiments on the Parallel Swing, USN-SAM and NASA Joint Rep. No. 86, Naval School of Aviation Medicine, Pensacola, Fla., 1963.
- 7-268. Guedry, F. E., Jr., Montague, E. K., Quantitative Evaluation of the Vestibular Coriolis Reaction, Aerospace Med., 32: 487-500, June 1961.
- 7-269. Guedry, F. E., Jr., Niven, J. I., Interaction of Vestibular Stimuli of Different Magnitudes and Opposite Direction. Part I. Perception of Visual Apparent Motion during Angular Accelerations, Joint Project Rep. No. NM001-063.01.36, Naval School of Aviation Medicine, Pensacola, Fla., Dec. 1954. (AD-620362).
- 7-270. Guedry, F. E., Jr., Richmond, G., Differences in Response Latency with Different Magnitude Angular Accelerations, AMRL-301, Army Medical Research Lab., Fort Knox, Ky., 1957.

- 7-271. Gurdjian, E. S., Experiences in Head Injury and Skeletal Research, in Impact Acceleration Stress Symposium, Brooks AFB, Texas, Nov. 27-29, 1961, NAS-NRC-977, National Academy of Sciences, National Research Council, Washington, D. C., 1962, pp. 145-157.
- 7-272. Gurdjian, E. S., Lissner, M. S., Patrick, L. M., Protection of the Head and Neck in Sports, JAMA, 182: 509-512, Nov. 1962.
- 7-273. Gurdjian, E. S., Webster, J. E., Lissner, H. L., Studies on Skull Fracture with Particular Reference to Engineering Factors, Amer. J. Surg., 78: 736-742, 1949.
- 7-274. Haber, F., Haber, H., Possible Methods of Producing the Gravity-Free State for Medical Research, J. Aviat. Med., 21: 395-400, 1950.
- 7-275. Haley, J. L., Jr., Turnbow, J. W., Test Results - Hemispherical Specimens, Supplement II to Helmet Design Criteria for Improved Crash Survival, Tech. Rep. 65-44B, Army Aviation Materiel Labs., Fort Eustis, Va., Jan. 1966.
- 7-276. Haley, J. L., Jr., Turnbow, J. W., Macri, S., Helmet Design Criteria for Improved Crash Survival, Tech. Rep. 65-44, Army Aviation Materiel Labs., Fort Eustis, Va., Jan. 1966.
- 7-277. Hallenbeck, G. A., Design and Use of Anti-G Suits and Their Activating Valves in World War II, AF-TR-5433, Air Materiel Command, Wright-Patterson AFB, Ohio, 1946. (ATI-25139).
- 7-278. Hallenbeck, G. A., Maaske, C. A., Martin, E. E., Evaluation of Anti-G Suits, Rep. No. 2, NRC-CAM-254, National Research Council, Comm. on Aviation Medicine, Dec. 12, 1943. (Wright-Patterson AFB, Ohio).
- 7-279. Hammer, L. R., Aeronautical Systems Division Studies in Weightlessness: 1959-1960, WADD-TR-60-715, Wright Air Development Division, Wright-Patterson AFB, Ohio, Dec. 1961.
- 7-280. Hanson, P. G., Maximum Voluntary Ventilation after +G_x Impact in Humans, ARL-TR-65-22, Aeromedical Research Lab., Holloman AFB, N. M., Nov. 1965.
- 7-281. Hardy, J. D., Acceleration Problems in Space Flight, presented at XXI Congreso Internacional de Ciencias Fisiologicas (21st International Congress of Physiological Science), Buenos Aires, Argentina, Aug. 1959.

- 7-282. Hardy, J. D., Clark, C. C., Gray, R. F., Acceleration Problems in Space Flight, NADC-MA-5909, Naval Air Development Center, Johnsville, Pa., Oct. 1959.
- 7-283. Hartzler, V. L., Roccaforte, P. A., Experimental Determination of Human Vestibular System Response through Measurement of Eyeball Counterroll, Thesis, GE/EE/65-11, Air Force Institute of Technology, Air University, School of Engineering, Wright-Patterson AFB, Ohio, Aug. 1965.
- 7-284. Hawkins, J. T., Hirsch, A. E., General Motors Energy-Absorbing Steering Column as a Component of Shipboard Personnel Protection, Naval Ship Research and Development Center, Washington, D. C., in Shock and Vibration and Associated Environments, Symposium, 37th, Oct. 1967 Pt. 4, pp. 79-84.
- 7-285. Hawkins, W. R., Lectures in Aerospace Medicine, Space Flight Dynamics, 11. Zero "G", in Lectures in Aerospace Medicine, School of Aviation Medicine, Brooks AFB, Texas, Jan. 11-15, 1960, Paper no. 11.
- 7-286. Headley, R. M., Human Tolerance and Limitations to Acceleration, in Bio-Assay Techniques for Human Centrifuges and Physiological Effects of Acceleration, Bergeret, P., (ed.), AGARDograph No. 48, Pergamon Press, N. Y., 1961.
- 7-287. Hellstrom, G., Closed Liver Injury: A Clinical and Experimental Study, Almqvist & Wiksell, Uppsala, Sweden, 1965.
- 7-288. Helson, H., Adaptation-Level Theory, Harper and Rowe, N. Y., 1964.
- 7-289. Hendler, E., Physiological Effects of a Simulated Space Flight Profile, Fed. Proc., 22(4): 1060-1063, 1963.
- 7-290. Henry, J. P., Studies of the Physiology of Negative Acceleration, Air Force Tech. Report 5953, Wright-Patterson AFB, Ohio, 1950.
- 7-291. Henry, J. P., Ballinger, E. R., Maher, P. J., et al., Animal Studies of the Sub-Gravity State during Rocket Flight, J. Aviat. Med., 23: 421-432, 1952.
- 7-292. Henzel, J. H., The Human Spinal Column and Upward Ejection Acceleration: An Appraisal of Biodynamic Implications, AMRL-TR-66-233, Aerospace Medical Research Labs., Wright-Patterson AFB, Ohio, Sept. 1967.

- 7-293. Henzel, J. H., Clarke, N. P., Mohr, G. C., Compression Fractures of Thoracic Vertebrae Apparently Resulting from Experimental Impact, A Case Report, AMRL-TR-65-134, Aerospace Medical Research Labs., Wright-Patterson AFB, Ohio, Aug. 1965.
- 7-294. Hershgold, E. J., Roentgenographic Study of Human Subjects during Transverse Accelerations, Aerospace Med., 31: 213-219, 1960.
- 7-295. Hewes, D. E., Spady, A. A., Jr., Harris, R. L., Comparative Measurements of Man's Walking and Running Gaits in Earth and Simulated Lunar Gravity, NASA-TN-D-3363, June 1966.
- 7-296. Higgins, L. S., Schmall, R. A., Cain, C. P., et al., The Investigation of the Parameters of Head Injury Related to Acceleration and Deceleration, TI-118-67-1, Technology, Inc., San Antonio, Texas, June 1967. (AD-659795).
- 7-297. Highly, F. M., Jr., Critz, G. T., Hendler, E., Determination of Human Tolerance to Negative Impact Acceleration: Phase I, Naval Air Engineering Center, Philadelphia, Pa., paper presented at the 34th Annual Meeting, Aerospace Medical Association, Los Angeles, Calif., Apr. 29- May 2, 1963.
- 7-298. Hirsch, A. E., Man's Response to Shock Motions, DTMB-1797, David Taylor Model Basin, Washington, D. C., Jan. 1964.
- 7-299. Hirsch, A. E., White, L. A., Mechanical Stiffness of Man's Lower Limbs, DTMB-1810, David Taylor Model Basin, Washington, D. C., Oct. 1964.
- 7-300. Hixson, W. C., Niven, J. I., Application of the System Transfer Concept to a Mathematical Description of the Labyrinth. I. Steadystate Nystagmus Response to Semicircular Canal Stimulation by Angular Acceleration, Project No. MR005.13-6001, Rep. 57, Naval School of Aviation Medicine, Pensacola, Fla., 1961.
- 7-301. Hixson, W. C., Niven, J. I., Frequency Response of the Human Semicircular Canals. II. Nystagmus Phase Shift as a Measure of Nonlinearities, Project No. MR005.13-6001, Rep. 73, Naval School of Aviation Medicine, Pensacola, Fla., 1962.
- 7-302. Hixson, W. C., Niven, J. I., Correia, M. J., Kinematics Nomenclature for Physiological Accelerations, Monograph 14, Naval Aerospace Medical Institute, Pensacola, Fla., 1966.

- 7-303. Holcomb, G. A., Human Experiments to Determine Human Tolerance to Landing Impact in Capsule Systems, paper presented at the Fifth Symposium on Ballistic Missile and Space Technology, Los Angeles, Calif., Aug. 1960.
- 7-304. Holcomb, G. A., Impact Studies of the United States Aerospace Industry, presented at the Symposium on Impact Acceleration Stress, Brooks AFB, San Antonio, Texas, Nov. 27-29, 1961.
- 7-305. Hollister, N. R., Jolley, W. P., Horne, R. G., et al., Biophysics of Concussion, WADC-TR-58-193, Wright Air Development Center, Wright-Patterson AFB, Ohio, 1958.
- 7-306. Holmes, A. E., Space Tool Kit Survey, Development, and Evaluation Program, Final Report, NASA-CR-65267, 1965.
- 7-307. Hoppin, F. G., Jr., Sever, R. J., Hitchcock, L., Jr., Pulmonary Function in Man under Prolonged Acceleration, II. Correlation of Arterial Blood Oxygen Saturation with Ventilation and Gas Being Breathed, NADC-MR-6519, Naval Air Development Center, Johnsville, Pa., Dec. 1965.
- 7-308. Hoppin, F. G., Jr., York, E., Kuhl, D. E., et al., Distribution of Pulmonary Blood Flow as Affected by Transverse (+G) Acceleration, Final Report, NADC-MR-6517, Naval Air^x Development Center, Johnsville, Pa., Dec. 1965.
- 7-309. Hunt, N. C., A Comparison of the Effects of Vasopressin and Positive Pressure Breathing on the Cardiovascular Deconditioning of Water Immersion, in Preprints of Scientific Program of the 38th Annual Scientific Meeting, Aerospace Medical Association, Washington, D. C., Apr. 10-13, 1967, pp. 52-53.
- 7-310. Hunt, N. C., Immersion Diuresis, Aerospace Med., 38: 176-180, Feb. 1967.
- 7-311. Hunt, N. C., Positive Pressure Breathing during Water Immersion Aerospace Med., 38(7): 731-735, 1967.
- 7-312. Hyatt, K. H., The Effects of Drugs on Post-Recumbency Orthostatic Intolerance, in Proceedings of a Research Contractors Conference, NASA-Manned Spacecraft Center, Houston, Texas, 1964, NASA-CR-67948, pp. 160-163.

- 7-313. Hyde, A. S., The Effect of Back Angle, Molded Supports, and Staged Evisceration upon Intrapulmonary Pressures in Dogs and a Monkey during Forward (+G_x) Acceleration, AMRL-TDR-62-106, Aerospace Medical Research Labs., Wright-Patterson AFB, Ohio, Sept. 1962.
- 7-314. Hyde, A. S., Cherniack, N. S., Lindberg, E. F., et al., Some Cardiorespiratory Responses of Flying and Non-Flying Personnel to Different Vectors of Acceleration with Correlation of these Responses to Other Variables, AMRL-TDR-62-151, Aerospace Medical Research Labs., Wright-Patterson AFB, Ohio, Dec. 1962.
- 7-315. Hyde, A. S., Raab, H. W., A Summary of Human Tolerance to Prolonged Acceleration, AMRL-TR-65-36, Aerospace Medical Research Labs., Wright-Patterson AFB, Ohio, Feb. 1965.
- 7-316. Igarashi, M., Dimensional Study of the Vestibular End Organ Apparatus, in Second Symposium on the Role of the Vestibular Organs in Space Exploration, NASA-Ames Research Center, Moffett Field, Calif., Jan. 25-27, 1966, NASA-SP-115, pp. 47-54.
- 7-317. Ivanov, K. V., Zhukov, M. K., Melchanova, M. G., Effect of Accelerations Produced during Irradiation of Animals on the Course of Acute Radiation Sickness, Patolog. Fiziol. i Eksper. Terap., 5: 74-75, 1962, English Abstract in Soviet Literature on Life Support Systems, A. Biosciences, LC-AID-P-63-91, Library of Congress, Washington, D. C., 1963, p. 12.
- 7-318. Jackson, M. S., Sears, C. W., Effect of Weightlessness upon the Normal Nystagmic Reaction, Aerospace Med., 37(7): 719-721, 1966.
- 7-319. Jarvis, C. R., Flight-Test Evaluation of an On-Off Rate Command Attitude Control System of a Manned Lunar-Landing Research Vehicle, NASA-TN-D-3903, Apr. 1967.
- 7-320. Johnson, L. B., Havener, P. W., Experimental Research Studies on Tools for Extravehicular Maintenance in Space, Phase II Final Report, NASA-CR-91052, Aug. 1967.
- 7-321. Johnson, W. H., Mayne, J. W., Stimulus Required to Produce Motion Sickness, Restriction of Head Movement as a Preventive of Airsickness Field Studies on Airborne Troops, J. Aviat. Med., 24(5): 400-411, 1953.

- 7-322. Jones, G. M., Comparison of Nystagmoid Responses to Rotational Stimuli about Vertical and Rolling Axis, J. Physiol., 154: 32P-33P, 1960.
- 7-323. Jones, G. M., Disturbance of Oculomotor Control in Flight, Aerospace Med., 36(5): 461-465, 1965.
- 7-324. Jones, G. M., Predominance of Anti-compensatory Oculomotor Response during Rapid Head Rotation, Aerospace Med., 35(10): 965-968, 1964.
- 7-325. Jones, G. M., Vestibular Inaptitude in the Environments of Flight and Space, J. Laryngol., 80(3): 207-221, 1966.
- 7-326. Jones, G. M., Vestibulo-ocular Disorganization in the Aerodynamic Spin, Aerospace Med., 36(10): 976-983, 1965.
- 7-327. Jones, G. M., Barry, W., Kowalsky, N., Dynamics of the Semicircular Canals Compared in Yaw, Pitch and Roll, Aerospace Med., 35(10): 984-989, 1964.
- 7-328. Jones, G. M., Milsum, J. H., Spatial and Dynamic Aspects of Visual Fixations, IEEE Trans. Bio-Med. Engr., BME-12(2): 54-62, 1965.
- 7-329. Kaehler, R. C., The Effects of Transverse Accelerations and Exponential Time-Lag Constants on Compensatory Tracking Performance, ASD-TR-61-457, Aeronautical Systems Div., Wright-Patterson AFB, Ohio, Sept. 1961.
- 7-330. Kaehler, R. C., Meehan, J. P., Human Psychomotor Performance under Varied Transverse Acceleration, WADD-TR-60-621, Wright Air Development Center, Wright-Patterson AFB, Ohio, Aug. 1960.
- 7-331. Kakurin, L. I., Akhrem-Akhremovich, R. M., Vanyushina, Yu. V., et al., The Influence of Restricted Muscular Activity on Man's Endurance of Physical Stress, Accelerations and Orthostatics, in Reports Presented at Soviet Conference on Space Biology and Medicine, Nov. 10-12, 1964, Lebedinskiy, A. V., Nefedov, Yu. G., Khazen, I. M., (eds.), JPRS-38596, Joint Publications Research Service, Washington, D. C., Nov. 1966, pp. 110-117.
- 7-332. Kasten, D. F., Interdisciplinary Measurement of Human Performance under Low and Zero Gravity Conditions, Aerospace Medical Research Labs., Wright-Patterson AFB, Ohio, 1964. (AD-620931).

- 7-333. Kas'yan, I. I., Kopanev, V. I., Mechanisms of the Physiological Effect of Weightlessness on the Human Body, in Space Flight Physiology, JPRS-29156, Joint Publications Research Service, Washington, D. C., Mar. 1965, pp. 11-20. (Translation of Izvestiya Akad. Nauk SSSR, Seriya Biologii Cheskaya, No. 1: 10-17, 1965).
- 7-334. Kas'yan, I. I., Kosolov, I. A., Lebedev, V. I., et al., Reactions of Astronauts during Parabolic Flight on Airplanes, Izv. Akad. Nauk. SSSR, Ser. Biol., No. 2: 169-181, 1965.
- 7-335. Kas'yan, I. I., Krasovskiy, A. S., Kolosov, I. A., et al., Certain Physiological Reactions of Man under Conditions of Brief Weightlessness, JPRS-33115, Joint Publications Research Service, Washington, D. C., Dec. 1965. (Translated from Izvest. Akad. Nauk SSSR, Ser. Biol., No. 5: 633-646, Sept.-Oct. 1965)
- 7-336. Keighley, G., Clark, W. G., Drury, D. R., Flicker Fusion Frequency Measurements on Man Subjected to Positive Acceleration on a Human Centrifuge, J. Appl. Physiol., 4: 57-62, 1951.
- 7-337. Keller, T., O'Hagan, J., Weston, R., A Study of the Mechanics of Human Balancing for Potential Application to the Control of Vehicles, Pt. I. Initial Investigation of Vertical Balancing in Earth Gravity, Research Department Memorandum RM-299, Grumman Aircraft Engineering Corp., Bethpage, N. Y., 1965.
- 7-338. Kellogg, R. S., Kennedy, R. S., Graybiel, A., Motion Sickness Symptomatology of Labyrinthine Defective and Normal Subjects during Zero Gravity Maneuvers, AMRL-TDR-64-47, Aerospace Medical Research Labs., Wright-Patterson AFB, Ohio, June 1964.
- 7-339. Kennedy, R. S., Graybiel, A., The Dial Test: A Standardized Procedure for the Experimental Production of Canal Sickness Symptomatology in a Rotating Environment, NSAM-930, Naval School of Aviation Medicine, Pensacola, Fla., June 1965.
- 7-340. Kennedy, R. S., Tolhurst, G. C., Graybiel, A., The Effects of Visual Deprivation on Adaptation to a Rotating Environment, NSAM-918, Naval School of Aviation Medicine, Pensacola, Fla., Mar. 1965.
- 7-341. Kerr, W. K., Bibliography of Canadian Reports in Aviation Medicine, 1939-1945, DR-153, Defense Research Board, Dept. of National Defence, Canada, Oct. 1962. (AD-290050).

- 7-342. Kerr, W. K., Report on the Visit to Wright Field, U. S. A., Aeromedical Lab., Acceleration Unit, [no number], Royal Air Force, Farnborough, Hants, England, 1943.
- 7-343. Khazen, I. M., Extralabyrinthine Symptoms of Motion Sickness under Space Flight Conditions, in Space Biology and Medicine, 1(4): 14-25, 1967, JPRS-43762, Joint Publications Research Service, Washington, D. C., 1967. (Translation of Kosmicheskaya Biologiya i Meditsina, 1(4): 11-18, 1967).
- 7-344. King, B. G., Physiological Effects of Postural Disorientation by Tilting during Weightlessness, Aerospace Med., 32: 137-140, Feb. 1961.
- 7-345. Kohler, I., Experiments with Prolonged Optical Distortions, presented at XIV International Congress of Psychology, Montreal, June 1954.
- 7-346. Kornhuaser, M., Impact Protection for the Human Structure, presented at the Western Regional Meeting of the American Astronautical Society, Palo Alto, Calif., 1958.
- 7-347. Kornhuaser, M., Structural Effects of Impact, Spartan Books, Inc., Baltimore, Md., 1964.
- 7-348. Kornhauser, M., Theoretical Prediction of the Effect of Rate of Onset on Man's G-Tolerance, Aerospace Med., 32: 412-421, 1961.
- 7-349. Kuehnegger, W., Study of Man's Physical Capabilities on the Moon, Vol. 2, Pt. 2. Biomechanics Research Program Appendices, NASA-CR-66118, July 1965.
- 7-350. Kulwicki, P. V., Peoples, G., Controlled Rotation and Stabilization for the Orbital Worker, AMRL-Memo-P-21, Aerospace Medical Research Labs., Wright-Patterson AFB, Ohio, Dec. 1962.
- 7-351. Kurzhals, P. R., Adams, J. J., Hodge, W. F., Space-Station Dynamics and Control, in A Report on the Research and Technological Problems of Manned Rotating Spacecraft, Langley Research Center Staff, NASA-TN-D-1504, Aug. 1962, pp. 71-83.
- 7-352. Ladell, W. S. S., The Effects of Water and Salt Intake upon the Performance of Men Working in Hot and Humid Environments, J. Physiol., 127(1): 11-46, 1955.

- 7-353. Lamb, L. E., An Assessment of the Circulatory Problem of Weightlessness in Prolonged Space Flight, Aerospace Med., 35: 413-419, 1964.
- 7-354. Lamb, L. E., Hypoxia - An Anti-Deconditioning Factor for Manned Space Flight, Aerospace Med., 36: 97-100, 1965.
- 7-355. Lamb, L. E., Status of Knowledge of Weightlessness 1965, in Space Research: Directions for the Future, Part 3, NASA-CR-70003, 1965.
- 7-356. Lamb, L. E., Johnson, R. L., Stevens, P. M., Cardiovascular Deconditioning during Chair Rest, Aerospace Med., 35: 646-649, 1964.
- 7-357. Lamb, L. E., Johnson, R. L., Stevens, P. M., et al., Cardiovascular Deconditioning from Space Cabin Simulator Confinement, Aerospace Med., 35: 420-428, 1964.
- 7-358. Lamb, L. E., Stevens, P. M., Influence of Lower Body Negative Pressure on the Level of Hydration during Bed Rest, Aerospace Med., 36: 1145-1151, 1965.
- 7-359. Lambert, E. H., Wood, E. H., Baldes, E. H., et al., Comparison of Protection against the Effects of Positive Acceleration Afforded by the Standard Gradient Pressure Suit (G. P. S.) and a Simplified Single Pressure Suit, NRC-CAM-308, National Research Council, Committee on Aviation Medicine, May 27, 1944.
- 7-360. Lamport, H., Hoff, E. C., Baldes, E. H., et al., Tests of Protection against the Effects of Acceleration Afforded the Human by the Use of the Latest Model of the Gradient Pressure Suit (G. P. S.) when Inflated by Three Different Pressure Arrangements, NRC-CAM-187, National Research Council, Committee on Aviation Medicine, Aug. 25, 1943.
- 7-361. Lamport, H., Hoff, E. C., Herrington, L. P., Review Methods of Applying Air Pressure to the Extremities for Protection against Acceleration with Measurements of the Effective Pressures on the Skin, NRC-CAM-228, National Research Council, Committee on Aviation Medicine, Nov. 24, 1944.
- 7-362. Lansberg, M. P., Guedry, F. E., Jr., Graybiel, A., The Effect of Changing the Resultant Linear Acceleration Relative to the Subject on Nystagmus Generated by Angular Acceleration, Project No. MR005.13-6001, Rep. 99, Naval School of Aviation Medicine, Pensacola, Fla., 1964. (See also: Aerospace Med., 36(5): 456-460, May 1965).

- 7-363. Larson, C. A., Space Station Design Parameter Effects on Artificial G Field, AIAA J., 2(8): 1454-1455, 1964.
- 7-364. Latham, F., A Study in Body Ballistics: Seat Ejection, Proc. Roy. Soc., London., Ser. B., 147: 121-139, 1957.
- 7-365. Lawton, R. W., Physiological Considerations Relevant to the Problem of Prolonged Weightlessness: A Review, Astron. Sci. Rev., 4: 1-16, 1962.
- 7-366. Lawton, R. W., Weightlessness, in Bioastronautics Data Book, Webb, P., (ed.), NASA-SP-3006, 1964, Section 4, pp. 53-62.
- 7-367. Lawton, R. W., Shepler, H. G., Bondurant, S., et al., Circulatory and Respiratory Effects of Acceleration: Mammals, in Environmental Biology, Altman, P. I., Dittmer, D. S., (eds.), AMRL-TR-66-194, Aerospace Medical Research Labs., Wright-Patterson AFB, Ohio, Nov. 1966, pp. 250-255.
- 7-368. Lawton, R. W., Smith, B. J., Ekberg, D. R., Bioengineering Problems in Early Manned Space Flight, Ann. N. Y. Acad. Sci., 84: 29-74, 1960.
- 7-369. Lebedev, V., State of Weightlessness and the "End of the World", Nauka i Tekhnika, No. 8: 27-29, 1965.
- 7-370. Ledoux, A., L'adaptation du Systeme Vestibulaire Peripherique, Acta Otolaryngol., 53: 307-315, 1961, (Translated by Federal Aviation Agency, Washington, D. C., FAA-T-78, Adaptation of the Peripheral Vestibular System).
- 7-371. Lessing, H. C., Coate, R. E., Simple Atmosphere Re-entry Guidance Scheme for Return from the Manned Mars Mission, NASA-TN-D-3422, May 1966.
- 7-372. Letko, W., Spady, A. A., Jr., Hewes, D. E., Problems of Man's Adaptation to the Lunar Environment, in Second Symposium on the Role of the Vestibular Organs in Space Exploration, Ames Research Center, Moffett Field, Calif., Jan. 25-27, 1966, pp. 25-32.
- 7-373. Levashov, M. M., Nystagmographic Analysis of the Fast Component of Vestibular Nystagmus Caused by Radial Acceleration, JPRS-29571, Joint Publications Service, Washington, D. C., Apr. 1965.
- 7-374. Linder, G. S., Mechanical Vibration Effects on Human Beings, Aerospace Med., 33: 939-950, 1962.

- 7-375. Lindgren, S. O., Experimental Studies of Mechanical Effects in Head Injury, Acta Chir. Scand., Suppl. 360; pp. 1-100, 1966.
- 7-376. Lindley, C. A., A New Concept in Artificial Gravity Systems, Aerospace Corporation, El Segundo, Calif., in AIAA Fourth Manned Space Flight Meeting, St. Louis, Mo., Oct. 11-13, 1965, pp. 189-196.
- 7-377. Ling-Temco-Vought, Inc., Astronautics Division, Summary of MMU Tether Study Results, LTV-335.19, Dallas, Texas, Dec. 1964.
- 7-378. Lipkin, M., Ratcliffe, H. L., Some Effects of Cyclic Acceleration on Rhesus Monkeys, J. Aviat. Med., 25: 594-599, 1954.
- 7-379. Lissner, H. L., Evans, F. G., Engineering Aspects of Fractures, Clin. Orthop., 8: 310-322, 1958.
- 7-380. Livshits, N. N., Combined Effects of Ionizing Radiation and Other Factors, NASA-TT-F-354, 1965. (Translated from Effects of Ionizing Radiation and of Dynamic Factors on the Functions of the Central Nervous System - Problems of Space Physiology, Livshits, N. N., (ed.), Science Publishing House, Moscow, 1964, pp. 1-23).
- 7-381. Loats, H. L., Jr., Mattingly, G. S., Brush, C. E., A Study of the Performance of an Astronaut during Ingress and Egress Maneuvers through Airlocks and Passageways, Vol. II. Technical Discussions, NASA-CR-66342, Apr. 1965.
- 7-382. Lockheed-California, Co., Study of a Rotating Manned Orbital Space Station, Final Report, Vol. XI. Summary, Burbank, Calif., NASA Contract NAS9-1665, Mar. 1964.
- 7-383. Loftus, J. P., (ed.), Symposium of Motion Sickness with Special Reference to Weightlessness, AMRL-TR-63-25, Aerospace Medical Research Labs., Wright-Patterson AFB, Ohio, June 1963.
- 7-384. Loftus, J. P., Hammer, L. R., Weightlessness and Performance: A Review of the Literature, ASD-TR-61-166, Aeronautical Systems Div., Wright-Patterson AFB, Ohio, June 1961.
- 7-385. Lombard, C. F., Roth, H. P., Tolerance to Abrupt Deceleration; Facilities and Research at AFFTC, Edwards AFB, 1947-1952, NSL-65-152, Northrop Space Labs., Hawthorne, Calif., Contract No. AT41(609)-2317, Oct. 1965.

- 7-386. Lombard, C. F., Roy, A., Beattie, J. M., et al., The Influence of Orientation and Support-Restraint upon Survival from Impact Acceleration, ARL-TR-66-20, Aeromedical Research Lab., Holloman AFB, N. M., Nov. 1966.
- 7-387. Lomonaco, T., Strollo, M., Fabris, L., Sulla Fisiopatologia Durante il Volo Nello Spazio. Comportamento della Coordinazione Motoria in Soggetti Sottoposti a Valori di Accelerazione Variante da 3 a Zero g, Riv. Med. Aeron., 20 Suppl. 1: 76-96, Jan.-Mar. 1957.
- 7-388. Loret, B. J., Optimization of Manned Orbital Satellite Vehicle Design with Respect to Artificial Gravity, ASD-TR-61-688, Aeronautical Systems Division, Wright-Patterson AFB, Ohio, 1961.
- 7-389. Lowenstein, O., The Functional Significance of the Ultra-structure of the Vestibular End Organs, in Second Symposium on the Role of the Vestibular Organs in Space Exploration, NASA-Ames Research Center, Moffett Field, Calif., Jan. 25-27, 1966, NASA-SP-115, pp. 73-90.
- 7-390. Lynch, T. N., Jensen, R. L., Stevens, P. M., et al., Metabolic Effects of Prolonged Bed Rest: Their Modification by Simulated Altitude, Aerospace Med., 38: 10-20, Jan. 1967.
- 7-391. McCally, M., Body Fluid Volumes and Renal Response of Human Subjects to Water Immersion, AMRL-TR-65-115, Aerospace Medical Labs., Wright-Patterson AFB, Ohio, 1965.
- 7-392. McCally, M., Plasma Volume Response to Water Immersion: Implications for Space Flight, Aerospace Med., 35: 130-132, Feb. 1964.
- 7-393. McCally, M., Graveline, D. E., Physiologic Aspects of Prolonged Weightlessness, New Eng. J. Med., 269: 508-516, 1963.
- 7-394. McCally, M., Piemme, T. E., Murray, R. H., Tilt Table Responses of Human Subjects Following Application of Lower Body Negative Pressure, Aerospace Med., 37: 1247-1249, 1966.
- 7-395. McCally, M., Shropshire, S., Relative Effectiveness of Selective Space Flight Deconditioning Countermeasures, presented at 38th Annual Scientific Meeting of the Aerospace Medical Association, Washington, D. C., Apr. 10-13, 1967.

- 7-396. McDonald, L. W., Plantz, R. G., Vestibular Organs: Radiation Effects on Structure and Function, in Joint NASA-AEC Program in Space Radiation Biology, Progress Report, Fall 1967, UCRL-17751, University of California, Lawrence Radiation Lab., Berkeley, Calif., Sept. 1967, pp. 117-122.
- 7-397. McFarland, R. A., Human Factors in Air Transportation, Occupational Health and Safety, McGraw-Hill, N. Y., 1953.
- 7-398. Machell, R. M., (ed.), Summary of Gemini Extravehicular Activity, NASA-SP-149, 1967.
- 7-399. McIntyre, A. K., Present Position of Anti-G Suits, Royal Australian Air Force FR-93, Flying Personnel Research Committee, Air Ministry, London, June 1944.
- 7-400. McIntyre, A. K., Preliminary Report on K. O. P. Anti-G Suits, Royal Australian Air Force FR-92, Flight Personnel Research Committee, Air Ministry, London, June 1944.
- 7-401. Mack, P. B., Vose, G. P., LaChance, P. A., Experiment M-6, Bone Demineralization on Gemini IV, in Manned Space Flight Experiments Symposium, Gemini Missions III and IV, Washington, D. C., Oct. 18-19, 1965, NASA-TM-X-56861, 1966, pp. 61-80.
- 7-402. Mack, P. B., Vose, G. P., Vogt, F. B., et al., Experiment M-6, Bone Demineralization, in Gemini Midprogram Conference, NASA-Manned Spacecraft Center, Houston, Texas, Feb. 23-25, 1966, NASA-SP-121, pp. 407-415.
- 7-403. Magid, E. B., Coermann, R. R., The Reaction of the Human Body to Extreme Vibrations, in Proceedings of the Meeting of the Institute of Environmental Sciences, Los Angeles, Calif., Apr. 1960.
- 7-404. Managan, R. F., Flagg, K. C., Duddy, J. H., et al., Evaluation of Two Cyclic-Strain Impact Attenuators, AMRL-TR-66-221, Aerospace Medical Research Labs., Wright-Patterson AFB, Ohio, May 1967.
- 7-405. Mann, C. W., Ray, J. T., Absolute Thresholds of Perception of Direction of Angular Acceleration, Project No. NM001-110-500, Rep. 41, Naval School of Aviation Medicine, Pensacola, Fla., May 1956.
- 7-406. Mann, C. W., Ray, J. T., The Perception of the Vertical: XIV. The Effect of the Rate of Movement on the Judgement of the Vertical, Project No. NM001-110-500, Rep. 40, Naval School of Aviation Medicine, Pensacola, Fla., 1956.

- 7-407. Manning, G. W., Stewart, W. G., The Effect of Body Position on the Incidence of Motion Sickness, J. Appl. Physiol., 1: 619-628, 1949.
- 7-408. Margaria, R., Cavagna, G. A., Human Locomotion in Sub-Gravity, Aerospace Med., 35: 1140-1146, 1964.
- 7-409. Marshall, J. E., Visual-Vestibular Interaction and Threshold for Angular Acceleration, AMRL-754, Army Medical Research Lab., Fort Knox, Ky., Oct. 1967.
- 7-410. Marton, T., Hunt, S. R., Klaus, T., et al., Neutral Buoyancy Submersion for the Analysis of Human Performance in Zero G, in AIAA Fourth Manned Space Flight Meeting, St. Louis, Mo., Oct. 11-13, 1965, pp. 127-133.
- 7-411. Mavriplis, F., Little, G., Roberge, A., et al., Investigation of Independent Structure (Space) Crew Escape Concepts, AFFDL-TR-65-226, Air Force Flight Dynamics Lab., Wright-Patterson, AFB, Ohio, Mar. 1966.
- 7-412. Mayne, R., Spatial Orientation in a Weightless Environment, NASA-CR-65429, Apr. 1966.
- 7-413. Mayo Clinic, Studies of the Effects of Acceleration on Cardiovascular and Respiratory Dynamics, Semi-Annual Status Report, NASA-CR-83323, Apr. 1967.
- 7-414. Mazy, R. S., Mattingly, T. E., Felder, J. W., Jr., et al., Development of an Internal Restraint System for an Integrated Restraint-Pressure Suit System, NASA-CR-718, Feb. 1967.
- 7-415. Meintel, A. J., Jr., Garren, K. R., Driscoll, N. R., Manual Control of High-Altitude Apollo Launch Abort, NASA-TN-D-3433, June 1966.
- 7-416. Meiry, J. L., The Vestibular System and Human Dynamic Space Orientation, NASA-CR-64545, June 1965.
- 7-417. Meiry, J. L., Young, L. R., Biophysical Evaluation of the Human Vestibular System, NASA-CR-82977, 1967.
- 7-418. Middleton, W. C., White, W. J., The Effects of Centrifuge Radius on the Performance of Entry Tasks, DAC-59274, Douglas Aircraft Co., Inc., Santa Monica, Calif., June 1966.
- 7-419. Miller, E. F., Counterrolling of the Human Eyes Produced by Head Tilt with Respect to Gravity, Acta Otolaryng., 54: 479-501, 1962.

- 7-420. Miller, E. F., Fregly, A. R., vanden Brink, G., et al., Visual Localization of the Horizontal as a Function of Body Tilt up to $\pm 90^\circ$ from Gravitational Vertical, NSAM-942, Naval School of Aviation Medicine, Pensacola, Fla., Aug. 1965.
- 7-421. Miller, E. F., Graybiel, A., Magnitude of Gravitoinertial Force, an Independent Variable in Egocentric Visual Localization of the Horizontal, NAV-SAM- and NASA Joint Rep. 98, Naval School of Aviation Medicine, Pensacola, Fla., July 1964.
- 7-422. Miller, E. F., Graybiel, A., Kellogg, R. S., Otolith Organ Activity within Earth Standard, One-Half Standard, and Zero Gravity Environments, NSAM-943, Naval School of Aviation Medicine, Pensacola, Fla., Aug. 1965.
- 7-423. Miller, H., Riley, M. B., Bondurant, S., et al., The Duration of Tolerance to Positive Acceleration, J. Aviat. Med., 30: 360-366, 1959.
- 7-424. Miller, P. B., Medical Problems of Weightlessness, SAM-TR-66-200, School of Aerospace Medicine, Brooks AFB, Texas, 1965.
- 7-425. Miller, P. B., Hartman, B. D., Johnson, R. L., et al., Modification of the Effects of Two Weeks of Bed Rest upon Circulatory Functions in Man, Aerospace Med., 35: 931-939, 1964.
- 7-426. Miller, P. B., Johnson, R. L., Lamb, L. E., Effects of Four Weeks of Absolute Bed Rest on Circulatory Functions in Man, Aerospace Med., 35: 1194-1200, 1964.
- 7-427. Miller, P. B., Johnson, R. L., Lamb, L. E., Effects of Moderate Physical Exercise during Four Weeks of Bed Rest on Circulatory Functions of Man, Aerospace Med., 36: 1077-1082, 1965.
- 7-428. Miller, P. B., Leverett, S. D., Jr., Tolerance to Transverse (+G_y) and Headward (+G_z) Acceleration after Prolonged Bed^x Rest, Aerospace Med., 36(1): 13-15, 1965.
- 7-429. Miller, P. B., Stevens, P. M., Johnson, R. L., et al., The Effect of Lower Body Negative Pressure during Prolonged Bed Rest on Circulatory Functions in Man, paper presented at the 36th Annual Scientific Meeting, Aerospace Medical Association, New York, N. Y., Apr. 26-29, 1965.
- 7-430. Mishkin, S., Jones, G. M., Predominant Direction of Gase during Slow Head Rotation, Aerospace Med., 37(9): 879-900, 1966.

- 7-431. Model, A. A., State of the Vestibular Analyzer in Persons Working with Sources of Ionizing Radiation, JPRS-32151, Joint Publications Research Service, New York, Sept. 1965. (Translation of Meditinskaya Radiologiya, 10(5): 71-74, May 1965).
- 7-432. Moore, E. W., Responses to Coriolis Stimulation in Flying Personnel with Different Levels of Proficiency, SAM-TR-66-36, School of Aerospace Medicine, Brooks AFB, Texas, Apr. 1966.
- 7-433. Moore, E. W., Cramer, R. L., Dowd, P. J., Effects of Motion Sickness on the Dynamic Characteristics of Responses, to Coriolis Stimulation, SAM-TR-65-67, School of Aerospace Medicine, Brooks AFB, Texas, Sept. 1965.
- 7-434. Morway, D., Lathrop, R., Chambers, R., et al., Effects of Prolonged Water Immersion on the Ability of Human Subjects to Make Position and Force Estimations, NADC-MA-6115, Naval Air Development Center, Johnsville, Pa., July 1963.
- 7-435. Moskalenko, Yu. Ye., Problems of Space Biology, Vol. 5. Dynamics of the Cerebral Blood Volume under Normal Conditions and Gravitational Stresses, NASA-TT-F-492, Feb. 1968. (Translation of Problemy Kosmicheskoy Biologii. Tom V. Dinamika Krovenapolneniya Golovnogo Mozga v Norme i Pri Gravitatsionnykh Nagruzkakh, Nauka Press, Leningrad, 1967).
- 7-436. Mueller, D. D., An Analysis of the Behavior of Long Tetherlines in Space, AMRL-TDR-62-123, Aerospace Medical Research Labs., Wright-Patterson AFB, Ohio, Nov. 1962.
- 7-437. National Academy of Sciences, National Research Council, Physiology in the Space Environment, Vol. II. Respiration, NAS-NRC-1485B, Washington, D. C., 1967. (Conference Report by the Space Science Board, NAS-NRC, Woods Hole, Mass., June-July 1966).
- 7-438. National Academy of Sciences, National Research Council, Symposium on Impact Acceleration Stress, with a Comprehensive Chronological Bibliography, Brooks AFB, Texas, Nov. 27-29, 1961, NAS-NRC-977, Washington, D. C., 1962.
- 7-439. National Academy of Sciences, National Research Council, United States Space Science Program Report to COSPAR Ninth Meeting, Vienna, Austria, May 1966, Space Science Board, Washington, D. C., 1966, pp. 227-233.

- 7-440. National Aeronautics and Space Administration, Biological Control Systems - A Critical Review and Evaluation, NASA-CR-59441, Nov. 1963.
- 7-441. National Aeronautics and Space Administration, Mercury Project Summary Including Results of the Fourth Manned Orbital Flight, May 15-16, 1963, NASA-SP-45, Oct. 1963.
- 7-442. National Aeronautics and Space Administration, Results of the Third U. S. Manned Orbital Space Flight, NASA-SP-12, 1962.
- 7-443. National Aeronautics and Space Administration, Second Symposium on the Role of the Vestibular Organs in Space Exploration, Ames Research Center, Moffett Field, Calif., Jan. 25-27, 1966, NASA-SP-115, 1966.
- 7-444. National Aeronautics and Space Administration, Space Medicine Directorate, Office of Manned Space Flight, A Review of Medical Results of Gemini 7 and Related Flights, Kennedy Space Center, Fla., Aug. 23, 1966.
- 7-445. National Aeronautics and Space Administration, A Study of the Dynamic Model Technique in the Analysis of Human Tolerance to Acceleration, NASA-TN-D-2645, Mar. 1965. (Stanley Aviation Corporation, Denver, Colo.).
- 7-446. Naval Air Development Center, Aviation Medical Acceleration Lab., Johnsville, Pa., Unpublished data on G Vectors and Error Performance, 1964.
- 7-447. Nesterenko, V. S., Effect of Coriolis Acceleration on Human Organism, JPRS-30927, Joint Publications Research Service, Washington, D. C., July 1965. (OTS-TT-65-31426).
- 7-448. Newberry, P. D., Johnson, W. H., Smiley, J. R., Effect of Hypoxic Hypoxia on Nystagmus Induced by Angular Acceleration, Aerospace Med., 36(11): 1090-1093, 1965.
- 7-449. Newsom, B. D., General Dynamics Corp., Convair Division, San Diego, Calif., personal communication on unpublished data, 1968.
- 7-450. Newsom, B. D., Physiological Considerations on Maintenance of Muscle Tone under Subgravity Conditions, General Dynamics/Astronautics, San Diego, Calif., in Transactions of the Ninth Symposium on Ballistic Missile and Space Technology, U. S. Naval Training Center, San Diego, Calif., Aug. 12-14, 1964, Aerospace Corp., Los Angeles, Calif., Vol. I, pp. 445-462.

- 7-451. Newsom, B. D., Brady, J. F., A Comparison of Performance Involving Head Rotations about Y & Z Cranial Axes in a Revolving Space Station Simulator, Aerospace Med., 37(11): 1152-1157, 1966.
- 7-452. Newsom, B. D., Brady, J. F., Observations on Subjects Exposed to Prolonged Rotation in a Space Station Simulator, GDC-ERR-AN-719, General Dynamics - Convair Division, San Diego, Calif., Feb. 1965.
- 7-453. Newsom, B. D., Brady, J. F., Observations on Subjects Exposed to Prolonged Rotation in a Space Station Simulator, in Symposium on the Role of the Vestibular Organs in the Exploration of Space, Pensacola, Fla., Jan. 20-22, 1965, NASA-SP-77, 1965, pp. 279-292.
- 7-454. Newsom, B. D., Brady, J. F., Goble, G. J., Equilibrium and Walking Changes Observed at 5, 7 1/2, 10 and 12 RPM in the Revolving Space Station Simulator, Aerospace Med., 36(4): 322-326, 1965.
- 7-455. Newsom, B. D., Brady, J. F., O'Laughlin, T. W., Final Report on a Study of Performance in a Revolving Space Station Simulator as a Function of Head Rotation about Y and Z Cranial Axes, GDC-DBD65-043-12, General Dynamics - Convair Division, San Diego, Calif., Nov. 1966.
- 7-456. Newsom, B. D., Brady, J. F., Shafer, W. A., et al., Adaptation to Prolonged Exposures in the Revolving Space Station Simulator, General Dynamics - Convair Division, San Diego, Calif., paper presented at the 36th Annual Scientific Meeting of the Aerospace Medical Association, New York, N. Y., Apr. 26-29, 1965.
- 7-457. Nicholson, A. N., Franks, W. R., Devices for Protection against Positive (Long Axis) Acceleration, in Environmental Biology, Altman, P. I., Dittmer, D. S., (eds.), AMRL-TR-66-194, Aerospace Medical Research Labs., Wright-Patterson AFB, Ohio, Nov. 1966, pp. 259-260.
- 7-458. Nicholson, J. F., Naas, D. W., Magnetic Shoes for Human Orientation in Space, WADC-TN-59-352, Wright Air Development Division, Wright-Patterson AFB, Ohio, Feb. 1960.
- 7-459. Niven, J. I., Hixson, W. J., Naval School of Aviation Medicine, Pensacola, Fla., unpublished data, 1964.

- 7-460. Niven, J. I., Hixson, W. C., Frequency Response of the Human Semicircular Canals. I. Steady-State Ocular Nystagmus Response to High Level, Sinusoidal Angular Acceleration, USN-SAM and NASA Joint Rep. 58, Naval School of Aviation Medicine, Pensacola, Fla., 1961.
- 7-461. Niven, J. I., Hixson, W. C., Correia, M. J., Elicitation of Horizontal Nystagmus by Periodic Linear Acceleration, NAMI-953, Naval Aerospace Medical Institute, Pensacola, Fla., Dec. 1965.
- 7-462. Niven, J. I., Whiteside, T. C. C., Graybiel, A., The Elevator Illusion: Apparent Motion of a Visual Target during Vertical Acceleration, NAV-SAM and NASA Joint Rep. 89, Naval School of Aviation Medicine, Pensacola, Fla., Oct. 1963.
- 7-463. Nolan, A. C., Marshall, H. W., Cronin, L., et al., Decreases in Arterial Oxygen Saturation and Associated Changes in Pressures and Roentgenographic Appearance of the Thorax during Forward (+G_x) Acceleration, Aerospace Med., 34: 797-813, 1963.
- 7-464. North American Aviation, Inc., Missile Division, Study in the Utilization of Hand Tools in Space, WADD-TDR-60-535, Wright Air Development Division, Wright-Patterson AFB, Ohio, Aug. 1960. (AD-259343).
- 7-465. Nungesser, W. C., Factors Influencing the Renal Regulation of Calcium - Implications of Prolonged Weightlessness, Aero-medical Review 2-65, School of Aerospace Medicine, Brooks AFB, Texas, May 1965.
- 7-466. Nuttall, J. B., The Problem of Spatial Disorientation, JAMA, 166(5): 431-438, Feb. 2, 1958.
- 7-467. Nyberg, J. W., Grimes, R. H., Finney, L. M., Modifications of the Effects of Recumbency upon Physiological Functions by Periodic Centrifugation, DAC-P-3871, Douglas Aircraft Co., Santa Monica, Calif., 1966.
- 7-468. Nyberg, J. W., Grimes, R. H., White, W. J., Consequence of Heart-to-Foot Acceleration Gradient for Tolerance to Positive Acceleration, DAC-P-3268, Douglas Aircraft Company, Santa Monica, Calif., Oct. 1965.
- 7-469. Oestreicher, H. L., Field and Impedance of Oscillating Sphere in Viscous-Elastic Medium with Applications to Biophysics, J. Acoust. Soc. Amer., 23: 707, 1951.

- 7-470. Ommaya, A. K., Hirsch, A. E., Martinez, J. L., The Role of Whiplash in Cerebral Concussion, in 10th Stapp Car Crash Conference, Holloman AFB, N. M., Nov. 8-9, 1966, pp. 197-203.
- 7-471. Ord, J. W., Cooper, K. H., Beller, B. M., et al., A Study Designed to Determine the Effectiveness of Vigorous Supine Exercise in Preventing Bed Rest Deconditioning: III. Body Composition, Blood Volume, Blood Gas Transport, and Flack Test Responses, paper presented at the 37th Annual Scientific Meeting, Aerospace Medical Association, Las Vegas, Nev., Apr. 18-22, 1966.
- 7-472. Panferova, N. Ye., Tishler, V. A., Popova, T. G., Effect of Prolonged Bedrest on the Dynamics of Cardiac Contractions in Man, in Space Biology and Medicine, 1(6): 117-123, 1967, JPRS-44732, Joint Publications Research Service, Washington, D. C., 1967. (Translation of Kosmicheskaya Biologiya i Meditsina, 1(6): 75-78, 1967).
- 7-473. Pao, Y. C., Mathematical Model Analysis of Underwater Simulation, (Study of Astronaut Capabilities to Perform Extravehicular Maintenance and Assembly Functions in Weightless Conditions), LS-66-0794, Garrett/AiResearch Mfg. Division, Los Angeles, Calif., Aug. 1966.
- 7-474. Parin, V. V., Volynkin, Y. M., Vassilyev, P. V., Manned Space Flight, USSR Academy of Sciences, Moscow, USSR, (presented at COSPAR Symposium, Florence, Italy), 1964.
- 7-475. Payne, P. R., An Analog Computer which Determines Human Tolerance to Acceleration, Rep. 101-1, Frost Engineering Development Corp., Denver, Colo., 1961.
- 7-476. Payne, P. R., The Dynamics of Human Restraint Systems, in Impact Acceleration Stress Symposium, Brooks AFB, Texas, Nov. 27-29, 1961, NAS-NRC-977, National Academy of Sciences, National Research Council, Washington, D. C., 1962, pp. 195-257.
- 7-477. Payne, P. R., Personnel Restraint and Support System Dynamics, AMRL-TR-65-127, Aerospace Medical Research Labs., Wright-Patterson AFB, Ohio, Oct. 1965.
- 7-478. Payne, P. R., Stech, E. L., Human Body Dynamics under Short-Term Acceleration, Tech. Rep. 115-2, Frost Engineering Development Corporation, Denver, Colo., June 1962.

- 7-479. Perey, O., Fracture of the Vertebral End Plate in the Lumbar Spine, Acta Orthop. Scand. Suppl. XXV, Stockholm, 1957.
- 7-480. Pesman, G. J., Acceleration Terminology, Table of Comparative Equivalents, in Principles of Biodynamics, Prolonged Acceleration: Linear and Radial, AGARD, Biodynamics Committee, NATO, 1968, Chapt. 1, pp. 1-6.
- 7-481. Pesman, G. J., Eiband, A. M., Crash Injury, NACA-TN-3775, 1956.
- 7-482. Pesman, G. J., Scherer, H. F., Jr., Extension of the Measured Experience of Human Impact Loads, NASA-Manned Spacecraft Center, Houston, Texas, presented at the 34th Annual Meeting, Aerospace Medical Association, Los Angeles, Calif., Apr. 29- May 2, 1963.
- 7-483. Peterson, R. L., Personnel Seating Research for Air Force Aerospace Vehicles, SAE-851C, Presented at the Air Transport and Space Meeting, N. Y., Apr. 27-30, 1964.
- 7-484. Pierce, B. F., Wolf, R. L., Casco, E. L., The Use of Space Suits in Water Immersion Studies, in A Collection of Papers on Space Suits and Human Performance, REL-HFG-65-1, Chrysler Corporation, Space Division, New Orleans, La., Aug. 1965, pp. 4-1 - 4-7.
- 7-485. Pierson, W. R., Geller, R. E., Work in Low Friction Environment, AIAA J., 3: 1074-1079, 1965.
- 7-486. Pigg, L. D., Kama, W. N., Visual Acuity in Relation to Body Orientation and G-Vector, AMRL-TDR-62-74, Aerospace Medical Research Labs., Wright-Patterson AFB, Ohio, 1962.
- 7-487. Pine, A., Survey and Summary of Man-in-Space Simulation Techniques and Limitations, SS-3933, Garrett/AiResearch Manufacturing Division, Los Angeles, Calif., Oct. 1965.
- 7-488. Pitts, D. G., Visual Illusions and Aircraft Accidents, SAM-TR-67-28, School of Aerospace Medicine, Brooks AFB, Texas, Apr. 1967.
- 7-489. Poli, C. R., A Study of Retrieval Techniques for Tethered Astronauts, SEG-TR-65-30, Systems Engineering Group, Wright-Patterson AFB, Ohio, July 1965.
- 7-490. Poli, C. R., Hanavan, E. P., Jr., A Three-Mass Retrieval Study for the Gemini Tethered Astronaut, SEG-TR-65-29, Systems Engineering Group, Wright-Patterson AFB, Ohio, July 1965.

- 7-491. Popov, V. A., Rozanov, Yu. A., Sil'vestrov, M. M., An Information Model of the Extravehicular Dynamics of Cosmonaut Body Movements and Spatial Orientation, NASA-TT-F-10407, Nov. 1966. (Translation of Russian paper presented at the 17th International Astronautical Congress, Madrid, Oct. 9-15, 1966).
- 7-492. Power, G. G., Jr., Hyde, R. W., Sever, R. J., et al., Pulmonary Function in Man during Prolonged Acceleration. I. Diffusing Capacity and Blood Flow, NADC-ML-6512, Naval Air Development Center, Johnsville, Pa., June 1965.
- 7-493. Preber, L., Vegetative Reactions in Caloric and Rotary Tests, Acta Oto-Laryngol., Suppl. 144, 1958.
- 7-494. Raymond, S. A., Greenleaf, J. E., Matter, M., Jr., Effects of Acute and Chronic Hypohydration on Tolerance to +G Acceleration in Man: II. Impressions of Subjects, NASA-TM-X-1255, Sept. 1966.
- 7-495. Rees, D. W., Copeland, N. K., Discrimination of Differences in Mass of Weightless Objects, WADD-TR-60-601, Wright Air Development Division, Wright-Patterson AFB, Ohio, Dec. 1960.
- 7-496. Richmond, D. R., Bowen, I. G., White, C. S., Tertiary Blast Effects: Effects of Impact on Mice, Rats, Guinea Pigs and Rabbits, DASA-1245, Defense Atomic Support Agency, Washington, D. C., Feb. 1961. (Also in Aerospace Med., 32: 789-805, 1961).
- 7-497. Roberts, J. F., Walking Responses under Lunar and Low Gravity Conditions, (M. S. Thesis), Air Force Institute of Technology, Wright-Patterson AFB, Ohio, 1962. (Also AMRL-TDR-63-112, Aerospace Medical Research Labs., Wright-Patterson AFB, Ohio, 1963).
- 7-498. Roberts, J. B., Hygh, A. B., Hygh, E. H., A Comparison of Methods for the Evaluation of Protective Headgear, Aerospace Med., 35(11): 1044-1047, 1964.
- 7-499. Roberts, V. L., Hodgson, V. R., Thomas, L. M., Fluid Pressure Gradients Caused by Impact to the Human Skull, ASME-66-Huf-1, American Society of Mechanical Engineers, N. Y., 1966.
- 7-500. Roman, J. A., Warren, B. H., Graybiel, A., The Sensitivity to Stimulation of the Semicircular Canals during Weightlessness, SAM-TDR-62-148, School of Aerospace Medicine, Brooks AFB, Texas, Feb. 1963.

- 7-501. Rose, B., Stewart, W. K., Review of the Practicability of and Necessity for Anti-G Devices in the RAF with Particular Reference to the Franks' Flying Suit Mk. III, FPRC-584, Flying Personnel Research Committee, Air Ministry, London, July 1944.
- 7-502. Ross, B. M., Chambers, R. M., Effects of Transverse G-Stress on Running Memory, NADC-MR-6712, Naval Air Development Center, Johnsville, Warminster, Pa., June 1967. (Also in Percept. and Motor Skills, 24: 423-435, 1967).
- 7-503. Roth, E. M., Bioenergetic Considerations in the Design of Space Suits for Lunar Exploration, NASA-SP-84, 1966.
- 7-504. Roth, E. M., Biological and Engineering Implications of Space-Cabin Atmospheres, Lovelace Foundation for Medical Education and Research, Albuquerque, N. M., 1967, paper presented at the Conference on Bioastronautics, Virginia Polytechnic Institute, Blacksburg, Va., Aug. 14-18, 1967.
- 7-505. Roth, E. M., Space-Cabin Atmospheres, Part I - Oxygen Toxicity, NASA-SP-47, 1964.
- 7-506. Roth, H. P., Chart prepared at the University of California, Los Angeles, Calif., 1949.
- 7-507. Rothe, W. E., Pope, E. E., Lim, S. T., Fletcher, J. G., Research on the Human Physiologic Response to Prolonged and Angular Acceleration, A. Engineering Activities. B. Physiologic Activities, SAM-TR-67-69, School of Aerospace Medicine, Brooks AFB, Texas, Sept. 1967.
- 7-508. Rothstein, J. D., Brown, W. K., Feasibility Study: Lateral Impact with Standard Aircraft Harness Configuration, ARL-TR-66-3, Aeromedical Research Lab., Holloman AFB, N. M., Feb. 1966.
- 7-509. Royal Air Force, Physiology Laboratory, Devices for Protecting Pilots from Effects of High Acceleration with Particular Reference to Trials of the Franks' Suit, FPRC-498, Flying Personnel Research Committee, Air Ministry, London, Nov. 1942.
- 7-510. Royal Air Force, Physiology Laboratory, Flight Tests on Franks' Hydrostatic Suit, FPRC-339, Flight Personnel Research Committee, Air Ministry, London, July 1941.

- 7-511. Rubin, W., Vestibular Mechanism, Motion Sickness, and Drug Therapy. Experimental and Clinical Evaluations, Arch. Otolaryng. (Chicago), 80: 431-439, 1964.
- 7-512. Ruff, S., Brief Acceleration: Less than One Second, Vol. I, Pt. VI-C of German Aviation Medicine, World War II, Dept. Air Force, Superintendent of Documents, Government Printing Office, Washington, D. C., 1950, pp. 584-599.
- 7-513. Rushmer, R. F., Cardiovascular Dynamics, 2nd Ed., W. B. Saunders, Philadelphia, Pa., 1961, Chapter 3.
- 7-514. Rushmer, R. F., Green, E. L., Kingsley, H. D., Internal Injuries Produced by Abrupt Deceleration of Experimental Animals, Project no. 401, Rep. 1, School of Aviation Medicine, Randolph Field, Texas, Jan. 15, 1946.
- 7-515. Sadoff, M., Effects of High Sustained Acceleration on Pilot's Performance and Dynamic Response, NASA-TN-D-2067, 1965.
- 7-516. Samueloff, S. L., Browse, N. L., Shepherd, J. T., Response of Capacity Vessels in Human Limbs to Headup Tilt and Suction on Lower Body, J. Appl. Physiol., 21: 47-54, 1966.
- 7-517. Sasaki, E. H., Donning and Doffing the "Phase B" Apollo Prototype Space Suit during Zero Gravity, AMRL-TDR-64-32, Aerospace Medical Research Labs., Wright-Patterson AFB, Ohio, Apr. 1964.
- 7-518. Sasaki, E. H., Effect of Transient Weightlessness on Binocular Depth Perception, AMRL-TDR-63-134, Aerospace Medical Research Labs., Wright-Patterson AFB, Ohio, Dec. 1963.
- 7-519. Sasaki, E. H., Feasibility of Using Handrails to Move along a Surface While Weightless, AMRL-TR-65-152, Aerospace Medical Research Labs., Wright-Patterson AFB, Ohio, Aug. 1965.
- 7-520. Schlei, E. J., Vergamini, P. L., Simons, J. C., Some Motion Characteristics of Tethered Free Floating Workers, AMRL-Memo-P-13, Aerospace Medical Research Labs., Wright-Patterson AFB, Ohio, Oct. 1962.
- 7-521. Schmitt, T. J., Wind-Tunnel Investigation of Air Loads on Human Beings, DTMB-Aero Rep. 858, David Taylor Model Basin, Washington, D. C., Jan. 1954.

- 7-522. Schock, G. J. D., Apparent Motion of a Fixed Luminous Target during Subgravity Trajectories, AFMDC-TN-58-3, Air Force Missile Development Center, Holloman AFB, N. M., Feb. 1958.
- 7-523. Schock, G. J. D., A Study of Animal Reflexes during Exposure to Subgravity and Weightlessness, Aerospace Med., 32: 336-340, Apr. 1961.
- 7-524. Schone, H., On the Role of Gravity in Human Spatial Orientation, Aerospace Med., 35(8): 764-772, 1964.
- 7-525. Seale, L. M., Bailey, W. E., Powe, W. E., Study of Space Maintenance Techniques, ASD-TDR-62-931, Aeronautical Systems Division, Wright-Patterson AFB, Ohio, May 1963.
- 7-526. Seeman, J. S., Smith, F. H., Mueller, D. D., A Technique to Investigate Space Maintenance Tasks, AMRL-TR-66-32, Aerospace Medical Research Labs., Wright-Patterson AFB, Ohio, Apr. 1966.
- 7-527. Seiff, A., Whiting, E., The Effect of the Bow Shock Wave on the Stability of Blunt-Nosed Slender Bodies, NASA-TM-X-377, 1960.
- 7-528. Selzer, M. L., Gikas, P. W., Huelke, D. F., The Prevention of Highway Injury, Proceedings of a Symposium, University of Michigan, Apr. 19-21, 1967, Highway Research Institute, Univ. of Michigan, Ann Arbor, Mich., 1967. (PB-176624).
- 7-529. Sem-Jacobsen, C. W., Recording of In-Flight Stress in Jet Fighter Planes, Aerospace Med., 31: 320, Apr. 1960.
- 7-530. Seminara, J. L., Lunar Simulation, LMSC-679964, Lockheed Missiles and Space Co., Sunnyvale, Calif., Dec. 1967.
- 7-531. Seminara, J. L., Kincaid, W. K., Jr., Control Task Performance in the Lunar Visual Environment, LMSC-685055, Lockheed Missiles and Space Co., Sunnyvale, Calif., Feb. 1968.
- 7-532. Senders, J. Frost, G., Crocker, J., The Human Operator, in Bioastronautics Data Book, Webb, P., (ed.), NASA-SP-3006, 1964, Section 18, pp. 343-361.
- 7-533. Sergeyev, A. A., Physiological Mechanisms of the Action of Accelerations, JPRS-43412, Joint Publications Research Service, Washington, D. C., Nov. 1967. (Translation of Russian book Fiziologicheskkiye Mekhanizmy Deystviya Uskoreniy, Nauka Publishing House, Leningrad, 1967, pp. 1-391).

- 7-534. Shapland, D. J., The Dynamic Model, An Engineering Approach to the Problem of Tolerance to Abrupt Accelerations, Stanley Aviation Corporation, paper presented at the Symposium on Impact Acceleration Stress, Brooks AFB, San Antonio, Texas, Nov. 27-29, 1961.
- 7-535. Sharp, E. D., Sears, C. W., Walking in Zero G Using Velcro, AMRL-Memo-P-23, Aerospace Medical Research Labs., Wright-Patterson AFB, Ohio, Jan. 1963.
- 7-536. Shavelson, R. J., Seminara, J. L., The Effect of Lunar Gravity on Man's Performance of Basic Maintenance Tasks, LMSC-6-77-96-0, Lockheed Missiles and Space Co., Sunnyvale, Calif., June 1967.
- 7-537. Shuster, D. H., Evaluation of Replacement Times of Spacecraft Radios under Simulated Weightlessness, in A Collection of Papers on Space Suits and Human Performance, REL-HFG-65-1, Chrysler Corporation, Space Division, New Orleans, La., Aug. 1965, pp. 5-1 - 5-15.
- 7-538. Sieker, H. O., Devices for Protection Against Negative Acceleration, Part 1; Centrifuge Studies, WADC TR-52-87, Wright Air Development Center, Wright-Patterson AFB, Ohio, June 1952.
- 7-539. Simons, J. C., Gardner, M. S., Weightless Man: A Survey of Sensations and Performance while Free-Floating, AMRL-TDR-62-114, Aerospace Medical Research Labs., Wright-Patterson AFB, Ohio, Mar. 1963.
- 7-540. Simons, J. C., Walk, D. E., Sears, C. W., Motion Performance of Pressure-suited Subjects under Zero and Lunar Gravity Conditions, Aerospace Med., 36(5): 406-414, 1965.
- 7-541. Simons, J. C., Walking in Zero G, WADC-TR-59-327, Wright Air Development Center, Wright-Patterson AFB, Ohio, Oct. 1959.
- 7-542. Sisakyan, N. M., Yazdovsky, V. I., The First Group Flight into Outer Space, JPRS-25272, Joint Publications Research Service, Washington, D. C. (Translated from Pervyye Gruppovoy Kosmicheskiy Polet, 1964, pp. 1-156).
- 7-543. Sisakyan, N. M., Yazdovsky, V. I., The First Manned Space Flights, FTD-TT-62-1619, Foreign Technology Division, Wright-Patterson AFB, Ohio, 1962. (Translation of Pervyye Kosmicheskiye Polety Cheloveka, Moscow, 1962).

- 7-544. Smedal, H. A., Creer, B. Y., Wingrove, R. C., Ability of Pilots to Perform a Control Task in Various Sustained Acceleration Fields, Aerospace Med., 31: 901-906, 1960.
- 7-545. Smedal, H. A., Creer, B. Y., Wingrove, R. C., Physiological Effects of Acceleration Observed during a Centrifuge Study of Pilot Performance, NASA-TN-D-345, Dec. 1960.
- 7-546. Smedal, H. A., Rogers, T. A., Duane, T. D., et al., The Physiological Limitations of Performance during Acceleration, Aerospace Med., 34: 48-55, 1963.
- 7-547. Smedal, H. A., Stinnett, G. W., Innis, R. C., A Restraint System Enabling Pilot Control under Moderately High Acceleration in a Varied Acceleration Field, NASA-TN-D-91, 1960.
- 7-548. Smedal, H. A., Vykukal, H. C., Gallant, R. P., et al., Crew Physical Support and Restraint in Advanced Manned Flight Systems, Amer. Rocket Soc. J., 31: 1544-1548, Nov. 1961.
- 7-549. Smith, J. L., Effect of Accelerations on the Vestibular Analyzer, LC-ATD-66-62, Library of Congress, Air Technology Division, Washington, D. C., June 1966.
- 7-550. Snively, G. G., Chichester, C. O., Impact Survival Levels of Head Accelerations, Aerospace Med., 32: 316-320, 1961.
- 7-551. Snyder, R. G., Human Tolerances to Extreme Impacts in Free-Fall, Aerospace Med., 34: 695-709, 1963. (Also Preprint ASMA-63-67, paper presented at the 34th Annual Meeting of the Aerospace Medical Association, Apr. 29-May 2, 1963, Los Angeles, Calif.).
- 7-552. Snyder, R. G., Physiological Effects of Impact: Man and other Mammals, in Environmental Biology, Altman, P. L., Dittmer, D. S., (eds.), AMRL-TR-66-194, Aerospace Medical Research Labs., Wright-Patterson AFB, Ohio, Nov. 1966, pp. 231-242.
- 7-553. Snyder, R. G., Survival of High-Velocity Free-Falls in Water, FAA-AM-65-12, Federal Aviation Agency, Oklahoma City, Okla., Apr. 1965.
- 7-554. Snyder, R. G., Snow, C. C., Young, J. W., et al., Experimental Comparison of Trauma in Lateral (+G_y), Rearward Facing (+G_x), and Forward Facing (-G_x) Body Orientations when Restrained by Lap Belt Only, Aerospace Med., 38(9): 889-894, 1967.

- 7-555. Society of Automotive Engineers, Inc., 10th Stapp Car Crash Conference, Holloman AFB, New Mexico, Nov. 8-9, 1966, N. Y., 1966.
- 7-556. Sohn, R. L., Design of Spacecraft for Manned Planetary Mission, paper presented at the 16th International Astronautical Congress, Athens, Greece, Sept. 15, 1965.
- 7-557. Sohn, R. L., Manned Mars Trips Using Venus Swingby Modes, in AIAA/NASA Third Manned Space Flight Meeting, Houston, Texas, Nov. 4-6, 1964, AIAA-CP-10, pp. 330-338.
- 7-558. Sonntag, R. W., Jr., Capt., USAF, 6571st Aeromedical Research Lab., Holloman AFB, N. M., unpublished data, 1968. (Also Sonntag, R. W., Jr., Intracranial Pressure in Macaca Speciosa during Controlled Abrupt Deceleration, in Preprints of Scientific Program, 1967 Annual Scientific Meeting, Aerospace Medical Association, Washington, D. C., Apr. 10-13, 1967, pp. 162-163).
- 7-559. Spady, A. A., Jr., Harris, R. L., Effects of Pressure Suits and Backpack Loads on Man's Self-Locomotion in Earth and Simulated Lunar Gravity, NASA-TN-D-4464, Apr. 1968.
- 7-560. Spady, A. A., Jr., Krasnow, W. D., Exploratory Study of Man's Self-Locomotion Capabilities with a Space Suit in Lunar Gravity, NASA-TN-D-2641, July 1966.
- 7-561. Spiegel, E. A., Sommer, I., Vestibular Mechanisms, in Medical Physics, Glasser, O., (ed.), Yearbook Publishers, Inc., Chicago, Ill., 1944, Vol. I, pp. 1638-1652.
- 7-562. Squires, R. D., Jensen, R. E., Sipple, W. C., et al., Electroencephalographic Changes in Human Subjects during Black-out Produced by Positive Acceleration, NADC-MA-6402, Naval Air Development Center, Johnsville, Pa., Apr. 1964.
- 7-563. Stapp, J. P., Collected Data on 46 Rocket Sled Experiments (Holloman AFB), NSL-65-94, Northrop Space Labs., Hawthorne, Calif., Contract No. AF41(609)-2317, May 1965.
- 7-564. Stapp, J. P., Effects of Mechanical Force on Living Tissues. I. Abrupt Deceleration and Windblast, J. Aviat. Med., 26: 268-288, 1955.
- 7-565. Stapp, J. P., Human Tolerance to Deceleration, Summary of 166 Runs, J. Aviat. Med., 22(1): 42-45, 1951.

- 7-566. Stapp, J. P., Whole Body Tolerance to Impact, in Environmental Biology, Altman, P. L., Dittmer, D. S., (eds.), AMRL-TR-66-194, Aerospace Medical Research Labs., Wright-Patterson AFB, Ohio, Nov. 1966, pp. 228-230.
- 7-567. Stapp, J. P., Blount, W. C., Effects of Mechanical Force on Living Tissues. III. A Compressed Air Catapult for High Impact Forces, J. Aviat. Med., 28: 281-290, 1957.
- 7-568. Stapp, J. P., Hughes, C. D., Effects of Mechanical Force on Living Tissues. II. Supersonic Deceleration and Windblast, J. Aviat. Med., 27: 407-413, 1956.
- 7-569. Stapp, J. P., Mosely, D., Lombard, C. F., et al., Analysis and Biodynamics of Selected Rocket-Sled Experiments, Northrop Space Labs., Hawthorne, Calif., Contract No. AF41(609)-2317, July 1964.
- 7-570. Stapp, J. P., Taylor, E. R., Space Cabin Landing Impact Vector Effects on Human Physiology, Aerospace Med., 35(12): 1117-1133, 1964.
- 7-571. Stech, E. L., The Effect of Age on Vertebral Breaking Strength, Spinal Frequency, and Tolerance to Acceleration in Human Beings, Tech. Note 122-101, Frost Engineering Development Corp., Englewood, Colo., Jan. 1963.
- 7-572. Stech, E. L., The Variability of Human Response to Acceleration in the Spinal Direction, Rep. 122-09, Frost Engineering Development Corp., Englewood, Colo., May 1963.
- 7-573. Steele, J. E., Motion Sickness and Spatial Perception, in Symposium on Motion Sickness with Special Reference to Weightlessness, AMRL-TR-63-25, Aerospace Medical Research Labs., Wright-Patterson AFB, Ohio, June 1963, pp. 43-65.
- 7-574. Steiner, S. H., Mueller, G. C. E., Heart Rate and Forward Acceleration, J. Appl. Physiol., 16: 1078-1080, 1961.
- 7-575. Stevens, P. M., Lamb, L. E., Effects of Lower Body Negative Pressure on the Cardiovascular System, Amer. J. Cardiol., 16: 506-515, 1965.
- 7-576. Stevens, P. M., Lynch, T. N., Effects of 9-Alphafluorohydrocortisone on Dehydration due to Prolonged Bed Rest, Aerospace Med., 36: 1151-1156, 1965.

- 7-577. Stevens, P. M., Lynch, T. N., Gilbert, C. A., Potential Uses of Lower Body Negative Pressure as an Anti-Deconditioning Measure during Weightlessness, in Preprints of Scientific Program, 37th Annual Scientific Meeting, Aerospace Medical Association, Las Vegas, Nev., Apr. 18-21, 1966, pp. 160-161.
- 7-578. Stevens, P. M., Lynch, T. N., Johnson, R. L., et al., Effects of 9-Alphafluorohydrocortisone and Venous Occlusive Cuffs on Orthostatic Deconditioning of Prolonged Bed Rest, Aerospace Med., 37(10): 1049-1056, 1966.
- 7-579. Stevens, P. M., Miller, P. B., Lynch, T. N., et al., Effects of Lower Body Negative Pressure on Physiologic Changes due to Four Weeks of Hypoxic Bed Rest, Aerospace Med., 37: 466-474, 1966.
- 7-580. Stewart, W. K., Effect of Abdominal Compression on Ability to Withstand G: Final Report, FPRC-300, Flying Personnel Research Committee, Air Ministry, London, May 1941.
- 7-581. Stewart, W. K., Efficiency of Abdominal Belts in the Prevention of Blacking-Out, FPRC-176, Flying Personnel Research Committee, Air Ministry, London, Aug. 1940.
- 7-582. Stewart, W. K., Franks' Suit: Progress Notes, FPRC-390, Flying Personnel Research Committee, Air Ministry, London, Dec. 1941.
- 7-583. Stewart, W. K., Investigation of Blacking-Out in Defiant L. 7024, FPRC-269, Flying Personnel Research Committee, Air Ministry, London, Mar. 26, 1941.
- 7-584. Stewart, W. K., Note on Spencer Acceleration Belt and Leggings USA Firm, FPRC-458, Flying Personnel Research Committee, Air Ministry, London, May 1942.
- 7-585. Stewart, W. K., Report on the Cotton Pneumodynamic Suit, FPRC-407, Flying Personnel Research Committee, Air Ministry, London, Jan. 1942.
- 7-586. Stiehm, E. R., Different Effects of Hypothermia on Two Syndromes of Positive Acceleration, J. Appl. Physiol., 18: 387-392, 1963.
- 7-587. Stoll, A. M., Human Tolerance to Positive G as Determined by the Physiological Endpoints, J. Aviat. Med., 27: 356-367, 1956.

- 7-588. Stone, R. W., Jr., Letko, W., Some Observations on the Stimulation of the Vestibular System of Man in a Rotating Environment, in Symposium on the Role of the Vestibular Organs in the Exploration of Space, Pensacola, Fla., Jan. 20-22, 1965, NASA-SP-77, 1965, pp. 263-278.
- 7-589. Stone, R. W., Jr., Letko, W., Tolerance to Vehicle Rotation of Subjects Using Turning and Nodding Motion of the Head While Performing Simple Tasks, AIAA-64-218, presented at the First Annual Meeting of the AIAA, June 28-July 2, 1964, Washington, D. C.
- 7-590. Stone, R. W., Jr., Letko, W., Hook, W. R., Examination of a Possible Flight Experiment to Evaluate an Onboard Centrifuge as a Therapeutic Device, in Second Symposium on the Role of the Vestibular Organs in Space Exploration, Ames Research Center, Moffett Field, Calif., Jan. 25-27, 1966, NASA-SP-115, 1966, pp. 245-256.
- 7-591. Stone, R. W., Jr., Piland, W. M., Factors Related to Weightlessness in Space: A Review of Potential Problems and Prospective Solutions, NASA-Langley Working Paper 425, July 6, 1967.
- 7-592. Stubbs, S. M., Dynamic Model Investigation of Water Pressures and Accelerations Encountered during Landings of the Apollo Spacecraft, NASA-TN-D-3980, Sept. 1967.
- 7-593. Stubbs, S. M., Landing Characteristics of the Apollo Spacecraft with Deployed-Heat-Shield Impact Attenuation Systems, NASA-TN-D-3059, Jan. 1966.
- 7-594. Swearingen, J. J., Evaluation of Various Padding Materials for Crash Protection, FAA-AM-66-40, Federal Aviation Agency, Oklahoma City, Okla., Dec. 1966.
- 7-595. Swearingen, J. J., Tolerance of the Human Face to Crash Impact, FAA-AM-65-20, Federal Aviation Agency, Oklahoma City, Okla., July 1965.
- 7-596. Swearingen, J. J., McFadden, E. B., Garner, J. D., et al., Human Voluntary Tolerance to Vertical Impact, Aerospace Med., 31: 989-998, 1960.
- 7-597. Swearingen, J. J., McFadden, E. B., Garner, J. D., et al., Protection of Shipboard Personnel against the Effects of Severe Short-Lived Upward Forces Resulting from Underwater Explosions, Federal Aviation Agency, Civil Aeromedical Research Inst., Oklahoma City, Okla., Jan. 1960. (Under Navy Contract NA-ONR-104-51).

- 7-598. Swet, C. J., Some Applications of Passive Spacecraft Orientation Techniques, Johns Hopkins University, Applied Physics Lab., Silver Spring, Md., SAE-Paper 857A, presented at the SAE Air Transport and Space Symposium, N. Y., Apr. 1964.
- 7-599. Taliaferro, E. H., Wempen, R. R., White, W. J., The Effects of Minimal Dehydration upon Human Tolerance to Positive Acceleration, DAC-P-3114, Douglas Aircraft Company, Los Angeles, Calif., 1964.
- 7-600. Taylor, E. R., Biodynamics: Past, Present and Future, ARL-TDR-63-10, Aeromedical Research Lab., Holloman AFB, N. M., Mar. 1963.
- 7-601. Taylor, E. R., Rhein, L. W., Carter, V. L., Jr., et al., The Effects of Severe Impact on Bears, ARL-TDR-64-6, Aeromedical Research Lab., Holloman AFB, N. M., July 1964.
- 7-602. Taylor, H. L., Henschel, A., Brozek, J., et al., Effects of Bed Rest on Cardiovascular Function and Work Performance, J. Appl. Physiol., 2: 223-239, 1949.
- 7-603. Taylor, J. W., X-Irradiation and Acceleration Stress, NADC-MA-6003, Naval Air Development Center, Johnsville, Pa., 1960.
- 7-604. Taylor, N. B. G., Hunter, J., Johnson, W. H., Antidiuresis as a Measurement of Laboratory Induced Motion Sickness, Canad. J. Biochem. Physiol., 35(11): 1017-1027, 1957.
- 7-605. Teichner, W. H., Craig, R. L., Human Tolerance Limits for Environmental Exposures with Special Reference to Apollo, Summary, Compendium, Critique, NASA Grant NGR 22-007-070, Guggenheim Center for Aerospace Health and Safety, Harvard School of Public Health, Boston, Mass., Mar. 1967.
- 7-606. Thompson, A. B., A Proposed New Concept for Estimating the Limit of Human Tolerance to Impact Acceleration, Aerospace Med., 33: 1349-1355, 1962.
- 7-607. Tieber, J. A., Lindemuth, R. W., An Analysis of the Inertial Properties and Performance of the Astronaut Maneuvering System, AMRL-TR-65-216, Aerospace Medical Research Labs., Wright-Patterson AFB, Ohio, Dec. 1965.
- 7-608. Torphy, D. E., Effects of Short-Term Bed Rest and Water Immersion on Plasma Volume and Catecholamine Response to Tilting, Aerospace Med., 37: 383-387, 1966.

- 7-609. Trout, O. F., Jr., A Water-Immersion Technique for the Study of Mobility of a Pressure-Suited Subject under Balanced-Gravity Conditions, NASA-TN-D-3054, Jan. 1966.
- 7-610. Turnbow, J. W., Impact Test Methods for Helmets, Supplement I to Helmet Design Criteria for Improved Crash Survival, Tech. Rep. 65-44A, Army Aviation Materiel Labs., Fort Eustis, Va., Jan. 1966.
- 7-611. Turnbow, J. W., Carroll, D. F., Haley, J. L., Jr., et al., Crash Survival Design Guide, USAAVLABS-TR-67-22, Army Aviation Materiel Labs., Fort Eustis, Va., 1967.
- 7-612. U. S. Air Force, Seat System, Upward Ejection, Aircraft, General Specifications for, MIL-S-9479A, 16 June 1967.
- 7-613. U. S. National Committee for the I. G. Y., Memorandum-TP-21, June 10, 1958. (Also USSR, Academy of Sciences, Pravda, Moscow, Apr. 27, 1958).
- 7-614. U. S. Navy, Vertigo, Approach Magazine, U. S. Naval Aviation Safety Review, NAVAER-00-75-510, Vol. 4(3): 28-33, Sept. 1958.
- 7-615. Urschel, G. W., Hood, W. B., Jr., Cardiovascular Effects of Rotation in the Z Axis, Aerospace Med., 37(3): 254-256, 1966.
- 7-616. Usami, M., Study of the Influence of Rotatory Stimulation upon Respiration, J. Oto-Rhino-Laryngological Soc. of Japan, 65(5): 662-671, 1962, DRB-T-84-J, Directorate of Scientific Information Services, Defence Research Board, Canada, Sept. 1964.
- 7-617. Useller, J. W., Algranti, J. S., Pilot Reaction to High Speed Rotation, Aerospace Med., 34: 501-504, 1963.
- 7-618. Vallbona, C., Spencer, W. A., Vogt, F. B., et al., The Effect of Bed Rest on Various Parameters of Physiological Function, Part IX: The Effect on the Vital Signs and Circulatory Dynamics, NASA-CR-179, 1965.
- 7-619. Vallbona, C., Vogt, F. B., Cardus, D., et al., The Effect of Bed Rest on Various Parameters of Physiological Function, Part I: Review of the Literature on the Physiological Effects of Immobilization, NASA-CR-171, 1964.

- 7-620. Van Patten, R. E., A Restraint System for Application in R_x and -G_x Acceleration Environments with Emphasis upon Knee and Lower Leg Restraints, AMRL-TR-64-144, Aerospace Medical Research Labs., Wright-Patterson AFB, Ohio, Dec. 1964.
- 7-621. Van Schaik, P. N., Test Results of the Astronaut Maneuvering Unit, ASD-TDR-63-71, Aeronautical Systems Division, Wright-Patterson AFB, Ohio, Mar. 1963.
- 7-622. Van Sickle, N. D., Modern Airmanship, 2nd ed., Van Nostrand & Co., N. Y., 1961.
- 7-623. Vasil'yev, P. V., Kotovskaya, A. R., Physiological Reactions of Man Subjected to Accelerations under Space Flight Conditions, NASA-TT-F-9597, Oct. 1965. (Translation of paper presented at the XVI International Aeronautical Congress, Athens, Greece, Sept. 13-18, 1965).
- 7-624. Vinacke, W. E., Aviator's Vertigo, J. Aviat. Med., 19: 158-170, 1948.
- 7-625. Vogt, F. B., Effect of Extremity Cuff-Tourniquets on Tilt Table Tolerance after Water Immersion, Aerospace Med., 36: 442-447, 1965.
- 7-626. Vogt, F. B., Effect of Intermittent Leg Cuff Inflation and Intermittent Exercise on the Tilt Table Response after Ten Days Bed Recumbency, Aerospace Med., 37: 943-947, 1966.
- 7-627. Vogt, F. B., An Objective Approach to the Analysis of Tilt Table Data, Aerospace Med., 37: 1195-1204, Dec. 1966.
- 7-628. Vogt, F. B., Plasma Volume and Tilt Table Response to Water - Immersion Deconditioning Experiments Using Extremity Cuffs, Aerospace Med., 38: 460-464, May 1967.
- 7-629. Vogt, F. B., Use of Extremity Cuffs as a Cardiovascular Reflex Conditioning Technique, NASA-CR-90248, Mar. 1967.
- 7-630. Vogt, F. B., Cardus, D., Vallbona, C., et al., The Effect of Bed Rest on Various Parameters of Physiological Function. Part VI: The Effect of the Performance of Periodic Flack Maneuvers on Preventing Cardiovascular Deconditioning of Bed Rest, NASA-CR-176, 1965.
- 7-631. Vogt, F. B., Johnson, P. C., Effectiveness of Extremity Cuffs or Leotards in Preventing or Controlling the Cardiovascular Deconditioning of Bed Rest, Aerospace Med., 38: 702-707, July 1967.

- 7-632. Vogt, F. B., Johnson, P. C., Plasma Volume and Extracellular Fluid Volume Change Associated with 10 Days Bed Recumbency, Aerospace Med., 38: 21-25, Jan. 1967.
- 7-633. Vogt, F. B., Johnson, P. C., Study of Effect of Water Immersion on Healthy Adult Male Subjects: Plasma Volume and Fluid Electrolyte Changes, Aerospace Med., 36: 447-451, May 1965.
- 7-634. Vogt, F. B., Mack, P. B., Beasley, W. G., et al., The Effect of Bed Rest on Various Parameters of Physiological Function. Part XII. The Effect of Bed Rest on Bone Mass and Calcium Balance, NASA-CR-182, 1965.
- 7-635. Vogt, F. B., Mack, P. B., Johnson, P. C., et al., Tilt Table Response and Blood Volume Changes Associated with Fourteen Days of Recumbency, Aerospace Med., 38: 43-48, 1967.
- 7-636. Vogt, F. B., Mack, P. B., Johnson, P. C., Tilt Table Response and Blood Volume Changes Associated with Thirty Days of Recumbency, Aerospace Med., 37: 771-779, Aug. 1966
- 7-637. Vogt, F. B., Spencer, W. A., Cardus, D., et al., The Effects of Bed Rest on Various Parameters of Physiological Function, Part XIII: A Review of Possible Mechanisms of Orthostatic Intolerance to Passive Tilt, NASA-CR-183, 1966.
- 7-638. Volynkin, Y. M., Yazdovskiy, V. I., The First Manned Space Flights, FTD-TT-62-1619, Foreign Technology Div., Wright-Patterson AFB, Ohio, Dec. 1962.
- 7-639. Voronin, G. V., Effect of an Electrical Stimulus on the Reaction of the Human Vestibular Apparatus Caused by Acceleration, in Space Biology and Medicine, 1(4): 142-152, 1967, JPRS-43762, Joint Publications Research Service, Washington, D. C., 1967. (Translation of Kosmicheskaya Biologiya i Meditsina, 1(4): 92-99, 1967).
- 7-640. Vought Astronautics, Study of Orbital Launch Operations, Vol. II, AST-EIR-13491, Dallas, Texas, June 1961.
- 7-641. Vykukal, H. C., Gallant, R. P., Stinnett, G. W., An Interchangeable, Mobile Pilot-Restraint System, Designed for Use in High Sustained Acceleration Force Fields, Aerospace Med., 33: 279-285, Mar. 1962.
- 7-642. Walsh, E. G., The Perception of Rhythmically Repeated Linear Motion in the Horizontal Plane, Brit. J. Psychol., 53: 439-445, 1962.

- 7-643. Walton, W. G., Compensatory Cyclo-torsion Accompanying Head Tilt, Amer. J. Optom., 25: 525, 1948.
- 7-644. Ward, J. L., Senders, J. W., Methodological Studies of Tracking Behavior: The Effect of Various Supplemental Information Feedbacks, BBN-1458, Bolt, Beranek and Newman, Inc., Cambridge, Mass., Dec. 1966.
- 7-645. Warzecha, L. W., Merrick, E. J., Criteria and Techniques for Maintenance, Repair, and Assembly in Manned Orbital Operations, General Electric Co., Philadelphia, Pa., IAS Paper 62-136, paper presented at the IAS National Summer Meeting, Los Angeles, Calif., June 19-22, 1962.
- 7-646. Watson, J. F., Cherniack, N. S., Effect of Positive Pressure Breathing on the Respiratory Mechanics and Tolerance to Forward Acceleration, ASD-TR-61-398, Aeronautical Systems Division, Wright-Patterson AFB, Ohio, Aug. 1961.
- 7-647. Watson, J. F., Cherniack, N. S., Zechman, F. W., Respiratory Mechanics during Forward Acceleration, J. Clin. Invest., 39: 1737-1743, 1960.
- 7-648. Watts, D. T., Mendelson, E. S., Hunter, H. N., Tolerance to Vertical Acceleration Required for Seat Ejection, J. Aviat. Med., 18: 554-564, 1947.
- 7-649. Webb Associates, Inc., Design, Fabricate, Test and Deliver a Cardiovascular Conditioning Suit, Malibu, Calif., NASA Langley Contract NAS1-6004, 1967.
- 7-650. Webb, P., Human Water Exchange in Space Suits and Capsules, NASA-CR-804, 1967.
- 7-651. Webb, P., Impact and Vibration, in Bioastronautics Data Book, Webb, P., (ed.), NASA-SP-3006, Section 5, 1964, pp. 63-85.
- 7-652. Webster, A. P., Hunter, H. N., Acceleration Chart, J. Aviat. Med., 25: 378-379, 1954.
- 7-653. Wegmann, H. M., Bruner, H., Klein, K. E., et al., Enzymatic and Hormonal Responses to Exercise, Lowered Pressure, and Acceleration in Human Plasma and Their Correlation to Individual Tolerances, Fed. Proc., 25: 1405-1408, 1966.
- 7-654. Weis, E. B., Jr., Clarke, N. P., Brinkley, J. W., Human Response to Several Impact Acceleration Orientations and Patterns, Aerospace Med., 34: 1122-1129, 1963.

- 7-655. Weis, E. B., Jr., Clarke, N. P., Brinkley, J. W., et al., Mechanical Impedance as a Tool in Research on Human Response to Acceleration, Aerospace Med., 35(10): 945-950, 1964.
- 7-656. Weis, E. B., Jr., von Gierke, H. E., Clarke, N. P., Mechanical Impedance as a Tool in Biomechanics, ASME-63-WA-280, 1963, American Society of Mechanical Engineers, Winter Annual Meeting, Philadelphia, Pa., Nov. 17-22, 1963.
- 7-657. Weiss, H. S., Edelberg, R., Charland, P. V., et al., Animal and Human Reactions to Rapid Tumbling, J. Aviat. Med., 25: 5-22, 1954.
- 7-658. Weiss, H. S., Edelberg, R., Charland, P. V., et al., The Physiology of Simple Tumbling, WADC-TR-53-139, Part 2, Wright Air Development Center, Wright-Patterson AFB, Ohio, 1954.
- 7-659. Wendt, G. R., The Nature of Adaptation to Oscillatory Rotation, in Symposium on the Role of the Vestibular Organs in the Exploration of Space, Pensacola, Fla., Jan. 20-22, 1965, NASA-SP-77, 1965, pp. 133-139.
- 7-660. Wendt, G. R., Studies of Adaptation to Bodily Rotation in Humans, Annual Progress Report, University of Rochester, Rochester, N. Y., May 1, 1964 - Apr. 1, 1965. (AD-461547).
- 7-661. Wendt, G. R., Vestibular Functions, in Handbook of Experimental Psychology, Stevens, S. S., (ed.), John Wiley and Sons, N. Y., 1951.
- 7-662. Wersall, J., Lundquist, P. G., Morphological Polarization of the Mechanoreceptors of the Vestibular and Acoustic Systems, in Second Symposium on the Role of the Vestibular Organs in Space Exploration, NASA-Ames Research Center, Moffett Field, Calif., Jan. 25-27, 1966, NASA-SP-115, pp. 57-72.
- 7-663. West, J. B., Dollery, C. T., Distribution of Blood Flow and the Pressure-Flow Relations of the Whole Lung, J. Appl. Physiol., 20: 175-183, 1965.
- 7-664. White, C. S., The Scope of Blast and Shock Biology and Problem Areas in Relating Physical and Biological Parameters, DASA-1856, Defense Atomic Support Agency, Washington, D. C., Nov. 1966.

- 7-665. White, C. S., Bowen, I. G., Richmond, D. R., Biological Tolerance to Air Blast and Related Biomedical Criteria, CEX-65-4, Atomic Energy Commission, Civil Effects Test Operation, Washington, D. C., Oct. 18, 1965.
- 7-666. White, P. D., Nyberg, J. W., Finney, L. M., et al., A Comparative Study of the Physiological Effects of Immersion and Bed Rest, DAC-59226, Douglas Aircraft Co., Inc., Santa Monica, Calif., June 1966.
- 7-667. White, P. D., Nyberg, J. W., Finney, L. M., et al., Influence of Periodic Centrifugation on Cardiovascular Functions of Man during Bed Rest, DAC-59286, Douglas Aircraft Co., Inc., Santa Monica, Calif., June 1966.
- 7-668. White, S. C., Johnston, R. S., Pesman, G. J., Review of Biomedical Systems for M-3 Flight, in Conference on Medical Results of the First U. S. Manned Suborbital Space Flight, National Aeronautics and Space Administration, Washington, D. C., June 1961.
- 7-669. White, W. J., Douglas Aircraft Co., Inc., Santa Monica, Calif., personal communication, 1967.
- 7-670. White, W. J., Acceleration and Vision, WADC-TR-58-333, Wright Air Development Center, Wright-Patterson AFB, Ohio, Nov. 1958.
- 7-671. White, W. J., Effects of Transient Weightlessness on Brightness Discrimination, Aerospace Med., 36(4): 327-331, 1965.
- 7-672. White, W. J., A Space-Based Centrifuge - 1965 Status Report, DAC-P-3436, Douglas Aircraft Company, Santa Monica, Calif., 1965.
- 7-673. White, W. J., Variations in Absolute Visual Threshold during Accelerative Stress, WADC-TR-60-34, Wright Air Development Center, Wright-Patterson AFB, Ohio, 1960.
- 7-674. White, W. J., Jorve, W. R., The Effects of Gravitational Stress upon Visual Acuity, WADC-TR-56-247, Wright Air Development Center, Wright-Patterson AFB, Ohio, Nov. 1956.
- 7-675. White, W. J., Monty, R. A., Vision and Unusual Gravitational Forces, in Visual Capabilities in the Space Environment, Baker, C. A., (ed.), Pergamon Press, N. Y., 1965, pp. 65-89.

- 7-676. White, W. J., Nyberg, J. W., White, P. D., et al., Biomedical Potential of a Centrifuge in an Orbiting Laboratory, SSD-TDR-64-209 Suppl., Space Systems Division, Los Angeles, Calif., July 1965.
- 7-677. White, W. J., Riley, M. B., The Effects of Positive Acceleration on the Relation between Illumination and Instrument Reading, WADC-TR-58-332, Wright Air Development Center, Wright-Patterson AFB, Ohio, 1958.
- 7-678. Whiteside, T. C. D., Hand-Eye Coordination in Weightlessness, Aerospace Med., 32: 719-725, Aug. 1961.
- 7-679. Whiteside, T. C. D., Graybiel, A., Niven, J. I., Visual Illusions of Movement, FPRC-1207, Flying Personnel Research Committee, Air Ministry, London, 1963.
- 7-680. Woellner, R. C., Graybiel, A., Counterrolling of the Eyes and Its Dependence on the Magnitude of Gravitational or Inertial Force Acting Laterally on the Body, J. Appl. Physiol., 14: 632-634, 1959.
- 7-681. Wood, C. D., Kennedy, R. S., Graybiel, A., Review of Anti-motion Sickness Drugs from 1954-1964, Aerospace Med., 36(1): 1-4, 1965.
- 7-682. Wood, E. H., Code, C. F., Baldes, E. H., Protection Afforded the Human by Hydrostatic as Compared to Pneumatic Anti-G Devices, NRC-CAM-207, National Research Council, Committee on Aviation Medicine, Nov. 12, 1943.
- 7-683. Wood, E. H., Nolan, A. C., Donald, D. E., et al., Influence of Acceleration on Pulmonary Physiology, Fed. Proc., 22: 1024-1034, 1963.
- 7-684. Wood, E. H., Nolan, A. C., Marshall, H. W., et al., Decreases in Arterial Oxygen Saturation as an Indicator of the Stress Imposed on the Cardio-Respiratory System by Forward Acceleration (+G_x), AMRL-TDR-63-104, Aerospace Medical Research Labs.,^xWright-Patterson AFB, Ohio, 1963.
- 7-685. Woodward, C., et al., Investigation, Design and Development of an F 7U-3 Ejection Seat Energy Absorption System of Protection of Crash Force Loads, NAMC-ACEL-335, Naval Air Material Center, Air Crew Equipment Lab., Philadelphia, Pa., June 1957.
- 7-686. Wortz, E. C., AiResearch Mfg. Co., Division of Garrett Corp., Los Angeles, Calif., personal communication on unpublished data, 1968.

- 7-687. Wortz, E. C., Browne, L. E., Shreck, W. H., et al., Study of Astronaut Capabilities to Perform Extravehicular Maintenance and Assembly Functions in Weightless Conditions, NASA-CR-859, Sept. 1967.
- 7-688. Wunder, C. C., A Survey of Chronic Weightlessness Simulation in Biological Research, AFSCM-TDR-64-1, Headquarters Air Force Systems Command, Andrews AFB, Md., 1964.
- 7-689. Young, L. R., Li, Y. T., Studies of Human Dynamic Space Orientation Using Techniques of Control Theory, NASA-CR-85781, Jan. 1967.
- 7-690. Yeremin, A., Training of a Human Being for Weightlessness, in Studies in Physical Training for Weightlessness, JPRS-30111, Joint Publications Research Service, Washington, D. C., May 1965, pp. 7-15.
- 7-691. Young, J. W., Smith, R. E., Jr., Trajectory Optimization for an Apollo-Type Vehicle under Entry Conditions Encountered during Lunar Return, NASA-TR-R-258, May 1967.
- 7-692. Young, L. R., A Sampled Data Model for Eye Tracking Movements, Doctoral Thesis, Massachusetts Institute of Technology, Cambridge, Mass., June 1962.
- 7-693. Young, L. R., Li, Y. T., Studies of Human Dynamic Space Orientation Using Techniques of Control Theory, NASA-CR-57292, Dec. 1964.
- 7-694. Young, L. R., Meiry, J. L., Li, Y. T., Control Engineering Approaches to Human Dynamic Space Orientation, in Second Symposium on the Role of the Vestibular Organs in Space Exploration, NASA-Ames Research Center, Moffett Field, Calif., Jan. 25-27, 1966, NASA-SP-115, pp. 217-227.
- 7-695. Yuganov, Ye.M., Gorshkov, A. I., Kasyan, I. I., et al., Vestibular Reactions of Cosmonauts during the Flight in the Voskhod Spaceship, Aerospace Med., 37(7): 691-694, 1966.
- 7-696. Yuganov, Ye. M., Siedl'nikov, I. A., et al., Sensory Reactions of Man and Sensitivity of the Vestibular Analyzer under Short-Term Weightlessness, FTD-TT-64-1052, Foreign Technology Division, Wright-Patterson AFB, Ohio, Dec. 1964.
- 7-697. Yuganov, Ye. M., Zakhmatov, D. M., Illusory Perceptions during Flight under Complex Meteorological Conditions, J. of Med. Military (Moscow), 4: 30, 1958.

- 7-698. Zarriello, J. J., Norsworthy, M. E., Bower, H. R., A Study of Early Grayout Threshold as an Indicator of Human Tolerance to Positive Radial Acceleratory Force, Project NM 11-02-11, Subtask 1, Report No. 1, U. S. Naval School of Aviation Medicine, Pensacola, Fla., 1958.
- 7-699. Zechman, F. W., Cherniack, N. S., Hyde, A. S., Ventilatory Response to Forward Acceleration, J. Appl. Physiol., 15: 907-910, 1960.
- 7-700. Zellmer, R. W., Granville, J. W., McNee, R. C., et al., Significance of Combined Stresses of G Forces and Irradiation, Aerospace Med., 34: 626-629, 1963.
- 7-701. Zim, M. H., Her Journey of No Return, Life Mag. 62: 64A-67, Mar. 24, 1967.
- 7-702. Zuckerman, S., Black, A. N., The Effect of Impact on the Head and Back of Monkeys, Rep. R. C. 124, Ministry of Home Security, Oxford, England, Aug. 1940.

8. VIBRATION

Prepared by

E. M. Roth, M. D., Lovelace Foundation
A. N. Chambers, Bellcomm, Inc.

TABLE OF CONTENTS

8.	VIBRATION	8-1
	Nomenclature and Principles	8-1
	Biomechanical Responses of Body to Vibration	8-6
	Longitudinal Vibrations ($\pm G_z$)	8-9
	a) Supine Vibrations ($\pm G_z$)	8-11
	b) Semi-Supine Vibrations	8-13
	Transverse Vibrations ($\pm G_x$)	8-19
	Vibrations Transmitted to the Hand	8-21
	Skull Vibrations	8-22
	Transfer Functions and Power Spectra of Random Vibration	8-22
	Tissue Impedance	8-32
	Ultrasonic Vibrations	8-33
	Patho-physiological Response to Vibration	8-34
	Permanent Pathological Changes	8-34
	Physiological Response	8-35
	Subjective Response	8-36
	Longitudinal or Vertical Vibration ($\pm G_z$)	8-36
	Semi-Supine and Other Vibrational Axes	8-41
	Threshold of Vibration Sensation	8-46
	The Cardiovascular System and Blood	8-48
	Respiratory Physiology.	8-48
	Metabolic Factors.	8-51
	Human Tolerance to Vibration	8-51
	Visual Effects.	8-67
	Visual Acuity	8-67
	Effects on Visual Tasks	8-75
	Vigilance, Concentration and Reaction Time During Vibration.	8-78

Simple Motor Performance	8-78
Performance of Complex Tasks	8-79
Performance Under Combined Vibration and Linear G	8-89
Performance on Launch Towers During Horizontal Oscillation	8-91
Protection Against Vibration	8-91
References	8-95

The vibration environment in space operations covers a wide range of amplitudes and frequencies. One must consider vibration due to spacecraft booster and control rockets, aerodynamic loading, cabin machinery, and equipment, as well as vibration in land and water surface vehicles supporting operations. Much can be preplanned regarding the vibration environment but unexpected contingency resonances, especially in emergency modes of operation, may suddenly appear on the scene. A study of the accuracy of vibration predictions in spacecraft design is available (14).

Vibration seldom occurs in the operational situation as a single isolated variable. Other environmental variables such as weightlessness, linear acceleration, etc., can be expected to interact with vibration to either reduce or increase the debilitating effects. Equipment variables include such things as size of graduations or illumination of instruments, inflated pressure suits, etc.; procedural variables include such things as task load, variations in time of task performance, etc.; and finally, personal variables, such as fatigue and deconditioning from weightlessness or inactivity, etc., all may have effects. The effects of some of these can be predicted at this time; others must await further research.

After a review of nomenclature and principles, data will be presented on the biomechanical characteristics of the human; the physiological and biochemical response, and finally, degradation of performance in response to vibration.

NOMENCLATURE AND PRINCIPLES

Vibration is defined as the periodic motion of the particles of an elastic body or medium in alternately opposite directions from the position of equilibrium when that equilibrium has been disturbed. The vibration, therefore, may occur in air, liquid, or solid media; however, the primary concern here is with the oscillation of solid or semisolid bodies (e.g., structures of the spacecraft) in contact with the human body. Some nonauditory effects on the body are produced by transmission of vibration through the air; however, most of this occurs in the audio range and therefore is covered in Sound and Noise, (No. 9).

The parameters of vibration which are significant for an understanding of the effects of vibration on the human body are as follows:

Frequency

Frequency is usually specified in cycles per second (cps) or Hertz (Hz) and may extend from greater than zero to the megacycle range. The band of concern with respect to the effects on the human body is usually confined to that less than 1000 Hz. Most of the significant effects of vibration occur

within the 0.5 to 50 Hz range. Within this range the human body responds as a complex system of masses, elasticities, and dampers having lumped parameters. Above 50 Hz, it is more appropriate to regard the body as a continuous viscous-elastic medium for vibration applied to the surface of the body. Below 0.5 Hz vibration is experienced as single jolts and as such, may be experienced as motion sickness. See Acceleration, (No. 7).

Displacement

Displacement, which is usually expressed in inches or centimeters, is defined as the maximum half-wave (single amplitude) or full-wave (double amplitude) displacement. The term amplitude is not synonymous with displacement. One refers to displacement amplitude or acceleration amplitude.

Velocity

Velocity, in inches/second or cm/second, is the first derivative of displacement and ordinarily is not used in describing the effects of vibration on the human body.

Acceleration

Acceleration inches/second² or cm/second², is the second time derivative of displacement and ordinarily is expressed as maximum or peak g. For sinusoidal vibration:

$$G = \frac{A(2\pi f)^2}{386} \quad (1)$$

Where A = single amplitude of displacement in inches

f = frequency in Hz

For random vibration the acceleration is given as root mean square (r.m.s.) acceleration, or r.m.s. per frequency band.

Jolt

Jolt, in inches/second³, is the third derivative of amplitude. The rate of onset of linear impact is a significant factor in evaluation of human tolerance to vibration of low frequency such as the 1/2 cycle vibration of impact.

Duration

Duration of vibration, in seconds or minutes, is important in establishing the effects of vibration. This includes short-term exposures, long-term exposures (over 1 hour) for which there is very little research data, and repeated exposures for which there is even less.

Figure 8-1 represents the relationship of some of these parameters. Vibrations may be considered sinusoidal when composed of a single sine wave; complex, when composed of any other wave form; and non-periodic, which may approach randomness, when composed of waves which do not repeat systematically. Random, or semirandom waves, are usually characterized in terms of a power density curve (PSD) which is derived from the frequency bands that characterize the random vibrations.

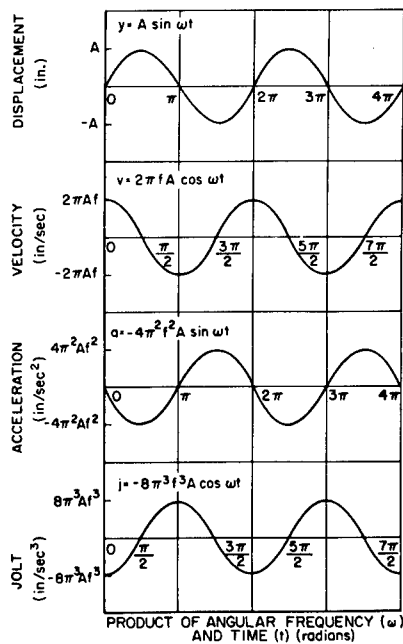


Figure 8-1

Relationship of the Parameters of Sinusoidal Vibration

(After Morgan et al (eds.)⁽¹¹⁴⁾)

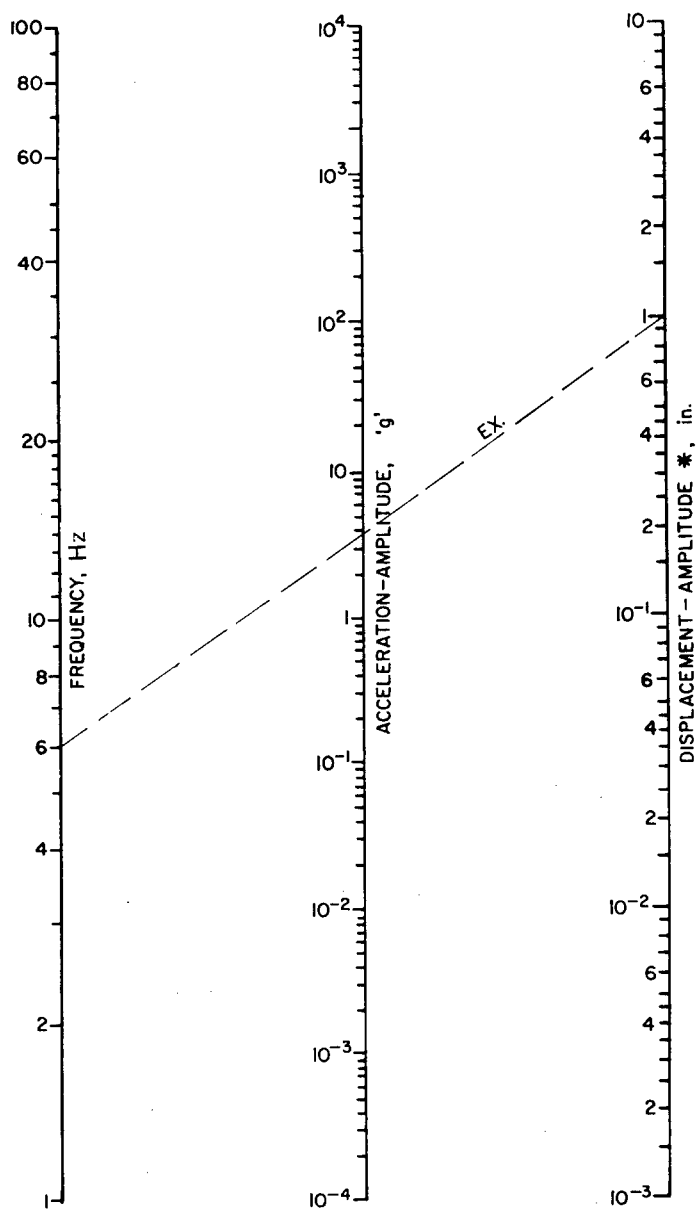
Figures 8-2a and b represent a nomogram allowing interconversion of frequency, amplitude, and acceleration factors in sinusoidal vibration.

The transmission of vibration to and within the human body is dependent on the following:

- Direction of application of vibration to the human body which includes one, or any combination of the axes of the body. (See Figure 7-1 in Acceleration, (No. 7) for nomenclature of axes). Most vibration research has been confined to the longitudinal axis (Z) of the body, since this has been the most common condition in most vehicles. However, in space vehicles, vibration can be expected to also occur in the direction of the fore-aft (X) axis of the body, or laterally along the Y axis.
- Point of application of vibration to the human body which includes whole body vibration transmitted through seats (when subject is seated), through the feet (when standing), through the length of the body (when reclining), or combinations of these. Also, vibration may be transmitted via a body part such as the hand (when holding a vibrating control). Vibration of instruments may also be included in the latter category where the effects are primarily confined to the visual system.

Figure 8-2

Interconversion of Physical Factors in Vibration



* = HALF PEAK-TO-PEAK AMPLITUDE

Example of use: To determine the acceleration-amplitude of a vibration of 6 Hz at 1 in. (half-wave) amplitude (i.e. 2 in. peak-to-peak), lay a straight-edge across the chart joining 6 Hz with 1 in. amplitude.

Answer: The acceleration-amplitude is 4 g (approximately)

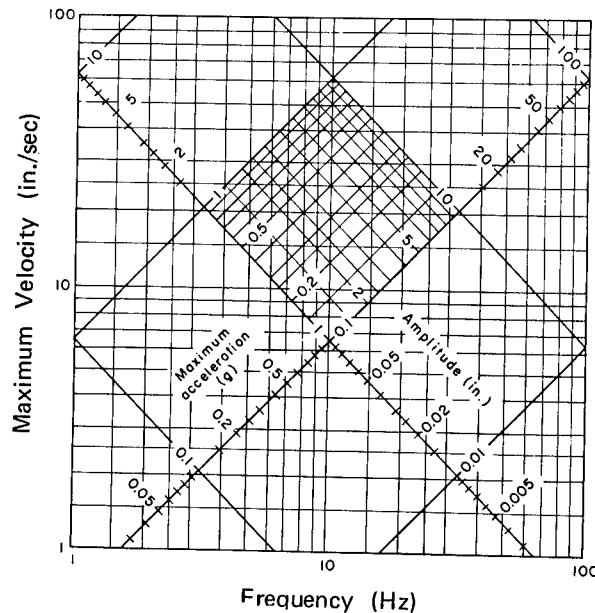
- a. Nomogram of Frequency, Displacement-Amplitude and Acceleration-Amplitude for Sinusoidal Vibration

(After Guignard⁽⁸⁰⁾)

Figure 8-2 (continued)

b. Conversions Between the Parameters of Vibration

(After Morgan et al (eds.)⁽¹¹⁴⁾)



- Position of the body also determines the effects of vibration on the body and is related to the point of application. Effects are different depending on whether the person is seated, standing, reclining, prone, supine, or crouched.
- Materials interposed between the body and source of vibration affects transmission of vibration to the body. This includes the effects of padding on seats, spring mountings, etc.
- Restraint of the body may attenuate or increase the effects of vibration depending on the frequency and amplitude. This includes the restraint of the person by seat belts and harnesses against a vibrating seat, support for the arm in operating a control, wearing of girdles (which restrain the abdominal region), etc.
- Interaction with other environmental variables may also enhance or reduce vibration and vibration effects. The presence of acceleration forces (e.g., linear $+G_z$), reduced gravitation, and null gravity can be expected to affect the transmission characteristics.

The transmission of vibration within the human body is dependent on the following:

- Body size, build, and weight with greater attenuation involving larger masses and densities
- Posture, whether erect or slumped; and
- Muscular tension and fatigue (91).

The response of the human body, which establishes the criteria for this Compendium, can be considered under the headings of physical or biomechanical, pathological, physiological, and performance. Of these, the biomechanical responses, which cause discomfort and pain, establish most of the physiological tolerance limits to vibration. Each of these responses will be described in some detail below.

BIOMECHANICAL RESPONSES OF BODY TO VIBRATION

Basic concepts in the biomechanical structure of the body have been covered under impact in Acceleration, (No. 7).

The physical responses of the body are primarily the result of the body acting as a complex system of masses, elasticities, dampings, and couplings in the low frequency range (i.e., up to 50 Hz). The impedance of the body and its parts and organs damp vibration over certain frequency and amplitude ranges. For certain other frequency/amplitude ranges, there are resonances which amplify the vibration within various portions or all of the body. In general, the impedance of the body and its parts and inherent resonance factors influence the transmission characteristics of the vibration through the body (137, 139).

Figure 8-3 is a model of the dynamic mechanical properties of the human body. The body system for the low-frequency range below 100 Hz can be approximated partially or in toto by a lumped-parameter system, i.e., a system consisting of rigid bodies and restraining elements of negligible mass.

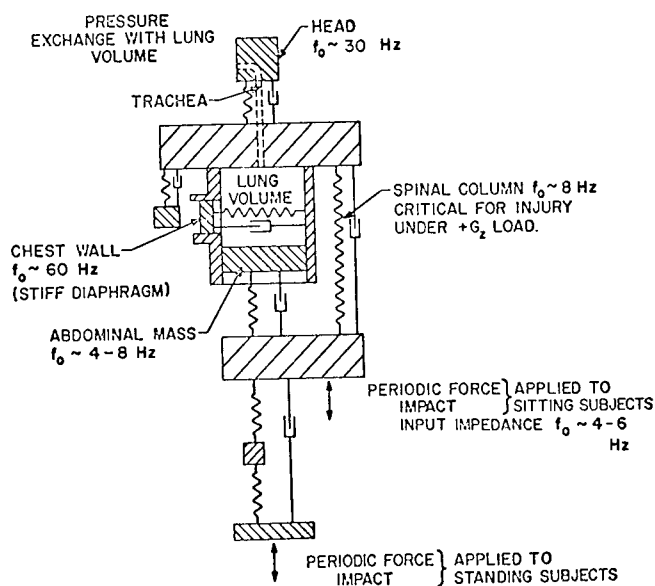


Figure 8-3

Mechanical Model for the Human Body for G_z
Vibration and Impact Loads and External
Pressure Loads (Acoustic, Blast, Decompression)

(After von Gierke⁽⁶⁷⁾)

Calculation of the response of such a system to static, transient or dynamic forces presents a "network" rather than a field problem. The characteristics of such a system can be determined experimentally by studying its resonance behavior when exposed to steady state vibrations of varying frequency (33).

The smaller the masses involved, the higher is the resonant frequency of the subsystem. The main torso resonances of the sitting or standing man are between 4 and 6 Hz, whereas the resonance of the head relative to the shoulder is in the order of 20-30 Hz (30, 33).

Mechanical energy, per se, transferred from the environment to the man is primarily deterministic of biologic effects (69, 179, 180, 182). The impedance model, then, is essentially an energy transfer model. As such, its purpose is to delineate the energy exchange characteristics of the human body. There are several pertinent aspects to the energy characteristics: the distribution of the real or dissipated energy over the frequency range, the distribution of the reactive or stored energy over the frequency range and the total amount of each. The model defines the energy transfer patterns and, while it gives no a priori estimate of absolute levels, it does indicate that certain types of environments will be more likely to present tolerance problems than others.

Also, the energy transfer to the human from the environment can be given in terms of the impedance and the power density spectrum of the velocity (105, 140, 141, 142, 143, 144, 171). This means that one can reduce a particular acceleration-time history to its power spectrum in order to judge its effect. This has the advantage that it eliminates the need for approximating very erratic acceleration-time histories. Therefore, knowledge of impedance and phase angles permits calculation of the coupling of mechanical energy transmitted to the body under different modes of application and protection. (See Figure 8-10.) (137, 139)

This approach is especially useful in non-sinusoidal forms of vibration as are often met in operational situations. In the case of the steady state non-sinusoidal excitation it is necessary to resolve the force and velocity wave forms into a finite or infinite (Fourier) series of sinusoidal components. In the case of the transient excitation it is necessary to break the aperiodic waveform into an infinite series of sinusoidal components by means of the Fourier integral. In the case of random excitation the problem is more difficult because the waveform cannot be broken into sinusoidal components. However, it is still possible to calculate the impedance factors by dealing with the auto- and cross-correlation functions of force and velocity. These functions are actually definitions of the average characteristic of the signals and they do have Fourier integrals. The electric analogues of these problems in power circuits have been amenable to computer treatment (85, 142, 179).

Above roughly 100 Hz, lumped-parameter models become more and more unsatisfactory; a distributed-constant, continuous medium must be introduced to describe the wave phenomena observed in these frequency ranges (68). The characteristics of their propagation and the internal damping of vibrations at higher frequencies tend to localize effects of such stimuli. For higher frequencies, through the audio-frequency range and up to about 100 kHz, the wave propagation of vibratory energy becomes more and more important but the type of wave propagation (shear waves, surface waves, or compressional waves) is strongly influenced by boundaries and geometrical configurations. Above 100 kHz and up into the MHz range, compression waves predominate and are propagated in a beam-like manner. This viewpoint permits not only a phenomenological description of the body's mechanical properties but, in an increasing number of cases, forms the basis for attempts to explain the behavior of tissue in terms of microscopic tissue- and cell-structure.

Vibration measurements of the body's response are usually made whenever possible by non-contact methods. New cinerentgenographic methods have been used successfully to measure the displacement of internal organs, while optical, cinematographic, and stroboscopic observation can give the displacement amplitudes of larger parts of the body (106, 181). Small vibrations can sometimes be measured without contact by capacitive probes located at small distance from the (grounded) body surface. The probe forms a condenser with the body; capacity changes due to vibrations can be measured in a high frequency carrier system. If vibration pickups in contact with the body are used, they must be small and light enough so as not to introduce a distorting mechanical load. This usually places a weight limitation on the pickup of a few grams or less, depending on the frequency range of interest and the effective mass to which the pickup is attached. For example, Figure 8-16b illustrates the effect of weight and size on the response of accelerometers attached to the skin overlying soft tissue.

New laser techniques are being developed to detect and measure vibration of mechanical structures (119). Measurement of transmission of external force through fluid systems of the body under vibration is currently under study (15).

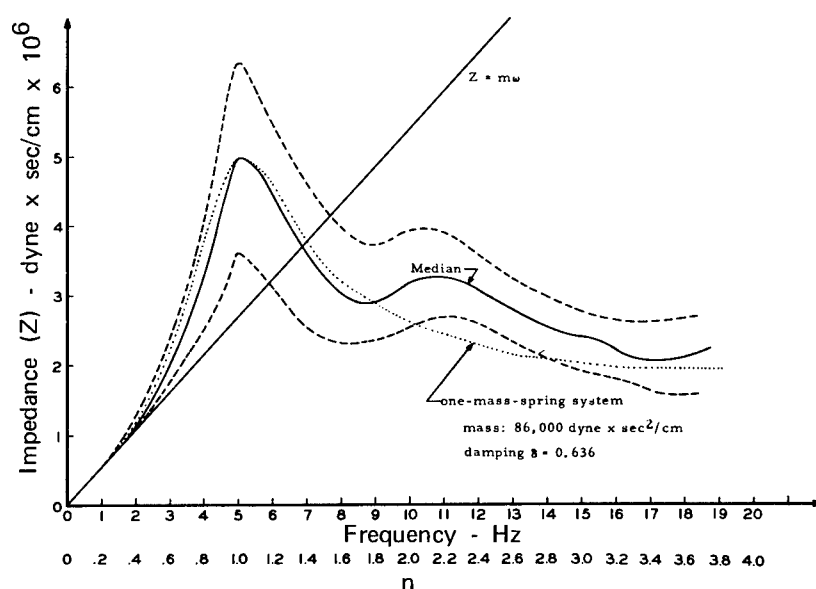
Living organisms have linear characteristics only in the low frequency range and for very small deformation. (See discussions of Figures 8-17 and 8-18.) For higher frequencies and large forces, a non-linear response must be expected. The damping coefficients, for instance, may depend on the instantaneous velocity of the organ displacements. This deviation from the assumed viscous damping and the participating mass may change with higher accelerations. There will be a difference, therefore, between the response of an organism to steady-state vibration with relatively low acceleration and to impact pulses with short, high accelerations (27). This consideration holds for the responses of the whole body as well as for a single organ or organ complex.

Since the natural frequency of the studied organ system in a given animal differs much from the related organ of man, their responses to a certain form of excitation cannot be compared. Also the posture of the living subject will have an influence on his dynamic response, necessitating a careful control of the subject's position during the test. Establishing tolerance criteria for man, using animals as substitutes, presumes that the tissue strength in animals is the same as in man. This is not a too unreasonable assumption (133). Scaling factors are now under study (66). In evaluating impedance curves, it should be kept in mind that the impedances, reflecting resonances and tissue damping are not independent of the shaking intensity whether expressed in terms of amplitudes or peak velocity or peak accelerations. It has been shown that the force between subject and support does not increase linearly with these parameters (24, 48, 103, 185). (See Figure 8-9a.) The nature of the padding material between shaker and subject as well as the level and direction of linear acceleration bias can influence the determination of the resonance spectrum of the body (26, 48). (See Figure 8-11a and b.)

Excellent reviews of impedance and transmission parameters of man are available from which the following discussion is taken (27, 28, 29, 33, 179, 180).

Longitudinal Vibrations ($\pm G_z$)

The average response of sitting human subjects to steady-stage vibration in the frequency range 0 to 20 Hz is illustrated in Figure 8-4. Up to two Hz, the impedance of the whole body is the same as the impedance of a pure mass ($m\omega$), indicating that the body moves as a whole unit. Around 5 Hz, a resonance peak produces the greatest deformation of the whole body, and a second peak around 10.5 Hz demonstrates a resonance of a subsystem in the body.



Median and the twentieth and eightieth percentile of the impedance of eight different subjects, compared with the impedance of a pure mass ($m\omega$) and a one-mass-spring system with damping.

Figure 8-4
Impedance of a Sitting Man
(After Coermann et al(28, 29))

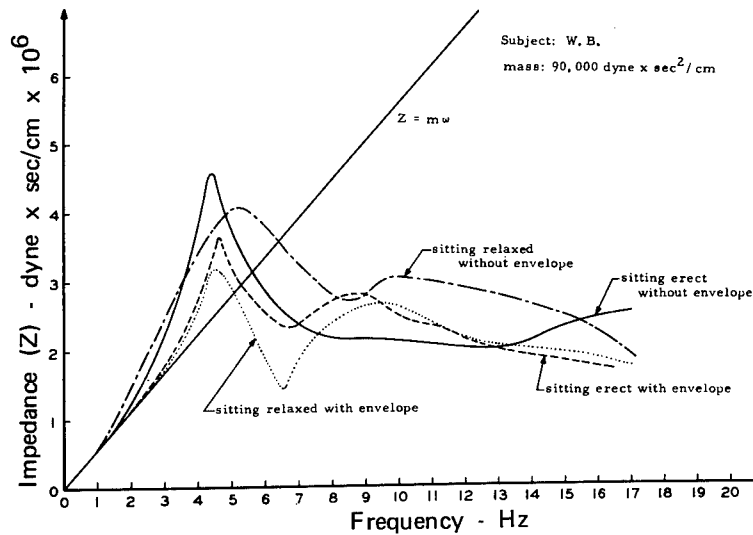
The calculation of the parameters for these two resonances leads to a model consisting of two mass-spring systems with dampers. The first system (dotted line) (Figure 8-4) represents about 90 percent of the body mass, has an elasticity of about 685 lbs per inch and a damping factor of about 0.32 of the critical damping; the second represents about 10 percent of the body mass, has an elasticity of about 186 lbs per inch and a damping factor of about 0.13 of the critical.

These parameters change considerably if the subject assumes a relaxed position or if the abdomen of the subject is restrained by a semi-rigid envelope (Figure 8-5a). While the first resonance frequency changes only little, the damping factor for this resonance varies over a wide range, indicating that the body reacts almost as a pure mass for frequencies up to

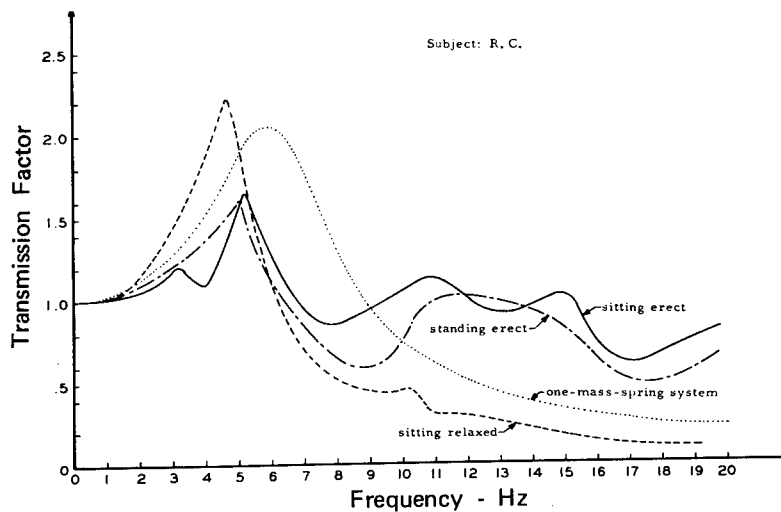
Figure 8-5

The Effect of Posture, Clothing or Envelopes, and Relaxation
on Impedance and Transmission of Vibration in Man

(After Coermann et al(27, 33))



- a. The Effect of a Semi-rigid Envelope Around the Abdomen on the Impedance of One Sitting Subject at Erect and Relaxed Postures



- b. The Transmission of Vibrations from the Seat to the Head of One Subject at Varied Body Postures Compared with the Transmission Factor of a One-Mass-Spring System with Damping

6 Hz. The second resonance practically disappears. The same effect can be seen if the transmission of vibration from the seat to the head of a sitting subject is measured (Figure 8-5b). The peak of the fundamental resonance at around 5 Hz is reduced in a relaxed posture, and the higher resonances become insignificant. (See also Figure 8-10 comparing impedance in the semisupine seated and standing man.)

The greatest loads occur in the region of the eleventh thoracic to the second lumbar vertebra which can therefore be assumed as the hinge area for flexion of the upper torso. Since the center of gravity of the upper torso is considerably forward of the spine, flexion movement will occur even with the force applied parallel to the axis of the spine. Changing the direction of the force so that it includes an angle with the spine (for example by tilting the torso forward) influences this effect considerably. Similarly, the center of gravity of the head can be considerably in front of the neck joint which permits forward-backward motion. This situation results in forward-backward rotation of the head instead of pure vertical motion. Examples of relative amplitudes for different parts of the sitting and standing body are shown in Figure 8-6. The curves show an amplification of motion in the impedance resonance range and a decrease at higher frequencies. The impedances and the transmission factors are changed considerably by individual differences in the body and its posture, as well as support by a seat or back rest of a sitting subject; or by the state of the knee or ankle joints of a standing subject. The resonance frequencies remain relatively constant whereas the transmission ratio varies (for the condition of Figure 8-6b). Transmission factors as high as 4 have been observed at 4 Hz (145). Above approximately 10 Hz vibration amplitudes of the body are smaller than the amplitudes of the exciting table and decrease continuously with increasing frequency. The attenuation of the vibrations transmitted from the table to the head is illustrated in Figure 8-7. At 100 Hz this attenuation is around 40 dB. The attenuation along the body at 50 Hz is shown, although not for pure longitudinal excitation. (See Figure 8-8).

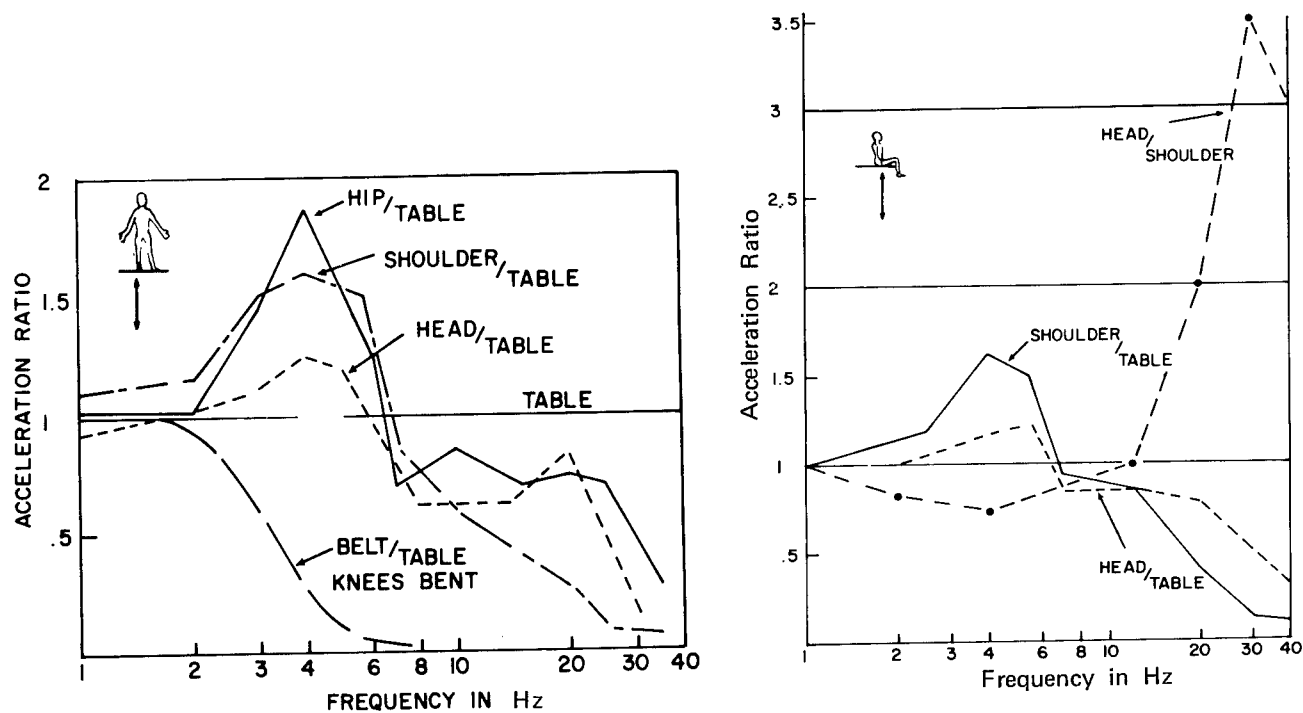
In the seated position, between 20 and 30 Hz, the head exhibits a resonance as can be seen clearly in Figure 8-6b. In this range the head amplitude can exceed the shoulder amplitude by a factor of 3. This resonance is of importance in connection with the deterioration of visual acuity under the influence of vibration. Another frequency range of disturbances between 60 and 90 Hz suggests an eyeball resonance (30). (See also Figs. 8-17 and 8-18.)

Maxima in horizontal seat-to-head transmissibility have been reported in the range 1.5 to 2.5 Hz (40, 91). Resonance near 2 Hz is the dominant mode in horizontal vibration of the seated man. If the seated subject is vibrated in more than one plane simultaneously, his physical response and subjective appreciation of the motion depend upon the amplitude and phase relationships between the component vibrations.

a) Supine $\pm G_z$

The impedance of the human body lying on its back on a rigid surface and vibrating in the direction of its longitudinal axis has been determined by ballistocardiograph studies (73, 187). The total mass of the body forms a

Figure 8-6
Transmission of Vertical Longitudinal Vibration to Body Parts
in Standing and Sitting Subjects



a. Transmission of Vertical Vibration from Table to Various Parts of the Body of a Standing Human Subject

(After Dieckmann⁽⁴¹⁾, data for transmission to belt after Radke⁽¹⁴⁵⁾)

b. Transmission of Longitudinal Vertical Vibration from Table to Various Parts of Body of Seated Human Subject

(After Dieckmann⁽⁴¹⁾)

Figure 8-7
Attenuation of Vertical and Horizontal Vibration for Standing and Sitting Human Subjects

(Continuous lines after von Békésy⁽⁵⁾.
Shaded area is range of values for 10 subjects after Coermann⁽³⁰⁾)

(After von Gierke⁽⁷⁰⁾)

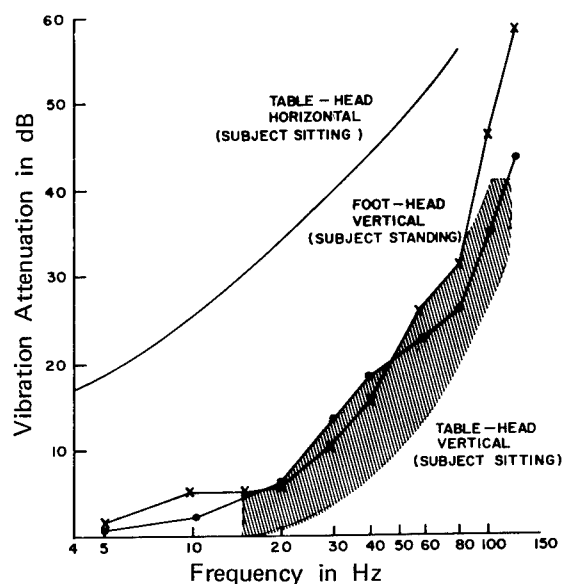
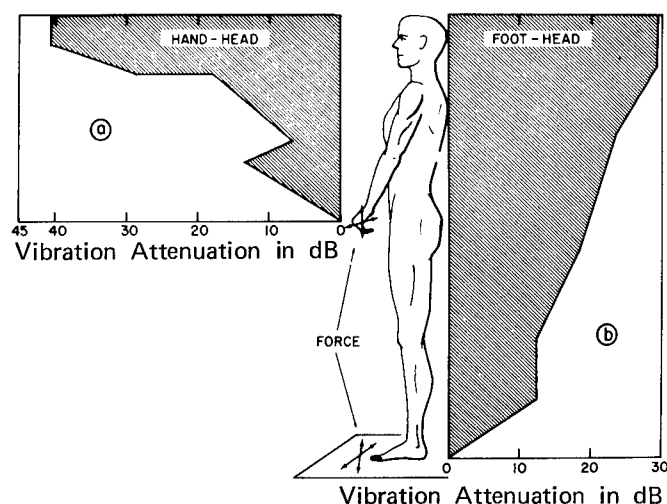


Figure 8-8

Attenuation of Vibration at 50 Hz Along Human Body

Excitation of a) hand and b) platform on which subject stands.

(After von Gierke⁽⁷⁰⁾, adapted from von Békésy⁽⁵⁾)



simple mass-spring system with the elasticity and resistance of the skin for tangential vibration. For the average subject the resonant frequency is between 3 and 3.5 Hz and the Q of the system is about 3. Q is defined as the rate of increase caused by resonance of the amplitude of an oscillating system and is measured as the ratio of the mass or spring reactance at resonance frequency to damping resistance. Restricting the subject's mobility by clamping the body at the feet and shoulders between plates connected with the table changes the resonant frequency to approximately 9 Hz and the Q to about 2.5. More recent studies on shake tables in the 0.2 to 0.5 g range indicate that at 4-8 Hz, as in the sitting position, subjects can tolerate less intensity than at other frequencies. Tension-relaxation factors also hold here. These results are indicated in Figures 8-9a and b. In Figure 8-9a the nonlinearities of the intensity response are noted as g-load is increased.

b) Semi-Supine

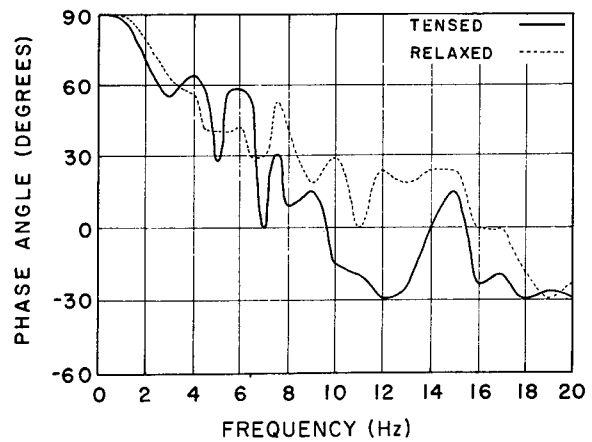
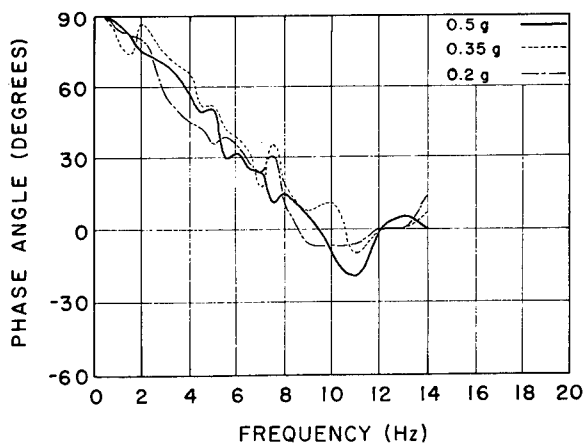
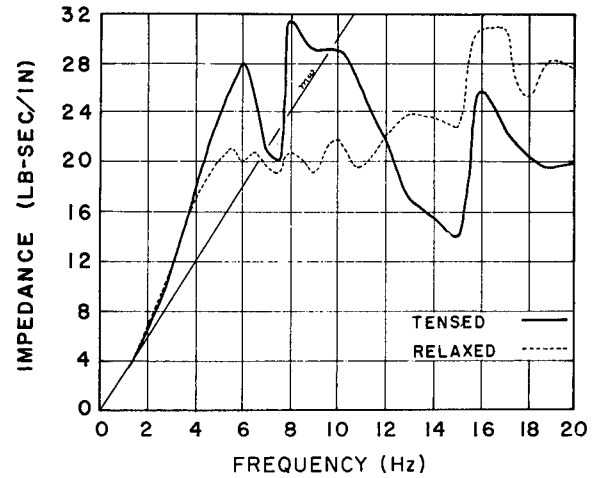
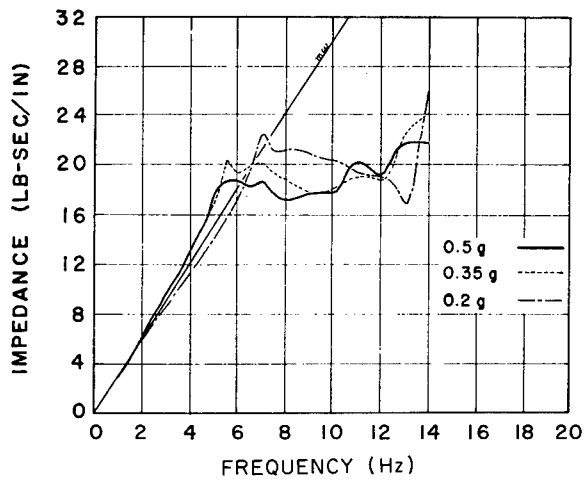
In semi-supine position used in spacecraft liftoff, the response of the human body to steady-state sinusoidal vibration is definitely different, as shown in Figure 8-10 (middle curve). The general course of the impedance curve follows very closely the $m\omega$ -line up to about 15 Hz, except at around 8 Hz where a slight peak due to a resonance in the pelvic area becomes evident. The second enhancement of the curve around 14 Hz indicates a very high damping in the body, and the phase angle signifies the domination of the damping forces at higher frequencies. The other curves of Figure 8-10 can be used to compare the impedance factors for steady-state sinusoidal, longitudinal vibration in the seated, semi-supine and standing human.

Figures 8-11a and b indicate the effect of a constant, linear-G bias on semi-supine impedance and resonance peaks (176). The subjects were placed in a seat position similar to that described in Figure 8-24a and vibrated in the Z axis, exposed to vibration (± 0.4 G at 2-1/2 to 20 Hz in 1/2 Hz increments) combined with linear acceleration of 1, 2-1/2, and 4 G. The absolute quantities (impedance magnitude and phase angle) shown in Figure 8-11a and 8-11b for one of the subjects are the magnitudes of the undistorted fundamental

Figure 8-9

Mechanical Impedance in the Supine Position

(After Edwards and Lange⁽⁴⁸⁾)



a. Whole-Body Mechanical Impedance Versus Frequency, with Table Acceleration Level as a Parameter, Subject RGE, Supine Relaxed

b. Whole-Body Mechanical Impedance Versus Frequency, Subject RGE, Supine Tensed and Supine Relaxed

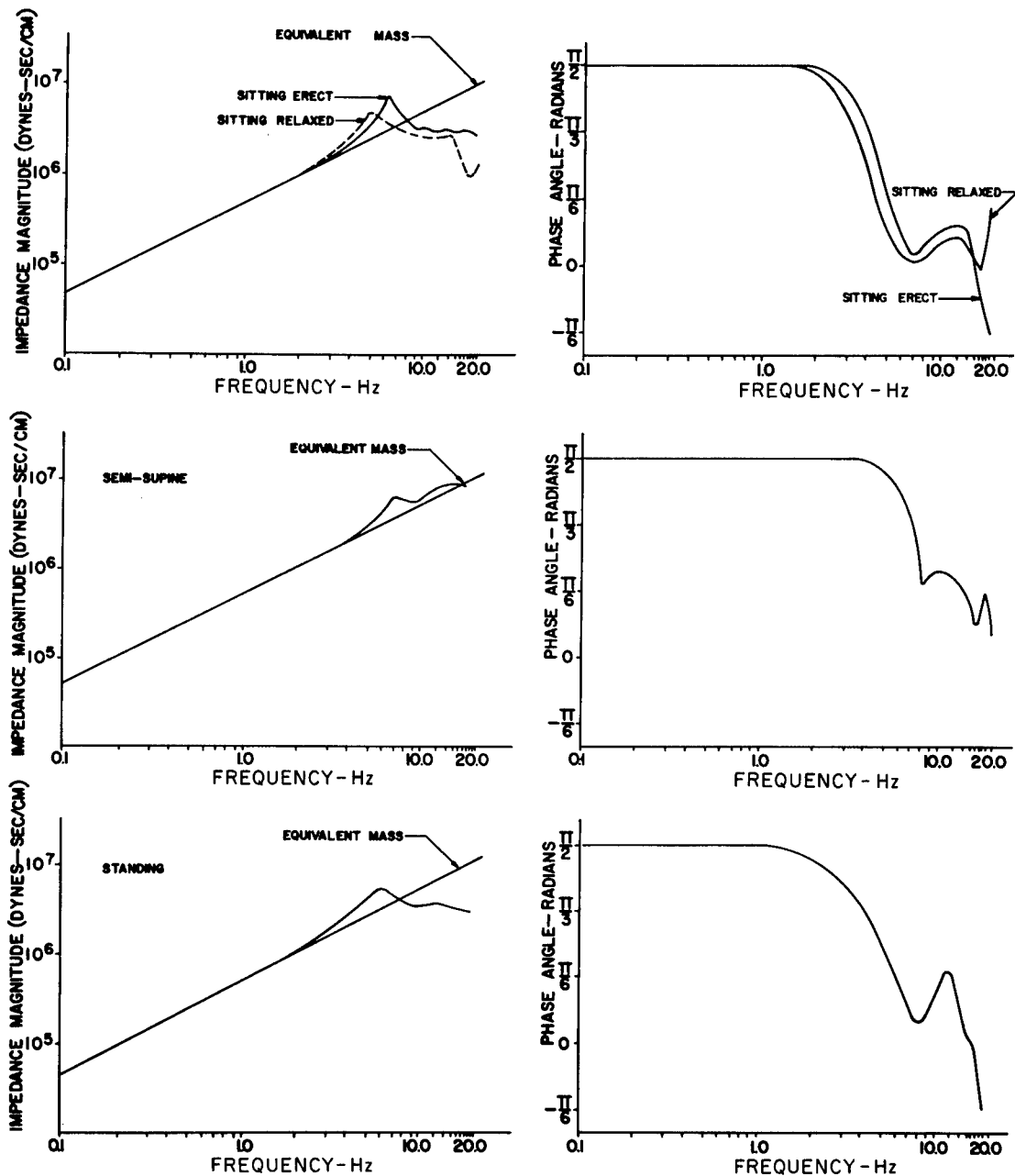


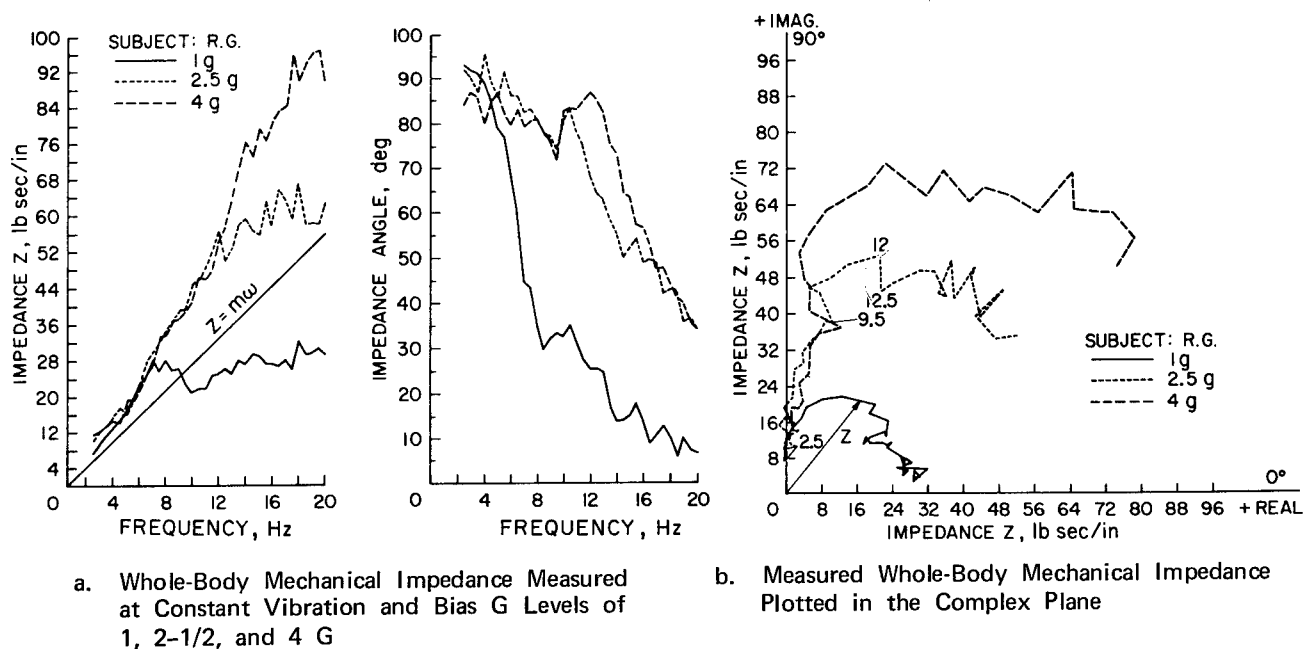
Figure 8-10

Human Mechanical Driving Impedance in the Steady-State Sinusoidal (Vibration) Environment

(After Weis et al⁽¹⁷⁹⁾, from data of Coermann⁽²⁷⁾)

Figure 8-11
Effect of Linear G Bias on Vibrational Impedance

(After Vykukal⁽¹⁷⁶⁾)



waveforms of the frequencies tested. As shown by these results, the influence of an increased bias G on the dynamics of the human body is quite significant. The differences in the nature of the body position and seat damping structure are probably responsible for the difference in impedance between the 1 G condition in 8-11a and 8-11b. Resonances at 7, 11, 13, 15, and 18 Hz were detected as expected (48, 179).

The complex plane or polar coordinate representation of impedance data in Figure 8-11b allows for a more detailed analysis of the system dynamics. Resonances and curve trends appear as deviations from ideal element responses (mass, spring, dampers). As noted, the resonances indicated appear as small loops (actions of subsystems resonating by themselves); the major loop trend represents whole body response in the frequency range tested.

The most significant effects of increased bias G on dynamics of the body are increased stiffness, reducing damping, and higher energy transmission to internal organs. The observance of pain by the subjects at certain measured resonant frequencies would indicate a lower tolerance to vibration at that frequency when combined with higher linear accelerations. No significant subjective impressions were noted at the 1-G bias level. However, at 2.5 and 4g, the subject became dramatically aware of local resonances, such as in the abdomen, chest, and extremities. Visual decrements were also noted. The correlation of resonance measurements and subjective impressions is quite significant. For example, in the frequency range of 9.5 to 12.5 Hz at 2.5-G bias, the subject noted the following sensations: at 9.5 Hz, "awareness of stomach vibrating," 11.5 Hz, "stomach vibration continued," 12.5 Hz,

"stomach sensations decreasing." The polar plot (Figure 8-11b) indicates a deviation from the major loop in this frequency range. Subjective observations indicate a direct relationship with other deviations also shown in Figure 8-10c. Additional studies are needed to determine the effects of increasing the vibration G magnitude on impedance for higher bias-g levels simulating booster liftoff to orbital insertion.

One of the most important subsystems of the body, which is excited in the standing and sitting position as well as in the lying position is the thoraco-abdomen system (151, 187). The abdominal viscera have a high mobility due to the very low stiffness of the diaphragm and the air volume of the lungs and the chest wall behind it. Under the influence of both longitudinal and transverse vibration of the torso, the abdominal mass vibrates in and out of the thoracic cage. These vibrations not only take place in the (longitudinal) direction of excitation but, during that phase of the cycle when the abdominal contents swing towards the hips, the abdominal wall is stretched outward and the abdomen appears larger in volume; at the same time the downward deflection of the diaphragm causes a decrease of the chest circumference. At the other end of the cycle the abdominal wall is pressed inward, the diaphragm upward, and the chest wall is expanded. This periodic displacement of the abdominal viscera has a sharp resonance between 3 and 3.5 Hz. (See Figure 8-12.) Oscillations of the abdominal mass are coupled with the air oscillations of the mouth-chest system (8, 15). Measurements of the impedance of the latter system at the mouth (by applying oscillating air pressure to the mouth) shows that the abdominal wall and the anterior chest wall respond to this pressure. The impedance has a minimum and the phase angle is zero between 7 and 8 Hz. The abdominal wall shows maximum response between 5 and 8 Hz, the anterior chest wall between 7 and 11 Hz. Vibration of the abdominal system resulting from exposure of a sitting or standing subject is clearly detected as modulation of the flow velocity through the mouth. (At large amplitudes, speech can be modulated at the exposure frequency.) Electrical equivalent circuits and mechanical models for the abdomen-chest-mouth system are available (8, 67, 73).

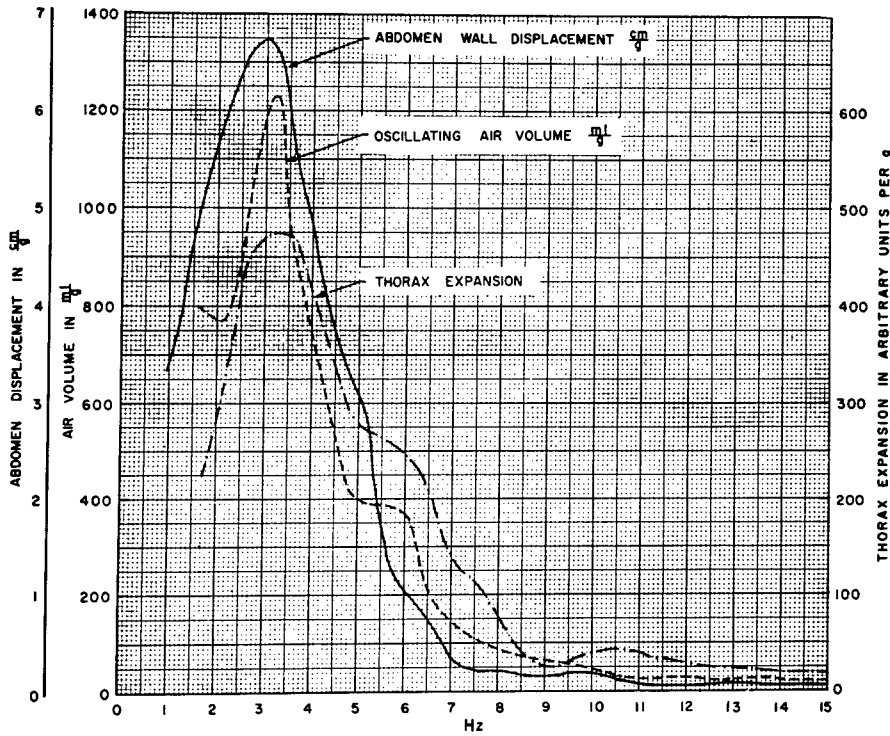
Recent studies focused on the transmission of sinusoidal abdominal pulses to the cerebrospinal fluid of animals suggest that the amplitude ratio of intracranial pressure to the airflow velocity is relatively constant for 2-30 Hz driving frequencies (15).

The bear is often used as a substitute for man in vibration and impact research because it is assumed that his body structure is most similar to that of man. In the steady-state impedance curve of a 126-lb Himalayan bear, the first resonance frequency is a little lower than that of the average man but still in the range of the standard deviation. Also at higher frequencies the characteristic of the impedance curve is similar if the difference in weight is considered.

An anatomical review of organ morphology related to vibration is available (73). The movements of the visceral organs can be a limiting factor for human tolerance to steady-state vibration in the frequency range 4 to 8 Hz. To measure the resonant frequencies of the thoraco-abdominal system as a whole, an air-filled balloon on a catheter was inserted in the

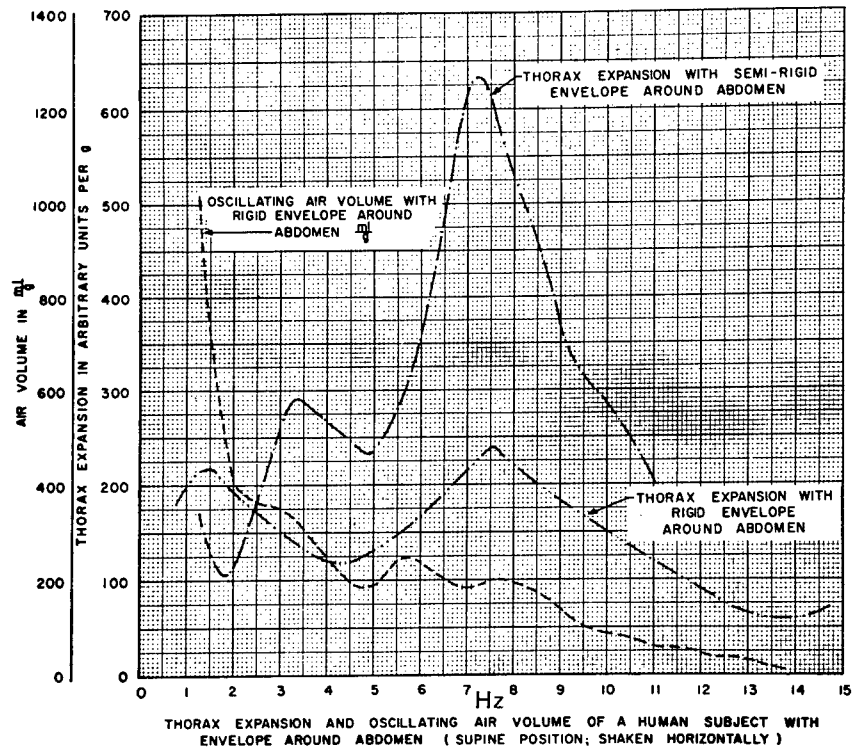
Figure 8-12

Thorax Expansion and Oscillating Air Volume of a Human Subject
with and without Envelope Around Abdomen
(supine position, shaken horizontally)
(After Coermann et al⁽³³⁾)



a. Without Envelope about Abdomen

b. With Envelope about Abdomen



colon of human and animal subjects sitting on a vertically vibratory shake table (185). The changes of the pressure within the balloon and the phase of this pressure relative to the movement of the shaker were recorded at frequencies from 1 to 20 Hz. In Figure 8-13 the pressure changes per G of the shaker are plotted versus frequency for a man sitting erect, sitting relaxed, and semi-supine, as well as for a sitting rhesus monkey and mouse.

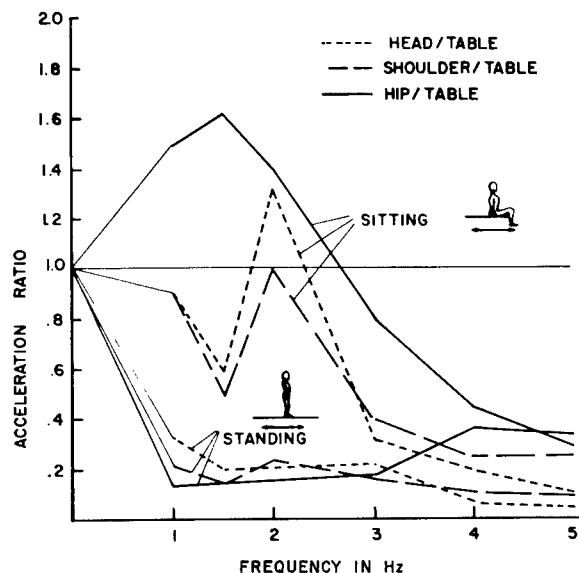


Figure 8-13

Transmission of Transverse, Horizontal Vibration from Table to Various Parts of Sitting and Standing Human Subject

(After Goldman and von Gierke⁽⁷³⁾, adapted from Dieckmann⁽⁴⁰⁾)

Man and monkey show in the sitting position main resonances between 4 and 5 Hz, while the man in semi-supine position has maximum movements of the thoraco-abdominal viscera between 7 and 8 Hz. The abdominal viscera of other animals have different resonance systems (131, 132, 150). Thus, before animals are used to study the influence of transient forces on the abdominal organs, it must be assured that their thoraco-abdominal systems have dynamic characteristics similar to those of man. There appears to be little evidence that anesthesia, 100% oxygen, or feeding have significant effects on resonant frequency of organs in animals (130).

Transverse Vibrations ($\pm G_x$)

The physical response to transverse vibration -- i.e., horizontal in the normal upright position -- is quite different from that described for vertical vibration (73). Instead of thrust forces acting primarily along the line of action of the force of gravity on the human body, they act at right angles to this line. The direction of the body masses along this line is therefore of the utmost importance and greater differences must be expected between sitting and standing subjects than for vertical vibration where the supporting structure of the skeleton and especially the spine have been designed for vertical loading.

Impedance measurements for transverse vibration are available. In fore-and-aft vibration, the resonant frequency occurs due to flexion of the lumbro-dorsal spine and articulation at the hip joints. There is also a lateral bending mode at 1.6 Hz (80).

The transmission of vibration along the body is illustrated in Figure 8-14 (40). For a standing subject the shoulder and head amplitudes are of the order of 20 to 30 percent of the table amplitude at about 1 Hz and decrease

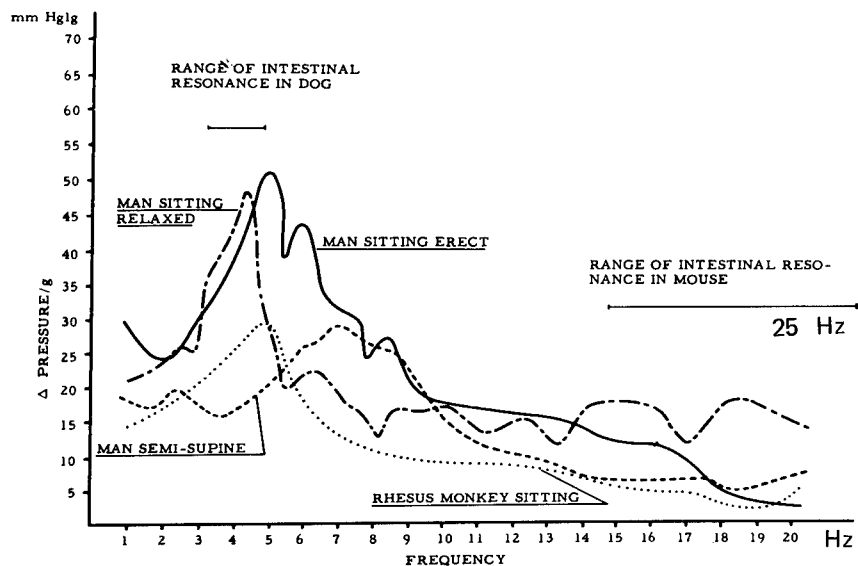


Figure 8-14

Comparison of Intestinal Pressure Change During Sinusoidal Vibration in Man at Different Postures and in Rhesus Monkeys (Anesthetized)

(After Coermann (27))

with increasing frequency. Relative maxima of shoulder and head amplitudes occur at 2 and 3 Hz respectively. The sitting subject exhibits amplification of the hip (1.5 Hz) and head (2 Hz) amplitudes. All critical resonant frequencies appear to be between 1 and 3 Hz. Investigation of experimental results of the type of Figure 8-10 in connection with phase measurements shows that the transverse vibration patterns of the body can be described as standing waves, i.e., as a rough approximation one can compare the body with a rod in which transverse flexural waves have been excited. One has, therefore, in agreement with the experimental results, nodal points on the body which become closer to the feet as the frequency increases since the phase shift between all body parts and the table increases continuously with increasing frequency. At the first characteristic frequency at 1.5 Hz, the head of the standing subject is observed to have a 180° phase shift compared with the table; between 2 and 3 Hz this phase shift becomes 360° (40).

There are longitudinal head motions excited by the transverse vibration in addition to the transverse head motions shown in Figure 8-14. The head performs nodding motion due to the anatomy of the upper vertebrae and the location of the head's center of gravity. Above 5 Hz the head motion for the sitting and standing subjects is predominantly vertical of the order of 10 to 30 percent of the horizontal table motion.

Many kinematic processes, physical loadings, and gross destructive anatomical effects can be studied on dummies which approximate a human being in size, form, mobility, total weight, and weight distribution in body segments (27). Several such dummies are commercially available. They have been used extensively in aviation and automotive crash research and in other studies to precede work with human subjects and to study protective seats and harnesses. Such dummies attempt to match the "resiliency" of human flesh by some kind of padding, but they are crude simulations at best and the dynamic mechanical properties are, if at all, only reasonably matched in a very narrow low frequency range (27). This and the passiveness of such dummies must be kept in mind as important mechanical differences between them and living subjects.

Vibrations Transmitted to the Hand

In connection with studies on the use of vibrating hand tools, several measurements have been made of vibration transmission from hand to arm and body (2, 6, 39). The impedance measured on a hand grip for a specific condition representative of hand tool use is presented in Figure 8-15.

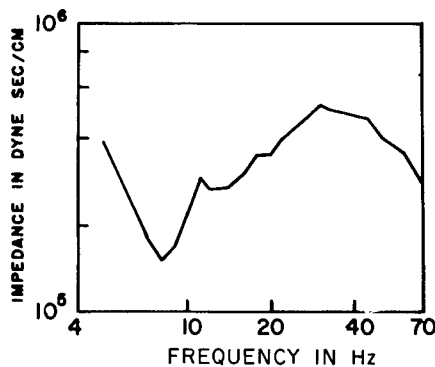


Figure 8-15

Impedance and Phase Angle of Arm Measured at a Vibrating Hand Grip

Elbow flexion 20° to 25° , static pressure on grip 22 lbs. Measurements on one subject.

(After Goldman and von Gierke⁽⁷³⁾, adapted from Dieckmann⁽³⁹⁾)



The impedance has one maximum in the range below 5 Hz probably determined by the natural frequencies for transverse excitation of the human body between 1 and 3 Hz. A second strong maximum appears between 30 and 40 Hz; the effective mass of the hand (approximately 2.2 lbs. 1 kg.) is here in resonance with the elasticity of the soft parts on the inside of the hand. This elasticity between force and hand has been estimated at $2 \cdot 10^{-8}$ cm/dyne. With a practical hand tool, which operates between 40 and 50 Hz, it has been found that the vibration amplitude decreases from the palm to the back of the

hand by 35 to 65 percent. Further losses occur between the hand and the elbow and the elbow and the shoulder. Figure 8-8 which shows this decrease of vibration amplitude from the hand to the head, indicates that the strongest attenuation occurs in the shoulder joint.

Thresholds of sensitivity to vibrating tools vary with age, experience, and simultaneous exposure to noise (172).

Skull Vibrations

The vibration pattern of the skull agrees approximately with the pattern of a spherical elastic shell (7, 57). The nodal lines observed suggest that the fundamental frequency lies between 300 and 400 Hz with resonances for the higher modes around 600 and 900 Hz. The frequency ratio between the modes is approximately 1.7 while the theoretical ratio for a sphere is 1.5. From the observed resonances, the elasticity of skull bone can be calculated. The value obtained for Young's modulus (1.4×10^{10} dynes/cm²) agrees fairly well with static test results on dry skull preparations. (See also Sound and Noise, (No. 9). Vibrations of the lower jaw with respect to the skull can be explained by a simple mass-spring system, which has a resonance, relative to the skull, between 100 and 200 Hz (35).

Transfer Functions and Power Spectra of Random Vibrations

Recent studies have attempted to quantitate responses to random vibration from power-frequency encountered in ground vehicle simulators (88, 174). Random vibrations best describe the environment in most transportation systems. Power-spectral histories and other techniques such as time histories, peak distribution, and probability records describe the vibratory input to the subject but often fail to quantitate the response especially where angular mode such as pitch and roll are also present. Transfer functions relating "average absorbed power" to onset of fatigue have received preliminary study (140, 142). Since absorbed power is a time-sensitive scalar quantity it is hoped that this parameter may be summed in complex multidegree of freedom environments and symptoms related to this value.

The essential premise controlling the use of the transfer function is that the system be linear. Therefore, application of the transfer function to human dynamics requires the establishment that man behave as a linear system within the bounds of interest. The body cannot always be treated as a linear, passive mechanical item. Linearity is an idealization which holds only for relatively small amplitudes. Nonlinearity must be kept in mind if mechanical injury to tissue is considered (73). There is actually considerable non-linearity of response well below amplitudes required for the production of damage. An example of this is given in Figure 8-16a. Studies at 0.2, 0.35, and 0.5 g indicate not only that non-linearities exist between intensity and impedance, but that the non-linear response is most prominent at resonance frequencies (48). Animal data up to 3 g's have corroborated these findings (24, 103, 185). Another variable controlling impedance and resonance

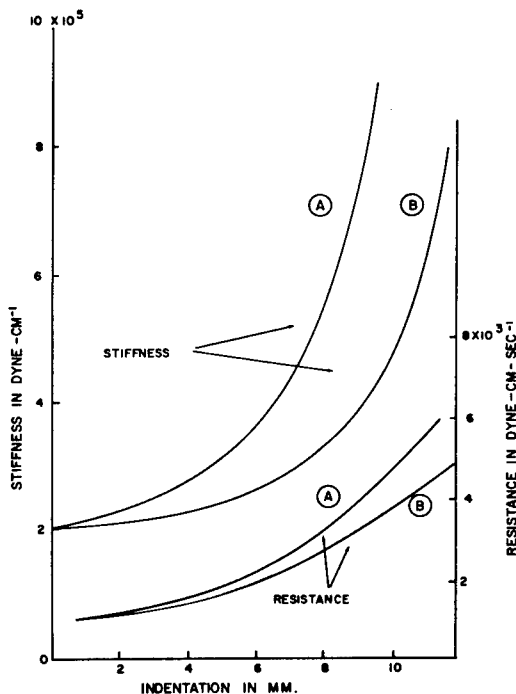
patterns is the nature of the absorbing medium between shaker and subject (48). A technique should really be developed by which the impedance of the padding may be subtracted from the total impedance to yield that of the subject alone, principally in the same manner by which the impedance of the mass of the support is now subtracted (179). The adjusted impedance of the subject may then be compared to that of the impedance of the subject without padding, and consequently a true measure of the force-transmitting characteristics of the padded support may be obtained. Distortions also arise from the effects of the mass of the accelerometer (Figure 8-16b).

Studies have recently been performed in an attempt to define the range of linearity of the human response to $\pm G_z$ vibration for subsequent determination of transfer functions (144). The following discussion is taken directly from these studies.

To gather response data concerning random vibration, experiments were conducted using a uniform spectrum, white-noise vibration filtered through a 2-Hz band-width filter at center frequencies of 3, 5, 7, 10, 13, 15, 20, 25,

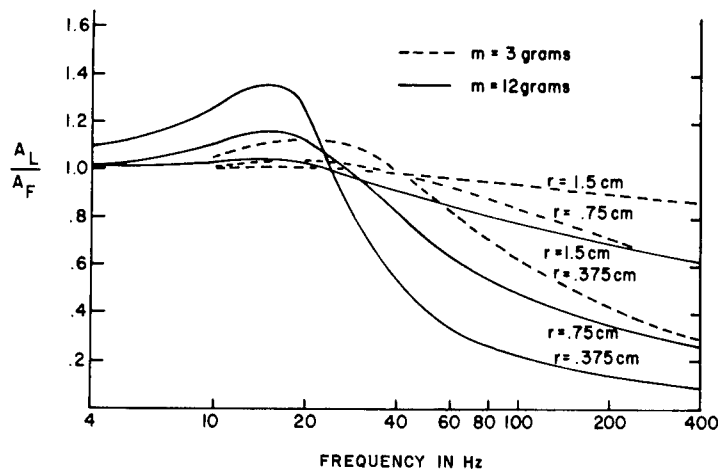
Figure 8-16

Measurement Distortion and Non-Linearity of Tissue Response to Vibration



a. Effect of Loading Distortion of Body Surface on Surface Impedance of Soft Tissue for Two Experimental Human Subjects A and B

(After Goldman and von Gierke⁽⁷³⁾, adapted from Franke⁽⁵⁶⁾)



b. Amplitude Distortion Due to Size and Weight of Accelerometer Attached to Body Surface Over Soft Tissue of Human Subject Exposed to Vibration

This graph gives the ratio, $\frac{A_L}{A_F}$, of the response of a loaded accelerometer of mass m and radius r of contact surface area for several values of m and r .

(After Goldman and von Gierke⁽⁷³⁾)

and 30 Hz. The tolerance condition was a combination of vibration severity where pain, loss of physical stability, or advanced stages of blurred vision were considered unacceptable. When tolerance was reached, the subject actuated a buzzer which began the rms data collection procedure. Each subject was held at the tolerance level for 20-60 sec. The time interval was dependent upon the stability of rms data. In order to examine more carefully human response to random vibration of greater frequency content, a third experiment was conducted using 10 subjects exposed to random motions filtered with a 10 Hz band width filter. These data established the upper boundary of human response in accordance with the experimental control described for tolerance testing. To validate the hypothesis that whole body response is linear below this level, tests were performed at seven different acceleration levels to very low intensity. Regression analysis (Figure 8-17a) indicated strong linearity throughout the frequency spectrum.

To evaluate the variability of human response with changes in wave form, the same test was conducted using white noise passing through 2 and 10 Hz band-width filters. A comparison of the response at a center frequency of 5 Hz is shown in Figure 8-17b. Although response varied with the three types of input, strong linear characteristics were evident for each input.

The study of linearity was also approached in a manner analogous to that of a constant-rate spring:

$$k = \sqrt{(F/D)^2 - (\delta\omega)^2} \quad (2)$$

Where D = Deformation - (deflection)

F = Force

k = Spring constant

δ = Damping

$\omega = 2\pi f$

For head acceleration responding to body displacement or deflection, D, (see Figure 8-18a):

$$D = \frac{(A_{in} - A_H) 386}{4\pi^2 f^2} \quad (3)$$

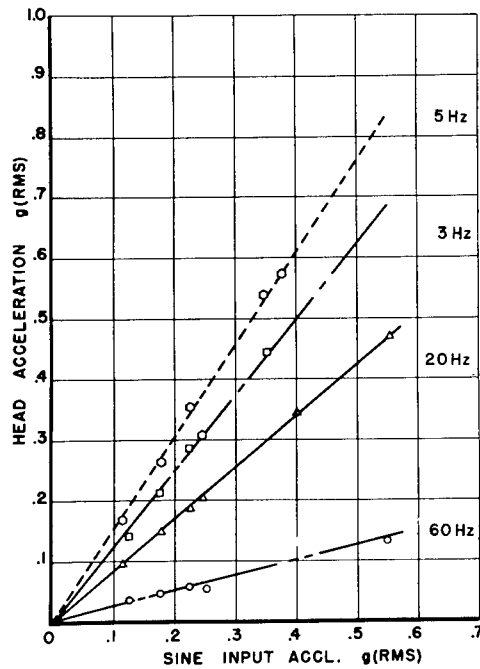
Where A_H = Head acceleration

A_I = Input acceleration

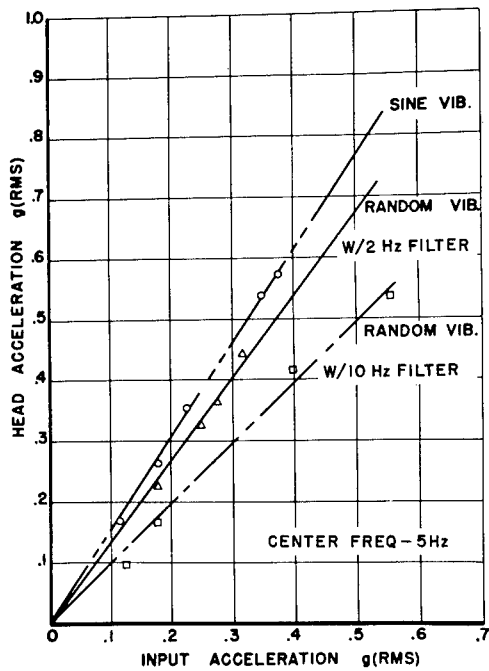
f = Frequency, Hz.

When the applied or restoring force is proportional to the spring deformation, the system is considered to be linear. However, if the force magnitude is not proportional to the displacement, or if the damping is not proportional to the velocity, the system is nonlinear. Figure 8-17c describes the use of

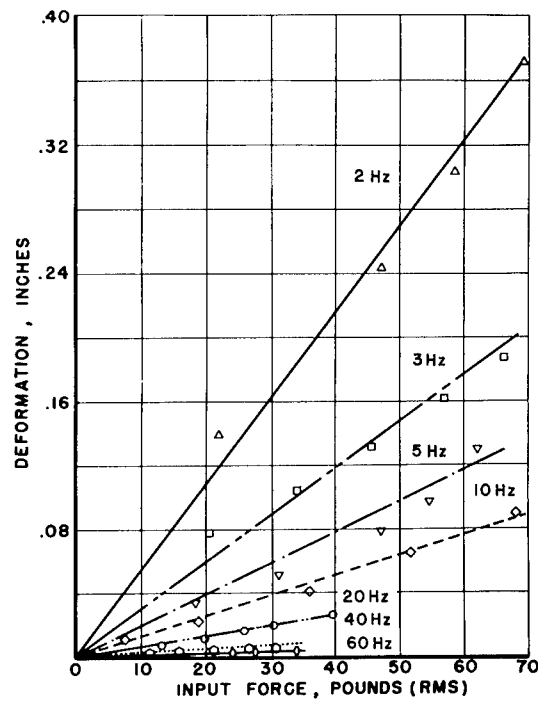
Figure 8-17
Determination of Acceleration Transfer Functions from Human Tolerance
Data to Random Vibration in the $\pm G_z$ Axes (Seated)
(After Pradko et al⁽¹⁴⁴⁾)



a. Frequency Response Comparison



b. Response of Human Head to Different Types of Vibration in the $\pm G_z$ Axis (Seated)



c. Human Deflection Characteristics in the $\pm G_z$ Axis (Seated)

Equation (3) again verifying the previous findings that the mechanical response characteristic of man in a seated erect position within the limits of this evaluation may be treated as a linear system.

With the establishment of linearity, the transfer function can be experimentally determined. Transfer functions are expressed as continuous functions, using the Laplace transform. The schematic representation is shown as

$$[\text{Input, } I(s)] \times \left[\begin{array}{c} \text{Element transfer} \\ \text{function, } G(s) \end{array} \right] = \text{Output, } O(s)$$

$$G(s) = \frac{\text{Output (s)}}{\text{Input (s)}} = \frac{O(s)}{I(s)} \quad (4a)$$

where $I(s)$ = Laplace transform of the input

$O(s)$ = Laplace transform of the output

$G(s)$ = Transfer function

The general form of the transfer function $G(s)$ is the ratio of output to input transform,

$$G(s) = \frac{\text{Response function}}{\text{Input function}} = \frac{O(s)}{I(s)} \quad (4b)$$

A graph of the ratio of the output to the input is a graph of the transfer function. The curve is then mathematically fitted by a ratio of polynomials. The early manual techniques of curve matching were laborious and now have been replaced and simplified by computer methods (50). For the specific case the data used were the means of rooted values. The transmissibility of head acceleration to input acceleration gave a curve similar to the dashed line of Figure 8-5b. From the ratio described in Equation 5a, the complex variable (S) is obtained:

$$G_A(S) = \frac{A_{\text{head}}}{A_{\text{input}}} (S) \quad (5a)$$

where $G_A(S)$ = Acceleration transfer function

(S) = Complex variable

This transfer function, under both sinusoidal and random vibration, should be in good agreement with experimental data.

The force transfer function, $G_F(S)$, can be defined as

$$G_F(S) = \frac{F_{\text{input}}}{A_{\text{head}}} (S) \quad (5b)$$

The $G_F(S)$ can be determined from characteristic curves of F/A_{input} and F/A_{output} shown in Figure 8-18a to c.

By combining Equations 5a and 5b, the analytical transfer function can be obtained. There is close agreement between the statistical impedance data collected during these experiments (similar to dash dot line of Figure 8-5a) and the response calculated from the analytical transfer function. It is thus concluded that human response to sinusoidal and random vibration displays linear characteristics in the range where equilibrium or physical self-control is maintainable; transmissibility ratios of force and motion are sufficiently stable to be used for determining human transfer functions in the 1-60 Hz frequency spectrum; and transfer function statements of motion and force accurately describe human response to sinusoidal and random vibrations.

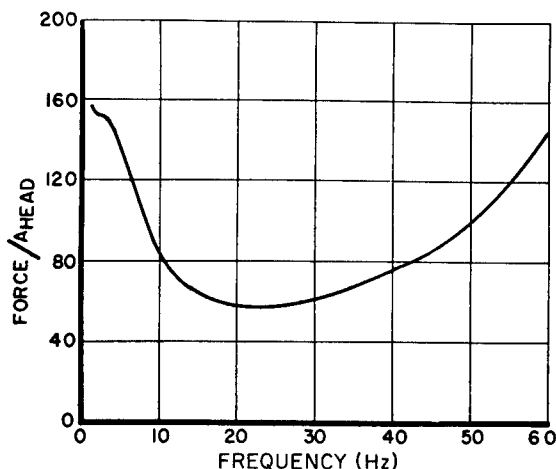
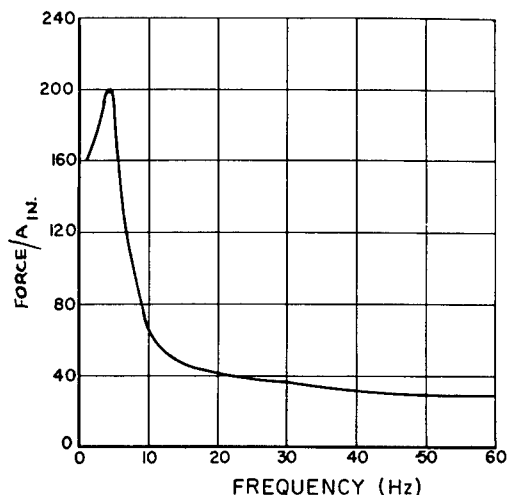
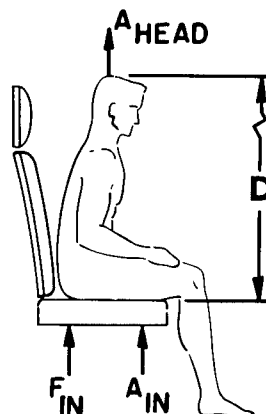
Transfer functions allow analytical solutions for the dynamic response of the human body, but the transfer functions do not give any apparent way to determine the severity of the vibration. A parameter that will relate the vibration to the subjective response is required. Extensive testing has shown

Figure 8-18

Force to Input and Output Acceleration Ratios Used in Calculation of Force Transfer Functions

(After Pradko et al⁽¹⁴⁴⁾)

- a. (right) Diagram of Force Accelerations and Deformation, D
- b. (bottom left) Force Input Acceleration Characteristics
- c. (bottom right) Force Output Characteristics for Head



that the rate of flow of energy becomes the parameter that characterizes the interaction of the vibrating human and the environment. The energy flow takes place as a result of the complex damped elastic properties of the anatomy. This energy flow has been designated as average "absorbed power" (105, 143).

These are two distinct concepts employed to obtain the analytical solution for a vibration environment: the transfer function and the absorbed power. The utility of the transfer function is manifested in the assessment of human response for skewed or oblique orientations (141). On the other hand, the absorbed power concept is a self-contained procedure that correlates with the nonlinear subjective response to vibration intensity (143).

The transfer function describes the mechanical response characteristics analytically as effective mass and inertial. These functions provide the means of conducting vibration analysis mathematically without using human test subjects in laboratory experimentation. The transfer functions were developed for a normal seated position without armrests or backrests. Consequently, when attempting to assess these or other specific features of seating arrangements, one must resort to direct measurement of absorbed power. It was noted that under linear vibration conditions when seat belts were used, absorbed power was not appreciably affected. When man is seated, the vibration input to the feet becomes significant when the frequency is above 10 Hz. This is especially true when the man is seated on a cushioning device. In this case the input to the feet should be included in the analysis.

Absorbed power has a physical significance and interpretation. Consequently, it is possible to measure the variation of this parameter for different people and different seating arrangements. A muscular person generally has, for the same body weight, a lower absorbed power for the same vibration than a more obese person. On the other hand, if a rigid mass were used in place of a human test subject, the rate of flow of energy would be zero because of its rigid, inelastic properties. A contoured seat generally has a larger contact area than one that is not contoured. This larger area will reduce body movement, owing to its elastic properties, and thus generally produce a lower absorbed power. Under very severe conditions where the man moves relative to the seat, the assumption of linear equations is no longer valid; consequently, transfer functions and absorbed power cannot be used under these conditions. Under normal vibration conditions, using absorbed power as a criterion, one can modify the input or a seating arrangement and measure directly the effect upon comfort. This versatility of absorbed power is not realized in other known methods of determining human discomfort due to vibration. If one is using sinusoidal boundary curves to assess the effects of various seating arrangements and positions, for the same vibration input, the curves are not helpful. Sinusoidal boundary curves are a function of the vibration input and are not sensitive to position and seating arrangement.

Because of the importance of this approach, the following discussion is taken directly from Reference (105). In the time domain, absorbed power can be written for an infinite time or a finite averaging time. For an infinite averaging time it is

$$\text{Average absorbed power} = \lim_{T \rightarrow \infty} \frac{1}{T} \int_0^T F(t) V(t) dt \quad (6)$$

where $F(t)$ = Input force

$V(t)$ = Input velocity

For a finite averaging time, it can be written in the form of a differential equation as follows:

$$\frac{d^2 P_{av}(t)}{dt^2 W_n^2} + \frac{dP_{av}(t)}{dt} \left(\frac{2\delta}{W_n} \right) + P_{av}(t) = KF(t) V(t) \quad (7)$$

where $P_{av}(t)$ = Finite average absorbed power

δ = Damping factor

W_n = Lowest frequency to be averaged, rad/sec

$F(t)$ = Input force

$V(t)$ = Input velocity

K = Conversion constant

Absorbed power can also be described in the frequency domain. It is computed as the product of the mean squared acceleration A_i^2 rms and the parameter K_i , at each frequency "i". K_i is a function of frequency, but does not vary at any one frequency (143).

$$P_{av} = \sum_{i=0}^N K_i A_i^2 \text{ rms} \quad (8)$$

Since absorbed power is a scalar quantity, it possesses the desirable feature of being directly additive. For multidegree of freedom systems, the individual absorbed power values are readily summed for a single quantitative and qualitative measure of human vibration. From the previous equations it becomes apparent that absorbed power can be determined in both the time domain and the frequency domain. When absorbed power is determined in the time domain, it can be determined by direct measurement of force and acceleration or by obtaining force from the transfer functions. Absorbed power can be determined from the output of a triaxial accelerometer, utilizing the transfer functions to generate the force. (See Reference 105). Filters can be included only if one is interested in determining the contribution of specific frequencies to the absorbed power.

For many purposes it is convenient to describe vibration in terms of its frequency domain characteristics. For deterministic vibrations this is usually done by stating the time-domain equations; for example, Fourier

series, single sinusoids, or line-spectra graphs. Random vibration characteristics, however, are commonly described in the time domain by correlation functions and in the frequency domain by power spectral density.

Absorbed power can be calculated for each of these conditions when the K_i in Equation 8 are known at each frequency, or are known as a function of frequency. Transfer functions that relate force to acceleration can be manipulated to give phase angle, force, and power by the following three equations: (143).

$$\sin \phi = \frac{(F_2 F_3 - F_1 F_4) w}{\sqrt{(w^2 F_4^2 + F_3^2)(F_1^2 + w^2 F_2^2)}} \quad (9)$$

$$\text{Force} = K_0 \sqrt{\frac{F_1^2 + w^2 F_2^2}{F_3^2 + w^2 F_4^2}} A_i \text{ rms} \quad (10)$$

$$\text{Power} = \sum_{i=0}^N K_1 k_0 \frac{(F_1 F_4 - F_2 F_3)}{(F_3^2 + w^2 F_4^2)} A_i^2 \text{ rms} \quad (11)$$

The F quantities that appear in Equations 9-11 are the F that are given with the constant power graphs, Figures 8-38a to d. In the equations, ϕ is the angle between acceleration and force, force is in pounds when $A_i \text{ rms}$ is in feet per square second, and power is in watts when K_1 is equal to 1.356.

The F and numerical constants are derived from experimental data. For vertical vibration they are ($\pm G_Z$)

$$\begin{aligned} F_1 &= -0.10245296 \times 10^{-9} w^6 + 0.17583343 \times 10^{-5} w^4 \\ &\quad - 0.44600722 \times 10^{-2} w^2 + 1 \\ F_2 &= 0.12881887 \times 10^{-7} w^4 - 0.93394367 \times 10^{-4} w^2 \\ &\quad + 0.10543059 \\ F_3 &= -0.45416156 \times 10^{-9} w^6 + 0.37667129 \times 10^{-5} w^4 \\ &\quad - 0.56104406 \times 10^{-2} w^2 + 1 \\ F_4 &= -0.21179193 \times 10^{-11} w^6 + 0.5172811 \times 10^{-7} w^4 \\ &\quad - 0.17946748 \times 10^{-3} w^2 + 0.10543059 \end{aligned}$$

and

$$W = 2\pi f, \quad K_0 = 4.35373, \quad K_1 = 1.356$$

The F and numerical constants for the feet are

$$\begin{aligned} F_2 &= -0.18706955 \times 10^{-4} w^2 + 0.074036789 \\ F_3 &= 0.33913154 \times 10^{-6} w^4 - 0.23697592 \times 10^{-2} w^2 + 1 \\ F_4 &= 0.17013499 \times 10^{-8} w^4 - 0.39439090 \times 10^{-4} w^2 \\ &\quad + 0.074036789 \end{aligned}$$

and

$$W = 2\pi f, \quad K_0 = 1.182, \quad K_1 = 1.356$$

The above analysis assumes that the vibration input is the same for both feet. Where this is not the case, K_0 must be divided by 2 and the transfer function used for each individual foot.

The F and numerical constants for the fore and aft motion ($\pm G_x$) are:

$$\begin{aligned} F_1 &= 1 \\ F_2 &= 0.219106 \\ F_3 &= -0.0185309w^2 + 1 \\ F_4 &= -0.000618934w^2 + 0.219106 \end{aligned}$$

and

$$W = 2\pi f, \quad K_0 = 4.3532, \quad K_1 = 1.356$$

The F and numerical constants derived for the side to side motion ($\pm G_y$) are:

$$\begin{aligned} F_1 &= 0.24052124 \times 10^{-3} w^4 - 0.066974483w^2 + 1 \\ F_2 &= 0.57384538 \times 10^{-5} w^4 - 0.50170413 \times 10^{-2} w^2 \\ &\quad + 0.33092592 \\ F_3 &= -0.14979958 \times 10^{-5} w^6 + 0.001008882w^4 \\ &\quad - 0.10108617w^2 + 1 \\ F_4 &= -0.17137490 \times 10^{-7} w^6 + 0.53137351 \times 10^{-4} w^4 \\ &\quad - 0.011096507w^2 + 0.33092592 \end{aligned}$$

and

$$W = 2\pi f, \quad K_0 = 4.353, \quad K_1 = 1.356$$

Inserting these F into Equations 9-11, one can solve for phase angle, force, power, or acceleration for any frequency, sum of frequencies, or power spectral density (PSD). This calculation is best performed on a digital computer. However, tables of constants are available for hand calculation of several different problems relating to comfort threshold. These are seen in Figure 8-38. Examples of these calculations are available (105, 141).

Tissue Impedance (73)

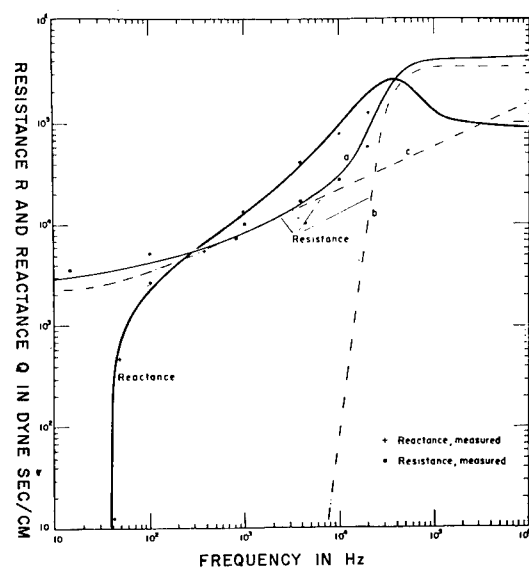
The mechanical properties of body tissue are summarized in Table 7-74 of Acceleration, (No. 7). Whereas bone behaves more or less like a normal solid, soft elastic tissues, such as muscle, tendon, and connective tissue, resemble elastomers having similar Young's moduli, S-shaped stress-strain relations and high stretchabilities. Their properties have been studied in connection with the quasistatic pressure-volume relations of hollow organs such as arteries, the heart, the urinary bladder, etc. (160), but linear properties have always been assumed when dynamic responses were studied. Soft tissue can then be described phenomenologically as a visco-elastic medium and plastic deformation has to be considered only if injury occurs.

Impedance measurements of small areas (1 to 17 cm^2) over soft human tissue have been made with vibrating pistons between 10 Hz and 20 kHz . This impedance starts out at low frequencies as a large elastic reactance. With increasing frequency the reactance decreases, becomes zero at a resonance frequency, and becomes a mass reactance with still further increase in frequency. (See Figure 8-19a.) (64, 71). These data cannot be explained by simple lumped-parameter models, but require a theory of wave propagation in a visco-elastic medium, such as the tissue constitutes for this frequency range (71). The high viscosity of the medium makes possible the use of simplified theoretical assumptions such as a homogeneous isotropic infinite medium and a vibrating sphere instead of a circular piston. The results of such a theory agree well with the measured characteristics. As a consequence it has been possible to assign absolute values to the shear viscosity and the shear elasticity of soft tissue. (See Table 7-74 in Acceleration, No. 7.) The theory, together with the measurements, shows that over the audio-frequency range most of the vibratory energy is propagated through the tissue in the form of transverse shear waves and not in the form of longitudinal compression waves. Such shear waves have a much smaller propagation velocity (and therefore wave length) than sound and a strong dispersion. The velocity is about 20 m/sec. at 200 Hz and increases approximately with the square root of the frequency. This may be compared with the constant sound velocity of about 1500 m/sec. for compressional waves. Some energy is propagated along the body surface in the form of surface waves which have been observed optically. Their velocity is of the same order as the velocity of shear waves.

From the mechanical impedance of the body surface one can calculate the acoustic absorption coefficients. This indicates what percentage of an incident air-borne sound wave is absorbed at the body surface and propagated through the tissue and what percentage is reflected (64). At 100 Hz a small area of the forehead or of soft tissue absorbs only about 2 percent of the incident

Figure 8-19

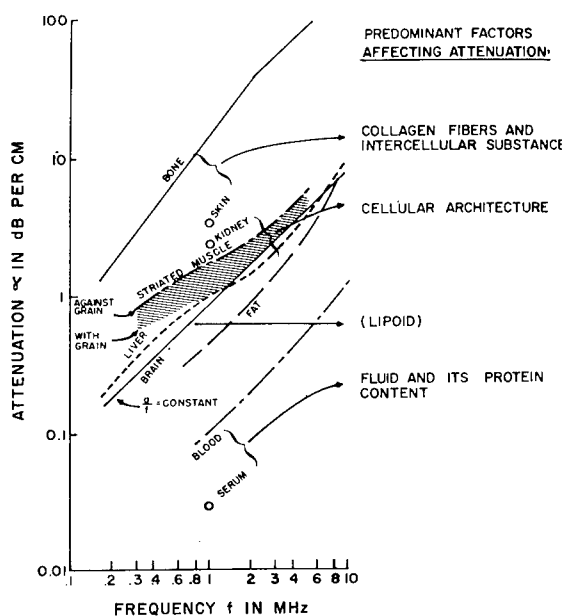
Response of Body Tissues to High Frequency Vibrations



a. Resistance and Reactance of Circular Area 2 cm. Diameter, of Soft Tissue Body Surface

Smooth curves calculated for 2 cm. sphere vibrating in a) visco-elastic medium with properties similar to soft tissue, b) frictionless compressible fluid, c) incompressible fluid.

(After Goldman and von Gierke⁽⁷³⁾, adapted from von Gierke et al⁽⁷¹⁾)



b. Approximate Values of High Frequency Sound Attenuation in Various Tissues

(After Goldman and von Gierke⁽⁷³⁾, adapted from Goldman and Hueter⁽⁷⁴⁾, and Dussik et al⁽⁴⁷⁾)

sound energy. At higher frequencies a still smaller percentage is absorbed. Only the specialized structure of the ear allows a small area of the body surface, the tympanic membrane, to absorb much more energy; for example, at 1000 Hz, 50 to 80 percent. This is achieved by the middle ear transformer action which matches the tissue structures of the inner ear to the characteristic impedance of air. (See Sound and Noise, No. 9, for aural, local, and diffuse body effects.)

Ultrasonic Vibrations (73)

Above several hundred kHz in the ultrasound range, most of the vibratory energy is propagated through tissue in the form of compressional waves and geometrical acoustics offers a good approximation for the description of their path (20, 156). Since the tissue dimensions under consideration are almost always large compared with the wavelength (about 1.5 mm at 1 m Hz) the mechanical impedance of the tissue is equal to the characteristic impedance, i.e., sound velocity times density. This value for soft tissue differs only slightly from the characteristic impedance of water (74). The most important factor in this frequency range is the tissue viscosity, which brings about an increasing energy absorption with increasing frequency. At very high frequencies this viscosity also generates shear waves at the boundaries of the

medium, at the boundary of the acoustic beams, and in the areas of wave transition to media with somewhat different constants, (e.g., boundary muscle to fat tissue, or soft tissue to bone). These shear waves are attenuated so rapidly that they are of no importance for energy transport but are noticeable as increased local absorption, i.e., heating.

From 500 kHz to 10 m Hz the attenuation coefficient describing the decrease of the sound intensity in a plane ultrasound wave, is only in fair agreement with the value one would calculate from the tissue viscosity measured in the audio-frequency range. The tissue deviates in this frequency range from the behavior of a medium with constant viscosity. In Figure 8-19b, attenuation coefficients measured in different types of tissue are summarized (47, 74). On this graph a curve, $\frac{\alpha}{f^2} = \text{constant}$, would be indicative of classical viscous absorption with constant shear viscosity. A smaller slope, or a change in slope, indicates a change in viscosity with frequency (relaxation phenomenon). The graph gives only a few examples and typical functions from a large body of attenuation data available. The absorption of most soft tissues is in the range from 0.5 to 2dB/cm/m Hz. The order of increasing absorption is: brain tissue, liver tissue, striated muscle, smooth muscle, kidney, skin and tendon. Bone has the highest value with approximately 10 dB/cm.

PATHO-PHYSIOLOGICAL RESPONSE TO VIBRATION

The effects of vibration on the physiological functioning of the body may be considered in two categories: a) those changes which are directly attributable to the differential vibratory movement or deformation of particular body structures giving permanent or transient damage, and b) generalized responses to vibration as a non-specific stress. These are more dependent on magnitude and duration and less on frequency than the primary effects.

Permanent Pathological Changes

Permanent pathological changes may follow very severe vibration. Animals can be killed by vibration (73). There is a poorly defined dependence on frequency of the lethal accelerations above 10 G which coincides with the resonant displacement of the visceral organs (116). Post-mortem examination of these animals usually shows lung damage, often heart damage, and occasionally brain injury. The injuries to heart and lungs probably result from the beating of these organs against each other and against the rib cage. The brain injury, which is a superficial hemorrhage, is not yet interpretable in definite terms; it may be due to relative motion of the brain within the skull, to mechanical action involving the blood vessels or sinuses directly or to secondary mechanical effects transmitted through the cerebrospinal fluid (15). Tearing of intra-abdominal membranes is rarely seen. Exposure for several minutes to peak acceleration of about 5 g often produces heart damage as indicated by delayed changes in the electrocardiogram. An increase in body temperature is found on exposure to vibration. Since this occurs also in dead animals it is probably mechanical in origin. Calculations

of heat absorption based on body impedance data suggest that appreciable heat can be generated at large amplitudes. Exposure of monkeys to 5g at 10 and 20 Hz for several hours seems to produce some damage to the vestibular system but these findings require confirmation (148).

Rarely has permanent damage been produced in humans by total body vibration. Observations on man have been made in a few instances and indicate that above about 3g, sharp pain in the chest may occur (184, 193). Traces of blood have occasionally been found in the feces after exposure of 6g at 20 to 25 Hz for about 15 minutes suggesting mechanical damage to the intestine or rectum. (See Figure 8-31 - uppermost curve.)

At very severe levels of vibration, chromosomal changes have been produced in microbes and insects along with mutations (3, 100). The significance of these changes to man is not clear.

Chronic injuries may be produced by vibration exposure of long duration at levels which produce no apparent acute effects (73). In practice, such effects are usually found after exposure to repeated blows or to random jolts rather than to sinusoidal motion. When such shocks or blows are applied to the human body at relatively short intervals, the relation of the interval to tissue response times becomes very important. Exposure to such forces frequently occurs in connection with the riding of vehicles. Buffeting in aircraft or in high-speed small craft on the water, and shaking in heavy vehicles on rough surfaces, give rise to irregular jolting motion. Acute injuries from exposure to these situations are rare but complaints of discomfort and chronic minor injury are common. Truck and tractor drivers often have sacroiliac strain. Minor kidney injuries are occasionally suspected and, rarely, traces of blood may appear in the urine. The length of exposure and the details of the ways in which the body is supported play an important role.

Chronic injuries are also produced by localized vibration, such as the pain and numbing of the fingers on exposure to cold which affects many people after several months of using such equipment as pneumatic hammers and drills or hand-held grinders or polishers (58, 71). The heavier, slow-moving devices appear to produce more severe jolting. Little is known of the mechanism of the injury or of the actual forces responsible, although many high frequency components may be present (2). The repeated insults to the tissues directly or through vasoconstrictor responses seem to gradually affect the arterioles, capillaries, and their nerve supply giving a Renaud's syndrome (58). Repeated vasoconstriction in response to high intensity sound may also increase the incidence of this syndrome (97). Injuries resembling these have been produced in the feet of rats exposed to 60 Hz at 8 to 9 g for 10 to 12 hours per day up to about 1000 hours (84). This vascular condition has been treated with ultrasound (156, 191).

Physiological Response

The primary physiological responses to vibration include:

- Subjective sensation of pain and discomfort.
- Neurological function,—including the perception of vibration and regulation of posture.
- Cardiovascular changes in blood pressure, electrocardiographic outputs, and blood cell counts.
- Respiratory changes in tidal volumes, rates, and valsalva response.
- Metabolic imbalances.
- Endocrine malfunction.

Subjective Response

The nature of the subjective response varies with the axis of vibration.

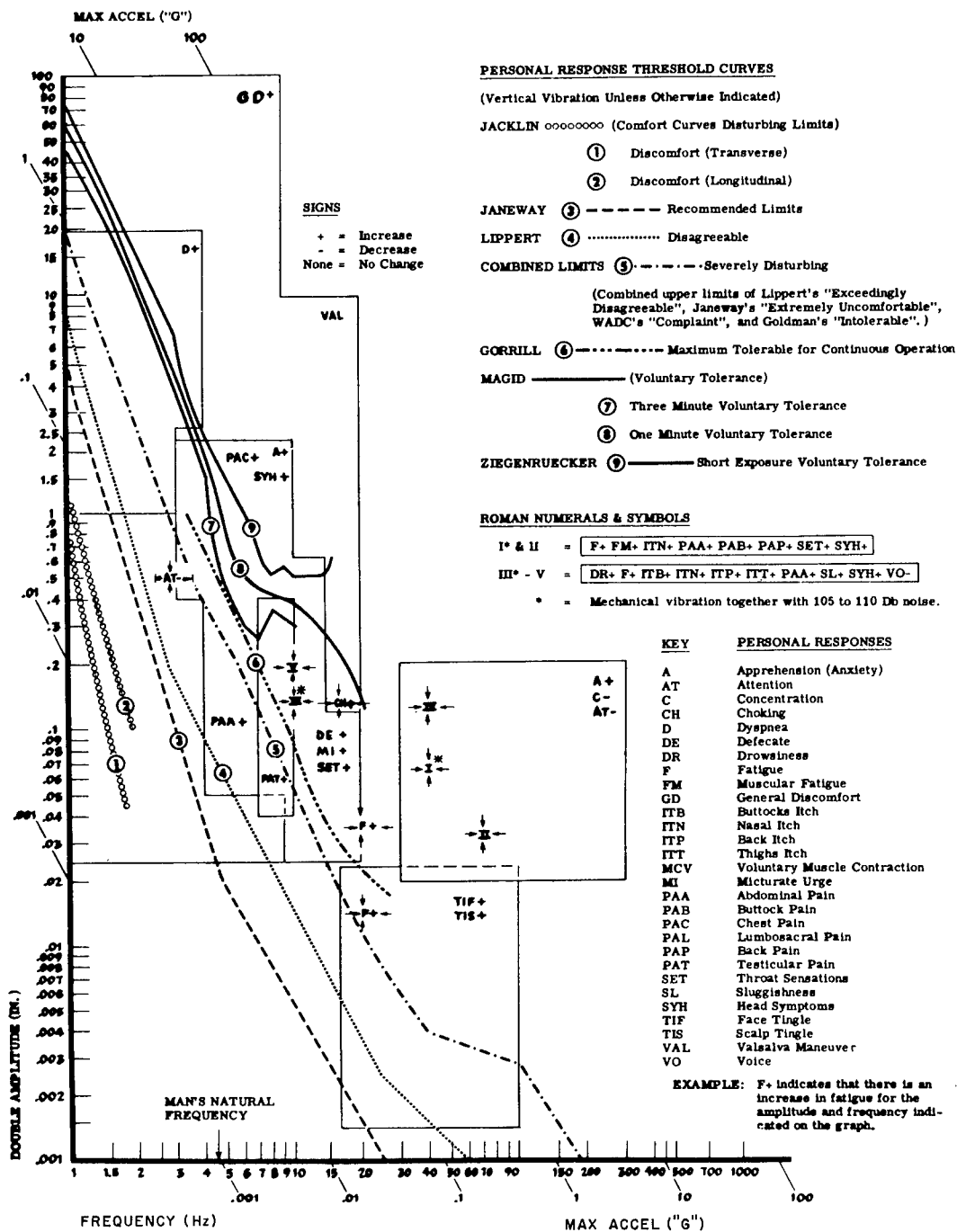
Longitudinal or Vertical Vibration ($\pm G_z$)

The subjective and symptomatic responses to vertical sinusoidal vibration are reviewed in Figures 8-20 and 8-31 (70, 94, 96, 107, 123, 168, 178, 193). The subjective responses of the subjects range from the perception of feeling through discomfort, apprehension to pain and are the primary sensations correlated with the physical response of the body. Most tolerance criteria are based on these subjective responses. Testing to the point of serious physical or physiological damage to the body is, of course, unacceptable for human subjects. It may be assumed that, in most cases, these levels are well below those that would cause damage to bodily tissue. Table 8-20 indicates the gross variability in previous attempts to set thresholds for tolerance to vibration.

Table 8-21 is a descriptive summary of the symptoms during vertical vibration plotted in Figure 8-22.

Generally there are three apparently simple criteria: the threshold of perception, of unpleasantness, and of tolerance. The latter two are difficult to identify and reproduce, although agreement to within a factor of about 3 has been obtained. In studies lasting up to 20 minutes, no single subjective end point is found for a whole population, although some reactions are more common than others (115, 126, 193). There is a general tendency for those body organs with high mobility to give symptoms at low frequency and those with little mobility to be affected at higher frequencies. Very long exposure to vibration much above the level of perception seems to be irritating and fatiguing.

Subjective responses to vertical sinusoidal vibration while standing have been studied (19, 41). In general, standing subjects tolerate this form of vibration more readily than when sitting, probably because of the damping factor of leg flexion (90°). Except for body sway and balance difficulty, physiological effects are similar. Figure 8-23a compares the subjective symptom threshold for standing and sitting subjects with acceleration recorded on the shake table. Figure 8-23b gives the body areas affected. At the higher



This chart summarizes the reported reactions to a wide range of vibrations, plus some objective signs of physiological change, as reported in the literature up to 1960.

Figure 8-20

Subjective Response to Vibration

(After Webb⁽¹⁷⁸⁾, adapted from Linder⁽¹⁰⁷⁾)

Table 8-21

Regional Symptomatology During Vertical Vibration

(After Magid et al⁽¹¹⁷⁾)

HEAD-NECK

Head Sensations	Vibration or "tight" sensation of facial skin
Pharynx	Pharyngeal tug or "lump in throat"
Jaw	Sensation of vibration
Speech	Lower frequencies secondarily affected due to reactions of thorax and abdomen, high frequencies due to superimposed transmitted vibrations to laryngeal tissues and possibly main stem bronchi

THORAX

Respiration	Decreased ability to perform physiological respiratory movements of the thoracic cage due to superimposed forces from oscillating platform
Dyspnea	Actual air hunger
Valsalva	Partial or complete closure of glottis resulting in increased intrathoracic and intra-abdominal pressure
Pain	Dull-to-severe pain of the precordium occasionally radiating to the sternum, no other radiations, pain subsiding immediately after cessation of vibration

ABDOMEN

Voluntary Abdominal Musculature Contraction	Degree of contraction or "bearing down"
Pain	Usually periumbilical with tendency to radiate to right lower quadrant

SKELETAL MUSCULATURE

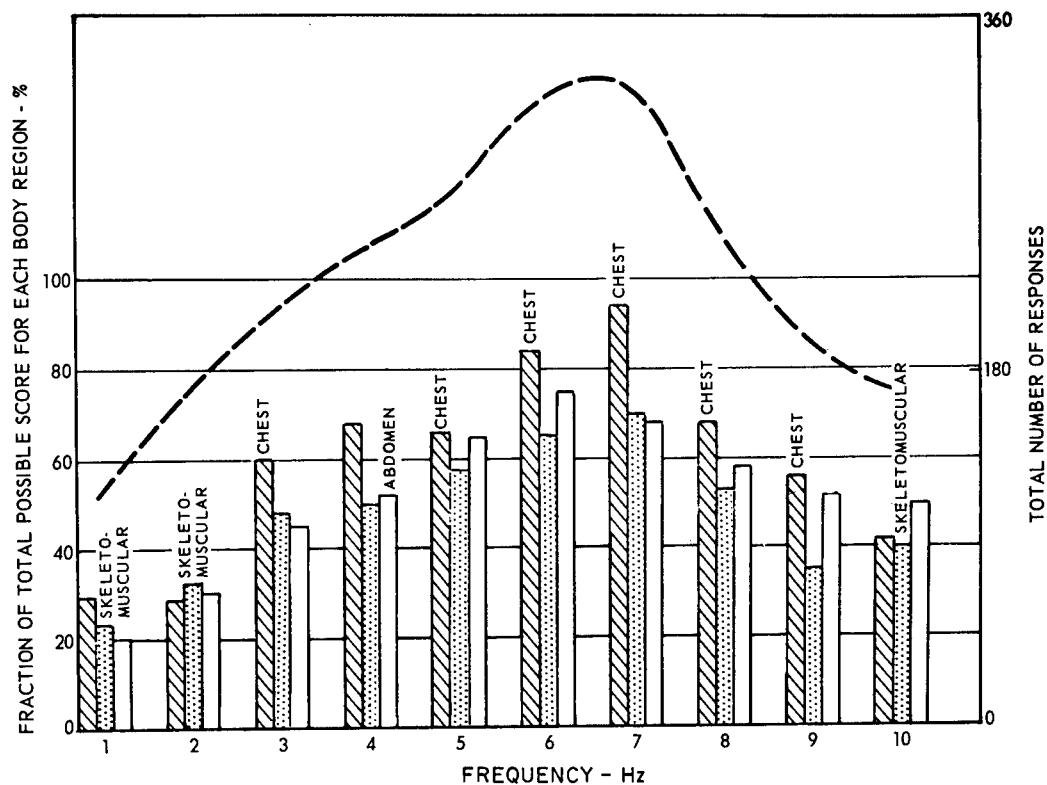
Skeletal Musculature	Sensation of "muscle tightness" or possibly increased muscle tone primarily of the lower extremities, dorsum, and neck
Voluntary Muscle Contraction of Extremities	Muscular contraction in an effort to counteract movements of oscillating platform
Lumbosacral Pain	Dull-to-severe pain at midline with bilateral radiation, subsiding immediately after cessation of vibration

PELVIC-PERINEAL COMPLEX

Micturate (Urge)	Mechanical stimulation of bladder neck and proximal portion of urethra
Defecate (Urge)	Mechanical stimulation of distal portion of sigmoid colon and rectum

GENERAL DISCOMFORT

Overall estimation of each frequency ridden



This chart summarizes the subjective responses of ten experienced subjects exposed to vertical sinusoidal vibrations ranging from 35 inches double amplitude at 1 Hz to about 1/4" double amplitude at 6-10 Hz, which produced accelerations of 1.2 ± 0.6 G. They were seated on a hard surfaced aircraft seat and were restrained by a lap belt and shoulder harness. The total number of subjective responses for each frequency was summed; they reached a peak at 6 and 7 Hz, as shown by the upper dashed curve and the right hand vertical scale. The vertical bars show the approximate magnitude of the following groups of symptoms:

Chest (cross-hatched bars) - Respiratory difficulty, pain, and breath holding (Valsalva maneuver).

Skeletomuscular (stippled bars) - Muscle pain, back pain, general discomfort.

Abdomen (open bars) - Contraction, pain.

The words above each set of bars state what symptoms set the limit for voluntary tolerance for that particular frequency.

Figure 8-22

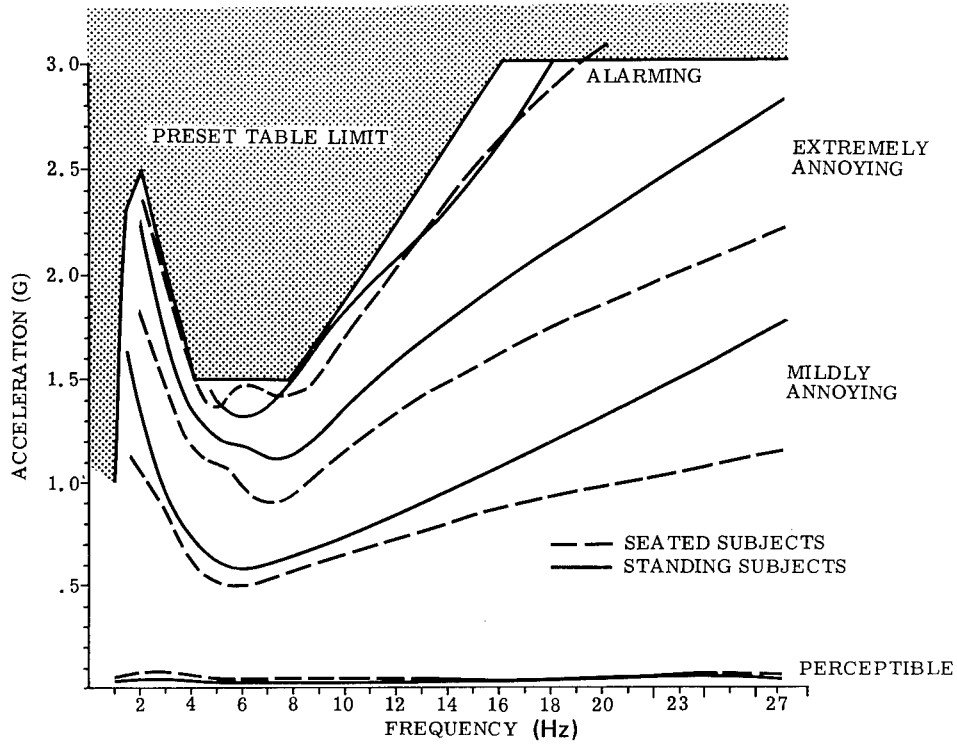
Subjective Responses to Vertical Vibration While Seated

(After Webb⁽¹⁷⁸⁾, adapted from Magid et al^(115, 117))

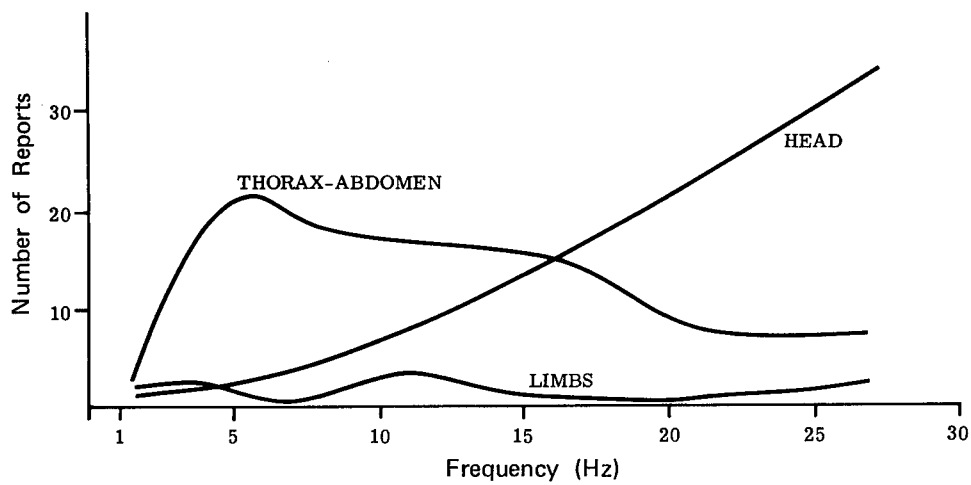
Figure 8-23

Subjective Reactions and Body Areas Affected by Vibration in Seated and Standing Subjects

(After Chaney⁽¹⁹⁾)



a. Subjective Reaction Curves - Seated and Standing Subjects



b. Relationship Between Body Areas Affected by Vibration When Standing

frequencies, a higher acceleration is generally accepted on the second encounter with a given frequency.

Semi-Supine and Other Vibrational Axes

There are few data available on symptoms during semi-supine vibration. In transverse vibration (in the fore-aft direction) of a seated subject, there is a shearing force applied to the buttocks which must be considered (80). Data are available on symptoms during sinusoidal vibration in the X, Y and Z axes in contoured and adjustable couches proposed for spacecraft use. A detailed review will be presented of this study with the acceleration of gravity vectored through the X-axis. The contoured couch was similar to the project Mercury couch. Restraint was provided by two-inch straps; no helmet was used; the head was unrestrained. The adjustable couch had leg and foot supports, torso and lower extremity support straps, and provided closer coupling than the contoured couch. During exposures in the contoured couch each subject was told to maintain his position in the couch with his head in the headrest as long as possible by whatever bracing or straining maneuvers that were useful. However, if head buffeting against the headrest contour did become intolerable before other symptoms became tolerance limiting, he was to lift his head from the headrest and continue until forced to stop by other symptoms. In the contoured couch the head was restrained. Pertinent angles and g-load nomenclature are noted in Figure 8-24a.

At a preset frequency, the double amplitude of sinusoidal vibration was increased at a rate of 0.75 mm per second until the subject signaled that he had reached his limit of voluntary tolerance. The acceleration level thus reached was considered a subjective tolerance value for that frequency.

Curves describing the averages of these acceleration and velocity-time tolerance levels at each of the frequencies studied in the contoured couch are presented in Figure 8-24b and d. This figure reveals that the Y and Z axis curves are similar throughout their extent, rising from the 2 G level at the low frequencies to the 12 to 14 G level at 20 Hz. The X axis curve is slightly higher than the other two below 8 Hz but rises more slowly as frequency increases above this point, reaching a maximum of only about 50% of the Y and Z axis values at 20 Hz. The X axis curve is slightly higher than the other two below 8 Hz but rises more slowly as frequency increases above this point, reaching a maximum of only about 50% of the Y and Z axis values at 20 Hz.

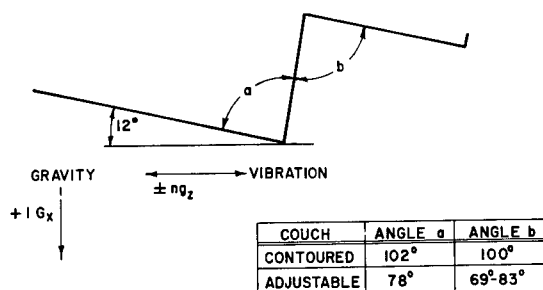
Curves tracing the average values of accelerations and velocity seconds tolerated in the adjustable couch are shown in Figure 8-24c and e. Although representing fewer data points, they permit axis tolerance above 8 Hz with a slight improvement below this frequency. The X axis curve is considerably higher below 12 Hz but flattens out at the higher frequencies. Except for some drop-off above 15 Hz, Z axis tolerance is quite similar to that attained in the contoured couch.

Table 8-25a summarizes the symptoms occurring during X axis exposures. With both couches, the principal focus of complaints was the thorax. Using the contoured couch, these complaints were present throughout the frequency

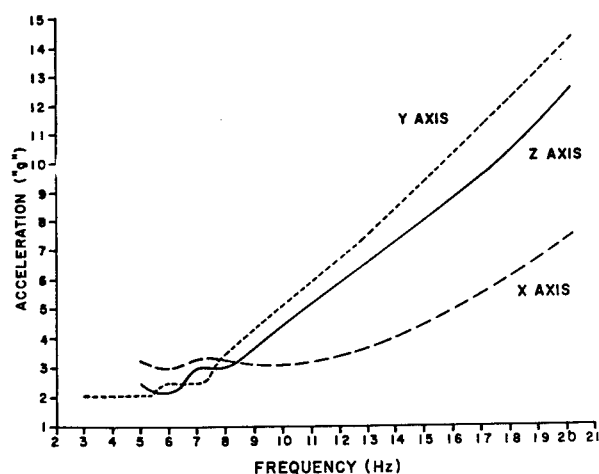
Figure 8-24

Couch Parameters and Tolerance Levels During Vibration in the X, Y, and Z Axes

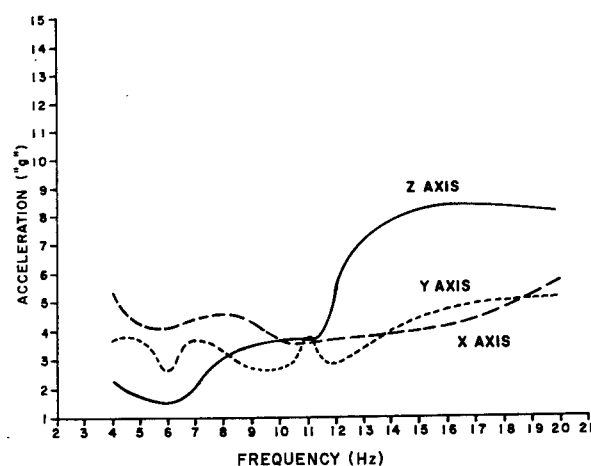
(After Temple et al⁽¹⁶⁸⁾ and Weis et al⁽¹⁷⁹⁾)



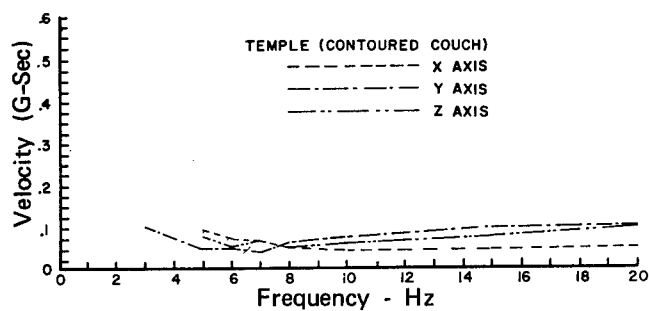
a. General Orientation of the Body (Semisupine) and the Principal Body Angles in Both Couches



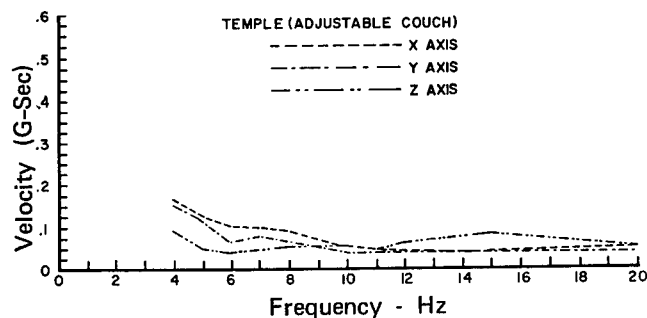
b. Average Levels of Acceleration Tolerance in the Contoured Couch



c. Average Levels of Acceleration Tolerance in the Adjustable Couch

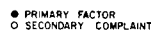
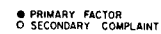


d. Velocity - Time Plots of Tolerance in Contoured Couch



e. Velocity - Time Plots of Tolerance in Adjustable Couch

● PRIMARY FACTOR
○ SECONDARY COMPLAINT



range studied but with the adjustable couch they occurred at, and below, 12 Hz. In both systems the majority of the complaints were of pain or a poorly defined "pressure" referred to the substernal area. Considerable difficulty with respiration, particularly inspiration, was encountered in both couches. In the contoured couch this difficulty was almost invariably associated with abdominal or other thoracic symptoms. Complaints referable to the abdomen were relatively more frequent in the adjustable couch, occurring at and below 12 Hz, but with no predominant localization. These complaints were in the nature of a poorly defined "dull discomfort." There were complaints of headache in the contoured couch, occurring across the frequency range, but head complaints were relatively more common in the adjustable couch, almost entirely at the frequencies above 14 Hz. These included headaches and poorly characterized, transitory feelings of "confusion" or "disorientation" which cleared almost immediately upon cessation of the exposure. Sharp, repetitive impact of various body segments, occurring alternately against couch and restraint with each vibratory cycle, caused considerable difficulty in the adjustable couch at frequencies up to 15 Hz. This "banging," as it was described by the subjects, was a particular problem in the sacral area where, apparently, point-loading was occurring. "Banging" was not encountered in the contoured couch in this axis.

Symptoms occurring during Y axis exposures are summarized in Table 8-25b. Again, with the contoured couch, the thorax was a major source of difficulty. In this instance, however, the complaints were primarily of a "pressure" referred subcostally. As in the X axis respiratory difficulties were present, albeit not quite as frequently, and were associated again with abdominal or other thoracic symptoms. Thoracic and respiratory symptoms were relatively less frequent with exposures in this axis in the adjustable couch and, with both couches, the symptoms were largely confined to the frequency range below 10 Hz. Abdominal complaints were more frequent in both couches here than in the X axis. They were present across the frequency range in the contoured couch but were largely limited to the region below 12 Hz in the adjustable couch. The symptoms were, again, poorly described "pressures" or discomforts. In the contoured couch, below 9 Hz, they were largely referred to the epigastrium and, above this level, to the suprapubic area while in the adjustable couch they were principally referred to the epigastrium and periumbilical area. In the frequency range 3 to 6 Hz subjects in the contoured couch frequently complained of significant general fatigue and neck muscle soreness and "spasm." There were some complaints referred to the head, principally headache, in the adjustable couch at and above 10 Hz. Another problem of significance in the contoured couch in this axis was that of frictional rubbing against the couch or restraint straps, giving rise to erythema and abrasions (occasionally blisters) of the hips, thighs, and calves and other areas underlying the restraint straps. This was occasionally associated with reports of "banging" such as were previously encountered in connection with the adjustable couch in the X axis. Both problems became more severe as the frequency increased.

Symptoms occurring during Z axis exposures are seen in Table 8-25c. There were more complaints referable to the head in this axis in both couches than had been previously noted. In the contoured couch these consisted primarily of headache and neck-muscle soreness in the 5 to 10 Hz range; and

instances of "confusion" or "disorientation," such as occurred in the X axis, scattered across the frequency range. In the adjustable couch the head symptoms occurred almost completely below 12 Hz and included headache, "confusion" or "disorientation," some head "banging" and general unpleasantness. There was a major difficulty with respiration, particularly inspiration, in the adjustable couch in this axis. This was quite often unassociated with any other complaints, in contrast with the other two axes, and occurred across the frequency range. Complaints of this nature were much less frequent in the contoured couch. Thoracic complaints were similar with both couches but were noted up to a slightly higher frequency in the adjustable couch. Abdominal symptoms in both couches followed patterns very similar to those present for the respective couches in the Y axis. In the contoured couch, below 9 Hz, the complaints were again referred to the epigastrium while above 6 Hz testicular symptoms, described as "fullness," "tapping," or "squeezing," replaced the suprapubic symptoms noted in the Y axis. These testicular symptoms occurred very infrequently in the adjustable couch. A number of subjects in the contoured couch stopped simply because they had just "had enough." This complaint was not frequency-related.

Almost all symptoms, such as thoracic "pressure," abdominal discomfort, or headache, of which subjects complained following exposures in any of the axes were gone within 5 to 10 minutes. The abrasions and occasional blisters were medically treated and healed without complication. Infrequently, a headache or sore neck persisted beyond the immediate post-exposure period for 12 to 24 hours or, more rarely, for longer periods but no serious problems arose.

Further analysis of the contoured couch data directs attention to two factors that influenced the results. The first relates to the complaints of intolerable frictional rubbing (and, less frequently, "banging") of body segments against the couch or restraints which occurred, especially at the higher frequencies, in the Y and, to a lesser extent, the Z axis. Two conditions appear to have been responsible for this problem. One was the variable, occasionally loose, body-to-couch coupling which often resulted in dead space between subject and couch, or in unavoidable slackness in the restraint. The other, arising from the first, was the development during vibration of phase shifts between body segments and the couch due to the mechanical response characteristics of the system.

The second factor pertains to the lack of head restraint. One objective of the contoured couch exposures had been to determine the desirability of raising the head, when its buffeting against the couch became unbearable, in an attempt to prolong the duration of the exposure and increase the level of acceleration reached. It appears, however, that the benefits accruing to this procedure were negated by the resulting fatigue and the precipitation of, or accentuation of, head, neck, and thoracoabdominal symptoms.

In composite vibration, the direction and magnitude of the resultant acceleration are important in determining its subjective acceptability (76). If a subject is exposed to simultaneous vertical and horizontal (fore-and-aft) vibrations of equal frequency and amplitude, a circular motion of the seat may be produced by suitable phasing of the two vibrations. It has been

demonstrated that, if the direction of circular motion of the seat is backward-running (i. e., anti-clockwise as viewed from the right), the subject's physical and subjective responses are essentially those characteristic of horizontal excitation; but, if the circular motion is forward-running, the response resembles that to vertical vibration (80).

Threshold of Vibration Sensation

Whole-body accelerations of sufficient intensity can be appreciated as oscillatory at frequencies down to 0.1 Hz, a frequency corresponding with the slowest, noticeable, heaving-movements of a large ship, and possibly lower. The threshold of sensation for linear oscillation in the long axis of the body, as determined by parallel swings, is about 0.005 g at frequencies of 1 Hz and below (177). At such frequencies, the sensation is mediated by the vestibular organs and by somatic receptors in the areas of application of the vibration to the body. The sensation of motion may, of course, be augmented by seeing surrounding objects in relative oscillation. At higher forcing frequencies, where body resonances and phase shifts in the transmission of vibration occur, the sensation of vibration is presumed to be mediated by mechano-receptors throughout the body. The threshold of perception of whole-body vertical vibration in the range 1 to 20 Hz lies between 0.01 and 0.002 g, with the lowest threshold (maximum sensitivity to vibrational acceleration) at 3 to 6 Hz (72). When standing, the sensitivity at low frequencies less than in the seated position is shown in Figure 8-23a.

The threshold of sensitivity of the finger tips to sinusoidal vibration is recorded in Figure 8-26. The difference limens (DL) for rate of intermittent stimuli at the finger tip in comparison with those of the ear are shown in Figure 8-27. The mechanism which allows these skin receptors to distinguish between rates in the vicinity of 300 Hz with less than a 10% error are under study (124). No gross change in sensitivity to vibration appears to be brought on by previous vibration exposure (80).

Even though the pattern of the vibration be quite complex, habituation to vibration occurs, as it does to noise, if the quality of the stimulus is constant. For example, one can quickly cease to notice considerable intensities of noise and vibration on board ship. Low frequency (1 to 2 Hz) steady-state oscillation of moderate intensity can be soporific in man, as exemplified by the practice of baby-rocking and the relaxation afforded by the rocking chair. Random vibration, on the other hand, tends to increase arousal, as does the sudden onset, alteration, or cessation of a particular condition of vibration. Irregularity and intermittency of stimulation oppose habituation. Habituation to sustained vibration is probably a central phenomenon, although some adaptation may occur at the receptor level. Sinusoidal oscillations at frequencies between 0.1 and 1 Hz, or random vibration with a spectral representation in that region, can induce motion sickness. (See Acceleration, No. 7).

The nature of the synchronous electrical activity which can be recorded from the brain during vibration remains an open question (1, 80). There is no published evidence that the human E. E. G. can be driven by low frequency vibration in a manner analogous to photic driving. The likelihood of motion

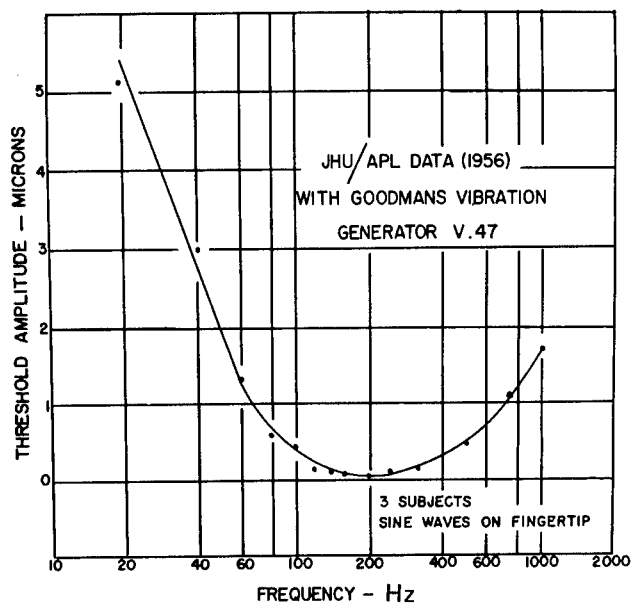


Figure 8-26

Observed Relation Between Threshold Amplitude of Vibration and the Frequency of Sine Waves for the Finger Tip

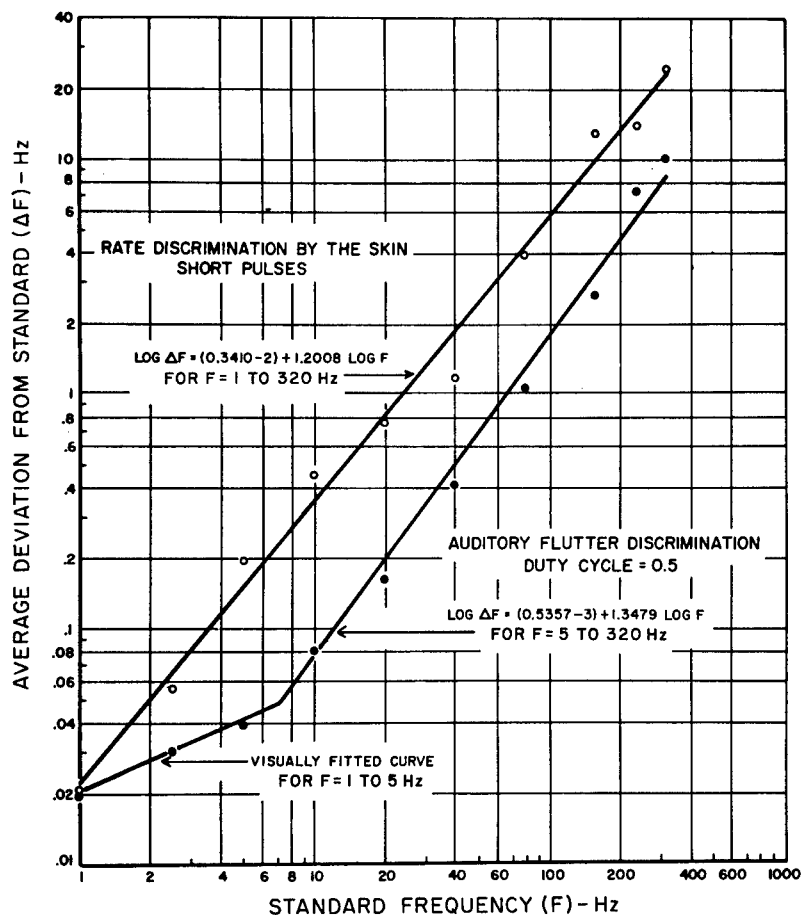
(After Mowbray and Gebhard⁽¹²⁴⁾)

Figure 8-27

Different Limens for Finger Tip Vibration Sensitivity and Acoustic Sensitivity

Upper curve: Relation Between Δf and $\log f$ for the tactile data.
Lower curve: The same relation for the auditory flutter data.

(After Mowbray and Gebhard⁽¹²⁴⁾)



artifacts and the possibility of E.E.G. changes produced by indirect physiological mechanisms, such as hyperventilation, should be borne in mind if abnormal E.E.G. recordings are seen during vibration.

The Cardiovascular System and Blood

In man, measurements of cardiovascular activity during whole-body vibration have generally been restricted to the pulse rate, the blood pressure and the electrocardiogram. The changes in pulse rate, blood pressure, and cardiac output reported in the literature have been varied and non-specific, resembling the responses associated with alarm or moderate exercise (23, 112, 149, 152). The rise in systolic radial arterial pressure during vibration at frequencies above 3 Hz was unaccompanied by a fall in the diastolic pressure (153). Figure 8-28a and b indicate the oxygen consumption and cardiovascular response to $+G_x$ vibration.

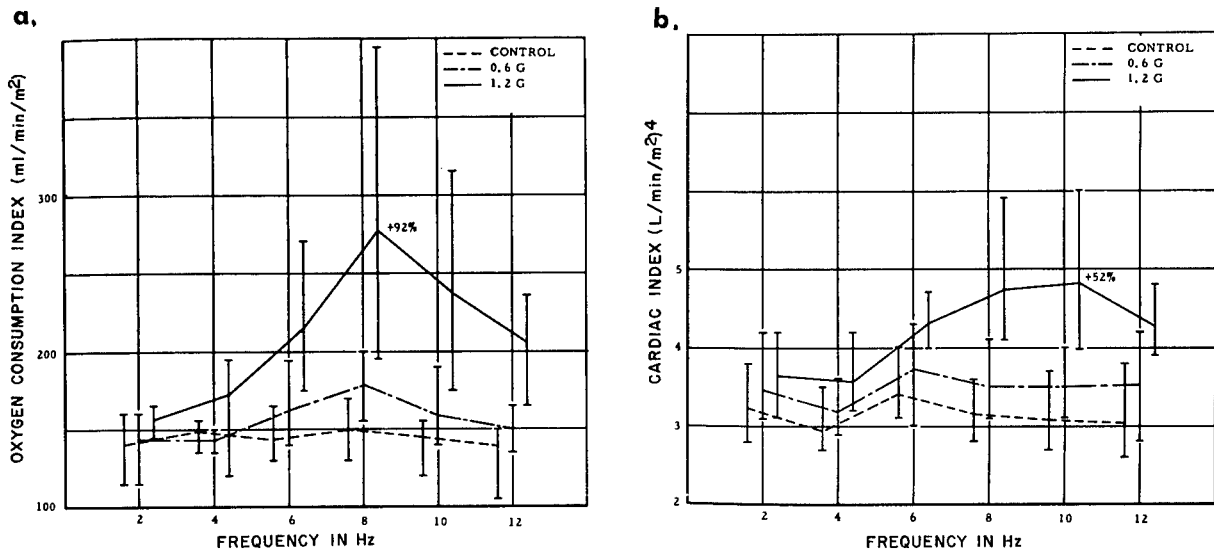
At low frequencies of vibration (2 to 3 Hz), beating has been observed between the pulse and vibration frequencies during arterial pressure recordings in the dog (4). A fall in the skin temperature has been noted in the lower limbs during whole body vibration of human subjects. Other changes in peripheral vasomotor activity, mediated by autonomic efferent impulses, have been demonstrated by workers using the galvanic skin reflex as a measure of vibration stress (41). Changes in the formed elements of the blood appear to be related to general stress response (80, 152). (See also Reynaud's phenomenon in section on permanent pathology.)

Respiratory Physiology

The increases in oxygen consumption and respiratory quotient have been attributed to a raised metabolic activity due to the muscular effort of maintaining the posture during vibration. This explanation is supported by the fact that the increases in these respiratory indices were found to be greater when the subjects were standing up than when they were seated during low frequency vibration of the same intensity. The differences produced by varying g load and direction of vibration are seen in comparison of graphs in Figures 8-28a and 8-28c. Exposure to altitude above 10,000 feet lowers vibration resistance in animals (121).

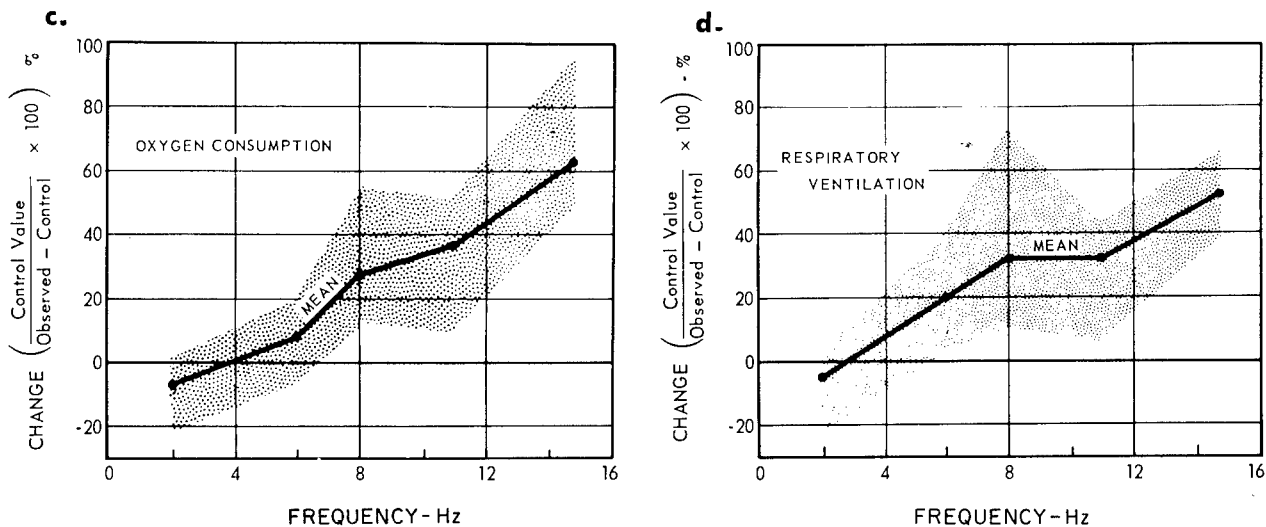
The relation of respiratory response to resonance is not clear in that a significant increase only at forcing accelerations exceeding 0.5 g at 9.5 Hz was recorded in one experiment (50, 51), while a fairly linear increase in oxygen consumption with increasing frequency from 6 to 15 Hz, at a fixed displacement-amplitude of 0.132 in. at 0.46 to 2.88 g was recorded in another (60). Increase in oxygen consumption has also been found to be greatest at the lowest frequencies of vibration, at constant acceleration-amplitude, in the range 2 to 7 Hz (46). Some of these responses are seen in Figures 8-28d and 8-29a and b. The changes are more pronounced early in the exposure and appear to be compounded of a passive mechanical effect added to a physiological response to vibration stress. Hyperventilation with hypocapnia, on occasion, may be caused by stress or discomfort; also increased muscular demand for oxygen may be augmented by superimposition

Figure 8-28
Cardiovascular and Respiratory Response to +G_z Vibration



Average oxygen consumption (a) and cardiac index (b) of four human subjects vibrated in the (front to back) direction. The subjects were in the semi-supine position and vibrated for 6 minutes at two vibration intensities (0.6G and 1.2G). (The bars indicate the range of the data).

(After von Gierke⁽⁶⁵⁾, from data of Clarke et al⁽²³⁾)

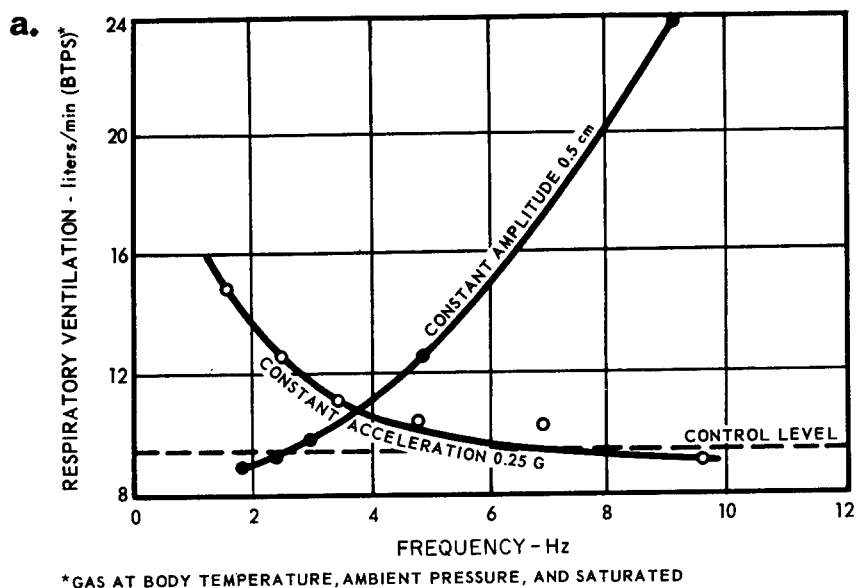


The change in oxygen consumption for four male subjects during vibration is shown in (c) as a percentage change from the control value, with the mean values being connected by a line and the range shown with shading. Similar data are shown in (d), where respiratory ventilation is also shown to increase as a function of frequency, when amplitude is held constant. The subjects were exposed to 20 minutes of G_z vibration at an amplitude of 0.132 inch while seated on a chair and entirely unrestrained.

(After Webb⁽¹⁷⁸⁾, adapted from Gaueman et al⁽⁶⁰⁾)

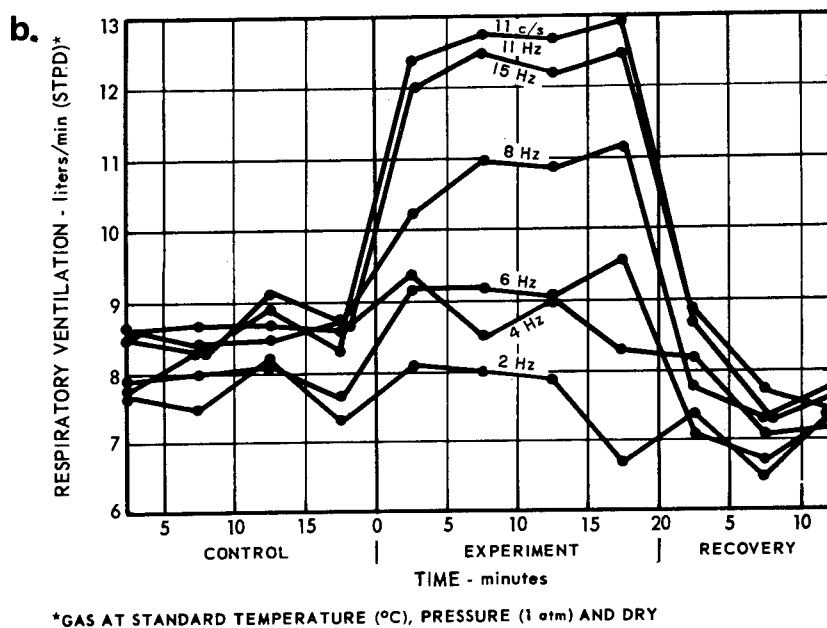
Figure 8-29

Respiratory Ventilation During Longitudinal Vibration While Seated



Average respiratory ventilation rates are shown for 12 men who were vibrated while seated on a hard platform at the amplitudes, rates, and acceleration shown.

(After Webb⁽¹⁷⁸⁾, adapted from Ernsting⁽⁵⁰⁾)



Mean values of respiratory ventilation are shown for 5 seated men exposed to a 20-minute period of vibration at 0.125 inch amplitude, at frequencies from 2 to 15 Hz as marked on each curve.

(After Webb⁽¹⁷⁸⁾, adapted from Hoover and Ashe⁽⁸⁹⁾)

of oscillations at forcing frequency (89, 192). Labyrinthine factors may be at play during very low frequencies of 1.76 Hz (52). The hypocapnia, occasionally seen, may affect performance (23, 42).

Metabolic Factors

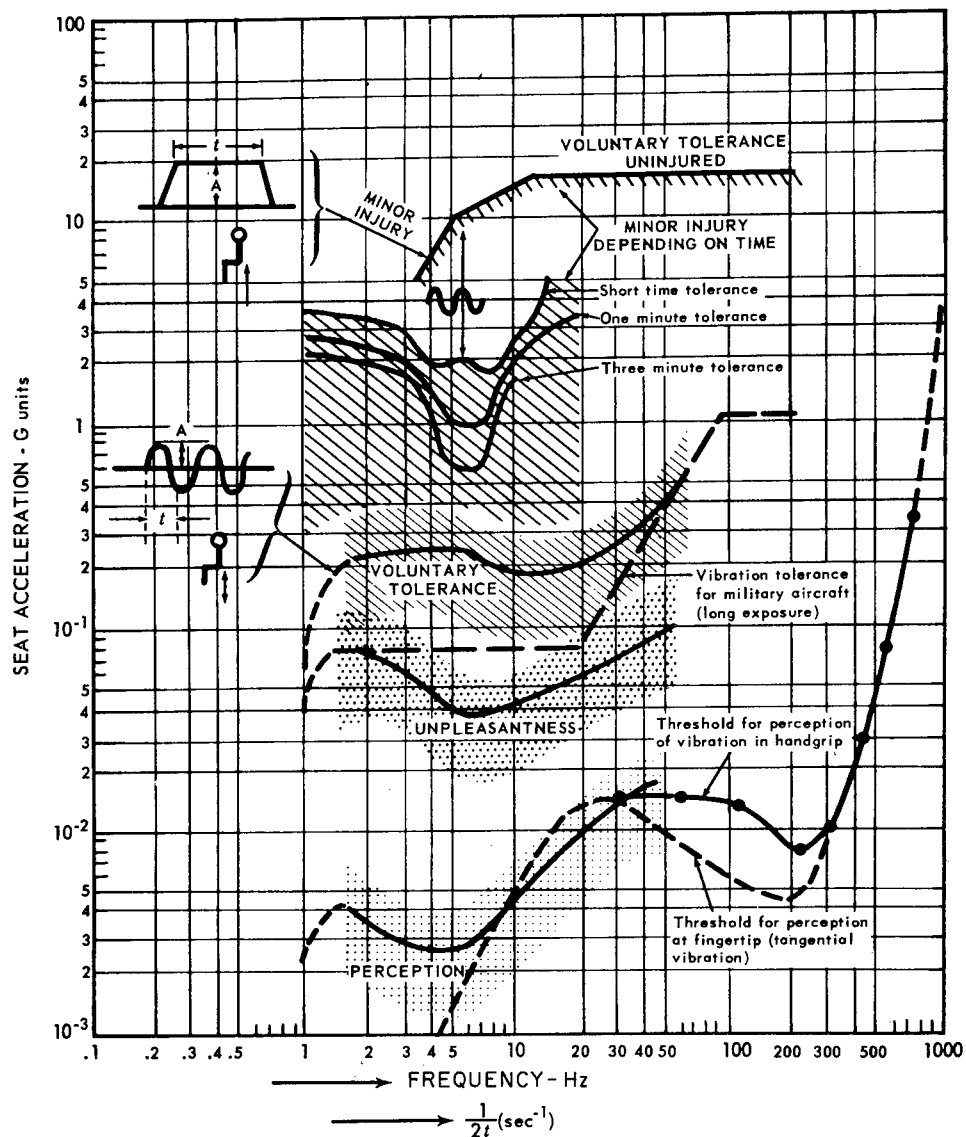
The increase in oxygen consumption and endocrine changes in animals have been attributed to several stress factors in chronic exposure to vibration (80). Loss of body weight can also be found (89). In humans, 9 minutes of vibration at the predicted 3 minute tolerances (118) (see curves in Figure 8-30) for selected frequencies ranging from 1-20 Hz produced statistically significant increase in 17-OHsteroids and 17-ketosteroids which were in the upper reaches of normal. No significant changes in serum PBI were noted (108).

Combinations of thermal and vibratory stress in mice tend to show synergistic effects (122). Hematocrit, hemoglobin and SGOT responses reflected this synergism.

HUMAN TOLERANCE TO VIBRATION

Tolerance criteria for vibration exposure established by various investigators agree only within certain limits since evaluation criteria, positioning and support of the subjects have a marked effect on such limits. Threshold data on longitudinal sinusoidal vibration while seated have been summarized in Figure 8-30. Figures 8-31a and b elaborate on these thresholds with subjective and performance end points for several other vibration modes and conditions. Some past tolerance thresholds may be seen in Figure 8-20. Other reviews of tolerance criteria are available (10). Tolerance thresholds to vibration in the X, Y, and Z axes while sitting in contoured couches or adjustable vibration-absorbing devices in spacecraft liftoff position are found in Figures 8-24b and c. (See below for restraint variables.)

Sources of vibration in land and aircraft are seen in Figure 8-32. The range of vibration levels found in aircraft, trucks, and tractors is indicated in Figure 8-33. Individual points represent flight vibration data obtained in various types of military aircraft. The solid circles, squares, and triangles indicate vibrations at seat levels which were reported as excessive and undesirable in actual service; the open marks indicate conditions accepted as tolerable. The linearized dividing line between tolerable and excessive vibrations is the WADC tolerance criterion shown in Figure 8-30, used as a long-time vibration tolerance criterion in military aviation aircraft. This curve is based on subjective pilot comments with respect to tolerable and intolerable levels in military aircraft (62). Levels below this line are tolerated, in general, for long times (up to 8 hours) without observed detrimental effects on performance or health. For short flight durations (for example in helicopters) vibration levels considerably above this line but not above the voluntary tolerance area, are routinely tolerated.



This illustrates schematically a number of tolerance criteria for vibration. The four shaded zones represent: threshold for perception; the unpleasant area of vibration; the limits of voluntary exposure, unprotected, for 5-20 minutes; and the voluntary tolerance limits for subjects with lap belt and shoulder harness for three minutes, one minute, and less than one minute. Above this, minor injuries occur, depending on time. At the top of the chart is plotted the voluntary tolerance curve for impact, which may be considered to be half-cycle vibration of large magnitude. The conventional way of measuring durations (t) and amplitudes (A) is shown in the small diagrams at the left.

Figure 8-30

Criteria for Vibration Tolerance in Longitudinal Axis While Seated

(After Webb (178), adapted from von Gierke and Hiatt⁽⁷⁰⁾)

Figure 8-31

Reactions to Mechanical Vibrations

(After Mohr and von Gierke (123))

- a. Summary of Tolerance Limits to Sinusoidal, Whole-Body Vibration
(Numbers refer to Table 8-31b. See original source for references.)

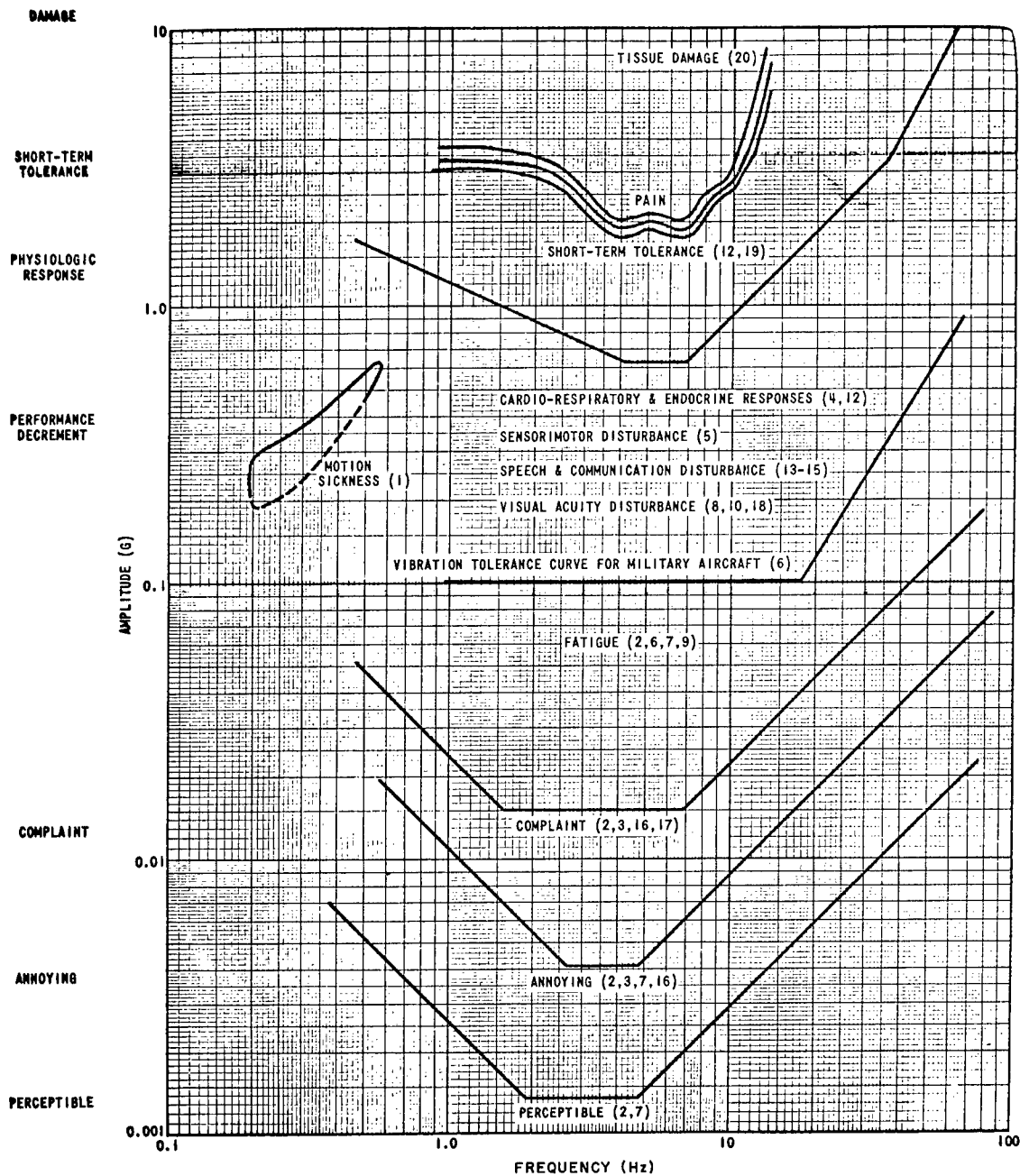


Figure 8-31 (continued)

b. Table of Experimental Conditions for Figure 8-31a

1. Seated subjects exposed for 20 min or less to vertical sinusoidal motion.
2. Standing and recumbent subjects exposed for short durations (5 min or less) to vertical and horizontal sinusoidal motion.
3. Standing, seated, and recumbent subjects exposed for short durations (<20 min) to vertical sinusoidal vibration.
4. Recumbent subjects exposed for short durations to vertical sinusoidal motion.
5. Seated subjects exposed for 10-min periods to vertical sinusoidal motion.
6. Subjects seated in military aircraft exposed for periods of approx 1 hr to flight-induced vibration, primarily in the vertical direction.
7. Standing, seated, and recumbent subjects exposed for periods of 5-20 min to vertical or horizontal vibration.
8. Seated subjects exposed for short durations to vertical vibration.
9. Standing and seated subjects exposed for periods of 5 min or less to vertical sinusoidal vibration.
10. Seated subjects exposed for periods of approx 1 min to vertical sinusoidal vibration.
11. Standing and seated subjects exposed for short durations to vertical or horizontal sinusoidal motion (summary combination of limits).
12. Seated subjects exposed for periods of 1 min to vertical sinusoidal vibration.
13. Seated subjects exposed for short durations to vertical vibration.
14. Seated subjects exposed for short durations to vertical vibration.
15. Recumbent subjects exposed for short durations to vertical and horizontal vibration.
16. Standing subjects exposed for short durations (<5 min) to vertical sinusoidal motion.
17. Airline passengers exposed for continuous periods of 100 min principally to vertical vibration.
18. Recumbent subjects exposed for periods of 1-2 min to vertical and horizontal vibration.
19. Recumbent subjects exposed to vertical and horizontal vibration at increasing amplitude up to the maximum voluntary tolerance.
20. Vibration limits (general summary).

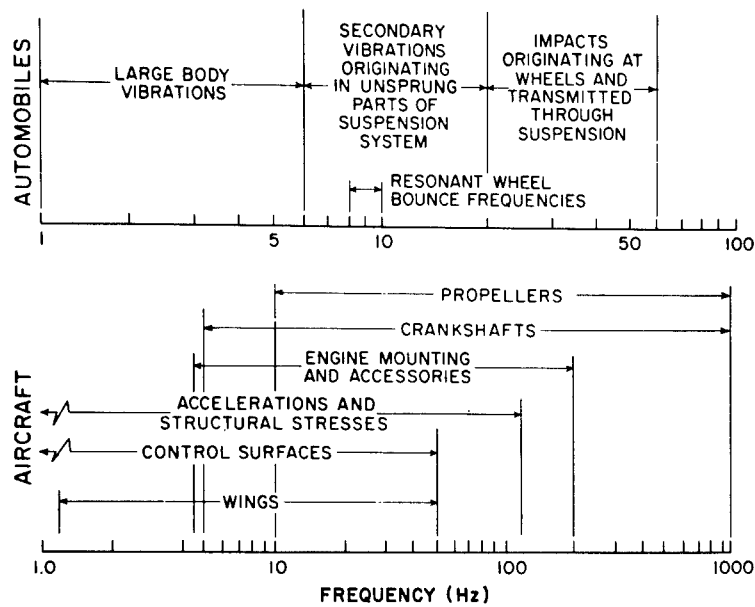


Figure 8-32

Vibration Frequencies Encountered in Aircraft and Automobiles

(After McFarland and Teichner⁽¹¹⁴⁾)

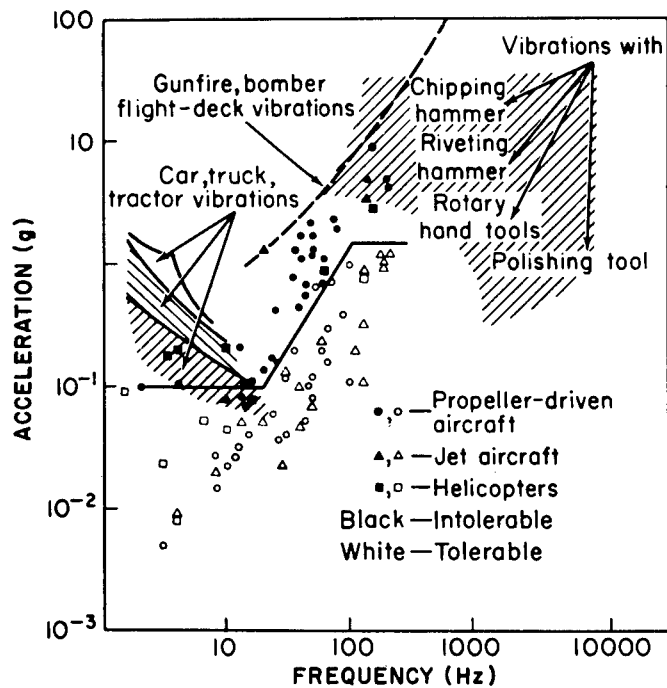


Figure 8-33

Vibration Environment for Various Transport Devices

(After Goldman and von Gierke⁽⁷³⁾)

Dangerous vibration levels in space vehicles will be restricted to the relatively short duration of takeoff and reentry. Review of past performance of astronauts during takeoff showed some difficulty in the visual area. (See Light, No. 2). No problems have arisen in the reentry phase of the profile, although it is possible that angular and linear buffeting patterns may be experienced during reentry emergencies in spacecraft or emergency capsules (120). The areas indicated for road vehicle vibration in Figure 8-33 are the range for the respective vibration maxima and do not represent spectral limits (41, 145). Most vehicles have very pronounced natural frequencies excited according to ground conditions. Very generally, rubber-tired tractors, as well as trucks, have the maximum of their vertical accelerations in the 2 to 6 Hz range; for large rubber-tired earth moving equipment the range is 1.5 to 3.5 Hz and for crawler type tractors it is near 5 Hz.

Tolerance thresholds to land vehicles producing random vibration over rough terrain have received recent review (142, 174). Data are also available on threshold to railroad vehicles and similar modes of mass commercial land and air transport (16, 109, 136, 159).

Excellent reviews have been made of tolerance to vibration on board ships at sea (11, 99). These relate tolerance criteria to ship configuration and state of the sea. Such data are of value in the design of tracking ship facilities for space operations.

Vibration levels observed on hands while operating various hand tools are also indicated in Figure 8-33. These levels are strongly dependent on tool design and type of operation. Most of the hand vibrations indicated are in the acceleration range at which chronic hand injuries may result (2, 58, 71).

The presence of gusts which buffet aircraft lead to random, single-shock pulses of repetitive nature (61, 135, 146). These are prominent in low altitude, terrain-following maneuvers where high wind shears are present. During search and rescue missions for returning spacecraft, these gusts are potential problems. A review of this problem is available with coverage of the gust response of many military aircraft (61). Figure 8-34 presents the most widely used summary of available information on human tolerance to aircraft gust response as a function of duration of exposure. These curves were based on considerable data for exposures up to approximately 10 minutes. From there on, the validity is based on relatively few points. A straight line extrapolation of the intolerance boundary indicates that the environment would become intolerable before one would experience performance decrement. These curves also show that vertical accelerations equal to 0.25 g (rms) hamper performance after several minutes. For durations of approximately one hour the performance boundary is 0.15 g (rms). For duration of three hours, a convenient estimate is approximately 0.1 g (rms).

Since atmospheric turbulence is random in nature, aircraft response should be considered in terms of the statistical probability of encountering various gust loads. Most of the current data on human buffet tolerance are extrapolated from short-time simulation studies and limited flight-test

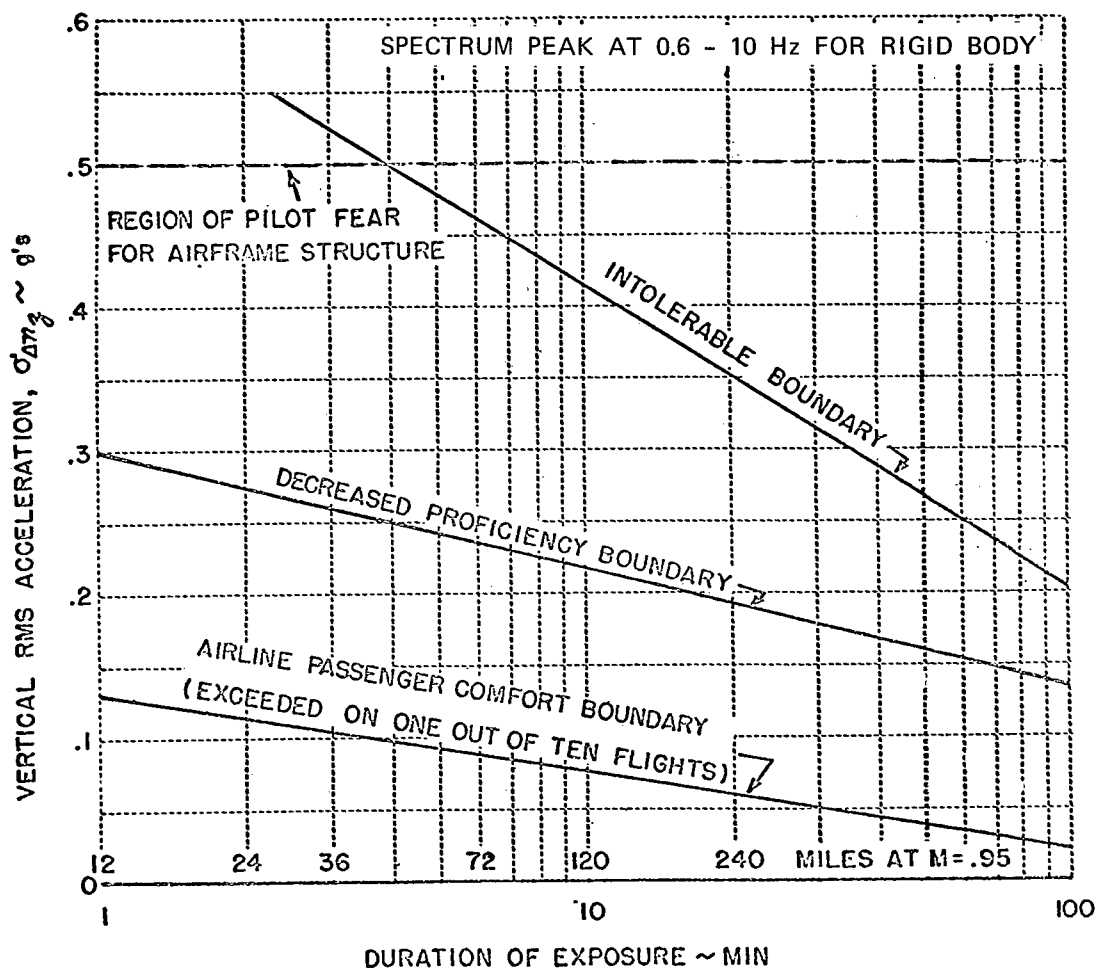


Figure 8-34

Time-Intensity Vibration Boundaries

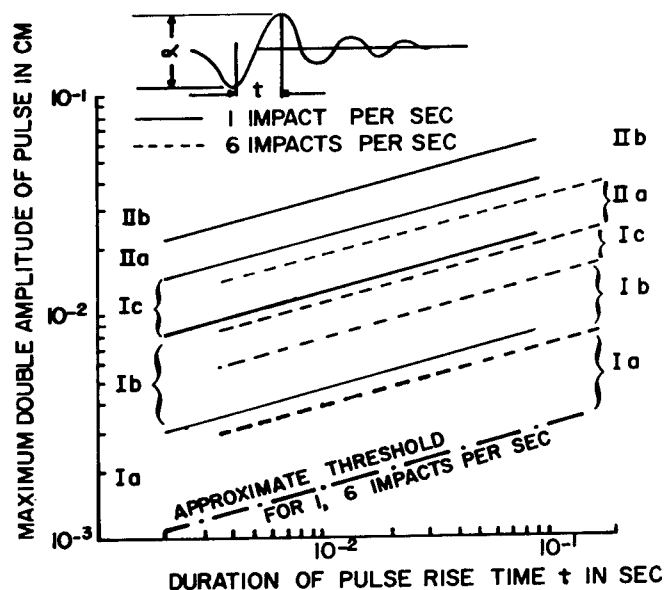
(After Gell⁽⁶¹⁾)

programs and must be extended to the durations proposed for future systems. (See Figure 8-50.)

For irregular, random vibrations the tolerance curves established for sinusoidal vibrations may serve as temporary guidelines for the time being, since little data exist. Single shock acceleration pulses as they occur as floor vibrations near drop forges or similar equipment were used in one study and some of the results are presented in Figure 8-35. The intolerable range in this series of experiments should probably be considered as conservative since experiments with sinusoidal vibrations by the same authors, which were included in the averages of Figure 8-30, gave relatively conservative tolerance levels (73).

Recent studies have shed some light on the relative importance of peak vs. rms acceleration in evaluation of tolerance in periodic low frequency vibration exposure (25). For various rms acceleration levels and frequency

Figure 8-35



Tolerance of Human Subjects in the Standing or Supine Position to Repetitive Vertical Impact Pulses

These are representative of impacts from pile drivers heavy tools, heavy traffic, etc. Subjective reaction is plotted as a function of the maximum displacement of the initial pulse and its rise time. The numbers indicate the following reactions: Ia, threshold of perception; Ib, of easy perception; Ic, of strong perception, annoying; IIa, very unpleasant, potential danger for long exposures; IIb, extremely unpleasant, definitely dangerous. The decay process of the impact impulses was found to be of little practical significance.

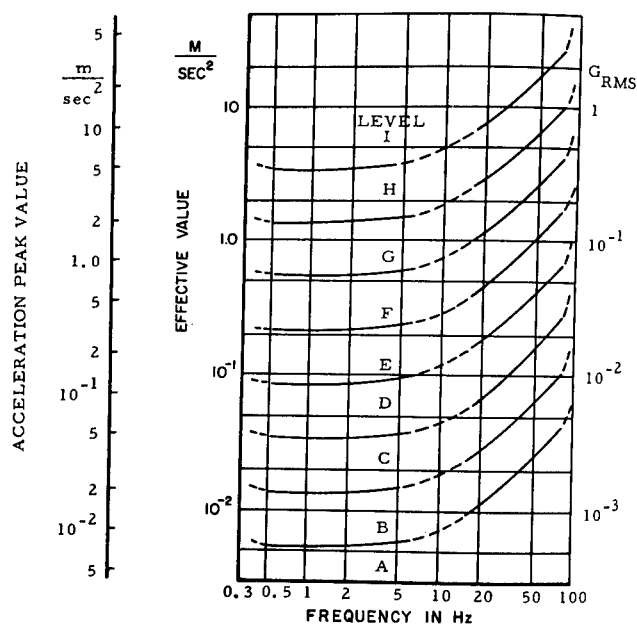
(After Goldman and von Gierke⁽⁷³⁾, adapted from Reiher and Meister⁽¹⁴⁷⁾)

contents, pairs of periodic vibration exposures having the same rms but different peak accelerations were evaluated using both a subjective severity rating and a measure of vibration induced hand motion. The higher peak acceleration of the various pairs having the same rms values was subjectively rated more severe in 32 of 40 observations. However, when attempting to hold the hand in a fixed position during vibration, the induced deviations from the null point, expressed either as average or peak-to-peak errors appeared to depend more on rms acceleration and frequency than on the small differences in peak acceleration studied here.

Efforts are underway to arrive at international agreement on vibration levels acceptable to man under various conditions (65, 93). The goal is to arrive at standard methods for rating environments with respect to human exposure (65, 93). The attributes, hazardous, acceptable and comfortable are not absolute qualities, but are dependent on innumerable biological, psychological, sociological, economic and technological variables. Most rating systems contain at least three criteria: thresholds of perception, unpleasantness, and tolerance. However, only perception can be recognized as a real threshold, whereas unpleasantness and tolerance are more or less subjective judgments and as such are certainly strongly dependent on motivation, the test structure, and the task being performed.

Many approaches have been attempted. The most applicable one is that of the German Engineering Society which gives 10 zones of equal perceptibility and tolerability. These are shown in Figure 8-36. The German standard (128) goes into considerably more detail with respect to evaluation of complex frequency spectra and direction of vibrations. It is hoped that an American standard similar to whatever will evolve as an international standard can be proposed. Soviet standards for industrial vibration exposure are available (190).

Unfortunately, time of exposure is not adequately covered by these standards. The time dependence of various responses to vibration, such as the curves for "fatigue times" and comfort limits, are illustrated in Figure 8-34



Perceived Intensity K	Level	Description of the Perception	Tolerance of Exposure
0.1	A	Not perceptible Barely perceptible	Threshold of perception
0.25	B	Living in dwellings with short or without interruptions*
0.63	C	Perceptible	Living in dwellings with prolonged interruptions*
1.6	D	Very perceptible	Physical labor without interruption*
4.0	E	Strongly perceptible	Physical labor with short interruptions*
10.0	F	Very strongly perceptible . . .	Rather long trips in trains and trucks.
25.0	G	Differentiated judgment no longer possible	Physical labor with prolonged interruptions**
63.0	H	Driving in self-propelled working machines.
	I	Trips in trains and trucks for a short time.

* The interruptions refer to the application of the vibration. "Short" in this context means that continuous oscillations are interrupted by occasional pauses of approximately 10 minutes in length. The relation of pauses to time of vibration should not exceed 0.1.

** "Prolonged" in this context means that the length of the pauses is at least one hour and that the relation of pauses to time of oscillation lies between 0.1 and 1.0.

The curves of equal perceived intensity (K-values) classify ranges (levels of A to I) of equal perception and tolerability.

Figure 8-36

German Standard for the Classification of Vibration Exposures

(After von Gierke⁽⁶⁵⁾, adapted from VDI⁽¹⁷⁵⁾)

and 8-37a. The acceptability vs. time curves of Figure 8-37a are for longitudinal (Z-axis) sinusoidal vibrations for a sitting subject. For lateral vibrations the equivalent tolerance or comfort levels are usually reported as being lower than for vertical vibrations by a factor 0.7 to 0.5. Similarly the corresponding root mean square (rms) value for random-type, broad-band vibrations appear lower than the same rating for the rms value of sine waves by a factor of approximately 0.6. With respect to these corrections, differences of opinion are not marked (65). Considering the limited data on which these curves are based, it is conceivable that one time-correction function would be satisfactory for all levels of vibration.

Figure 8-37b is a recent proposal by the ISO/TC 108 Working Group 7 for whole-body vibration in the range of 1 to 90 Hz related to the fatigue-decreased proficiency (f.d.p.) criteria (77, 78). The safe exposure limits have been temporarily set at 6 dB above corresponding f.d.p. limits. These draft limits apply to healthy people exposed to whole-body vibration while seated or standing in vehicles or industrial work places. It can be seen from Figure 8-37b that the acceptable level declines with increasing duration of exposure. Noise limits for hearing conservation are similarly related to time and it may be taken as a general rule that in occupational situations the required effectiveness of silencing or vibration control increases with the duration of exposure of personnel at risk. Tentative weighting forces, listed in Figure 8-37b, have been proposed for use in adapting the limits in the event of vibration acting transversely (i.e., athwart the body rather than vertically along the spinal axis), or when the criterion, instead of being working efficiency, is either the preservation of comfort or occupational health. Weighting factors for use when the oscillatory motion is complex or discontinuous are under consideration.

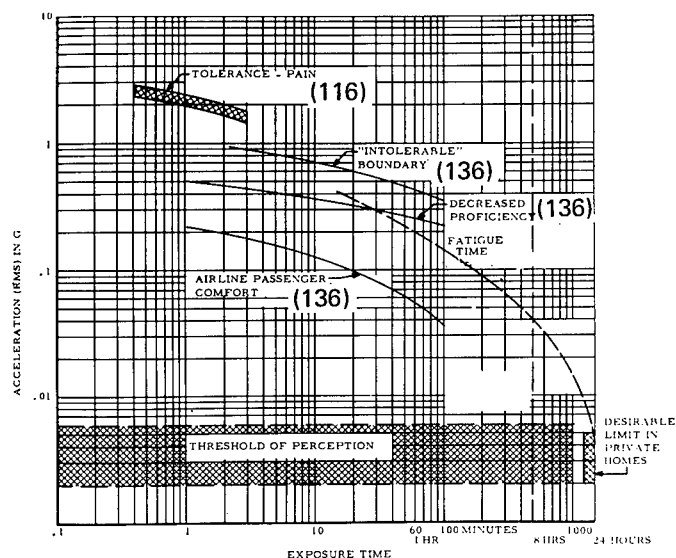
Attempts have been recently made to correlate tolerance with power input. This is of specific value during random vibration. Pages 8-22 to 8-32 cover the theory of absorbed power determinations. Figures 8-38a to d describe constant power graphs for vertical, ($\pm G_z$) fore and aft, ($\pm G_x$) side to side, ($\pm G_y$) vibration, and the vibratory response of the feet. The acceleration-frequency relationships are achieved by holding power constant and solving for the acceleration at each frequency. These graphs can then be interpreted as constant-comfort graphs for acceleration versus frequency. The dash line in Figure 8-38a is a constant power graph that includes both the seat and the feet input.

It is apparent from the functions described previously and from Equation 11 that absorbed power can be expressed, at a single frequency, as a product of a constant, K_i , and acceleration squared, A^2 . Consequently, it is possible to provide a table that supplies this constant along with effective mass G (jw) and phase angle ϕ , so that one can determine power, acceleration, or force at any frequency through very simple calculations. Tables 8-38c to h provide these constants for four vibration inputs and are used in the examples given in References (105, 141).

The information in Figure 8-38b includes both feet for a man in a seated position. This analysis assumes the vibration is the same for both feet.

Figure 8-37

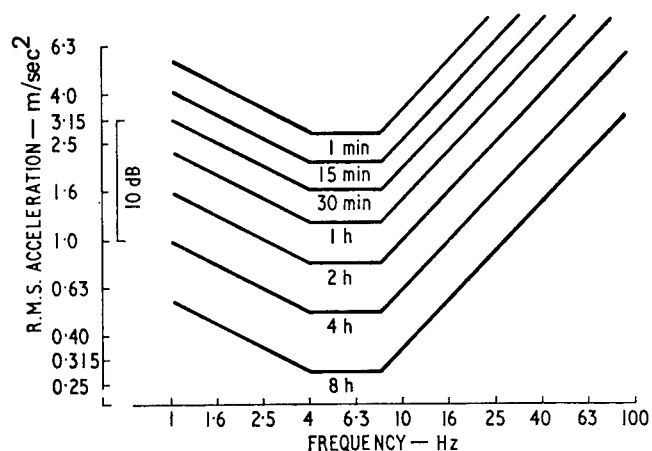
Vibration Limits as a Function of Exposure Time



The curves are valid for sinusoidal vibrations of approximately 1 Hz

a. Longitudinal Vibrations

(After von Gierke⁽⁷¹⁾, based on references 24, 131, 134, 136, and 137)



Proposed weighting factors for adaptation of the limits.

Transverse (horizontal) vibration	subtract 3 dB
Reduced comfort boundaries	subtract 10 dB
Safe exposure limits	add 6 dB

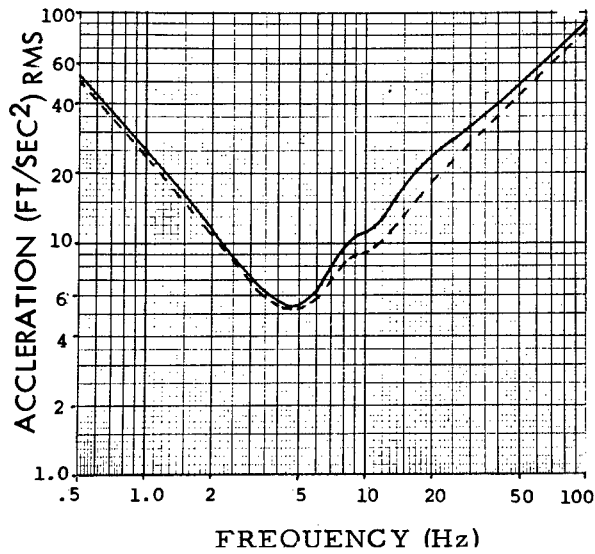
b. Proposed "Fatigue-Decreased Proficiency" Limits for Vertical Vibration in the Range 1 to 90 Hz; Weighting Factors Are Given in Table

(After Guignard⁽⁷⁹⁾, from ISO/TC108⁽⁹³⁾)

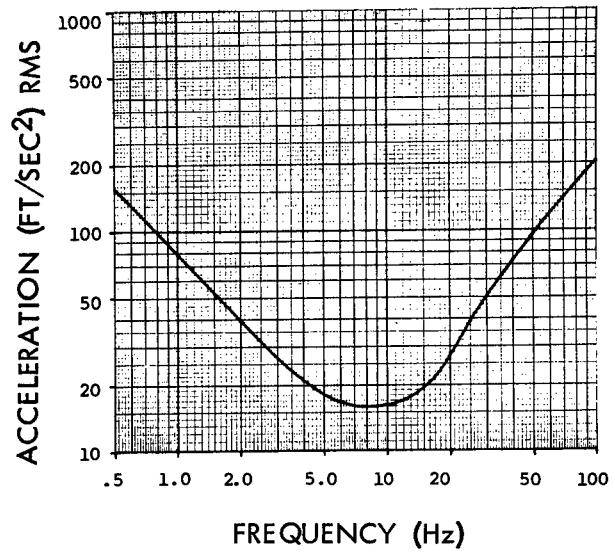
Figure 8-38

Constant Power Graphs for Comfort of Seated Man Undergoing Vibration
and Table of Constants

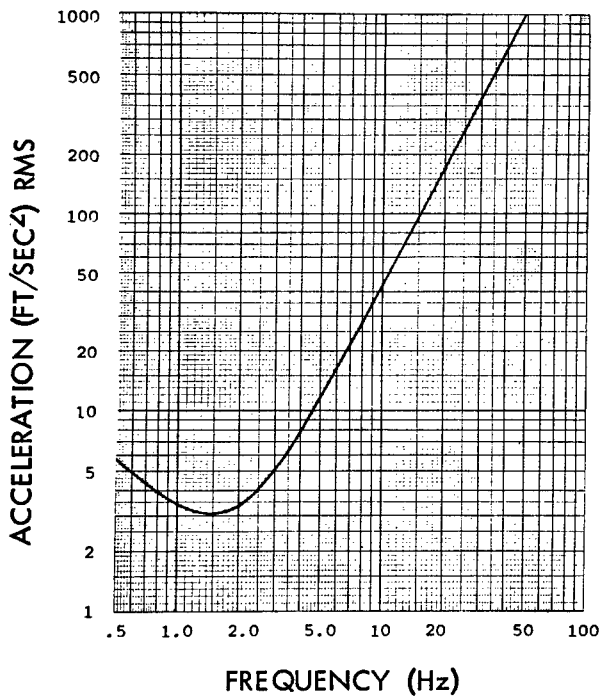
(After Lee and Pradko⁽¹⁰⁵⁾)



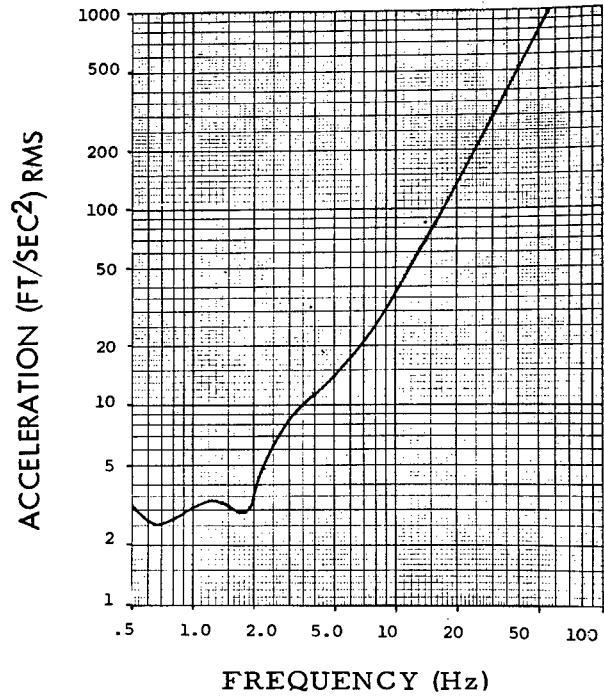
a. $\pm G_z$ Vibration
— seat input only
--- seat and feet input



b. $\pm G_z$ Vibration
(input from feet)




c. $\pm G_x$ Vibration




d. $\pm G_y$ Vibration

Figure 8-38 (continued)

e. Absorbed Power Constants: $\pm G_z$


$$P = \sum_{i=0}^N K_{iv} A_i^2$$


Frequency (Hertz)	K_{iv} Watts (Ft/Sec ²) ²	$ G(jw) $ (Slugs)	Φ Phase Angle (Radians)
0.00	.000000	4.3537	.000000
0.10	.000082	4.3557	.000009
0.20	.000330	4.3616	.000070
0.30	.000747	4.3716	.000237
0.40	.001338	4.3855	.000566
0.50	.002113	4.4035	.001111
0.60	.003080	4.4255	.001935
0.70	.004253	4.4517	.003099
0.80	.005645	4.4820	.004669
0.90	.007272	4.5166	.006714
1.00	.009149	4.5553	.009307
1.10	.011296	4.5983	.012522
1.20	.013731	4.6455	.016435
1.30	.016471	4.6969	.021125
1.40	.019535	4.7524	.026669
1.50	.022941	4.8118	.033143
1.60	.026705	4.8751	.040622
1.70	.030840	4.9419	.049177
1.80	.035359	5.0121	.058874
1.90	.040269	5.0853	.06977
2.00	.045576	5.1612	.08193
2.25	.060561	5.3595	.11808
2.50	.077843	5.5635	.16280
2.75	.097002	5.7629	.21616
3.00	.117336	5.9463	.27786
3.25	.137876	6.1018	.34721
3.50	.157454	6.2175	.42322
3.75	.174830	6.2833	.50463
4.00	.188845	6.2914	.58997
4.25	.198576	6.2372	.67765
4.50	.203469	6.1197	.76601
4.75	.203404	5.9417	.85332
5.00	.198689	5.7092	.93785
5.25	.189988	5.4309	1.01790
5.50	.178206	5.1176	1.09174
5.75	.164358	4.7812	1.15769
6.00	.149444	4.4340	1.21404
6.25	.134362	4.0880	1.25915
6.50	.119843	3.7550	1.2915
6.75	.106430	3.4454	1.3098
7.00	.094481	3.1687	1.3137
7.25	.084182	2.9321	1.3035
7.50	.075581	2.7408	1.2811
7.75	.068618	2.5965	1.2500
8.00	.063152	2.4973	1.2151
8.25	.058994	2.4378	1.1813
8.50	.055923	2.4100	1.1528
8.75	.053709	2.4046	1.1328
9.00	.052125	2.4124	1.1222
9.25	.050964	2.4255	1.1211
9.50	.050041	2.4375	1.1283
9.75	.049205	2.4436	1.1426
10.00	.048340	2.4408	1.1623
10.50	.046233	2.4026	1.2117
11.00	.043455	2.3218	1.2661
11.50	.040109	2.2077	1.3175
12.00	.036470	2.0734	1.3607

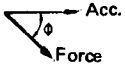
f. Absorbed Power Constants $\pm G_z$ (Foot Response)


$$P = \sum_{i=0}^N K_{if} A_i^2$$


Frequency (Hertz)	K_{if} Watts (Ft/Sec ²) ²	$ G(jw) $ (Slugs)	Φ Phase Angle (Radians)
0.00	.000000	1.1820	.000000
0.10	.000009	1.1822	.000004
0.20	.000029	1.1829	.000030
0.30	.000087	1.1840	.000103
0.40	.000155	1.1856	.000243
0.50	.000243	1.1877	.000473
0.60	.000349	1.1901	.000816
0.70	.000475	1.1930	.001293
0.80	.000621	1.1964	.001923
0.90	.000785	1.2001	.002729
1.00	.000969	1.2043	.003729
1.10	.001172	1.2088	.004942
1.20	.001394	1.2137	.006385
1.30	.001635	1.2190	.008077
1.40	.001894	1.2247	.010032
1.50	.002172	1.2307	.012265
1.60	.002468	1.2370	.014791
1.70	.002782	1.2437	.017621
1.80	.003114	1.2506	.020767
1.90	.003462	1.2578	.024239
2.00	.003828	1.2652	.028045
2.25	.004813	1.2847	.039068
2.50	.005890	1.3052	.052299
2.75	.007047	1.3263	.067759
3.00	.008270	1.3476	.085416
3.25	.009542	1.3687	.105185
3.50	.010843	1.3891	.126935
3.75	.012153	1.4085	.150494
4.00	.013451	1.4266	.175659
4.25	.014716	1.4431	.202203
4.50	.015929	1.4576	.229885
4.75	.017073	1.4701	.258464
5.00	.018133	1.4806	.287704
5.25	.019100	1.4882	.317383
5.50	.019967	1.4951	.347303
5.75	.020731	1.4993	.377291
6.00	.021391	1.5016	.407202
6.25	.021951	1.5023	.436924
6.50	.022416	1.5014	.466369
6.75	.022791	1.4993	.495483
7.00	.023086	1.4959	.524231
7.25	.023307	1.4916	.552601
7.50	.023462	1.4865	.580601
7.75	.023561	1.4806	.608250
8.00	.023609	1.4742	.635580
8.25	.023613	1.4673	.662630
8.50	.023579	1.4599	.689444
8.75	.023512	1.4522	.716067
9.00	.023416	1.4442	.742546
9.25	.023294	1.4358	.768927
9.50	.023149	1.4271	.795251
9.75	.022984	1.4181	.821557
10.00	.022799	1.4088	.847875
10.50	.022374	1.3889	.900654
11.00	.021880	1.3674	.953720
11.50	.021316	1.3438	1.007090
12.00	.020683	1.3178	1.060673


Figure 8-38 (continued)

g. Absorbed Power Constants: $\pm G_X$


$$P = \sum_{i=0}^N K_i A_i^2$$


Frequency (Hertz)	$\frac{K_{if} \cdot a}{(Ft/Sec^2)^2}$ (Watts)	$ G(jw) $ (Slugs)	Φ Phase Angle (Radians)
0.00	.000000	4.3532	.000000
0.10	.007986	4.3848	.000844
0.20	.031531	4.4763	.006528
0.30	.069418	4.6188	.020894
0.40	.119689	4.7995	.046237
0.50	.179748	5.0039	.83320
0.60	.246496	5.2171	.131737
0.70	.316507	5.4257	.190360
0.80	.386231	5.6176	.257704
0.90	.452216	5.7832	.332167
1.00	.511349	5.9148	.412159
1.10	.561072	6.0071	.496171
1.20	.599565	6.0573	.582807
1.30	.625846	6.0647	.670801
1.40	.639787	6.0306	.759027
1.50	.642028	5.9580	.846508
1.60	.633817	5.8513	.932423
1.70	.616810	5.7157	1.016109
1.80	.592853	5.5567	1.097054
1.90	.563802	5.3798	1.11749
2.00	.531380	5.1902	1.24936
2.25	.444761	4.6900	1.42020
2.50	.361943	4.1928	1.56942
2.75	.290275	3.7293	1.69887
3.00	.231488	3.3130	1.81097
3.25	.184614	2.9465	1.90839
3.50	.147747	2.6272	1.99340
3.75	.118894	2.3505	2.06800
4.00	.096307	2.1109	2.13385
4.25	.078565	1.9030	2.19232
4.50	.064556	1.7224	2.24452
4.75	.053425	1.5649	2.29138
5.00	.044521	1.4269	2.33366
5.25	.037349	1.3057	2.37192
5.50	.031533	1.1987	2.40686
5.75	.026783	1.1040	2.43874
6.00	.022879	1.0197	2.46799
6.25	.019650	0.9445	2.49491
6.50	.016963	.87707	2.51977
6.75	.014714	.81649	2.54280
7.00	.012821	.76187	2.56418
7.25	.011220	.71245	2.58410
7.50	.009859	.66761	2.60269
7.75	.008696	.62682	2.62008
8.00	.007698	.58960	2.63639
8.25	.006838	.55556	2.65171
8.50	.006094	.52465	2.66613
8.75	.005448	.49567	2.67972
9.00	.004885	.46926	2.69256
9.25	.004392	.44488	2.70470
9.50	.003959	.42234	2.71621
9.75	.003578	.40145	2.72713
10.00	.003242	.38206	2.73749
10.50	.002679	.34725	2.75675
11.00	.002233	.31695	2.77426
11.50	.001876	.29044	2.79024
12.00	.001587	.26710	2.80489

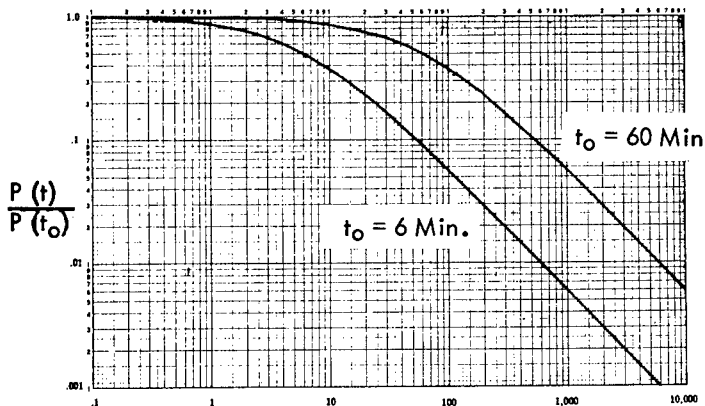
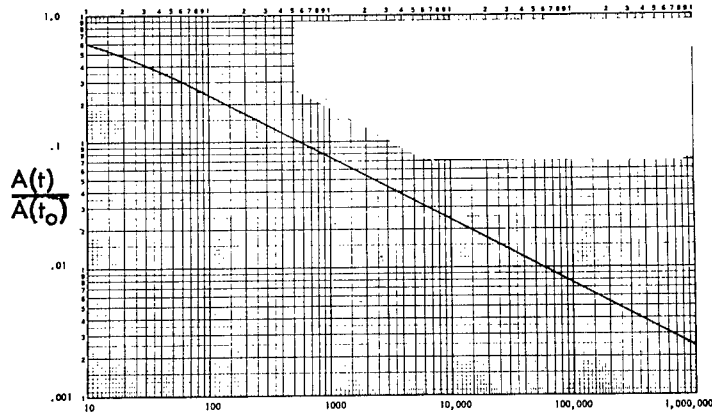
h. Absorbed Power Constants: $\pm G_Y$


$$P = \sum_{i=0}^N K_i A_i^2$$


Frequency (Hertz)	$\frac{K_{is}}{(Ft/Sec^2)^2}$ (Watts)	$ G(jw) $ (Slugs)	Φ Phase Angle (Radians)
0.00	.000000	4.3530	.000000
0.10	.012617	4.41226	.001325
0.20	.056579	4.59712	.011406
0.30	.152512	4.92206	.043086
0.40	.336090	5.37203	.116218
0.50	.618917	5.79730	.249935
0.60	.875526	5.86860	.427688
0.70	.929853	5.48783	.581862
0.80	.834987	4.98867	.669312
0.90	.718723	4.62680	.704698
1.00	.630460	4.44417	.717277
1.10	.575382	4.41090	.727329
1.20	.549073	4.49642	.746387
1.30	.547652	4.68182	.781883
1.40	.568966	4.95442	.840497
1.50	.610599	5.29472	.929863
1.60	.664520	5.65275	1.058335
1.70	.708175	5.91674	1.230978
1.80	.703578	5.91849	1.440331
1.90	.628075	5.5513	1.65955
2.00	.508018	4.9033	1.85402
2.25	.260384	3.2238	2.14049
2.50	.152064	2.1955	2.21043
2.75	.105940	1.6455	2.17949
3.00	.082866	1.3463	2.11488
3.25	.069233	1.1759	2.05159
3.50	.059955	1.0715	2.00434
3.75	.052919	1.0006	1.97603
4.00	.047168	0.9466	1.96438
4.25	.042241	0.9012	1.96568
4.50	.037906	0.8602	1.97640
4.75	.034040	0.8216	1.99367
5.00	.030573	0.7846	2.01533
5.25	.027458	0.7488	2.03975
5.50	.024660	0.7142	2.06579
5.75	.022152	0.6808	2.09262
6.00	.019906	0.6487	2.11967
6.25	.017899	0.6180	2.14652
6.50	.016107	.58865	2.17290
6.75	.014509	.56073	2.19863
7.00	.013084	.53423	2.22360
7.25	.011813	.50912	2.24773
7.50	.010681	.48537	2.27099
7.75	.009669	.46293	2.29337
8.00	.008768	.44175	2.31487
8.25	.007961	.42177	2.33551
8.50	.007240	.40292	2.35531
8.75	.006594	.38515	2.37430
9.00	.006155	.36839	2.39251
9.25	.005496	.35258	2.40998
9.50	.005028	.33767	2.42674
9.75	.004608	.32360	2.44282
10.00	.004228	.31032	2.45826
10.50	.003576	.28591	2.48733
11.00	.003042	.26409	2.51419
11.50	.002601	.24453	2.53905
12.00	.002235	.22696	2.56212

Figure 8-38 (continued)

- i. Normalized Acceleration Factors for
Constant Time-Dependent Power
(See text)
 $t_0 = 6 \text{ min.}$



- j. Normalized Power Factors for
Constant Time-Dependent Power (See text)

Where this is not the case the numerical constant K_0 for the feet must be divided by 2 and the transfer function used for each foot. Similar tables in Reference (141) provide for frequencies up to 100 Hz for pitch and roll vibrations.

As would be expected from the previous discussion, the physical surroundings in which the vibration occurs have a strong influence on what is an acceptable or unacceptable vibration power. For example, an upper acceptable absorbed power for automobile ride may be 0.2-0.3 W. If one were to ride in an automobile about this level, the opinion would very likely be that the ride is rough and the vehicle uncomfortable. On the other hand, the upper acceptable limit for off-road vehicles may be 6-10 W, and if one were to experience a ride in the 0.5-1.0 W range, the opinion would likely be that the ride is very comfortable. The measurement of the absorbed power for each application allows comparison on an absolute scale.

For vibrations of short duration, absorbed power can be used as a measurement of vibration severity, but frequently it is desired to determine a vibration comfort level for a longer period of time. The amount of available information for the effect of long time vibration is very sparse. (See Figure 8-37.) One can easily deduce why the amount of information is very limited. There are several parameters that affect the comfort level. These parameters are frequency, amplitude, environment, and a certain amount of fatigue or discomfort with the passage of time, even when there is no vibration present.

Since absorbed power accurately measures vibration severity for short term vibration, it can be deduced that for long term vibration, a term can be added to this power that may be similar to energy absorbed.

If this is done, an empirical expression for power becomes

$$P_T = P + \frac{1}{t_0} \int_0^t P dt \quad (12)$$

where P_T = Long term absorbed power

P = Average power

t_0 = Time scale factor, approximate onset of fatigue

Power need not remain constant, but if it does, Equation 12 takes the form

$$P_T = P + P \frac{t}{t_0} \quad (13)$$

Substituting KA^2 for power, (See Equation 8)

$$P_T = KA^2 \left[1 + \frac{t}{t_0} \right] \quad (14)$$

An acceleration-time relationship is given by

$$A(t) = \sqrt{\frac{P_T}{K(1 + (t/t_0))}} \quad (15)$$

At $t = 0$, $P_T = P_{av}$. Therefore, setting $P_T/K = A^2(t_0)$, which is the short-term acceleration, gives

$$A(t) = \frac{A(t_0)}{\sqrt{1 + (t/t_0)}} \quad (16)$$

This equation describes degradation of acceleration for constant comfort when time is considered. If one divides both sides of Equation 16 by $A(t_0)$

$$\frac{A(t)}{A(t_0)} = \frac{1}{\sqrt{1 + (t/t_0)}} \quad (17)$$

Figure 8-38i is a graph of Equation 17 with $t_0 = 6$ minutes.

If both sides of Equation 17 are squared, the equation is then absorbed power or comfort:

$$\frac{P(t)}{P(t_0)} = \frac{1}{1 + (t/t_0)} \quad (18)$$

This equation is graphed in Figure 8-38j with $t_0 = 6$ minutes and 60 minutes.

PERFORMANCE DURING VIBRATION

The effects on performance may be considered as direct mechanical interferences with performance, or indirect effects resulting from physiological alterations. Some of the types of performance which are significantly affected by vibration include (80, 114, 188).

- a. Visual tasks including effects on visual acuity and eye movements. Direct effects are primarily mechanical (resonance) for certain g-vector and frequency combinations; indirect include pain for other g-vector/frequency combinations.
- b. Vigilance, concentration, and reaction time.
- c. Simple motor tasks such as operation of switches.
- d. Speech.
- e. Complex motor tasks such as tracking.

Figures 8-39a and b review the general trends in psychophysical and performance tolerance under vibration in the longitudinal axis of a seated subject. Figure 8-31a and b also cover performance thresholds of an even more general nature. These figures and tables may be used as a general guide to the type of data available from experimental study.

Visual Effects

Visual impairment is a major psychophysical defect expected from vibration in a spacecraft (158). Unfortunately, most studies have been performed during G_z vibration in the seated position. This will be assumed in the text unless otherwise stated.

Visual Acuity

Vibration of either the viewer or the object can blur vision over certain frequency and acceleration ranges and is usually attributed to movement of the retinal image at a speed too great to be followed by the eye (80, 167). In general, there is no clear-cut evidence that decrement in acuity is either purely frequency dependent or amplitude dependent. The evidence is conflicting because the same methods for measuring visual acuity or the same conditions of vibration have not always been held constant during the tests. Some,

Figure 8-39

Psychomotor Performance During Longitudinal Vibration
(After Linder⁽¹⁰⁷⁾. References available in original document.)

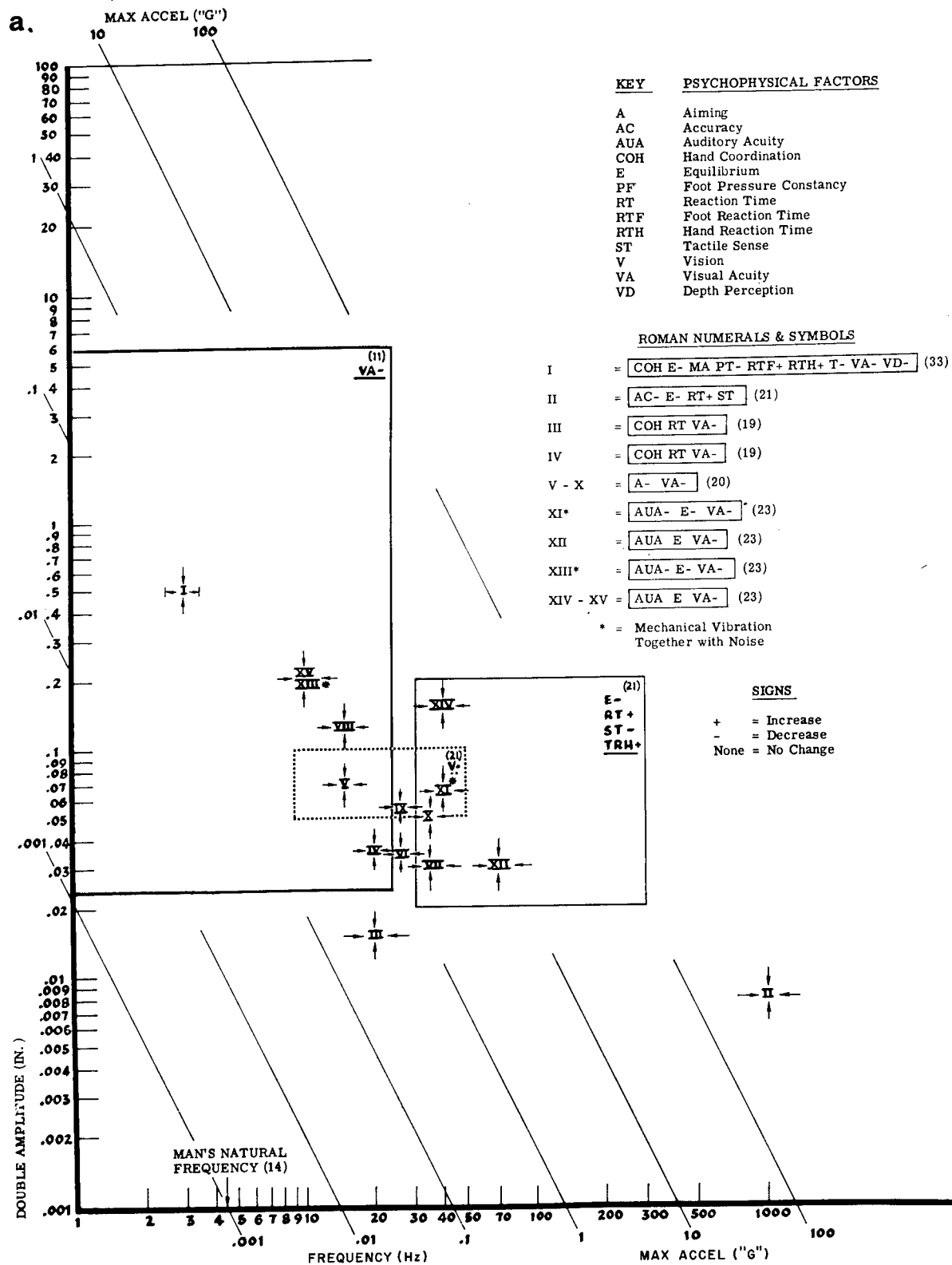
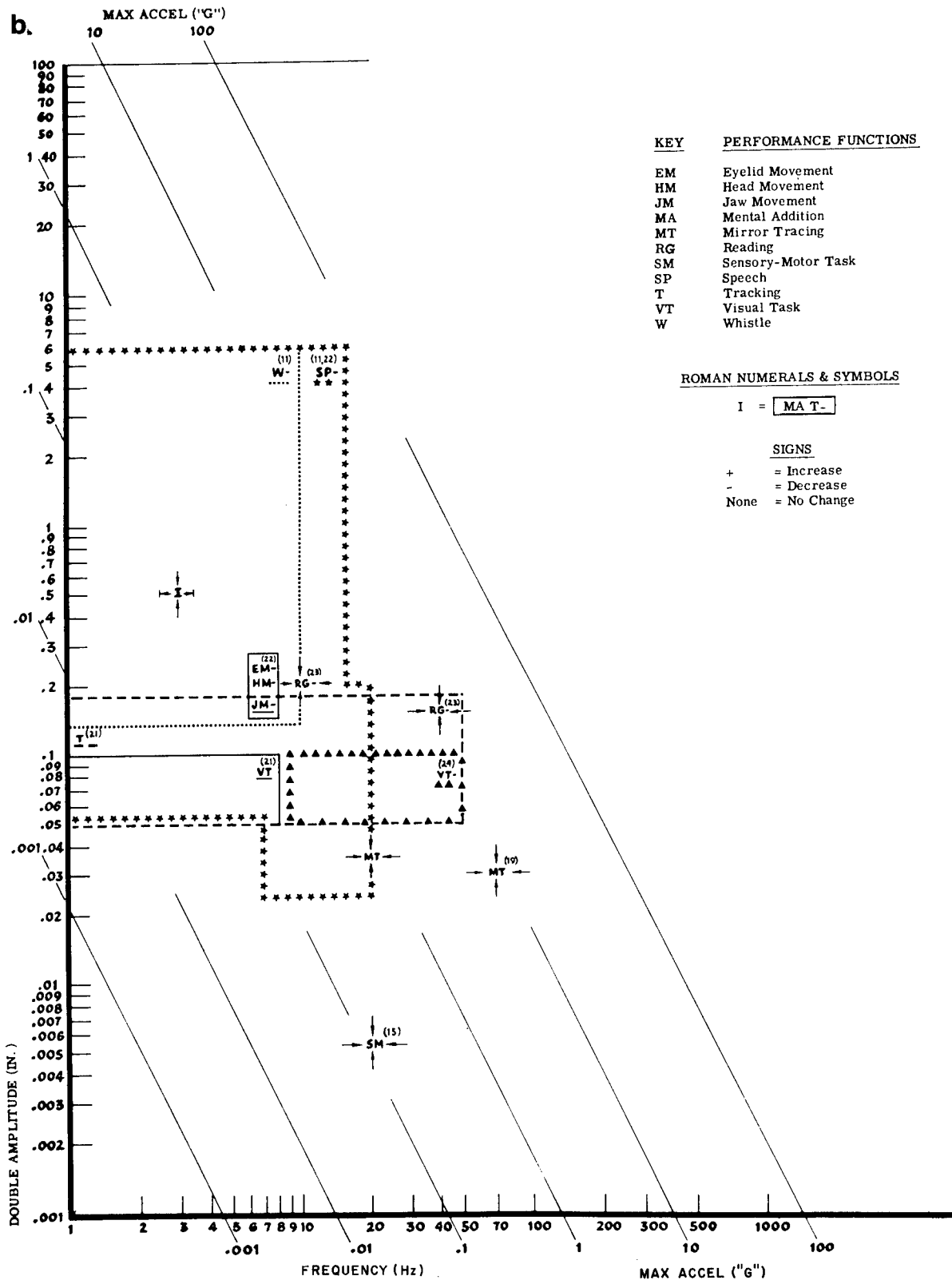


Figure 8-39 (continued)



for example, have applied a constant displacement-amplitude at all frequencies, others have reduced amplitude at the higher frequencies (110, 125).

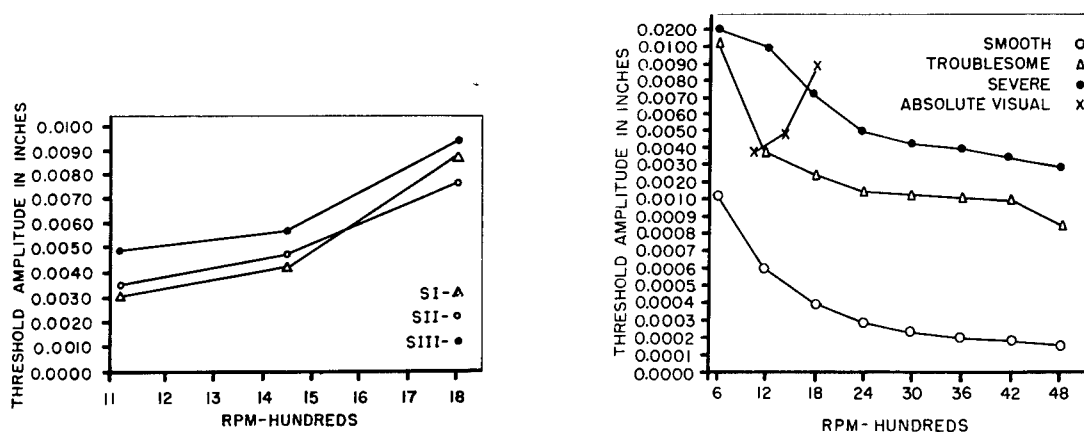
The tests of visual acuity under vibration have included the use of:
a) Landolt C (38, 44, 154), b) variable coarseness gratings, such as the Clason acuity meter (111), c) the separation of diverging lines (31), and the reading of printed numbers of letters to study the legibility of test material vibrated with the observer stationary (34, 36, 45, 79, 98, 125).

The sensitivity to vibration in the visual field is a factor of interest (34, 169, 189). The results of a determination of the minimum amplitudes of vibration in the visual field which are just perceptible at various frequencies are shown in Figure 8-40a. Stimuli were printed materials in six- and eight-point type viewed at a reading distance of 14 inches under 13.0 and 23.5 ft-L. The amplitude threshold increased with frequency, and the average amplitude threshold is in the neighborhood of 0.0056 inch. The threshold increased with decreasing brightness, but the type size variable was not found to affect the threshold through the range tested. The visual threshold to total body vibration as related to subjective threshold of vibration in the visual field is noted in Figure 8-40b.

Visual acuity is degraded during vertical sinusoidal vibration at frequencies above 15 Hz, particularly in the frequency bands of 25 to 40 Hz and 60 to 90 Hz, and in a third band for some subjects at 50 to 55 Hz (31). Within a limited range, the decrement in acuity increases with increasing amplitude of vibration reaching the head. This is interpreted as the result of mechanical

Figure 8-40

Thresholds of Perceptibility of Vibration in the Visual Field
for $\pm G_z$ (Seated Subjects)
(After Wulfek (189))



a. Amplitude Threshold at Three Frequencies for Three Subjects (First Order Interaction: Frequency X Subjects) (See text)

b. Amplitude Thresholds to Vibration

These curves compare subjective response to total body vibration with the amplitude required for detection of vibration in the visual field. (X)

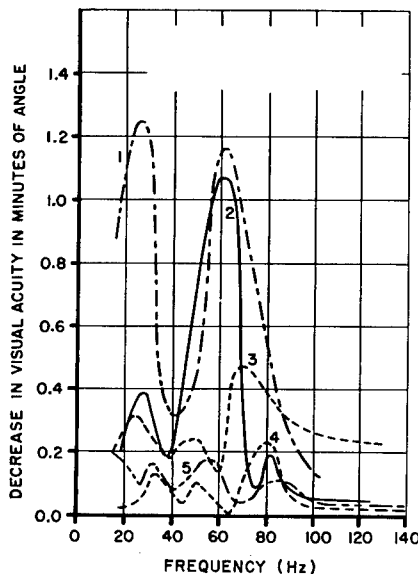
body resonances. The decrement in the 60 to 90 Hz band is caused by resonance of the eyeball or its adnexa within the orbit. Also the reduction in acuity in the range of 20 to 40 Hz is attributed to passive movement of the eyes produced by resonance of the soft tissues of the face and scalp (37).

Figure 8-41a shows binocular visual acuity at various frequencies of head vibration for five subjects. At particular frequencies there appear to be resonance points at which acuity was most affected. The first point might be due to difficulty in fixating the vibrating test object. The remaining peaks may be due to the effects of complex sympathetic vibrations produced at resonance in the musculature of the eye, compounded with the fundamental vibration of the test object. The results are clear in indicating that vibration of the body and test object impairs visual efficiency. The results do not, however, permit an evaluation of the effects of vibration in the visual field as opposed to those of vibration impressed directly upon the body. The subject-to-subject variability is clear.

Visual acuity has also been shown to be degraded by vertical, whole-body vibration at acceleration-amplitudes between 0.1 and 0.75 g in the frequency range from 4 to 40 Hz (36, 38, 104, 111, 125). The effect of whole-body vibration on the ability of humans to read digits of an aircraft mileage indicator

Figure 8-41

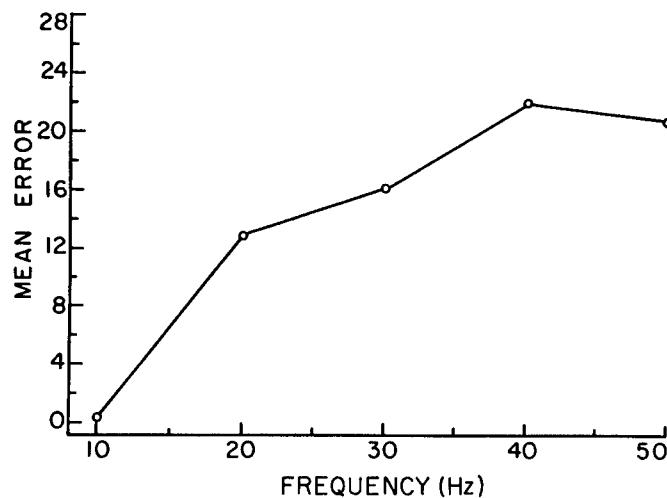
Effect of Whole-Body Exposure to $\pm G_z$ Vibration (Seated) to Visual Performance



a. Person to Person Variability

The curves show that during 2 hrs. of exposure to vibration visual acuity decreases, particularly at two distinct ranges of frequency. The five curves are for different subjects.

(After Wulfeck⁽¹⁸⁹⁾, adapted from MacFarland⁽¹¹³⁾)



b. Increase in Errors of Reading of Dial Digits with Forcing Frequency During Vibration at Constant Displacement-Amplitude of 0.05 Inches

(After Mozell and White⁽¹²⁵⁾)

is shown in Figure 8-41b (125). Vertical sinusoidal frequencies between 8 and 50 Hz with displacements of 0.05, 0.1 and 0.16 in. double amplitude were used but only those of 0.05 is recorded in the figure.

Orientation of test materials with respect to the direction of vibration also have been shown to influence acuity. Using the Ronchi type of test-objects, it has been found that visual performance decreased when the lines of the grating were placed athwart the direction of vibration (111,161). This is interpreted as being the result of the blurring of the margins between the lines of the grating and the intervening spaces, whereas this does not occur when the vibration is parallel with the lines of the grating.

Increase in the level of illumination reduces the amount of impairment of visual acuity (34, 36, 38). The visual acuity decrements produced by vibration can be compensated for by increased luminance of the displays (34). Figure 8-42 indicates that as luminance increases from 0.046 ft-L to 15.0 ft-L,

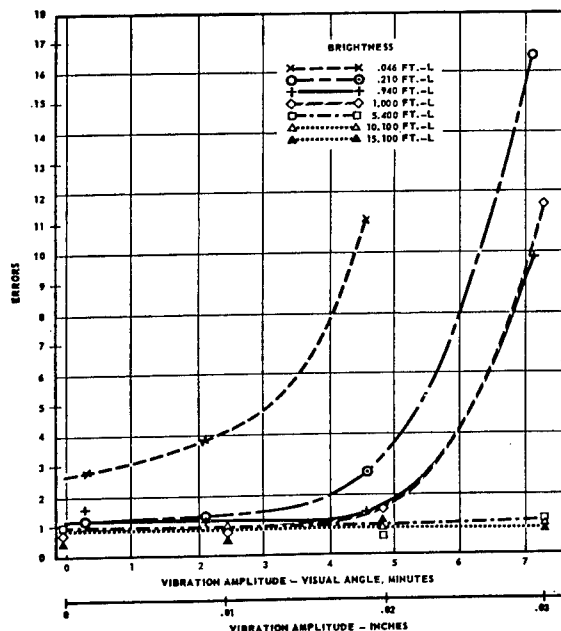


Figure 8-42

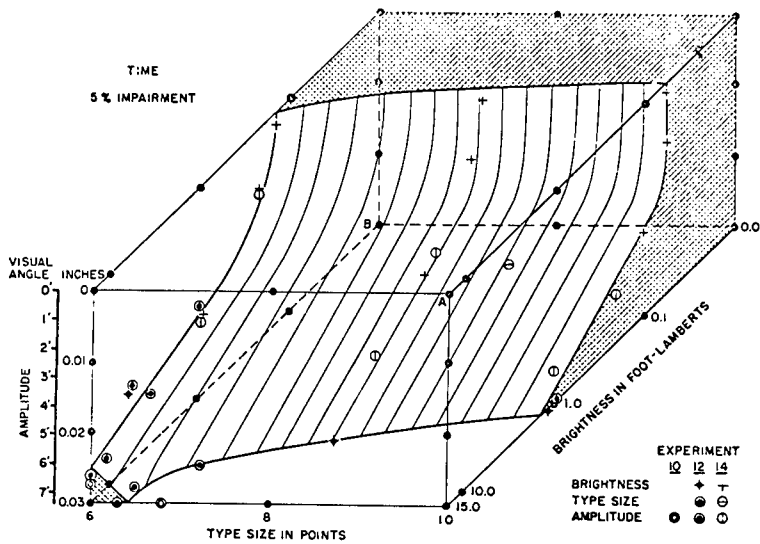
Effect of Vibration Amplitude (1050 cpm) on Reading Accuracy for Various Luminances

(After Urmer and Jones⁽¹⁷³⁾ , adapted from Crook et al⁽³⁴⁾)

performance is significantly improved, although the difference in errors between luminances of 5.4 ft-L and 15.10 ft-L is not marked. The subjects performed simple mental arithmetic on printed numbers (34). The effect on the subjects' speed and accuracy has been measured as vibration was varied in frequency, amplitude and form, and as the printed material was varied in brightness, contrast and type size. Of these variables, amplitude of vibration, brightness and type size seem to be the most critical. The results of experiments on these variables are summarized in Figures 8-43a and b, for a mid-frequency value of 1050 cpm. The three variables interact to produce given decrements in speed and accuracy of performance. The authors conclude that:

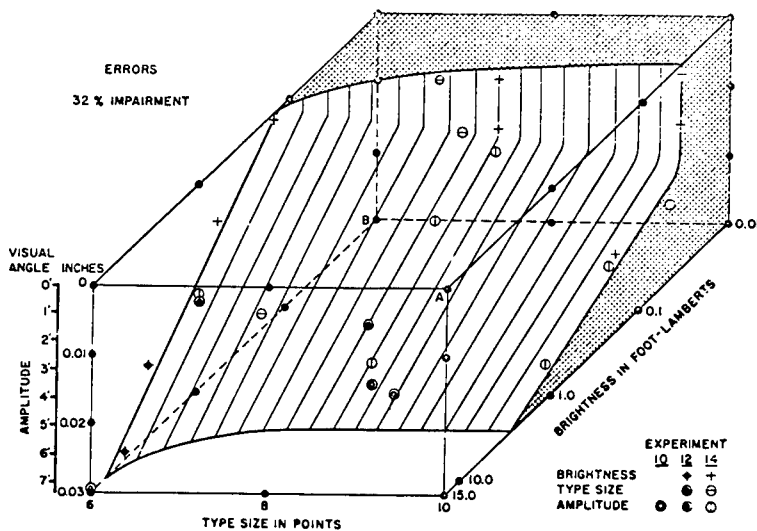
Figure 8-43
Effects of Amplitude, Brightness, and Type Size on Visual Performance During Vibration

(After Crook et al⁽³⁴⁾)



- a. Combinations of Amplitude, Brightness, and Type Size Producing a Constant Impairment in Time Scores

In the solid figure, corner A represents the most favorable conditions, B the least favorable. The curved surface is the boundary at which time is increased 5% as conditions become less favorable. Based on results from 12 subjects each.



- b. Combinations of Amplitude, Brightness, and Type Size Producing a Constant Impairment in Error Scores

In the solid figure, corner A represents the most favorable conditions, B the least favorable. The curved surface is the boundary at which errors are increased 32% as conditions become less favorable. Based on results from 12 subjects each.

- On a numeral-reading task involving simple mental arithmetic, performance is not significantly impaired by decrease of brightness to 0.05 ft-L, decrease of type size to 6-point or below, or increase of amplitude of visual vibration produced by rotating prisms at 1050 cycles per minute to 0.02 inch, if only one factor is varied at a time.
- Two of these values, in combination, impair time scores from 0 to 40 percent and error scores from 0 to 190 percent. All three, in combination, impair time and error scores 130 and 1100 percent, respectively.
- Certainly for brightness, and possibly for type size, the range within which performance is not affected is broader than for reading of verbal material.
- Performance as a function of any one variable, especially when all other conditions are favorable, tends to improve rapidly to a critical value and then levels off sharply.
- Impairment caused by the visual vibration introduced by means of prisms is considerably less than would be caused by vibration of the head at the same amplitude, to judge from previous work on the relation of head vibration to acuity.
- Because of this factor and the possible interaction of various other unfavorable conditions, the results of these experiments should be considered as indicating the minimum impairments that would probably be produced in the most similar practical situation.
- The effect of head vibration can be assumed to be greater than that of exclusively visual vibration, for the same amplitude of relative vibratory movement. In some operational situations the visual vibration might be the more troublesome, because vibration of the viewing surfaces would cause excessive amplitudes of relative movement. For this reason separate estimates of the two factors would be desirable in practical application.
- As far as relative vibratory movement alone is concerned, under daylight or high levels of artificial illumination, the reading of printed numerical materials at 14 inches would not be affected by vibration amplitudes up to 0.02 inch nor of dial numerals by amplitudes up to 0.04 inch. Under night illumination designed to protect dark adaptation the tolerances would be much less. A drop in brightness to 0.046 ft-L, for example, puts a premium on printed numerals above 8-point in size, and brings the critical amplitude down to perhaps 0.01 inch for the larger type sizes; in the case of dials at the same brightness, the corresponding critical numeral size would be about 5/32 inch and the critical amplitude 0.02 inch; for 1/8 inch dial numerals a brightness drop to 0.2 ft-L would bring critical amplitude to 0.02 inch.

These data, the data on visual thresholds to vibration, and the data on discomfort thresholds can be used to establish some general principles for

avoiding or compensating for the effects of vibration in the visual field on visual performance. Maybe the most significant of these is that if brightness can be kept above 0.1 ft-L, type size above 8-point, and vibration of material in the visual field less than that which would be judged "severe" (0.0200 inch) anywhere in the frequency range of total body $\pm G_z$ vibration, there would be no impairment of legibility due to vibration.

Eye movements in response to sinusoidal oscillation of either a subject with stationary test material or a vibrating test object with a stationary subject have been studied (54, 82, 83, 98, 134, 163, 170). Figure 8-44 shows the movement of the eyes during sinusoidal vibration. The ability of the human eye to follow a sinusoidal relative movement of a target begins to break down at 1 to 2 Hz and is practically lost by 4 Hz. Figures 8-44, 8-45 and 8-46 show this effect.

Experiments have recently been carried out in which the effects upon visual performance of whole-body vibration have been compared with the effects of vibrating the visual object itself (37). At 6 Hz, using similar angular displacements, vibration of the visual object was found to result in higher impairment of vision than vibration of the human subject. At 14, 19, and 27 Hz the converse was found to be the case; results which support previous theories of resonance of eyeball or facial tissue to account for the sensitivity of visual performance to whole-body vibration at these higher frequencies (34).

Effects on Visual Tasks

Figure 8-51a summarizes the threshold factors in degradation of visual tasks (see discussion). Several complex visual tasks have been studied in detail. In Figure 8-47, subjects were given two separate tasks to perform (scanning and placing) in the seated position while being vibrated in the frequency range in which significant body resonances occur (81). Vibration frequencies ranged from 2.4 to 9.5 Hz. "Scanning" required the subject to scan blocks of type script letters "c" and to count randomly placed anomalous letters "o". "Placing" required the subject to pick four markers off the periphery of a 16 inch diameter disc in front of him and to place them precisely on spots, providing 1/32 inch clearance, one inch from the center of the disc. Errors and time to complete task are given in Figure 8-47 which presents only the mean time to completion (in seconds) rather than errors since very few errors were made under any conditions. Correlation with velocity and amplitude of head and eye movements is noted.

Data on visual acuity of different digit heights at periodic, vertical, low-frequency vibration are available (104, 127). Data are also available on random vibration effects in aircraft flight during gusty conditions with emphasis on letter-height factors (92).

Control of the axis of vibration and reduction of the vibration transmitted to the head reduces impairment of visual acuity (36, 38). This is particularly significant in the design of head restraints (164, 165). (See below.) Subjects were studied in the adjustable couch described in Figure 8-24a.

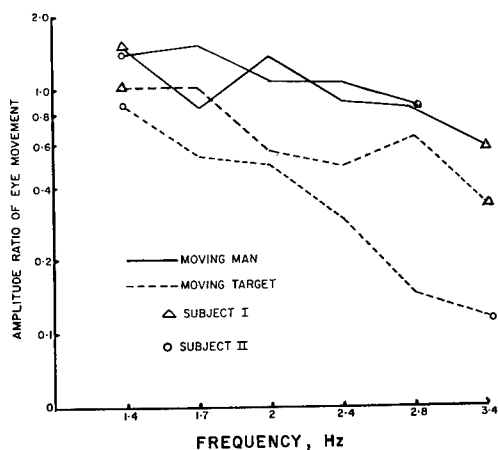


Figure 8-44

Frequency Response of the Oculomotor System Fixating a Stationary Target During Whole-Body Vibration (peak-to-peak displacement 5 mm) Giving Relative Angular Displacement of Target at 0.08 Degree of Arc

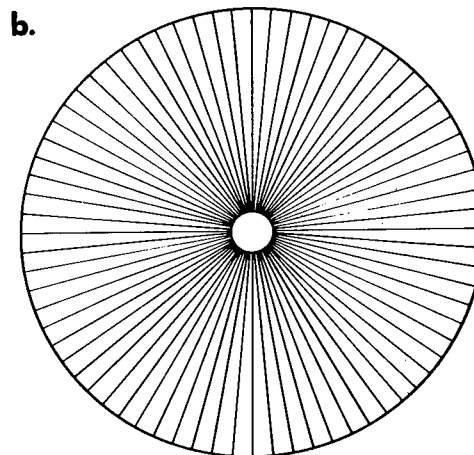
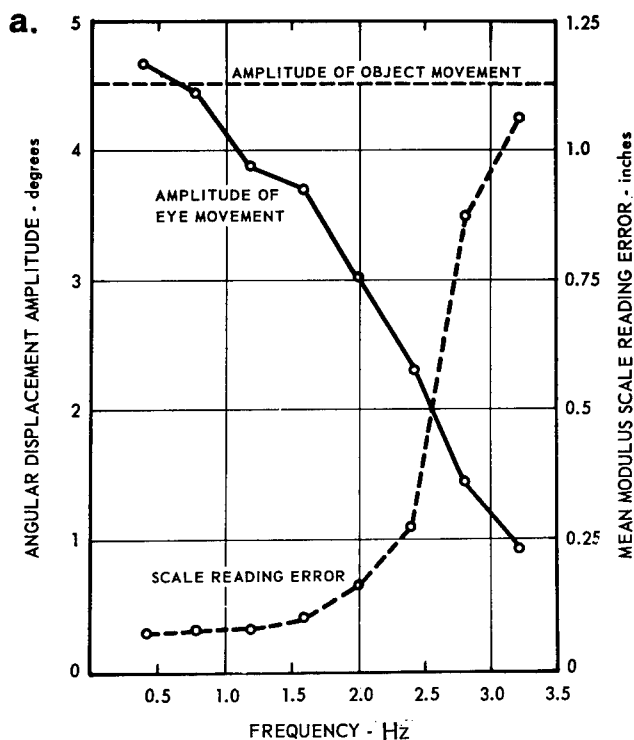
Note that the amplitude ratio of eye movement shows a greater decline with frequency when the target is vibrated than when the subject is vibrated with respect to a stationary target (continuous lines).

(After Guignard and Irving⁽⁸³⁾)

Figure 8-45

The Effect of Vibration of Target on Visual Performance

(After White⁽¹⁸⁶⁾, adapted from Jones and Drazin⁽⁹⁸⁾)



The diagrams show scale reading error and eye movements when viewing vibrating targets, a radial line disk, (b), and a horizontal scale, (a). The subject's head was fixed, and he was asked to follow the motions of the disk and scale at the frequencies shown, the excursion of the targets being 4.5 min of arc. The subject's eyes moved with the target at frequencies below 0.5 Hz, but less and less as the frequency increased. Distortion of the radial lines also increased with frequency. Errors in reading the position of markers on the horizontal scale also increased as the frequency increased.

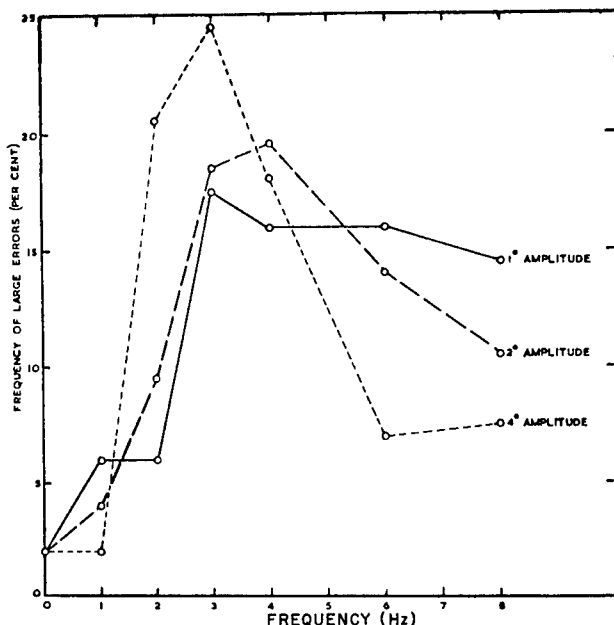


Figure 8-46

Variation of Large Dial Reading Errors (greater than 0.5 scale division) with Frequency and Amplitude of Sinusoidal Dial Vibration

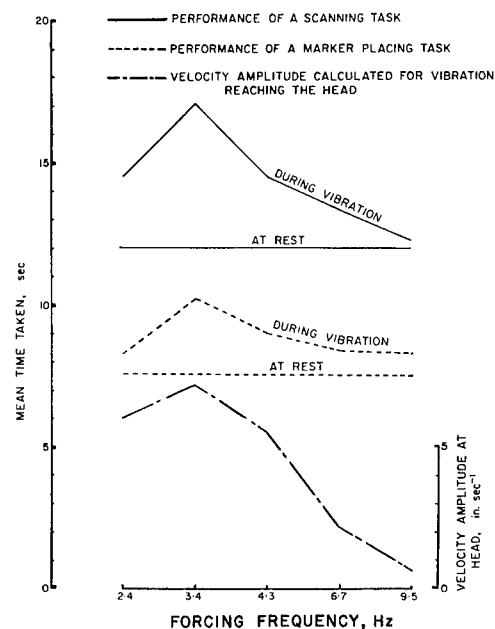
(After Drazin (45))

Figure 8-47

Effects of Vertical Sinusoidal Whole-Body Vibration on Performance.

Average times taken to complete accurately the scanning of printed material (continuous lines) and the placing of markers on a board (finely hatched lines), plotted against frequency of vibration. The horizontal lines indicate the control times taken in the absence of vibration. The lowermost curve (coarsely hatched line) shows the calculated velocity-amplitude of vibration reaching the subjects head. (See text)

(After Guignard and Irving⁽⁸¹⁾)



Performance at 6, 11, and 15 Hz was compared at various levels of acceleration with and without use of a helmet restraint. Results indicate that performance of an easy dial reading task was relatively unaffected, but a more difficult dial test incurred performance decrease as the g-load was increased from 0.3 to 2.4 g. Helmet restraint and frequency factors depended on axis of vibration. Helmet restriction improved performance at all frequencies when vibration was in the X axis; improved performance at 6 Hz but degraded it at 11 Hz and 15 Hz in the Y axis; and had no effect in the Z axis. At $1G_x \pm 1.1G_x$, use of an X-axis piston-spring damper isolation system resulted in less errors than use of an X-axis rigid system at 6 and 11 Hz (164). At 15 Hz, at this vibration intensity, both the pure piston and pure spring systems were effective in the X-axis. A Z-axis restraint had an effect only at 15 Hz. Free

movement of head was better than Z-axis restraint at this frequency. More work is needed on the relative eye movement during restraint in this form of vibration exposure, with special emphasis on cross-axis motions and combinations including roll movements before optimum restraints are possible.

The effects of in-flight vibration on visual function of astronauts of the Mercury and Gemini programs are covered in Light, (No. 2).

Vigilance, Concentration and Reaction Time During Vibration

These functions have been tested by many investigators during low frequency, whole-body vibration but there is no unequivocal evidence that they are directly impaired (31, 91, 104, 111, 154, 161). Choice reaction time with either transverse or longitudinal motion usually shows no relationship to frequency or intensity of motion. No difference from the pre-vibration control level was noted during vibration. However, reaction time significantly increases (subjects slow down) following exposure to transverse vibration (91, 155). This may or may not be due to drop in motivation. It has been suggested that if situations are such that hasty decisions are required of vehicle occupants after a vertical or transverse vibration experience, it can be expected that they will respond slower than normal, and even slower than during such vibration (91). Although it is widely believed that environmental vibration contributes to the lowering of performance by fatigue, the specific mechanisms by which it does so are unknown.

Simple Motor Performance

Measurements of simple motor performance during whole-body vibration have yielded varied results depending more upon the nature of the tests than upon the quality of the environmental stress. In general, those tests which call for maintained intensity rather than precision of volitional activity, for example, strength of grip or speed of tapping, reveal little or no decrement in performance during low frequency vibration (111). On the other hand, tests which call for precise muscular coordination, and positional control of the limbs and extremities, do show adverse effects. The reduction of manual and bodily steadiness has already been mentioned. Large-amplitude vibration or jostling of the body interferes mechanically with fine muscular actions. The performance of tasks involving precise muscular action, such as controlled depression of an accelerator pedal, accurate placing of markers on a screen, throwing switches on a console or using hand-held navigational aids, has been shown to be degraded most by vibration at low frequencies in the region of the major body resonances (81, 91, 154). This is explained by the vibratory excitation of large and rapid differential movements between the operating limb and the point of contact with the task. Fine movements of the hand and wrist, such as in writing, or in turning control knobs on electronic apparatus, in which there is only light pressure of application of the hand to the task, are easily disturbed by vibration. Tasks in which the control may be firmly gripped and provides a greater resistance to operation are less likely to be severely hindered.

Speech, which can be regarded as a special form of coordinated postural activity, can be seriously disturbed by heavy vibration and jolting of the body. This can add to the difficulties of communication by aircrew in flight. Interference with speech by continuous vibration is caused by modulation of the flow of air through the respiratory passages and by vibratory deformation of the organs of speech. The degree of interference is related to the periodicity and intensity of vibration, the dynamic properties of the buccal, cervical and thoraco-abdominal structures involved in speech, and the time-course and duration of the spoken syllables. The disturbance of speech during whole-body vibration is worst at forcing frequencies between about 3 and 15 Hz. Within this band, intelligible speech becomes very difficult at acceleration-amplitudes exceeding 0.5 g (80, 166).

Performance of Complex Tasks.

Whole-body sinusoidal vibration at acceleration-amplitudes exceeding 0.1 g in the frequency range 1 to 30 Hz can produce significant increases in the error scores in compensatory tracking tasks (17, 55, 59, 75, 91, 125, 138, 154). There is considerable divergence between the conclusions reached by different workers, particularly on the relative importance of intensity and frequency of vibration in producing the performance decrement. Some of this conflict of opinion arises from differences in method. Not all investigators have used constant amplitudes of vibration over the frequency band studied; in some experiments the man and the display were vibrated together, while in others the man was vibrated but not the display; and there has been no standardization of either the nature of the display or the type of control used.

It is generally agreed that error scores in tracking tasks rise with increasing frequency at a constant displacement-amplitude, and with increasing amplitude at a given frequency of vibration. It is easy to conclude from this that performance during whole-body vibration depends largely upon the intensity (acceleration-amplitude) of the vibration. However, other factors also contribute. There is a dearth of reliable information about the frequency-dependence of the decrement in performance during continuous vibration. Performance at a task involving the adjustment of knobs on a console vibrated with the man is particularly impaired by resonance of the shoulder-girdle at frequencies around 4 Hz (138).

Transverse vibration or sway (Figure 8-48) lowers most performance more significantly than does vertical vibration (91). The frequency of 1.5 Hz is considered to be a particularly disturbing frequency of vibration in this plane. Fore-and-aft vibration (surge) at 0.15 g may impair tracking performance. Figure 8-48b shows that performance over comparatively long periods of vibration (30 min) deteriorated with the passage of time during continuous steady-state vibration. Tracking ability was also found to be worse during the immediate post-vibration period than during the preliminary control test. While part of the decrement in performance during vibration can be explained as simple mechanical interference with the task; other factors, including the motivation of the subject during prolonged periods of working under environmental stress, must also operate.

A systematic study of tracking performance during vibration at frequencies from 2 to 12 Hz and amplitudes from 0.0625 to 0.25 in., showed that the decrement in performance is a function of amplitude and a fractional exponent of frequency (59). (See Figure 8-49). The error score was reported to be approximately proportional to $A\sqrt{f}$, where A is the displacement-amplitude of vibration and f is the forcing frequency. However, a generalization that tracking error scores are proportional to displacement amplitude times the sq. rt. of frequency may be an erroneous concept in view of what is known concerning the relationships between body resonance phenomena and tracking performance (63). The presentation of data at constant displacement amplitudes and varying frequencies obscures the fact that there is tremendous variation in the resultant acceleration levels and could lead to obfuscation and misinterpretation of frequency effects. No theory has been presented to support this relationship. Tracking ability when the man and the display are vibrated together were compared with that when the man alone was vibrated relative to a static display. The latter condition created greater difficulty for the subjects and increased the error scores.

The direction of the tracking task relative to the direction of vibration appears to be a factor in performance. A comparative study has been made of the effects of whole-body vertical vibration at frequencies of 5, 7, and 11 Hz from 25-35 percent of the human tolerance levels (defined by amplitude levels within each frequency in Reference (26) on performance of tasks representative of those encountered in aerospace flight (12). Within the limits of the vibration conditions studied, it was found that while the most pronounced decrements occur in vertical tracking, decrements in horizontal tracking, especially at 5 Hz were quite large. Vertical tracking errors ranged from 34 to 70 percent greater under vibration than under vibration-free conditions in the first experiment, although there was some adaptation on the part of the subjects since the magnitude of the vertical tracking performance decrement was lower in each treatment cell. However, the smallest vertical tracking decrement observed was still about 23 percent. Horizontal tracking decrements ranged from 10 to 48 percent with very little change between experiments. The magnitude of the tracking performance decrements was related to the magnitude of integrated absolute G_z (output) measured at the sternum. More procedural errors were committed under vibration than under static conditions. This degree of degradation is likely to reach unsatisfactory levels of decrement in an operational situation. This reach has been extended to include a study of the effects of tracking performance at vertical peak acceleration values of 25%, 20%, 15%, and 10% of the one-minute tolerance level at 5 Hz (86). (See the squares in Figure 8-51b). It was determined that a statistically significant decrement at 5 Hz began at 0.20 g or 20% of the one-minute tolerance level. No significant decrement in performance occurred at 15% and 10% tolerance. Another significant effect in this experiment was that due to trails. The performance of the subjects improved through each 5-trial testing period. Trials were three minutes in length and five trials were presented during 20 minutes of continuous vibration. It would be tempting to postulate that the disruptive effects of vibration, of the g levels used in this experiment, are temporary, and the subject adapts to them. There was a trend (not significant) for greater adaptation to take place for the two higher amplitudes than for the two lower ones.

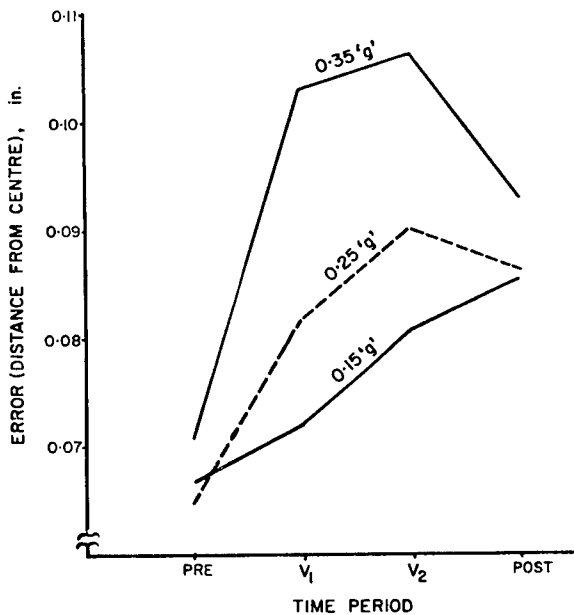
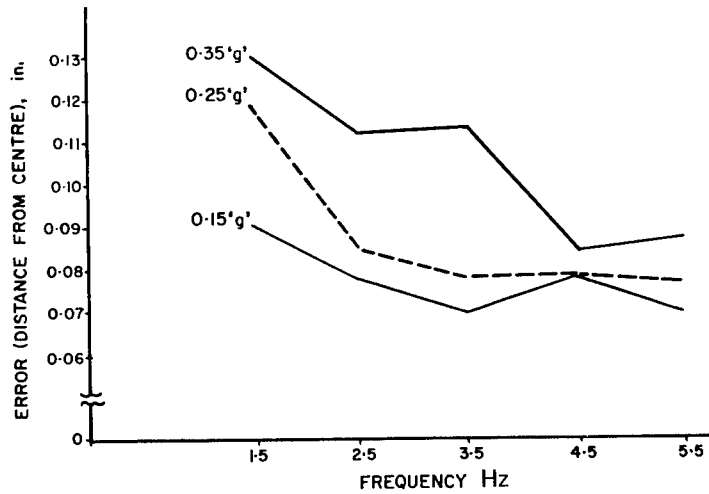
Figure 8-48

Effect of G Load, Frequency, and Duration on a Compensatory Tracking Task

(After Hornick et al⁽⁹¹⁾)

- a. Performance of a Compensatory Tracking Task as a Function of Frequency and Intensity of Transverse Whole-Body Vibration (acceleration-amplitude is the parameter).

Note that the error scores are greatest at 1.5 Hz and increase with increasing acceleration-amplitude.



- b. Performance of a Compensatory Tracking Task as a Function of Intensity and Time Period for Transverse Whole-Body Vibration (acceleration-amplitude is the parameter).

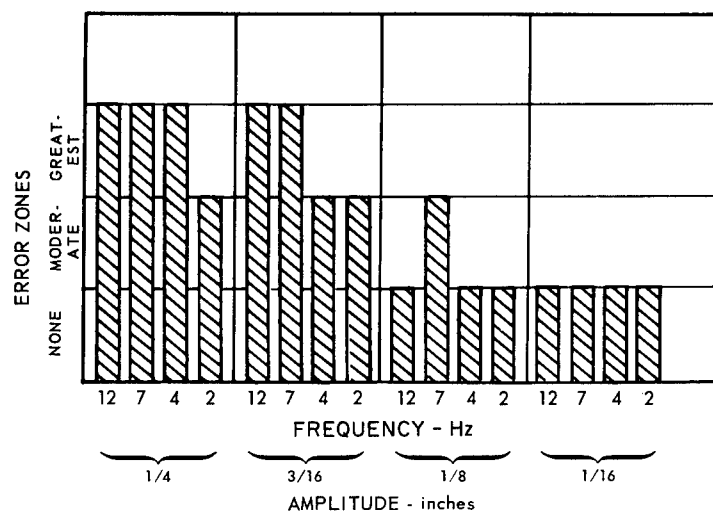
Note that performance worsens (error scores increase) during the second half of a 30-min. period of vibration and that some deterioration, compared with the control period, is present immediately after vibration has ceased.

Figure 8-49

Tracking Performance During Vertical Sinusoidal Vibration While Unrestrained

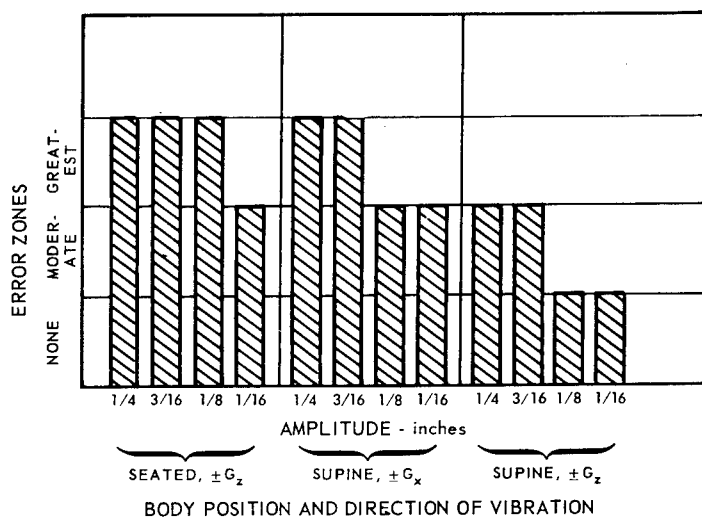
(After Webb⁽¹⁷⁸⁾, adapted from Fraser et al⁽⁵⁹⁾)

a.



The averaged effects of both amplitude and frequency of sinusoidal vibrations on error in a tracking task are shown for four subjects who were entirely unrestrained. Maximum accelerations were 3.63 G.

b.



The effects of the direction of vibration and of amplitude are shown for the same experimental situation as in a.

Recent comparisons have been made of the effect of whole-body vertical vibration on tracking performance with compensatory wheel, column, and foot systems (20) in 4 subjects at frequencies ranging from 1 through 27 Hz. A good correlation was found between general subjective experience and tracking performance. Maximum effects were noted in the 10-20 Hz range. Within the limits of this experiment and over the entire range of vibration frequency and intensity, increased force requirements in foot tracking produced the lowest degree of error but are increasingly affected by vibration. Thus, if precision is of utmost importance and the environment is to contain little vibration, higher force values (150 lbs.) are recommended; whereas, if vibration is to be present and consistency in performance is the objective, lower values (50 lbs.) appear most appropriate. Foot pressure constancy is most severely affected at 1.5 and 2.5 Hz at 43 lb./inches during transverse, and at 3.5 Hz during longitudinal vibration (91). Error increases with intensity. There is no trend of error over time, and recovery is virtually complete following exposure. The frequency dependence may vary with pressure.

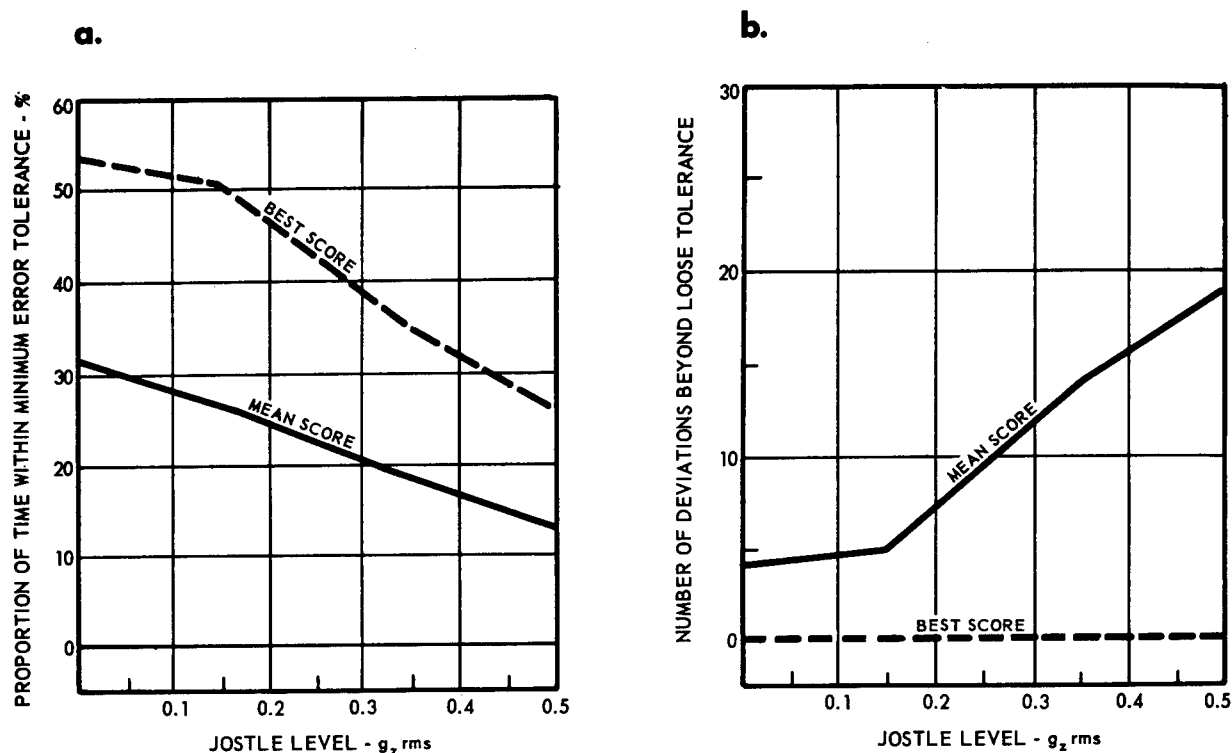
The effects of random vibrations or jostle on control tasks are seen in Figure 8-50. The difference between sinusoidal, random-amplitude and random amplitude-and-frequency vibration has received study (20, 25, 138). A comparison has been made of tracking ability during sinusoidal, narrow-band and wide-band random vertical vibration, produced by a dynamic flight simulator (20). The three types of vibration were equated in terms of their rms displacement-amplitude. The random vibration represented flight through turbulence having characteristic modes of vibration at 0.75 and 2.5 Hz and had a power spectral density representation with peaks at about 0.01 g^2/Hz at 1 and 2.5 Hz. Sinusoidal vibration was applied at 0.75 and 2.5 Hz, which were also the nominal frequencies of the narrow-band random vibrations used. The report revealed no clear-cut difference in tracking performance during sinusoidal and random vibrations of the same rms intensity. Under the conditions of the trial, significant differences were found only when the design of the display was important in relation to the direction of vibration. A marked decrement in performance was measured during steady-state vibration at 2.5 Hz and 0.54 in. amplitude when the task involved vertical tracking with a control-display feedback delay. The time-constant of the feedback delay was 2 sec, which is representative of an aircraft control system.

In another set of experiments an attempt was made to study human subjects under whole-body vertical vibration to compare effects on performance of 5 Hz sinusoidal, 5 Hz random amplitude, and 4-12 Hz random vibration equated on the basis of power, and determine acceleration levels at which significant performance decrements are found for each type of vibration (183). The complex experimental task required two-dimensional compensatory tracking, visual monitoring, and auditory monitoring during 20-minute vibration exposures at levels equated to 5, 15, 25, and 30 percent of the 1-minute human tolerance values for 5 Hz sinusoidal vibration. Performance decrements under vibration were restricted to tracking, the most demanding component of the task complex. Tracking performance deteriorated with increasing acceleration levels of each type of vibration. Overall performance differences associated with the different types of vibration equated on the basis of power were not significant. A number of task and procedural variables,

Figure 8-50

Tracking Performance During Vertical Jostle

(After Webb⁽¹⁷⁸⁾, adapted from Clark⁽²²⁾)



These two figures illustrate the increasing difficulty of performing a demanding control task as random vertical vibrations ("jostle") increased in magnitude. Pilots were held by a Navy torso restraint device in the North American Aviation "G-seat," which was then programmed to move in the $\pm G_z$ direction with an electrical white noise input, and jostle levels of: 0.15 G_z rms (root mean square) described by the pilots as similar to flying through mild turbulence; 0.35 G_z rms, described as severe turbulence; and 0.50 G_z rms, in which the largest jolts were classed as one-of-a-kind in a real flight. Power density spectra peaked near 1 Hz. A panel-mounted accelerometer showed maximum and minimum accelerations of 0 to 2.5 G_z for 0.15 G_z rms; -1.2 to 4.0 G_z for 0.35 G_z rms; and -2.5 to 5.0 G_z for 0.5 G_z rms. The demanding control task was to track in pitch, shown on a 5-inch oscilloscope screen, and hold roll to 0. Fourteen highly motivated and skilled Navy pilots made 70 runs; they tolerated the random vibrations well, although they had to brace themselves against the larger seat movements to avoid slapping of the head or body against the structure. Longer runs - 15 to 30 minutes at 0.35 G_z rms - produced muscular fatigue.

Chart a shows what tracking error occurred as the jostle levels increased; the minimum tolerance for error was set to be 1/12 of the task amplitude. Chart b shows that as jostle increased, more and more tracking deviations appeared beyond the loose tolerance level of 5/6 of the task amplitude.

including task difficulty, work-rest cycle, and prior experience appear to be important determinants of performance capabilities and fatigue effects found in vibration studies, indicating a need for further investigation of these variables. For various pairs of periodic vibration exposure having the same rms but different peak accelerations, subjective severity ratings seem to depend on differences in peak acceleration but motor functions such as holding hand and arm in fixed position depend on rms values. The evidence presented above indicates that differences in bandwidth and spectral density characteristics of vibration conditions equated on the basis of power (mean square acceleration) are of far less importance in determining performance capabilities than other experimental variables. Inasmuch as the vibration conditions tested cover a significant portion of the 1-20 Hz range in which the more significant effects of vibration are found, further study should be undertaken to test the generality of this finding. If performance equivalence of power values is found to hold within a number of frequency bands spanning the 1-20 Hz range, the way will be open to utilize data derived from tests with simple sinusoidal vibration in predicting performance under more complex spectra.

A major difficulty of research in this area still centers on selection of performance tests representative of operational tasks for which difficulty levels and operator loading can be specified. If unitary activities such as tracking or visual monitoring are tested in isolation, measurement problems are simplified, but task difficulty must be increased in order to achieve adequate sensitivity to stress effects. An alternative is to employ complex tasks which require time-sharing of attention among several activities. The use of tasks of this type, which simulate more closely operational situations, will be facilitated if some effort is devoted to establishing the difficulty level of the total task complex and each of its component activities. One approach which merits consideration is the use of secondary task scores to measure operator workload. Techniques are available for deriving quantitative estimates of operator loading in a complex task by measuring ability to perform an auxiliary task concurrently (49, 101, 102).

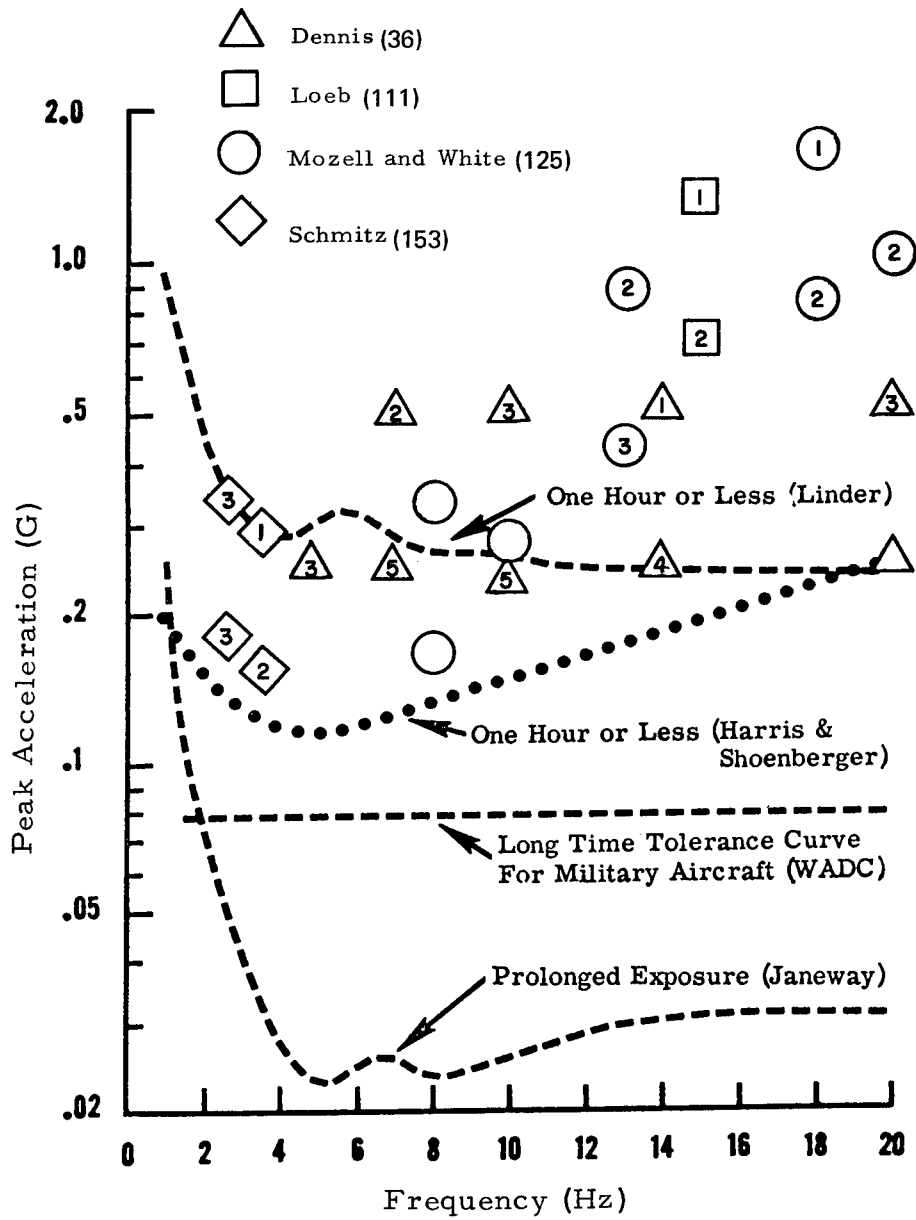
An interesting comparison has been made between the long-time tolerance limits proposed and the result of visual acuity tests and tracking performance as shown in Figures 8-51a and b. The curves offer an excellent opportunity for display of the effect which experimental variables may have on the setting of performance thresholds. The following discussion is taken from this review (87).

In Figure 8-51a, the geometric symbols refer to the studies of particular authors and their locations on the figure indicate the levels of vibration at which visual acuity was tested. The numbers inside the symbols show the relative level of decrement obtained within any one study. Number 1 denotes the greatest decrement with successive numbers indicating decreasing decrement. The absence of a number means that no decrement was obtained. There is nothing to indicate that visual acuity will be adversely affected at the levels of the two long-term exposure curves at the bottom of the figure. Of course, no data are presented at these levels. However, it seems extremely unlikely that visual acuity would be significantly affected at these low g values. (See also Figure 8-23a.)

Figure 8-51

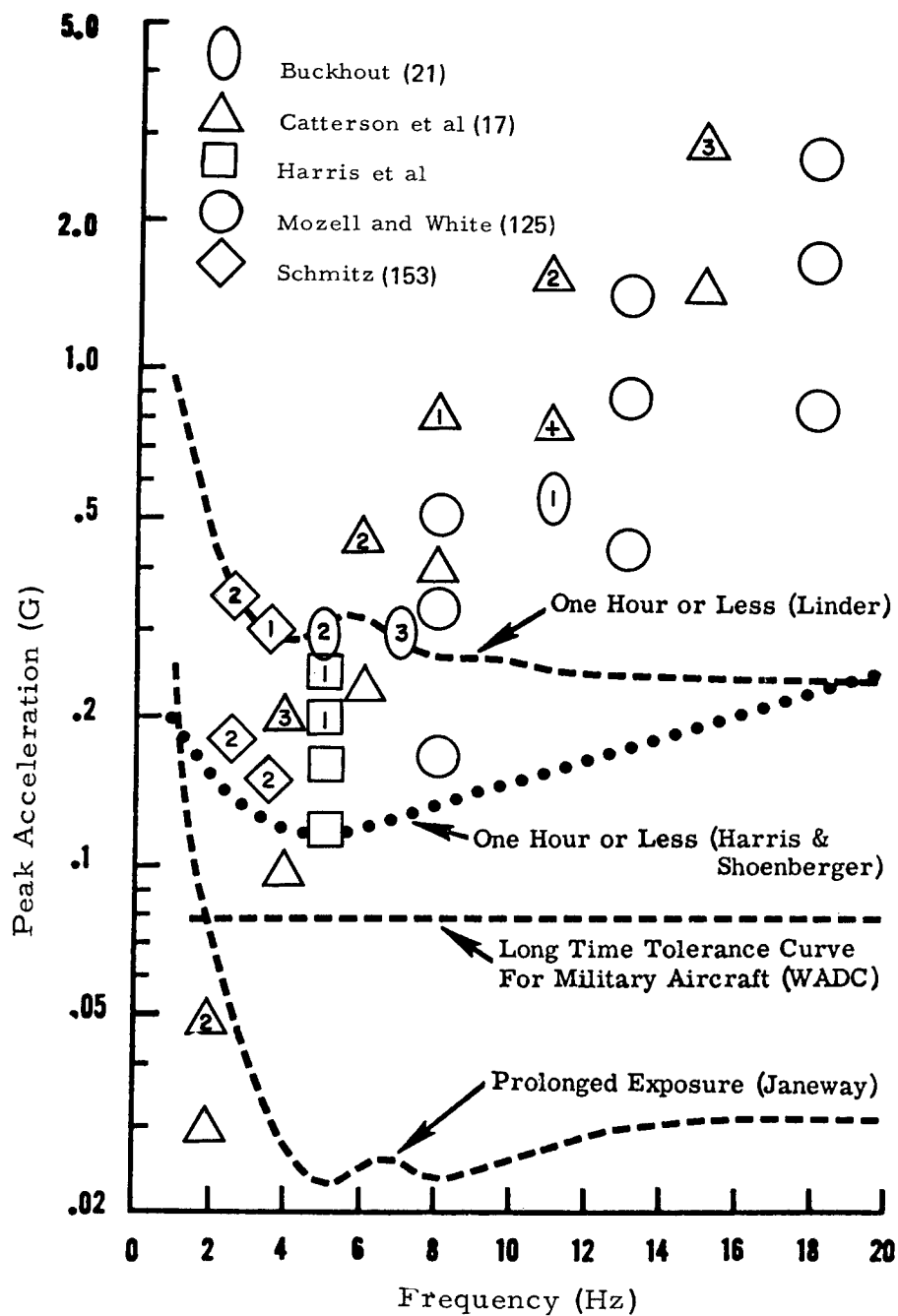
Performance During Vibration in Relation to Long-Time Recommended Limits

(Adapted from Harris and Schoenberger (87))



a. Performance on Visual Acuity Tasks (See text)

Figure 8-51 (continued)



b. Performance on Tracking Tasks (See text)

The upper curve (one hour recommended limit) has numerous data points surrounding it; some showing decrements and some showing no decrements in visual acuity. Of particular interest are the data presented by Dennis because they follow the recommended one hour exposure curve rather closely. The greatest decrement occurred at the 0.25 g level at 5 Hz, with less decrement occurring at 14 Hz, still less decrement at 10 Hz and at 7 Hz, and finally none at all at 20 Hz. Thus these data look pretty good in relation to a body resonance hypothesis and would suggest an alteration of the curve more in line with body resonance. However, the situation is complicated by the data points indicated by the circles (Mozell and White). At 8 and 10 Hz at g values higher than used by Dennis, no decrement in visual acuity was obtained. There are data by Schmitz at lower frequencies of 2.5 Hz and 3.5 Hz indicating a decrement in visual acuity at the level of the curve. These data are also in line with body resonance in that a greater decrement in visual acuity was obtained at the frequency value closer to body resonance, that is, a greater decrement was obtained at 3.5 Hz than at 2.5 Hz.

All of the remaining data points on the graph are above approximately 0.4 g and all indicate a decrement in visual acuity. Of interest again are the data obtained by Dennis at 0.5 g, since he held peak acceleration constant and varied the frequency. At 0.5 g the greatest decrement occurred at 14 Hz, the next at 7 Hz and the next and last ones at this g level are 10 and 20 Hz. An interesting comparison is that as much error occurred at 0.25g at 5 Hz as occurred at 0.5 g at the frequencies of 10 and 20 Hz. The contradiction between the Mozell and White data and the Dennis data can be easily explained. A comparison of the data of these investigators shows that Dennis used a much more difficult task for measuring visual acuity than did Mozell and White. Dennis found about 15% error in visual acuity during control conditions, and Mozell and White found essentially no error in visual acuity for the control conditions in their study.

In Figure 8-51b, tracking performance data obtained under many different conditions is presented for comparison with the recommended long-term tolerance curves. Perhaps the most striking aspect of this figure is the fact that Mozell and White found no decrements in tracking performance at any combination of frequency and peak acceleration used. Many of these data points of Mozell and White are at levels where other investigators found tracking ability adversely affected; and also, from the preceding figure, it can be seen that consistent losses in visual acuity occurred at much lower levels than those at which Mozell and White failed to find tracking performance decrement. In reality, the simplicity and grossness of the display and the simplicity and crudeness of the motor response account for this discrepancy (87, 125).

The subjects in the study by Catterson et al were not restrained, while the subjects of all of the other investigators represented on this figure were. Overall, the data of Catterson et al seem to correspond fairly well with body resonance except for the two data points at 2 Hz. At this frequency, 0.05 g produced a decrement in tracking performance where 0.03 g at the same frequency did not. While it is difficult to explain the difference in performance obtained between these small g levels, it is perhaps possible to understand why decrements could occur at such low values. The authors state, "there is

objective evidence of a sedative and somnolent effect of vibration at 2 Hz (17). This could explain the decrement which occurred at 2 Hz and would suggest that it occurred for a very different reason than the decrements at other frequencies. However, one doesn't have to look far for another unusual finding in these data. Catterson et al found an improvement in performance at 11 Hz at approximately 0.7 g. Buckhout found a large performance decrement at the same frequency at approximately 0.5 g.

There does not seem to be any generalized information that can be gleaned from this figure except for some suggestive evidence that tracking performance is more likely to be affected around body resonance, 3-8 Hz; however, as with the visual acuity data presented in Figure 8-51a, inconsistency exists here also. Considering both the visual acuity and the tracking data, about the only thing one can say about Linder's recommended 1 hour tolerance curve is that the g values seem too high at the low frequency end of the curve. One might also say that the g values appear to be too low at the high frequency end of the curve. In view of the fact that these studies lasted less than 1 hour, it would seem advisable to err on the side of conservatism, and to suggest further that Linder's curve is too high throughout the frequency range. Harris and Schoenberger curves for exposure times up to 1 hour are presented as the dotted line in Figures 8-51a and b. It represents somewhat of a compromise between Linder's curve and the WADC curve. Although the acquisition of new data will undoubtedly necessitate changes in this curve, it is believed to be a more realistic estimate than the one presented by Linder. In the absence of data to indicate otherwise, one may also suggest the WADC curve as a design guideline for long-term exposure, in preference to Janeway's curve.

Performance under Combined Vibration and Linear G

The effect of combined linear and oscillatory acceleration of liftoff and reentry patterns on pilot attitude-control capabilities are of interest. One might expect different resonance spectra under zero gravity and g loading superimposing vibration at 11 Hz onto a steady linear acceleration on the tracking ability of a human pilot in a stability- and rate-augmented vehicle with dynamics typical of a large high-thrust rocket (43). The linear accelerations ranged from 1 to 3.5 g and the oscillatory stresses varied from 0 to ± 3.0 g at 11 Hz. A random-appearing compensatory tracking problem was presented to the pilot in the pitch plane, although the pilot controlled both pitch and yaw. No attempt was made to simulate additional pilot tasks such as monitoring of critical launch vehicle and spacecraft performance and status displays which would be required in the real situation. Various damper-failure situations were investigated, and certain characteristics due to nonlinearities of the autopilot were studied. Effects on the tracking efficiency of dividing the pilot's attention between pitch and yaw channels were also examined. Both performance measures and subjective opinion indicated substantial degradation in pilot tracking effectiveness above vibration levels of ± 1.5 g at 11 Hz. The pilots were almost completely ineffective at ± 3.0 g vibration.

Under vibration, the pilots reached the limit stops of the engine-servo rate and position often enough that a linear analysis of the pilot describing

function was difficult. Pilot comments indicate that they could not perceive rate information from the visual display (rate of needle motion). It is therefore assumed that the pilots were unable to generate the lead time constant usually necessary in this type of tracking. The engine-servo rate and position limits were chosen to simulate a typical large high-thrust booster rocket. The problem often arises in a study of this type that the vehicle and control dynamics are not compatible with the "standard" task. However, the task was selected so that comparisons could be made with previous studies. The highest frequencies of the present task were somewhat too high for the air-frame-autopilot combination used and it was suggested that increasing the engine-servo rate limit would permit the pilot to improve his performance. Limiting the rapidity with which the control system under the pilot's direction can act also prevents him from tracking rapidly. Hence, the portion of the input not filtered by the system, the remnant, would tend to increase the error. To determine the magnitude of this effect in the present study a series of runs were made for three values of servo rate limits under 1 g static conditions using one above-average pilot. The results indicate an improvement between 5°/sec and 20°/sec with a modest improvement up to 50°/sec. A brief investigation of the pilot's ability to cope with sudden changes in the controlled element was made by simulating pitch damper failures. The period of temporary adaptation required was approximately 15 seconds at a 3.0 +G_x linear acceleration and ±2.0 G_z vibration, while for a +1 G_z acceleration, it was 5 seconds.

Dial reading has been studied in the semi-supine position of Figure 8-24 as a function of the level of 11 Hz G_x vibration and the size of the dial, where a bias acceleration of 3.75 G_x was superimposed on the vibration (26). Dial reading errors were inversely related to the arc length of the interval between dials and directly related to the amplitude of vibration. There was approximately 50% distortion of the 11 Hz vibration acceleration, which markedly influences the interpretation of results and their comparison to measurements of visual decrements from 11 Hz vibrations with 1 G_x bias loads. In most general terms, however, the 3.85G_x bias, and/or the unidirectional force (i.e., the resultant acceleration was always greater than 0G) creates a subjectively more tolerable environment than with a 1 G bias. Vibrations of 3.85G_x ±3.0g_x were without serious subjective effects in exposures of 90 seconds duration. Gross comparisons of dial reading performance under the two conditions provide some indication that the greater bias acceleration is associated with less visual decrement, probably as a result of alteration in resonance peaks at the eye.

The increase in the tolerance seen from trial to trial during studies of performance is of interest from the point of view of training to vibration tolerance (86). Also of interest is the fact that when an intensity range is reached that produces significant increments in error, the standard deviation is much larger than would be expected from the increase in the size of the mean (32, 87). The major reason for the large increase in variability is that some individuals show a tremendous increase in error while other individuals in the same experiment show little or no increase in error. This result has been obtained even for experienced pilots (146). This fact suggests that one may select individuals for those missions with a greater potential for vibration hazard, such as those with boosters giving severe POGO effects. (See Light, No. 2.)

Performance on Launch Towers During Horizontal Oscillation

Preliminary attempt has been made to determine on-tower-limitations of the capabilities of standing workers performing servicing tasks in the arms of the tower about the Saturn V Vehicle at a firing site on Launch Complex 39 (157). It was determined that horizontal, linear, sinusoidal oscillation-frequencies of 0.33 Hz and 0.80 Hz were satisfactory samples of the wind conditions that could be expected (162). The corresponding amplitudes of ± 6.3 inches and ± 7 inches could be expected at the uppermost level. Three tasks were performed at each of the frequencies and amplitudes: a hand accuracy test for nut and bolt assembly; a hand-probe steadiness test; and a visual acuity test. No significant differences were found in the results of the tests at 0.33 Hz, but significant decrements of performance appeared at 0.80 Hz, especially in precision tasks which cannot be done readily at this frequency. There were significant differences between G_x and G_y axes in these tests. More time is needed for tasks that do not require precision, but at 0.80 Hz, an increase of time does not result in an increase of performance accuracy of precision tasks. Visual acuity is lessened at 0.80 Hz only when worker-subject is oscillated from shoulder-to-shoulder. It was recommended that performance-time at 0.80 Hz should be limited to compensate for increased human error from fatigue which is seen at this frequency.

PROTECTION AGAINST VIBRATION

Techniques for reducing the transmission of vibration to vehicle-mounted equipment apply equally to man. These include vibration isolation, the use of nodal positions, and attention to the immediate routes of entry of vibration into the body. Protection against vibrations is so far mainly achieved by vibration isolation, a method relatively effective, economical, and requiring little space at the higher frequencies (13, 41, 70, 73, 80, 85, 129).

Vibration of the support structures at frequencies near the resonant frequency of a mass-spring system is made worse by spring isolation. Damping must therefore be included but unfortunately, the greater the amount of damping, the less attenuation is achieved at higher frequencies. There is also conflict between the demands of an isolation system for continuous vibration (a low frequency suspension with light damping) and those of a system for discrete impacts (a stiff suspension with fairly heavy damping). This problem is not easily resolved and passenger vehicle suspension systems represent a practical compromise. Motor car and railway carriage suspension systems have been found empirically to give the best overall ride with a natural frequency of 1 to 1.5 Hz and damping between 0.5 and 0.7 of critical for viscous damping or its equivalent. Such a system may slightly augment vertical oscillations near the resonant frequency. Suspensions with resonant frequencies below 1 Hz give a smoother ride but tend to make passengers motion sick.

The human may be passively isolated by means of a suspension seat or similar device. As a rough rule, the loaded system should have a resonant frequency not exceeding one half of the lowest frequency from which it is desired to isolate the load. For man, in vertical excitation, the latter may

be taken to be 3 to 4 Hz, so that the resonant frequency of an occupied suspension seat should lie between 1 and 2 Hz. The precise spring stiffness and damping appropriate to particular conditions are a problem for individual solution. Provision should be made for the independent varying of stiffness and damping to suit the individual user and the particular circumstances. More practicable, although limited, advantages can be gained by fitting non-linear springs of the "hard" type to suspension seats. The stiffness of such springs increases with deflexion, so that displacement of the load is reduced for heavier vibration. A combination of non-linear stiffness and suitable damping can be obtained in rubber suspensions, or in spring and damper systems embodying special features such as recruitment. Pneumatic springs and other active isolation devices, in which displacement of the load is opposed under servo control by power supplied to the system, may also have applications in suspension systems.

The vibration of instruments, making them difficult to read, is reduced by placing the instrument or instrument panel on anti-vibration mountings. The resonant frequency of the loaded mountings should not fall within the range which is critical for instrument legibility. Design for operation by wrist and finger movements, rather than by extended movements of the whole arm, will improve the vibration resistance of control systems.

Below 5 to 10 Hz the large space required to compensate amplitudes at tolerance limits often prohibits application of isolation methods in aerospace-craft. Improved body restraint and suppression of individual resonances is a promising approach in this frequency range. The effects of such protective restraints, enclosures and supports have only been investigated in a very preliminary way (118, 168). Some increase in tolerance appears possible, although some supports such as integrated impact protective devices in suits can keep subject from relaxing and produce a less favorable coupling with the vibration source. Mice have been protected from damage from 20 Hz vibration at 7 G (rms) by positive pressure breathing at 3.75 and 6.00 inches of H₂O, but no direct extrapolation of efficacy to man is possible (9).

Contoured and adjustable couches have been used in spacecraft. In experiments with these adjustable couches (reviewed in Figure 8-24 and Table 8-25) the role of restraints becomes obvious in the discussion which is recorded here (168).

A structure is needed which will more effectively couple the head to the vibration source, and provide better body-to-couch coupling by reducing dead space, minimizing restraint slackness and lessening the possibilities for body-couch phase shift. The adjustable couch was designed to answer these needs and does provide considerable improvement in body-to-couch coupling. However, it does not completely solve the coupling problem. Further, the more positive restraint and protection that it provides for the helmeted head is only partly successful in improving tolerance.

The problem of operational head restraint and protection is a particularly difficult one. During the departure and reentry phases of space flight, the sustained linear acceleration, or deceleration, and associated severe vibrations will make head protection very important. Despite adequate restraint the head

may still be subjected to severe uncontrolled, and possible injurious buffeting under some circumstances. In the study of Figure 8-24, with the head helmeted and well coupled to the couch, the symptoms limiting tolerance at the low frequencies seem to have been minimized. However, the coupling appears to have accentuated head discomfort and caused lower tolerances at the higher frequencies, particularly in the X and Y axes. This is in contrast to exposures in the contoured couch when raising the unrestrained, unhelmeted head from the couch helped to isolate it from the vibration source, contributing to better tolerance levels at the higher frequencies. It is possible that, in the adjustable couch, the mass of the head may have been resonating with the helmet and elastic liner, magnifying the vibration input to the head and causing lower tolerances. However, a study on the subjective tolerance of the restrained head vibrated alone at frequencies between 10 and 30 Hz, helmeted and unhelmeted, revealed that use of the helmet did afford an advantage in isolation and protection of the head when compared with results obtained under the same conditions without a helmet (168).

The significance of the observed relationship between head restraint and frequency in the response of the head to vibration has been given some emphasis by the results of a series of dial reading performance studies recently completed utilizing the adjustable couch in essentially the same configuration as used in this study (165). (See above.) One of the questions asked in these studies concerned the influence of head restraint on dial reading accuracy. It was demonstrated that accuracy below 8 Hz was greater with the head restrained than if it were unrestrained. The opposite was the case above this frequency range. These results held true for the X and Y axes, but not for the Z axis. A broad generalization concerning the interrelationships of head restraint, frequency and tolerance is not warranted on the basis of this study. Given the results obtained with this particular system, however, it appears that a head restraint should provide close coupling to the vibration source at frequencies up to about 10 Hz, and should provide isolation from the source at frequencies between 10 and 20 Hz. (Preliminary test of this idea was covered in the section on dial reading, page 8-90.)

One can look at protection from an impedance point of view (128, 179). Vibration tolerance, in terms of velocity, is relatively lower at the higher frequencies as shown in Figure 8-24d and e. In fact, the tolerance curves are strikingly similar in form to the inverse ($1/|Z(\omega)|$) of the impedance magnitude. The velocity tolerance appears to be lowest where impedance is highest and vice versa (179). There are also perturbations in the tolerance curve corresponding to the critical frequencies. In comparison to the effect of other frequencies, the perturbation in the velocity tolerance curves due to resonant frequencies is not as impressive as it is in the acceleration tolerance curves.

Acting on these facts, one can approach the problem of protection system design (179). The basic problem is to minimize the amount of power exchange by the human with the environment (105, 140, 141, 142, 143, 171). In other words, the protection system should have a characteristic such that, when interposed between the human and the environment, it modifies the environment to minimize transmittal of energy at the frequencies where the impedance is absolutely or relatively highest. Therefore, on accepting the premise that

the mechanical energy, per se, damages the human, one would try to design a protection system whose velocity transfer characteristics attenuates 7 and 12 Hz energy and high frequency energy while passing low frequency energy. In fact, the protection system velocity transfer function could be the reciprocal of the impedance magnitude. There is an aspect of protection system design which cannot be specified by the impedance method. This is the absolute level or the total energy or power which can be transmitted with safety. In other words, there is no specification on how much energy the protection system must dissipate within itself. Also, in the real-world situation, both impact and vibration must be considered in design of the ideal restraint system and the appropriate tradeoffs mode. (See Impact section in Acceleration, No. 7.)

The most recent work on vibration isolation for aerospace pilot protection under low-altitude, high-speed flight suggests that passive systems cannot provide the required degree of isolation while simultaneously limiting maximum displacement to desired values (13). An active hydraulic system employing acceleration and displacement feedback mechanisms has been proposed.

REFERENCES

- 8-1. Adey, W. R., French, J. D., Kado, R. T., et al., EEG Records from Cortical and Deep Brain Structures during Centrifugal and Vibrational Accelerations in Cats and Monkeys, IRE Trans. Biomed. Electr., BME 8: 182-188, 1961.
- 8-2. Agate, I. N., Druett, H. A., A Study of Portable Vibrating Tools in Relation to Clinical Effects Which they Produce, Brit. J. Indust. Med., 4: 141-163, 1947.
- 8-3. Antipov, V. V., Delone, N. L., Parfyonov, G. P., et al., Results of Biological Experiments Carried Out under Conditions of Flight in Ship Vostok with Participation of Cosmonauts A. G. Nikolayev, P. R. Popovich, and V. F. Bykovsky, in A Session of the Fifth International Space Science Symposium, Florence, Italy, May 12-16, 1964, Life Sciences and Space Research III, John Wiley & Sons, Inc., N. Y., 1965, pp. 215-229.
- 8-4. Ashe, W. F., Physiological and Pathological Effects of Mechanical Vibration on Animals and Man, OSU-RF-862-4, Ohio State University, Research Foundation, Columbus, Ohio, Sept. 1961.
- 8-5. von Bekesy, G., Uber die Empfindlichkeit des Stehenden und Sitzenden Menschen Gegen Sinusformige Erschutterungen, Akust. Ztschr., 4: 360, 1939.
- 8-6. von Bekesy, G., Uber die Vibrationsempfindung, Akust. Ztschr., 4: 316, 1939.
- 8-7. von Bekesy, G., Vibration of the Head in a Sound Field and Its Role in Hearing by Bone Conduction, J. Acoust. Soc. Amer., 20: 749, 1948.
- 8-8. Bowen, I. G., Holladay, A., Fletcher, E. R., et al., A Fluid-Mechanical Model of the Thoraco-Abdominal System with Applications to Blast Biology, DASA-1675, Defense Atomic Support Agency, Washington, D. C., June 1965.
- 8-9. Brady, J. F., Newsom, B. D., Effect of Positive Pressure Breathing on the Vibration Tolerance of the Mouse, Aero-space Med., 37(1): 40-45, 1966.

- 8-10. Bryce, W. D., A Review and Assessment of Criteria for Human Comfort Derived from Subjective Responses to Vibration, NGTE-R-286, National Gas Turbine Establishment, Ministry of Aviation, Pyestock, Hants, Dec. 1966.
- 8-11. Buchmann, E., Criteria for Human Reaction to Environmental Vibration on Naval Ships, DTMB-1635, David Taylor Model Basin, Washington, D. C., June 1962.
- 8-12. Buckhout, R., Effect of Whole Body Vibration on Human Performance, Human Factors, 6(2): 153-157, Apr. 1964.
- 8-13. Calcaterra, P. C., Schubert, D. W., Research on Active Vibration Isolation Techniques for Aircraft Pilot Protection, AMRL-TR-67-138, Aerospace Medical Research Labs., Wright-Patterson AFB, Ohio, Oct. 1967.
- 8-14. Callahan, J. A., Gemini Spacecraft Flight Vibration Data and Comparison with Predictions, in The Shock and Vibration Bulletin, Bull. 35, Pt. 7, Naval Research Lab., Washington, D. C., Apr. 1966, pp. 67-76.
- 8-15. Carmichael, J. B., Jr., Henzel, J. H., Mohr, G. C., et al., On the Measurement of the Transmission of External Force Through Fluid Systems in Primates, AMRL-TR-66-44, Aerospace Medical Research Labs., Wright-Patterson AFB, Ohio, Mar. 1967.
- 8-16. Carstens, J. P., Kresge, D., Literature Survey of Passenger Comfort Limitations of High Speed Ground Transports, Rep. No. D-910353-1, United Aircraft Corporation, Research Labs., East Hartford, Conn., July 1965.
- 8-17. Catterson, A. D., Hoover, G. N., Ashe, W. F., Human Psychomotor Performance during Prolonged Vertical Vibration, Aerospace Med., 33: 598-602, May 1962.
- 8-18. Chaney, R. E., Subjective Reaction to Whole Body Vibration, BOE-D3-6474, Boeing Co., Wichita, Kan., Sept. 1964.
- 8-19. Chaney, R. E., Whole Body Vibration of Standing Subjects, BOE-D3-6779, Boeing Co., Wichita, Kan., Aug. 1965.
- 8-20. Chaney, R. E., Parks, D. L., Tracking Performance during Whole-Body Vibration, BOE-D3-3512-6, Boeing Co., Wichita, Kan., Nov. 1964.
- 8-21. Chaney, R. E., Parks, D. L., Visual-Motor Performance during Whole-Body Vibration, BOE-D3-3512-5, Boeing Co., Wichita, Kan., Nov. 1964.

- 8-22. Clark, C. C., Human Control Performance and Tolerance under Severe Complex Waveform Vibration with a Preliminary Historical Review of Flight Simulation, MAR-ER-12406, Martin Co., Baltimore, Md., 1962.
- 8-23. Clark, J. G., Williams, J. D., Hood, W. B., Jr., et al., Initial Cardiovascular Response to Low Frequency Whole Body Vibration in Humans and Animals, Aerospace Med., 38(5): 464-467, 1967.
- 8-24. Clark, W. S., Lange, K. O., Coermann, R. R., Deformation of the Human Body due to Unidirectional Forced Sinusoidal Vibration, Human Factors, 4: 255-274, Apr. 1962. (Also in Human Vibration Research, Lippert, S., (ed.), Pergamon Press, Oxford, England, 1963, pp. 1-28).
- 8-25. Clarke, N. P., Mohr, G. C., Brinkley, J. W., et al., Evaluation of Peak vs. RMS Acceleration in Periodic Low Frequency Vibration Exposures, AMRL-TR-65-67, Aerospace Medical Research Labs., Wright-Patterson AFB, Ohio, Nov. 1965. (Also in Aerospace Med., 36(11): 1083-1089, 1965).
- 8-26. Clarke, N. P., Taub, H., Scherer, H. F., et al., Preliminary Study of Dial Reading Performance during Sustained Acceleration and Vibration, AMRL-TR-65-110, Aerospace Medical Research Labs., Wright-Patterson AFB, Ohio, Aug. 1965.
- 8-27. Coermann, R. R., Comparison of the Dynamic Characteristics of Dummies, Animals and Man, in Impact Acceleration Stress, Proceedings, Brooks AFB, Texas, Nov. 27-29, 1961, NAS-NRC-977, National Academy of Sciences, National Research Council, Washington, D. C., 1962, pp. 173-184.
- 8-28. Coermann, R. R., The Mechanical Impedance of the Human Body in the Sitting and Standing Position and Its Significance for the Subjective Tolerance to Vibrations, paper presented at the 3rd Annual Meeting of the Biophysical Society, Pittsburgh, Pa., Feb. 1959.
- 8-29. Coermann, R. R., The Mechanical Impedance of the Human Body in Sitting and Standing Position at Low Frequencies, ASD-TR-61-492, Aeronautical Systems Div., Wright-Patterson AFB, Ohio, Sept. 1961.
- 8-30. Coermann, R. R., Untersuchungen uber die Einwirkung von Schwingungen auf den Menschlichen Organismus, Jahrbuch Deutsch. Luftfahrtforsch., 3: 111, 1938.

- 8-31. Coermann, R. R., Untersuchungen uber die Einwirkung von Schwingungen auf den Menschlichen Organismus, Luftfahrtmedizin, 4: 73-122, 1940.
- 8-32. Coermann, R. R., Magid, E. B., Lange, K. O., Human Performance under Vibrational Stress, Human Factors, 4: 315-324, Oct. 1962.
- 8-33. Coermann, R. R., Ziegenruecker, G. H., Wittwer, A. L., et al., The Passive Dynamic Mechanical Properties of the Human Thorax-Abdomen System and of the Whole Body System, Aerospace Med., 31: 443-455.
- 8-34. Crook, M. N., Harker, G. S., Hoffman, A. C., et al., Effect of Amplitude of Apparent Vibration, Brightness, and Type Size on Numeral Reading, AF-TR-6246, Wright Air Development Center, Wright-Patterson AFB, Ohio, Sept. 1950.
- 8-35. Dart, E. E., Effect of High Speed Vibratory Tools on Operators Engaged in Airplane Industry, Occup. Med., 1: 515-550, 1946.
- 8-36. Dennis, J. P., The Effect of Whole Body Vibration on a Visual Performance Task, Rep. 104, Clothing and Equipment Physiological Research Establishment, Ministry of Supply, Farnborough, England, 1960. (AD-247249).
- 8-37. Dennis, J. P., Some Effect of Vibration upon Visual Performance, J. Appl. Psychol., 49(4): 245-252, 1965.
- 8-38. Dennis, J. P., Elwood, M. A., The Effects of Vibration Experienced in Different Seating Positions, Rep. 78, Clothing and Equipment Physiological Research Establishment, Ministry of Supply, Farnborough, England, 1958.
- 8-39. Dieckman, D., Ein Mechanisches Modell fur das Schwingungserregte Hand-Arm-System des Menschen, [A Mechanical Model for the Hand-Arm-System Set in Motion by Oscillation], Int. Z. Angew. Physiol., 17: 125-132, 1958.
- 8-40. Dieckman, D., Einfluss Horizontaler Mechanischer Schwingungen auf den Menschen, [Influence of Horizontal Mechanical Swinging on Man], Int. Z. Angew. Physiol., 17(1): 83-100, 1958.
- 8-41. Dieckman, D., Einfluss Verticaler Mechanischer Schwingungen auf den Menschen, [Influence of Vertical Mechanical Oscillations in Man], Int. Z. Angew. Physiol., 16(6): 519-564, 1957.

- 8-42. Dixon, M. E., Stewart, P. B., Mills, F. C., et al., Respiratory Consequences of Passive Body Movement, J. Appl. Physiol., 16: 30-34, 1961.
- 8-43. Dolkas, C. B., Stewart, J. D., Effect of Combined Linear and Oscillatory Acceleration on Pilot Attitude-Control Capabilities, NASA-TN-D-2710, Mar. 1965.
- 8-44. Drazin, D. H., Effects of Low-Frequency High-Amplitude Whole Body Vibration of Visual Acuity, FPRC-Memo-128, Flying Personnel Research Committee, Air Ministry, London, Nov. 1959.
- 8-45. Drazin, D. H., Factors Affecting Vision during Vibration, Research, (London), 15: 275-280, 1962.
- 8-46. Duffner, L. R., Hamilton, L. H., Schmitz, M. A., Effect of Whole Body Vertical Vibration on Respiration on Human Subjects, J. Appl. Physiol., 17: 913-916, 1962.
- 8-47. Dussik, K. T., Measurement of Arterial Tissue with Ultrasound, Amer. J. Phys. Med. (Baltimore), 37: 160-165, 1958. (Presented at the International Conference of Ultrasonics in Medicine, Los Angeles, Calif., Sept. 6-7, 1957).
- 8-48. Edwards, R. G., Lange, K. O., A Mechanical Impedance Investigation of Human Response to Vibration, AMRL-TR-64-91, Aerospace Medical Research Labs., Wright-Patterson AFB, Ohio, Oct. 1964.
- 8-49. Ekstrom, P. J., Analysis of Pilot Loads in Flight Control Systems with Different Degrees of Automation, paper presented at the IRE International Congress on Human Factors Engineering in Electronics, Long Beach, Calif., May 3-4, 1962.
- 8-50. Ernsting, J., Respiratory Effects of Whole Body Vibration, FPRC-1164, Flying Personnel Research Committee, Air Ministry, London, 1961.
- 8-51. Ernsting, J., Respiratory Effects of Whole Body Vibration, RAF-IAM-179, Royal Air Force, Institute of Aviation Medicine, Farnborough, England, May 1961.
- 8-52. Ernsting, J., Guignard, J. C., Some Effects of Low Frequency Vibration on Vision, in Proceedings, Fifth European Congress of Aviation Medicine, London, Aug. 29- Sept. 2, 1960, Human Problems of Supersonic and Hypersonic Flight, Barbour, A. B., Whittingham, H. E., (eds.), Pergamon Press, Oxford, England, 1962, pp. 339-342.

- 8-53. Electro Scientific Industries, Inc., ESIAC Algebraic Computer Applications Bulletin, Portland, Ore., Oct. 1963.
- 8-54. Fender, D. H., Nye, P. W., On Investigation of the Mechanisms of Eye Movement Control, Kybernetik, 1: 81-88, 1961.
- 8-55. Forbes, A. R., Survey of the Effects of Buffeting and Vibration on Human Behavior, FPRC-Memo-105, Flying Personnel Research Committee, Air Ministry, London, 1959.
- 8-56. Franke, E. K., Mechanical Impedance Measurements of the Human Body Surface, AF-TR-6469, Wright-Patterson AFB, Ohio, Apr. 1951.
- 8-57. Franke, E. K., The Response of the Human Skull to Mechanical Vibrations, WADC-TR-54-24, Wright Air Development Center, Wright-Patterson AFB, Ohio, Nov. 1954.
- 8-58. Franke, E. K., Hildreth, K. M., Local Vascular Response to Vibrations, WADC-TN-56-297, Wright Air Development Center, Wright-Patterson AFB, Ohio, July 1956. (AD-97106).
- 8-59. Fraser, T. M., Hoover, G. N., Ashe, W. F., Tracking Performance during Low Frequency Vibration, Aerospace Med., 32(9): 829-835, 1961.
- 8-60. Gaeuman, J. V., Hoover, G. N., Ashe, W. F., Oxygen Consumption during Human Vibration Exposure, Aerospace Med., 33(4): 469-474, 1962.
- 8-61. Gell, C. F., Human Tolerance and Performance in High Speed Low Level (HSL) Flight, ASCC Working Party 61 - Project 61/3, Ling-Temco-Vought, Astronautics Div., Dallas, Texas. [no date]
- 8-62. Getline, G. L., Vibration Tolerance Levels in Military Aircraft, Shock and Vibration Bulletin No. 22, Supplement, Dept. of Defense, Washington, D. C., 1955.
- 8-63. von Gierke, H. E., Chief of the Biodynamics and Bionics Division, Aerospace Medical Research Labs., Wright-Patterson AFB, Ohio, personal communication, 1968.
- 8-64. von Gierke, H. E., Measurement of Acoustic Impedance and Acoustic Absorption Coefficient of the Surface of Human Body, AF-TR-6010, Wright-Patterson AFB, Ohio, Mar. 1950.

- 8-65. von Gierke, H. E., On Noise and Vibration Exposure Criteria, Arch. Environ. Health, 11: 327-339, Sept. 1965.
- 8-66. von Gierke, H. E., Response of the Body to Mechanical Forces, An Overview, in Lectures in Aerospace Medicine, Sixth Series, Feb. 6-9, 1967, School of Aerospace Medicine, Brooks AFB, Texas, pp. 325-344.
- 8-67. von Gierke, H. E., Response of the Body to Mechanical Forces - An Overview, paper presented at the Conference on Prevention of and Protection against Accidental Explosion of Munitions, Fuels and Other Hazardous Mixtures, New York, Oct. 10-13, 1966, New York Academy of Sciences, N. Y.
- 8-68. von Gierke, H. E., Transmission of Vibratory Energy through Human Body Tissue, in Medical Physics, Glasser, O., (ed.), The Yearbook Publishers, Inc., Chicago, Ill., 1960, Vol. 3, pp. 661-669.
- 8-69. von Gierke, H. E., Coermann, R. R., The Biodynamics of Human Response to Vibration and Impact, Indust. Med. Surg., 32(1): 30-32, 1963.
- 8-70. von Gierke, H. E., Hiatt, E. P., Biodynamics of Space Flight, in Progress in the Astronautical Sciences, Singer, S. F., (ed.), North-Holland Publishing Co., Amsterdam, 1962, Vol. I, Chapt. VII, pp. 343-401.
- 8-71. von Gierke, H. E., Oestreicher, H. L., Franke, E. K., et al., Physics of Vibration in Living Tissues, J. Appl. Physiol., 4(12): 886-900, June 1952.
- 8-72. Goldman, D. E., Effects of Vibration on Man, in Handbook of Noise Control, Harris, C. M., (ed.), McGraw-Hill, N. Y., 1957, Chapt. 11, pp. 1-20.
- 8-73. Goldman, D. E., von Gierke, H. E., The Effects of Shock and Vibration on Man, Lecture and Review Series No. 60-3, Naval Medical Research Institute, Bethesda, Md., Jan. 1960.
- 8-74. Goldman, D. E., Hueter, T. F., Tabular Data of the Velocity and Absorption of High Frequency Sound in Mammalian Tissues, J. Acoust. Soc. Amer., 28: 35-37, 1956.
- 8-75. Gorrill, R. B., Snyder, F. W., Preliminary Study of Aircrew Tolerance to Low Frequency Vertical Vibration, BOE-D3-1189, Boeing Co., Seattle, Wash., July 1957.

- 8-76. Grant, W. J., A Study to Correlate Flight Measured Helicopter Vibration Data and Pilot Comments, WADD-TR-61-66, Wright Air Development Division, Wright-Patterson AFB, Ohio, Aug. 1961.
- 8-77. Guignard, J. C., Defining Limits of Human Exposure to Vibration, Institute of Sound and Vibration Research, University of Southampton, paper read at the Environmental and Human Factors in Engineering Meeting, Southampton, England, Apr. 10-14, 1967.
- 8-78. Guignard, J. C., Human Response to Intense Low-Frequency Noise and Vibration, P 3/68, Preprint of paper to be published in the Institution of Mechanical Engineers Proceedings, 182 Part 1: 1967-68.
- 8-79. Guignard, J. C., The Physical Response of Seated Men to Low-Frequency Vertical Vibration, FPRC-1062, Flying Personnel Research Committee, Air Ministry, London, Apr. 1959. (AD-229171).
- 8-80. Guignard, J. C., Vibration, in A Textbook of Aviation Physiology, Gillies, J. A., (ed.), Pergamon Press, Oxford, England, 1965, Chapt. 29, pp. 813-894.
- 8-81. Guignard, J. C., Irving, A., Effects of Low Frequency Vibration on Man, Engineering (London), 190: 364-367, 1960.
- 8-82. Guignard, J. C., Irving, A., Human Frequency Response to Vibration, unpublished work read at the Space Medicine Symposium, Eleventh International Astronautical Congress, Stockholm, Sweden, Aug. 1960.
- 8-83. Guignard, J. C., Irving, A., Measurements of Eye Movements during Low Frequency Vibration, Aerospace Med., 33(10): 1230-1238, 1962.
- 8-84. Guillermin, V., Jr., Wechsberg, P., Physiological Effects of Long Term Repetitive Exposure to Mechanical Vibration, Aviation Med., 24: 208-221, 1953.
- 8-85. Harris, C. M., Crede, C. E., (eds.), Handbook of Shock and Vibration, McGraw-Hill, N. Y., 1961.
- 8-86. Harris, C. S., Chiles, W. D., Touchstone, R. M., Human Performance as a Function of Intensity of Vibration at 5 CPS, AMRL-TR-64-83, Aerospace Medical Research Labs., Wright-Patterson AFB, Ohio, Sept. 1964.

- 8-87. Harris, C. S., Shoenberger, R. W., Human Performance during Vibration, AMRL-TR-65-204, Aerospace Medical Research Labs., Wright-Patterson AFB, Ohio, Nov. 1965.
- 8-88. Holland, C. L., Jr., Cote, L. J., Bogdanoff, J. L., Some Aspects of Human Response to Random Vibration, ATAC-TR-9010 (LL 105), U. S. Army Tank Automotive Center, Warren, Mich., Aug. 1965.
- 8-89. Hoover, G. N., Ashe, W. F., Respiratory Response to Whole Body Vertical Vibration, Aerospace Med., 33: 980-984, 1962.
- 8-90. Hornick, R. J., Vibration Isolation in the Human Leg, in Human Vibration Research (A Collection of Articles sponsored by the Human Factors Society), Lippert, S., (ed.), Pergamon Press, N. Y., 1963.
- 8-91. Hornick, R. J., Boettcher, C. A., Simons, A. K., The Effect of Low Frequency, High Amplitude, Whole Body, Longitudinal and Transverse Vibration upon Human Performance, Contract No. DA-11-022-509-Ord-3300, Project No. TEI-1000, Bostrom Research Labs., Division of Bostrom Corp., Milwaukee, Wis., July 1961.
- 8-92. Hurt, G. J., Rough-air Effect on Crew Performance during a Simulated Low-Altitude High-Speed Surveillance Mission, NASA-TN-D-1924, Aug. 1963.
- 8-93. International Standard Organization, Technical Comm. ISO/TC108: Mechanical Vibration and Shock; Working Group 7: Thresholds of Mechanical Vibration and Shock Acceptable to Man, (USA participation through the American Standards Association, Sectional Committee, S3, Bioacoustics. [no date])
- 8-94. Jacklin, H. M., Liddel, G. J., Riding Comfort Analysis, Engineering Bulletin Research Series No. 44, Purdue University, Lafayette, Ind., May 1933.
- 8-95. Janeway, R. N., Passenger Vibration Limits, SAE J., 56: 48, 1949.
- 8-96. Janeway, R. N., Ride and Vibration Data, Special Publication SP-6, Society of Automotive Engineers, N. Y., 1950.
- 8-97. Jansen, G., Zur Entstehung Vegetativer Funktionsstorungen durch Larmeinwirkung, Arch. Gewerbepath. Gewerbehyg., 17: 238-261, 1959.
- 8-98. Jones, G. M., Drazin, D. H., Oscillatory Motion in Flight, FPRC-1168, Flying Personnel Research Committee, Air Ministry, London, July 1961.

- 8-99. Kanazawa, T., A Proposal for the Vibration Limits of Ships, Schiff und Hafen, H. 7: July 1961.
- 8-100. Knepton, J. C., Influence of Vibrations on Chromosomes, Aerospace Med., 37(6): 608-612, June 1966.
- 8-101. Knowles, W. B., Operator Loading Tasks, Human Factors, 5: 155-161, 1963.
- 8-102. Knowles, W. B., Rose, D. J., Manned Lunar Landing Simulation, paper presented at IRE 1963 National Winter Convention on Military Electronics, Los Angeles, Calif., Jan. 30-Feb. 1, 1963.
- 8-103. Krause, H. E., Lange, K. O., Nonlinear Behavior of Biomechanical Systems, ASME-63-WA-278, American Society of Mechanical Engineers, Winter Annual Meeting, Philadelphia, Pa., Nov. 17-22, 1963.
- 8-104. Lange, K. O., Coermann, R. R., Visual Acuity under Vibration, Human Factors, 4: 291-300, 1962.
- 8-105. Lee, R. A., Pradko, F., Analytical Analysis of Human Vibration, SAE-680091, Society of Automotive Engineers, N. Y., Automotive Engineering Congress, Detroit, Mich., Jan. 8-12, 1968.
- 8-106. Leysath, W., Weis, E. B., Jr., X-Ray Motion Monitor: Low Dosage, Wide-Variable Field Television Radiograph for Biodynamic Analysis, AMRL-TR-66-104, Aerospace Medical Research Labs., Wright-Patterson AFB, Ohio, Dec. 1966.
- 8-107. Linder, G. S., Mechanical Vibration Effects on Human Beings, Aerospace Med., 33(8): 939-950, 1962.
- 8-108. Litta-Modignani, R., Blivaiss, B. B., Magid, E. B., et al., Effects of Whole Body Vibration of Humans on Plasma and Urinary Corticosteroid Levels, Aerospace Med., 35(7): 662-667, 1964.
- 8-109. Loach, J. C., A New Method of Assessing the Riding of Vehicles and Some Results Obtained, J. Inst. Locomotive Engrs., 48: 183-240, 1958-1959.
- 8-110. Loeb, M., A Further Investigation of the Influence of Whole Body Vibration and Noise on Tremor and Visual Acuity, AMRL-165, Army Medical Research Lab., Fort Knox, Ky., 1955.

- 8-111. Loeb, M., A Preliminary Investigation of the Influence of Whole Body Vibration and Noise, AMRL-145, Army Medical Research Lab., Fort Knox, Ky., 1954.
- 8-112. Loeckle, W. E., The Physiologic Effects of Mechanical Vibration, in German Aviation in World War II, Vol. 2, 1950, pp. 716-722. (U. S. Government Printing Office, Washington, D. C.).
- 8-113. McFarland, R. A., Human Factors in Air Transportation: Occupational Health and Safety, McGraw-Hill, N. Y., 1952.
- 8-114. McFarland, R. A., Teichner, W. H., Effects of Environment on Human Performance, Chapter 10, in Human Engineering Guide to Equipment Design, Morgan, C. T., Cook, J. S., Chapanis, A., Lund, M. W., (eds.), McGraw-Hill, N. Y., 1963, Chapter 10, pp. 411-484.
- 8-115. Magid, E. B., Coermann, R. R., Human Response to Vibration, Chapter 5, in Human Factors in Technology, Bennett, E., Degan, J., Spiegel, J., (eds.), McGraw-Hill, N. Y., 1963, pp. 86-119.
- 8-116. Magid, E. B., Coermann, R. R., The Reaction of the Human Body to Extreme Vibrations, in Proceedings of the Institute of Environmental Science, National Meeting, 1960, pp. 135-153.
- 8-117. Magid, E. B., Coermann, R. R., Lowry, R. D., et al., Physiological and Mechanical Response of the Human to Longitudinal Whole Body Vibration as Determined by Subjective Response, MRL-TDR-62-66, Aerospace Medical Research Labs., Wright-Patterson AFB, Ohio, June 1962.
- 8-118. Magid, E. B., Coermann, R. R., Ziegenruecker, G.H., Human Tolerance to Whole Body Sinusoidal Vibration, Aerospace Med., 31(11): 915-924, 1960.
- 8-119. Massey, G. A., Study of Vibration Measurement by Laser Methods, NASA-CR-985, Jan. 1968.
- 8-120. Mavriplis, F., Little, G., Roberge, A., et al., Investigation of Independent Structure (Space) Crew Escape Concepts, AFFDL-TR-65-226, Air Force Flight Dynamics Lab., Wright-Patterson AFB, Ohio, Mar. 1966.
- 8-121. Megel, H., Wozniak, A. B. E., Frazier, A. B., et al., Effect of Altitude upon Tolerance of Rats to Vibration Stress, Aerospace Med., 34(4): 319-321, 1963.

- 8-122. Megel, H., Wozniak, H., Sun, L., et al., Effects on Rats of Exposure to Heat and Vibration, J. Appl. Physiol., 17(5): 759-762, 1962.
- 8-123. Mohr, G. C., von Gierke, H. E., Reactions to Mechanical Vibrations: Man, in Environmental Biology, Altman, P. L., Dittmer, D. S., (eds.), AMRL-TR-66-194, Aerospace Medical Research Labs., Wright-Patterson AFB, Ohio, Nov. 1966, pp. 217-221.
- 8-124. Mowbray, G. H., Gebhard, J. W., Sensitivity of the Skin to Changes in the Rate of Intermittent Mechanical Stimuli, TG-282, Johns Hopkins University, Applied Physics Lab., Silver Spring, Md., July 1957.
- 8-125. Mozell, M. M., White, D. C., Behavioral Effects of Whole Body Vibration, J. Aviat. Med., 29: 716-724, 1958.
- 8-126. National Aeronautics and Space Administration, Human Engineering Design Criteria Study, MSFC-STD-267A, Manned Space Flight Center, Houston, Texas, Jan. 1966. (prepared by Douglas Aircraft Co., Inc.).
- 8-127. National Aeronautics and Space Administration, Saturn V Service Arms, Preliminary Engineering Report, Complex 39, Launch Operations Center, Tech. Rep. 4-4-2-D, Washington, D. C., June 15, 1963.
- 8-128. National Aeronautics and Space Administration, A Study of the Dynamic Model Technique in the Analysis of Human Tolerance to Acceleration, NASA-TN-D-2645, Mar. 1965. (Stanley Aviation Corporation, Denver, Colo.).
- 8-129. Naval Research Lab., The Shock and Vibration Bulletin, Bull. 35, Pt. 7, Apr. 1966, Washington, D. C. (35th Symposium on Shock, Vibration and Associated Environments, New Orleans, La., Oct. 25-28, 1965).
- 8-130. Nickerson, J. L., A Study of the Effects of Anesthesia, High Oxygen and Feeding upon the Resonant Frequencies of Visceral Organs, AMRL-TDR-64-14, Aerospace Medical Research Labs., Wright-Patterson AFB, Ohio, Apr. 1964.
- 8-131. Nickerson, J. L., Coermann, R. R., Internal Body Movements Resulting from Externally Applied Sinusoidal Forces, AMRL-TR-62-81, Aerospace Medical Research Labs., Wright-Patterson AFB, Ohio, July 1962.

- 8-132. Nickerson, J. L., Drazic, M., Internal Body Movement along Three Axis Resulting from Externally Applied Sinusoidal Forces, AMRL-TR-66-102, Aerospace Medical Research Labs., Wright-Patterson AFB, Ohio, July 1966.
- 8-133. Nickerson, J. L., Drazic, M., Young's Modulus and Breaking Strength of Body Tissues, AMRL-TDR-64-23, Aerospace Medical Research Labs., Wright-Patterson AFB, Ohio, Mar. 1964.
- 8-134. Niven, J. I., Hixson, W. C., Frequency Response of the Human Semicircular Canals. I. Steady State Ocular Nystagmus Response to High Level, Sinusoidal Angular Acceleration, USN-SAM and NASA Joint Rep. 58, Naval School of Aviation Medicine, Pensacola, Fla., 1961.
- 8-135. Notess, C. B., A Triangle-Flexible Airplane, Gusts, Crew, Full Scale Division Memo No. 343, Cornell Aeronautical Lab., Inc., of Cornell University, Buffalo, N. Y., May 1963.
- 8-136. Notess, C. B., Gregory, P. C., Requirements for the Flight Control System of a Supersonic Transport, SAE-679C, Society of Automotive Engineers, paper presented at the SAE- American Society of Naval Engineers Forum, Washington, D. C., Apr. 8-11, 1963.
- 8-137. Office of the Secretary of Defense, Research and Engineering, Shock, Vibration and Associated Environments Part II, Bulletin 30, Washington, D. C., Jan. 1962. (AD-273514). (30th Symposium on Shock, Vibration, and Associated Environments, Oct. 10-12, 1961, Detroit, Mich.).
- 8-138. Parks, D. L., A Comparison of Sinusoidal and Random Vibration Effects of Human Performance, BOE-D3-3512-2, Boeing Co., Seattle, Wash., July 1961.
- 8-139. Plunkett, R., (ed.), Mechanical Impedance Methods for Mechanical Vibrations, Colloquium, presented at the American Society of Mechanical Engineers Annual Meeting, Dec. 2, 1958, N. Y.
- 8-140. Pradko, F., Lee, R. A., Vibration Comfort Criteria, Publication No. 660139, Society of Automotive Engineers, N. Y., Jan. 1966.
- 8-141. Pradko, F., Lee, R., Kaluza, V., Theory of Human Vibration Responses, Army Tank-Automotive Center, Warren, Mich., July 1967.

- 8-142. Pradko, F., Lee, R., Kaluza, V., Theory of Human Vibration Response, U. S. Army Tank Automotive Center, Warren, Mich., in Army Science Conference, U. S. Military Academy, West Point, N. Y., June 14-17, 1966, pp. 215-228. (AD-634632).
- 8-143. Pradko, F., Lee, R. A., Kaluza, V., Theory of Human Vibration Response, U. S. Army Tank-Automotive Center, Warren, Mich., ASME Paper 66-WA/BHF-15, presented at the Winter Annual Meeting and Energy Systems Exposition, Nov. 27 - Dec. 1, 1966, N. Y.
- 8-144. Pradko, F., Orr, T. R., Lee, R. A., Human Vibration Analysis, SAE-650426, Society of Automotive Engineers, N. Y. [no date]
- 8-145. Radke, A. O., Vehicle Vibration, Man's New Environment, Bostrom Research Labs., Milwaukee, Wis., ASME-Paper-No. 57-A-54, presented at the ASME Annual Meeting, N. Y., Dec. 3, 1957.
- 8-146. Rawson, H. E., Flight Simulator Study of Human Performance during Low Altitude, High-Speed Flight, TRECOM-TR-63-52, Army Transportation Research Command, Fort Eustis, Va., Nov. 1963.
- 8-147. Reiher, H., Meister, F. J., Die Empfindlichkeit des Menschen gegen Stosse, Forsch. Geb. Ingenieurwesens, 3: 177, 1932.
- 8-148. Riopelle, A. J., Hines, M., Lawrence, M., Effects of Intense Vibration, AMRL-358, U. S. Army Medical Research Labs., Fort Knox, Ky., Oct. 1958.
- 8-149. Roberts, L. B., Dines, J. H., Cardiovascular Effects of Vibration, NASA-CR-80356, Oct. 1966.
- 8-150. Roman, J. A., Effects of Severe Whole Body Vibration on Mice and Protection from Vibration Injury, WADC-TR-58-107, Wright Air Development Center, Wright-Patterson AFB, Ohio, Dec. 1957. (AD-151070).
- 8-151. Roman, J. A., Coermann, R. R., Ziegenruecker, G. J., Vibration, Buffeting and Impact Research, J. Aviat. Med., 30(2): 118-125, 1959.
- 8-152. Schaeffer, V. H., Ulmer, R. G., A Representative Bibliography of Research in Low Frequency Mechanical Vibration, AMRL-405, Army Medical Research Lab., Fort Knox, Ky., Nov. 1959.

- 8-153. Schmitz, M. A., The Effect of Low Frequency, High Amplitude Whole Body Vertical Vibration on Human Performances, Rep. 128, Bostrom Research Labs., Milwaukee, Wis., 1959.
- 8-154. Schmitz, M. A., Simons, A. K., Man's Response to Low Frequency Vibration, Rep. 125, Bostrom Research Labs., Milwaukee, Wis., Aug. 1959. (Paper proposed for ASME Annual Meeting, Atlantic City, N. J., Nov. 29-Dec. 4, 1959).
- 8-155. Schmitz, M. A., Simons, A. K., Boettcher, C. A., The Effect of Low Frequency, High Amplitude, Whole Body Vertical Vibration on Human Performance, Rep. 130, Bostrom Research Labs., Milwaukee, Wis., Jan. 1960.
- 8-156. Schwan, H. P., Biophysics of Diathermy, in Therapeutic Heat, Licht, S., (ed.), Elizabeth Licht, Publisher, New Haven, Conn., 1965, pp. 63-125.
- 8-157. Seeman, J. S., Williams, R. B., Deck Motion Simulator Program, NASA-TN-D-3594, Oct. 1966.
- 8-158. Snyder, F. W., Vibration and Vision, in Visual Capabilities in the Space Environment, Baker, C. A., Pergamon Press, N. Y., 1965, pp. 183-201.
- 8-159. Sperling, E., Betzholt, C., Contribution to the Evaluation of Comfortable Running of Railway Vehicles, Monthly Bulletin of the International Railway Congress Association (Belgium), 34: 672-678, 1957.
- 8-160. Stacy, R. W., Williams, D. T., Worden, R. E., et al., Essentials of Biological and Medical Physics, McGraw-Hill, N. Y., 1955.
- 8-161. Stevens, S. S., The Effects of Noise and Vibration on Psychomotor Efficiency, OSRD-274, National Research Council, Office of Scientific Research and Development, (Harvard Psychoacoustic Lab.), Washington, D. C., 1941.
- 8-162. Strickland, Memorandum M-P&VE-VA-139-63, Vehicle Wind-Induced Oscillations and Deflections for the Saturn V Vehicle and Preliminary Structural Loads and Deflections for the Saturn V Operations Nuclear Vehicle, June 13, 1963, NASA-George C. Marshall Space Flight Center, Huntsville, Ala.
- 8-163. Sunderhauf, A., Untersuchungen uber die Regelung der Augenbewegungen, Klin. Mbl. Augenheilk., 136: 837, 1960

- 8-164. Taub, H. A., Dial-Reading Performance as a Function of Frequency of Vibration and Head Restraint System, AMRL-TR-66-57, Aerospace Medical Research Labs., Wright-Patterson AFB, Ohio, Apr. 1966.
- 8-165. Taub, H. A., The Effects of Vibration on Dial Reading Performance, AMRL-TDR-64-70, Aerospace Medical Research Labs., Wright-Patterson AFB, Ohio, July 1964.
- 8-166. Teare, R. J., Human Hearing and Speech during Whole Body Vibration, BOE-D3-3512-3, Boeing Co., Wichita, Kan. Apr. 1963.
- 8-167. Teare, R. J., Parks, D. L., Visual Performance during Whole Body Vibration, BOE-D3-3512-4, Boeing Co., Wichita, Kan., Nov. 1963.
- 8-168. Temple, W. E., Clarke, N. P., Brinkley, J. W., et al., Man's Short-Time Tolerance to Sinusoidal Vibration, Aerospace Med., 35(10): 923-930, Oct. 1964.
- 8-169. Tinker, M. A., Effect of Vibration upon Reading, Amer. J. Psychol., 61(3): 386-390, July 1948.
- 8-170. Trincker, D., Sieber, J., Bartual, J., Schwingungs-Analyse der Vestibular, Optokinetisch und durch Elektrische Reizung Ausgelosten Augenbewegungen beim Menschen, Kybernetik, 1: 21, 1961.
- 8-171. Truxal, J. G., Electrical and Electronic Engineering Series, McGraw-Hill, N. Y., 1955.
- 8-172. Tsysar', A. I., The Combined Effect of Noise and Vibration on the Vibration Sensitivity of Adolescents, Gigiyena i Sanitariya, No. 6: 30-36, 1965.
- 8-173. Urmer, A. H., Jones, E. R., The Visual Sub-System Concept and Spacecraft Illumination, in Visual Capabilities in the Space Environment, Baker, C. A., (ed.), Pergamon Press, Oxford, England, 1965, pp. 101-109.
- 8-174. Van Deusen, B. D., A Study of the Vehicle Ride Dynamics Aspect of Ground Mobility, Vol. II. Human Response to Vehicle Vibration, Contract Rep. No. 3-114, Chrysler Corporation, Highland Park, Mich., work conducted for U. S. Army Engineer Waterways Experiment Station, Corps of Engineers, Vicksburg, Miss., Mar. 1965.

- 8-175. Verein Deutscher Ingenieure-Richtlinie 2057: Beurteilungsmasstab für die Einwirkung Mechanischer Schwingungen auf den Stehenden und Sitzenden Menschen, Dusseldorf, 1958, Revision 1961.
- 8-176. Vykukal, H. C., Dynamic Response of the Human Body to Vibration when Combined with Various Magnitudes of Linear Acceleration, in Preprints of Scientific Program, 37th Annual Scientific Meeting, Aerospace Medical Association, Las Vegas, Nev., Apr. 18-21, 1966, pp. 64-65.
- 8-177. Walsh, E. G., Role of the Vestibular Apparatus in the Perception of Motion on a Parallel Swing, J. Physiol. (London), 155: 506-513, 1961.
- 8-178. Webb, P., Impact and Vibration, in Bioastronautics Data Book, Webb, P., (ed.), NASA-SP-3006, 1964, Chapt. 5, pp. 63-85.
- 8-179. Weis, E. B., Jr., Clarke, N. P., Brinkley, J. W., et al., Mechanical Impedance as a Tool in Research on Human Response to Acceleration, Aerospace Med., 35(10): 945-950, 1964.
- 8-180. Weis, E. B., Jr., von Geirke, H. E., Clarke, N. P., Mechanical Impedance as a Tool in Biomechanics, ASME-63-WA-280, 1963, American Society of Mechanical Engineers, Winter Annual Meeting, Philadelphia, Pa., Nov. 17-22, 1963.
- 8-181. Weis, E. B., Jr., Leysath, W. Q., Horning, K. R., Development of a Pulsed X-Ray Television Fluoroscope for Biodynamic Research, AMRL-TR-66-189, Aerospace Medical Research Labs., Wright-Patterson AFB, Ohio, Mar. 1967.
- 8-182. Weis, E. B., Jr., Primiano, F. P., The Motion of the Human Center of Mass and Its Relationship to the Mechanical Impedance, AMRL-TR-65-50, Aerospace Medical Research Labs., Wright-Patterson AFB, Ohio, June 1966.
- 8-183. Weisz, A. Z., Goddard, C., Allen, R. W., Human Performance under Random and Sinusoidal Vibration, AMRL-TR-65-209, Aerospace Medical Research Labs., Wright-Patterson AFB, Ohio, Dec. 1965.
- 8-184. White, D. C., Mozell, M. M., Whole Body Oscillation; Preliminary Report, NADC-MA-LR23, Naval Air Development Center, Johnsville, Pa., Apr. 1957.

- 8-185. White, G. H., Lange, K. O., Coermann, R. R., The Effects of Simulated Buffeting on the Internal Pressure of Man, Human Factors, 4: 275-290, Apr. 1962. (Also in Vibration Research, Lippert, S., (ed.), Pergamon Press, Oxford, England, 1963).
- 8-186. White, W. J., Vision, Douglas Aircraft Corp., in Bioastronautics Data Book, NASA-SP-3006, 1964, Chapter 17, pp. 307.
- 8-187. Wittern, W. W., Ballistocardiography with Elimination of Influence of Vibration Properties of Body, Amer. Heart J., 46: 705-714, 1953.
- 8-188. Woodson, W. E., Conover, D. W., Human Engineering Guide for Equipment Designers, University of California Press, Berkeley, Calif., 1964.
- 8-189. Wulfeck, J. W., The Minimum Amplitude of Vibration Visually Perceptible as Related to Frequency of Vibration and Other Variables, Dept. of Psychology, Tufts College, Medford, Mass., 1948.
- 8-190. Yanin, L. V., (ed.), Labor Hygiene and Industrial Sanitation, A Collection of the Principal Official Publications, Part 2, AEC-TR-6467/2, U. S. Atomic Energy Commission, Washington, D. C., 1967, pp. 20-72. (Translation of Sbornik Vazhneishikh Ofitsial'nykh Materialov po Voprosam Gigieny Truda i Proizvodstvennoi Sanitarii, Yanin, L. V., (ed.), Gosudarstvennoe Izdatel'stvo Meditsinskoi Literatury, Moskva, 1962).
- 8-191. Zakharov, A. V., The Use of Ultrasonic Treatment of Vibration Sickness, FASEB-S852-4, (Federation of American Societies for Experimental Biology), TT-65-62371, Clearinghouse for Federal Scientific and Technical Information, Springfield, Va., June 1965, (Translated from Vrachebnoe Delo, No. 9: 81-84, 1964).
- 8-192. Zechman, F. W., Jr., Peck, D., Luce, E., Effect of Vertical Vibration on Respiratory Airflow and Transpulmonary Pressure, J. Appl. Physiol., 20(5): 849-854, 1965.
- 8-193. Ziegenruecker, G., Magid, E. B., Short Time Human Tolerance to Sinusoidal Vibrations, WADD-TR-59-391, Wright Air Development Division, Wright-Patterson AFB, Ohio, 1959.

9. SOUND AND NOISE

Prepared by

E. M. Roth, M. D., Lovelace Foundation
A. N. Chambers, Bellcomm, Inc.

TABLE OF CONTENTS

9.	SOUND AND NOISE	9-1
	Nomenclature and Units	9-1
	Sound Perception and Space Operations	9-3
	The Acoustic Environment	9-5
	Absolute Threshold for Intensity and Frequency	9-11
	Difference Thresholds for Intensity and Frequency	9-12
	Pitch	9-17
	Masking of Sound Signals by Noise	9-17
	Monaural (Pure Tone) Masking	9-17
	Masking by Narrow-Band Noise	9-18
	Masking by Wide-Band Noise	9-18
	Localization of Sound	9-20
	Speech	9-21
	Speech Spectra	9-21
	Intelligibility of Speech	9-24
	Articulation Index	9-24
	Conversion of AI to Speech Intelligibility Scores	9-30
	The Speech Interference Level (SIL)	9-30
	Interference with Speech by Secondary Environmental	
	Factors	9-31
	Simultaneous Speech	9-31
	Ambient Atmosphere	9-31
	Ear Plugs and Helmets	9-31
	Speaker Training	9-35
	Microphone and Electronic Processing in Speech	
	Intelligibility	9-35
	Biological Responses to Noise Exposure and Tolerance	9-40
	Physiological Effects of Noise	9-40
	Ear and Hearing	9-40
	Discomfort to the Ear	9-40

Ear Damage - Temporary and Permanent	
Hearing Loss	9-41
Non-Aural Effects	9-47
Effects of Noise on Performance	9-49
Low Frequency and Infra-audible Sound	9-52
Sonic Booms.	9-56
Ultrasound	9-56
Noise Control and Protection	9-58
Noise Reduction	9-59
Personal Protective Equipment	9-78
Analysis of Sound and Noise Factors in Astronaut	
Performance	9-81
References.	9-83

SOUND AND NOISE

Sound and noise problems arise at several points in space operations. Sound energy generated by boosters on the launch pad affects the crew on board the vehicle as well as ground personnel. Sound is also a critical factor in the design of communication systems. Excessive exposure to noise in the many facets of space operations can lead to temporary or permanent damage to the ear and interfere indirectly with the performance of critical tasks. The only novelty to the acoustic environment in space operations is limited to the role of high-energy, low-frequency (under 50 Hz) sound. Noise problems of the space age will probably be much more serious for ground support personnel than for the astronauts.

NOMENCLATURE AND UNITS

Sound is generally used to refer to any vibration or passage of zones of compression and rarefaction through the air or any other physical medium which is sufficient to stimulate the receptors of the ear or other body tissue.

Hearing refers to the response of the auditory system to sound. In order to be heard, these fluctuations must be of sufficient intensity to stimulate the cochlear receptors and they must also fall within, or contain frequency components within the spectral range of human hearing. This is commonly referred to as the audio-frequency range and may be considered to extend from about 16 to 20,000 Hz. Pressure oscillations at frequencies above this range are called ultrasonics. They cannot be heard by man but may nevertheless exert biological effects and are discussed briefly later in this section. At frequencies below 16 Hz such pressure oscillations can also exert biological effects and are, therefore, legitimately considered under the heading of "noise."

Signal is any pure tone or narrow frequency band that is used to convey information.

Speech refers to the human capability for generating meaningful sounds.

Noise refers to any undesirable sound or sound which does not convey information and can be produced by a single tone, a narrow frequency band, or a wide frequency band. All can vary in amplitude. The presence of noise with a signal tends to raise the minimum audible intensity of signal or speech above that in quiet surroundings. The phenomenon is called masking.

The basic dimensions or parameters of sound and hearing concerned with the pure tones are intensity (or amplitude), frequency, and duration as expressed in physical terms; and loudness, pitch, and duration as expressed in psychological (or subjective) terms. Other physical dimensions such as wave-form, etc., are mixtures of the basic dimensions of intensity and frequency. The existence of these two sets of measures indicates the lack

of linearity between sound and hearing. Table 9-1 summarizes these terms and units.

Table 9-1
Terms and Units Used in Audition

Physical		Psychological	
Term	Unit/Measure	Term	Unit/Measure
Frequency	Cycles per second or Hertz	Pitch	Mel
Amplitude	Decibel $L = 20 \log(p_1/p_2)$	Loudness	Phon Sone
Duration	Seconds/Minutes	Duration	Seconds/Minutes

The unit used to measure intensity, L , in physical units is the decibel (dB) and is expressed as:

$$L = 20 \log (p_1/p_0) \quad (1)$$

where p_1 = the sound pressure level (SPL) to be measured;
 p_0 = a reference pressure, usually 0.0002μ bars
or dyne/cm^2 .

The difference between two sound pressure levels is expressed as:

$$L_2 - L_1 = 20 \log (p_2/p_1) \quad (2)$$

The speed of passage of the zones of compression or rarefaction represents the velocity of sound, which is characteristic of the medium of propagation in given conditions. The separation of corresponding points in successive zones is the wavelength, which is inversely proportional to the frequency, according to the relationship:

$$\text{Wavelength } (\tau) = \frac{\text{Velocity of Sound } (V)}{\text{Frequency } (\eta)} \quad (3)$$

For example, taking the velocity of sound in air at 0°C to be 1087 ft/sec, a 100 Hz tone will generate a disturbance with a wavelength of 10.87 ft.

The measure of frequency is simply cycles per second or Hz. A range of frequency may be indicated by the octave, which is the interval between any two frequencies having a ratio of 2 to 1. The duration is expressed in seconds or minutes.

The psychological measures of loudness are the phon and sone. The phon is merely a transformation of the sone into a logarithmic scale related in specific ways to the sound pressure level of a reference sound. Sounds that have equal sone value or phon value or presumed to be equally loud, and discriminations between the loudness of sounds can be reported in either sones or phones (see Figure 9-6). The mel is used as a subjective measure of

differences in frequency between sounds. The psychological measures will be covered below.

The performance capabilities of the human ear for the reception of tones that are of primary concern here are the various thresholds for absolute and difference discrimination of intensity and frequency levels, both in quiet surroundings and with noise, as well as certain other complex discriminations. The thresholds include: (1) the absolute threshold which is the intensity at which a sound can just be discriminated from silence, (2) the difference thresholds which are the minimal differences (i. e., just noticeable differences) in intensity or frequency between signals that can be discriminated by the listener, and (3) the discomfort and damage thresholds which are the levels of intensity which, if of sufficient duration, will cause discomfort to the listener and, for higher levels, may cause pain and temporary or permanent reduction in hearing capability. The other capabilities for discrimination of sound are the localization of sound, both monaurally and binaurally, and the number of intensities or frequencies or combinations that can be discriminated both on an absolute or on a comparative basis. These capabilities are not of particular interest in space operations.

The representation of speech can be expressed as a function of time only (i. e., waveform), or as a function of frequency only (i. e., spectrum), or as a function of both time and frequency (i. e., intensity-frequency-time pattern). The capabilities of the human ear for the reception of speech of interest here have to do primarily with its intelligibility. The Articulation Index (AI) is the measure that ordinarily is used to compute the intelligibility of speech. The AI is defined as a weighted fraction representing, for a given speech channel and noise condition, the effective proportion of the normal speech signal which is available to the listener for conveying speech intelligibility (121).

Several general reviews of sound, noise, and audition are available (12, 13, 35, 65, 66, 82, 85, 155, 165). Standards for the physical measurement of sound are published (3).

SOUND PERCEPTION AND SPACE OPERATIONS

The human auditory system shown schematically in Figure 9-2 is adapted to respond to changes of air pressure at frequencies that range from about 16 to 20,000 Hz (upper limits are more variable than lower) and at root mean square pressures from about 10^{-4} to 10^3 dynes/cm². The pressure changes move the tympanic membrane (ear drum), and this motion is modulated and transmitted through the "middle ear" by the lever action of three small bones, the auditory ossicles. The motion is transmitted to the cochlea (inner ear) as mechanical vibration and displacements of a membrane (the basilar membrane). The displacements generate electrical effects in sensory cells on the membrane which, in turn, generate patterns of nerve impulses in the neural parts of the auditory system. This is the physical basis for hearing. Signal processing characteristics of the peripheral auditory system are under study (76).

Figure 9-2

Anatomy of the Auditory Mechanism

(After Jerison⁽¹⁰⁴⁾, drawing of ear adapted from Gardner⁽⁶³⁾ (original by Max Brodel); upper diagram redrawn from Morgan et al (eds.)⁽⁶⁶⁾)

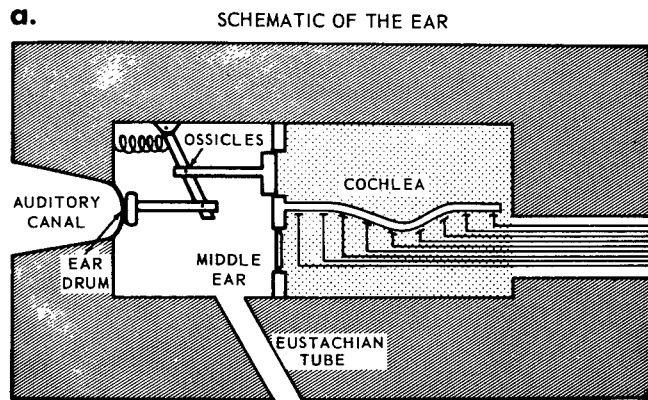


Figure a is a mechanical schematic of the major parts of the ear, showing the conversion of sound pressure waves into nerve impulses to the brain. The auditory canal acts as a resonating chamber, amplifying sound frequencies between about 2000 Hz and 5000 Hz by from 5 to 10 dB. The peak human sensitivity to such tones, as shown in Fig. 9-9a (bottom curve) is due to this amplification.

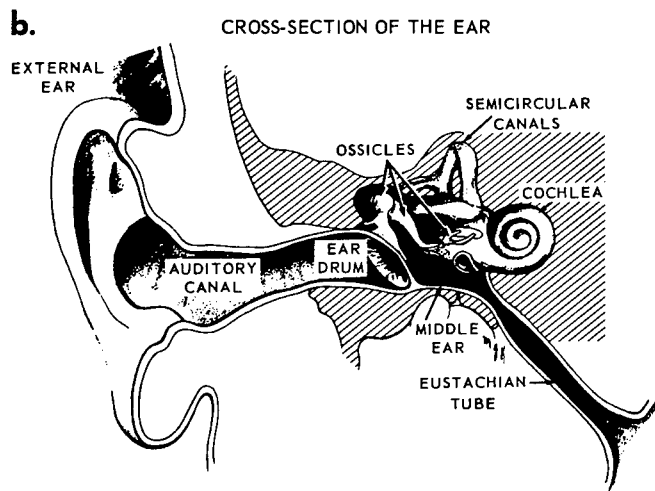
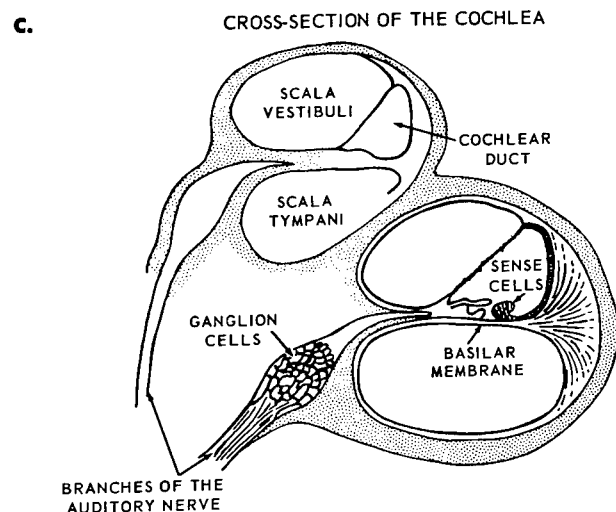


Figure b is a simplified drawing of the ear. The eardrum is a tough thin membrane that transmits pressure changes from the external ear to the middle ear bones or ossicles. The ossicles – the malleus (hammer), incus (anvil), and stapes (stirrup), weighing together about 50 mg – are the smallest bones in the human body. They transmit and transform the vibrations of the 75 mm² eardrum into vibrations of the 3 mm² oval window. The oval window is at one end of the internal ear or cochlea, a snail-shaped tube. Sound waves reaching the oval window by the motion of the stapes produce complex wave motions in an incompressible fluid in the cochlea.



The cochlea is presented in magnified section in Figure c, which shows the four large chambers filled with the fluid which carries the vibrations to the sense cells. These sense cells, about 30,000 in all, can transmit this information as patterns of excitation in the auditory nerve, and eventually as patterns of excitation in the brain.

At another level of analysis, the neural response to patterns of pressure changes may be considered as a "message" that is encoded, decoded, fed back to the sense cell, and transformed into other messages to the machinery of the body. The complete analysis of this response requires the tools of electrophysiology and experimental psychology. At very basic points in the neural network one discovers complex interactions; for example, the sensitivity of the sense cell, which might appear to depend only on its physical properties, turns out to depend also on whether or not the observer is paying attention.

The analysis of hearing can also be accomplished by treating the human observer as a black box to be analyzed in input-output terms. This is the psychophysical approach of experimental psychology. It is concerned with the relationship between an observer's behavior (including his reports about his experience) and the physically defined stimulus.

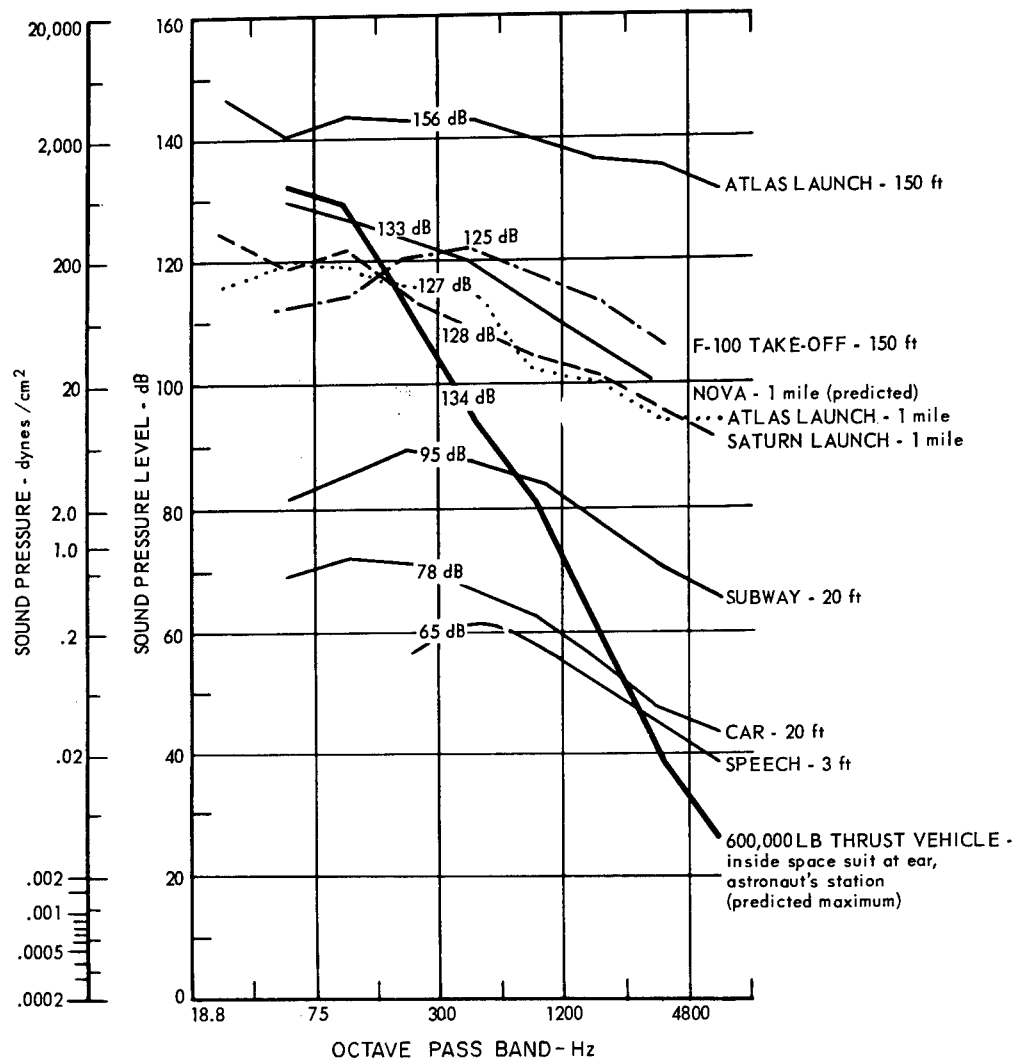
During space missions the major concerns will be to protect the auditory system from damage from excessive sound, and to provide an environment that will permit auditory communications. For these purposes the most important facts come from the "black box" approach. Data from this approach will be emphasized here, but some results of other levels of analysis of the auditory system will also be presented.

In order to facilitate evaluation of the acoustic environments in the space program, an electronic dummy or manikin which represents the average male torso from the xiphoid process upward is under development (26). Providing an exact replica of the human head, including the simulation of natural flesh impedances, the dummy features an artificial voice which produces levels up to 100 dB SPL at six inches, and a highly advanced artificial ear which measures sound pressures at the eardrum or the entrance to the ear canal. A unique hearing-mode amplifier optionally provides automatic and continuously variable loudness-contour equalization.

The Acoustic Environment

Sounds of the sort that will be and have been encountered in aerospace operations, as well as some everyday sounds, are described in Figure 9-3. The rocket noise levels in this figure were from early prediction studies and should not be used in any calculations (vide infra).

The external sound field of a space vehicle during the launch is filled principally by the jet noise of the booster rockets (32, 69, 81). Prediction of near field noise has received analytic study (150). Because of the directivity of the jet noise, the zone of maximum sound intensity produced on the ground is in the form of a ring which spreads outwards from the launching pad as the vehicle ascends in a vertical launch. Once it is well clear of the ground, the rocket emits noise as a practically spherical radiation. The noise grows fainter and changes to a muted, low-frequency rumble heard from below as the rocket gains altitude. The sound attenuation and fall in pitch with increasing distance are augmented by the rarefaction of the atmosphere and the gathering speed of the vehicle, the noise of which often appears to a listener on the ground to disappear abruptly. As the vehicle accelerates off the pad, noise



This graph shows physical descriptions of some common and uncommon sounds. Measurements with commercial sound level meters and octave band analyzers give sound pressure level (SPL) in decibels (dB) relative to the reference level, and the ordinate can serve as a nomogram for converting from one measure to the other. (The conversion is logarithmic). Overall sound pressure level of each curve is shown numerically on the curve. The source of each curve and the distance between the point of measurement and the noise source are indicated at the right. Major differences between rocket noises from either Atlas, Saturn, or (predicted) Nova and other sources are in the very high energies of the rockets at frequencies below 75 Hz. The very unusual spectrum of noise predicted for the Mercury astronauts was based on the sound shielding properties of the capsule, space suit, helmet, and earphones of the Mercury configuration. These attenuate higher frequency sound more effectively than lower frequency sound.

Figure 9-3
Rocket Noise and Everyday Sounds

(After Jerison⁽¹⁰⁴⁾, from the data of Cole et al⁽³³⁾, Hoeft and Leech⁽⁹⁷⁾,
Cole et al⁽³¹⁾, Clark⁽²⁸⁾, Bonvallet⁽¹⁴⁾, and French and Steinberg⁽⁵⁹⁾)

from this source extends far into the surrounding community but quickly diminishes within the crew compartment. With increasing airspeed, however, the crew compartment receives aerodynamic noise generated by boundary layer turbulence. This boundary layer noise reaches its maximum level as the vehicle passes through the range of maximum dynamic pressure ($\max q$) and progressively decreases thereafter. It becomes insignificant as a noise source within approximately two minutes after lift-off. Aerodynamic noise also increases in level and peaks at lower frequency as vehicles are larger. For capsules in the size range of Apollo and greater, noise at maximum dynamic pressure will peak below 100 Hz (see Figure 9-4).

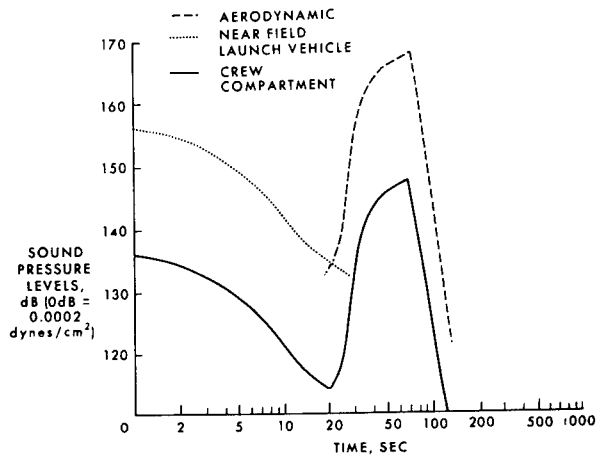
The acoustic environments generated by aerospace systems in being and under development are or will be, more severe in the low frequency range than any previously encountered (138, 150). Because there are no large rotating or reciprocating parts in a rocket engine, the noise of rocket vehicles does not normally contain discrete frequency components. However, structural resonances excited by distributed noise and transients, or by auxiliary sources such as pumps in liquid-fueled machines, can contribute to the internal sound field of rocket-propelled vehicles. The level of very low frequency noise (1-100 Hz) produced by the turbulent mixing of the booster propulsive flow with the surrounding atmosphere generally rises as the booster increases in size and thrust. It has been estimated that the very large super boosters of the future (e. g., Nova) will produce their maximum noise energy in the infrasonic range (below 20 Hz) (143). Occasionally, a periodicity can develop in primary rocket engine noise, due to unstable conditions. The directivity of rocket noise in the far field is less marked than that of turbojet engine noise, although a similar postero-lateral directivity maximum does occur.

Figure 9-4a presents a predicted (by calculation) time-history of external and crew compartment noise during a typical spacecraft launch for a system of the Apollo size (57, 106, 141, 142, 148, 149). Figure 9-4b shows the actual overall sound-pressure levels measured during the launch. The topmost curve is the external noise that has been measured on the command-module shoulder. These data were collected during Apollo boilerplate development missions and are scaled to a nominal Saturn launch-vehicle trajectory (57, 141, 142). As predicted from wind-tunnel data, the noise became significant approximately 20 seconds after lift-off, and increased to a sound pressure level of 162 decibels (106, 149). The noise remained intense throughout the high dynamic pressure region and became insignificant 100 seconds after lift-off. The curve labeled "crew station" shows the overall time-history of sound pressures expected in the crew compartment. These data were calculated by subtracting the overall noise reduction that had been measured during a command-module ground test from the external noise levels. Since the crewmen will be wearing space suits during launch, the noise reduction measured for the helmet (see Figure 9-52) and space suit was subtracted from the crew-station noise levels. The curves labeled "stomach" and "ear" represent an estimate on the crewmen's environment during launch. These data clearly demonstrate that a crewman will be exposed to overall sound-pressure levels of 95 decibels or more for about 60 seconds. For the trajectory considered, the maximum sound-pressure level will occur 60 seconds after lift-off.

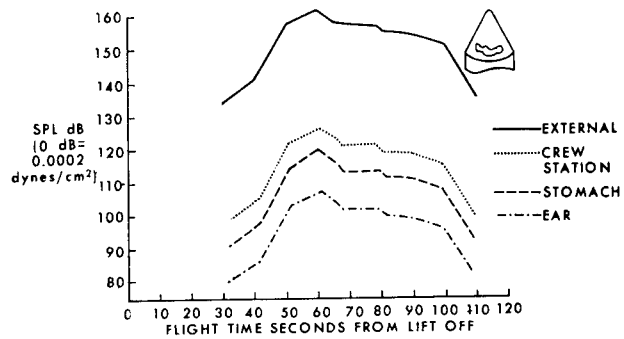
Figure 9-4

Predicted Sound Pressure Environment Inside and Outside
Apollo Spacecraft at Launch (See text)

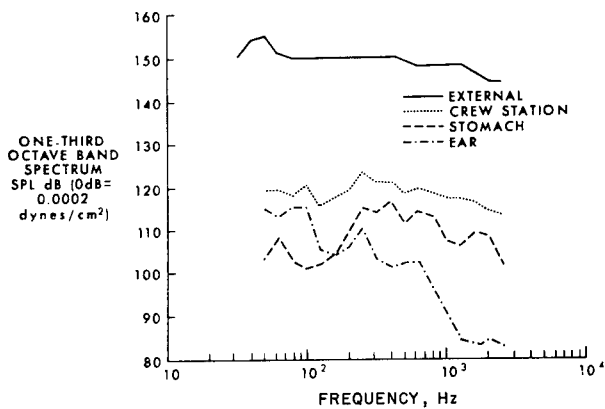
(After French⁽⁵⁷⁾)



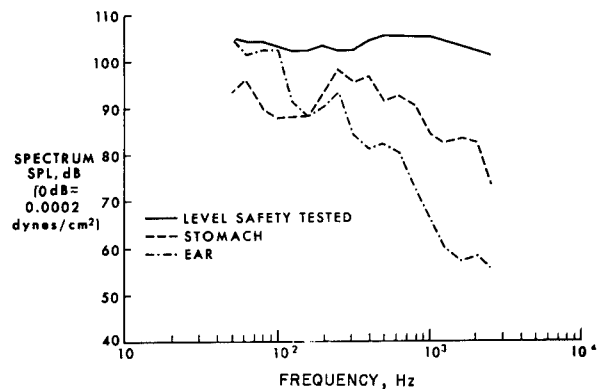
a. Predicted Overall Time History of External and Crew Compartment Noise (Calculated)



b. Overall Sound-Pressure-Level Time Histories for Apollo Mission (Measured)



c. One-Third Octave-Band Frequency Spectra for Apollo Mission at T + 60 Seconds (Measured)



d. Spectrum Sound Pressure Levels for Apollo Mission at T + 60 Seconds (Measured)

Figure 9-4c presents a one-third octave-band frequency analysis for this flight time. The curves are labeled to correspond with the overall levels shown in Figure 9-4b. The external noise levels were recorded in flight, reduced to one-third octave-band levels, and corrected to a nominal trajectory. The crew-station noise levels were calculated by subtracting the noise reduction of the command module at each one-third octave-band from the external noise levels. The spectra for the stomach and ear were obtained by subtracting the one-third octave-band noise reduction measured for the suit and helmet from the crew-station levels. These data show that the external noise spectrum is flat with a maximum of 155 decibels around 50 Hz. After the noise has been transmitted through the spacecraft, the spectrum is still reasonably flat, but the maximum sound-pressure level of 123 decibels occurs at 250 Hz. The spectrum on the stomach has the highest sound-pressure levels in the 250 to 800 Hz range, and the maximum of 116 decibels occurs at 400 Hz. The spectrum at the ear is unique in that the maximum noise level of 115 decibels occurs at 50 Hz and the sound-pressure level decreases as the frequency increases. It is also important to notice that the overall sound-pressure level calculated by using the measured overall noise reduction. The difference is due to the dynamic response of the helmet at frequencies below 200 Hz (see Figure 9-52).

The one-third octave-band spectra at the stomach and ear, shown in Figure 9-4c were converted to spectrum levels or sound-pressure level per cycle and presented in Figure 9-4d. The curve marked "level safely tested" is the sound-pressure level per cycle tested during the program where adverse physiological effects and performance decrements were not reported for a 1-minute exposure. (See below under discussion of Figure 9-36).

During reentry of a capsule, boundary-layer turbulence again generates an internal sound field containing broadband noise of high intensity (69). The sound pressure levels reached are comparable with those produced during the maximum dynamic pressure period at launch but high intensities may be maintained for longer periods during reentry. Current, overall, ambient noise level for the Apollo spacecraft is estimated at 87 dB. This level is relatively consistent throughout all phases of the mission with the exception of the launch phase.

During captive firing of rocket engines in ground installations, continuous broadband noise is emitted for as long as the test is continued. The spatial distribution of this noise in the surrounding field depends upon the factors affecting the propagation of sound through the air and the directivity of the source. Exhaust blast deflectors and diffusers are commonly used in captive firing installations and can modify considerably the basic directivity (30, 151). A proportion of the noise from ground firing can be propagated for considerable distances as ground-borne vibration, which can be disturbing both mechanically and as the source of re-radiated acoustic noise.

Figure 9-5 represents a summary of the frequency environments experienced in operational situations as well as in test facilities for low frequency noise.

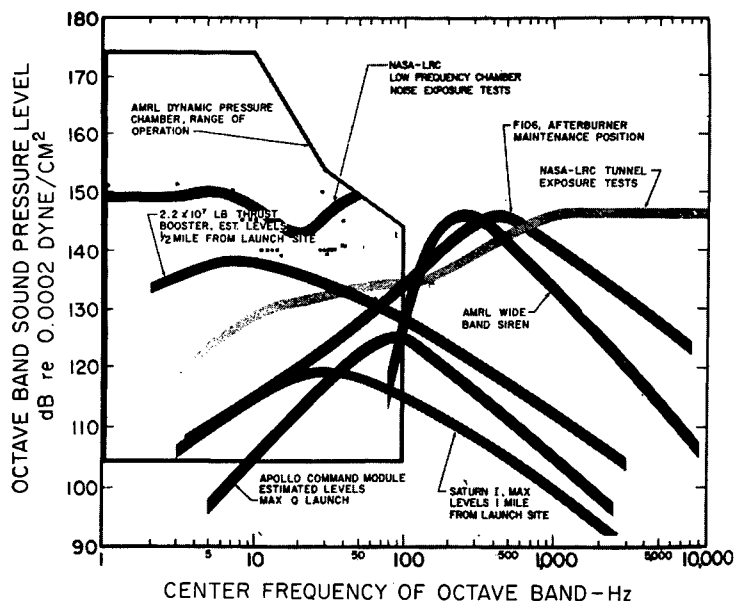


Figure 9-5

Low Frequency Noise Experiments Used in Human Exposure Tests

In a series of tests, a limited number of healthy human subjects safely tolerated, without gross performance decrements, the sound spectra indicated. The dots indicate the individual exposures to the NASA-Langley Research Center Low-Frequency Chamber. The measured spectrum for a Saturn booster and the estimated spectrum for a 2.2×10^7 lb thrust booster are to indicate the shift of the noise spectrum to lower frequencies with increasing thrust.

(After von Gierke⁽⁶⁸⁾, adapted from Mohr et al (138))

Factors affecting the propagation of sound in air have been studied (28, 82, 84, 169, 170). Theoretically, the spherical radiation of sound waves from a point source obeys an inverse square law of intensity, so that the sound pressure amplitude is inversely proportional to distance from the source. In other words, the SPL drops by 6 dB for each doubling of distance (the divergence decrease). An additional attenuation of sound in air is brought about by molecular damping processes, the effect of which is strongest at high frequencies. In practice, the pattern of propagation of sound is further complicated by atmospheric inhomogeneity and movement, as well as by obstacles in the sound field.

The attenuation of sound in air takes place through energy-dissipative processes (viscous, thermal and relaxational) occurring both within and between the molecules of the medium. An important part of the acoustical damping in air is due to a relaxation effect between the vibrational states of the oxygen molecule. This effect is strongly enhanced by the presence of water molecules, with the result that sound attenuation in the atmosphere is increased when the humidity is high (84). Fine particulate moisture (fog, drizzle, light snow) produces a negligible attenuation, however, and indeed a paradoxical increase in noise propagation can be observed in these conditions. This is attributable to other factors, present at the same time, which encourage the propagation of sound, such as thermal homogeneity and the absence of wind.

The velocity of sound, c , depends upon the air temperature, according to the formula:

$$c = c_0 (T/T_0)^{1/2} \quad (4)$$

in which T is the absolute temperature of the air under consideration. Because the air temperature normally decreases with altitude, sound radiated from a source near the ground is refracted upwards. A temperature inversion produces the opposite effect and can give rise to a paradoxical increase in noise with increased distance from the source.

When a wind is blowing, the pattern of sound propagation is distorted. A sound shadow is created upwind from the sources. In moderate wind, SPL differences of as much as 30 dB can be measured between upwind and downwind positions at the same distance from the source of sound. Sound is also reflected and diffracted by obstacles in the sound field (169). The scattering of sound by buildings, hillocks, and other surface features reduced the overall propagation of noise into the far field. Roughness of the ground and vegetation also produce losses by the absorption and scattering of sound waves passing over the terrain (208). Considerable losses by scattering can result from meteorological turbulence (99).

Data are available on levels, spectra, and acceptability of noise from ground vehicles (14, 24, 152). It is clear from the above discussion that most of the inflight problems associated with the ear and hearing will probably be concerned with the efficiency of the auditory system for communications work. The following discussion is intended to summarize present knowledge of the biological aspects of auditory communication.

Absolute Threshold for Intensity and Frequency

The auditory response to the frequency of pure tones is commonly accepted as falling between about 16 and 20,000 Hz as indicated in Figure 9-6.

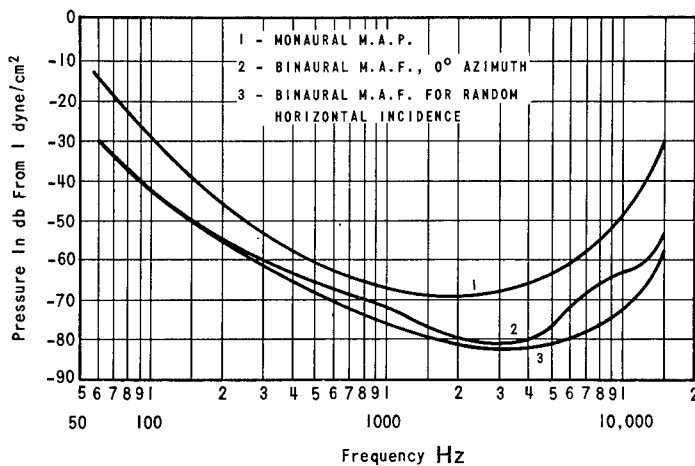


Figure 9-6

Absolute Thresholds for Reception of Signals

M.A.P. stands for "Minimum Audible Pressure".

M.A.F. stands for "Minimum Audible Field".

(After Sivian and White (175))

The limits for response to intensity vary as a function of frequency. They are often different for different individuals and the threshold may vary from time to time in the same individual (86). The limits for response to intensity extend from the minimum level (i.e., absolute threshold) at which a sound can be heard to intensities where feeling and discomfort begin. The minimum intensities to which the ear will respond vary as much as 80 dB with the greatest sensitivity between 2000 and 4000 Hz. Individual differences in absolute thresholds vary as much as 20 dB and can vary as much as 5 dB within a short period of time.

The audibility of a signal depends on the duration since the response of the ear is not instantaneous. For pure tones, about 200-300 msec. are required for buildup and approximately 140 msec. to decay. Thus, tones of

less than 200-500 msec. do not sound as loud and are not as audible in noise background as sounds of longer duration.

Difference Thresholds for Intensity and Frequency

Detectability of just-noticeable-differences (JND'S) in intensity is dependent on both intensity and frequency (87). At sensation levels of 20 decibels or less, the intensity increment that is just noticeable as a loudness change is comparatively large, being on the order of 2 to 6 decibels, depending on the frequency. Above a sensation level of about 20 decibels an intensity increment of about 1/2 to 1 decibel is detectable, except at the frequency extremes, where the increment is somewhat larger. Within the frequency limits of about 500 to 1,000 Hz, just-noticeable-differences of intensity are smallest. The curves for difference thresholds are presented in Figure 9-7.

The frequency difference required to produce a just-noticeable-difference in pitch varies essentially according to frequency at low frequencies. Smaller differences in frequency are detected at high than at low frequencies. This just-noticeable-difference of pitch is not wholly dependent on frequency in that the sensation level is a contributing factor. Below a sensation level of 20 dB, the ear rapidly loses its ability to detect frequency changes; above this level, the ear will fairly consistently detect a change of 3 Hz in a tone of 1000 Hz or less. Beyond this frequency, the just-noticeable-difference remains fairly constant at 0.3 of one percent of the tone's frequency.

The difference thresholds for frequency are presented in Figure 9-8. Carrying capacity of the auditory system for pure tones is such that about seven distinct pitches and seven distinct loudnesses, or about 49 pure tones all told, can be identified on an absolute basis. Figure 9-9 presents equal-loudness contours for pure tones (66,104). Figure a is in a free field, and figure b is with headphones. The numbers on the curves are their loudness levels in phons. The phon-unit was developed to identify tones according to their loudness as perceived by people rather than their sound energy as sensed by instruments. It was determined by matching the loudness of each tone with a 1000 Hz tone. The loudness of the tone is defined as the same number of phons as the number of dB SPL (sound pressure level) of the 1000 Hz tone that matched it. The bottom curve in figure a is the pure tone threshold for hearing which varies with age (190).

As an example, an engineer is required to construct a two-tone signal of constant loudness. If the tones are 100 Hz and 500 Hz in a free field and the higher tone is set at 60 dB, this tone will have a loudness of about 64 phons. A 64-phon 100 Hz tone in a free field, according to figure a would have to be at an SPL of about 70 dB. The two tones should therefore be 70 and 60 dB, respectively, to be perceived as equally loud.

To compare tones at different loudnesses, it is necessary to state the relationships of the loudnesses, and this can be done with the sone-scale. Sones are related to phons logarithmically and the conversion can be accomplished with

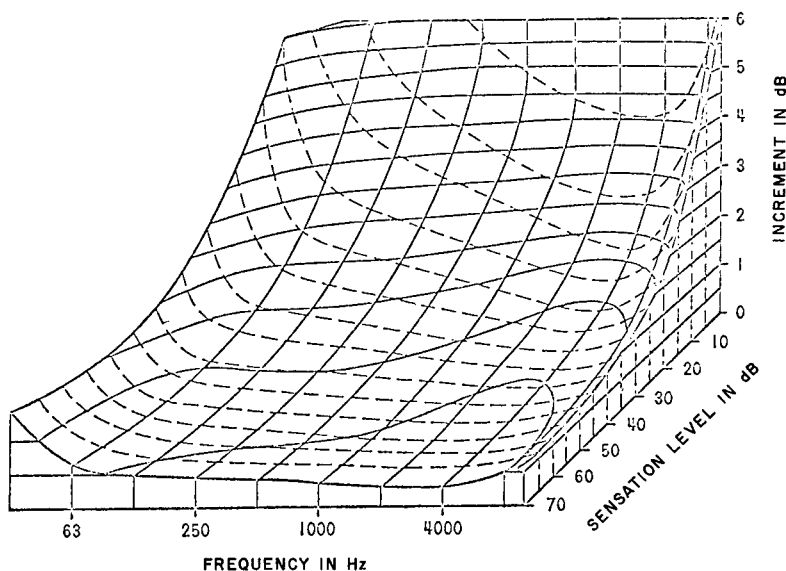


Figure 9-7

Difference Thresholds for Intensities of Signals

Three-dimensional surface showing the differential intensity thresholds as a function of the frequency and the intensity of the standard tone. The threshold is represented as the difference in decibels between the standard intensity and the standard plus the increment. Following the contour lines from 1000 Hz and 30 dB, one sees, by way of illustration, that the intensity of a 1000-Hz tone must be raised 1.0 dB from a level of 30 dB above threshold before the average observer can detect the change. If one starts with levels 60 or 70 dB above threshold, he finds that an increment of less than 0.5 dB is detectable.

(After Stevens⁽¹⁸³⁾, from the data of Riesz⁽¹⁶¹⁾)

Figure 9-8

Difference Thresholds for Frequency of Signals

Three-dimensional surface showing the differential frequency threshold as a function of the frequency and the intensity of the standard tone. Frequency discrimination is poor at intensity levels near the absolute threshold (rear part of figure) and at high frequencies (right-hand part of figure). At sensation levels above 30 dB and at frequencies below 1000 Hz, however, a change of about 3 Hz can be detected.

(After Stevens⁽¹⁸³⁾, from the data of Shower and Biddulph⁽¹⁷⁶⁾)

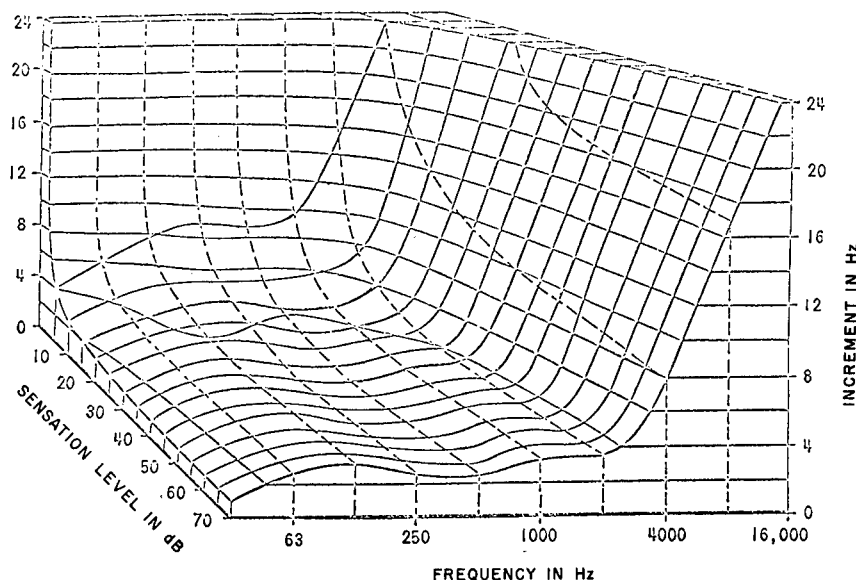
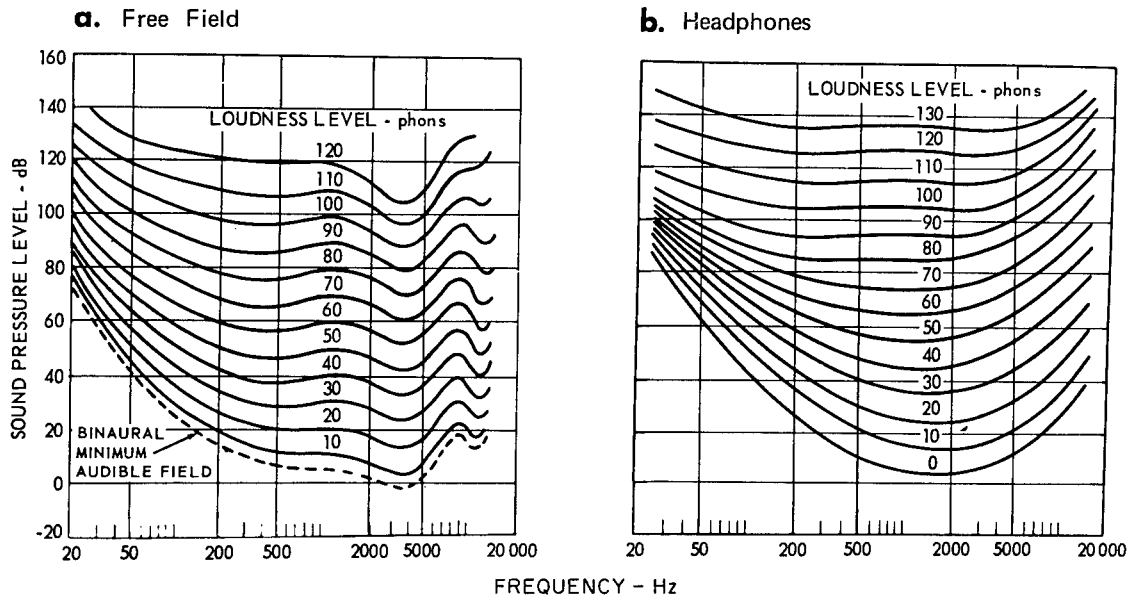


Figure 9-9
Sound Perception of Pure Tones
(After Gales et al⁽⁶⁶⁾)



the nomogram in Figure 9-10a. By international agreement, 1 sone has been defined as the relative loudness of a sound whose equivalent loudness is 40 phons. In exponential form:

$$\text{Number of sones} = 2^{(p-40)/10} \quad (5)$$

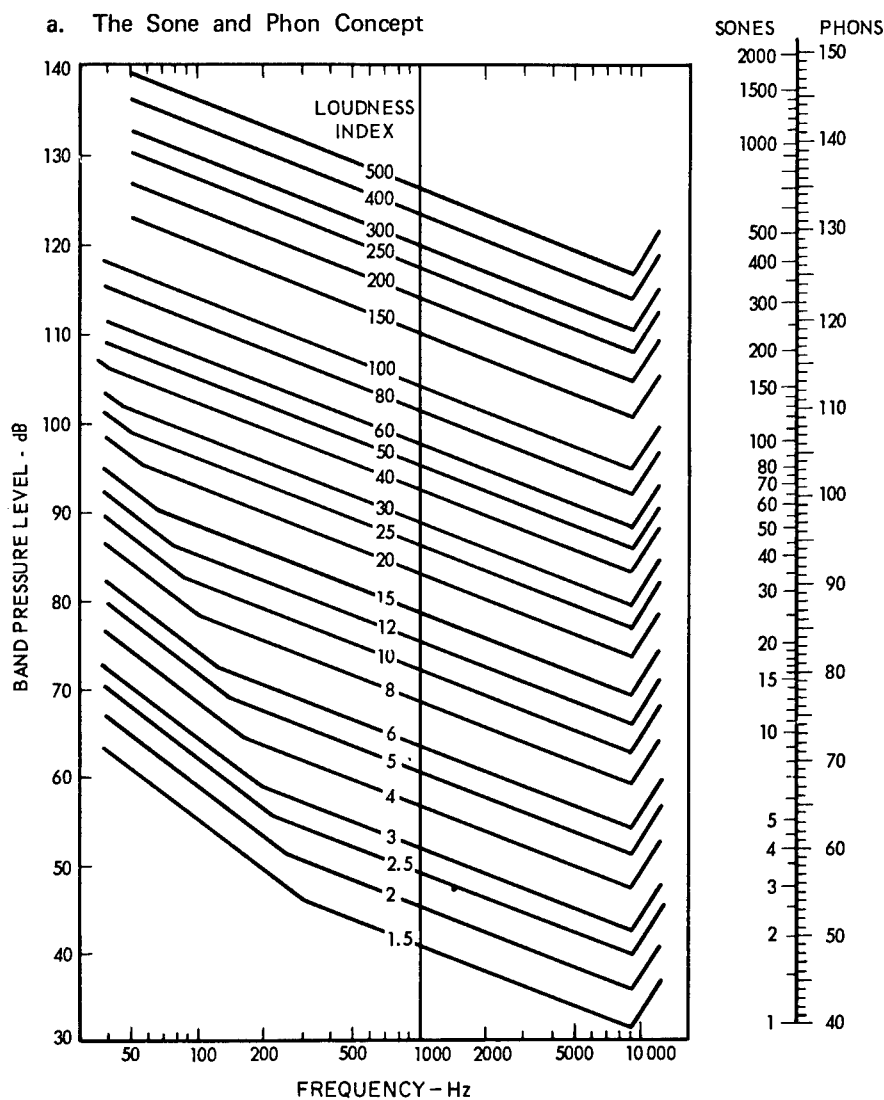
where p is the number of phons. The sone scale permits one to compare directly the intensities of experience. That is the purpose of this scale. The decibel equivalent or phon scale does not permit such a comparison. The resulting relationship between phons and sones is illustrated in Table 9-10b which also indicates some representative loudnesses of familiar noises.

One can illustrate the use of the sone concept by the following. Example: To double the loudness of the tones in the preceding example, 64 phons first are converted to sones. The nomogram in Figure 9-10a shows that 64 phons = 5.2 sones. Twice the loudness would be equal to 10.4 sones. This in turn is seen from the nomogram to be 73 phons. From figure a, one can determine that the new signal would have the 100 Hz tone at about 80 dB and the 500 Hz tone at about 68 dB by finding the SPL's of tones at these frequencies that lie slightly above the 70-phon curve.

To illustrate the calculation of loudness with the chart and formula of Figure 9-10a, the data on sound pressure levels at an astronaut's ear and from a Century series fighter, as presented in Figure 9-3, are analyzed by the steps laid out in Table 9-10c. Octave bands are shown in column (1), and the geometric mean frequency of each band in column (2). Sound pressure level in decibels for each band, as estimated from Figure 9-3, is shown in column (3). The formula shown under Figure 9-6 for adding sones takes $F = 0.3$ because the data are in octave bands. The formula of Figure 9-10a is as follows:

Figure 9-10

Perception of Sound Loudness



$$S_t = S_m + F(\Sigma S - S_m)$$

This figure and the accompanying equation are used to estimate how loud a complex sound such as rocket noise will seem to an observer. To use the figure, one must have physical measures of the noise from a sound level meter and sound analyzer or one must be able to predict values for those measures. The figure gives the loudness index for bands of noise at the indicated geometric mean frequencies and band pressure level (total SPL for the band); for example, a band with a geometric mean at 200 Hz and SPL of 100 dB will have a loudness index of about 40. When the results of a particular sound analysis are available, the total loudness (subjective "intensity") of the sound can be calculated with the equation.

In the equation, S_t is the total loudness in sones, S_m is the highest loudness index measured, ΣS is the sum of the loudness indices for all of the bands of noise. The Factor, F , is 0.3 if the analysis is by octave bands, 0.2 for half-octave bands, and 0.15 for third-octave bands. The nomogram at the right of the figure permits conversion of sones to phons, which are related to the familiar decibel scale of sound pressure level.

(After Jerison⁽¹⁰⁴⁾, from Stevens⁽¹⁸⁴⁾)

Figure 9-10 (continued)

b. Representative Levels of Equivalent and Relative Loudness

Equivalent loudness (phons)*	Relative loudness (sones)	Example of noise at particular level	Facility of conversation
140	—	Large Rocket Engine at 100 yd 50 h.p. Victory Siren at 100 ft Approximate Threshold of Aural Pain	
130	—	Jet Engine at 50 ft	
120	256	Carrier Island during Jet Operations Close to Rivetter at Work Boiler Shop, Weaving Shed	Impossible
110	128	Near Orchestra in Loud Symphonic Finale Loud Motor Horn at 20 ft	
100	64	Light Aircraft Engine at 50 ft Inside Propeller-driven Airliner	By shouting
90	32	Inside Underground Train at Speed Busy Motor Traffic passing at 20 ft	
80	16	Cocktail Party Moderately Loud TV or Radio playing Indoors	By raised voice
70	8	Normal Conversational Speech at 3 ft Inside Railway Sleeping Car	Normal
60	4	Inside Quiet Saloon Motor-car	
50	2	Quiet Office or City Street at Night (Ambient)	
40	1	Average Level in Quiet Residence (Children Asleep)	
30	0.5	Broadcasting Studio (Ambient) Quiet Whisper	By whispering
20	0.25	Quiet Countryside at Night (Ambient)	
10	—	Rustling Leaves	
0	—	Silence (Approximate Threshold of Hearing)	

* Numerically equal to dB re 0.0002 b at 1000 Hz only.

(After Guignard⁽⁸²⁾, Crown copyright)

c. Example of Band Analysis of Loudness Perception

(1) Octave Band	(2) Geometric mean frequency	(3) (4) Mercury Astronaut's Ear (estimated)		(5) (6) Century Fighter 150 feet overhead	
		Band Pressure	Loudness Index	Band Pressure	Loudness Index
37.5-75	53	133	300	113	70
75-150	106	130	300	115	100
150-300	212	113	120	120	180
300-600	425	95	37	123	275
600-1200	850	82	18	118	240
1200-2400	1700	60	5	113	200
2400-4800	3400	40	2	108	175
4800-9600	6800	26	0	---	---
Σ S (sum of loudness indices)			782	1240	

(After Jerison⁽¹⁰⁴⁾)

For Astronaut: $S_t = 300 + [0.3 (782-300)] = 445 \text{ sones} = 128 \text{ phons}$
by nomogram 9-10a.

For Century Fighter: $S_t = 275 + [0.03 (1240-275)] = 565 \text{ sones} = 131 \text{ phons}$
by nomogram 9-10a.

Since 445 sones is about 80 percent of 565 sones, the apparent loudness of the Mercury rockets in the capsule at lift-off should be about 80 percent of the loudness in the cabin of a Century fighter flying overhead at 150 feet under full military power.

Pitch

Pitch, like loudness, is also a subjective attribute of sound. It is determined primarily by frequency, although it is affected somewhat by loudness, spectrum, etc. (123, 147). A scale for the quantitative rating of the magnitude of pitch in a manner similar to that described above for loudness has been established (66). The unit of this scale is the mel, which is defined as the pitch of a 1,000 Hz pure tone at a level 40 dB above absolute threshold.

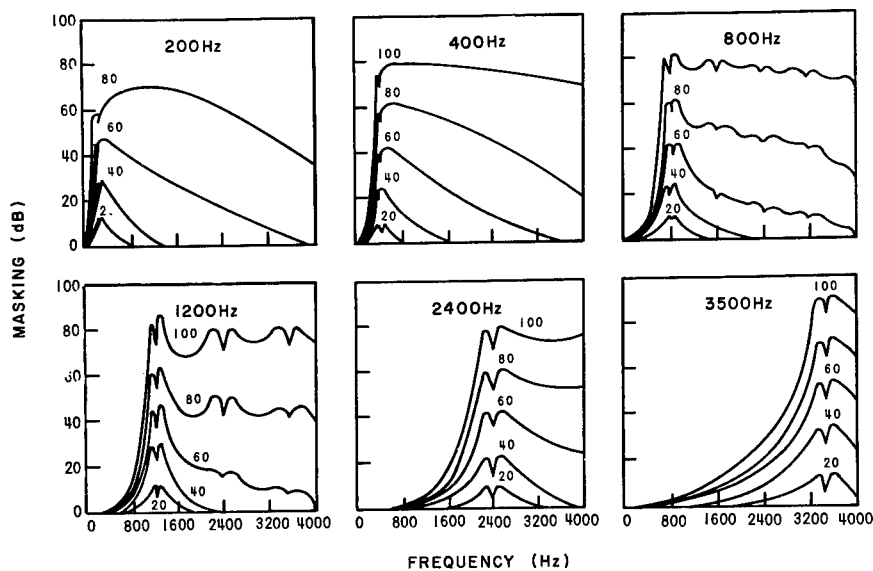
Masking of Sound Signals by Noise

Because few environments are free of noise, noise is usually a limiting factor in a signal-processing system. Design of a signal-processing system must separate signal from noise. Noise mixed with a signal tends to raise the threshold for hearing that signal above the threshold in quiet, or absolute threshold. This phenomenon is called masking, and the elevated threshold is known as the masked threshold.

Monaural (Pure Tone) Masking

The masking of a signal, basically a pure tone, by another pure tone must be determined experimentally. The masking thresholds of signals for various representative frequencies and amplitudes as they are affected by pure tones of various frequencies and amplitudes are depicted in Figure 9-11. These are based on monaural reception of signals and noise. It will be noted from these curves that the masking effect is greatest when the signal and noise are of similar frequencies and is greater for noise frequencies below the signal frequency than for noises above the signal frequency. At relatively high intensities, however, the masked threshold of signals that are some integral multiple of the masking tone is raised more than the threshold of those signals having no harmonic relationship to the masking tone.

In interaural masking (i. e., when the signal is fed into one ear and the noise into the other) no masking occurs when the noise SPL is relatively low (below 40 or 50 dB). When the noise SPL is above 50 dB, the sound is con-



Masking as a function of frequency for masking by pure tones of various frequencies and levels. Number at top of each graph is frequency of masking tone. Number on each curve is level above threshold of masking tone.

Figure 9-11

Masking of a Signal by Pure Tones
(After Wegel and Lane⁽²⁰⁶⁾)

ducted through the bone of the skull to the opposite ear to produce masking as in the monaural case.

Masking by Narrow-Band Noise

The masking of a signal by narrow-band noise is similar to those for pure-tone masking except that the sharp dips caused by harmonics are absent. Figure 9-12 shows representative curves for monaural reception.

Masking by Wide-Band Noise

Figure 9-13 shows the masked thresholds for a pure tone masked by wide-band noise of uniform spectrum (i. e., white noise). The amount of masking of a signal by wide-band noise can be predicted if the spectrum level of the noise is known at the frequency of the signal tone. In making such a prediction it is assumed that the masking is caused by noise frequencies which lie in a band near that of the signal. When used to predict masking, this critical band-width is so defined that the SPL of the noise in the critical band is just equal to the SPL of the signal at its masked threshold. Figure 9-14 shows the generally accepted values of critical band-width as function of frequency.

The prediction of masking threshold at a given signal frequency (f) may be determined by measuring the spectrum level of the wide-band noise at the frequency of the signal. Correct this measured level to the level in the

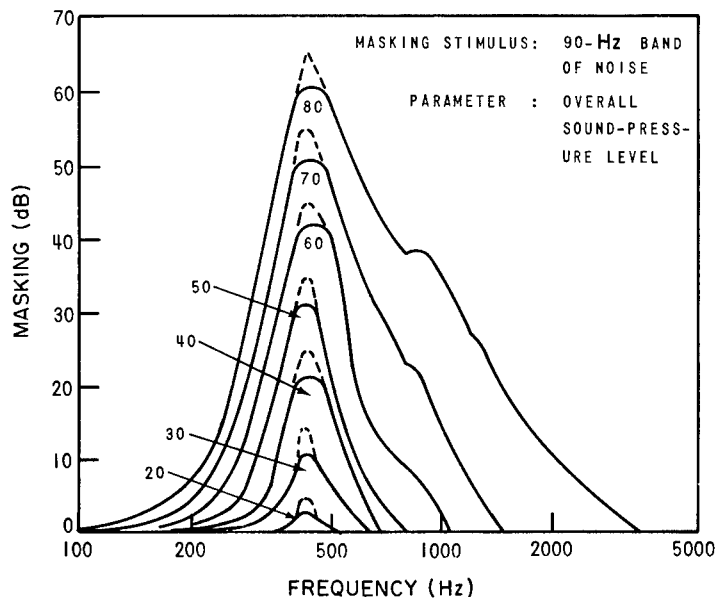
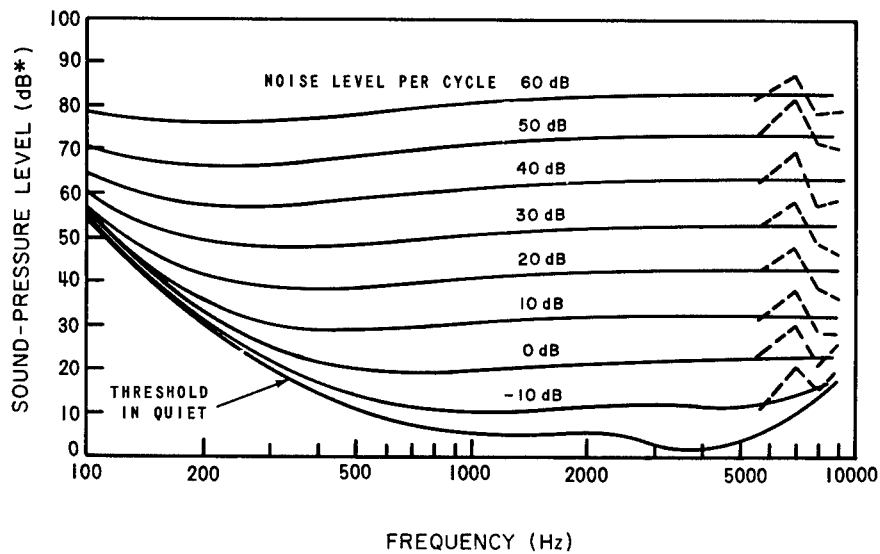


Figure 9-12

Masking of a Signal by Narrow-Band Noise
(After Egan and Hake⁽⁴⁶⁾)



* Re 0.0002 μ BAR

Figure 9-13

Masking of a Signal by Wide-Band Noise
(After Hawkins and Stevens⁽⁸⁹⁾)

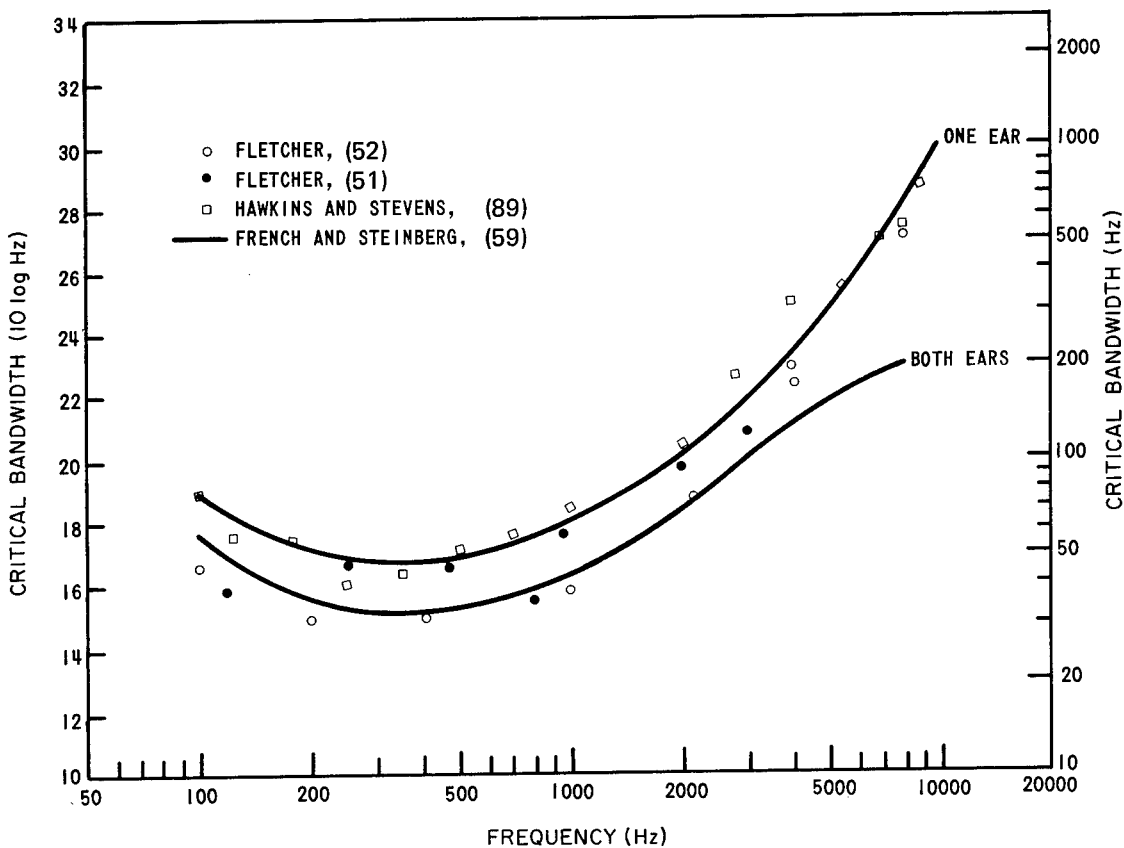


Figure 9-14
Critical Masking Bandwidth as a Function of Frequency
(After Gales et al⁽⁶⁶⁾)

critical band at f by adding the 10 log of the critical band-width. This correction can be read directly from the left-hand ordinate in Figure 9-14. The corrected value is the masked threshold at f if the value is more than 20 dB above the absolute threshold at f . If it is less than 20 dB, a correction must be made for non-linearity in the masking versus noise level function near the absolute threshold. To correct for masked threshold below 20 dB absolute threshold, use the curve in Figure 9-15.

The effect of masking on evaluation of loudness function has been studied recently (92). Techniques for the improvement of signal to noise ratio by altering the signal or by filtration of masking noise are available (66).

Localization of Sound

Localization of sound appears not to be a significant problem in space operations. A Naval study has been directed to this subject (8).

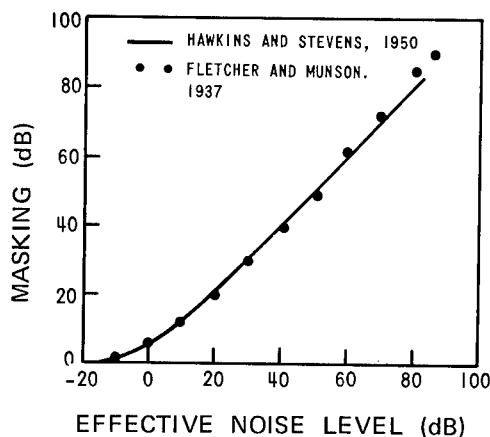


Figure 9-15

Masking as a Function of Noise Level
in the Critical Band

(After Gales et al⁽⁶⁶⁾)

SPEECH

The vibration of the vocal cords or resonance of the air column in the mouth and nasal passages determines the nature of speech. Speech patterns may be quantitated by recording instantaneous speech pressure with time or by determining the rms speech pressure at a given frequency band in a stated time interval. Much of the material in this section is taken directly from a fine review of speech physiology (120). Data are currently being gathered on typical astronaut speech patterns (188,189); on the characterization of speech sources in terms of genetic operating characteristics (178); and on the words used most frequently in aerospace communications (49).

Speech Spectra

When filters one-octave wide are used, the function relating the spectral coefficients to the center or boundary frequencies of the octave is called the octave-band spectrum. It often simplifies a calculation, dimensionally, to divide the rms pressure in each band by the width of the band in cycles per second (Hz). When that quotient is translated into decibels, the result is called the spectrum level. An overall level of speech covers the spectrum across the audio-frequency range. Typical octave-band spectra of adult males are available (66). The overall speech level is 65 dB relative to 0.0002 μ bar, a representative level for male speakers using a moderate level of vocal effort. The spectrum produced by female speakers is roughly similar in shape, but the overall level of female speech is, on the average, 2 or 3 dB lower.

For some purposes it is important to examine changes of speech pressure with time while simultaneously retaining the analysis of the speech wave into several or many bands of frequency. One way of accomplishing this is to divide the speech signal into a number of frequency bands (by means of band-pass filters) and then to divide the component signals - the individual signals in the several bands - into segments of 1/8-sec duration.

Measurements have been made in the manner described above with octave-band and half-octave-band filters. The maximum instantaneous pressure in each 1/8-sec segment, and, also, the rms pressure in each 1/8-sec segment, are determined. Spectrum levels are derived by dividing the squares of the instantaneous pressure and the rms pressure by the filter band-width and then converting the quotients into decibels.

Four curves relating sound-pressure level to frequency are shown in Figure 9-16. Curve A shows, for each frequency band of 1 Hz width, the

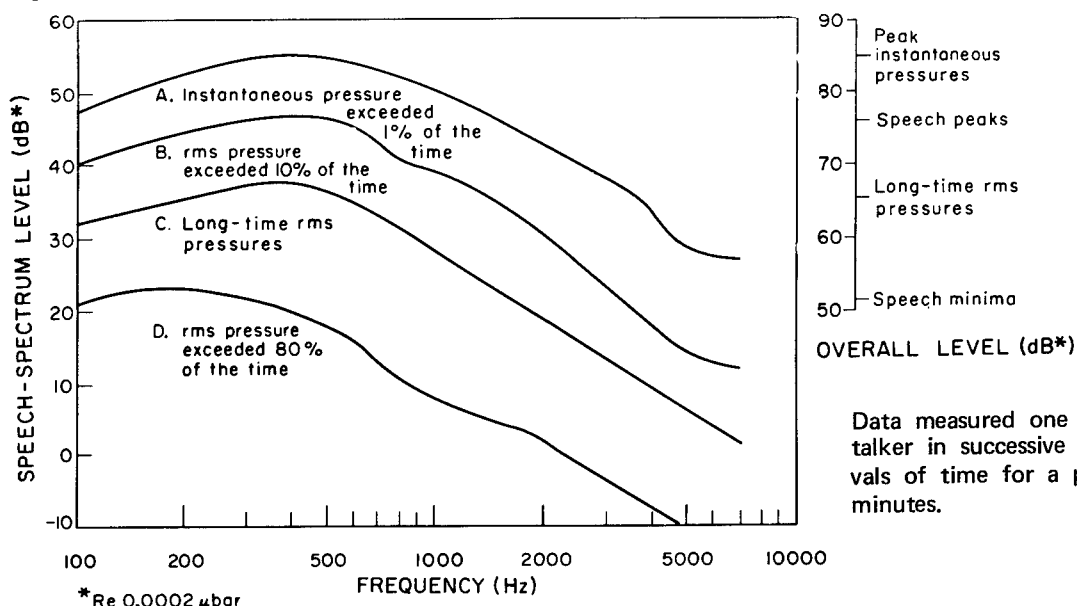


Figure 9-16

Spectrum Level of Instantaneous and RMS Pressures of Speech Uttered
at a Conversational Level of Effort

(After Gales et al⁽⁶⁶⁾, from the data of Dunn and White⁽⁴³⁾)

instantaneous pressure that was exceeded in only 1 percent of the 1/8-sec intervals. This curve is, in a sense, a "peak-instantaneous-pressure" curve. Curve B shows, for each frequency band, the root-mean-square pressure that was exceeded in only 10 percent of the 1/8-sec intervals. One can call this one the curve of "speech peaks." Curve C is the long-time-rms pressure. Curve D shows, for each frequency band, the rms pressure that was exceeded in 80 percent of the 1/8-sec intervals. Inasmuch as about one-fifth of ordinary conversational speech is dead time, this lowermost curve represents, in a sense, the rms pressure of the weakest sounds. One can refer to this curve as the "speech minima" curve. At the right-hand side of the graph are represented the corresponding overall levels - the values for unanalyzed, unfiltered speech.

If the speech is too soft, it will be masked by noise in the communication system. If it is too loud, it will overload the system. Dynamic range is the difference, in decibels, between the pressure level at which overload occurs (according to some overload criterion) and the pressure level of the noise in the system. Obviously, the dynamic range is not, in general, the same for all points in the communication system. Usually, it is the dynamic range at the listener's ear that is most important.

To determine the dynamic range required of a communication system, the engineer must take into account the variations in pressure level from speech sound to speech sound, condition to condition, and talker to talker.

Several key speech ranges have been noted from the weakest to the strongest (66):

- The range of fundamental speech-sound level is 0-28.2 dB.
- The range (difference) from speech minima with minimum normal vocal effort to peak instantaneous pressures with maximum normal effort is 60 dB (39-99).
- The range (difference) from speech minima to peak instantaneous pressures is about 40 dB for a given level of vocal effort.
- The range of variations of talkers in normal conversation is 20 dB.

Table 9-17 covers some of the typical speech levels 1 m from the talker.

Table 9-17
Sound-Pressure Levels of Speech 1 m from the Talker
(After Gales et al⁽⁶⁶⁾)

Measure of sound pressure	Whisper (dB)	Normal level (dB)			Shout (dB)
		Minimum	Average	Maximum	
Peak instantaneous pressures	70	79	89	99	110
Speech peaks	58	67	79	87	98
Long-time rms pressures	46	55	65	75	86
Speech minima	30	39	49	59	70

Critical design recommendations for dynamic range in speech communication have been recorded (66).

- For very high-quality communication, the dynamic range should be 60 dB.
- For commercial broadcast purposes, the dynamic range can be 40-45 dB.
- If a mechanism for compensating for variations in average speech levels among talkers is provided in the system, a dynamic range of 30 dB is adequate for essentially perfect speech communication.

- With practiced talkers and listeners, communication can be quite effective in a system providing a dynamic range of only 20 dB.
- Because most communication systems include microphones and/or background noise, it is appropriate to identify "normal" with 65 dB relative to 0.0002 μ bar, one meter in front of the talker.

Intelligibility of Speech

In designing a speech-communication system, many design decisions must be made on the basis of the intelligibility of speech in a given system. Two procedures are available for measuring speech intelligibility. One procedure, the one the design engineer can use most often, is characterized by calculating a predictive measure of intelligibility. The other procedure involves measuring intelligibility directly through intelligibility testing.

Both of the above procedures have their limitations. For example, the calculated, predictive measure of intelligibility breaks down under extreme conditions of noise masking, frequency distortion, and certain kinds of amplitude distortion and is not applicable to the evaluation of systems involving complex processing of speech. When confronted with such problems, it is necessary to resort to empirical data derived from intelligibility tests to provide the basis for engineering decision, but intelligibility testing requires careful laboratory methods involving the control of a number of factors (45, 55, 59). (An aerospace word list is available (49).

Articulation Index (66)

Many design decisions can be made on the basis of calculated, predictive measures of intelligibility. One such measure is the articulation index (AI), and there are two methods of calculating it; one (the 20-band method) is more detailed and accurate than the other (the weighted-octave-band method). A second measure is really an inverse measure of intelligibility and is called the speech inference level (SIL) of noise. The articulation index should be used in all carefully designed speech-communication systems. The speech interference level can serve as a rule-of-thumb guide in making some engineering decisions regarding face-to-face communication.

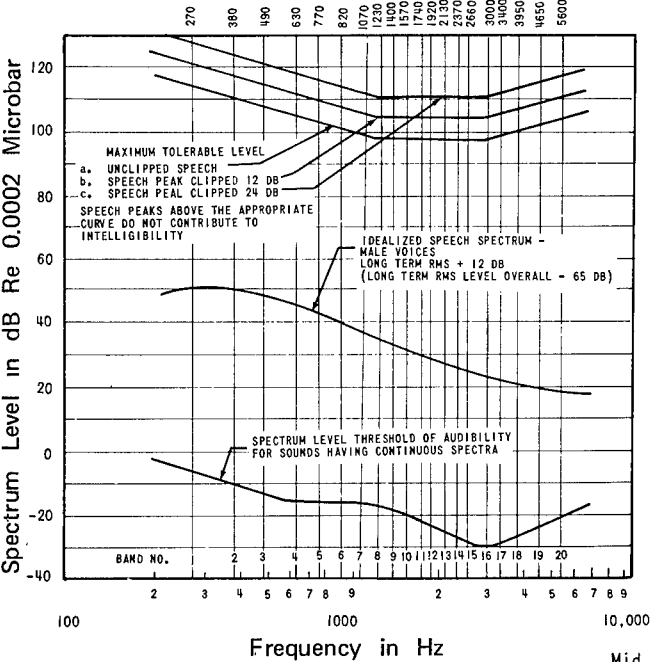
For speech-communication systems, the AI can be used as the predictive measure of intelligibility. The articulation-index formulation is based on the fact that, to obtain high intelligibility, one must deliver a considerable fraction of the total speech band-width to the listener's ear and, also, that the signal-to-noise ratio at the listener's ear must be reasonably high. If the speech peaks are 30 dB or more above the noise throughout the frequency band from 200-6,000 Hz, the listener will make essentially no errors (AI = 1.00). If the speech peaks are less than 30 dB above the noise in any part of the speech band, the listener will make some mistakes (AI < 1.00). If the speech peaks are never above the noise at all (ratio of speech peaks to rms noise less than 0 dB), the listener will rarely be able to understand anything (AI = 0).

Details regarding the establishment of the AI index by the two major methods and variants under different noise conditions are available (2, 10, 11, 25, 43, 59, 66, 113, 118, 154, 204). Figure 9-18a is an example of the basic worksheet for the 20-band method giving the baseline data needed. Figure 9-18b is an example of the calculation of the AI by the 20-band method

Figure 9-18

Calculation of Articulation Index by the 20-Band Method

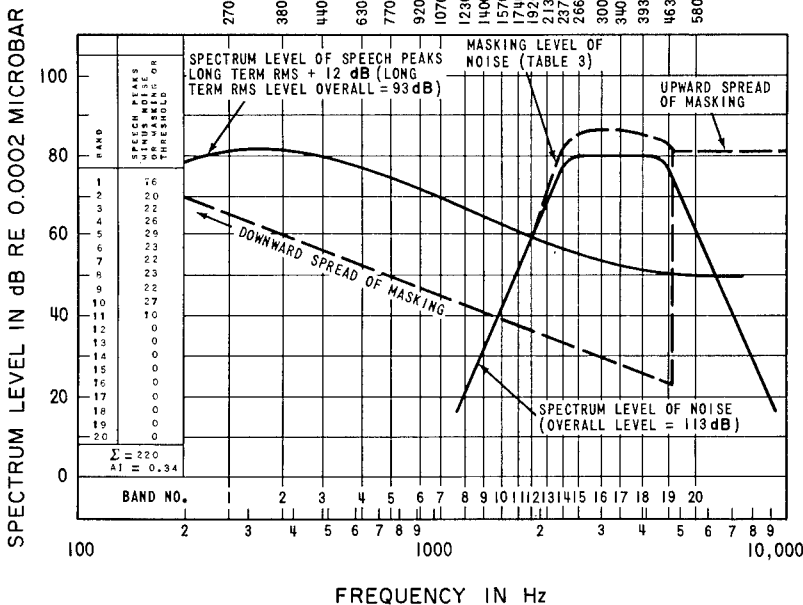
Mid Frequencies of 20 Bands Contributing Equally to Speech Intelligibility with Male Voices



a. Worksheet for the 20-Band Method

Mid Frequencies of 20 Bands Contributing Equally to Speech Intelligibility With Male Voice

b. Sample Calculation by the 20-Band Method



from data on the masking level of a sample 113 dB noise (overall level) with upward and downward spread of the masking.

Speech-intelligibility test scores are influenced by a number of distortion and stress conditions imposed upon the speech signal during its transmission. The effects of a number of such factors can be quantitatively evaluated by the appropriate use or modification during use of AI (117). Further, the effect on speech intelligibility can be properly predicted by an AI when only one factor is present or when several such factors are operating simultaneously. AI's adequately predict either the effects of wideband, continuous-spectrum noise or the effects of bands of noise as narrow as 200 Hz wide, in the frequency range from about 200 Hz to 6000 Hz and for sound-pressure levels up to approximately 125 dB.

Speech may be masked by non-steady-state noise. The duty cycle is that fraction of the time that a masking noise is on and affects speech intelligibility (135). Whenever the noise is not steady-state and the on-off duty cycle is known, the appropriate effective AI can be determined by calculating the AI as though the noise were steady-state and then applying a correction to the resulting AI as indicated in Figure 9-19. This procedure may be followed where the noise falls during the "off" periods to a level at least 20 dB below the level of the noise during the "on" periods.

The rate of interruption of the noise is also to be considered. The effective AI found for a communications system in which a noise having a definite on-off duty cycle is present should be further adjusted in accordance with the functions shown in Figure 9-20. The vertical ordinate gives the effective AI to be expected for a given parameter when the masking noise is interrupted at the rates shown on the abscissa.

Frequency distortion, or the transmission of the signal with unequal gain as a function of frequency, usually affects the intelligibility of speech. These effects are accounted for with reasonable accuracy by AI provided that the unequal emphasis is applied to the appropriate frequency band component of the speech signal. However, the AI will not provide a valid means for estimating the intelligibility of speech that has a very irregular long-term spectrum, i. e., a spectrum that goes through a series of peaks and valleys, the slopes of which, on the average, exceed 18 dB/octave (119).

Amplitude distortion of the speech signal may also affect intelligibility. The effects of sharp symmetrical peak clipping (a noise-canceling method discussed below) can be estimated by use of a computed AI as follows (205):

- (1) Determine from Figure 9-21 the increase in the long-term rms of speech as the result of the particular amount of peak-clipping and post-clipping amplification present in a system (205).
- (2) Add the result of (1) above to the speech peaks (unclipped speech + 12 dB) that would reach the listener's ears without the peak-clipping and comparable post-clipping amplification. Post-clipping amplification is defined as the amount

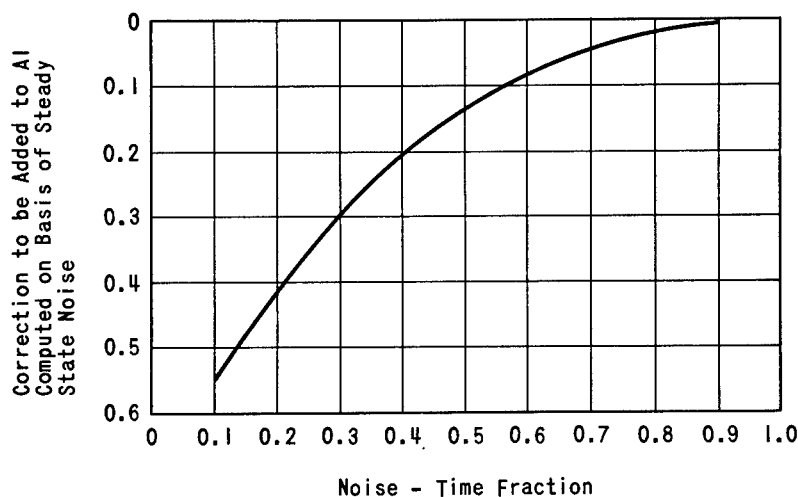


Figure 9-19

Correction of the Articulation Index for Intermittent Noise

The ordinate shows a correction to be applied to the articulation index computed on the assumption that a masking noise is steady-state for various noise-time fractions. The corrected AI cannot exceed 1.0

(After Gales et al⁽⁶⁶⁾, adapted from Miller (135))

Figure 9-20

The Effective AI as a Function of the Frequency with Which a Masking Noise is Interrupted

The parameter of the curves is the corrected AI calculated on the assumption that the masking noise is steady-state and then adjusted according to Figure 9-18 for the fraction of the time the noise is on.

(After Gales et al⁽⁶⁶⁾, adapted from Miller and Licklider⁽¹³⁷⁾)

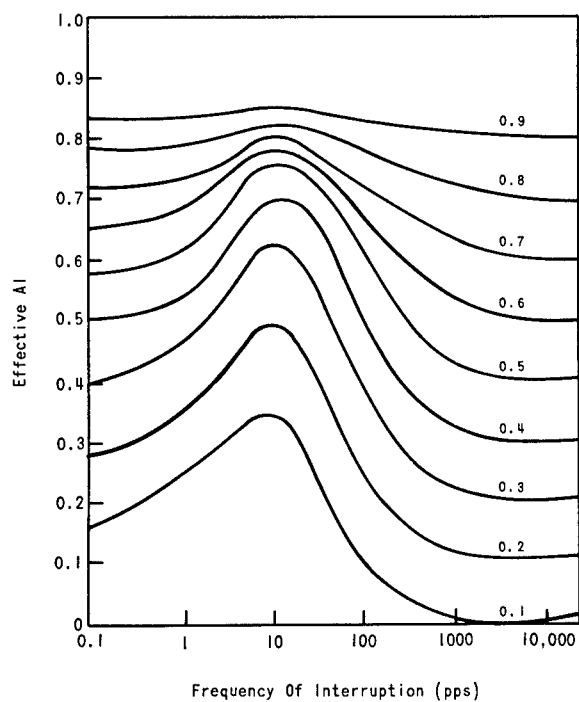
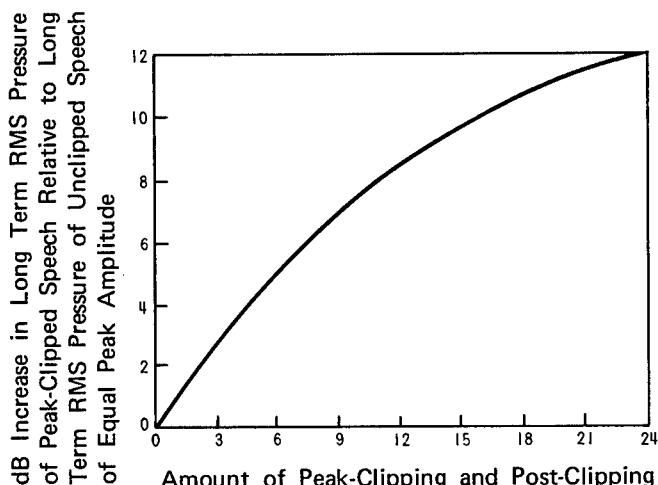


Figure 9-21

The Increase in RMS Speech Power as a Function of Clipping When Clipped Level is Raised to Clipping Reference Level

(After Wathen-Dunn and Lipke⁽²⁰⁵⁾)



Amount of Peak-Cropping and Post-Cropping Amplification in dB. (Peak amplitude defined by 0.001 probability level in distribution of instantaneous amplitudes.)

of amplification added to the system to achieve peak-to-peak amplitudes equal to the peak amplitudes that would be achieved without peak clipping. If the post-clipping amplification does not equal in decibels the amount of peak clipping applied to the speech signal, the increase in the long-term rms found in Step (1) should be reduced by a factor equal to the ratio between the decibel amount of peak-clipping and post-clipping amplification.

- (3) Plot the result of Step (2), (Figure 9-18a) and proceed to compute AI as one would for continuous noise. Note that the maximum tolerable level indicated in Figure 9-18a worksheets for the speech is higher for peak-clipped than for nonclipped speech. In general, peak clipping will be used only when the speech signal is relatively free of noise prior to reaching the processing unit. (see below).

Reverberation in a room in which a speech signal is presented will cause a decrease in intelligibility (109). The amount of degradation will be a function of the reverberation time of the room. For present purposes, reverberation time is defined as the time required for a steady-state pure tone of 512 Hz to decrease 60 dB after the source is stopped. It is possible to correct the AI found for a given speech communication system when the reverberation time is known by the use of Figure 9-22.

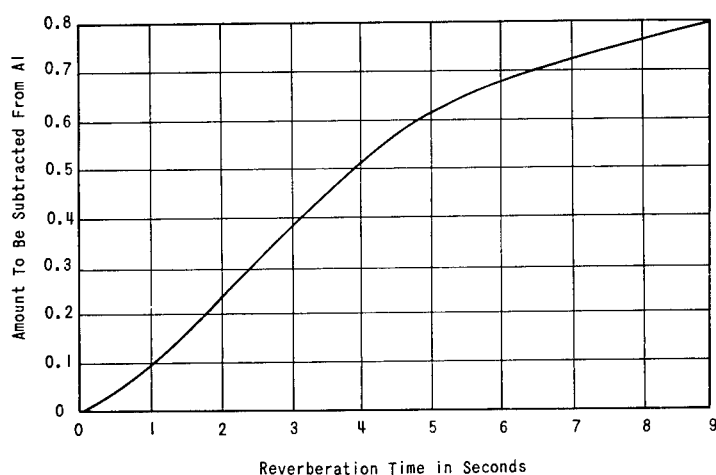


Figure 9-22

Effect of Reverberation Factors in the Intelligibility of Speech

The ordinate shows the amount to be subtracted from AI. AI cannot be less than 0.0.

(After Gales et al⁽⁶⁶⁾, from the data of Knudsen and Harris⁽¹⁰⁹⁾)

Very weak or very intense vocal efforts by a talker will tend to reduce speech intelligibility (153). A given AI value can be expected to be accurate, other factors held constant, when the vocal effort of the talker is maintained at a fairly consistent level somewhere between a measured long-term rms sound-pressure level with 50 to 85 dB measured one meter from the talker's lips. In systems where very strong or very weak vocal efforts are used the measured speech level should be changed into an effective speech level prior to the plotting of the speech spectrum on the AI worksheets. The relation between actual and effective speech levels is shown in Figure 9-23.

Visual cues from observing the talker's lips or face can contribute a great deal to the intelligibility of speech, particularly in the presence of noise (187). However, an AI can be modified or adjusted in accordance with Figure 9-24 into an "effective AI" to reflect the effect of visual cues upon speech intelligibility.

There are many other factors influencing speech communication that the AI as presently calculated does not evaluate. In particular, it should be noted that the method is designed for and has been validated principally against speech intelligibility tests involving male talkers. With what degree of accuracy AI would predict the relative intelligibility of speech of female talkers over different communication systems is not known. Also, the quantitative effects upon speech intelligibility to be obtained from listeners receiving a mixture

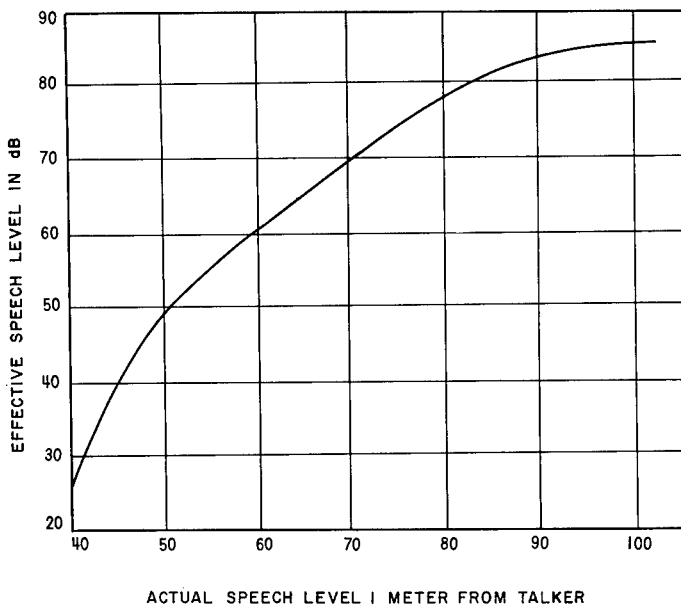


Figure 9-23

The Effective Speech Level as a Function of the Actual Speech Level Used by a Talker

Data are given as dB, long term (R.M.S.) re 0.0002 micro bars.

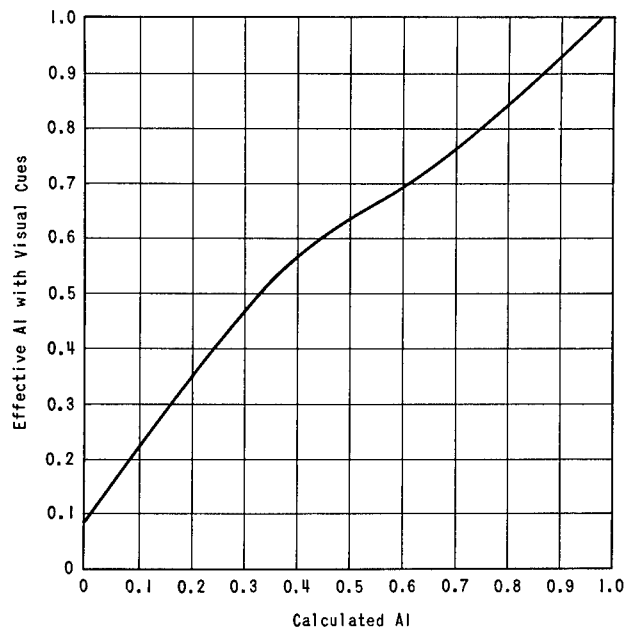
(After Gales et al (66))

Figure 9-24

Effect of Visual Cues on Intelligibility of Speech

Relation between calculated AI and effective AI for a communication system wherein the listener can see the lips and face of the talker.

(After Gales et al (66), from the data of Sumbly and Pollack (187))



of the speech signals directly from a talker and also from a loudspeaker are not known. Accordingly, AI should probably not be applied to such a system.

Conversion of AI to Speech Intelligibility Scores

AI's may be converted to estimated speech-intelligibility scores by use of Figure 9-25. It is to be especially noted that the intelligibility score (in

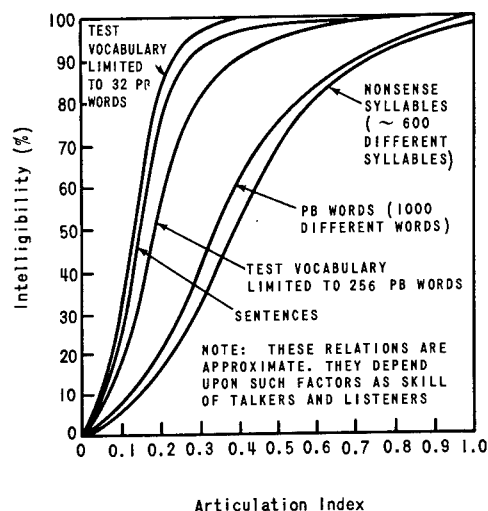


Figure 9-25

Relation Between the Intelligibility of Speech and the Articulation Index

(PB = phonetically balanced)

(After Gales et al⁽⁶⁶⁾, from the data of French and Steinberg⁽⁵⁹⁾)

percent correct) is highly dependent upon the constraints placed upon the message being communicated. The greater the constraints, i. e., the smaller the average information content (in information theory terms) associated with each item in the total ensemble of message, the higher the percent intelligibility score for a given AI. Typical constraints may consist of grammatical structure and context, such as found in sentences, limitations in vocabulary size, and in the syllabic length of words. See Ref. (49) for an aerospace word list.

No single AI value can be specified as a criterion for "acceptable" communications. The efficiency of communications as shown in Figure 9-25 is a function of the messages to be transmitted and the proficiency of the talkers and listeners involved. Furthermore, what level of performance is to be required over a given system is, of course, dependent upon factors whose importance can be evaluated only by the users of the communication system.

The Speech Interference Level (SIL)

A simpler, but less exact and less general method for predicting the intelligibility of face-to-face speech communication has been devised for use in situations where the noise has a relatively continuous spectrum (e. g., ventilation noise in offices, aircraft noise, the noise in most engine rooms, and the noise around milling machines) (66). The method, called the speech-interference-level (SIL) method, yields the maximum noise level that will permit correct reception of 75% of PB (phonetically balanced) words or about 98% of test sentences. This criterion is equivalent to an AI of about 0. 5.

To determine the SIL of a given noise, proceed as follows:

- Measure the sound-pressure level of the ambient noise in octave bands of 600-1,200; 1,200-2,400; and 2,400-4,800 Hz.
- Determine the arithmetic average of the decibel levels in the three octave bands. This average value is the SIL.
- Consult Figure 9-26a to find the maximum distance between talker and listener at which 75% of PB words will be heard correctly. Figure 9-26b summarizes the use of SIL in estimating speech interference.

Figure 9-27 summarizes the intelligibility of speech as related to the signal-to-noise ratio (see also Figure 9-33). In those situations where a low signal-to-noise ratio is unavoidable the use of standardized phrases or words may mean the difference between satisfactory and unsatisfactory performance.

Interference with Speech by Secondary Environmental Factors

Simultaneous Speech

A listener cannot listen to two simultaneous and non-redundant messages and receive full information from both messages. Instead, he switches attention from one to the other, with an attendant loss of information in both messages. In paying attention to one and disregarding the other, only the one message is understood. When more than a one-voice message exists simultaneously in a communication situation, the use of frequency-selective filters can give characteristic timbres to each of the several voices, thereby permitting reception of the relevant voice.

Ambient Atmosphere

The human voice, earphones, and loudspeakers become less efficient generators of sound as the ambient atmospheric pressure is reduced. The effect on the talker, microphone, and earphone, of reducing the ambient pressure from that of sea level to that of 40,000 ft is shown in Figure 9-28.

The effects of the gaseous composition, such as the helium content of the atmosphere, on sound propagation and intelligibility of speech is covered in Inert Gas (No. 11).

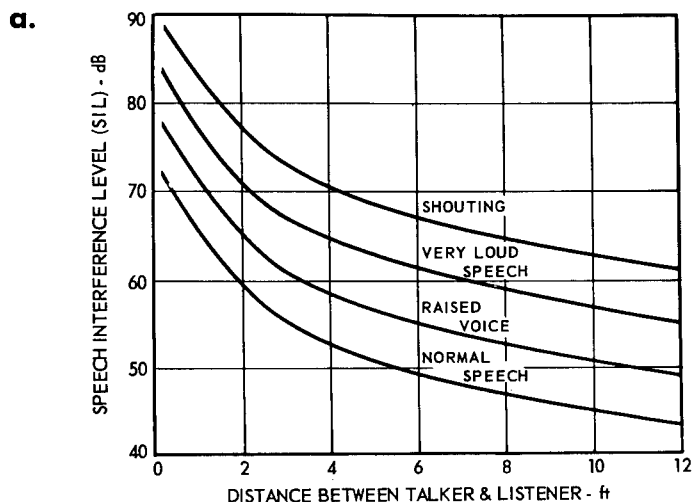
Ear Plugs and Helmets

Under most noise conditions, a listener can wear ear plugs without reducing the intelligibility of speech. Ear plugs attenuate the speech and the noise by the same amount so that the signal-to-noise ratio at the listener's eardrum is the same with the ear plugs as without them. When speech level exceeds 85 dB, ear plugs cause an increase in intelligibility, whether or not there is background noise. This is depicted in Figure 9-29. The noise reduction by typical helmets is seen in Table 9-50c and in Figures 9-51 and 52.

Figure 9-26

Speech Interference Levels

(After Jerison⁽¹⁰⁴⁾, data for graph from Gales et al. (eds.)⁽⁶⁶⁾,
table from Rosenblith and Stevens⁽¹⁶⁶⁾)



Speech Interference Level (SIL) is a readily calculated index of the degree to which a complex sound or noise will interfere with speech. It is also often used as a rough estimate of the comfort or acceptability of a potentially annoying noise. SIL is defined as the arithmetic mean of the sound pressure levels (dB re 0.0002 dyne/cm²) within three octave bands: 600-1200 Hz, 1200-2400 Hz, and 2400-4800 Hz. The chart shows the maximum permissible SIL for normal and raised speech associated with various distances between speaker and listener. It should be kept in mind that the SIL is accurate only for broad-band noises with fairly typical spectra. With atypical noises such as those shown by the Mercury astronaut curve in (9-3) SIL may not be strictly appropriate, but will probably be used until better measures are developed.

SIL of the noise estimated at the astronaut's ear during lift-off may be calculated from the dB levels within the three octave bands between 600 and 4800 Hz as shown in 9-3. These are 81, 60, and 41 dB. SIL is the arithmetic mean of these numbers; therefore, $SIL = (81 + 60 + 41)/3 = 61$ dB. For the Century fighter overflight shown in 9-10c, $SIL = (118 + 113 + 108)/3 = 113$ dB.

Speech communication criteria associated with various SIL levels are shown in the following table:

b.

Speech Communication Criteria			
SIL dB	Voice Level and Distance	Nature of Possible Communication	Type of Working Area
45	Normal voice at 10 ft.	Relaxed conversation	Private offices; conference rooms
55	Normal voice at 3 ft; raised voice at 6 ft; very loud voice at 12 ft.	Continuous communi- cation in work areas	Business, secretarial, control rooms of test cells, etc.
65	Raised voice at 2 ft; very loud voice at 4 ft; shouting at 8 ft.	Intermittent communication	
75	Very loud voice at 1 ft; shouting at 2-3 ft.	Minimal communication (danger signals; restricted prearranged vocabulary desirable)	

Figure 9-27

The Role of Signal-to-Noise Ratio in Speech Intelligibility

(Adapted from Jerison⁽¹⁰³⁾; (a) after Pollack⁽¹⁵⁸⁾; (b) after Miller et al⁽¹³⁶⁾; and (c) after Gales et al⁽⁶⁶⁾)

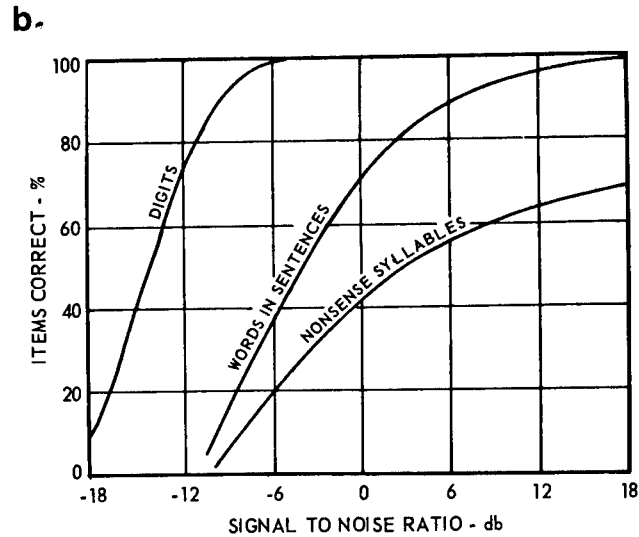
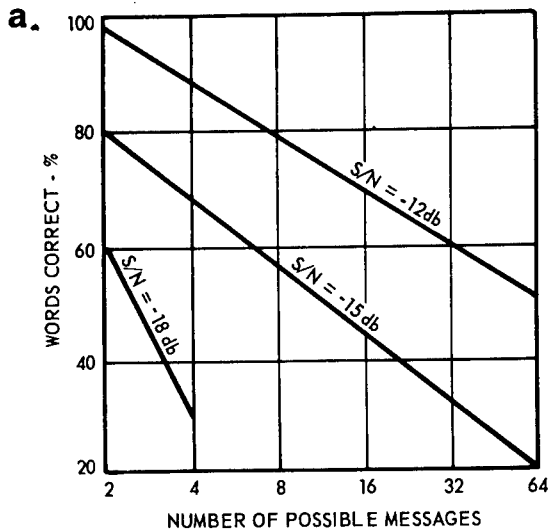
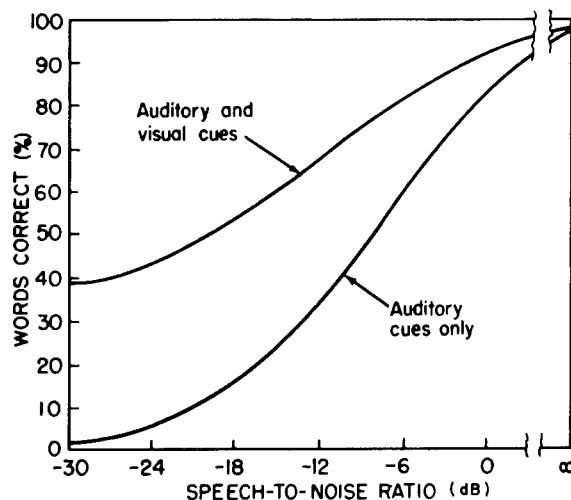


Figure a shows how the correct perception of spoken messages is affected by the diversity of responses required of the observer. As the number of possible messages (standard, two-syllable words) increases from 2 to 64, the percentage of correct reports about the messages drops. The relationship is poorer when the signal/noise ratio, shown here in dB, is lower.

Figure b shows similar effects with other materials graphed in a different way. It shows that single numbers (digits) are detected correctly more easily than are words in sentences, and words in sentences are detected correctly more easily than nonsense syllables. This is a special case of the effect shown in figure a. In General, the less "information" the sender-receiver system has to process, the more accurate the processing. In figure a, the system is processing from 1 to 6 "bits" of information (that is, 64 messages = 2^6 messages = 6 "bits"). In figure b, the amount of information processed varies from a little over 3 "bits" for digits to unknown but higher amounts for the other categories. It is clear that communications can be improved by using a limited vocabulary: the smaller the vocabulary, the better the system.

Figure c shows that the increment of intelligibility contributed by visual cues is a function of the prevailing speech-to-noise ratio; if the speech-to-noise ratio is high, the listeners hear the words clearly and therefore cannot take advantage of the cues provided by lip reading; if the speech-to-noise ratio is low, they need, and they in fact use, the visual cues.



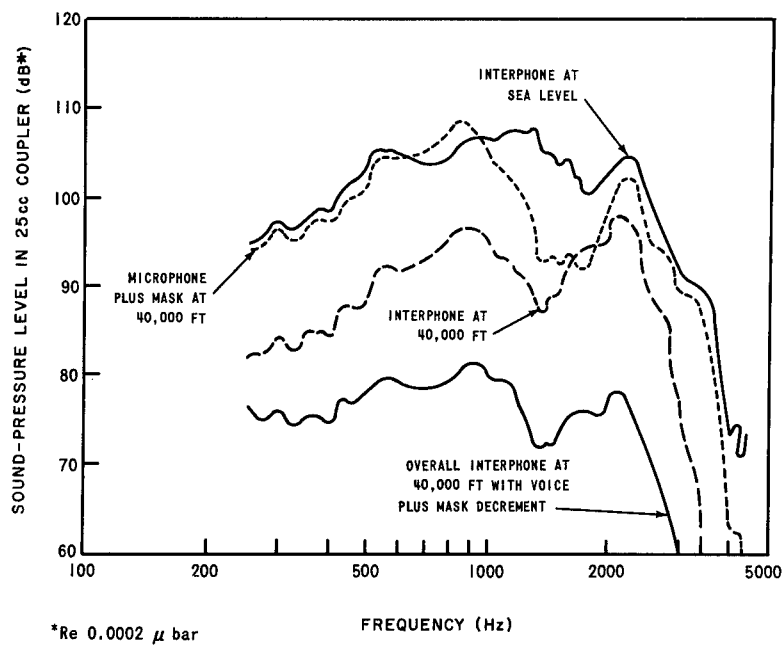
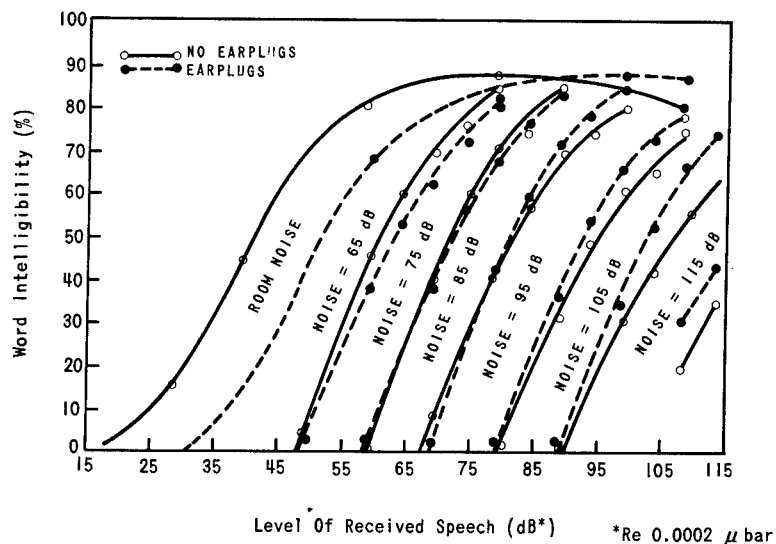


Figure 9-28
Effects of Ambient Atmospheric Pressure on Reception of Speech
at Sea Level vs 40,000 ft (2.7 psia or 141 mm Hg)

(After Kryter⁽¹¹⁰⁾)



Relation between PB-word intelligibility and speech level in various levels of masking noise with and without earplugs. (NDRC type V51R ear plugs were used). Data show higher intelligibility in presence of intense noise with ear plugs than without.

Figure 9-29
Effects of Ear Plugs on Intelligibility of Speech

(After Kryter⁽¹¹³⁾)

Speaker Training

Considerable increases in intelligibility are found whenever trained talkers are used to convey auditory information. This increase in intelligibility is more marked under noisy conditions than under more optimal ones. Characteristics which differentiated good from poor talkers are as follows:

1. Superior speakers speak with greater syllable intensity (decibels).
2. Superior speakers have longer average syllable durations.
3. Superior speakers have more pitch variability than poorer ones.
4. Superior speakers utilize proportionally more of total speech time with speech sounds and less with pauses.

Microphone and Electronic Processing in Speech Intelligibility (66)

Microphones are usually designed with the following characteristics:

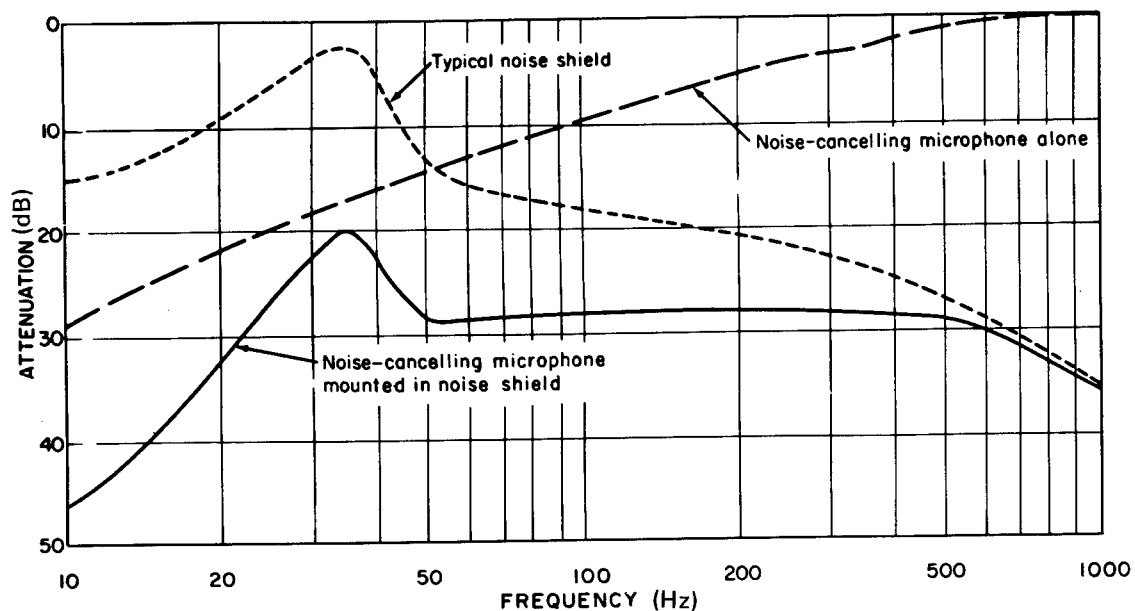
1. High sensitivity to acoustic speech signals.
2. Faithful transduction of the acoustic speech signal into an electric signal.
3. Ability to reject other acoustic signals and noises that are present at the location of the talker.

When the talker is in an intense noise field and the required space is available, the microphone should be put in a noise shield. A noise shield protects the microphone more from high-frequency than low-frequency noise; noise canceling does just the opposite. As shown in Figure 9-30a, a noise-canceling microphone in a noise shield can attenuate noise by 30 dB.

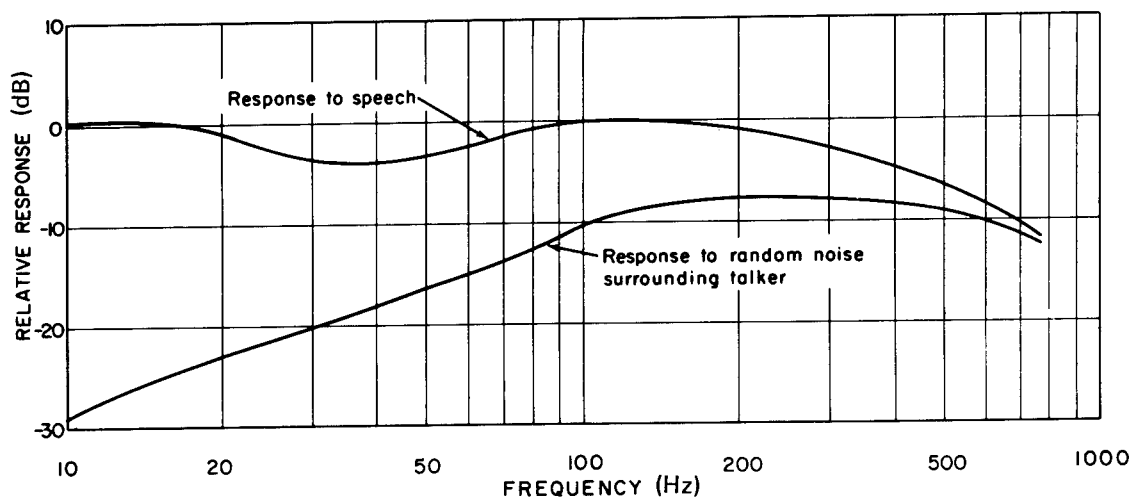
Many microphones are satisfactory insofar as frequency-response characteristics are concerned; few, however, are specifically designed to discriminate between the talker's speech signal and the ambient noise surrounding the talker. Microphones that are so designed are called noise-canceling microphones (90, 66). These microphones, also called differential or pressure-gradient microphones, are so constructed that sound waves can reach the diaphragm from the back as well as from the front of the microphone. When a microphone is placed directly in front of the lips of a person who is talking, it is in the spherically expanding part of the speech wave pattern, and there is a large gradient of speech pressure between the front and back of the diaphragm. Noise, on the other hand, usually comes from more distant sources. With noise-canceling microphones, this noise has equal access to both the back and front of the diaphragm and is thus largely "canceled" whereas the speech is not. The amount of discrimination that is available from a typical noise-canceling microphone placed 1/2 in. in front of the talker's lips is shown in Figure 9-30b. Noise-canceling microphones

Figure 9-30

Noise Attenuation and Speech Intelligibility with Noise-Shielding
and Noise-Canceling Microphones



a. Attenuation of Noise with Noise and Noise-Canceling Microphones
(After Hawley and Kryter⁽⁹⁰⁾)



b. Relative Response of Noise-Canceling Microphones to Speech
and Noise When Placed 1/2 Inch from Speaker's Lips
(After Gales et al⁽⁶⁶⁾)

must be held very close to the lips if the noise discrimination properties are to be realized; in most cases they should just touch the lips when being used.

Amplifiers, transmitters, and receivers to be used in speech-communication systems should have the following characteristics (66):

1. Sufficient band-width to provide a "flat" audiofrequency response from at least 250-4,000 Hz (preferably 200-6,100 Hz for intelligibility and 100-7,500 Hz for quality of reproduction).
2. Sufficient dynamic range and gain to handle the range of instantaneous pressures found in speech and to develop the necessary signal level at the headset or loudspeaker terminals. In addition, they should introduce less background noise than is introduced by the microphone.

Linear amplification is usually desirable for speech communication when both talkers and listeners are in relative quiet. In noise, however, it may be desirable to introduce nonlinearity deliberately. Two kinds of nonlinear amplification are of particular interest in this connection: automatic gain control (AGC), sometimes called automatic volume control (AVC); and peak clipping.

Automatic gain control and peak clipping have different actions and effects, but they can be used together. The one essential difference in the actions of the two is in their response times; ordinary AGC operates on relatively long-time measures of the intensity of a signal whereas a peak clipper can be thought of as an AGC that operates instantaneously.

The AGC system derives a measure of the average signal strength over a period of time, and this information is used to adjust the operating characteristic of the amplifier. Sustained, intense signals lead to reduction of the gain; sustained, weak signals lead to increase of the gain. The average output level is, therefore, about the same, no matter what the average input level. But AGC does not eliminate variations in intensity between parts of the signal that occur together in a short interval of time; the consonants remain weaker than the neighboring vowels, for example, because the AGC averages over an interval longer than a single speech sound.

A noise-controlled AGC system can provide high speech intelligibility during periods of intense noise and, at the same time, protect the hearing of the listeners from exposure to intense speech during periods of relative quiet.

The attack-and release-time constants usually employed in the "limiter" amplifiers used in commercial broadcast work are, typically, 10 msec and 600 msec, respectively. For some communication systems designed to operate in noise, it has been found that an attack time of about 0.1 sec and a release time of about 10 sec are most satisfactory. (When the release time is made appreciably shorter, there is an objectionable fluctuation in the transmitted background noise).

Peak clipping is simply clipping the peaks off the speech signal and leaving the remainder (66). Ordinarily, peak clipping involves clipping both the positive (upward) and negative (downward) peaks. For all practical purposes, peak clippers have no attack or release times; they operate instantaneously. Peak clipping alone often tends to reduce the amplitudes of the intense parts of speech (usually the vowels) down to the level of the weaker parts (consonants). Because of this, peak clipping is often used to make the various speech sounds more homogeneous in amplitude. If by reamplifying a signal that has been clipped so that the peak amplitude of the remnant is the same as the peak amplitude of the original wave before clipping, the intensity of the weak consonant sounds is increased. This is true even though the peak level of the speech and therefore, the peak power requirements of the amplifiers, radio transmitters, etc., is not increased. Figure 9-31 shows word intelligibility as a function of peak amplitude of received speech, with peak

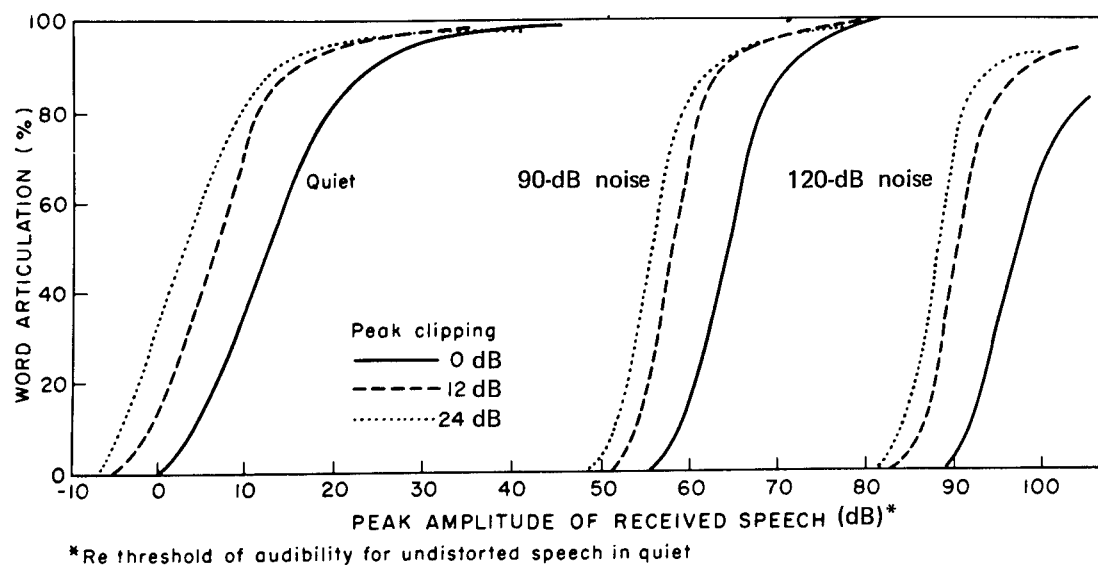


Figure 9-31

Word Intelligibility as a Function of Peak Amplitude of Speech
with Various Levels of Peak Clipping

(After Gales et al⁽⁶⁶⁾, from the data of Licklider⁽¹²⁶⁾)

clipping as the parameter. As can be seen, with equal peak-to-peak amplitude, clipped speech is much better understood than unclipped speech.

The clipped speech in a quiet environment has a harsh, unpleasant sound because of the distortion products that are introduced by the clipping. When listened to in noise that enters the system at a point following the clipper, the distortion products tend to be masked by the noise, and the speech sounds about as "clean" as unclipped speech in the same noise. Data are available on the optimum level of clipping for various noise conditions and electronic configuration in the communication system (66).

Calculation of the effect of peak clipping on the articulation index has been covered in Figures 9-18a and 9-21. Another way of avoiding some of the distortion products introduced by peak clipping is by using the heterodyne clipping. A single-sideband, suppressed-carrier modulation is used to shift the spectrum of the speech signal up the frequency scale by x Hz. The peaks are clipped and the sideband-modulated carrier is reamplified by the desired amount. By then passing the resulting signal through a bandpass filter (x to $x + 5,000$ Hz) and using the signal in an ordinary single-sideband suppressed-carrier transmission or, if an audio signal is required, demodulating with the aid of standard single-sideband suppressed-carrier technique, the clipped speech may be transmitted.

Because the distortion-product noise introduced by peak clipping consists of harmonics and intermodulation products, it will be largely very high and very low in frequency, relative to the shifted speech frequencies, and will, therefore, fall outside of the band of the bandpass filter (x to $x + 5,000$ Hz), and the transmitted signal will not contain the distortion products even though it has been clipped. Such a process will make the received signal sound "cleaner" and less harsh to a listener in quiet. Elimination of the distortion products that lie outside the filter bands, however, will affect the shape of the transmitted wave in such a way that less power is actually transmitted than would be transmitted by an ordinary pre-modulation peak-clipping system. Thus, heterodyne clipping does not improve the intelligibility of the speech received in noise quite as much as does peak clipping the speech prior to modulation.

Standardization of earphones and equipment for audiometric testing is under study. New approaches to the study of speech audiometry are underway (186, 212, 214). For the Apollo program it has been suggested that the microphones and earphones have the following characteristics (198):

a. Microphones

Output Level	0 dbm \pm 3 dB into a 600 ohm load for sound pressure level (SPL) of 106 dB 1/4 inch from the microphone.
Power Supply	14.0 to 20.5 volts.

b. Earphones

Output Level	At least 110 dB SPL (Reference 0.0002 dyne/cm ²) for 0.78 volts RMS drive into a 6 cc cavity.
Input Impedance	600 ohms.
Minimum Power	15 mw

BIOLOGICAL RESPONSES TO NOISE EXPOSURE AND TOLERANCE

The human response to noise has received recent review (68, 71, 82, 112, 138). The responses may be considered from the physiological and psychologic point of view.

Physiological Effects of Noise

Ear and Hearing

The primary effects of noise exposure are on the hearing organ and on the hearing function. Loudness perception, masking of other signals by noise, temporary hearing loss after occasional exposure to higher sound pressure levels, and finally permanent hearing loss caused by repeated exposures to noise for days and years, have been studied extensively in connection with the large scale problem of industrial noise exposure (114, 172). The gradual cumulative loss of hearing is apparently due to degeneration of the external hair cells in the cochlea and depends on the level of the noise, its frequency spectrum, the intermittency of exposure, the age and probably the susceptibility of the individual (122, 164).

Discomfort to the Ear

When a sound of high intensity (especially at low frequencies) enters the ear, a number of protective mechanisms come into operation to reduce the amplitude of vibration at the hearing organ (82). The immediate effects include a change in the mode of vibration of the stapes, due to subluxation of the incu-stapedal joint and, under extremely intense stimulation, the malleo-incudal joint. The foot of the stapes then performs a rocking motion in the oval window, the amplitude of the piston-like movement being reduced. Some acoustical energy is also dispersed by the excitation of harmonics in the transmission pathway medial to the tympanic membrane.

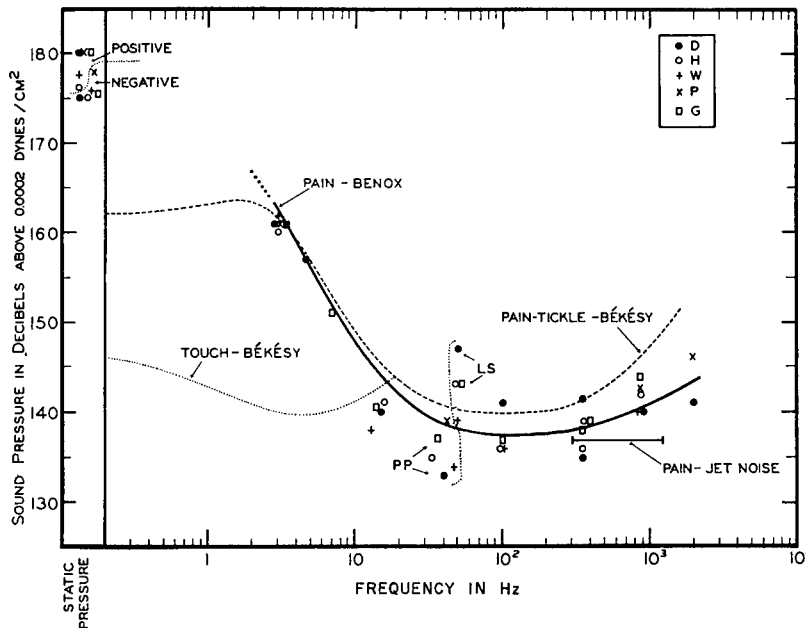
As an additional protective mechanism, the stapedius and tensor tympani muscles contract in response to a loud noise (or mechanical irritation of the external auditory canal, face, or neck). Anatomically, these little muscles have opposing actions: stapedius tends to withdraw the foot of the stapes from the oval window, while tensor tympani tends to pull the handle of the malleus (attached to the eardrum) inwards. The resulting effect of these actions is to produce an increase in stiffness and possibly in damping of the ossicular chain. Because the muscular action of the acoustic reflex is a physiological response with a latency of some 10 msec, it fails to protect the hearing organ from noises which are impulsive or of sudden onset (e. g., gunfire).

Intense noise (SPL greater than 100 dB re 0.0002 μ b), especially when it is of sudden onset, can provoke a generalized reflex response of tensing, grimacing, and covering the ears with the hands (86). In some individuals there is a compelling urge to avoid or escape from the noise.

Extremely high intensities of noise (> 135 to 140 dB) in the range of 20-2,000 Hz produce sharp pain in the ears, presumably due to stretching of the tissues of the eardrum and related structures, rather than to overstimulation of the hearing organ itself. It can be provoked in the totally deaf (1). For 15 Hz and below, 179 dB is the probably pain threshold (70). (See below).

Figure 9-32 represents the threshold for aural pain with high sound pressures. The following considerations apply to discomfort experienced from high intensity sound:

Figure 9-32



Thresholds for Aural Pain Produced by Pure Tones and Jet Noise

Points represent means of 3-4 determinations. Duplicate points represent means taken on different days. Positive and negative static pressures in the external ear canal are referred to atmospheric pressure. Line representing jet noise threshold is placed at overall sound pressure level and extends to the frequencies of the octave bands (300-600 and 600-1200) carrying most of the sound energy. (Touch and Pain-Tickle thresholds after Bekesy) (From reference 70). Solid line represents new contours proposed by CHABA Working Group 46. Broken line Glorig (A.A.O.O.), proposed by ISO (75).

(After von Gierke⁽⁶⁸⁾)

- Discomfort in the ear is felt after a few seconds exposure to noise fields exceeding 120 dB in the octave bands between 300 and 9,600 Hz.
- Annoyance is greater by a noise that is modulated in frequency and/or intensity than by a steady-state noise.
- Adaptation is greater to steady noise than it is to intermittent or irregular noise.
- Discomfort is avoided by setting a signal, whenever possible, at about 40-50 dB above absolute threshold.

Ear Damage - Temporary and Permanent Hearing Loss

Aftereffects of noise include temporary or permanent loss of hearing (112, 115). Good data have become available relating noise-induced permanent threshold shift (NIPTS) to broad-band steady noises experienced daily for eight hours over many years. The gap in knowledge with respect to intermittent, irregular exposures and short duration exposure has been filled by

the plausible assumption, supported by various bits of indirect evidence, that noise-induced temporary threshold shift (NITTS), i. e., auditory fatigue and complete recovery following each individual noise exposure, is an integral part of the NIPTS process (see Figure 9-33). Without NITTS no NIPTS will develop. The assumption now is that NIPTS progresses similarly to NITTS but with a different time scale. All types of noise exposures which produce equal amounts of NITTS are considered equally hazardous with respect to NIPTS. The relative effectiveness of different noise spectra and different exposure time patterns can, therefore, conveniently and without hazard, be studied in laboratory experiments on normal-hearing subjects (75).

The NITTS can be measured with pure tone audiometry (36, 73, 107). Figure 9-33a and b covers the NITTS as related to steady and pulsed noise. Figure 9-33c relates temporary loss to NIPTS. The NITTS found in young adults with normal hearing, from an eight-hour exposure to a noise has about the same numerical magnitude as the NIPTS in industrial workers exposed for 10 or more years, eight hours per workday, to about the same noise (112). NITTS data can be used as a reasonably valid secondary yardstick for assessing the potential damage risk for permanent threshold shifts due to exposure to noise. Figure 9-33d shows how loss of speech intelligibility is related to hearing loss. A detailed analysis of the relation of NITTS and NIPTS to speech intelligibility is available (112).

In considering the permanent hearing loss, one must be concerned with the effects of short-term (under 8 hours) and long-term (over 8 hours) exposures to pure tone, narrow-band, and broad-band noise which can cause temporary or permanent damage to the ear. Several new approaches have been recently suggested (68, 112, 139). These damage contours are discussed below under noise control and protection, Figure 9-39 to 9-49.

The normal hearing loss associated with aging in males is recorded in Figure 9-34a (147). These curves exclude all men exposed to noise or military service where gunfire may have been involved, as well as those with a history of ear pathology. Theories on the cause of hearing loss in older individuals not exposed to excessive noise are currently focused on the changes in the joints of the ossicle chain of the middle ear which reduce the transmission of higher frequencies. Figure 9-34b presents the average hearing thresholds obtained by several surveys. The L. S. curve represents a special group of commercial and test pilots who appear to have lower thresholds than the general population (190). Astronauts would probably fall into this group.

Data are available on the hearing levels of adult Americans (74). Figure 9-34c represents an estimate of speech reception thresholds from these data obtained by averaging the levels at the three pure-tone frequencies which include the range usually considered most important for understanding speech- 500, 1000, and 2000 cycles per second for the better ear. The patterns for men and women are similar. A steady increase with age from the youngest to the oldest age group can be noted in the estimated median thresholds for speech. Only in the age groups 60 years and over does the median threshold exceed audiometric zero. Some 8 percent of the adults in the U. S. A. or

Figure 9-33

After Effects of Noise

a.

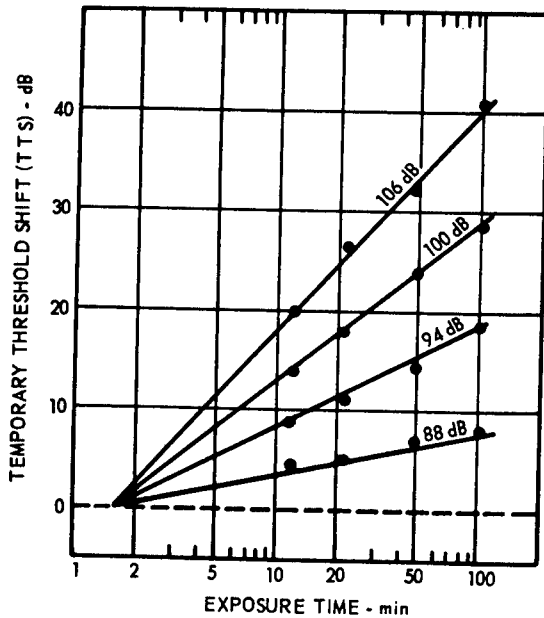


Figure a illustrates the increase in the amount of temporary threshold shift (TTS) for hearing a 4000 Hz tone as prior exposure to steady noise increases in duration. The effect is greater when the SPL of the noise is higher. For example, at 106 dB (top line) there is a more rapid increase in TTS than for the 100 dB noise, and so on. The amount of TTS is proportional to the logarithm of the duration of noise exposure.

b.

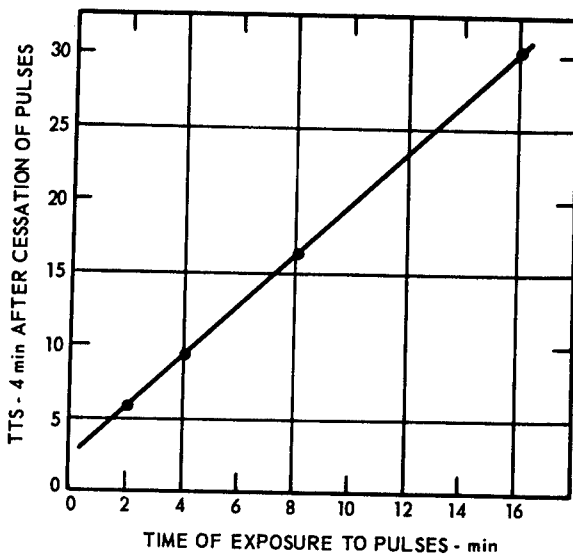


Figure b illustrates the increase in TTS when the exposure is to an intermittent noise -- clicks at 25 per minute -- and at an SPL of 140 to 155 dB. The curve is the average of tests at 3000, 4000, and 6000 Hz; TTS increases linearly (rather than logarithmically) as exposure time increases.

(Figures a and b after Jerison⁽¹⁰⁴⁾, adapted from Glorig et al⁽⁷⁵⁾, and Ward et al⁽²⁰³⁾)

Figure 9-33 (continued)

c.

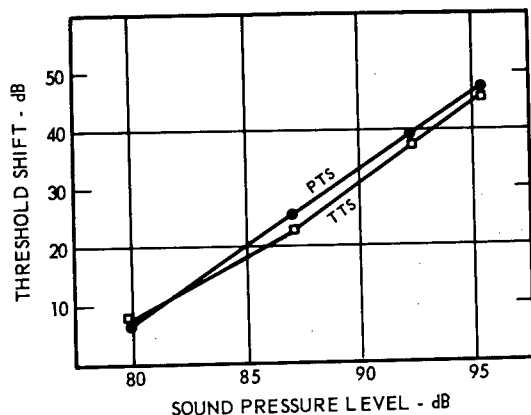


Figure c shows the relationship between TTS and permanent threshold shift (PTS) -- that is, partial deafness. The point in this figure is to emphasize that TTS, which is easily studied in the laboratory, is a valid measure of the permanent effect of a noise on hearing.

d.

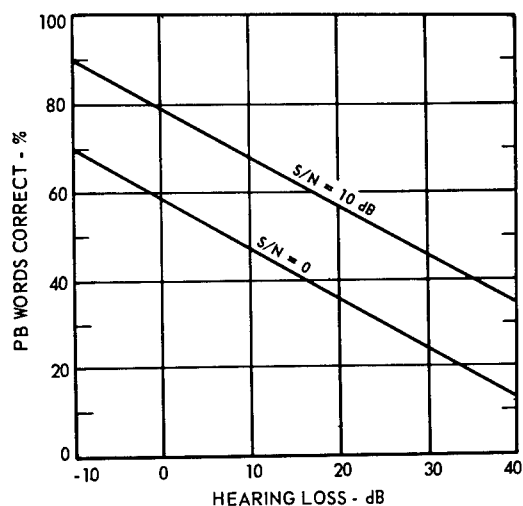
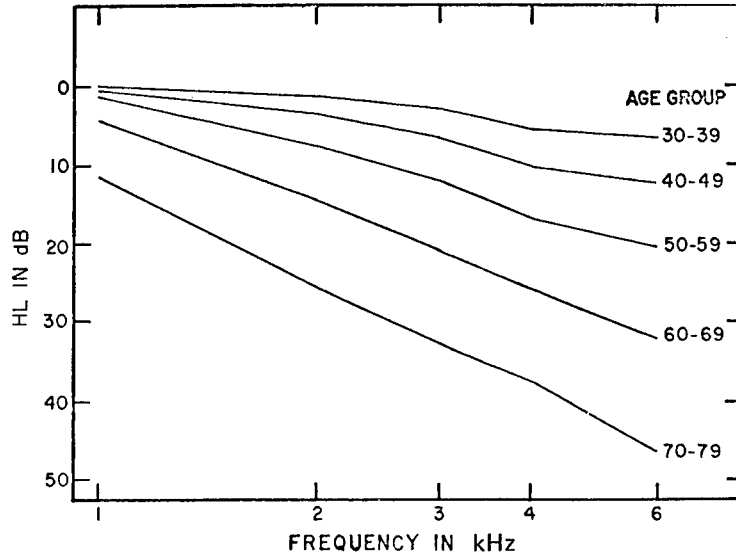


Figure d shows the relationship between partial deafness as measured by permanent threshold shifts (at 1000, 2000, and 3000 Hz) and the effectiveness of hearing for speech communication tested with PB (phonetically balanced) words. By combining the kind of information presented by these four charts, it is possible to set damage risk criteria as shown in Figure 9-40. The damage risk criteria are concerned with keeping permanent after effects of noise from damaging hearing, especially as used in speech communication.

(Figures c and d after Jerison⁽¹⁰⁴⁾, adapted from Glorig et al⁽⁷⁵⁾, and Kryter et al⁽¹²¹⁾)

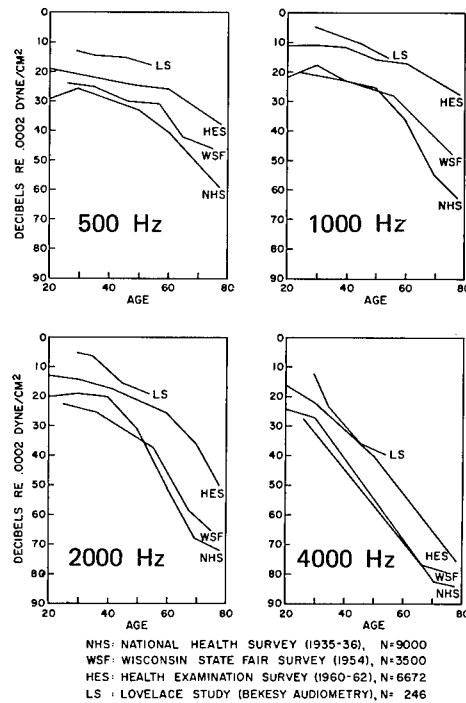
Figure 9-34

Loss of Hearing of Signals as a Function of Age



a. Hearing Loss of Tones in a Group of Males with No History of Ear Pathology or Exposure to Gunfire

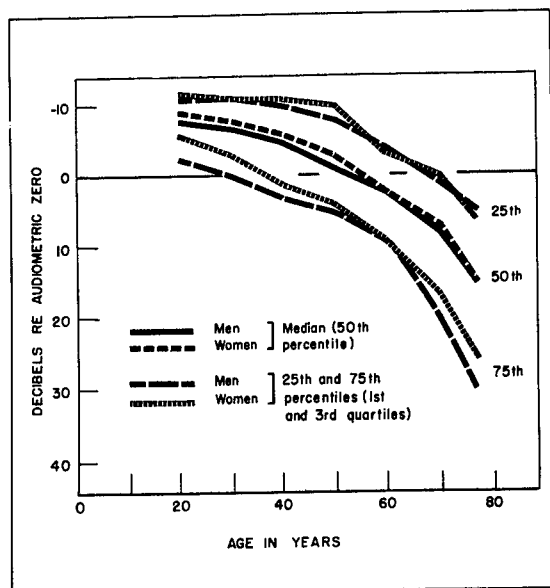
((After Nixon et al⁽¹⁴⁷⁾)



b. Comparison of Average Hearing Thresholds by Age at 500, 1000, 2000, and 4000 Hz for the "Better" Ear

(After Szafran⁽¹⁹⁰⁾)

Figure 9-34 (continued)

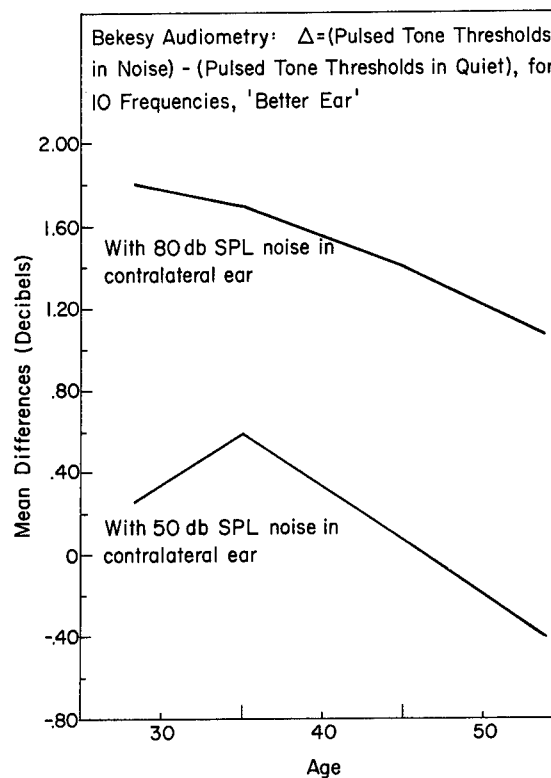


c. Medians and Quartiles from the Distribution of the Hearing Threshold Level for Speech (Average of Pure-Tone Levels at 500, 1000, and 2000 Hz) in the Better Ear for Men and Women, United States

(After Glorig⁽⁷⁴⁾)

d. Bekesy Audiometry: Pulsed Tones Threshold at 10 Frequencies in the Better Ear of a Select Group of Pilots

(After Szafran⁽¹⁹¹⁾)



9.2 million persons, have hearing levels in the better ear of 15 decibels or more above audiometric zero within the critical speech range. This includes persons with varying degrees of hearing handicap - ranging from some difficulty with faint speech to the inability to understand even amplified speech - which impairs their ability to hear everyday speech well enough to understand it.

In auditory perception studies using the Bekesy technique, many, though certainly not all older pilots of the L. S. curve of Figure 9-34b, do not show the traditionally expected unfavorable change of the effective threshold in the presence of 50-80 dB SPL white noise input to the contralateral ear (190, 191). The average difference between the pulsed tone thresholds in quiet and in noise for the better ear is plotted in Figure 9-34d.

Criteria for tympanic membrane rupture, when the ear is exposed accidentally to blast waves of different duration or to high intensity sound of varying duration, have been fully developed as a function of frequency, or pulse duration, or both (200). Levels above 155 dB for exposure to many sound cycles in the range of maximum ear sensitivity and above 175 dB for exposure to single blast pulses of low frequency content must be considered hazardous in this connection (34, 38, 94). (See also blast pathology in Pressure, No. 12).

Non-Aural Effects

During exposure to steady-state sound fields having an overall SPL of 120-150 dB or higher, undesirable, nonauditory effects are experienced, regardless of the ear protection provided (48, 82). Intense noise, especially at frequencies below 1000 Hz can be felt as well as heard. The threshold of feeling for airborne sound is some 10 dB lower than the threshold of aural pain in the middle audiofrequency range. By direct absorption through the body surface, airborne vibration can stimulate mechano-receptors throughout the body, including touch and pressure receptors and the vestibular organs. The sensations produced can be bizarre and disturbing. It has been suggested that, like mechanical vibration of the body, intense acoustical irradiation might interfere with postural activity, due to stimulation of the sensory pathways involved from several end organs (37, 38, 44).

The effect of high-intensity low-frequency noise on the respiratory system is reinforced in the 40-60 Hz range through mechanical resonance of the chest, the same resonance that determines the curve of safety criteria for emergency exposure of humans to blast waves of varying durations (17). Considering all such nonauditory mechanical effects on the body, it is important to keep in mind that dynamic mechanical response depends critically on body dimensions. Therefore, animal data are meaningless unless proper scaling laws have been applied (67). For example, the same chest resonance which occurs for human subjects between 40 and 60 Hz appears at over 400 Hz for a rabbit and at over 1,000 Hz for a mouse.

Vertigo and, occasionally, disorientation, nausea and vomiting can also be present. The order of sound pressure level necessary to provoke such

symptoms is 120 to 150 dB re 0.0002 μ b in the range 1.6 to 4.4 Hz (40,44). Severe symptoms are likely to arise during acoustical stimulation at SPLs greater than 140 dB if the noise is predominantly of low frequency, below 10 Hz (Figure 9-36). There is some evidence that noise-induced vertigo is due to direct stimulation of vibration-sensitive end organs in the vestibular apparatus. Nystagmus can be induced by noise of extreme intensities (over 150 dB) directed into the ears of deaf subjects (1). The vertigo and disorientation might result from irradiation of vestibular centers in the brain by the "overflow" of impulses from the intensely-stimulated auditory pathway. Feelings of rotation are not a feature of noise-induced vertigo (40).

Apart from subjective effects and interference with performance and communication, intense noise elicits certain central neurophysiological reactions. Very loud or sudden noises evoke fear and avoidance reactions in man and animals. Continuous loud jet noise (overall levels of 120 dB to 7,500 Hz) can produce irritability and a sense of fatigue (50,101), the neurophysiological basis of which is difficult to define. Experimental evidence exists, however, to show that, in addition to the direct sensory projection to the auditory cortex, the labyrinth projects to the reticular activating system of the brain stem, where an increase in activity is produced by intense acoustical stimulation (199).

Loud tonal signals produce arousal and have the effects of blocking alpha activity in the electroencephalogram and evoking on-and-off responses and auditory driving at 10 Hz (157). It is, of course, commonplace that noise awakens sleepers. It is most likely to do so during the early stages, before the sleep is deep (108). In certain animals (notably rats, mice, and other rodents), intense noise can induce epileptiform fits, or audiogenic seizures (6).

A variety of clinical and physiological indices have been observed to show changes in response to intense noise (50,82). These changes include fluctuations in respiratory rate, pulse rate and blood pressure (101, 124, 125), decreases in gastro-intestinal motility (179) and alterations in regional blood flow, including that in the cochlea itself (163).

There are many investigations, primarily European, dealing with physiological effects of noise on the circulatory and endocrine systems (68). These workers report constriction of peripheral blood vessels in the skin as the most consistent characteristic reaction of the sympathetic nervous system to noise (101,124,125). This increase in peripheral vascular flow resistance is followed by a general decrease in arterial blood flow. The degree of this reaction depends on the intensity of the noise, is independent of the frequency, but increases with the bandwidth of the noise. These reactions were found to start at loudness levels between 60 and 70 phons and remained unchanged throughout the exposure. Therefore, they are considered phenomena separate from startle reactions. They are independent of the subject's familiarity with the noise since they were also found in industrial noise workers when exposed to the same noise spectrum in which they had worked for years. These reactions are also reported to be present, to an even stronger degree, during sleep.

The time for peripheral circulation to return to normal was, for exposure up to one hour, always longer than the exposure time. An example of such noise effects on the finger pulse and its recovery time is illustrated in Figure 9-35. That continuous or too frequent activation of this normal, primitive emergency reaction can lead to permanent changes and effects is only inferred in some studies. A clinical study of 1,000 steel workers revealed a statistically significant increase of vascular disorders and cardiac arrhythmias among groups exposed to high noise environments (90-120 phons) for more than three years (101). Even after exclusion of workers using

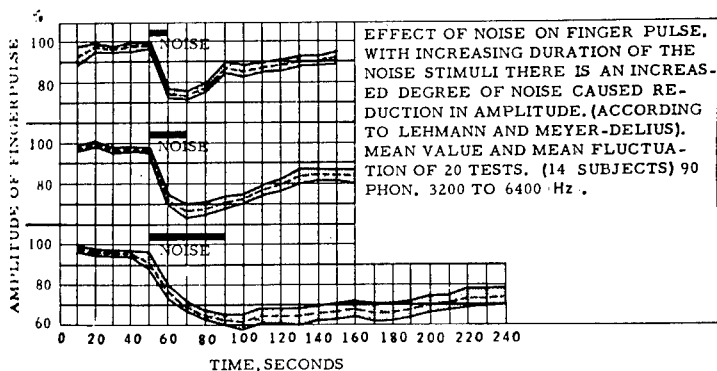


Figure 9-35

Effect of Noise on Peripheral Circulation
(After von Gierke⁽⁶⁸⁾, adapted from
Lehmann and Meyer-Delius⁽¹²⁴⁾)

pneumatic tools, symptoms similar to those in Raynaud's phenomenon were statistically more frequent among workers exposed to the highest noise level.

A battery of tests, including renal, electrocardiographic, electroencephalographic and haematological examinations have been performed on human subjects exposed to turbojet noise at an overall SPL of up to 120 dB (50). Their findings were largely negative and, although fluctuations in the fasting blood sugar level were recorded, the results of the experiments indicated complete physiological adaptation to the noise. In general, the non-aural physiological reactions to noise appear to be non-specific responses to startle, fear, or stress. Therefore, the metabolic and endocrinological effects of noise may generally be interpreted as non-specific responses to noise as a stress (82). A number of studies have been made of the adaptation response to noise, including measurements of blood eosinophil levels and adreno-cortical function (6, 50, 83). Weight losses ranging from 5.5 to 19 lbs in five out of nine human subjects exposed to jet noise for a total of 20 hr over a period of 6 weeks have been recorded (50). The causes of this weight loss are not entirely clear.

Effects of Noise on Performance

Effects of noise on nonauditory performance have been demonstrated (48, 79, 102, 103, 114, 138, 159, 163, 171). Work efficiency on tasks involving vigilance (alertness) over long time periods is reduced in noise environments of the order of 100 dB (48, 102). Levels of noise above 90 dB degrade performance of multiple-choice, serial-reaction tasks. High-pitched noise having a spectral preponderance above 2000 Hz had a more deleterious effect than low-pitched noise below 2000 Hz. Recently psychomotor performance

using Atsai-Partington test of 16 subjects was evaluated under four noise conditions, during four test sessions. Three experimental conditions each began with different intensities of noise (quiet, overall 85 dB, or overall 95 dB) extending over a band from 150 to 9,600 Hz. After 30 minutes exposure the noise was changed to a final high intensity level (110 dB), which lasted for 15 minutes. The fourth condition served as a control, in which quiet prevailed throughout the entire 45 minute period. The results partially supported the hypothesis that greater changes in noise levels produce greater decrements in performance. There was, however, a strong interaction between noise conditions and sessions. The nature of this interaction indicated that this phenomenon does not occur uniformly throughout the course of learning, and probably is of lesser importance for well learned tasks.

Psychomotor performance has also been measured on a rail test during free-field exposure to wideband noise at an overall level of 120 dB. Subjects wore various combinations of ear protectors to obtain experimental conditions of: (1) sound pressure levels equal in both ear canals (balanced condition) and (2) sound pressure level greater in one ear canal than in the other (unbalanced condition). Man's ability to maintain his equilibrium was adversely affected by the unbalanced noise condition. Future research will be directed to performance in exposure conditions higher than those employed in this study.

It has been concluded that in tasks calling for both speed and skill, noise increases the incidence of mistakes although the rate of working may remain unchanged (82). It has also been shown that vigilance suffers in the presence of intense noise (overall SPL \approx 114 dB re 0.0002 μ b). Time-judgment may also be altered by noise of a similar intensity in a complex manner (103,105). There is a possible connection between signal rate and the effects of noise in vigilance. Harmful effects of noise have been found on a task which involved a high signal rate coming from several sources of information, while no harmful effects of noise were found on a closely similar task with a low signal rate and only one source of information (103). It might well, however, have been division of attention rather than the presence of numerous signals, which made one of the tasks sensitive to noise, although doubt is shed on this hypothesis by a more recent study (19). In a task which always involved three sources of signals, it was shown that effects of noise were less likely to appear if note was taken only of those cases in which the subject was absolutely certain that he had seen the signal which his instructions required him to detect. If, however, note was taken of responses made with a low degree of confidence, effects of noise were more likely. This study in itself did not provide sufficient evidence to exclude altogether the role of division of attention. In a later experiment men were asked to watch a regularly flashing light and to report any flashes which were abnormally bright. Some subjects watched only one light and received a low frequency of signals; some subjects watched three lights, any one of which could deliver a signal, and each of which in fact delivered as many signals as the single light in the condition already described. A third group of subjects watched only one light but received as many signals as did the subjects who watched three lights. The clearest deterioration in performance in noise appeared in this latter group who did not have to divide attention but who did receive a high rate of signals. There was no sign of an effect upon the men who saw very few

signals, who were indeed, if anything, improved by a loud noise. The subjects dividing their attention between three sources of signals were in an intermediate condition.

The mechanism of the effect of noise is still ambiguous although the above physiological and psychological measures suggest that it is indeed arousing. Response-time in a vigilance task is lengthened during combination of noise and vibration, and combined environmental stresses (heat, noise, vibration, etc.) may be synergistic in their effects on performance (129). In a recent study, ten pilots were tested for 20 minutes under ten combinations of heat and noise (39). The subjects simultaneously performed two monitoring tasks and one tracking task. Data were also obtained on six physiological measures and two subjective measures. The study indicates that temperatures as high as 110°F (in combination with 50 percent relative humidity and 150 feet per minute air velocity) and noise as high as 110 dB result in no degradation in performance or thermal equilibrium. Heat was found to increase heart rate, axillary temperature, and thigh temperature, but did not affect rectal temperature. Noise was found to increase heart rate and respiratory rate. Interaction between noise and heat suggests that noise lowered thigh temperature at ambient temperatures in the vicinity of 100°F. The subjective data indicate that 80°F is the most comfortable temperature at levels of humidity and air velocity that were used. The subjects were unable to estimate the effects of heat on their performance, although they were able to estimate the effects of noise.

In general, it may be said that the effect of intense noise on work is distracting rather than disabling, and noise is most troublesome when it is irrelevant to the task in hand. Extremely high noise levels can interfere with the accuracy of precision manual-dexterity tasks through noise-induced vibrations of body parts. They can affect the sense of equilibrium, add to disorientation, motion sickness, etc., depending on the specifics of the environment and the type of noise. It should be remembered that the level of noise required to exert a measurably degrading effect on task-performance (overall SPL greater than 90 dB) is considerably higher than the highest levels which are acceptable according to other criteria (e. g., hearing conservation or communication) (82).

The possible use of noise and variations in noise patterns as positive psychological stimuli to alleviate isolation and monotony has been studied (19, 210). The masking of pain by noise, as recently applied in dental work (audio analgesia), is also an effect to be mentioned in connection with space missions (64).

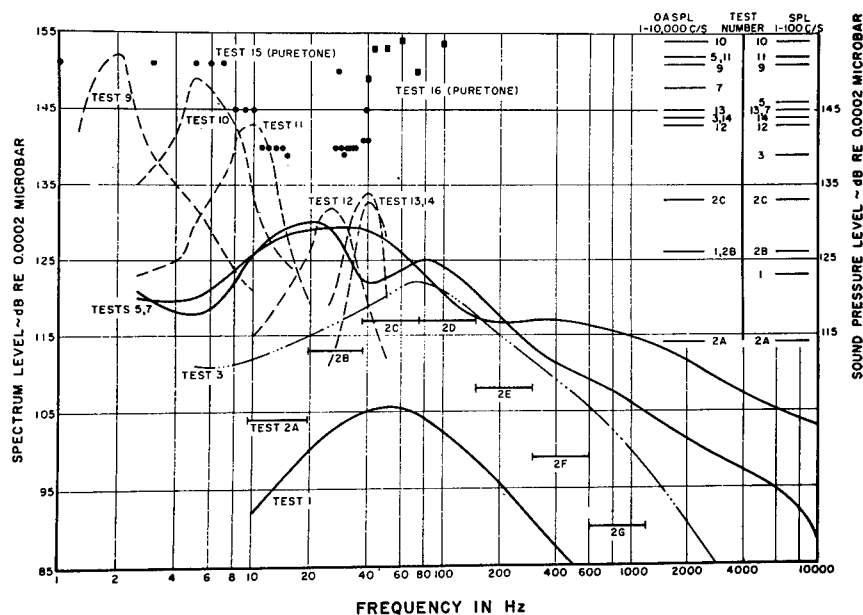
It is sometimes claimed by litigious farmers that aircraft noise so disturbs farm animals that chickens fail to lay, cows fail to yield milk, or pigs fail to fatten (209). Studies of the last phenomenon, supported by endocrinological investigations, yielded no evidence that the animals were adversely affected by repeated exposure to intense aircraft fly-over noise (209).

Low Frequency and Infra-audible Sound

Exposure to low-frequency, high-intensity noise has had little study prior to the space program (9, 70). Pain thresholds were recorded at approximately 179 dB for static pressure, 165 dB at 3 Hz, and decreasing to the range of 140 dB from 15 to well above 100 Hz. In the past, little comment was made on nonauditory effects. The noise-experienced subjects of the previous studies observed no sensations of disturbed equilibrium or nausea during exposures to tones below 30 Hz even at sound pressure levels inducing pain (9).

Recent studies cover the spectra noted in Figure 9-36a (138). For the sake of comparison, random noise exposures are plotted as spectrum level. Overall sound pressure levels and levels for the 1-100 Hz frequency range are indicated on the right ordinate. Five noise-experienced Air Force officers (4 males, 1 female, ages 24 to 26) comprised the subject panel for these tests. For exposure to the jet engine noise (test 3) heavy clothing was worn because of low ambient temperature; for the other tests, light clothing was worn. Standard Air Force ear protectors (earplugs, earmuffs or the two combined) were worn throughout the exposures to the jet engine (test 3), to the Thermal Structures Tunnel (tests 4-8) and to the RTD Low Frequency Siren (test series 16) because the sound pressure levels for the frequency

Figure 9-36
Response to High Intensity - Low Frequency Noise
(After Mohr et al(138))



a. Summary of Test Environments

Summary analysis of representative noise exposures for tests 1 to 16. Random noise exposures are plotted in spectrum level (left ordinate) with overall sound pressure levels indicated on right ordinate. Response to these spectra are given in Table 9-36b.

Figure 9-36 (continued)

b Table of Physiological and Performance Responses to Spectra of Figure a

Test 1 - At sound levels predicted for the crew compartment atop the Saturn Booster, subjects reported no significant disturbance of vision, verbal communication, spatial orientation or finger dexterity. Pulse rates remained stable with no significant fluctuations that could be ascribed to the noise exposure. Minor chest wall and body hair vibration were noted but were in no way considered distressing. All subjects concurred that the exposure was unquestionably tolerable.

Test 2 - Test was carried out in seven steps, during each of which the subjects were exposed for two minutes to a single octave band of white noise at a sound pressure level approximately 10 dB higher than the levels for the corresponding bands in the test 1 spectrum. All subjects reported the test environments as tolerable with no significant subjective responses other than mild chest wall and body hair vibration noted during the 35-70 Hz and 70-140 Hz band exposures. Objective observations were negative. Subjects' speech signals were being modulated somewhat by the noise, though intelligibility remained good. It was clear from the experiences of all subjects during these exposures that insert earplugs do provide substantial attenuation for noise of very low frequency. It was equally clear that none of the earmuff devices when worn alone gave significant reductions and that some models appeared to amplify the noise under the muff. Earmuffs placed over insert earplugs did seem to add to the attenuation achieved by plugs alone.

One subject wore no ear protection for considerable of the total exposure time in tests 1 and 2 and each of the others tried the various noise environments without protection for short intervals. It is assumed also that minimal or no protection was afforded when muffs only were worn. No shifts in auditory acuity were detected following the tests.

Test 3 - All subjects considered the noise environment as tolerable so long as ear protection was used. Visual acuity, spatial orientation and hand coordination were not subjectively affected. However, all subjects reported mild chest wall vibration and one subject reported "awareness" of his respiratory action. Speech sounds were completely masked by the higher frequency portion of the spectrum making direct verbal communication within the noise field impossible. Limited speech communications is carried out by maintenance men in similar noise fields through use of interphone systems incorporating noise-cancelling microphones.

Tests 4 & 5 - Test 4 was unremarkable. The test 5 environment contained the highest levels of low frequency noise to which the subject panel had yet been exposed, but also contained very high level energy throughout the audible spectrum. The speech signals recorded were completely masked despite the noise reduction provided by microphone and shield. Pulse rates were increased 10 to 40 percent over resting levels. Two subjects reported mild chest wall vibration, two others noted mild nasal cavity vibration, and one of these perceptible throat fullness. All agreed that the addition of the high level infrasound did not appear to modify the responses observed many times previously in noise fields having similar energy distribution through the higher frequency ranges.

Tests 6, 7 & 8 - These tests provided exposures which retained intense very low frequency noise components but had relatively less energy in the higher frequencies. All subjects considered the exposures tolerable for the short durations involved. Speech signals were completely masked, nevertheless, except those of one subject who was stationed inside a vehicle which afforded appreciable attenuation of the high frequencies. His speech was definitely modulated but the poor intelligibility achieved was attributed to the masking. All subjects reported mild to moderate chest wall vibration; two subjects noted throat pressure; three subjects experienced perceptible though tolerable interference with the normal respiratory rhythm. Pulse rates measured during test 7 exhibited no significant changes during the exposure.

Throughout these tests visual acuity, hand coordination and spatial orientation were subjectively normal.

Tests 9 - 11 - The most prominent effects attributable to the infrasonic noise spectra (test 9-11) occurred during exposures without ear protection. An uncomfortable sensation reflecting pressure build-up in the middle ear was elicited which required frequent Valsalva to relieve. This effect was almost entirely absent when insert earplugs were used. Although earmuffs alone proved no more effective in attenuating the low frequency noise than they had in tests 1 and 2, they did help prevent the middle ear pressure changes. Three subjects described an occasional tympanic membrane tickle sensation during these exposures without protection and one subject observed marked nostril vibration. Another noted mild abdominal wall vibration during exposure to the test 10 spectrum (5-10 Hz). No shifts in hearing threshold were detectable one hour following these exposures. When ear protectors were worn to lessen the middle ear pressure changes, exposures to infrasound of these levels were judged well within tolerance.

Tests 12-14 - The maximum intensity low sonic exposures produced moderate chest wall vibration, a sensation of hypopharyngeal fullness (gagging) and perceptible visual field vibration in all subjects. Two subjects experienced mild middle ear pain during brief periods without ear protection but a third had no sensation of tickle or pain. Recorded speech sounds exhibited audible modulation; however, the intelligibility scores were unchanged from the control values (control scores, 94-98 percent; exposure scores 93-98 percent). Post-exposure fatigue was generally present after a day of repeated testing. The exposures as a group were not considered pleasant; however, all subjects concurred that the environments experienced were within the tolerance range. No statistically significant objective effects were detected in tests 9-14, but the objective tests must be considered gross and would not necessarily detect minor decrements occurring below the threshold of subjective recognition.

Test 15 - Exposures to 24 discrete frequency noise fields showed both objective and subjective responses qualitatively similar to those elicited by the corresponding narrow band spectra. Pressure build-up in the middle ear was not a factor at 30 Hz and above but the gag sensation was magnified for at least one subject. Although all exposures were judged tolerable, it was noted that the subjective sensations rose to intensity very rapidly as sound pressure levels were increased above 145 dB.

Test 16 - Siren capability limited the maximum levels of exposure at 40 Hz and 43 Hz. Above this frequency range voluntary tolerance of the three subjects was reached at 50 Hz (153 dB), 60 Hz (154 dB), 73 Hz (150 dB), and 100 Hz (153 dB). The decision to stop exposures at these levels for the time being was based on the following subjectively alarming responses: mild nausea, giddiness, subcostal discomfort, cutaneous flushing and tingling occurred at 100 Hz; coughing, severe substernal pressure, choking respiration, salivation, pain on swallowing, hypopharyngeal discomfort and giddiness were observed at 60 Hz and 73 Hz. One subject developed a transient headache at 50 Hz; another developed both headache and testicular aching during the 73 Hz exposure.

A significant visual acuity decrement (both subjective and objective) occurred for all subjects during the 43, 50, and 73 Hz exposures. Speech sounds were perceptibly modulated during all exposures; however, analysis of the speech tapes revealed no decrement in intelligibility that could be primarily ascribed to the modulation effect. Intelligibility scores fell from a normal 95-100 percent to a low of 77-86 percent for the highest level exposures; a decrease of this magnitude would be expected to occur, however, due to the masking effect of the higher harmonics present in the noise environments.

All subjects complained of marked post-exposure fatigue. No shifts in hearing threshold were measurable two minutes post exposure; the earplug and muff combinations worn are known to provide sufficient protection against the higher harmonics of the noise fields and were apparently effective to an appreciable degree in attenuating the fundamental tones. Recovery from most of the symptoms was complete upon cessation of the noise. One subject continued to cough for 20 minutes, and one retained some cutaneous flushing for approximately four hours post exposure. Fatigue was resolved by a night's sleep.

range known to injure the organ of hearing were also very high. During exposures in the AMRL High Intensity Noise Chamber (tests 1-2) and in the NASA-LRC Low Frequency Noise Facility (tests 9-15), where the higher frequency components were relatively low in level, most subjects experimented with various combinations of protection as well as exposure with bare ears.

Although exposure times of at least two minutes each were desired, the period for test 3 (jet engine) was limited to one minute by ground operating restrictions on the engine. Durations of exposures to the Thermal Structures Tunnel noise (4-8) were determined by the blow-down time of the tunnel under the conditions used. For tests 4 and 5, exposure time was 60 seconds; for tests 6-8, durations were only 25 seconds. All other tests lasted a minimum of two minutes at each intensity level presented.

The following tests were performed: visual acuity (modified Snellen E); one-leg stand; finger to nose test; handwriting; finger dexterity; hand coordination; direct speech intelligibility; and objective intelligibility by a modified Rhyme Test of Word Intelligibility, scored by trained listeners using the subjects speech responses recorded on magnetic tape through noise-canceling microphones encased in acoustically isolated shields. The test results noted in Table 9-36b are taken directly from the report (138).

In summary, the maximum infrasonic exposure levels produced by the available simulation devices did not reach the voluntary tolerance limit for noise-experienced subjects; however, the unusual sensations excited by the oscillating pressure environment could be alarming to the naive observer. In the very low sonic frequency range, chest wall vibration, gag sensations, and respiratory rhythm changes were regularly observed. But the limits of voluntary tolerance were not exceeded by the exposure levels available from the various devices.

In the 50-100 Hz range, the simulator capability for discrete-frequency noise was sufficient to generate subjectively intolerable environments. Responses including headaches, choking, coughing, visual blurring, and fatigue were sufficiently alarming to preclude undergoing higher level exposures without more precise control of the noise environment and definition of the physiologic effects elicited.

The presently available data thus support the conclusion that noise-experienced human subjects, wearing ear protectors (145), can safely tolerate broad-band and discrete frequency noise in the 1-100 Hz range for short durations at sound pressure levels as high as 150 dB (138). At least for the frequency range above 40 Hz, however, such exposures are undoubtedly approaching the limiting range of subjective voluntary tolerance and of reliable performance. As would be expected, the responses reported by these five subjects during the various test series reflect considerable variability in the subjective effects. At present, the magnitude of possible individual and group variability cannot be accurately estimated.

Sonic Booms

Sonic booms are one form of noise which is of great current interest because of the potentially large percentage of the population affected by it and because of economic consequences (7, 16, 18, 23, 93, 131, 132, 144, 181). None of the response criteria discussed can be meaningfully applied to its evaluation. Disregarding the brief startle response, no damage to hearing or any other harmful physiological effect can be attributed to exposure to pressure waves of the magnitude experienced by communities. As shown in Table 9-37 there is hardly any noteworthy interference with most tasks or job pro-

Table 9-37

Measured or Predicted Effects of Overpressure from Supersonic Vehicles (Sonic Boom)

(After von Gierke⁽⁶⁸⁾, adapted from Nixon⁽¹⁴⁴⁾)

Peak Overpressure			Predicted and/or Measured Effects	
Lbs/In ²	Lbs/Ft ²	Dynes/cm ²		
0—7.10 ⁻²	0—1	0—478		No damage to ground structures. No significant public reaction, day or night.
7 × 10 ⁻² —1.05 × 10 ⁻²	1.0—1.5	478—717	Sonic booms from normal operational altitudes:	No damage to ground structures; probable public reaction.
1.05 × 10 ⁻² —1.4 × 10 ⁻²	1.5—2	717—957	Typical community exposures (seldom above 2 lbs/ft ²)	No damage to ground structures; significant public reaction, particularly at night.
1.4 × 10 ⁻² —3.5 × 10 ⁻²	2.0—5.0	957—2,393		Incipient damage to structures.
1.4 × 10 ⁻¹ —8.10 ⁻¹	20—120	9.57 × 10 ³ —5.74 × 10 ⁴	Measured sonic booms from aircraft flying supersonic speeds at minimum altitude: experienced by humans without injury.	
5	720	3.44 × 10 ⁵	Estimated threshold for eardrum rupture (maximum overpressure),	
15	2,160	1.033 × 10 ⁶	Estimated threshold for lung damage (maximum overpressure),	

ficiencies. In this area, tools are restricted to measuring the diffuse annoyance or complaint pattern of the population exposed to the boom and to arriving at operational criteria based on such data. This is the goal and purpose of the various sonic boom studies conducted by the US Air Force, NASA, and the FAA over the last ten years on an ever-increasing scale. These are not medical safety criteria, not task interference criteria, but expressions of the majority of a population showing that they are annoyed and willing to complain and act against such noise intrusion into their personal lives (68).

Ultrasound

The mechanics of the absorption of ultrasonic vibrations by body tissues have been covered in Vibration (No. 8). (See Figure 8-19). Data on the general acoustic properties of different human and animal tissues are also available (41, 77, 80).

Ultrasound has not been studied as a naturally occurring phenomenon (except for low-frequency, low-intensity emanations of animal origin) (20).

Information has been obtained in laboratory environments and almost entirely in animal rather than human experiments (42, 88). The most comprehensive investigations, with detailed histological studies, have been made on the central nervous system of the cat and other small animals (42, 60). The human brain has been modified at localized sites by intense ultrasound, but there has been insufficient material for extensive histological study (61). However, the dosage conditions employed to induce functional change, and the histological results available, indicate that the effects on the human brain are the same as those observed in the cat. Precisely placed ultrasonic lesions have been produced in a number of deep brain structures in man for treatment and relief of the signs and sensations associated with hyperkinetic, hypertonic, and intractable pain disorders (61, 62, 77, 134).

High-intensity ultrasound produces physiological changes which are observable immediately (60), but the effects of tissue structure, at dosages which produce selective irreversible changes, occur at sub-microscopic sites and cannot be seen in stained tissue sections until after a time interval of minutes to an hour after exposure. Acoustically induced cavitation has been eliminated as a primary factor in the development of irreversible changes, by producing lesions as well as motor deficits under a hydrostatic pressure sufficiently great to prevent tension forces from occurring in tissue. The fact that physiological changes are evident immediately after exposure, but that histological changes do not begin to appear until later, has led to investigations of the possible interaction of intense noncavitating ultrasound and biologically important molecular species in solution (78, 88, 91).

Damage from ultrasound in the space program may arise in exposure to rocket and jet noise. Ultrasonic vibrations are also used in non-destructive testing of metals, in cleaning baths, in measuring devices, in power and communication control, in drilling and welding processes, and in medical diagnosis (77, 80, 88, 168).

The effect of diffuse total body ultrasonic exposure from jet engines and other sources has been reviewed (195). Spectral analyses of the noise obtained near turbo-jet engines on the ground or aircraft in flight show that both sonic and ultrasonic vibrations are produced. Intensity levels appear to be reduced as engine speed decreases. There is evidence that, with increasing air speed, the overall intensity level of the noise increases and strong energy components may appear at ultrasonic frequencies as well as in the audible range. This tendency is exaggerated as the speed approaches a Mach number of 1.0. The effects upon man are alleged to involve nausea, disturbance of equilibrium, fatigue, mental confusion, headache, and auditory, visual, and motor disturbances. The effects are said to be transient. Disturbances of equilibration, fatigue, and confusion are the most frequently reported symptoms. These deleterious effects are attributed to ultrasonic vibrations. The logic by which ultrasonic vibrations become the cause is unclear in many of the reports and causal relationships have not been established. To date, such reports have not been based on systematic experimentation (78, 195). Clothing variables are a major factor not under control in the epidemiological studies. Response of animals to total body exposure cannot be directly extrapolated to man (78, 173). In animals, changes in the

hematopoietic, endocrine, and nervous system have been noted at levels as low as 95-100 dB at 54 kc for 1-3 hrs (78).

Warm skin sensation and bone pain from overheating of the periosteum appear to be the first local symptoms noted at high exposures (173). Energy fluxes of over 0.1 watts/cm² for over 10 minutes are probably required for local tissue damage (127, 173). The energies involved in the pulsed diagnostic technique vary from 0.004 to 0.04 watts/cm². At these levels no tissue damage has been observed (5, 58). When ultrasound has been used to produce tissue damage in therapeutic studies, the levels have ranged from 3 to 100 watts/cm² at a duration up to ten minutes (167). In these studies, there appears to be an outstanding deficiency in reporting how the energy levels of watts/cm² were determined. At present, there is no method available for determining this for pulsed waves; and only relative methods for continuous waves. In fact, only in the past years has it been possible to ascertain the electrical-physical continuity of ultrasonic transducers (130). The only way at present to express an energy value of any merit is to determine the energy in the electrical pulse to the transducer and multiply it by the measured, direct-energy conversion efficiency of the crystal; then divide by the area of the crystal. Caution must therefore be used in evaluating the older literature.

NOISE CONTROL AND PROTECTION

There now exists a substantial body of theoretical and technical knowledge about noise and its control (12, 85, 212). In order to reduce the harmful effects of noise, the first step must be to decide what are to be the criteria of acceptable noise exposure - that is to say, which effects of noise are to be protected against and how much noise control is necessary. The second step is to analyze and measure the offending noise, using the techniques already outlined or, when advance planning against noise is contemplated, to predict the acoustical power of the source or sources, the probable quality of the noise produced and its routes of propagation. From the information obtained in the first two steps, it is then possible to calculate the amount of noise reduction required. The final step is to select and apply the most appropriate and economical means of noise control. There are three principal ways in which noise may be attacked: by reduction at source, by reduction in the transmission pathway from the source to man, and by reduction of the effects produced by noise on man.

A number of attempts have been made over the past twenty years or so to specify the maximum levels and durations of various types of sounds that persons can tolerate without suffering some degree of permanent hearing loss. These specifications have usually been in the form of graphs or contours showing, as a function of either the frequency spectrum or the duration, the sound pressure levels considered tolerable. These contours often have been labeled "damage risk criteria," although strictly speaking the contours are not "criteria" - the criterion is the degree of permanent hearing loss in a given percentage of the exposed people that the person deriving the contours deems reasonable. It has been suggested that these be called "damage risk contours" (DRC's) and not damage risk criteria (112).

In the past, the criteria against which damage risk contours were drawn were not usually precisely stated. This was dictated primarily, of course, by the general lack of data available as to the precise effects of exposure to intense sound on hearing. In assessing human reactions to environmental stimuli as a basis for exposure criteria, it must be kept in mind that such reactions can be of completely different natures. For clarity these categories should be separated. Perhaps the best classification is by methods of measurement used; these are (a) objective physiological responses; (b) efficiency of job performance; and (c) subjective verbal response to stimuli. Each of these reactions can lead to different criteria. At question also is what percent of the population at risk should be protected against these criteria. Efforts are underway to arrive at international agreement on noise control and risk criteria in many different environments. (100, 155)

Noise Reduction

In the past, criteria for the prevention of permanent hearing loss took the following form (47, 71, 72, 112, 177, 192, 194). In setting limits for continuous daily exposure, it was assumed that the ears were unprotected and exposed continuously during normal work hours over a period of 25 years (177, 192). The limits for such exposure to broadband noise were approximately 85 dB in the octave bands 300-600, 600-1200, 1200-2400, and 2400-4800 Hz. For higher octave-band sound pressure levels, ear protection was recommended. For octave band sound pressure levels in excess of 95 dB, ear protection was considered mandatory. As noted above, the ear cannot tolerate pure tone (or discrete frequency) levels for as long an interval as broadband noise, so these limits were usually lowered by 10 dB, if the noise contained predominant narrow band components. The permissible sound pressure levels in the octave bands below 300 Hz were somewhat higher. Some criteria assumed that the contribution of noise in these frequency bands to hearing impairment was negligible. Other damage risk criteria made allowances for the natural loss of hearing acuity with age (presbycusis) and allowed, for example, instead of an average 85 dB for the octave bands 300 to 4800 Hz, levels of 92 dB for persons younger than 30 years and 80 dB for persons between 50 and 60 years old (111).

When the exposure was less than 8 hours, daily exposure to higher levels than those specified could be tolerated. The assumptions made were either that equal quantities of acoustic energy determined by constant product (exposure time \times square of sound pressure (47) or equal quantities of the product (exposure time \times sound pressure (111) were equally injurious to the ear. The "constant energy concept" is in widespread use but is probably on the conservative side. The results of studies relating temporary hearing loss to exposure time were in favor of the "constant exposure time \times pressure concept (180, 202). Using either one of these concepts, maximum exposures "equal" to the 8-hour, damage-risk contours discussed above were allowed. These short-time contours are illustrated in Figure 9-38. If several significant exposures at various intensities took place during a working day, these exposures were converted into "equivalent exposure time" (EET) for the criterion level for an 8-hour exposure. If all the equivalent exposure times

when added together, exceeded 480 minutes at the 8 hour criterion level, the daily exposure limit was exceeded (111, 192).

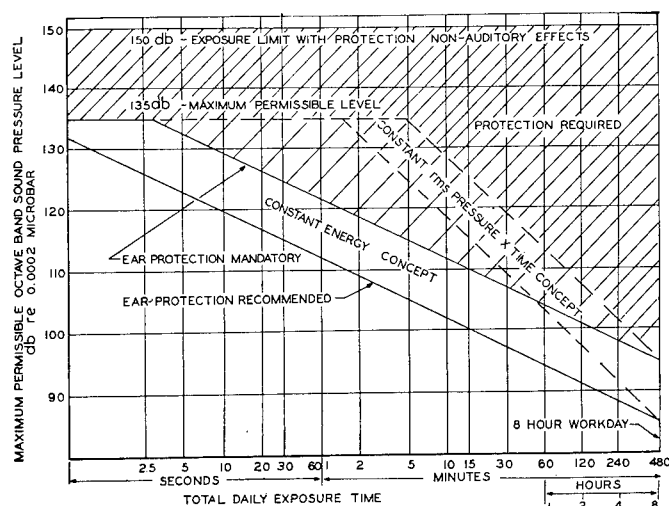


Figure 9-38

Damage Risk Contours for Short Term Exposure to Broad-Band Noise

The curves based on the "constant energy concept" and the "constant pressure times time concept," are shown. The curves designate the limits for safe daily exposure over a period of many years in terms of maximum permissible exposure time or sound pressure level in the octave bands of 300-600, 600-1200, 1200-2400, and 2400-4800 Hz. (For exposure to pure tone noise, the curves should be lowered by 10 dB, however, the maximum permissible level of 135 dB stays the same.

(After von Gierke and Hiatt⁽⁷¹⁾)

As more and more data on the hearing of persons exposed to intense sound have become available, a simpler and more significant concept has emerged on which meaningful criteria of the risk involved in exposure to sound can be based. These are as follows (112, 139):

- For a given population of people exposed to a given intense sound, some will suffer more hearing loss than others. In general, the damage risk contours developed in the past have been such that at least 50 percent of the people exposed to the so-called tolerable DRC's have suffered a significant permanent hearing loss.
- Practically speaking, courts of law, guided by otologists, have distinguished between hearing impairment and hearing handicap. By impairment is usually meant damage or a decrease in the ability of the auditory system to function normally, whereas handicap refers to the condition in which the impairment reaches the stage that the person, as a total organism, is not able to function normally in his everyday living. What is "normal" and what is a "handicap" are obviously subject to various interpretations, depending on value judgments of those attempting to define these terms.
- The only hearing handicap that is judged (according to most medical recommendations concerning industrial deafness) to be truly harmful to a person, and therefore possibly compensable according to law, is a hearing handicap for speech (128). "Impairment" is used by the AAO and AMA as meaning a range from beginning to total disability to hear everyday speech in sentence form. Amount of impairment is given in percent based on binaural hearing determined by a

formula devised by the Committee on Conservation of Hearing and now accepted by most authorities and compensation commissions.

Specifying a damage risk criterion in terms of the statistical nature of hearing losses and in terms of some specified handicap for understanding speech should be a straight-forward process, even though controlled by the value judgments of those making the specifications. Perhaps more difficult, at least in a technical or scientific sense, is the problem of drawing the damage risk contours that are deemed to be acceptable according to whatever criterion one chooses. This task is made complex and difficult because of the tremendous variety of spectral and temporal patterns of sound to which people may be exposed. Sufficient data are available to undertake this task only on so-called "steady-state" sounds; the effects on hearing of that class of sounds called "impulse" have not been studied enough to permit much to be said about what types of exposures are to be considered tolerable (95, 96).

An attempt has been made to describe and explain a set of damage risk contours for steady-state noise that are drawn to meet a criterion based on the concepts outlined above and on the basis of a joint consideration of data of temporary and permanent hearing loss, or threshold shifts, due to exposure to sound (112). These make use of the concepts of speech intelligibility and noise masking covered above. In brief, the suggestion is made that speech energy is to be found between 100 and 6000 Hz or so, but it is maximal in the frequency region below 1000 Hz. It has been found that the speech frequencies below about 1700 Hz are equally as important to the intelligibility of speech as the frequencies above that level. For speech in sentence form, the lower range is more important. For this reason, it is appropriate to protect the ear more with respect to lower frequencies, below, say, 2000 Hz than at the higher.

The sounds in the conversational speech of a single talker cover a range of intensities of over 30 dB. Typically, the weakest components in speech uttered at conversational level and perceived 3 or 4 feet from the talker will be 10 to 15 dB or so above the normal threshold of hearing.

These considerations provide at least a partial basis for explaining the recommendation that the handicap for hearing speech starts only when hearing loss found at 500, 1000, and 2000 Hz averages 15 dB (128). Although this so-called 15 dB audiometric "fence" for evaluating handicap for speech is open to experimental question, it is generally accepted by medical experts at the present time (116). The value of such an approach is now under study by several groups (100, 128, 139).

Figures 9-39 to 9-49 are examples of the more recent approach to long- and short-term exposures (75, 115, 139). These have been accepted by the CHABA Working Group No. 46. Although the damage risk contours presented in these following figures are in terms of pure tones or one-third and full octave bands of noise, these figures are to be used in the evaluation of noises that have greater bandwidths, i. e., extend over more than one octave. The level of each one-third or full octave band in a broader band noise of a speci-

fied duration is to be compared to the damage risk contours given in the figures which follow.

If any single band exceeds the damage risk contours specified, the noise can be considered as potentially unsafe. As progressively more one-third or octave bands of a broader band noise reach the damage risk contours, the hearing loss will become extended over a wider and wider range of the sound frequencies to which the ear is sensitive. Nevertheless, hearing loss at any one frequency region should not be significantly greater than that expected from exposure to a band of noise located about one-half octave below that particular frequency region (115).

Using Figures 9-39 and 9-40, one can find either maximum sound pressure levels for given durations or maximum once-per-day durations for given sound pressure levels for the octave and one-third octave or narrower bands of noise indicated. Figure 9-41 presents damage risk contours for pure tones only. Figures 9-39, 9-40, and 9-41, for single exposures, apply not only to noises whose level is constant over the exposure period, but also to those with a fluctuating level, provided that (a) the noise does not remain at a single level more than 2 min, and (b) the level never drops below the 480 min curves on Figures 9-40 and 9-41, i. e., the level that can be tolerated for a full work-day. The effective level of such a varying noise is equal to the average sound pressure level (SPL) of the noise over the exposure period. Several examples are given:

Example: The level of a noise whose maximum energy is in the 1200-2400 Hz octave band varies between 90 and 100 dB, 30 second (sec) bursts of 110 dB alternating with 90 sec intervals of 90 dB. The effective level is, therefore,

$$(30 \text{ sec} \times 110 \text{ dB} + 90 \text{ sec} \times 90 \text{ dB}) / (30 \text{ sec} + 90 \text{ sec}) = 95 \text{ dB SPL.}$$

From Figure 9-40, the maximum tolerable exposure to this noise is seen to be about 35 min.

Example: A generator with a pronounced whine at 1000 Hz varies in output level between 100 and 120 dB. Measurement shows that the time distribution of the levels is as follows: 120 dB, 25 percent of the time, 110 dB 40 percent, and 100 dB 35 percent. The average level is, therefore, $120 \times 0.25 + 100 \times 0.40 + 100 \times 0.35 = 109 \text{ dB}$. Figure 9-41 indicates that the maximum tolerable exposure to this whine is about 5 min.

Figures 9-42 through 9-49 provide functions showing damage risk contours for interrupted exposures to bands of noise. Figures 9-42 to 9-45 are used for the appropriate band limits or band center frequencies to show the maximum tolerable sound pressure levels for bands of noise having certain center frequencies or to show the maximum duration of daily exposure for bands of noise having certain center frequencies and known sound pressure levels and known on-fraction. The use of Figures 9-42 to 9-45 is limited to situations in which (a) there is alternation between noise and effective quiet

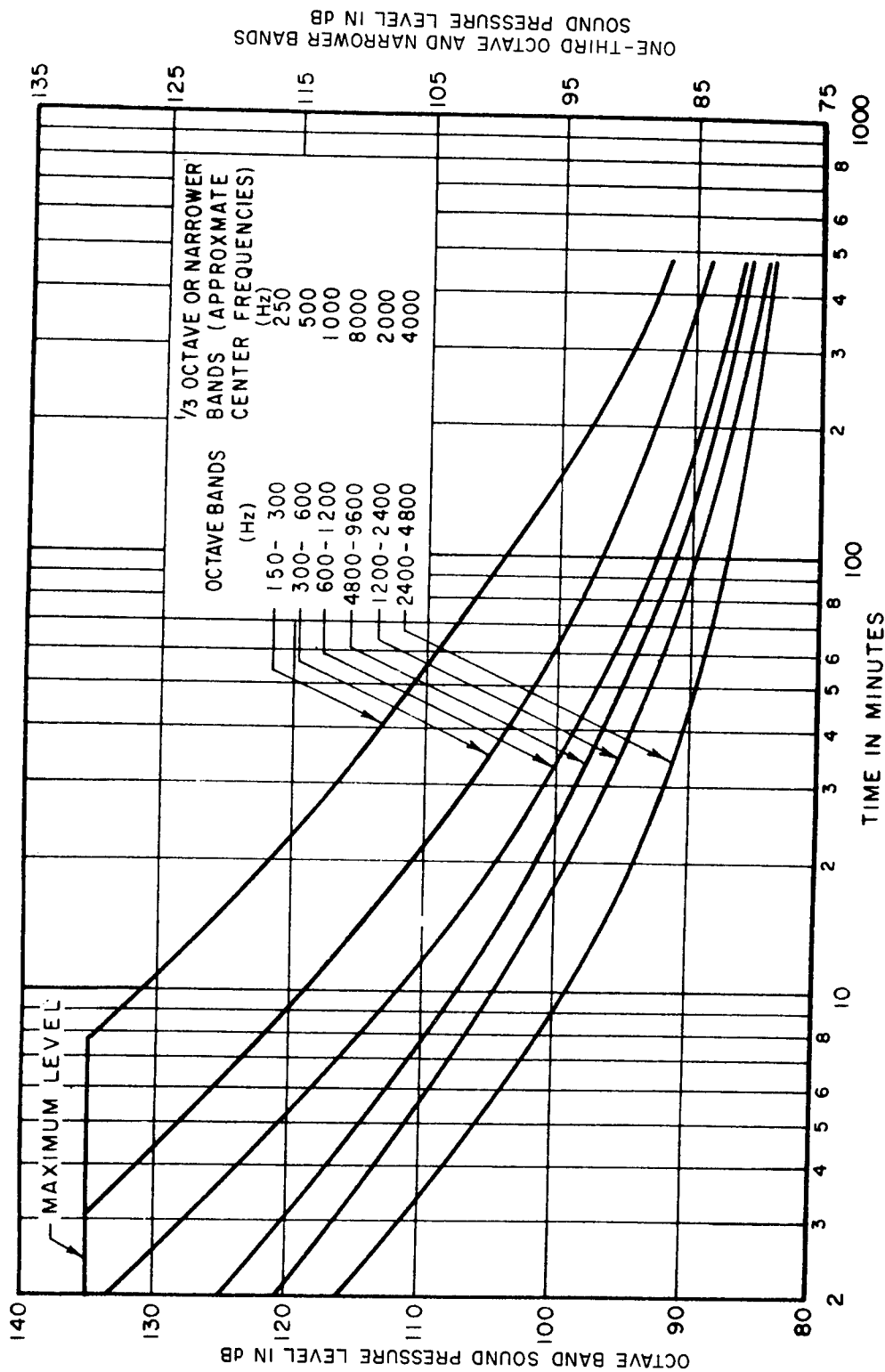


Figure 9-39

Damage Risk Contours for One Exposure Per Day to Certain Octave (left-hand ordinate) and Certain One-Third Octave or Narrower (right-hand ordinate) Bands of Noise

This graph can be applied to individual band levels present in broad band noise

(After Kryter - CHABA(139))

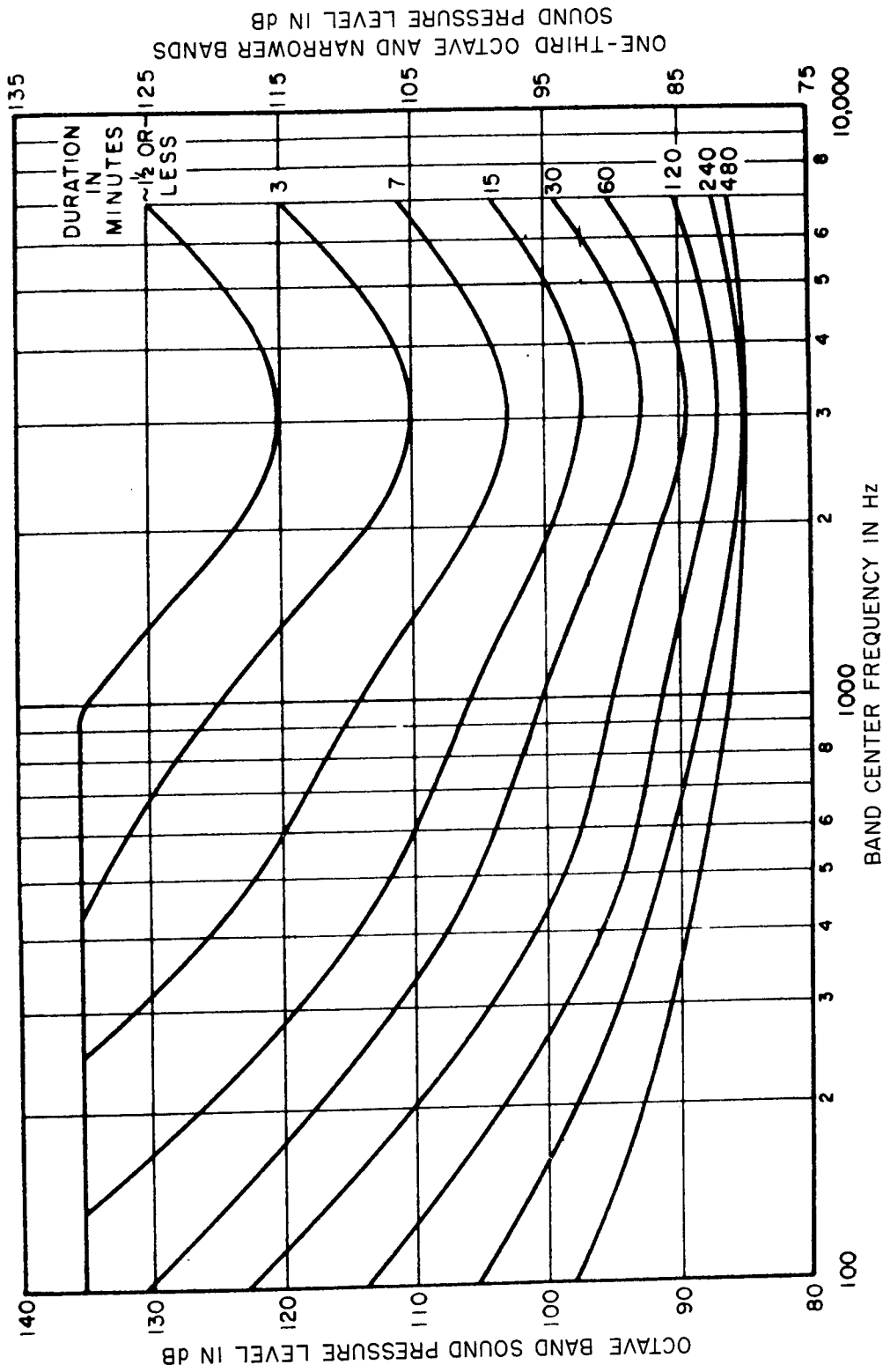


Figure 9-40

Damage Risk Contours for One Exposure Per Day to Octave (left-hand ordinate) and One-Third Octave or Narrower (right-hand ordinate) Bands of Noise

This graph can be applied to individual band levels present in broad band noise.

(After Kryter - CHABA⁽¹³⁹⁾)

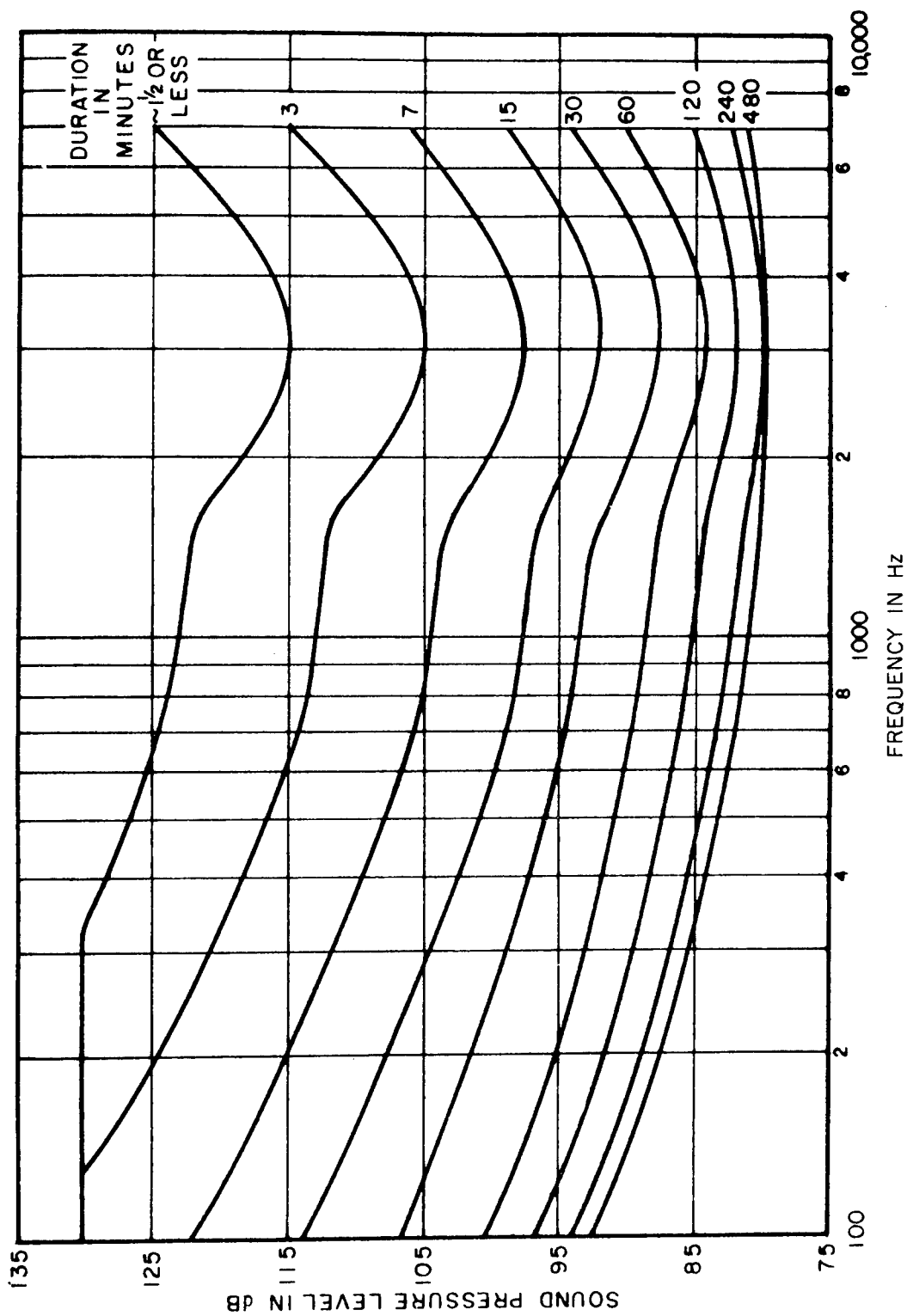


Figure 9-41

Damage Risk Contours for One Exposure Per Day to Pure Tones

(After Kryter - CHABA(139))

throughout the duration of daily exposure, and (b) individual noise bursts do not exceed 2 min in duration. "Effective quiet" exists when the noise level drops below the 480 min curves of Figures 9-40 and 9-41; the "duration of daily exposure" consists of the sum of the durations of the noise bursts and the effective quiet. "On-fraction" (the parameter of Figures 9-42 to 9-45) is the ratio of noise burst duration to duration of daily exposure; thus, it is not the ratio of noise time to quiet time, but the noise time divided by the noise-time-plus-quiet-time.

Example: The maximum tolerable level of the 300-600 Hz octave band of noise that is on for 1 min periods followed by 1 min periods of relative quiet (an on-fraction of 0.5) and a total period of exposure that continues for 60 min is found by entering Figure 9-42 on the vertical line for 60 min. This line crosses the curve for an on-fraction of 0.5 at a sound pressure level of approximately 127 dB (left-hand ordinate of Figure 9-42), the maximum tolerable level for the 300-600 Hz octave band, during the "on" period. The maximum tolerable level in a 300-600 Hz octave band of noise would be 89 dB during the "off" period in this case.

Figures 9-46, 9-47, 9-48, and 9-49 may be used to show the interval of effective quiet that must follow an exposure to an octave band or one-third octave or narrower band of noise having a specified sound pressure level and duration, before the exposure can be repeated during the work day. Effective quiet, again, exists whenever the noise level drops below the contour in Figure 9-40 for 480 min. These figures are to be used when the noise bursts are longer than 2 min in duration.

Example: A 300-600 Hz octave band of noise (Figure 9-46) having a sound pressure level of 115 dB (fourth contour from the left, as indicated by the top row of numbers on Figure 9-46), and a duration of 10 min would require 45 min of effective quiet following the noise burst before a person could be exposed again to the noise, throughout the 480 min work day. Thus, an individual could be exposed eight or nine times to this 10 min noise during the work day, provided he was given a 45 min rest between each exposure.

Example: A one-third octave band of noise with a center frequency of 2000 Hz displays the following time course. For 10 min the noise level alternates regularly between 90 and 100 dB, then drops to 70 dB (effective quiet) for 30 min. The effective level of the noise during the 10 min is thus 95 dB; Figure 9-48 indicates that a 10 min exposure to 95 dB (third contour from the left, indicated by the second row of numbers at the top of Figure 9-48), need be followed by only about 16 min of effective quiet. Therefore, the observed pattern (10 min noise, 30 min quiet) is tolerable over the 8 hr work day.

Example: A noise having its maximum energy in the octave band 2400-4800 Hz has an effective level of 100 dB and must be on for 10 min. The intersection of the 100 dB octave band contour in Figure 9-49 and the 10 min burst duration (abscissa) cannot be

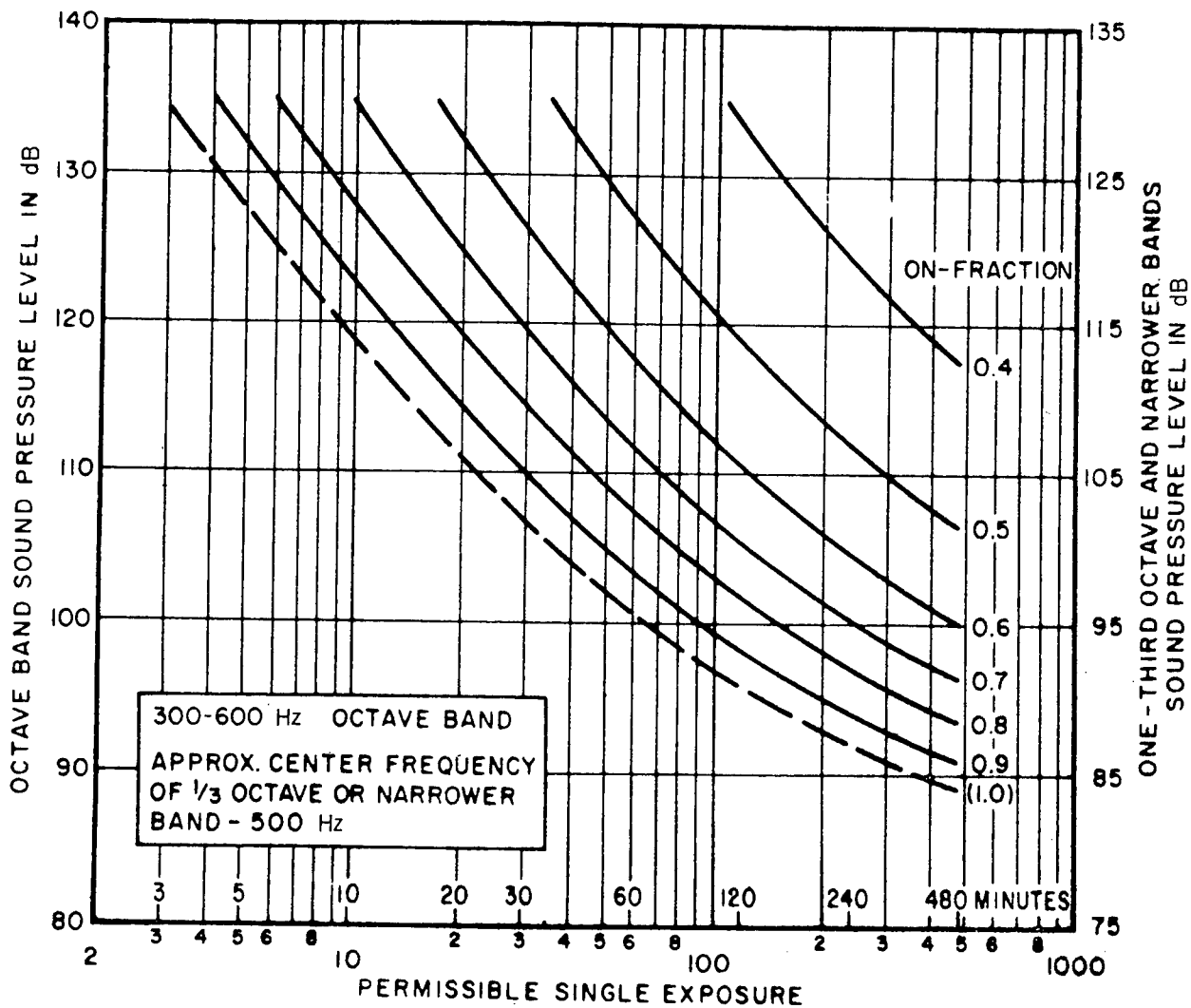


Figure 9-42

Damage Risk Contours for Short-Burst-Duration Intermittent Noise
(Noise bursts 2 minutes or less in duration)

(After Kryter - CHABA⁽¹³⁹⁾)

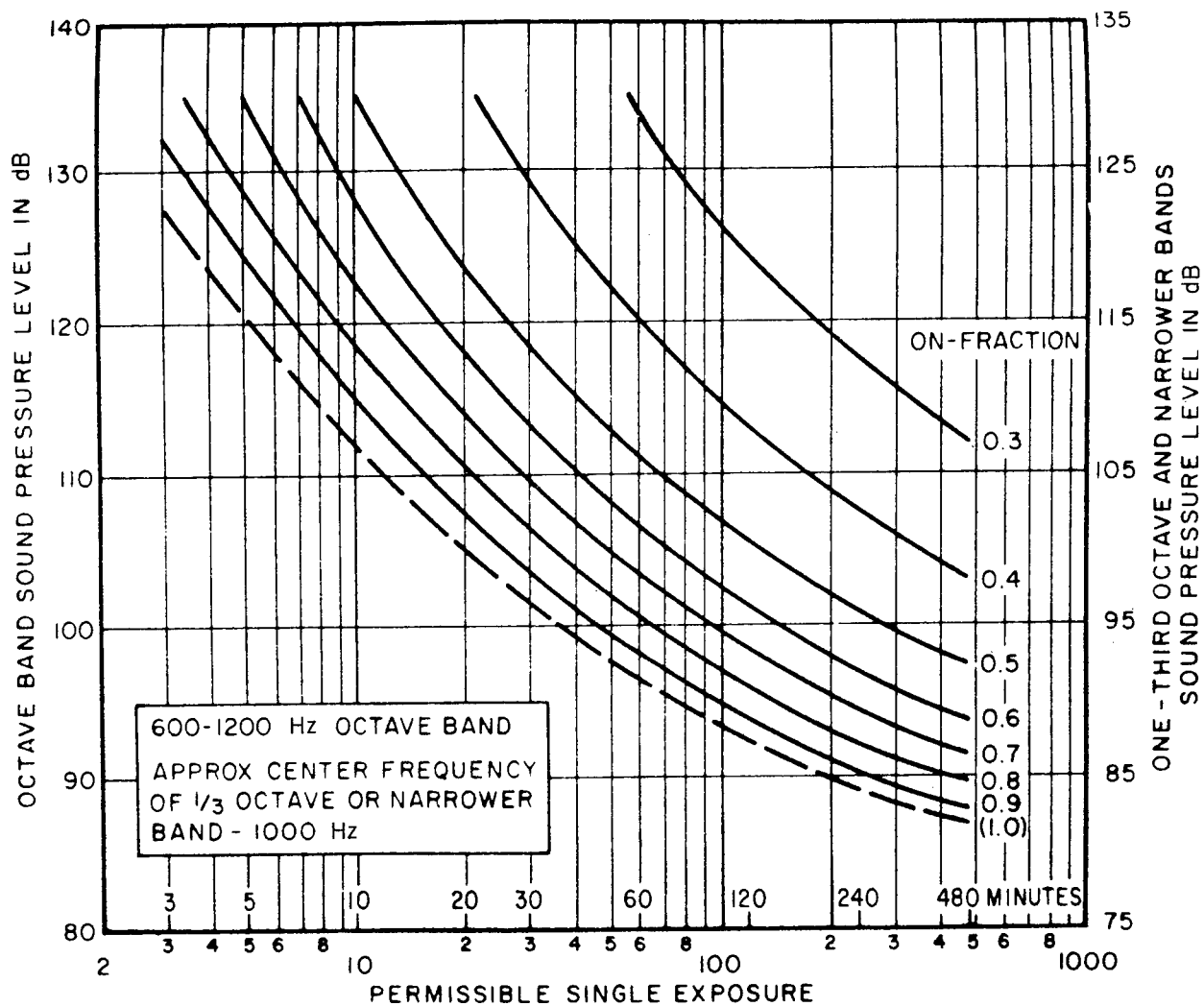


Figure 9-43

Damage Risk Contours for Short-Burst-Duration Intermittent noise
(Noise bursts 2 minutes or less in duration)

(After Kryter - CHABA⁽¹³⁹⁾)

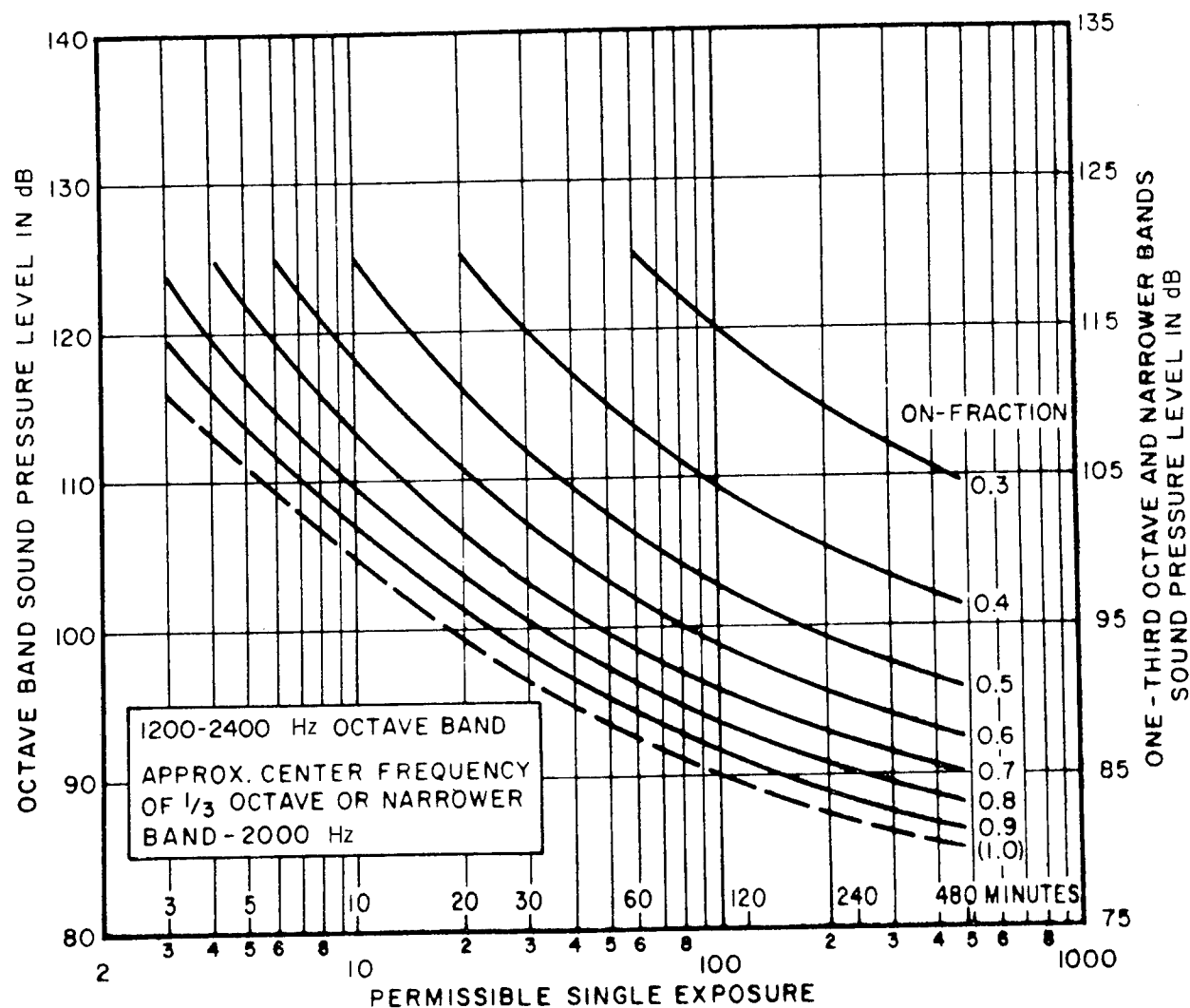


Figure 9-44

Damage Risk Contours for Short-Burst-Duration Intermittent Noise
(Noise bursts 2 minutes or less in duration)

(After Kryter - CHABA⁽¹³⁹⁾)

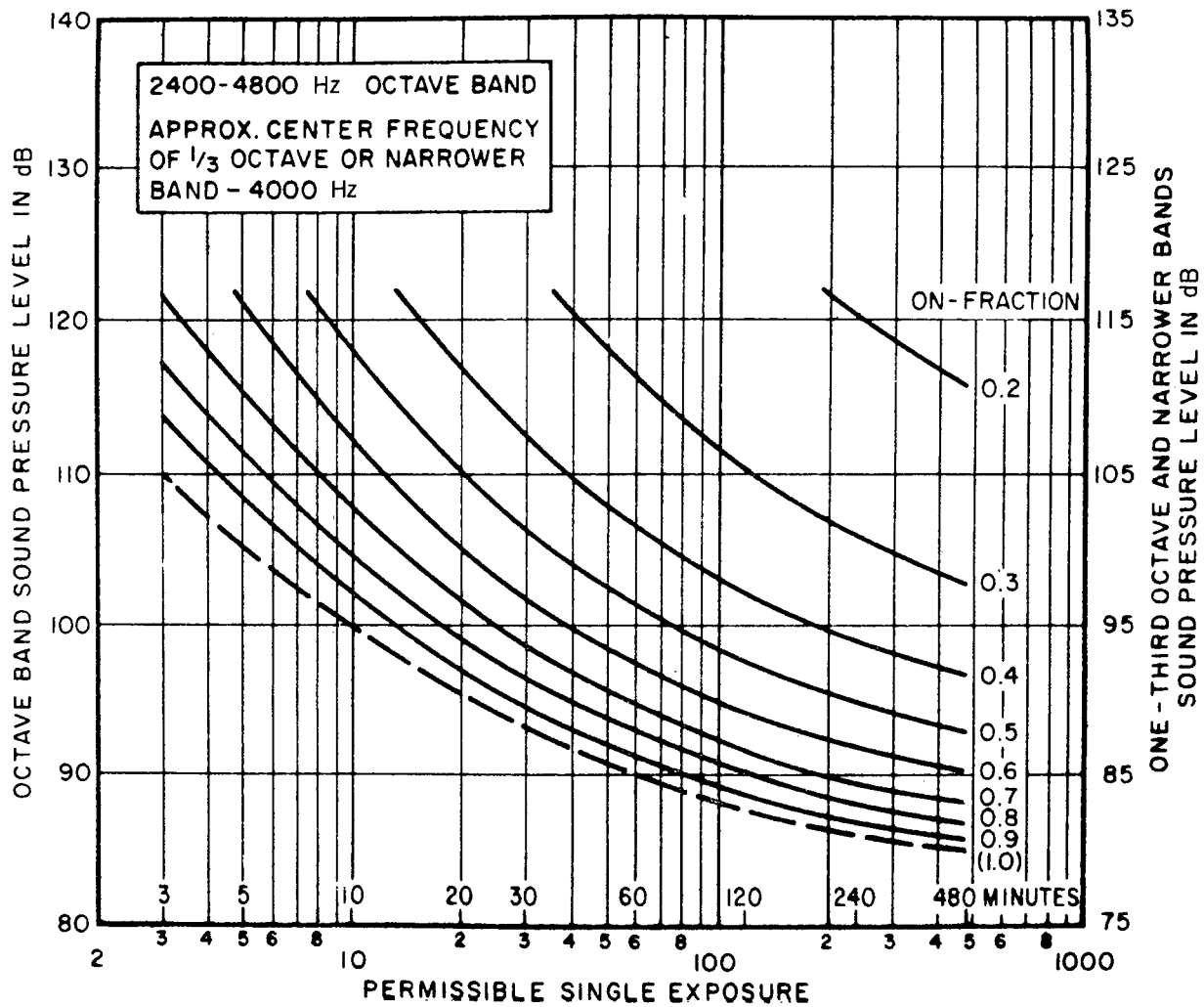


Figure 9-45

Damage Risk Contours for Short-Burst-Duration Intermittent Noise
(Noise bursts 2 minutes or less in duration)

(After Kryter - CHABA⁽¹³⁹⁾)

OCTAVE BAND:	130	125	120	115	110	105	100	95 dB
1/3 OCTAVE OR								
NARROWER BAND:	125	120	115	110	105	100	95	90 dB

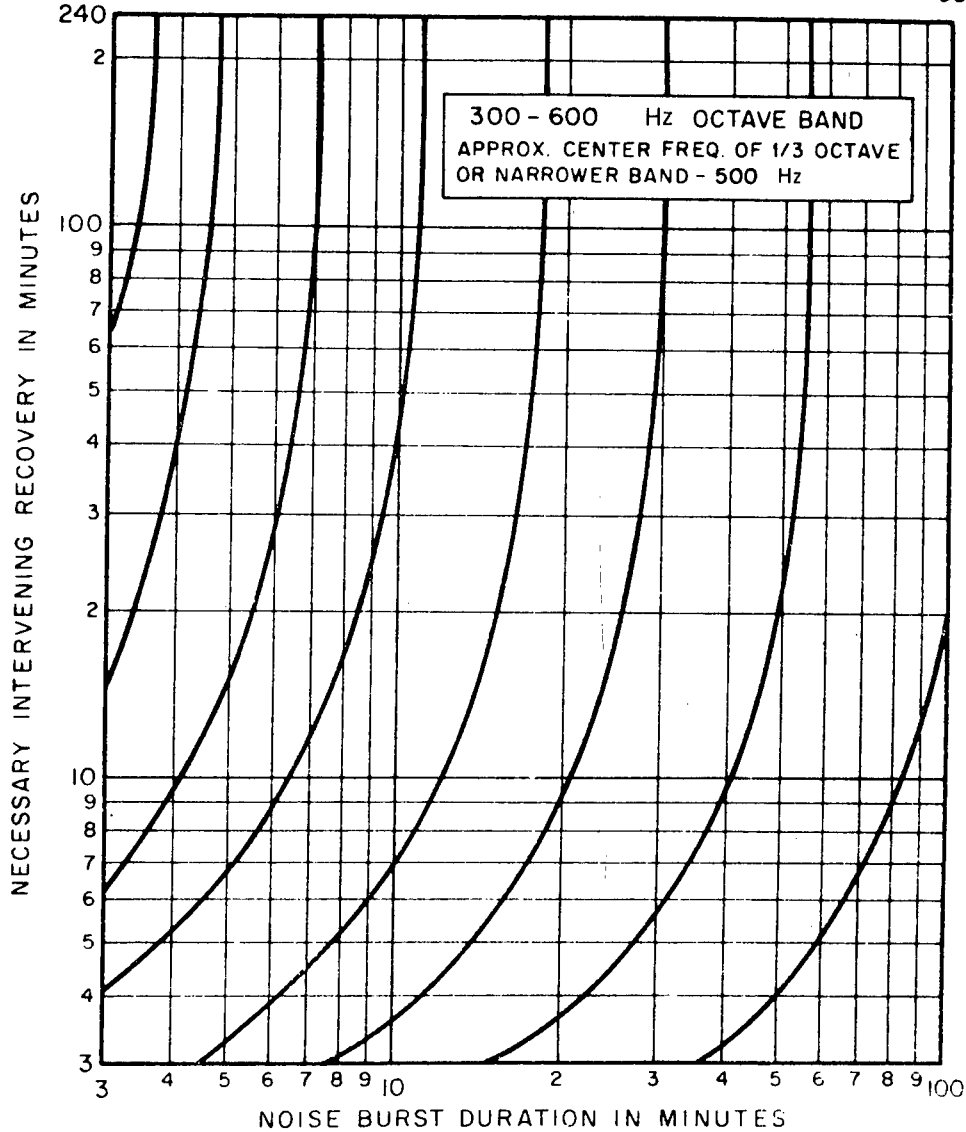


Figure 9-46

Damage Risk Contours for Long-Burst-Duration Interrupted Noise Parameter; Band SPL

(After Kryter - CHABA⁽¹³⁹⁾)

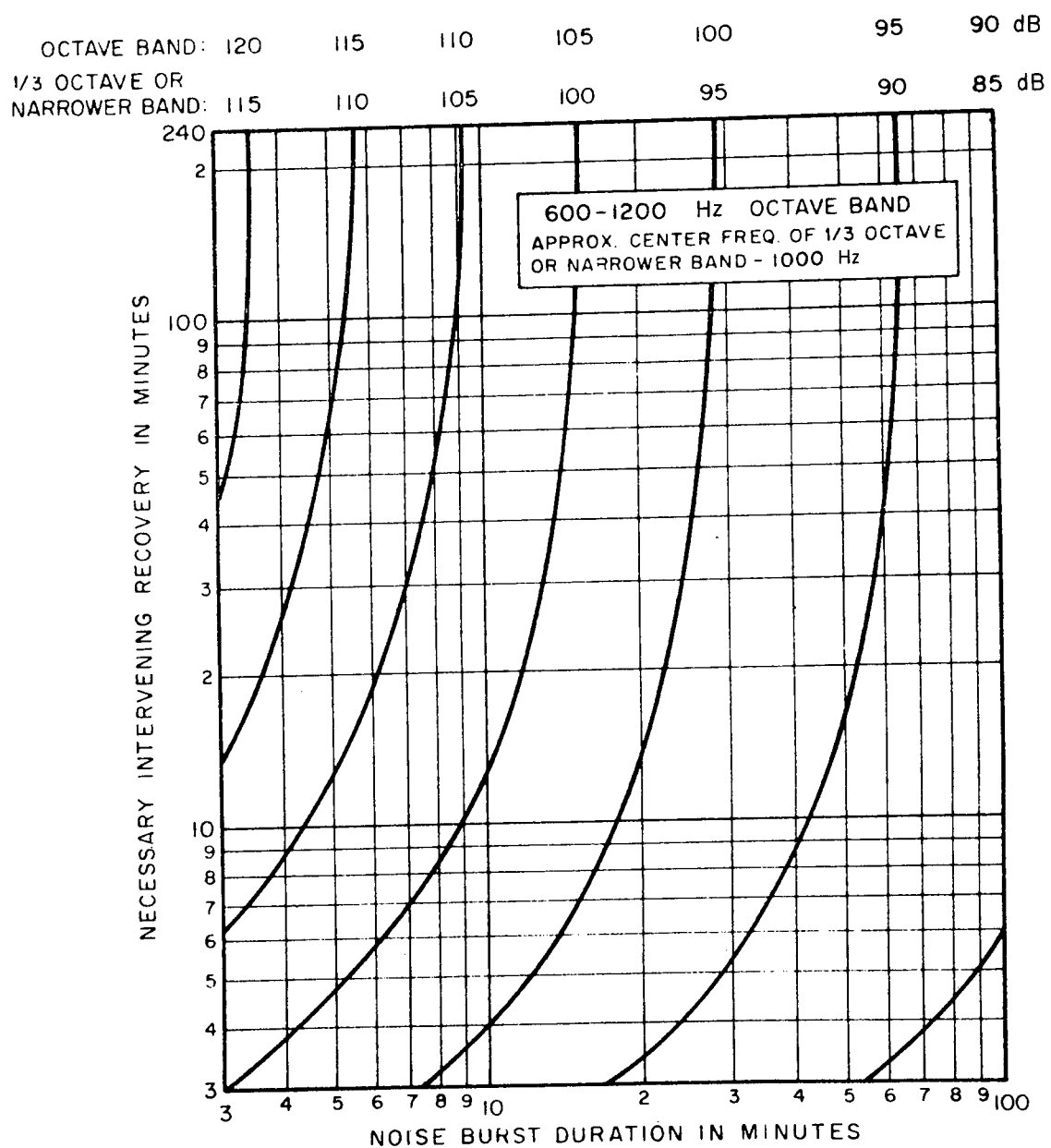


Figure 9-47

Damage Risk Contours for Long-Burst-Duration Interrupted Noise Parameter: Band SPL

(After Kryter - CHABA⁽¹³⁹⁾)

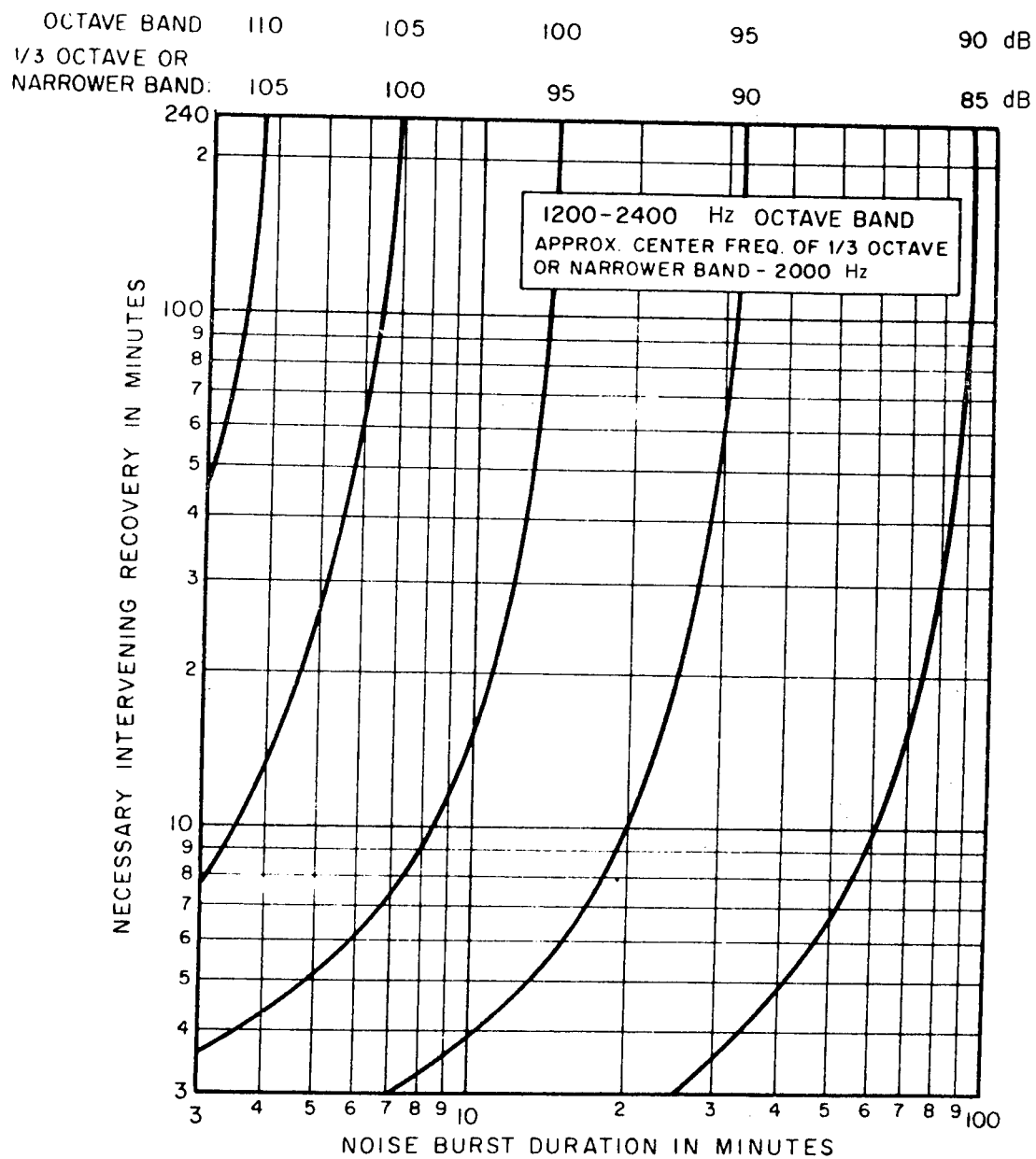


Figure 9-48

Damage Risk Contours for Long-Burst-Duration Interrupted Noise Parameter: Band SPL

(After Kryter - CHABA⁽¹³⁹⁾)

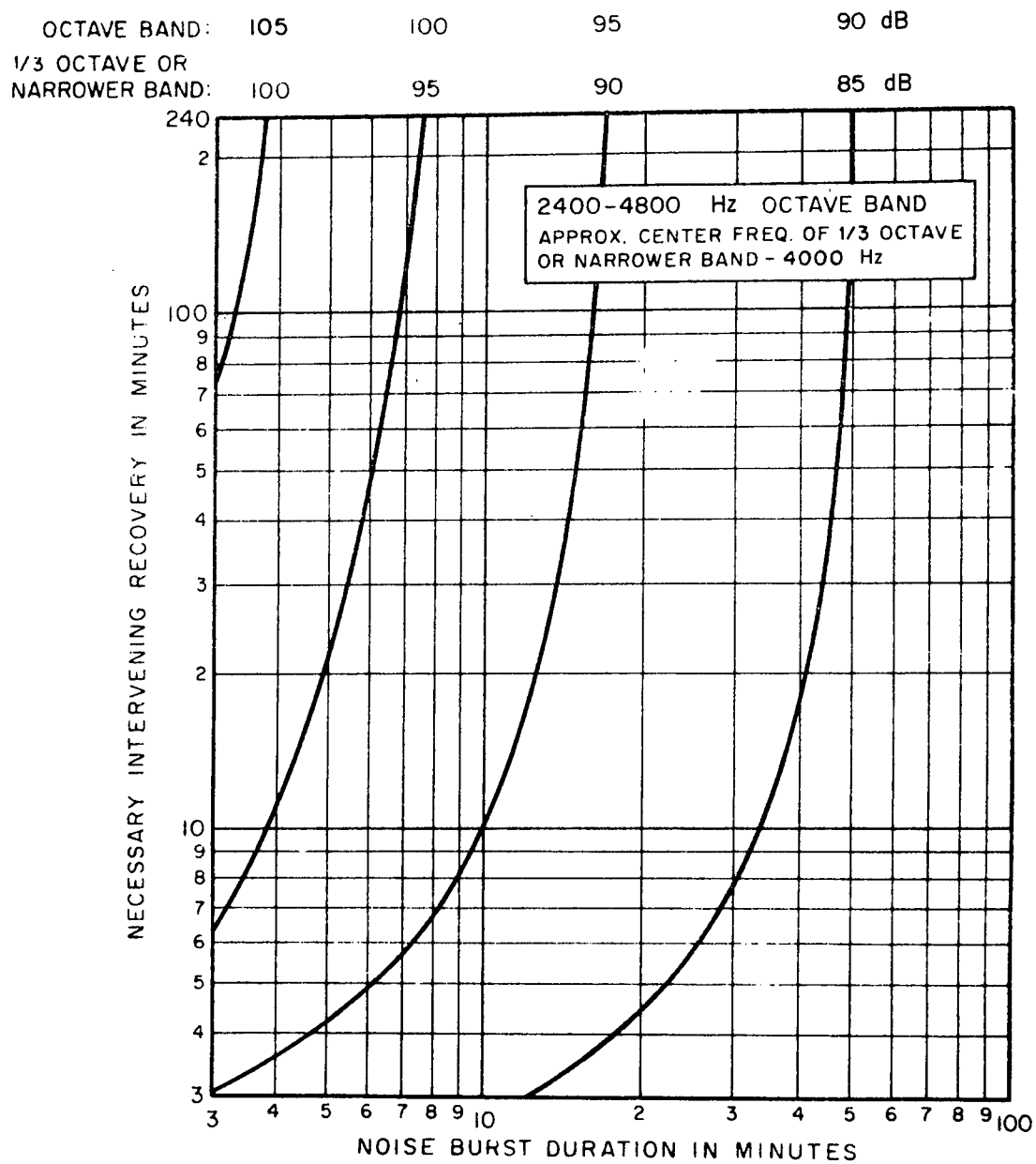


Figure 9-49

Damage Risk Contours for Long-Burst-Duration Interrupted Noise Parameter: Band SPL

(After Kryter - CHABA⁽¹³⁹⁾)

found on the graph, suggesting that a single 10 min exposure will probably exceed the criterion. This is verified by consulting Figure 9-39, which shows that a single 9 min exposure is all that can be tolerated in a single day.

Relations shown in Figures 9-39 to 9-49 are based either upon direct measures of temporary threshold shifts or permanent noise-induced losses in hearing resulting from exposure to sound or extrapolations from such data as are available. In general, there has been a sufficient amount of research in this problem area so that both the data points and extrapolations have been verified to a reasonable extent by one or more independent investigations. However, some of the relations are based on less evidence than others. For example:

- The maximum levels to be allowed regardless of duration (the top curves of Figures 9-39 and 9-41) are estimates that are not supported by direct experimental data.
- The data supporting the damage risk contours for pure tones are not as extensive as those for the octave or one-third octave bands of noise, and as such may be subject to change. Because of the extensiveness and similarity of results found with bands of noise by various investigators, it is felt that the damage risk contours for bands of noise are valid.
- As yet, there are very few data on the effects of sounds below 100 Hz and above about 7000 Hz. (See Figure 9-36a and b). In the opinion of the Working Group, there is at the present time insufficient evidence to warrant extrapolating the damage risk contours as a function of frequency beyond the frequencies mentioned.
- It is found that noises that are one octave in width will provide a degree of shift in threshold of audibility similar to that resulting from exposure to a one-third octave band having the same center frequency, but 5 dB less intense than the octave band of noise (112, 116). Further verification of this result is needed, however, before this difference between the effect on hearing of one-third and octave bands of noise having the same center frequency can be considered as proven.

As will be seen from a comparison of Figures 9-40 and 9-41, the ear is less tolerant of low-frequency pure tones than it is to narrow bands of noise in the same frequency region. The explanation for this difference is apparently to be found in the actions of the aural reflex (200, 201). This reflex is such that when the ear is exposed to intense bands of noise, it can provide, depending on the level, as much as 15 dB or so of effective protection for low-frequency sounds being transmitted to the inner ear. However, the reflex is not maintained by pure tones, and as a result the tolerable sound pressure level for low-frequency tones below 1000 Hz is much less than it is for bands of noise with frequencies below 1000 Hz.

Data are available on the center and cutoff frequencies of commercially available filters for noise control work (139).

Since pain is produced by overall sound pressure levels exceeding 135 dB, the unprotected ears should not be exposed to levels exceeding this level, no matter how short the exposure period. Because of nonauditory effects (possible disorientation, nausea, vomiting) exposure of personnel is usually restricted to noise levels below 150 dB, no matter how short the exposure time nor how much the noise level in the ear canal is reduced by ear protectors. In experiments with special precautions and close observation, people have been exposed with ear protection to higher levels without harm (see Figure 9-36).

If the combination of ambient noise levels and exposure times exceeds the damage risk criteria discussed, reduction of the ambient noise or personally worn ear protective devices are necessary to reduce the noise received by the ear to levels below the exposure criteria.

In reality, the damage risk contours discussed above have no sharp limits but are based on rather broad probability distributions. Therefore, they cannot be taken too literally (68). Nevertheless these contours serve as helpful guides for the advisability of noise control measures, the wearing of personal protection equipment or for reducing the exposure time. These criteria should be applied only for almost daily, repeated, routine exposures as applicable to aircraft ground crew or rocket test crews. They could be exceeded, if necessary, for short, infrequent special operations.

Routine exposure of personnel to hazardous noise levels as discussed here should always be monitored by a medical hearing-conservation program (192, 194). The intricate problem of the intrusion of aerospace noise into communities has been reviewed in detail (15, 28, 48, 82, 156, 182). (See also sonic booms above). Control of booster noise at launch complexes and test stands should make use of these principles.

Recent recommendations for control of noise in military aircraft and helmets have been published (196). They should be valid for use in NASA support aircraft. Table 9-50 covers these data. The acoustical noise level in any part of the aircraft intended for occupancy by the crew or other personnel cannot exceed the values specified in Table 9-50a, Part I (preferred) or Table 9-50a, Part II, during conditions of maximum continuous power. For takeoff, afterburner operation and other conditions normally not exceeding 5 minutes continuous duration the acoustical noise level in any part of the aircraft intended for occupancy by the crew or other personnel cannot exceed the values specified in Table 9-50b, Part I (preferred) or Table 9-50b, Part II.

In aircraft in which personnel must necessarily wear helmets at all times and communicate by electronic means (e. g., single place fighter aircraft), the acoustical noise level cannot exceed the values specified in Table 9-50c, Part I (preferred) or Table 9-50c, Part II during conditions of maximum continuous power. The acoustical noise level in any part of the aircraft intended for occupancy by the crew or other personnel cannot exceed the values specified in Table 9-50d, Part I (preferred) or Table 9-50d, Part II, during conditions of normal cruise power.

Table 9-50

Allowable Acoustical Noise Levels in Military Aircraft and Helmets (See text)

(After MIL-A-8806A (196))

a. Maximum Acceptable Noise Level at Maximum Continuous Power

I			II	
Frequency (Hz)		Max. acceptable noise level (dB)	Frequency bands (Hz)	Max. acceptable noise level (dB)
Band	Center			
Overall		113	Overall	113
22.4 - 45	31.5	111	37.5 - 75	111
45 - 90	63	111	75 - 150	111
90 - 180	125	111	150 - 300	111
180 - 355	250	111	300 - 600	105
355 - 710	500	105	600 - 1200	99
710 - 1400	1000	99	1200 - 2400	93
1400 - 2800	2000	93	2400 - 4800	87
2800 - 5600	4000	87	4800 - 9600	87
5600 - 11200	8000	87		

b. Maximum Acceptable Noise Level Under Short Duration Conditions

I			II	
Frequency (Hz)		Max. acceptable noise level (dB)	Frequency bands (Hz)	Max. acceptable noise level (dB)
Band	Center			
Overall		120	Overall	120
22.4 - 45	31.5	118	37.5 - 75	118
45 - 90	63	118	75 - 150	118
90 - 180	125	118	150 - 300	118
180 - 355	250	118	300 - 600	112
355 - 710	500	112	600 - 1200	106
710 - 1400	1000	106	1200 - 2400	100
1400 - 2800	2000	100	2400 - 4800	94
2800 - 5600	4000	94	4800 - 9600	94
5600 - 11200	8000	94		

c. Maximum Acceptable Noise Level with Protective Helmets or Devices

I			II	
Frequency (Hz)		Max. acceptable noise level (dB)	Frequency bands (Hz)	Max. acceptable noise level (dB)
Band	Center			
Overall		113	Overall	113
22.4 - 45	31.5	111	37.5 - 75	111
45 - 90	63	111	75 - 150	111
90 - 180	125	111	150 - 300	111
180 - 355	250	111	300 - 600	109
355 - 710	500	109	600 - 1200	106
710 - 1400	1000	106	1200 - 2400	100
1400 - 2800	2000	100	2400 - 4800	94
2800 - 5600	4000	94	4800 - 9600	94
5600 - 11200	8000	94		

d. Maximum Acceptable Noise Level at Normal Cruise Power

I			II	
Frequency (Hz)		Max. acceptable noise level (dB)	Frequency bands (Hz)	Max. acceptable noise level (dB)
Band	Center			
Overall		106	Overall	106
22.4 - 45	31.5	104	37.5 - 75	104
45 - 90	63	104	75 - 150	104
90 - 180	125	104	150 - 300	104
180 - 355	250	104	300 - 600	96
355 - 710	500	96	600 - 1200	90
710 - 1400	1000	90	1200 - 2400	86
1400 - 2800	2000	86	2400 - 4800	75
2800 - 5600	4000	75	4800 - 9600	75
5600 - 11200	8000	75		

A Soviet analysis of the acoustical environment for space cabins is available (211).

Personal Protective Equipment

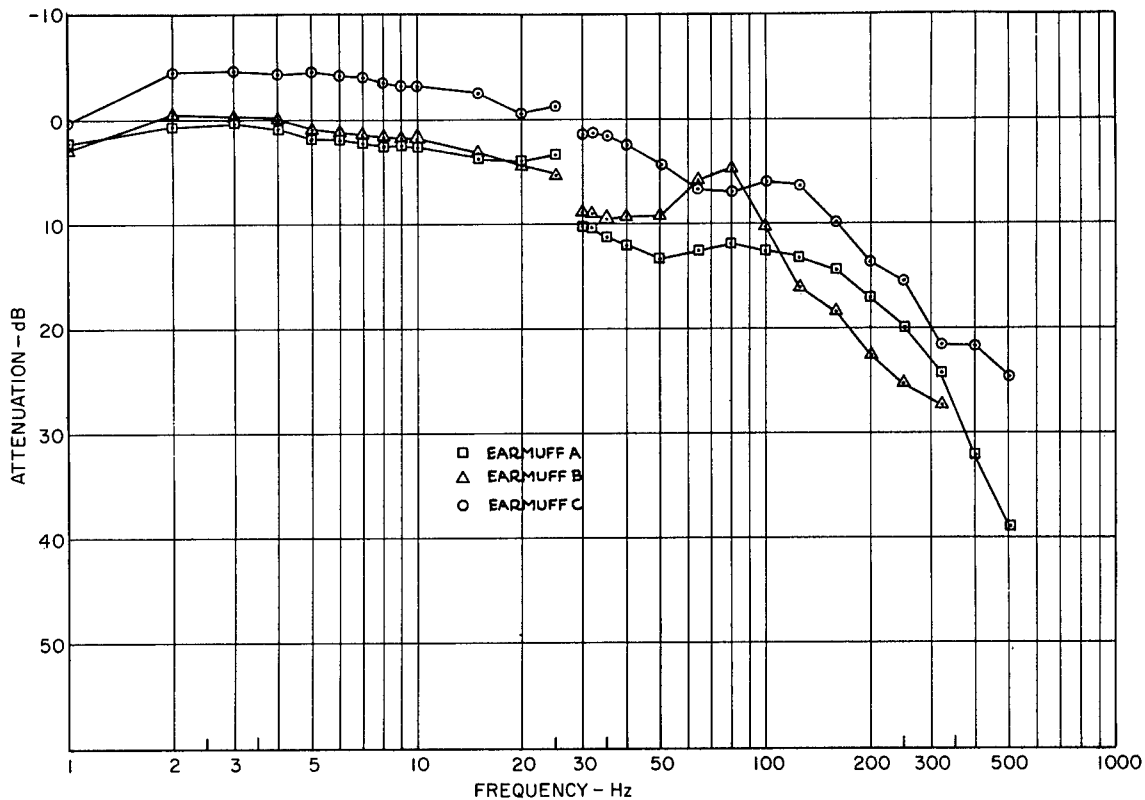
Personal protective equipment against degradation of performance by noise appears to be an optimum approach in many aspects of controlling the sound environment. In general there is no difficulty in providing adequate protection by comfortable personal equipment (earplugs, earmuffs, or properly designed and fitted helmets). Their effectiveness has been shown to be almost ideal and can hardly be improved (21, 22, 29, 56, 66, 71, 82, 133, 146, 160, 174, 213). Electroacoustic ear protectors are under design for impulse noise (197). Data are available on the effect of earmuffs in the low and infrasonic frequencies (145). (Figure 9-51a). The findings of this investigation demonstrate that "good" present-day earmuff protectors provide about 10 dB of sound attenuation at frequencies between 20 and 100 Hz and very little attenuation below 20 Hz. For optimum ear protection in intense sound fields with high concentrations of acoustic energy in the low audio frequency and infrasonic regions, good insert earplugs are recommended for short duration exposures. For long-time exposures, the use of good earmuffs in combination with insert earplugs is recommended. These data confirm, quantitatively, subjective observations (Figures 9-36a and b) of the performance of muff-type ear protectors in intense infrasonic and low audio-frequency noise environments.

The use of ear protection improves the intelligibility of direct voice communication in high noise environments (90). For space cabins, helmets to be worn during high-noise phases of the mission (boost phases and reentry) and the communication system have to be designed so that these criteria can be met. The reduction of ambient noise achieved by various representative earmuffs and helmets is illustrated in Figure 9-51b. Figure 9-29 covers the effect of earplugs on improving the intelligibility of speech in noisy environments. Figure 9-52 presents the nominal noise reduction values for a NASA helmet and earmuffs combination (194). Oxygen masks or the face plates of pressure helmets can give approximately 15 dB or more attenuation in the speech frequency range. (See also Table 9-50c)

Auditory signals for malfunction must be audible in the presence of external noise on liftoff. In general, auditory warning signals on spacecraft must be easily detectable, must hold the operator's attention, and must be quickly and accurately identifiable (198). The signal should therefore be easily distinguishable from background noises. Warbling or wailing tones may be used in order to be distinguishable from ambient noises. The sound should be at least 20 decibels above threshold and frequencies below 500 cycles per second should not be used. It is also recommended that signals which cause operator discomfort; e. g., continuous high pitched tones of frequencies above 200 cycles per second, not be used. The signal should be as brief as possible but still be identifiable.

Figure 9-51

Attenuation of Noise by Earmuffs and Helmets



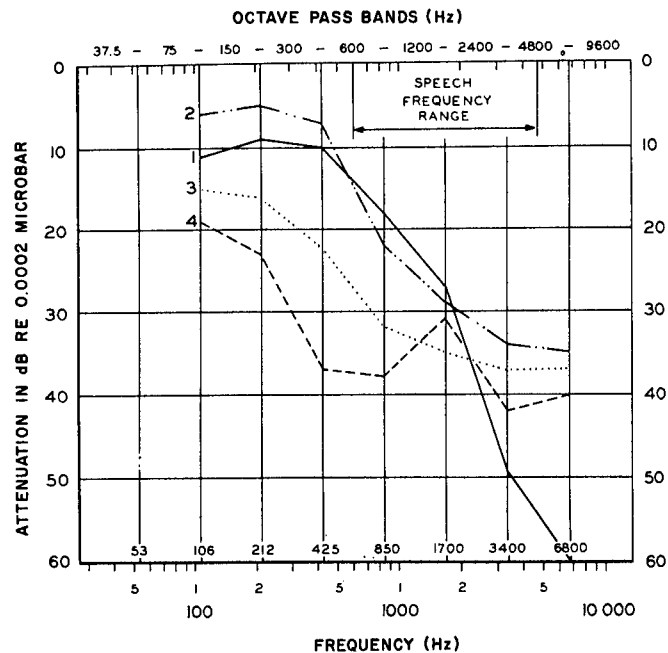
a. Physical Measurement of Earmuff Attenuation of Low Frequency Sound

(After Nixon et al⁽¹⁴⁵⁾)

b. Reduction of Ambient Noise of Different Frequencies Provided by Various Types of Helmets and Earmuffs

1. Full pressure helmet with earmuffs inside providing a poor seal around the ear (thin sponge rubber seal).
2. Protective flying helmet with earmuffs inside (thin sponge rubber cushion; poor seal).
3. Protective flying helmet with effective earmuffs (liquid filled cushion; good seal)⁽²⁰⁹⁾.
4. Effective earmuffs (liquid filled cushion; good seal) with headset inside for use by ground crews. This earmuff has a larger air volume under the muff than the earmuff used in the protective helmet above⁽¹¹⁾ and therefore it provides more attenuation.

(After von Gierke and Hiatt⁽⁷¹⁾)



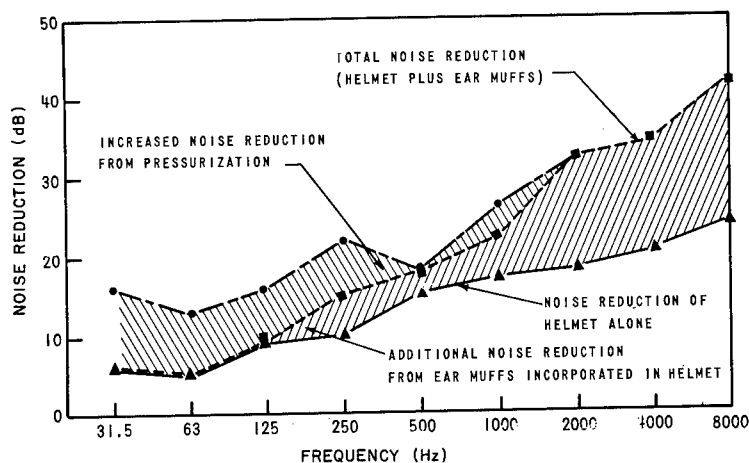


Figure 9-52

Nominal Noise Reduction Values
for the Addition of Ear Muffs
to NASA Helmets

(After AFSCM (194))

In the Apollo spacecraft Caution and Warning Subsystem, in addition to indicator lights for malfunctions, an audible signal is provided to alert the crew to existing out-of-tolerance conditions. The intensity level of the audio tone is 78 dB as measured at the instrument panel. It is a two-tone alternating signal, consisting of tones of 2000 and 750 Hz, with 2-1/2 switches per second. The Caution and Warning audio tone on-board the LEM is a single tone signal of 3200 Hz also at 78 dB measured at the instrument panel.

As covered in the section on speech intelligibility, filters in communications systems can be used for enhancing the audibility of signals in the presence of noise. This is accomplished by the passing of certain wanted frequencies and the exclusion of unwanted ones. Two types of signal masking can be reduced by filtering:

1. Masking produced by components within a critical bandwidth centered at the signal frequency (direct masking) and,
2. Masking effects of tonal noises on signals lying outside the critical band (remote masking).

For reduction of direct masking, very narrow band-pass filters that reject noise within the critical band should be used to reduce masking of wide-band on a tone that lies on a frequency which is within the noise spectrum. This band-pass filter must be narrower than the critical band or else it will only reject noise that has no masking effect.

The role of noise shields and noise-canceling microphones has been covered in the section on speech intelligibility. Figure 9-30 presents quantitative data on these effects. Recommendations for microphones and earphones in Apollo are indicated on page 9-39.

Specification of sound levels during extravehicular operations on the lunar surface indicate that acoustical levels generated by the PLSS shall not exceed the noise sound pressure level of 80 dB overall and 55 dB in the 300-4800 Hz range within the PGA helmet (198).

ANALYSIS OF SOUND AND NOISE FACTORS IN ASTRONAUT PERFORMANCE

The design and operation of the following systems and equipment are involved in the auditory performances and tolerances of the astronauts;

- Control and display system of command modules and secondary vehicles
- Intercommunications equipment
- Cabins
- Helmet and earplugs

The auditory performances and tolerances of the astronauts are considered to be a function of several factors. The basic auditory capabilities and tolerances of the astronaut population (or equivalent population) must be measured under standard conditions. To this is added or subtracted, as appropriate, the effects of the environment (e. g., the ambient noise levels, pressure levels, etc.); the equipment (e. g., signal-to-noise ratio of the intercommunication equipment, attenuation of noise by helmets, etc.); the operations (e. g., whether face-to-face verbal communications or intercommunication equipment are used, etc.); and personnel variables (e. g., attention, age fatigue, etc.).

There are some areas where it may be possible to construct mathematical models which will permit the handling of the complex interactions that are involved in many of the areas. Such models will have the advantage of indicating how individual variables can be manipulated in order to provide more than one way of arriving at an acceptable design endpoint in noise control.

As a first approach to this problem, the ambient noise levels expected within the spacecraft during all modes of an operation should be estimated as precisely as they can be at this time. This should include the spectral characteristics of the noise and the durations. Also, the noise attenuation characteristics of the environment and equipment planned for the specific system should be determined; e. g., effects of pressure levels in the cabins and pressure suit, use of earphones and helmet, etc.

A determination should then be made of transmission characteristics of the voice communication equipment. This involves determination of the signal-to-noise ratio, type of speech processing, frequency characteristics, and microphone and earphone noise pickup characteristics, etc., specified for the voice communication equipment, including the ground-to-spacecraft between command and secondary modes and between both primary and secondary modules and lunar or planetary surfaces.

Based on the task analyses available, those tasks which involve auditory performances should be identified. This includes: (1) the characteristics of the tasks (e. g., language content, redundancy, frequency of communication, etc.), (2) relationship to the other tasks, and (3) the environmental conditions which can be expected to exist at the same time.

Once the performances that are expected of the astronauts and the conditions under which they must be performed have been identified, then these should be compared with the performance and tolerance factors contained in this compendium. Comparison of the compendium with the performances, environments, etc., should indicate whether:

- The sound level of the auditory signal devices is sufficiently above the ambient noise levels to permit reception of the signal.
- The auditory devices are sufficiently distinctive to permit discrimination between them under all ambient noise conditions.
- The ambient noise level is sufficiently low in either the shirtsleeve or pressure suit environments, to permit face-to-face verbal communications when required with an acceptable level of intelligibility, with half effort.
- The signal-to-noise ratio and bandwidth for the intercommunication equipment is sufficiently high to permit an acceptable level of intelligibility.
- The ambient noise level does not exceed intensity levels and durations which cause undue discomfort or could be expected to cause temporary or permanent damage.

Based on these comparisons if there are any areas disclosed in which performance and or tolerance limits are exceeded or marginal, analyses should be performed to determine where corrections can be made. These include:

- Reduction of the ambient noise level at its source.
- Reduction of the ambient noise level in the cabins through the use of sound absorbing materials.
- Reduction of the ambient noise level at the ear through the use or modifications of helmet, earphones, and/or earplugs.
- Modification of the auditory signal devices to increase the signal-to-noise ratio and/or distinctiveness.
- Modification of the intercommunication equipment to increase the intelligibility.
- Modification in the mode of operation to be less dependent on auditory signal devices and/or verbal communications, with the appropriate programming of face-to-face and interphone modes.

REFERENCES

- 9-1. Ades, H. W., Central Auditory Mechanisms, in Handbook of Physiology, Section I: Neurophysiology, Vol. I, Field, J., Magoun, H. W., Hall, V. E., (eds.), American Physiological Society, Washington, D. C., 1959, pp. 585-613.
- 9-2. American Standards Association, Inc., American Standard for Acoustical Measurements, ASA - S1.6-1960, N. Y., 1960.
- 9-3. American Standards Association, Inc., American Standard Method for the Physical Measurement of Sound, ASA-S1.2-1962, (sponsored by Acoustical Society of America) N. Y., Aug. 1962.
- 9-4. American Standards Association, Inc., The Relations of Hearing Loss to Noise Exposure, Z24-X2, N. Y., 1954.
- 9-5. Andersson, T. P., Wakim, K. G., Herrick, J. F., et al., An Experimental Study of the Effects of Ultrasonic Energy on the Lower Part of the Spinal Cord and Peripheral Nerves, Arch. Phys. Med., 32: 71-83, 1951.
- 9-6. Anthony, A., Ackerman, E., Stress Effects of Noise in Vertebrate Animals, WADC-TR-58-622, Wright Air Development Center, Wright-Patterson AFB, Ohio, Sept. 1959.
- 9-7. Baron, M. L., Bleich, H. H., Wright, J. P., Investigation of Ground Shock Effects due to Rayleigh Waves Generated by Sonic Booms, NASA-CR-451, May 1966.
- 9-8. Batteau, D. W., Plante, R. L., Spencer, R. H., et al., Localization of Sound, Pt. 5, Auditory Perception, NOTS-TP-3109 (Pt. 5), Naval Ordnance Test Station, China Lake, Calif., Jan. 1965.
- 9-9. von Békésy, G., Über die Hörschwelle und Fuhlgrenze Langsamer Sinusformiger Luftdruckschwankungen, Ann. Physik, 26: 554-566, 1936.

- 9-10. Belger, R. C., Hirsh, I. J., Masking of Tones by Bands of Noise, J. Acoust. Soc. Amer., 28: 623-630, 1956.
- 9-11. Beranek, L. L., The Design of Speech Communication Systems, Proc. IRE, 35: 880-890, 1947.
- 9-12. Beranek, L. L., (ed.), Noise Reduction, McGraw-Hill, N. Y., 1960.
- 9-13. van Bergeijk, W. A., Pierce, J. R., David, E. E., Jr., Waves and the Ear, Anchor Books, Doubleday & Co., Inc., N. Y., 1960.
- 9-14. Bonvallet, G. L., Levels and Spectra of Traffic Vehicle Noise, J. Acoust. Soc. Amer., 22: 201-205, 1950.
- 9-15. Borsky, P. N., Community Reactions to Air Force Noise, Pt. 2. Data on Community Studies and Their Interpretation, WADD-TR-60-689 (Pt. 2), Wright Air Development Division, Wright-Patterson AFB, Ohio, Mar. 1961.
- 9-16. Borsky, P. N., Community Reactions to Sonic Booms in the Oklahoma City Area, Vol. 2. Data on Community Reactions and Interpretations, AMRL-TR-65-37(v.2), Aerospace Medical Research Labs., Wright-Patterson AFB, Ohio, Oct. 1965.
- 9-17. Bowen, I. G., Holladay, A., Fletcher, E. R., et al., A Fluid-Mechanical Model of the Thoraco-Abdominal System with Applications to Blast Biology, DASA-1675, Defense Atomic Support Agency, Washington, D. C., June 1965.
- 9-18. Broadbent, D. C., Effects of Noise on Behavior, in Handbook of Noise Control, Harris, C.M., (ed.), McGraw-Hill, N. Y., 1957, Chapt. 10, pp. 1-34.
- 9-19. Broadbent, D. E., On the Dangers of Over-Arousal, IAA Preprint 1, Applied Psychology Research Unit, Medical Research Council, Cambridge, England, paper presented at Second International Symposium on Basic Environmental Problems of Man in Space, Paris, June 14-18, 1965, International Astronautical Federation and International Academy of Astronautics, 1965.
- 9-20. Busnel, R. G., (ed.), Acoustic Behaviour of Animals, Elsevier, Amsterdam, 1963.

- 9-21. Camp, R. T., Jr., Keiser, R. L., Sound Attenuation Characteristics of the Navy SPH-3 (Modified) (LS) Helmet, USAARU-67-8, Army Aeromedical Research Unit, Fort Rucker, Ala., May 1967.
- 9-22. Camp, R. T., Jr., Tolhurst, G. C., Greene, J. W., Sound Attenuation Characteristics of the Project Mercury Pre-production Full Pressure Suit Helmet, SR-60-7, Naval School of Aviation Medicine, Pensacola, Fla., Sept. 1960.
- 9-23. Carlson, H. W., Sonic Boom, Int. Science and Tech., No. 55: 70-72, 74, 77-80, July 1966.
- 9-24. Carstens, J. P., Kresge, D., Literature Survey of Passenger Comfort Limitations of High Speed Ground Transports, Rep. D-910353-1, United Aircraft Corp., Research Labs., East Hartford, Conn., July 1965.
- 9-25. Carter, N. L., Kryter, K. D., Masking of Pure Tones and Speech, J. Auditory Res., 2: 66-98, 1962.
- 9-26. CBS Laboratories, Development of an Electronic Dummy for Acoustical Testing (Incorporating Manual of Operation and Design), NASA-CR-65348, A Division of Columbia Broadcasting System, Inc., Stamford, Conn., Mar. 28, 1966.
- 9-27. Chambers, A., Bellcomm, Inc., 1100 17th Street, N. W., Washington, D. C. 20036, personal communication, 1967.
- 9-28. Clark, W. E., Noise from Aircraft Operations, ASD-TR-61-611, Aeronautical Systems Div., Wright-Patterson AFB, Ohio, Nov. 1961.
- 9-29. Clarke, D. P. J., Acoustic Properties of Headgear: XXIII. The Anticoustic Co. Nosonic MK IX Earmuff with Ear-Phones and Liquid-Filled Ear Seals; and General Textile Mills Co., Helmet with Modified Sound Valve and Liquid-Filled Ear Seals, DRML-TM-643, Defense Research Medical Labs., Toronto (Ontario), Aug. 1966.
- 9-30. Cole, J. N., England, R. T., Powell, R. G., Effects of Various Exhaust Blast Deflectors on the Acoustic Noise Characteristics of 1,000 Pound Thrust Rockets, WADD-TR-60-6, Wright Air Development Div., Wright-Patterson AFB, Ohio, Sept. 1960.
- 9-31. Cole, J. N., Hille, H. K., Powell, R. G., et al., Noise Produced during Launchings of Rocket Power Vehicle and Human Factor Sitting Considerations, in Proceedings of Fourth International Congress on Acoustics, Copenhagen, Denmark, 1962.

- 9-32. Cole, J. N., Mohr, G. C., Guild, E., et al., The Effects of Low Frequency Noise on Man as Related to the Apollo Space Program, AMRL-Memo-B-66, Aerospace Medical Research Labs., Wright-Patterson AFB, Ohio, Mar. 1964.
- 9-33. Cole, J. N., Powell, R. G., Hille, H. K., Acoustic Noise and Vibration Studies at Cape Canaveral Missile Test Annex, Atlantic Missile Range. Vol. I. Acoustic Noise, ASD-TR-61-608 (I), Aeronautical Systems Div., Wright-Patterson AFB, Ohio, Dec. 1962.
- 9-34. Coles, R. R. A., Rice, C. G., Considerations on Auditory Effects from Nuclear Blast, RNMS-8/66, Royal Naval Medical School, Alverstoke, Hampshire, England, Oct. 1966.
- 9-35. Committee on Hearing and Bio-Acoustics, Bibliography of Reports Acquired by CHABA, Washington, D. C., Jan. 1963.
- 9-36. Davis, H., (ed.), Application of the ISO Standard Reference Zero (Audiometric), Report of Working Group 51, National Academy of Sciences, National Research Council, Committee on Hearing, Bioacoustics and Biomechanics, Washington, D. C., Sept. 1967. (AD-822535).
- 9-37. Davis, H., Survey of the Problem, in Benox Report, An Exploratory Study of the Biological Effects of Noise, University of Chicago, Dec. 1953, pp. 12-20. (Contract No. N6 ori-020, Task Order 44, ONR Proj. No. 144079).
- 9-38. Davis, H., Parrack, H. O., Eldredge, D. H., Hazards of Intense Sound and Ultrasound, Ann. Otol., 58: 732-738, 1949.
- 9-39. Dean, R. D., McGlothlen, C. L., Monroe, J. L., Effects of Combined Heat and Noise on Human Performance, Physiology, and Subjective Estimates of Comfort and Performance, BOE-D2-90540, Boeing Co., Seattle, Washington, May 1964.
- 9-40. Dickson, E. D. C., Some Effects of Intense Sound and Ultrasound on the Ear, Proc. Roy. Soc. Med., 46: 139-148, 1953.
- 9-41. Dunn, F., Fry, W. J., Physical Acoustic Properties: Mammalian Tissues, in Environmental Biology, Altman, P. L., Dittmer, D. S., (eds.), AMRL-TR-66-194, Aerospace Medical Research Labs., Wright-Patterson AFB, Ohio, Nov. 1966, pp. 197-198.

- 9-42. Dunn, F., Fry, W. J., Tissue Changes in Central Nervous System after Exposure to Ultrasound: Cat, in Environmental Biology, Altman, P. L., Dittmer, D. S., (eds), AMRL-TR-66-194, Aerospace Medical Research Labs., Wright-Patterson AFB, Ohio, Nov. 1966, pp. 198-199.
- 9-43. Dunn, H. K., White, S. D., Statistical Measurements on Conversational Speech, J. Acoust. Soc. Amer., 11: 278-288, 1940.
- 9-44. Edwards, D. A. W., Some Observations on the Effects on Human Subjects of Air and Structure Borne Vibrations of Various Frequencies, FPRC-753, Flying Personnel Research Committee, Air Ministry, London, 1950.
- 9-45. Egan, J. P., Articulation Testing Methods, Laryngoscope, 58: 955-991, 1948.
- 9-46. Egan, J. P., Hake, H. W., On the Masking Pattern of a Simple Auditory Stimulus, J. Acoust. Soc. Amer., 22: 622-630, 1950.
- 9-47. Eldred, K. M., Gannon, W. J., von Gierke, H. E., Criteria for Short Time Exposure of Personnel to High Intensity Jet Aircraft Noise, WADC-TN-55-355, Wright Air Development Center, Wright-Patterson AFB, Ohio, Sept. 1955.
- 9-48. Elliot, L. L., Hearing of Air Force Pilots: 1955-1962, SAM-TDR-62-127, School of Aerospace Medicine, Brooks AFB, Texas, Dec. 1962.
- 9-49. Fascenelli, F. W., Rogers, N., An Aerospace Word List for Speech Discrimination Testing, Aerospace Med., 38: 1164-1166, Nov. 1967.
- 9-50. Finkle, A. L., Poppen, J. R., Clinical Effects of Noise and Mechanical Vibrations of a Turbo-Jet Engine on Man, J. Appl. Physiol., 1: 183-204, 1948.
- 9-51. Fletcher, H., Auditory Patterns, Rev. Modern Phys., 12: 47-65, 1940.
- 9-52. Fletcher, H., Loudness, Masking and Their Relation to the Hearing Process and the Problem of Noise Measurement, J. Acoust. Soc. Amer., 9: 275-293, 1938.
- 9-53. Fletcher, H., Munson, W. A., Loudness, Its Definition, Measurement and Calculation, J. Acoust. Soc. Amer., 5: 82, 1933.

- 9-54. Fletcher, H., Munson, W. A., Relation between Loudness and Masking, J. Acoust. Soc. Amer., 9: 1-10, 1937.
- 9-55. Fletcher, H., Steinberg, J. C., Articulation Testing Methods, Bell. Syst. Tech. J., 8: 806, 1929.
- 9-56. Forshaw, S. E., The Significance of Variances in the Real-Ear Sensitivity of a Circumaural Earphone, DRML-RP-625, Defence Research Medical Labs., Toronto (Ontario), Sensory Capacities Section, Feb. 1966.
- 9-57. French, B. O., Appraisal of Apollo Launch Noise, Aerospace Med., 38(7): 719-722, 1967.
- 9-58. French, L. A., Wild, J. J., Neal, D., Attempts to Determine Harmful Effects of Pulsed Ultrasonic Vibrations, Cancer, 4: 342-344, 1951.
- 9-59. French, N. R., Steinberg, J. C., Factors Governing the Intelligibility of Speech Sounds, J. Acoust. Soc. Amer., 19: 90-119, 1947.
- 9-60. Fry, W. J., Intense Ultrasound in Investigation of the Central Nervous System, Ad. Biol. Med. Phys., 6: 281-348, 1958.
- 9-61. Fry, W. J., Meyers, R., Ultrasonic Method of Modifying Brain Structures, Confin. Neurol. (Basel), 22: 315-327, 1962.
- 9-62. Fry, W. J., Meyers, R., Fry, F. J., et al., Topical Differentia of Pathogenetic Mechanisms Underlying Parkinsonian Tremor and Rigidity as Indicated by Ultrasonic Irradiation of the Human Brain, Trans. Amer. Neurol. Assoc., 83rd., Atlantic City, pp. 16-24, 1958.
- 9-63. Gardner, E., Fundamentals of Neurology, W. B., Saunders Co., Philadelphia, Pa., 1963, pp. 187-188.
- 9-64. Gardner, W. J., Licklider, J. C. R., Follow-Up Report on Audio Analgesia, J. Acoust. Soc. Amer., 31: 850-851, 1959.
- 9-65. Garner, W. R., Hearing, Ann. Rev. Psychol., 3: 85-104, 1952.
- 9-66. Gales, R. S., Auditory Presentation of Information, U. S. Navy Electronics Lab., in Human Engineering Guide to Equipment Design, Morgan, C. T., Cook, J. S., Chapanis, A., Lund, M. W., (eds.), McGraw-Hill, N. Y., 1963, Chapt. 3., pp. 123-216.

- 9-67. von Gierke, H. E., Biodynamic Response of the Human Body, Appl. Mech. Rev., 17(12): 951-958, 1964.
- 9-68. von Gierke, H. E., On Noise and Vibration Exposure Criteria, Arch. Environ. Health, 11: 327-339, Sept. 1965.
- 9-69. von Gierke, H. E., Vibration and Noise Problems Expected in Manned Space Craft, Noise Control, 5(3): 8-16, 1959.
- 9-70. von Gierke, H. E., Davis, H., Eldredge, D. H., et al., Aural Pain Produced by Sound, in Benox Report, An Exploratory Study of the Biological Effects of Noise, University of Chicago, Dec. 1953, pp. 29-36. (Contract No. N6 ori-020, Task Order 44, ONR Proj. NR 144079).
- 9-71. von Gierke, H. E., Hiatt, E. P., Biodynamics of Space Flight, in Progress in the Astronautical Sciences, Singer, S. F., (ed.), North-Holland Publishing Co., Amsterdam, 1962, Vol. I, Chapt. VII, pp. 345-401.
- 9-72. von Gierke, H. E., Pietrasanta, A. C., Acoustical Criteria for Work Spaces, Living Quarters and other Areas on Air Bases, WADC-TN-57-248, Wright Air Development Center, Wright-Patterson AFB, Ohio, 1957.
- 9-73. Glorig, A., (ed.), Audiometry: Principles and Practices, The Williams & Wilkins Co., Baltimore, Md., 1965.
- 9-74. Glorig, A., Roberts, J., Hearing Levels of Adults by Age and Sex, United States - 1960-1962, Publication No. 1000, Series 11-11, Public Health Service, U. S. Department of Health, Education and Welfare, Washington, D. C., Oct. 1965.
- 9-75. Glorig, A., Ward, W. D., Nixon, J., Damage Risk Criteria and Noise-Induced Hearing Loss, Arch. Otolaryng., 74: 413-423, 1961.
- 9-76. Goblick, T. J., Jr., Pfeiffer, R. R., Signal Processing Characteristics of the Peripheral Auditory System, MIT-LL-TN-1966-50, Massachusetts Institute of Technology, Lincoln Lab., Lexington, Mass., Sept. 1966. (AD-645781).
- 9-77. Gorodetskiy, A. A., (ed.), Biological Action of Ultrasound and Super-High Frequency Electromagnetic Oscillations, JPRS-30860, Joint Publications Research Service, Washington, D. C., June 1965. (Translation of Biologicheskoye Deystviye Ultrazvuka i Sverkhvyschkoshastotnykh Elektromagnitnykh Kolebaniy Kiev, Academy of Sciences, Ukrainian SSR, 1964, pp. 3-120).

- 9-78. Gorshkov, S. I., Gorbunov, O. N., Nikol'skaya, Certain Aspects of the Biological Action of Ultrasonics in Connection with Its Application in Industry, in JPRS-26305, Joint Publications Research Service, Washington, D. C., Sept. 1964, pp. 21-29. (Translation of article in Gigiyena i Sanitariya, 29: 37-42, 1964.)
- 9-79. Grimaldi, J. V., Sensorimotor Performance under Varying Noise Conditions, Ergonomics, 2: 34-43, 1958.
- 9-80. Grossman, C. C., Holmes, J. H., Joyner, C., Purnell, E. W., Diagnostic Ultrasound, Proceedings of the First International Conference, University of Pittsburgh, 1965, Plenum Press, N. Y., 1966.
- 9-81. Guest, S., Jones, J. H., Far-Field Acoustic Environmental Predictions for Launch of Saturn V MLV Configuration, NASA-TN-D-4117, Sept. 1967.
- 9-82. Guignard, J. C., Noise, Chapter 30, in A Textbook of Aviation Physiology, Gillies, J. A., (ed.), Pergamon Press, London, 1965, pp. 895-967.
- 9-83. Hale, H. B., Adrenalcortical Activity Associated with Exposure to Low Frequency Sounds, Amer. J. Physiol., 171: 732 (abstract), 1952.
- 9-84. Harris, C. M., Absorption of Sound in Air Versus Humidity and Temperature, NASA-CR-647, Jan. 1967.
- 9-85. Harris, C. M., (ed.), Handbook of Noise Control, McGraw-Hill, N. Y., 1957.
- 9-86. Harris, D. J., Audible Sound Pressure Levels, in Environmental Biology, Altman, P. L., Dittmer, D. S., (eds.), AMRL-TR-66-194, Aerospace Medical Research Labs., Wright-Patterson AFB, Ohio, Nov. 1966, pp. 191-196.
- 9-87. Harris, D. J., Loudness Discrimination, NMRL-417, Naval Medical Research Lab., New London, Conn., Dec. 1963.
- 9-88. Hatfield, T. R., Evaluation of a Method for the Determination of Injury Risk of Ultrasonic Radiation in a Liquid Medium, (Master's Thesis), Ohio State University, Columbus, Ohio, 1965. (Prepared under Contract AF-33(608)-1095). (AD-620435).
- 9-89. Hawkins, J. E., Stevens, S. S., The Masking of Pure Tones and of Speech by White Noise, J. Acoust. Soc. Amer., 22: 6-13, 1950.

- 9-90. Hawley, M. E., Kryter, K. D., Effects of Noise on Speech, in Handbook of Noise Control, Harris, C. M., (ed.), McGraw-Hill, New York, 1957, Chapt. 9, pp. 1-26.
- 9-91. Hawley, S. A., Macleod, R. M., Dunn, F., Degradation of DNA by Intense Non-Concentrating Ultrasound, J. Acoust. Soc. Amer., 35: 1285-1287, 1963.
- 9-92. Hellman, R. P., Zwislocki, J., Loudness Function of a 1000 CPS Tone in the Presence of a Masking Noise, J. Acoust. Soc. Amer., 36(9): 1618-1627, 1964.
- 9-93. Hilton, D. A., Huckel, V., Maglieri, D. J., Sonic-Boom Measurements during Bomber Training Operations in the Chicago Area, NASA-TN-D-3655, Oct. 1966.
- 9-94. Hirsch, F. G., Effects of Overpressure on the Ear, A Review, Lovelace Foundation for Medical Education and Research, Albuquerque, N. M., presented at Conference on the Prevention of and Protection against Accidental Explosion of Munitions, Fuels and Other Hazardous Mixtures, New York Academy of Sciences, N. Y., Oct. 1966.
- 9-95. Hodge, D. C., McCommons, R. B., A Behavioral Study of the Sound-Shadow Effect in Impulse Noise, HEL-TM-12-67, Human Engineering Labs., Aberdeen Proving Ground, Md., July 1967.
- 9-96. Hodge, D. C., McCommons, R. B., Growth of Temporary Threshold Shift from Impulse Noise: A Methodological Study, HEL-TM-10-67, Human Engineering Labs., Aberdeen Proving Ground, Md., May 1967.
- 9-97. Hoeft, L. O., Leech, F. J., Noise and Vibration Environments Connected with Missiles and Space Vehicle Operations, in ARDC Science and Engineering Symposium Proceedings, Andrews AFB, Washington, D. C., Sept. 1958.
- 9-98. Hosey, A. D., Powell, C. H., (eds.), Industrial Noise, A Guide to Its Evaluation and Control, PHS-1572, Public Health Service, U. S. Dept. of Health, Education, and Welfare, Washington, D. C., 1967.
- 9-99. Ingard, U., A Review of the Influence of Meteorological Conditions on Sound Propagation, J. Acoust. Soc. Amer., 25: 405-411, 1953.

- 9-100. International Standard Organization, Technical Committee ISO/TC43: Acoustics; Working Group 8 - Industrial and Residential Noise; Working Groups 12 and 13 - Measurement and Assessment of Aircraft Noise. (USA Participation through the American Standards Association, Sectional Committee S3, Bioacoustics, [no date]).
- 9-101. Jansen, G., Zur Entstehung Vegetativer Funktionsstorungen durch Larmeinwirkung, Arch. Gewerbepath. Gewerbehyg., 17: 238-261, 1959.
- 9-102. Jansen, G., Schulze, J., Beispiele von Schlafstörung durch Geräusche, Klin. Wschr., 42: 132-134, 1964.
- 9-103. Jerison, H. J., Effects of Noise on Human Performance, J. Appl. Psychol., 43(2): 96-101, 1959.
- 9-104. Jerison, H. J., Hearing, in Bioastronautics Data Book, Webb, P., (ed.), NASA-SP-3006, 1964, Section 16, pp. 291-306.
- 9-105. Jerison, H. J., Wing, S., Effects of Noise and Fatigue on a Complex Vigilance Task, WADC-TR-67-14, Wright Air Development Center, Wright-Patterson AFB, Ohio, Jan. 1957.
- 9-106. Jones, G. W., Faugner, J. J., Jr., Investigation of Buffett Pressures on Models of Large Manned Launch Vehicle Configuration, NASA-TN-D-1633, May 1963.
- 9-107. King, P. F., Auditory Perception in Aircrew, in A Textbook of Aviation Physiology, Gillies, J. A., (ed.), Pergamon Press, Oxford, England, 1965, Chapter 31, pp. 968-988.
- 9-108. Kleitman, N., Sleep and Wakefulness, The University of Chicago Press, Chicago, Revised and Enlarged Edition, 1963.
- 9-109. Knudson, V. O., Harris, C. M., Acoustical Designing in Architecture, John Wiley & Sons, Inc., N. Y., 1950.
- 9-110. Kryter, K. D., Articulation Test Comparison of Six Signal Corps Aircraft Interphones at Low and High Altitudes, OSRD Rep. No. 1974, Office of Scientific Research and Development, National Defense Research Committee, Psycho-Acoustic Lab., Harvard University, Cambridge, Mass., 1944.
- 9-111. Kryter, K. D., Damage Risk Criteria for Hearing, in Noise Reduction, Beranek, L. L., (ed.), McGraw-Hill, N. Y., 1960.

- 9-112. Kryter, K. D., Damage Risk Criterion and Contours Based on a Permanent and Temporary Hearing Loss Data, Amer. Industr. Hyg. Ass. J., 26: 34-44, 1965.
- 9-113. Kryter, K. D., Effects of Ear Protective Devices on the Intelligibility of Speech in Noise, J. Acoust. Soc. Amer., 18: 413-417, 1946.
- 9-114. Kryter, K. D., The Effects of Noise on Man, J. Speech and Hearing Dis., Suppl I: 1-95, 1950.
- 9-115. Kryter, K. D., Exposure to Steady-State Noise and Impairment of Hearing, J. Acoust. Soc. Amer., 35: 1515-1525, 1963.
- 9-116. Kryter, K. D., Hearing Impairment for Speech, Arch. Otolaryng., 77: 598-602, 1963.
- 9-117. Kryter, K. D., Human Engineering Principles for the Design of Speech Communication Systems, AFCRC-TR-58-62, Air Force Cambridge Research Labs., L. G. Hanscom Field, Bedford, Mass., 1958.
- 9-118. Kryter, K. D., Methods for the Calculation and Use of the Articulation Index, J. Acoust. Soc. Amer., 34(11): 1689-1697, Nov. 1962.
- 9-119. Kryter, K. D., Validation of the Articulation Index, J. Acoust. Soc. Amer., 34: 1698-1702, 1962.
- 9-120. Kryter, K. D., Licklider, J. C. R., Speech Communication, in Human Engineering Guide to Equipment Design, Morgan, C. T., Cook, J. S., Chapanis, A., Lund, M. W., (eds.), 1963, Chapt. 4, pp. 161-216. (This chapter is based, in part, on material prepared by Webster, J. C., and Hawley, M.).
- 9-121. Kryter, K. D., Williams, C., Green, D. M., Auditory Acuity and the Perception of Speech, J. Acoust. Soc. Amer., 34: 1217-1223, 1962.
- 9-122. Lawrence, M., The Effect of Overstimulation and Internal Factors on the Function of the Inner Ear, Rep. 03032-1-F, University of Michigan, Kresge Hearing Research Institute, Ann Arbor, Mich., Apr. 1966.
- 9-123. Lawson, R. B., Pitch Perception, HEL-TN-7-65, Human Engineering Labs., Aberdeen Proving Ground Md., Oct. 1965. (AD-639109).

- 9-124. Lehmann, G., Meyer-Dlius, J., Gefassereaktionen der Korperperipherie bei Schalleinwirkung, Forschungberichte des Wirtshcafts und Verkehrsministeriums Nordrhein-Westfalen No. 517, 1958.
- 9-125. Lehmann, G., Tamm, J., Ueber Veränderungen der Kreislaufdynamik des Ruhenden Menschen unter Einwirkung von Gerauschen, [Changes of Circulatory Dynamics of Resting Men under the Effect of Noise], Int. Z. Angew. Physiol., 16: 217-227, 1956.
- 9-126. Licklider, J. C. R., The Effects of Amplitude Distortion upon the Intelligibility of Speech, J. Acoust. Soc. Amer., 18: 429-434, 1946.
- 9-127. Liebesny, P., Athermic Short Wave Therapy, Arch. Phys. Ther., 19: 736-740, 1938.
- 9-128. Lierle, D. M., (Chairman), Committee on Conservation of Hearing Subcommittee on Noise: Guide for the Evaluation of Hearing Impairment, Trans. Amer. Acad. Ophthal. Otolaryng., 63: 236-238, 1959.
- 9-129. Loeb, M., Jeantheau, G., Weaver, L. A., A Field Study of Vigilance Task, AMRL-230, Army Medical Research Lab., Fort Knox, Ky., 1956.
- 9-130. McElroy, J. T., Automation Industries, Research Lab., Boulder, Colo., personal communication, Apr. 1964.
- 9-131. McLean, F. E., Some Nonasymptotic Effects on the Sonic Boom of Large Airplanes, NASA-TN-D-2877, June 1965.
- 9-132. McLean, F. E., Carlson, H. W., Influence of Airplane Configuration on the Shape and Magnitude of Sonic-Boom Pressure Signatures, AIAA-65-803, presented at the AIAA/RAES/JSASS Aircraft Design and Technology Meeting, Los Angeles, Calif., Nov. 15-18, 1965.
- 9-133. Myers, C. K., An Evaluation for Use in Audiometry of the Noise Attenuation of Three Types of Circumaural Earmuffs, NMRL-MR-67-1, Naval Submarine Medical Center, Submarine Base, Groton, Conn., Jan. 1967.
- 9-134. Meyers, R., Fry, W. J., Fry, F. J., et al., Early Experiences with Ultrasonic Irradiation of the Pallidofugal and Nigral Complexes in Hyperkinetic and Hypertonic Disorders, J. Neurosurg., 16: 32-54, 1959.

- 9-135. Miller, G. A., The Masking of Speech, Psychol. Bull., 44: 105-129, 1947.
- 9-136. Miller, G. A., Heise, G. A., Lichten, W., The Intelligibility of Speech as a Function of the Context of the Test Materials, J. Exp. Psychol., 41: 329-335, 1951.
- 9-137. Miller, G. A., Licklider, J. C. R., The Intelligibility of Interrupted Speech, J. Acoust. Soc. Amer., 22: 167-173, 1950.
- 9-138. Mohr, G. C., Cole, J. N., Guild, E., et al., Effects of Low Frequency and Infrasonic Noise on Man, Aerospace Med., 36(9): 817-824, 1965.
- 9-139. National Academy of Sciences, National Research Council, Hazardous Exposure to Intermittent and Steady-State Noise, Report of Working Group 46, Committee on Hearing, Bioacoustics and Biomechanics (CHABA), Washington, D. C., Jan. 1965.
- 9-140. National Aeronautics and Space Administration, Nondestructive Testing: Trends and Techniques, Proceedings of the Second Technology Status and Trends Symposium, Marshall Space Flight Center, Huntsville, Ala., Oct. 26-27, 1966, NASA-SP-5082, 1967.
- 9-141. National Aeronautics and Space Administration, Results of the First Saturn I Launch Vehicle Test Flight SA-1, MPR-SAT-64-14, Marshall Space Flight Center, Huntsville, Ala., Apr. 1964. (Supersedes MPR-SAT-WF-61-8, 1961).
- 9-142. National Aeronautics and Space Administration, Results of the Second Saturn I Launch Vehicle Test Flight SA-2, MPR-SAT-63-13, Marshall Space Flight Center, Huntsville, Ala., Oct. 1963.
- 9-143. National Aeronautics and Space Administration, Safety and Design Considerations for Static Test and Launch of Large Space Vehicles, Part II B, Acoustic Hazards and Design Data, Joint Air Force NASA Hazards Analysis Board, NASA-MSFC, Washington, D. C., 1961.
- 9-144. Nixon, C. W., Human Response to Sonic Boom, Aerospace Med., 36(5): 399-405, 1965.
- 9-145. Nixon, C. W., Hille, H. K., Kettler, L. K., Attenuation Characteristics of Earmuffs at Low Audio and Intrasonic Frequencies, AMRL-TR-67-27, Aerospace Medical Research Labs., Wright-Patterson AFB, Ohio, May 1967.

- 9-146. Nixon, C. W., Sommer, H. C., Cashin, J. L., Use of Aural Reflex to Measure Ear-Protector Attenuation in High Level Sound, J. Acoust. Soc. Amer., 35(10): 1535-1543, 1963.
- 9-147. Nixon, J. C., Glorig, A., High, W. S., Changes in Air and Bone Conduction Thresholds as a Function of Age, J. Laryngol., 76(4): 288-298, 1962.
- 9-148. North American Aviation, Inc., Apollo Spacecraft Launch Vehicle Integration, NAA-SID-62-148, Space and Information Systems Division, Downey, Calif., May 1962.
- 9-149. North American Aviation, Inc., Transient Pressures on the 0.055 Scale Mdl. (PSTL-1) in NAA Trisonic Wind Tunnel - Preliminary Report, SID-62-1151, Space and Information Systems Division, Downey, Calif., Sept. 1962.
- 9-150. Ollerhead, J. B., On the Prediction of the Near Field Noise of Supersonic Jets, NASA-CR-857, Aug. 1967.
- 9-151. Oslake, J. J., Haight, N. L., Oberste, L. J., Acoustical Hazards of Rocket Boosters, Vol. I. Physical Acoustics, Rep. U-108-96, Aeronutronic Div., Ford Motor Co., Newport Beach, Calif., Nov. 1960.
- 9-152. Pearsons, K. S., Horonjeff, R. D., Category Scaling Judgement Tests on Motor Vehicle and Aircraft Noise, FAA-DS-67-8, Federal Aviation Administration, Dept. of Transportation, Aircraft Development Service, Washington, D. C., July 1967. (AD-658755).
- 9-153. Pickett, J. M., Effect of Vocal Force on the Intelligibility of Speech, J. Acoust. Soc. Amer., 28: 902-905, 1956.
- 9-154. Pickett, J. M., Pollack, I., Prediction of Speech Intelligibility at High Noise Levels, J. Acoust. Soc. Amer., 30: 955-963, 1958.
- 9-155. Pierce, J. R., David, E. E., Jr., Man's World of Sound, Doubleday & Co., Inc., N. Y., 1958.
- 9-156. Pietrasanta, A. C., Stevens, K. N., Guide for the Analysis and Solution of Air Base Noise Problems, WADC-TR-57-702, Wright Air Development Center, Wright-Patterson AFB, Ohio, Nov. 1961.
- 9-157. Plutchik, R., Frequency Analysis of Electroencephalographic Rhythms in Humans Exposed to High Intensity, Intermittent Auditory Inputs, Percept. Motor Skills, 23: 955-962, 1966.

- 9-158. Pollack, I., Message Uncertainty and Message Reception, J. Acoust. Soc. Amer., 31: 1500-1508, 1959.
- 9-159. Pollock, K. G., Bartlett, F. C., Psychological Experiments on the Effect of Noise, in Two Studies in the Psychological Effects of Noise, IHRB-65, Industrial Health Research Board, H. M. Stationary Store, London, 1932.
- 9-160. Ramsey, R. C., Design of Helmets, Earphones and Microphones Status Report No. 8, Electro-Voice, Inc., Buchanan, Mich., Dec. 1964. (Prepared under Contract AF-33(615)-1295).
- 9-161. Riesz, R. R., Differential Intensity Sensitivity of the Ear for Pure Tones, Phys. Rev., 31: 867-875, 1928.
- 9-162. Robinson, D. W., Dadson, R. S., Threshold of Hearing and Equal-Loudness Relations for Pure Tones and the Loudness Function, J. Acoust. Soc. Amer., 29: 1284, 1957.
- 9-163. Robinson, F. R., Cleary, J. P., Effects of High Intensity Sound on Circulation of the Inner Ear of the Guinea Pig, ASD-TN-61-58, Aeronautical Systems Division, Wright-Patterson AFB, Ohio, May 1961.
- 9-164. Rosenblith, W. A., The Relation of Hearing Loss to Noise Exposure, Report of the Exploratory Subcommittee Z24-X-2, American Standards Association, Inc., N. Y., 1954.
- 9-165. Rosenblith, W. A., (ed.), Sensory Communication, MIT Press, Cambridge, Mass., 1961.
- 9-166. Rosenblith, W. A., Stevens, K. N., Handbook of Acoustic Noise Control, Vol. II. Noise and Man, WADC-TR-52-204, (V.2), Wright Air Development Center, Wright-Patterson AFB, Ohio, June 1953.
- 9-167. Rosenthal, H., Ultrasonics in Clinical Medicine, Aviat. Med., 21(3): 265-272, June 1950.
- 9-168. Rowley, B. A., A Brief on the Feasibility of Ultrasonic Uses in Medicine, The Lovelace Foundation for Medical Education and Research, Albuquerque, N.M., Sept. 1964, unpublished report.
- 9-169. Rudnick, I., Propagation of Sound in the Open Air, in Handbook of Noise Control, Harris, C. M., (ed.), McGraw-Hill, N. Y., 1957, Chapt. 3, pp. 1-17.

- 9-170. Sabine, H. J., Sound Propagation Near the Earth's Surface as Influenced by Weather Conditions, WADC-TR-57-353(Pt. 4), Wright Air Development Center, Wright-Patterson AFB, Ohio, Jan. 1961.
- 9-171. Sanders, A. F., The Influence of Noise on Two Discrimination Tasks, Ergonomics, 4: 253-258, 1961.
- 9-172. Sateloff, J., Industrial Deafness, McGraw-Hill, N. Y., 1957.
- 9-173. Schwan, H. P., Biophysics of Diathermy, in Therapeutic Heat and Cold, Licht, S. H., (ed.), Published by Elizabeth Licht, New Haven, Conn., 2nd Edition, 1965, pp. 63-126.
- 9-174. Sergeant, R. L., Harris, J. D., Supra-Aural Cushions in Audiometry, NMRL-Memo-61-10, Naval Medical Research Lab., New London, Conn., Nov. 1961.
- 9-175. Sivian, L. J., White, S. D., On Minimum Audible Sound Fields, J. Acoust. Soc. Amer., 4: 288-321, 1933.
- 9-176. Shower, E. G., Biddulph, R., Differential Pitch Sensitivity of the Ear, J. Acoust. Soc. Amer., 3: 275-287, 1931.
- 9-177. Slavin, J. J., Soviet Tentative Standards and Regulations for Restricting Noise in Industry Approved by USSR Ministry of Health, Noise Control, 5(5): 44-49, 64, 1959.
- 9-178. Smith, C. P., Characterization of Speech Sources in Terms of Genetic Operating Characteristics, AFCRL-67-0309, Air Force Cambridge Research Labs., Bedford, Mass., May 1967.
- 9-179. Smith, E. L., Laird, D. A., The Loudness of Auditory Stimuli Which Affects Stomach Contractions in Healthy Human Beings, J. Acoust. Soc. Amer., 2: 94-98, 1930.
- 9-180. Spieth, W., Trittipee, W. J., Intensity and Duration of Noise Exposure and Temporary Threshold Shifts, J. Acoust. Soc. Amer., 30: 710-713, 1958.
- 9-181. Stanford Research Institute, Sonic Boom Experiments at Edwards Air Force Base, NSBEO-1-67, National Sonic Boom Evaluation Office, Arlington, Va., July 28, 1967. (Prepared under Contract AF 49(638)-1758).
- 9-182. Stevens, K. N., (ed.), Effects of Aircraft Noise in Communities, National Academy of Sciences, National Research Council, Committee on Hearing and Bio-acoustics: Report of Working Group 34, Washington, D. C., 1961.

- 9-183. Stevens, S. S., Handbook of Experimental Psychology, John Wiley and Sons, Inc., N. Y., 1951.
- 9-184. Stevens, S. S., Procedures for Calculating Loudness: Mark VI, J. Acoust. Soc. Amer., 33: 1577-1585, 1961.
- 9-185. Stevens, S. S., Volkman, J., The Relation of Frequency: A Revised Scale, Amer. J. Psychol., 53: 329-353, 1940.
- 9-186. Stover, W. R., Auditory Evaluation, NADC-AC-6709, Naval Air Development Center, Johnsville, Warminster, Pa., Nov. 1967.
- 9-187. Sumbly, W. H., Pollack, I., Visual Contribution to Speech Intelligibility in Noise, J. Acoust. Soc. Amer., 26: 212-215, 1954.
- 9-188. Surgent, L. V., Acoustical Analysis of Astronaut Speech, General Dynamics/Electronics, Rochester, N. Y., Feb. 1967. (Prepared under NASA contract NASw-1252).
- 9-189. Surgent, L. V., Acoustical Analysis of Astronaut Speech, Prog. Rep. for July 23 to Oct. 23, 1965, General Dynamics, Rochester, N. Y., Nov. 1965. (Prepared under NASA Contract NASw-1252).
- 9-190. Szafran, J., Psychophysiological Studies of Aging in Pilots, Lovelace Foundation for Medical Education and Research, Albuquerque, N.M., presented at the 38th Annual Scientific Meeting of the Aerospace Medical Association, Lovelace Memorial Session on the Aging Pilot, Washington, D. C., Apr. 12, 1967. (Submitted to Aerospace Medicine, May 1968).
- 9-191. Szafran, J., Psychophysiological Studies of Aging in Pilots, Lovelace Foundation for Medical Education and Research, Albuquerque, N. M., in Human Behavior and Aging: Recent Advances in Research and Theory, Talland, G. A., (ed.), Academic Press, N. Y., 1968.
- 9-192. U. S. Air Force, Hazardous Noise Exposure, Air Force Regulation, AFR-160-3, Washington, D. C., Oct. 1956.
- 9-193. U. S. Air Force, Human Engineering Design Criteria for Aerospace Systems and Equipment, Part 2. Aerospace System Facilities and Facility Equipment, MIL-STD-803A-2(USAF) Military Standards, Washington, D. C., Dec. 1, 1964.

- 9-194. U. S. Air Force Systems Command, Headquarters, Handbook of Instructions for Aerospace Personnel Subsystem Design, Chapt. 5. Human Performance Capabilities and Limitations, AFSCM-80-3, Washington, D. C., Apr. 15, 1965.
- 9-195. U. S. Naval Training Device Center, The Effects of Ultrasonic Vibrations on Man, NAVTRADEVCEEN-151-1-15, Port Washington, N. Y., Apr. 1948, (Reprinted Dec. 1959).
- 9-196. U. S. Navy, Acoustical Noise Level in Aircraft, General Specification for, MIL-A-8806A, July 11, 1966. (Supersedes MIL-A-8806(ASG), Oct. 25, 1956.
- 9-197. University of Pittsburgh, Electroacoustic Ear Protector, MX-7307()/UIC, Interim Report, TIR-30.0.3.5, Contract DA-49-186-AMC-214(D), Dec. 1966. (AD-809029).
- 9-198. Van Dyke, W. J., Performance/Design and Product Configuration Requirements, Extravehicular Mobility Unit for Apollo Block II Missions. Master End Item Specification, NASA-EMU-CSD-A-096, Manned Spacecraft Center, Houston, Texas, Jan. 1966.
- 9-199. Ward, A. A., Central Nervous System Effects, in Benox Report, An Exploratory Study of the Biological Effects of Noise, University of Chicago, Dec. 1953, pp. 73-80. (Contract No. N6-ori-020, Task Order 44, ONR Proj. Nr. 144079).
- 9-200. Ward, W. D., Damage-Risk Criteria for Line Spectra, J. Acoust. Soc. Amer., 34: 1610-1619, 1962.
- 9-201. Ward, W. D., Studies on the Aural Reflect. II. Reduction of Temporary Threshold Shift from Intermittent Noise by Reflex Activity; Implications of Damage-Risk Criteria, J. Acoust. Soc. Amer., 34: 234-241, 1962.
- 9-202. Ward, W. D., Glogig, A., Sklar, D. L., Dependence of Temporary Threshold Shift at 4 kc on Intensity and Time, J. Acoust. Soc. Amer., 30: 944-954, 1958.
- 9-203. Ward, W. D., Selters, W., Glogig, A., Exploratory Studies on Temporary Threshold Shift from Impulses, J. Acoust. Soc. Amer., 33: 781-793, 1961.
- 9-204. Waring, C. E., (ed.), Transformation and Reception of Sounds under Combat Conditions, TIPU-1130, Office of Scientific Research and Development, Office of Naval Research, Washington, D. C., 1946.

- 9-205. Wathen-Dunn, W., Lipke, D. W., On the Power Gained by Clipping Speech, J. Acoust. Soc. Amer., 30: 36-40, 1958.
- 9-206. Wegel, R. L., Lane, C. E., The Auditory Masking of One Pure Tone by Another and Its Probable Relation to the Dynamics of the Inner Ear, Phys. Rev., 23: 266-285, 1924.
- 9-207. Weinreb, L., Improved Ear Cushions for a Flying Helmet, WADD-TR-60-568, Wright Air Development Center, Wright-Patterson AFB, Ohio, 1960.
- 9-208. Wiener, F. M., Keast, D. N., Experimental Study of the Propagation of Sound Over Ground, J. Acoust. Soc. Amer., 31: 724-733, 1959.
- 9-209. Winchester, C. F., Campbell, L. E., Bond, J., et al., Effects of Aircraft Sound on Swine, WADC-TR-59-200, Wright Air Development Center, Wright-Patterson AFB, Ohio, Aug. 1959.
- 9-210. Wyatt, S., Langdon, J. N., Fatigue and Boredom in Repetitive Work, IHRB-77, Industrial Health Research Board, H. M. Stationary Office, London, 1937.
- 9-211. Yuganov, Ye. M., Drylov, Yu. V., Kuznetsov, V. S., Optimal Acoustic Environment for Spacecraft Cabins, NASA-TT-F-10980, June 1967. (Translation of Izv. Akad. Nauk SSSR, Ser. Biol., 31(1): 14-20, 1966).
- 9-212. Zwislocki, J. J., (ed.), Couplers for Calibration of Earphones; Review of Existing Situation and Recommendations for Needed Research and Development Work, Report of Working Group 48, National Academy of Sciences, National Research Council, Committee on Hearing, Bioacoustics and Biomechanics, Washington, D. C., Sept. 1967. (AD-658726).
- 9-213. Zwislocki, J. J., Ear Protectors, in Handbook of Noise Control, Harris, C. M., (ed.), McGraw-Hill, N. Y., 1957, Chapt. 8, pp. 1-27.
- 9-214. Zwislocki, J. J., (ed.), Feasibility of Intra-Service Standardization of Audiometric Tests and Testing Procedures; Current Status and Recommendations for Standardization, Report of Working Group 43, National Academy of Sciences, National Research Council, Committee on Hearing, Bioacoustics and Biomechanics, Washington, D. C., Sept. 1967. (AD-658725).